

Antimalarial Natural Product Cladosporin: Synthesis of Stereoisomeric Library, Lead Optimization, Co-crystallization, and Biological Evaluation and Synthesis of Related Macrocyclic Natural Products

by

Pronay Das
10CC15A26015

A thesis submitted to the
Academy of Scientific & Innovative Research
for the award of the degree of

DOCTOR OF PHILOSOPHY

in

SCIENCE

Under the supervision of
Dr. D. Srinivasa Reddy



CSIR-National Chemical Laboratory, Pune



Academy of Scientific and Innovative Research
AcSIR Headquarters, CSIR-HRDC campus
Sector 19, Kamla Nehru Nagar,
Ghaziabad, U.P. – 201 002, India

March, 2021

Certificate

This is to certify that the work incorporated in this Ph.D. thesis entitled, “Antimalarial Natural Product Cladosporin: Synthesis of Stereoisomeric Library, Lead Optimization, Co-Crystallization and Biological Evaluation and Synthesis of Related Macrocyclic Natural Products”, submitted by Pronay Das to the Academy of Scientific and Innovative Research (AcSIR) in fulfillment of the requirements for the award of the Degree of Doctor of philosophy in science, embodies original research work carried-out by the student. We, further certify that this work has not been submitted to any other University or Institution in part or full for the award of any degree or diploma. Research material(s) obtained from other source(s) and used in this research work has/have been duly acknowledged in the thesis. Image(s), illustration(s), figure(s), table(s) etc., used in the thesis from other source(s), have also been duly cited and acknowledged.



Pronay Das
(Research Student)
28.02.2021



Dr. D. Srinivasa Reddy
(Research Supervisor)
28.02.2021

STATEMENTS OF ACADEMIC INTEGRITY

I Pronay Das, a Ph.D. student of the Academy of Scientific and Innovative Research (AcSIR) with Registration No. 10CC15A26015 hereby undertake that, the thesis entitled “Antimalarial Natural Product Cladosporin: Synthesis of Stereoisomeric Library, Lead Optimization, Co-Crystallization and Biological Evaluation and Synthesis of Related Macrocyclic Natural Products” has been prepared by me and that the document reports original work carried out by me and is free of any plagiarism in compliance with the UGC Regulations on “*Promotion of Academic Integrity and Prevention of Plagiarism in Higher Educational Institutions (2018)*” and the CSIR Guidelines for “*Ethics in Research and in Governance (2020)*”.



Signature of the Student

Date : 28.02.2021

Place : Pune

It is hereby certified that the work done by the student, under my/our supervision, is plagiarism-free in accordance with the UGC Regulations on “*Promotion of Academic Integrity and Prevention of Plagiarism in Higher Educational Institutions (2018)*” and the CSIR Guidelines for “*Ethics in Research and in Governance (2020)*”.



Signature of the Supervisor

Name : Dr. D. Srinivasa Reddy

Date : 28.02.2021

Place : Jammu

Acknowledgement

During the entire period of my doctoral research, I have been acquainted, accompanied and supported by many people. Herein I take this opportunity to express my heart felt gratitude to all of them.

*First of all, I would like to express my heart felt thanks to my supervisor, **Dr. D. Srinivasa Reddy**, for his constant support and guidance throughout this journey. His precious knowledge, wise advices about life and generous help has significantly shaped the course of my doctoral journey and made me grow, not only as a researcher, but also as a wise and responsible human being. I feel immensely privileged to be a part of his esteemed research group at CSIR-National Chemical Laboratory, where I have been constantly motivated to achieve my goals. It is this very place, where I have learned to nurture a blend of hard work and discipline to shape my professional and personal aspects of life. It is under his supervision and guidance, where I have not only learned the art of culturing science, but also the art of thinking out of the box. What all I have gained and learned from him can never be repayed in any possible forms. I believe, a better way of thanking him would be through my future contributions to the scientific community. I wish him best of luck in his quest to perturb the limits of chemistry, and may nothing but great things happen to him and his family.*

I owe to thank my doctoral advisory committee (DAC) members, Dr. Mugdha Gadgil, Dr. Ravindar Kontham and Dr. G. J. Sanjayan for their constant support extended with guidance and suggestions. I am grateful to Prof. Dr. Ashwini K. Nangia (Director, CSIR-NCL), Prof. Dr. Sourav Pal (Former Director, CSIR-NCL), Dr. Pradeep Kumar (Former HoD, Division of Organic Chemistry, CSIR-NCL), Dr. S. P. Chavan (Former HoD, Division of Organic Chemistry, CSIR-NCL) and Dr. Narshinha P. Argade (HoD, Division of Organic Chemistry, CSIR-NCL) for giving me this opportunity and providing me with advanced research infrastructure and facilities.

I would like to express my gratitude to Dr. P. R. Rajamohanam, Dr. Uday Kiran Marelli, Dr. Ajith Kumar, Dinesh, Satish, Varsha, Meenakshi, Pramod for their timely support in recording NMR spectra. I would also like to express my gratitude to Mrs. Kunte and Mr. Sadafule for helping in HPLC analysis, Mrs. Santhakumari for HRMS facility. This list will be incomplete without expressing words of appreciation for Mr. Sridhar Thorat,

Acknowledgement

Mr. Sameer Shaikh and Dr. Rajesh Gonnade for diffracting and solving X-ray crystal structure of crucial compounds.

Herein I would also like to express my deep gratitude to my collaborators Dr. Dhanasekaran Shanmugam (CSIR-NCL) and Dr. Amit Sharma (International Center for Genetic Engineering and Biotechnology, New Delhi) for biological evaluations of synthesized compounds and co-crystallization. Besides I would once again like thank Dr. Amit Sharma for his valuable support and suggestions that has really shaped the entire structure of my doctoral work. In this context, I feel extremely happy to express a deep sense of gratitude to Miss. Palak Babbar for conducting and discussing biological experiments related to my doctoral work. Besides, she has always been there as a friend in need in tough times.

My list of acknowledgement would be incomplete without mentioning the name of Dr. Indrapal Singh (IIT Madras) who had effectively incepted in me a deep sence of interest in the field of medicinal chemistry and drug development. Besides, he has also provided me with the valuable knowledge regarding the art of organic synthesis that has helped me in this very journey. I would also like to thank Dr. Nandita Madhavan (IIT Bombay), under the guidance of whome I got my first exposure and experience in laboratory chemistry and research during my M. Sc. Dissertation.

It's my immense pleasure to thank my lab mates Dr. Kashinath, Dr. Gajanan, Dr. Kishore, Dr. Vasudevan, Dr. Satish, Dr. Remya, Dr. Santu, Dr. Seetharam, Dr. Gorakhnath, Dr. Vidya, Dr. Mahender, Dr. Rahul, Dr. Rohini, Dr. Hanuman, Dr. Srinivas, Dr. Giri, Dr. Madhuri, Dr. Gangadurai, Dr. Ramesh, Pankaj, Ganesh, Namrata, Monica, Paresh, Akshay, Rahul, Suhag, Dattatraya, Yash, Vishal, Swati, Sunil, Laxmikant, Satish, Grace, Neha, Sneha, Rini, Aman, Priyanka, Rahul Lagade for devoting their precious time and providing me with valuable suggestions. I am also grateful to my lab mates, Dr. Gorakhnath, Paresh, Rahul, Dr. Vidya for proof reading sections of my thesis. A special thanks also goes to my co-authors namely, Palak Babbar, Nipun Malhotra, Manmohan Sharma, Dr. Gorakhnath R. Jachak, Yash Mankad, Swati Yadav, Karl Harlos, Manickam Yogavel for their help in cladosporin related project. I would especially like to thank Dr. Gorakhnath Jachak, Dr. Santu Dhara, Dr. Satish Chandra Philkhana, Paresh Athawale, Rahul Choudhury for their

Acknowledgement

fruitful suggestions and moral support throughout my research time. I would also like to express my heartfelt thanks to Yash Mankad and Swati Yadav for assisting me in my research projects.

No words are sufficient to acknowledge my prized friends in and out of NCL who have helped me at various stages of my life and my research work. I would love to thank Dr. Krisahnu Mondal, Dr. Arijit Mallik, Dr. Munmun Ghosh, Dr. Shaibal Bera, Dr. Subhrata Mondal, Kaushik Majhi, Abhijit Bera, Debranjana Mondal, Ashish Bera, Tapas Haldar, Tamal Das, Mahesh Shinde, Sibadatta Senapati, Pawan Dhote, Swapnil Halnor, Nitin Jadav for being a valuable part of my NCL family. Besides, I would like to express a deep sense of gratitude to Sanjukta Pahar for her immense moral support throughout my masters (M. Sc.) and research tenure. I would also like to thank my friend out side of NCL, namely, Sameer Paranjape, Homith Bakshi, Rimjhim Barkakati, Bruhad Mankad, Prosonjit Paul, Sowmini Paul for being their as a constant moral support. I really enjoyed the time that I spent with these awesome people. I would also like to express my gratitude to Dr. Hina Khan for being there in the time of need as a best friend and an incomparable moral support during hard times. Apart from these, I want to thank my old friends namely, Dr. Asik Hossain, Subhankar Panda, Soumalya Bhattacharya, Suman Gomostha, Sutirtha Bhattacharya who had inspired me in the field of research. Last but not the least, I want to thank my childhood friends namely, Bodhayan Bhattacharya, Sourajit Mukherjee and Rupam Koner or always being there.

Without the funding that I have received, this Ph. D. would not have been possible. Hence I would like to express my sincere appreciation to CSIR-University Grants Commission (CSIR-UGC) for awarding me with JRF followed by SRF fellowship.

Words are inadequate to express my feelings and gratitude to my family for their unconditional love, care and support throughout my life. I would not have achieved anything without the support of my mom and dad, who gave me the freedom to explore my world and to explore who am I. With immense gratitude and reverence, I acknowledge my mom, Mrs. Krishna Das and my dad, Mr. Paritosh Kumar Das for shaping my life and making me who I am today.

Acknowledgement

Finally, with immense respect and gratitude, I bow down in front of the almighty for all that has been offered to me. I am, and will remain thankful for everything that has ever happened in my life, the good and the bad; for everything that I have achieved and few that I have lost. Some were blessings and some were lessons worth learning.

Pronay Das

Abbreviations

AcOH	acetic acid
AcCl	acetyl chloride
Ac ₂ O	acetic anhydride
Å	angstrom
Ar	aryl
MeCN	acetonitrile
Bn	benzyl
Boc	<i>tertiary</i> -butyloxycarbonyl
Br	bromo
brs	broad singlet
Bu	butyl
<i>t</i> -Bu	<i>tertiary</i> -butyl
calcd.	Calculated
cm ⁻¹	1/centimeter
C–C	carbon-carbon
C–H	carbon-hydrogen
C–N	carbon-nitrogen
C–O	carbon-oxygen
CH ₂ Cl ₂	Dichloromethane
CHCl ₃	Chloroform
DBU	1,8-diazabicyclo[5.4.0]undec-7-ene

Abbreviations

DMAP	4-dimethyl aminopyridine
DMF	<i>N,N</i> -dimethylformamide
DMSO	dimethylsulphoxide
DMSO- <i>d</i> ₆	deuteriated dimethylsulphoxide
dd	doublet of doublet
d	doublet (in NMR) or day(s) (in Scheme)
Et	ethyl
EtOAc	ethyl acetate
EtOH	ethanol
equiv	equivalent
g	gram(s)
h	hour(s)
Hz	hertz
IR	infrared
<i>J</i>	coupling constant (in NMR)
mass (ESI+)	electron spray ionization mass spectroscopy
min	minute(s)
m	multiplet
mL	milliliter(s)
mmol	millimole(s)
mp	melting point
m/z	mass to charge ratio

Abbreviations

Me	methyl
MHz	megahertz
N	normality
nM	nanomolar(s)
NMR	nuclear magnetic resonance
Ph	phenyl
ppm	parts per million
Pr	propyl
q	quartet
R _f	retention factor
rt	room temperature
s	singlet
S _N	nucleophilic substitution
<i>sec</i>	secondary
t	triplet
<i>tert</i>	tertiary
THF	tetrahydrofuran
TFA	trifluoroacetic acid
TLC	thin layer chromatography
UV	ultraviolet
v/v	volume by volume
wt/v	weight by volume

Abbreviations

°C	degree celsius
μM	micromolar
mg	Milligram
μmol	Micromolar
in vitro	Outside a living organism
in vivo	Inside a living organism


General Remarks

- All reagents, starting materials, and solvents were obtained from commercial suppliers and used as such without further purification. Solvents were dried using standard protocols or through MBRAUN (MB SPS-800) solvent purification system (SPS).
- All reactions were carried out in oven-dried glassware under a positive pressure of argon or nitrogen unless otherwise mentioned with magnetic stirring.
- Air sensitive reagents and solutions were transferred via syringe or cannula and were introduced to the apparatus via rubber septa.
- Progress of reactions were monitored by thin layer chromatography (TLC) with 0.25 mm pre-coated silica gel plates (60 F254). Visualization was accomplished with either UV light, Iodine adsorbed on silica gel or by immersion in ethanolic solution of phosphomolybdic acid (PMA), *p*-anisaldehyde, 2,4-DNP, KMnO₄, Ninhydrin solution followed by heating with a heat gun for ~15 sec.
- Column chromatography was performed on silica gel (100-200 or 230-400 mesh size).
- Melting points of solids were measured using scientific melting point apparatus (Buchi 565).
- Deuterated solvents for NMR spectroscopic analyses were used as received.
- All ¹H NMR, ¹³C NMR spectra were obtained using a 200 MHz, 400 MHz, 500 MHz spectrometer. Coupling constants were measured in Hertz. The following abbreviations were used to explain the multiplicities: s = singlet, d = doublet, t = triplet, q = quartet, m = multiplet, br = broad.
- HRMS (ESI) were recorded on ORBITRAP mass analyzer (Thermo Scientific, QExactive).
- Infrared (IR) spectra were recorded on a FT-IR spectrometer as a thin film.
- Optical rotation values were recorded on P-2000 polarimeter at 589 nm.
- Chemical nomenclature (IUPAC) and structures were generated using Chem Bio Draw Ultra.



Synopsis



	Synopsis of the thesis to be submitted to the Academy of Scientific and Innovative Research for award of the degree of Doctor of philosophy in Chemical Sciences
Name of the Candidate	Mr. Pronay Das
Enrollment No. and Date	Ph. D in Chemical Sciences (10CC15A26015); August, 2015
Title of the Thesis	Antimalarial Natural Product Cladosporin: Synthesis of Stereoisomeric Library, Lead Optimization, Co-Crystallization and Biological Evaluation and Synthesis of Related Macrocyclic Natural Products
Research Supervisor	Dr. D. Srinivasa Reddy
Research Co-Guide	

1. Introduction and Statement of Problem

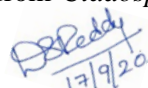
Parasitic diseases pose considerable threat in the global health concern accounting for more than one million casualties worldwide. Among the wide variety of parasitic diseases, malaria, caused by *Plasmodium falciparum*, remains as the most prevalent one with an estimate of 228 million cases worldwide in 2018 with a death of more than 4,00,000. Though several anti-malarial drugs have emerged throughout the timeline, most of them are discontinued owing to the emerging scenario of parasitic resistance. Artemisinin-based combination therapies (ACTs) are recommended by WHO as the first and second line treatment for *P. falciparum* malaria as well as for chloroquine-resistant *P. vivax* malaria. But cases of ACT resistant malarial parasite have been reported in several countries, as a result of which development of new and novel antimalarial lead molecule is crucial. In this context, Cladosporin, a fungal secondary metabolite isolated from *Cladosporium cladosporioides* and *Aspergillus flavus*, exhibits potent anti-plasmodial activity through targeting parasite cytosolic lysyl-tRNA synthetase (*PfKRS*), an enzyme central to protein biosynthesis. Besides, the molecule is >100 selective towards parasitic *PfKRS* over human KRS (*HsKRS*). Having such impressive anti-malarial potency with excellent parasitic selectivity, cladosporin surely holds a promising potential in the domain of anti-malarial drug development.

2. Objectives

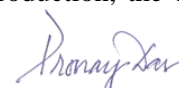
- Identifying the role of specific stereoisomeric conformation in the drug potency of cladosporin scaffold against *P. falciparum*.
- Developing a modified synthetic protocol for accessing gram scale quantities of cladosporin for in-depth pharmacokinetic (PK) studies.
- Synthesis and biological evaluation of cladosporin inspired library of compounds towards "lead identification".
- Synthesis of twelve membered macrocyclic natural products (Resorcylic Acid Lactones) structurally related to cladosporin.

3. Methodology

The thesis is divided into two major chapters. Initial part (**Section A**) of **Chapter 1** mainly deals with an introduction to cladosporin, a potent and selective anti-malarial natural product isolated from *Cladosporium cladosporioides* and *Aspergillus flavus*. Following introduction, the chapter


17/9/20

Signature of the Supervisor



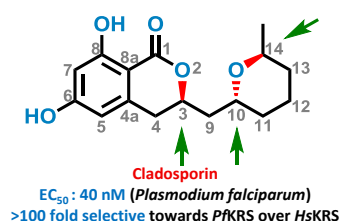
Signature of the Candidate

further discusses a divergent synthetic route to access all the possible stereoisomers of cladosporin. Through in depth biological evaluations including enzymatic and cell based assays and X-ray co-crystals, the crucial role of stereochemistry in anti-malarial drug potency has been deciphered in molecular level. **Section B** of this chapter deals with an efficient and modified synthetic route to access multi gram scale of Cladosporin. **Section C** further deals with the synthesis of analogue library around cladosporin scaffold, their biological evaluation, lead optimization and co-crystallization. In **Chapter 2**, deals with the synthesis of Cladosporin related macrocyclic natural products, specifically twelve membered Resorcylic Acid Lactones or RAL₁₂.

Chapter 1: Section A: Synthesis of entire stereoisomeric set of anti-malarial natural product cladosporin, their biological evaluation, and co-crystallization.

Cladosporin, an antifungal antibiotic and plant growth regulator isolated from *Cladosporium cladosporioides* and *Aspergillus flavus* in 1971^{1,2} is a chiral isocoumarin based scaffold that exhibited promising and selective (>100 folds in *Plasmodium falciparum* over humans) anti-plasmodial activity in nano molar range against both liver and blood stage *Plasmodium falciparum*.

To decipher the role of chirality in anti-malarial potency of cladosporin, we planned to synthesized all the possible stereoisomers of the same and screen them in vitro against *Plasmodium falciparum* and *Homo sapiens* KRS enzyme (*PfKRS* and *HsKRS*) along with in vivo parasite inhibition assay. The synthesized stereoisomers of cladosporin were further co-crystallized with *PfKRS* and the XRD analysis of the same revealed the structural bases of enzymatic binding of the isomers.



Herein, we developed a novel divergent synthetic route (Figure 1, 2, 3) to access all possible stereoisomers of the three chiral centered anti-malarial natural product cladosporin using chiral propylene oxide as the chiral source and assessed their inhibitory potency through parasite-, enzyme- and cell-based assays.

Synthesis

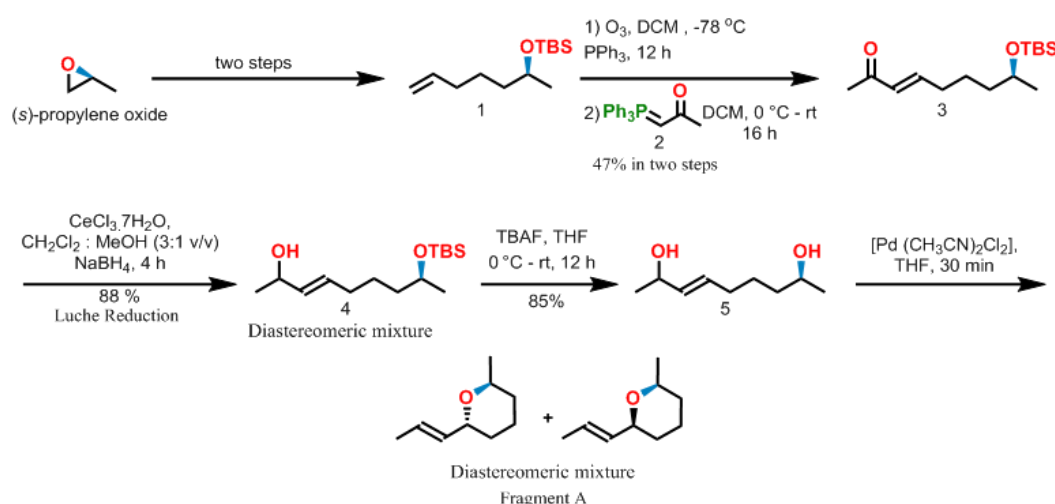


Figure 1. Synthesis of diastereomeric mixture of fragment A.

Dr. P. S. Reddy
17/9/20

Signature of the Supervisor

Pranay Son

Signature of the Candidate

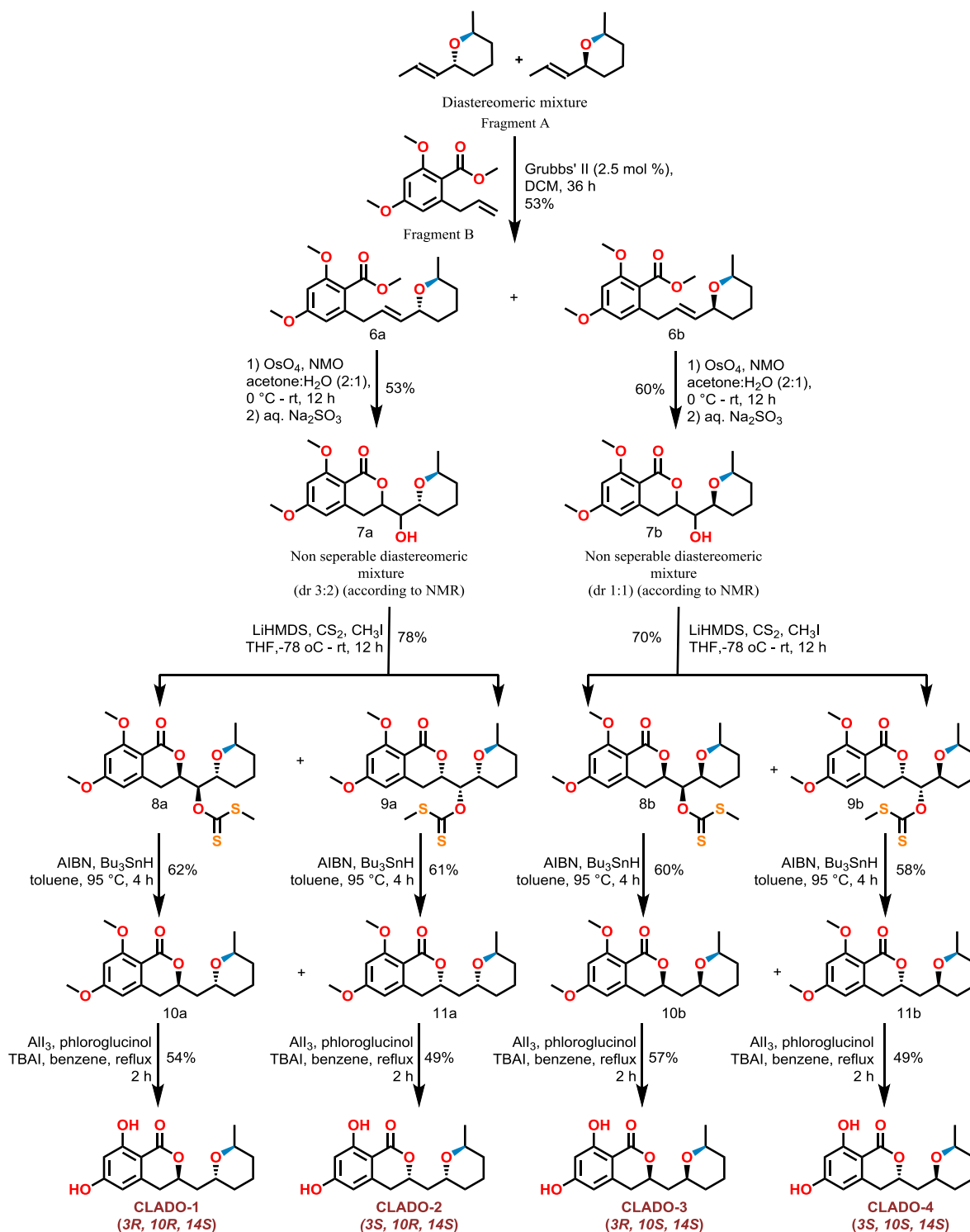


Figure 2. Synthesis of Cladosporin (CLADO-1) and three of its stereoisomers.

Dr. P. Reddy
17/9/20

Signature of the Supervisor

Kronay

Signature of the Candidate

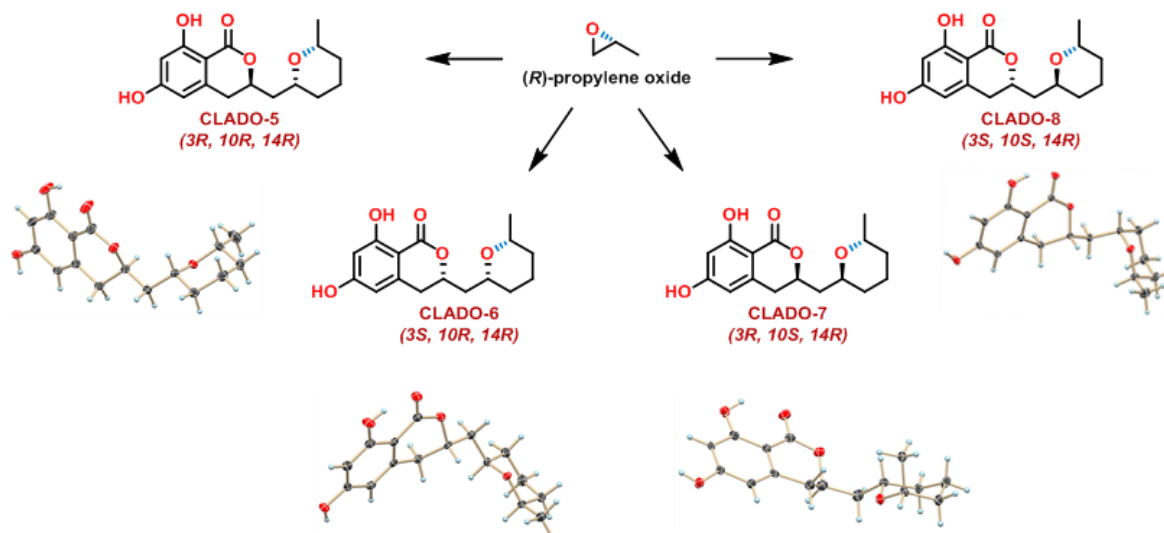


Figure 3: Synthesis of four stereoisomers of cladosporin from (*R*)-propylene oxide.

On the basis of drug-binding characteristics of the eight cladologs, we were able to assign CLADO-1 (cladosporin) and CLADO-5 as strong binders to *Pf*KRS, CLADO-2, CLADO-3, CLADO-7 as moderate binders, CLADO-6 and CLADO-8 as poor; whereas all the eight stereoisomers demonstrated pretty weak binding with *Hs*KRS indicating a high selectivity towards parasitic protein thus demonstrating a high selectivity index. Enzymatic and parasitic assays reflected similar trends in IC_{50} and EC_{50} values as well. The IC_{50} range for the best (CLADO-1) to poorest stereoisomer (CLADO-8) spanned a striking ~500- fold difference, which is pretty intriguing and interesting considering the fact that CALDO-1 and CLADO-8 are enantiomers of each other. To explore the structural basis of cladolog selectivity in a molecular level, we undertook the co-crystallization of six stereoisomers. After thorough analysis of the diffraction data we concluded on steric grounds that an *R* stereochemistry is necessary at C3 and C10 of the active cladosporin scaffold for retaining its anti-malarial potency; whereas stereochemistry at C14 is not a key detrimental factor for potency. Compilation and correlation of all the biological data led us to successfully categorize the entire stereochemical library of cladosporin in three different groups as depicted in figure 4.

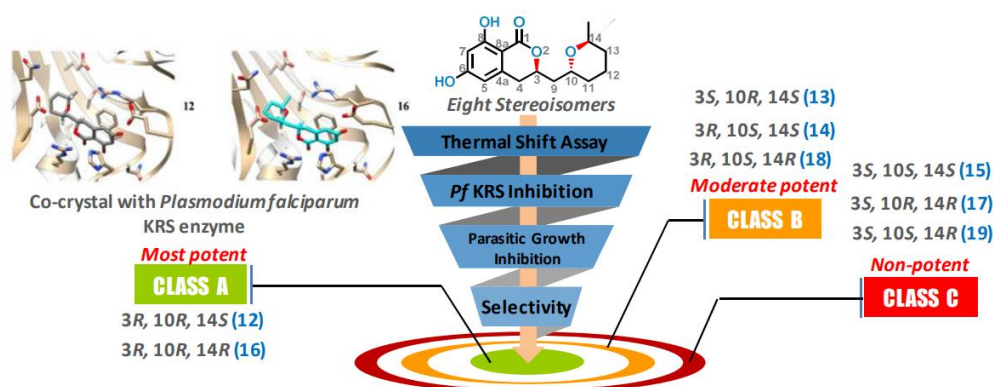


Figure 4. Summary of work and categorical distribution of cladologs.

DR Paddy
17/9/20

Signature of the Supervisor

Kronay Dor

Signature of the Candidate

Chapter 1: Section B: Gram scale synthesis of cladosporin

Cladosporin, a secondary metabolite isolated from fungal sources was found to exhibit selective nano-molar activity against malarial parasite, *Plasmodium falciparum* by inhibiting parasitic protein biosynthesis. In addition, this natural product has a broad range of bioactivities including, anti-parasitic, anti-fungal², anti-bacterial³ as well as plant growth inhibition^{1,4}. However, the quantities available from the natural sources are limited. To access sufficient quantities of cladosporin, we have developed a scalable synthetic route for the same. Gram-scale operations, Mitsunobu inversion to convert undesired alcohol to required one and palladium-catalyzed carbon monoxide insertion reaction to form six-membered lactone ring are the highlights of the present work. Now we have more than two grams of material in hand which is sufficient for further profiling such as in-depth assessment of the pharmacokinetics and pharmacodynamics. Furthermore, the synthetic protocol described herein is amiable for further scale up.

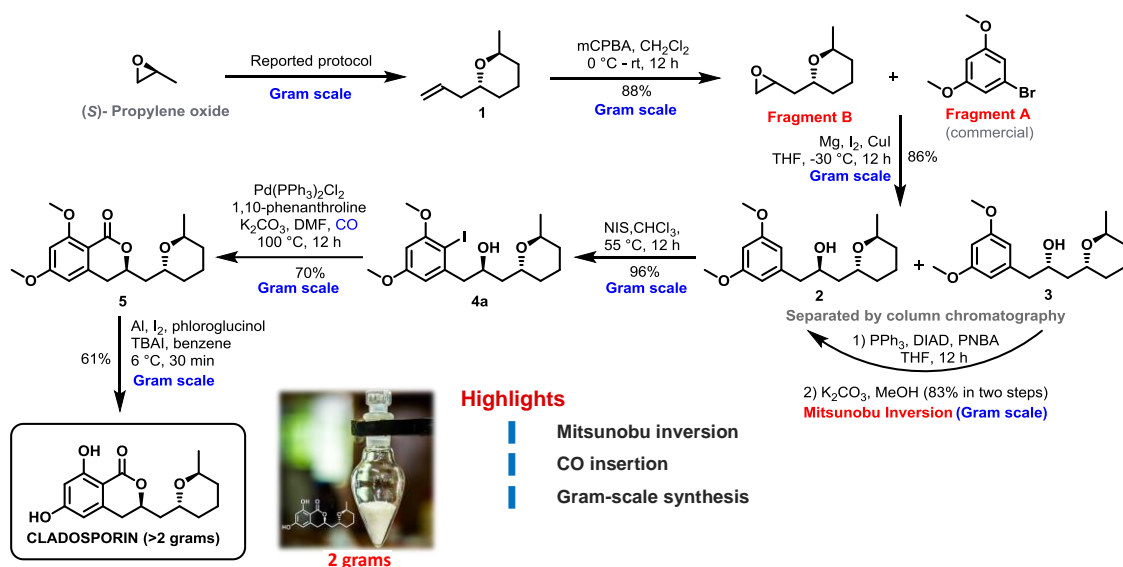


Figure 5: Gram scale synthesis of cladosporin.

Chapter 1: Section C: Design, Synthesis, Biological Evaluation of lysyl tRNA synthetase (KRS) Inhibitors based on Cladosporin Scaffold towards Identification of Antimalarial Leads

Cladosporin, an antifungal and antiparasitic natural products has proven to be a valuable target for the development of new and novel antimalarials. As no systematic SAR (Structure Activity Relationship) studies on this natural product have been reported in the literature so far, a proper and in depth assessment of the molecule is necessary for the identification of novel antimalarial leads. Hence, we planned to access a broad class of analogue library around cladosporin scaffold and screen them all in relevant biological assays so as to have an in depth understanding of its related SAR and develop a new lead that can be taken forward for the development of new antimalarials. All the possible and planned variation around the scaffold for a systematic SAR study has been depicted in figure 6.

Dr. P. S. Reddy
17/9/20

Signature of the Supervisor

Pranay Kumar

Signature of the Candidate

THIS WORK

- Variation in dihydroisocoumarin moiety
- Variation in tetrahydropyran moiety
- Modification of linker
- Other modifications and combinations

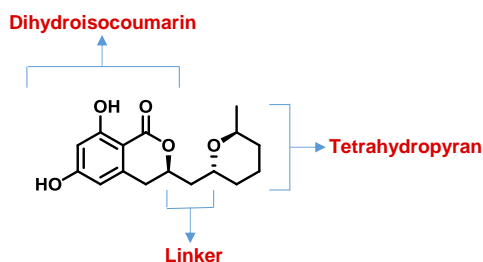


Figure 6. Possible modification around cladosporin scaffold.

Following the possible variations as depicted in figure 6, we generated a vast library of analogues around cladosporin scaffold. The structural modifications that has been incorporated in the active Cladosporin scaffold are depicted in the following figures.

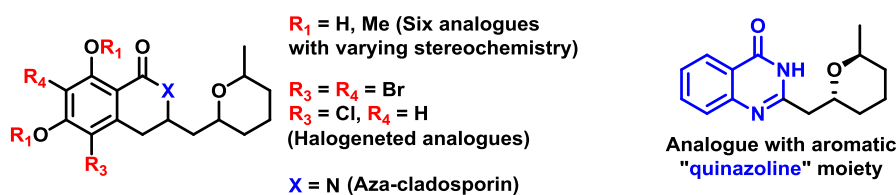


Figure 7a. Analogues with variations in isocoumarin moiety.

We also generated several analogues by modifying the THP moiety in the scaffold.

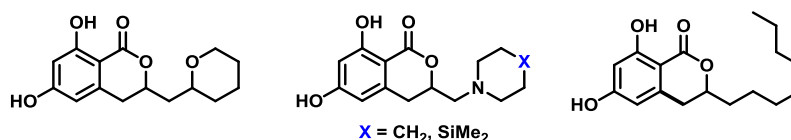


Figure 7b. Analogues with variations in THP moiety.

We also did some major changes in the core structure of cladosporin through multi-parameter modification and combination as follows.

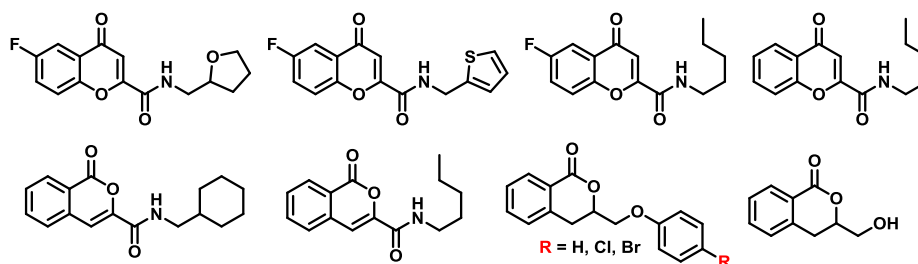


Figure 7c. Other modifications and combinations.

After close scrutiny of the co-crystal structure of cladosporin with *Pf*KRS we deciphered a promising possibility of introduction of hydroxyl group in the linker carbon of cladosporin scaffold. As a part of which we initially synthesized racemic (diastereomeric mixture) version of the hydroxy analogue (CL-1) of cladosporin which turned out to be promisingly potent (IC_{50} : 0.17 μM ; EC_{50} : 0.1 μM). This interesting observation intrigued us to synthesized chiral pure version of the concerned analogue. As a part of our plan, we synthesized both the diastereomers of the concerned analogue in chiral pure form (Figure 8). Biological profiling revealed CL-2 to be the potent isomer due to extra hydrogen bonding interaction of the added $-\text{OH}$ group with the active site residues. Besides, this analogues, CL-2 is metabolically more stable than cladosporin as evident from liver microsomal stability experiment.

Dr. P. S. Reddy
17/9/20

Signature of the Supervisor

Pronay Das

Signature of the Candidate

Herein we generated a vast library (~30 compounds) of related analogues of cladosporin, and following in depth anti-malarial screening, we came up with CL-2 as an active lead which can now be further modified towards new anti-malarials.

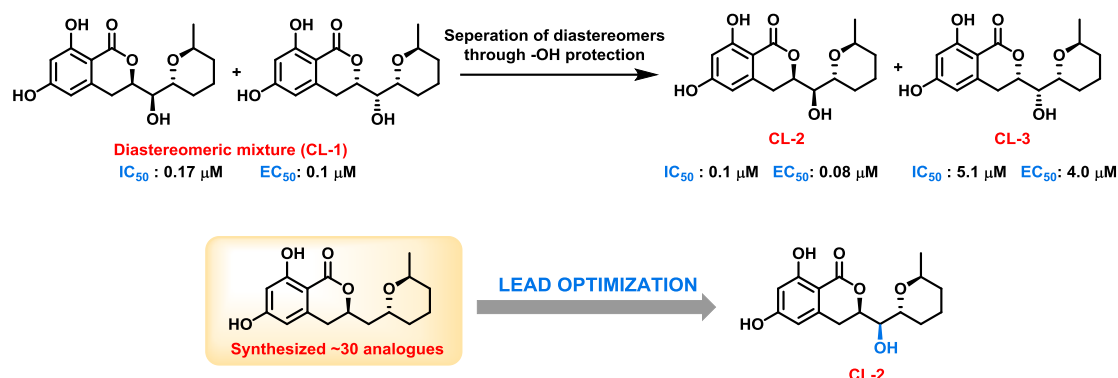


Figure 8. Analogues with -OH functionality at the linker carbon.

Chapter 2: Total Synthesis of Cladosporin related twelve membered macrocyclic natural products

Naturally occurring macrolides usually have significant and diverse bioactivities, which have potentially provided small-molecule entities for developing clinical drugs.⁵ Moreover, macrolides possessing lactone core fused to resorcinol fragment usually exhibited a wide spectrum of biological properties, including anti-tumour, anti-bacterial, anti-malarial activities^{6,7} In this context, we selected four, twelve membered macrolides (Figure 9), namely, Peniciminolide A, Peniciminolide B, (*R*)-Resorcyclide and (*R*)-Dihydroresorcyclide. All these natural products holds an in-depth structural similarity with Cladosporin as depicted in figure 10.

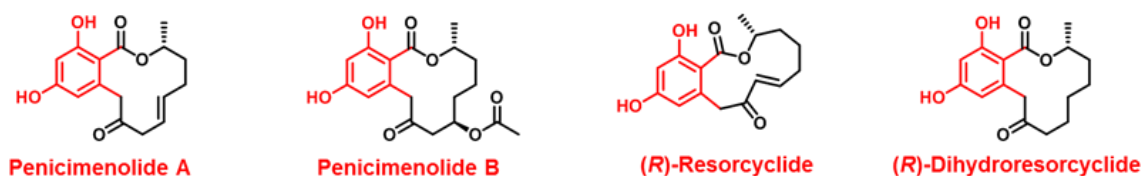


Figure 9. Structures of targeted macrocyclic natural products.

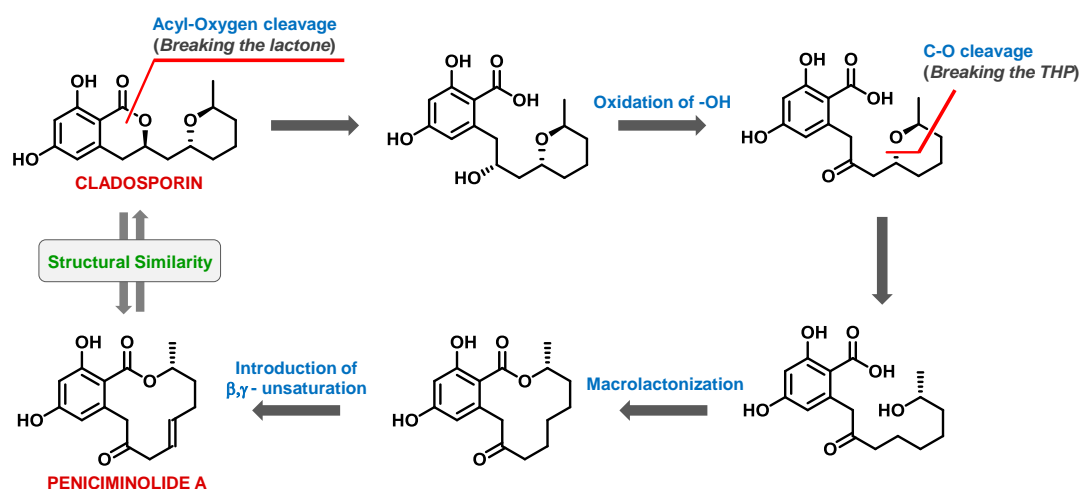


Figure 10. Structural similarity of Peniciminolide A with Cladosporin.

As a part of our work, we have accomplished the first total synthesis of Peniciminolide A in nine linear steps with moderate to high yields in each step. Exceptional low yield was observed in the final AlI_3 mediated exhaustive demethylation step owing to the formation of several unwanted by-products.

After synthesizing Peniciminolide A, we further hydrogenated the olefin functionality in the macrocyclic natural product which afforded yet another similar natural product, (*R*)-dihydroresorcyclide, a resorcinol-fused twelve-membered macrolide isolated from the fermentation extracts of an endophyte *Acremonium zeae*.⁸ Synthesis of other macrocyclic natural products are ongoing.

4. Summary

- We developed a divergent synthetic route for accessing all the stereoisomers of potent anti-malarial natural product cladosporin and assessed their inhibitory potency through parasite-, enzyme- and cell-based assays. X-ray diffraction study of co-crystals of the stereoisomers with *Pf*KRS further gave an insight about the structural bases of enzymatic binding of the isomers.
- We further utilized a modified synthetic protocol to access >2 grams of Cladosporin.
- In this work, we have studied the Structural Activity Relationship (SAR) of a broad library of analogues, designed and synthesized based on Cladosporin scaffold, in anti-malarial potency. In this exercise, we identified a lead compound (CL-2) having similar potency to that of cladosporin with an increased metabolic stability. The *Pf*KRS-CL-2 co-crystal structure reveals new features of enzyme drug interactions.
- Total synthesis of peniciminolide A and (*R*)-dihydroresorcyclide was accomplished. These macrocycles have an in-depth structural similarity with cladosporin.

5. Future directions

To accomplish the synthesis of other twelve membered Resorcyclic Acid Lactone (RAL₁₂) having structure compliance with cladosporin.

6. Publications

- Das, P., Babbar, P., Malhotra, N., Sharma, M., Jachak, G. R., Gonnade, R. G., Shanmugam, D., Harlos, K., Yogavel, M., Sharma, A., and Reddy, D. S. Specific Stereoisomeric Conformations Determine the Drug Potency of Cladosporin Scaffold against Malarial Parasite. *J. Med. Chem.* **2018**, *61*, 5664-5678.
- Das, P., Mankad, Y., Reddy, S. Scalable synthesis of cladosporin. *Tetrahedron lett.* **2019**, *12*, 831-833.

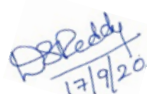
7. References

- Springer, J. P.; Cutler, H. G.; Crumley, F. G.; Cox, R. H.; Davis, E. E.; Thean, J. E. *J. Agric. Food Chem.* **1981**, *29*, 853–855.
- Scott, P. M.; Van Walbeek, W.; Maclean, W. M. *J. Antibiot.* **1971**, *24*, 747–755.
- Anke, H. *J. Antibiot.* **1979**, *32*, 952-958
- Kimura, Y.; Shimomura, N.; Tanigawa, F.; Fujioka, S.; Shimada, A.; *Z Naturforsch C.* **2012**, *67*, 587
- Yeung, K.S.; Paterson, I. *Chem. Rev.* **2005**, *105*, 4237.

Signature of the Supervisor

Signature of the Candidate

- 6) Jiang, C.S.; Liang, L.F. Guo, Y.W. *Acta Pharmacol. Sin.* **2012**, 33, 1217.
- 7) Winssinger, N.; Barluenga, S. *Chem. Commun.* **2007**, 171, 22.
- 8) Poling, S.M.; Wicklow, D.T.; Rogers, K.D.; Gloer, J.B. *J. Agric. Food. Chem.* **2008**, 56, 3006.


17/9/20

Signature of the Supervisor



Signature of the Candidate

Table of Content

Chapter 1

Section A: Synthesis of Entire Stereoisomeric Set of Anti-Malarial Natural Product Cladosporin, their Biological Evaluation, and Co-Crystallization

1.1.1. Introduction	1
1.1.1.1. An introduction to cladosporin	5
1.1.1.2. Highlights of reported synthesis of cladosporin	7
1.1.1.3. Highlights of reported synthesis of isocladosporin	8
1.1.2. Results and discussion	11
1.1.2.1. Synthesis of Fragment A from (S)-propylene oxide	11
1.1.2.2. Synthesis of Fragment B	12
1.1.2.3. Synthesis of Fragment A' from (R)-propylene oxide	16
1.1.2.4. Biological assessment of synthesized cladologs	21
1.1.2.4.1. Thermal Shift Assay (TSA)	21
1.1.2.4.2. Aminoacylation assay	22
1.1.2.4.3. Parasite growth inhibition assay	23
1.1.2.5. Structural bases for cladolog-KRS binding	26
1.1.3. Conclusions	30
1.1.4. Experimental section	32
1.1.5. References	58
1.1.6. Copies of ^1H and ^{13}C NMR spectra of selected compounds	63

Section B: Gram scale synthesis of cladosporin

1.2.1. Introduction	82
1.2.2. Results and discussion	84
1.2.2.1. Synthesis of key alcohol fragment	85
1.2.2.2. Optimization of Grignard reaction	85
1.2.3. Conclusion	89
1.2.4. Experimental Section	90

Table of Content

1.2.5. References	96
1.2.6. Copies of ¹ H and ¹³ C NMR spectra of selected compounds	99
Section C: Design, Synthesis, Biological Evaluation of lysyl tRNA synthetase (KRS) Inhibitors based on Cladosporin Scaffold towards Identification of Antimalarial Leads	
1.3.1. Introduction	104
1.3.2. Synthesis of analogue library around cladosporin scaffold	106
1.3.2.1. Modifications at linker	107
1.3.2.2. Modifications at dihydroisocoumarin moiety	109
1.3.2.3. Modifications at tetrahydropyran moiety	113
1.3.2.4. Other modifications	117
1.3.3. Biological assessment of synthesized analogues	122
1.3.3.1. Structure activity relationship (SAR) study	122
1.3.3.2. In vivo pharmacokinetics	127
1.3.3.3. Structural interactions in the CL-2-KRS complex	128
1.3.4. Conclusion	129
1.3.5. Experimental section	133
1.3.6. References	161
1.3.7. Copies of ¹ H and ¹³ C NMR spectra of selected compounds	166

Chapter 2

Total Synthesis of Cladosporin Related Twelve Membered Macrocyclic Natural Products

2.1. Introduction	193
2.1.1. Structural similarity between cladosporin and (<i>R</i>)-penicimenolide A	194
2.2.2. Selected previous synthesis of related compounds	195
2.2. Results and discussion	198
2.2.1. Retrosynthetic analysis of (<i>R</i>)-penicimenolide A , (<i>R</i>)-dihydroresorcyclide and (<i>R</i>)- <i>trans</i> -resorcyclide	198
2.2.2. Total synthesis of (<i>R</i>)-penicimenolide A	199
2.2.3. Total synthesis of (<i>R</i>)-dihydroresorcyclide	202
2.2.4. Total synthesis of (<i>R</i>)- <i>trans</i> -resorcyclide	203
2.2.4.1. Efforts towards olefin migration	203

Table of Content

2.2.4.2. Revision of the retrosynthetic scheme for (<i>R</i>)- <i>trans</i> -resorcyclide	206
2.3. Conclusion	209
2.4. Experimental section	210
2.5. References	224
2.6. Copies of ^1H and ^{13}C NMR spectra of selected compounds	227



FIRST CHAPTER

Section A



**Synthesis of Entire Stereoisomeric Set of Anti-
Malarial Natural Product
Cladosporin, their Biological Evaluation and
Co-Crystallization**

Chapter 1 (Section A): Synthesis of Entire Stereoisomeric Set of Anti-malarial Natural Product Cladosporin, their Biological Evaluation and Co-crystalization

1.1.1. Introduction

Natural products possess unique and diverse structural features with intricate carbon skeletons, which in turn makes them a validated starting point for medicinal chemistry and drug discovery program as well.¹ Besides, natural products have several advantages over synthetic drug like molecule which includes the presence of larger fraction of sp³-hybridized bridge-head atoms as compared to its synthetic congeners and a lower nitrogen content and higher oxygen content on an average.^{2,3} Considering these advantages, significant efforts have been devoted by medicinal chemists over the past few decades in developing drugs that target well known and crucial diseases like cancer, cholesterol, diabetes etc. Sufficient funding have also been contributed towards the successful discovery of several blockbuster drugs in the past years.⁴

In this context, parasitic infections hold a special mention with more than a million deaths occurring worldwide per year.⁵ Among the broad variety of parasitic infections, malarial happens to be a major one with 229 million cases globally including ~4,00,000 deaths.⁵ Since, the origin and emergence of malarial, several treatment regimens have been developed with time that significantly reduced the number of active malaria cases. Several drugs have been developed for serving the purpose of treatment as well. In the present times, malaria appears to be a pretty well controlled disease with a variety of in-hand available and affordable treatment options. Like many other infectious diseases, discovery of antimalarial drugs has been immensely benefited from nature and its natural resources.

One of the most prominent anti-malarial scaffolds derived from nature is quinoline extracted from the bark of *Cinchona sp.* also known as “fever tree”.⁶ In the course of time this scaffold inspired the development of several anti-malarial drugs as well (Figure 1). While developing new antimalarial compound based on quinoline scaffold, Bayer led to the discovery of one of the most popular and important quinoline based anti-malarial compound, chloroquine. In 1947 chloroquine entered clinical practice and turned out to be the most widely used anti-malarial until 1970s, in spite of having a poor therapeutic index. A decade later, first resistant *P. falciparum* were identified

Chapter 1 (Section A): Synthesis of Entire Stereoisomeric Set of Anti-malarial Natural Product Cladosporin, their Biological Evaluation and Co-crystalization

leading to ineffectiveness of the same.⁶ Following this several synthetic approaches have been adopted to produce derivatives of the same so as to tackle the issue of parasitic resistance (Figure 1).

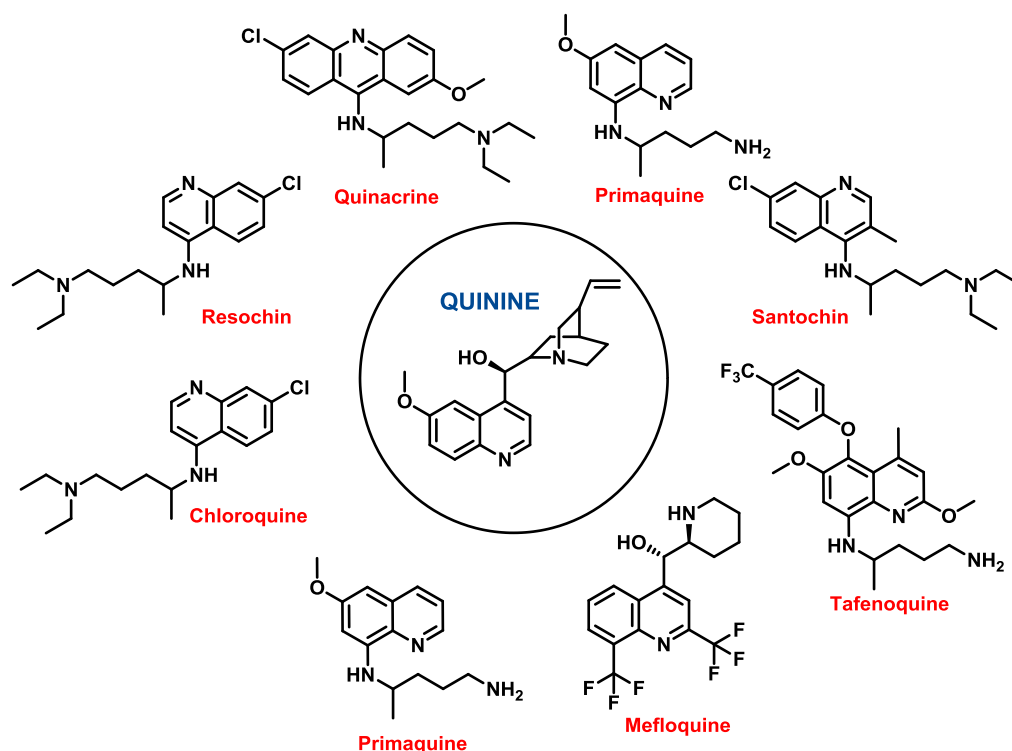


Figure 1. Structures of synthetic quinolines.

Febrifugine is yet another natural product, isolated from Chinese herb *Dichroa febrifuga* Lour, and was identified to have promising potency in the treatment of malarial infection.⁷ But alongside, severe liver toxicity, complemented with gastrointestinal irritation were evident in humans and various animal models. Till then, several medicinal chemistry approaches have been adopted to modify the core structure of the active natural product so as to deliver an optimized scaffolds with enhanced therapeutic index. In the 1960s halofuginone, a synthetic derivative of febrifugine was discovered by the U. S. Army Medical Research Command, which exhibited enhanced anti-malarial activity with a better safety window (increased therapeutic index). The core scaffold of febrifugine showed inherent toxicity owing to the spontaneous

Chapter 1 (Section A): Synthesis of Entire Stereoisomeric Set of Anti-malarial Natural Product Cladosporin, their Biological Evaluation and Co-crystallization

isomerization of the core to isofebrifugine through a potential reactive intermediate as depicted in figure 2.

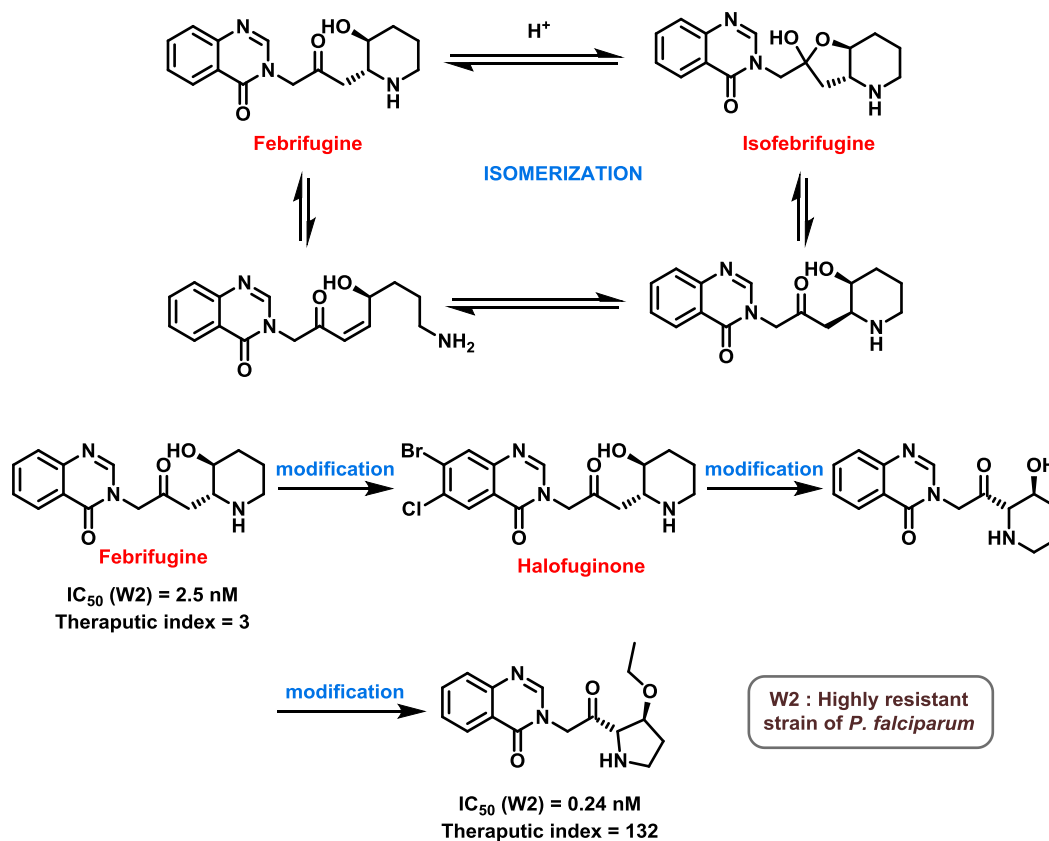


Figure 2. Isomerization and modifications of febrifugine.

To stop the isomerization process, removal of the methylene group between the carbonyl functionality and the piperidine moiety has turned out to be effective. Besides the piperidine moiety is also susceptible for further modifications like ring contraction to pyrrolidine and alkylation of the free hydroxyl group to form corresponding ethers. These efforts in turn afforded analogues of the same with increased efficacy. Alongside, combination of all these significant modifications further furnished analogues with excellent in vivo efficacy against *P. falciparum* infected *Aotus* monkeys (Figure 2).

Alongside the antimalarials discussed so far, several other unique chemical scaffolds appeared in the timeline (Figure 3). In the quest for synthetic anti-malarials that can

Chapter 1 (Section A): Synthesis of Entire Stereoisomeric Set of Anti-malarial Natural Product Cladosporin, their Biological Evaluation and Co-crystallization

satisfy the existing and increasing demand of anti-malarial agents, Paul Ehrlich came up with the discovery of methylene blue in the late 19th century.⁸ This compound could be manufactured in large quantities which successfully overcame the paucity of

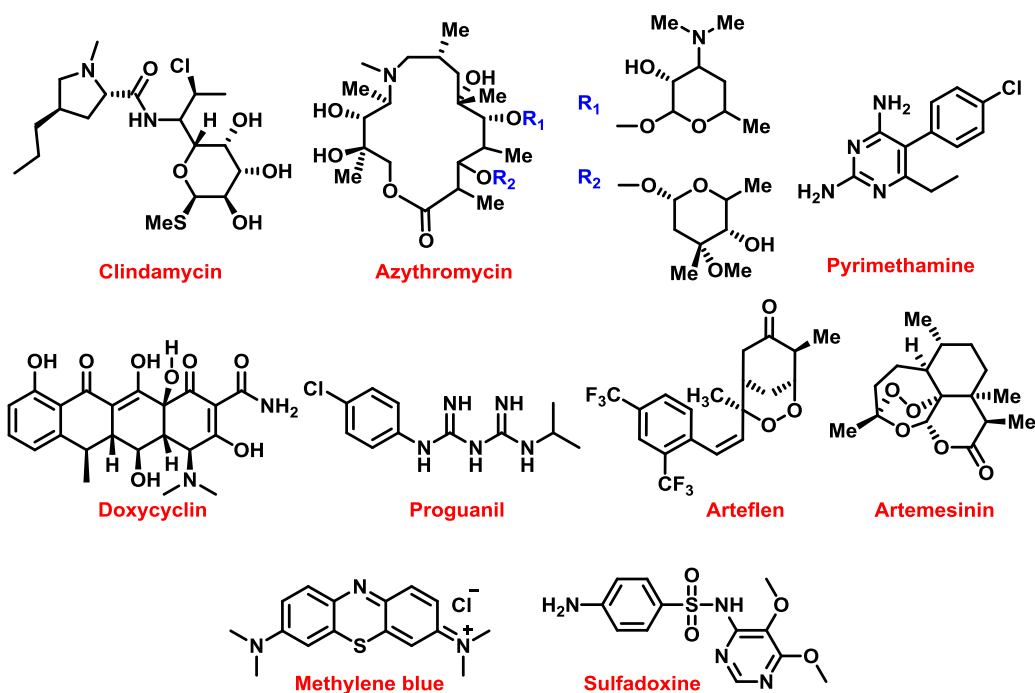


Figure 3. Other anti-malarial scaffolds in the pipeline.

quinine isolated from natural sources at that point of time. Proguanil, a pyrimidine derivative, emerged as an antimalarial drug during the time of World War II.⁹ Owing to the success of Proguanil in this aspect, further study was conducted on this scaffold which led the development of Pyrimethamine.⁹ Sulfones and sulfonamides were later used in combination with other mono-therapies to tackle the phenomenon of emerging resistance. Apart from these, the development of anti-malarials from antibiotics also holds significant advantages owing to their well-known and understood mechanism of action and well-defined pharmacokinetics and toxicological profiles.¹⁰ In the present scenario, artemisinin prevails as the most modern anti-malarial treatment. Artemisinin based combination therapies (ACTs) are endorsed by the World Health Organisation to treat malarial infection caused by *P. falciparum* as well as chloroquine-resistant *P. vivax*. Unfortunately, partial resistance to artemisinin appeared likely before 2001, and

Chapter 1 (Section A): Synthesis of Entire Stereoisomeric Set of Anti-malarial Natural Product Cladosporin, their Biological Evaluation and Co-crystalization

the widespread deployment of ACTs with cases of partial artemisinin resistance being confirmed in five countries.¹¹ In this concern, the World Health Organization (WHO) says “*The geographic scope of the problem could widen quickly and have important public health consequences: the spread or independent emergence of partner drug resistance or multidrug resistance globally could pose a public health threat, as no alternative anti-malarial medicine is available at present with the same level of efficacy and tolerability as ACTs.*”¹¹ Hence the need for a new and novel anti-malarial drug is of adequate importance and definitely holds a global urgency.

1.1.1.1. An introduction to cladosporin

Cladosporin, an anti-fungal antibiotic and a plant growth regulator, isolated from *Cladosporium cladosporioides* and *Aspergillus flavus* in 1971^{12, 13} is a chiral complex isocoumarin based scaffold which happens to be a promising lead molecule with potent anti-malarial activity against both blood and liver stage *Plasmodium falciparum* (*Pf*). Protein bio-synthesis is a process which is significantly crucial for the sustenance of life form. Several enzymes and cellular bio-mechanics are involved in this process of protein translation or protein bio-synthesis. One of such crucial enzyme involved in this process is Lysyl-tRNA synthetase or KRS. KRS is a class of enzyme responsible for the attachment of specific amino acid to the cognate tRNA. Cladosporin is found to target the parasite cytosolic lysyl-tRNA synthetase (*PfKRS*), an enzyme crucial for parasitic protein translation, hence terminating the process of protein biosynthesis.^{14, 15, 16, 17} The active scaffold of the natural product consists of a 6,8-dihydroxylisocoumarin ring linked to tetrahydropyran moiety bearing a methyl functional group. The dihydroxylisocoumarin effectively mimics adenosine moiety of the natural substrate ATP and the tetrahydropyran moiety binds to the ribose recognizing site of *PfKRS* and thus leading to a competitive inhibition of enzyme activity (Figure 4).¹⁵ Apart from *PfKRS*, cladosporin is also found to inhibit KRSs from several other species, which includes helminth parasites like *Schistosoma mansoni* (*Sm*) and *Loa loa* (*Ll*).¹⁸ Cladosporin further exhibits an intriguing selectivity (more than 100 folds) for the parasite lysyl-tRNA synthetase over human enzyme. This species specific selectivity

Chapter 1 (Section A): Synthesis of Entire Stereoisomeric Set of Anti-malarial Natural Product Cladosporin, their Biological Evaluation and Co-crystalization

of cladosporin has been formerly assigned through comprehensive sequence alignment, where the residues ser346 and val329 present in the active site of the target enzyme happen to be crucial for accommodating the methyl moiety of THP ring.¹⁵

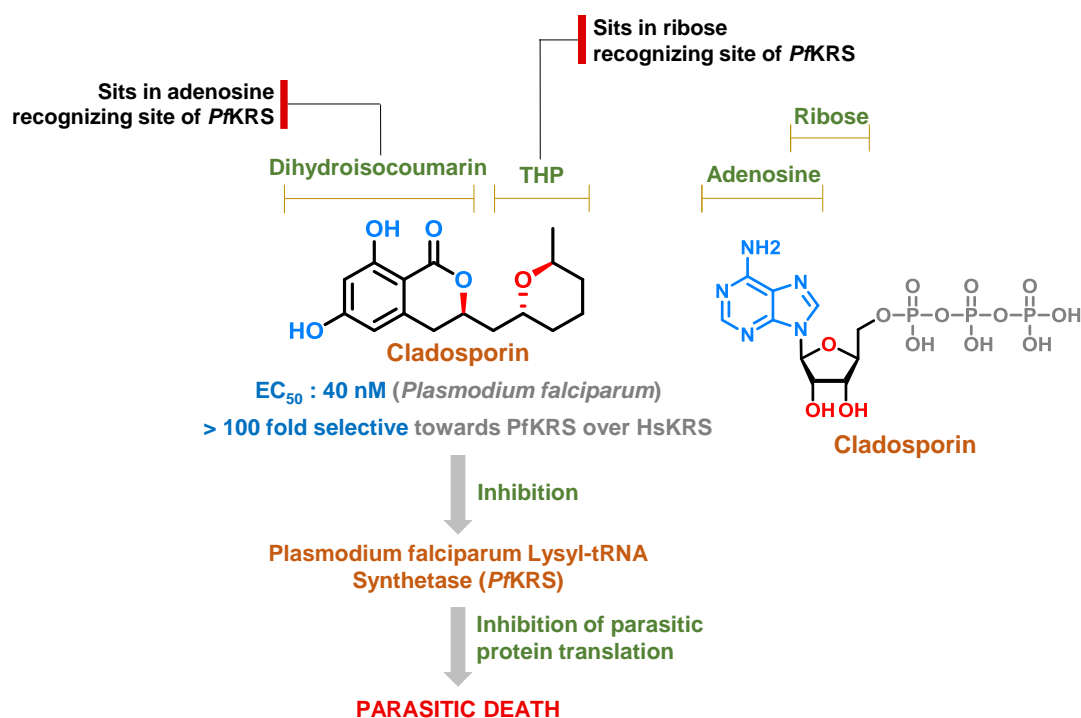


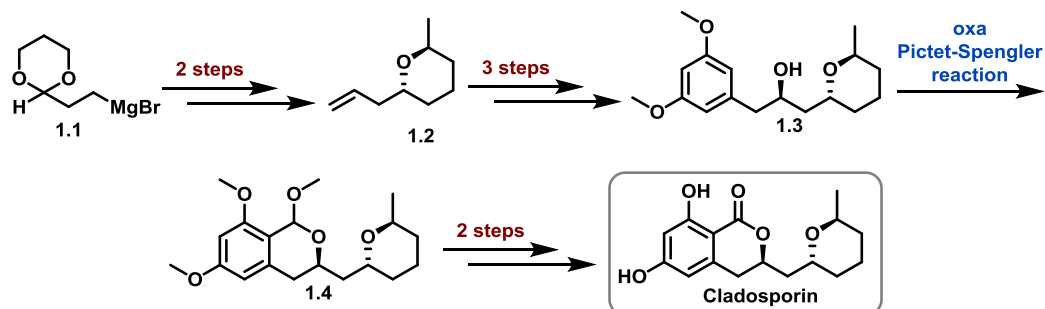
Figure 4. Structure and mode of action of cladosporin.

Potent anti-malarial activity, exquisite parasitic selectivity and a novel mode of action undoubtedly makes cladosporin an intriguing scaffold for the development of new anti-malarials. To date, one total synthesis by She et al. in 2013¹⁹ followed by a formal synthesis by Mohapatra et. al²⁰ in the same year has been documented in the literature. Apart from the reports on total synthesis, no proper medicinal chemistry or drug development approach (including Structure Activity Relationship (SAR) study) has yet been conducted on this active anti-malarial scaffold till date. Hence, exploring this molecule on the grounds of medicinal chemistry and drug discovery can be fruitful in the context of new and novel anti-malarial drug development.

Chapter 1 (Section A): Synthesis of Entire Stereoisomeric Set of Anti-malarial Natural Product Cladosporin, their Biological Evaluation and Co-crystallization

1.1.1.2. Highlights of reported synthesis of cladosporin

Total synthesis of cladosporin by She et. al (8 step asymmetric synthesis)



Formal synthesis of cladosporin by Mohapatra et. al (8 step asymmetric synthesis)

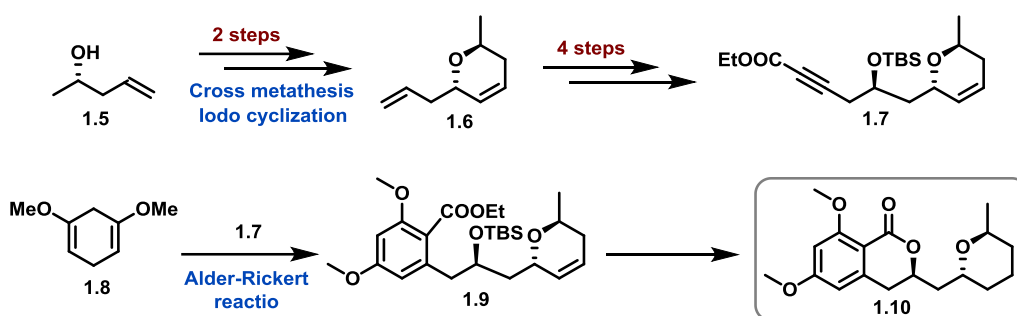


Figure 5. Reported syntheses of cladosporin.

Till date one total synthesis by She et al.¹⁹ followed by a formal synthesis of cladosporin by Mohapatra et al.²⁰ has been documented in the literature (Figure 5). She et. al envisioned the synthesis of cladosporin in a eight-step linear sequence using oxa-Pictet-Spengler reaction as key step.¹⁹ The elegant synthesis of cladosporin began with compound **1.2** which was synthesized from commercially available starting material. In the same year, Mohapatra et. al published an elegant formal stereoselective synthesis of cladosporin using cross-metathesis and iodocyclization reaction to access the *trans*-2,6-disubstituted dihydropyran ring system and an Alder–Rickert reaction to construct the aromatic ring.²⁰ Mohapatra et. al adopted an eight-step synthetic sequence starting with commercially available homoallylic alcohol **1.5** which upon cross metathesis followed by iodocyclization afforded THP fragment **1.6** in a diastereospecific fashion, which was further converted to **1.7** in a three-step sequence. Alder–Rickert reaction of

Chapter 1 (Section A): Synthesis of Entire Stereoisomeric Set of Anti-malarial Natural Product Cladosporin, their Biological Evaluation and Co-crystalization

1.7 with commercially available compound 1.8 followed by relevant functional group incorporation and interconversion afforded the final cladosporin precursor 1.10 (Figure 5).

1.1.1.3. Highlights of reported synthesis of isocladosporin

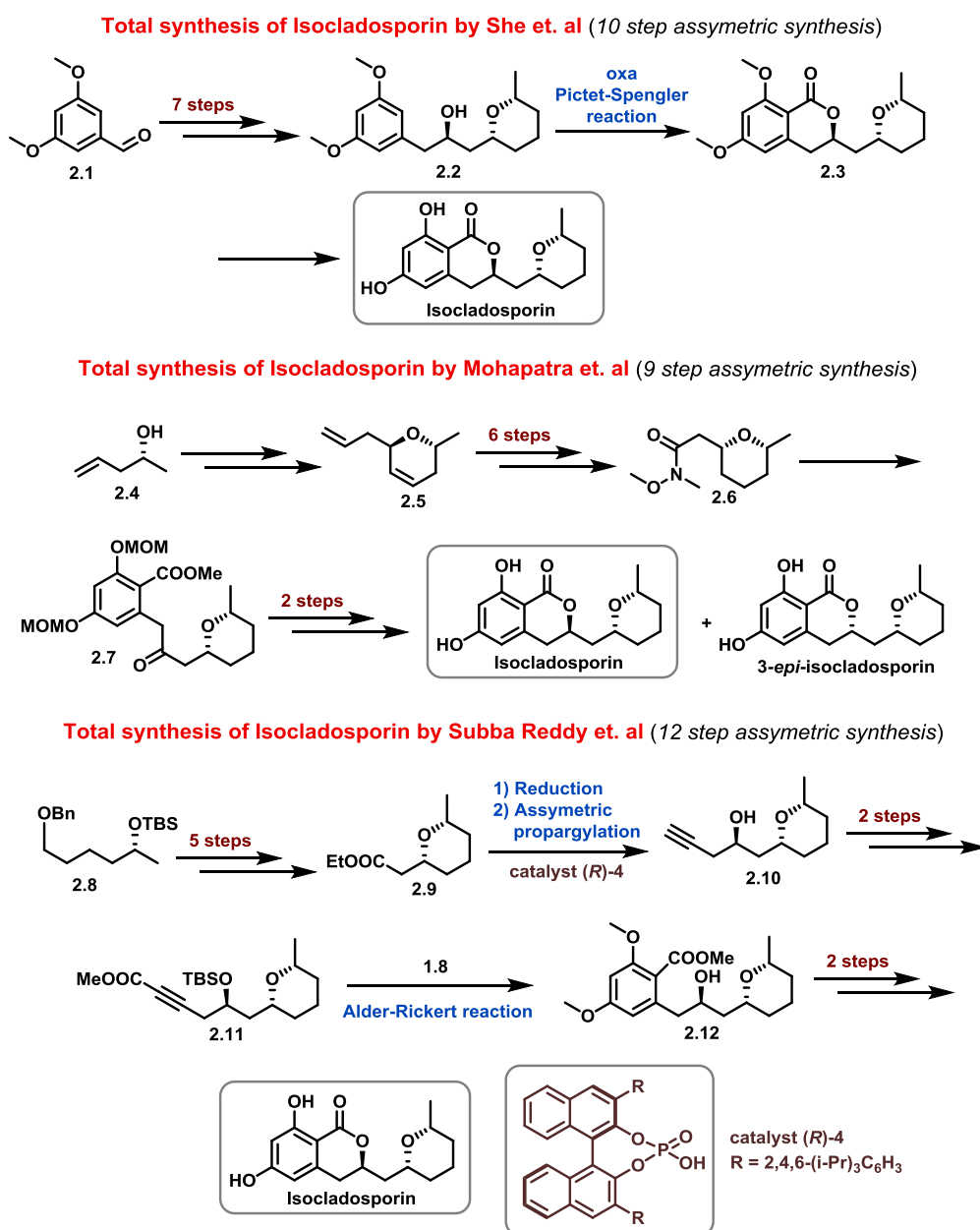


Figure 6. Reported syntheses of isocladosporin.

Chapter 1 (Section A): Synthesis of Entire Stereoisomeric Set of Anti-malarial Natural Product Cladosporin, their Biological Evaluation and Co-crystalization

Several groups have also reported the synthesis of yet another similar natural product, isocladosporin which has been isolated from the same fungal source (*Cladosporium cladosporioides*) as that of cladosporin. Isocladosporin happens to be a stereoisomer of cladosporin with an *R*-stereochemistry at C14 centre unlike cladosporin which possess an *S*-stereochemistry. Hence, synthetic approach towards the same are worth mentioning. Till date three total syntheses of isocladosporin have been documented in the literature.^{19, 21, 22} The first synthesis appeared from She et al. where they have utilized a ten-step linear asymmetric synthetic sequence to access the natural product using oxa-Pictet-Spengler reaction as the key step.¹⁹ Following this Mohapatra et al. reported the total synthesis of isocladosporin and 3-*epi*-isocladosporin in a nine-step linear synthetic sequence.²¹ The synthesis commenced with compound **2.5** which was synthesized from allylic alcohol **2.4** using previously developed protocol in his group. Subba Reddy et al. further reported an elegant synthesis of isocladosporin using a twelve-step linear synthetic sequence where Alder-Rikert reaction and asymmetric propargylation are the key highlights of the synthesis (Figure 6).²²

Considering the promising anti-malarial potency, parasitic selectivity and novel mode of action of cladosporin, it surely holds a strong foundation for the development of new and novel anti-malarial drug. Till date no in depth biological profiling or systematic structure activity relationship (SAR) studies have been thoroughly conducted on this potent NP. Owing to these facts, we planned to conduct a thorough systematic medicinal chemistry program on this active anti-malarial scaffold.

“Chirality” or in simple terms, the spacial arrangements and orientations of atoms of a molecule in three dimensional (3D) space manifests significant and curtail effects in the pharmacological properties of a drug. Ever since the invention of chirality in chemistry by Louis Pasteur, its significance in biology and pharmaceutical sciences has been repeatedly emphasized. The role of chiral chemistry and enantiomeric separation was further emphasized with the award of 2001 Nobel Prize in chemistry to Sharpless, Noyori and Knowles for the development of new synthetic methodologies using chiral catalyst to furnish single enantiomeric product. Most natural products appear in the

Chapter 1 (Section A): Synthesis of Entire Stereoisomeric Set of Anti-malarial Natural Product Cladosporin, their Biological Evaluation and Co-crystalization

nature as unique enantiomeric configuration and more than 50% of the approved human drugs are chiral pure entities. Although there are many drugs that are administered as racemates of equimolar enantiomers. This can in turn be severe and may exhibit serious side effects as well.^{23, 24} Despite having identical chemical connectivity of all the sets of atoms, different stereoisomers of a drug display significant differences in vital properties like pharmacokinetics, pharmacology, metabolism and toxicology.²⁵ Considering these crucial differences, it is not surprising that different stereoisomers of the same drug display stereoselective toxicity as well, as evident from the examples of thalidomide²⁶ and pain killer ibuprofen.²⁷ In view of the pivotal role of chirality in drug like properties of a molecule, we planned to conduct a thorough investigation of the role of “specific stereoisomeric configuration in the drug potency of cladosporin scaffold against malarial parasite”. From a structural stand point, cladosporin clearly indicates the presence of three chiral centres in the scaffold, and hence 2^n ($n = 3$), i.e.; eight stereoisomers are possible for the same (Figure 7).

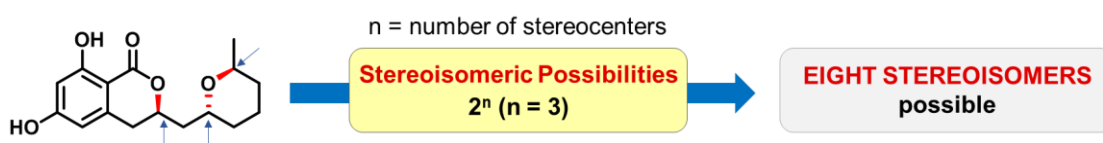


Figure 7. Stereoisomeric possibility of cladosporin scaffold.

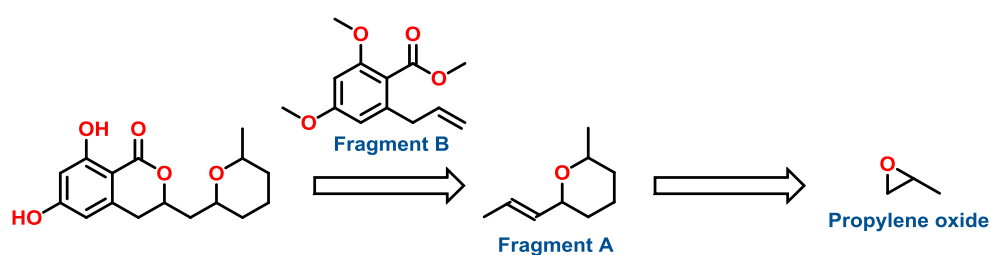
Considering the above facts we objectified our work as per the following points.

- Development of a novel divergent synthetic route to access all possible stereoisomers (called as “cladologs” herefrom) of cladosporin.
- Identification, purification and thorough characterization of all the cladologs using spectroscopic, spectrometric and crystallographic tools.
- Biological evaluation of the entire set of stereoisomers (cladologs) in enzyme- and cell-based parasitic inhibition assay to assess the role of chirality/stereochemistry in anti-malarial potency.
- Deciphering the structural basis of cladolog-*PfKRS* binding, through analysis of X-ray co-crystal structures of the stereoisomers with target enzyme *PfKRS*.

Chapter 1 (Section A): Synthesis of Entire Stereoisomeric Set of Anti-malarial Natural Product Cladosporin, their Biological Evaluation and Co-crystalization

1.1.2. Results and discussion

We envisioned the synthesis of cladosporin and seven of its stereoisomers from two key fragments using cross metathesis reaction, which was followed by relevant functional group interconversion (Scheme 1). Fragment A can be synthesized from propylene oxide of appropriate chirality, whereas fragment B can be obtained following standard reaction protocol.

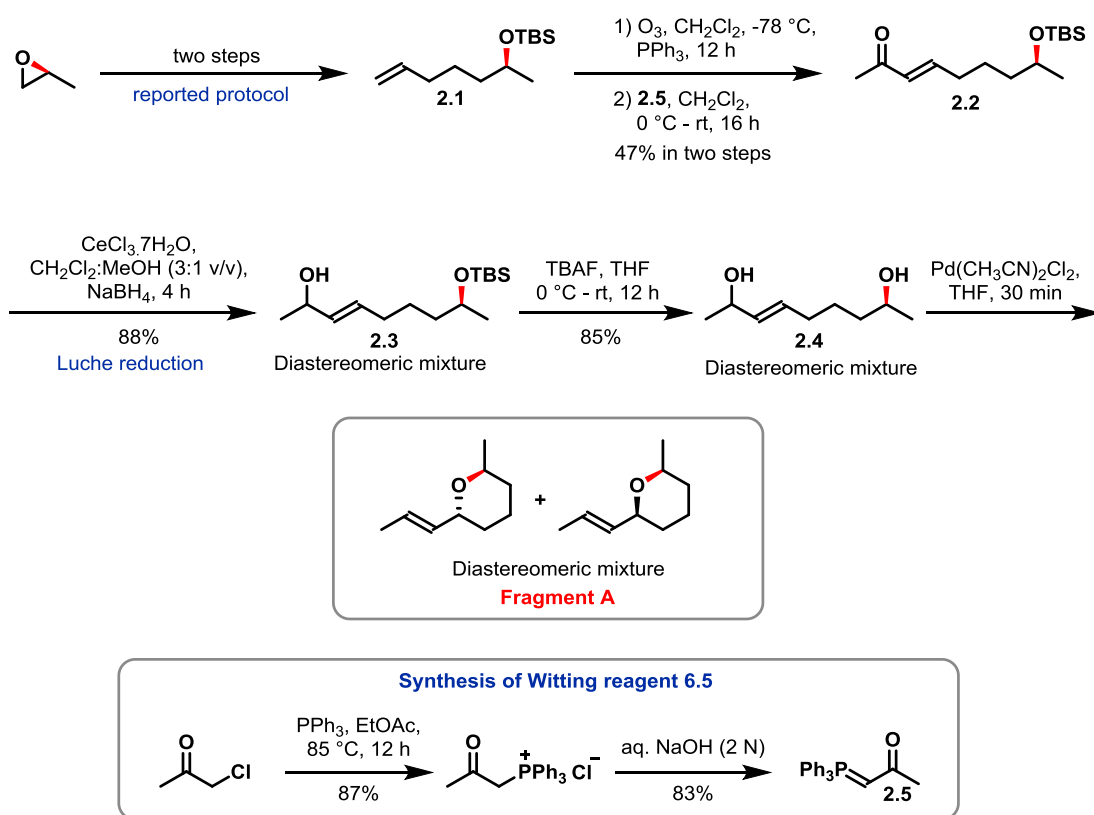


Scheme 1. Retrosynthetic scheme of cladosporin and its stereoisomers.

1.1.2.1. Synthesis of key fragment A from (*S*)-propylene oxide

Our synthesis started with (*S*)-propylene oxide as the chiral source which was converted to its corresponding TBS ether **2.1** following reported procedure.²⁸ One-pot ozonolysis of compound **2.1** followed by Wittig reaction with **2.5** (synthesized from chloroacetone in two steps) furnished α,β -unsaturated ketone **2.2** in 47% yield which was subjected to Luche reduction condition ($\text{CeCl}_3 \cdot 7\text{H}_2\text{O}$ and NaBH_4) to afford 1:1 diastereomeric mixture (by NMR) of allylic alcohol **2.3** with a yield of 88%. Reaction of alcohol **2.3** with tetra-*n*-butylammonium fluoride (TBAF) afforded diol **2.4** in 85% yield which was subjected to palladium-catalyzed intramolecular Tsuji–Troost type cyclization to furnish key fragment A as a 1:1 mixture of diastereomers (Scheme 2). Owing to the high volatility of the fragment, purification through column chromatography was deliberately avoided. Although, the formation of the compound was confirmed using High Resolution Mass Spectrometry (HRMS) where an $[\text{M}+\text{H}]^+$ 141.1274 was cleanly noticeable.

Chapter 1 (Section A): Synthesis of Entire Stereoisomeric Set of Anti-malarial Natural Product Cladosporin, their Biological Evaluation and Co-crystallization

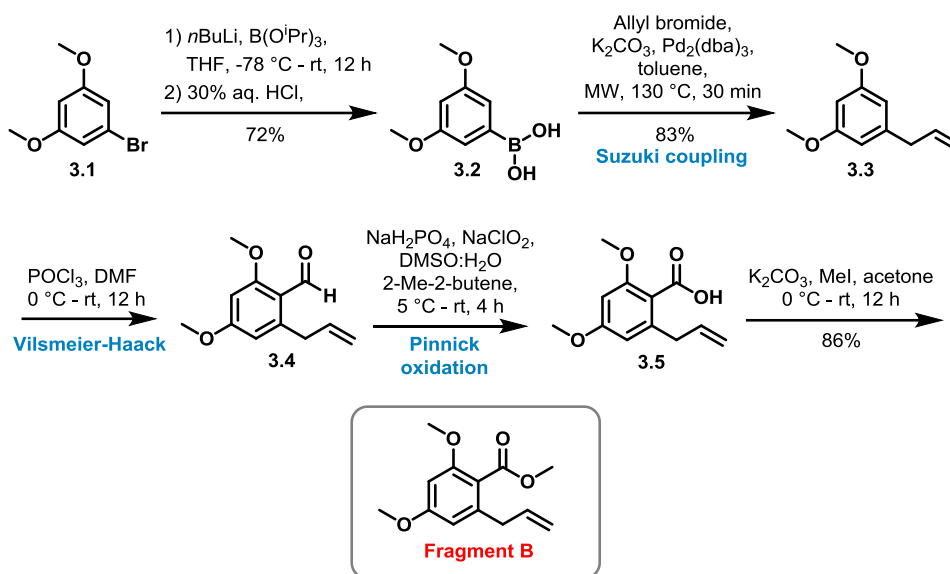


Scheme 2. Synthesis of key fragment A.

1.1.2.2. Synthesis of key fragment B

Synthesis of fragment B commenced with commercially available starting material 1-bromo-3,5-dimethoxybenzene **3.1** which upon lithium-halogen exchange using *n*BuLi followed by quenching the generated anion with triisopropyl borate furnished corresponding boronic ester which was in turn hydrolyzed using aq. HCl to give the required boronic acid derivative **3.2**. Microwave irradiated Suzuki cross coupling reaction was conducted between boronic acid fragment **3.2** and allyl bromide in presence of Pd₂(dba)₃ to afford allyl fragment **3.3**. Subsequent formylation (following Vilsmeier Haack protocol) followed by Pinnick oxidation led to the formation of aromatic acid **3.5** which was then esterified in presence of K₂CO₃ and methyl iodide to afford key fragment B (Scheme 3).

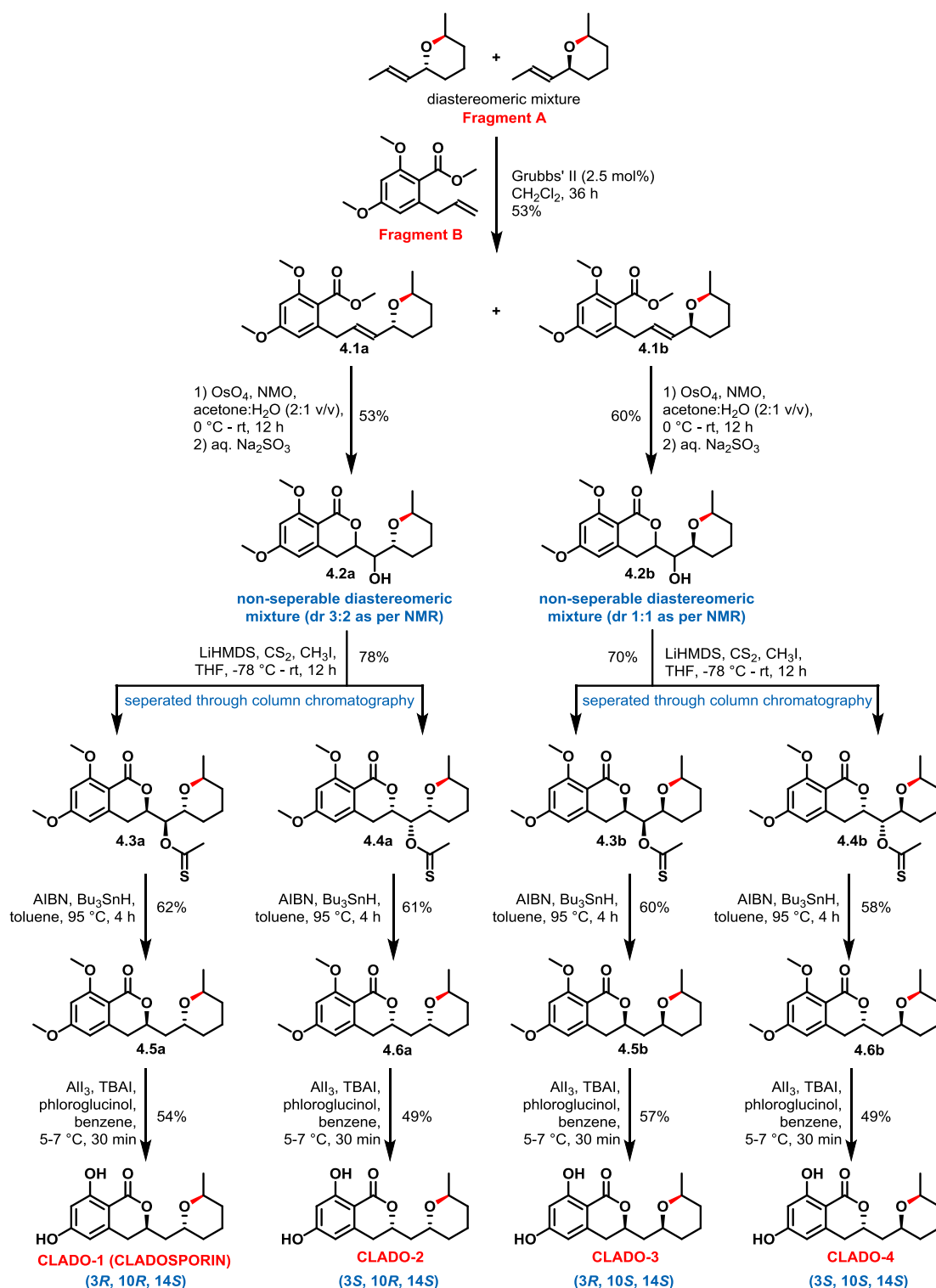
Chapter 1 (Section A): Synthesis of Entire Stereoisomeric Set of Anti-malarial Natural Product Cladosporin, their Biological Evaluation and Co-crystalization



Scheme 3. Synthesis of key fragment B.

After synthesizing both the key fragments (fragment A and B) they were treated with Grubbs' 2nd generation catalyst (2.5 mol %) in CH_2Cl_2 to undergo cross metathesis reaction which led to the formation of compound **4.1a** and **4.1b** in 53% yield.²⁹ Both the diastereomers were cleanly separated using column chromatography. It is worth mentioning here that the equivalence of the key fragments and the mode of addition of the Grubbs' catalyst is significantly crucial for the reaction. After several attempts to improve the yield of the reaction we came up with an optimized protocol where 1 equivalent of fragment B and 2.5 equivalent of fragment A were used. The optimized equivalence of starting materials manifested in a considerable improvement of the yield. Besides, the nature of addition of the Grubbs' catalyst also contributed to the yield enhancement. An overall of 2.5 mol% of Grubbs' catalyst was added consecutively in two equal portions in a time gap of 12 h. After initial addition of the catalyst, the conversion process gets sluggish after 10-12 h of reaction time. Fresh catalyst loading after 12 h was found to assist the reaction to reach completion with complete consumption of the limiting reagent (fragment B). The formation of the products **4.1a** was confirmed by the disappearance of terminal olefinic pattern and appearance of new olefinic peaks at 5.73-7.60 ppm in ^1H NMR along with singlet methyl ester peak at 3.85 ppm.

Chapter 1 (Section A): Synthesis of Entire Stereoisomeric Set of Anti-malarial Natural Product Cladosporin, their Biological Evaluation and Co-crystallization



Scheme 4. Synthesis of cladosporin and three of its stereoisomers from (*S*)-propylene oxide.

Chapter 1 (Section A): Synthesis of Entire Stereoisomeric Set of Anti-malarial Natural Product Cladosporin, their Biological Evaluation and Co-crystalization

Besides the presence of single proton peaks at 4.32 ppm and 3.87 ppm corresponding to oxygen attached proton in the THP moiety further confirms the success of cross metathesis reaction. Similar spectral pattern was also noticed in the case of **4.1b**. The formation of the **4.1a** and **4.1b** was further confirmed through HRMS which showed an m/z peak of $[M + H]^+$ at 335.1839. After thoroughly characterizing both the diastereomers, they were separately treated with osmium tetroxide mediated dihydroxylation protocol in presence of NMO as a co-oxidant in a mixture of acetone and water, to furnish corresponding diols. While monitoring the reaction progress using thin layer chromatography (TLC), a new polar spot corresponding to the required diol was noticed. After quenching the reaction with saturated aqueous Na_2SO_3 , disappearance of the polar spot was observed with a simultaneous appearance of a new spot which was more polar in nature as per TLC study. The final polar spot thus obtained was carefully isolated and thoroughly characterized. After interpreting the spectral data of the product, we deciphered that the diol intermediate got lactonized in situ to afford hydroxy-lactone intermediate **4.2a** with a diastereomeric ratio (dr) of 3:2 and **4.2b** with 1:1 diastereomeric ratio as per NMR spectral data.

To figure out whether the quenching reagent, Na_2SO_3 is leading to an in situ lactonization, we set up a control experiment where we quenched a separate batch of the same reaction with only water. Owing to our surprise, similar phenomenon of in situ lactonization was observed in this case as well. This clearly rules out the possibility of Na_2SO_3 facilitating the lactonization process. Probably, a change in polarity of the reaction mixture on addition of excess water was driving the lactonization phenomenon. The formation of lactonized product was further evident from the appearance of NMR peak corresponding to lactone attached proton at 4.68 - 4.39 ppm for compound **4.2a**. Identical spectral trend was also noticed in case of the other diastereomeric compound **4.2b**.

Following this, the hydroxy compound **4.2a** was converted to corresponding xanthate ester to furnish compound **4.3a** and **4.4a** with 78% yield. It was fortuitous that we were able to separated both the diastereomers (**4.3a** and **4.4a**) using flash chromatography.

Chapter 1 (Section A): Synthesis of Entire Stereoisomeric Set of Anti-malarial Natural Product Cladosporin, their Biological Evaluation and Co-crystalization

Hydroxy compound **4.2b** was also converted to its corresponding xanthate esters **4.3b** and **4.4b** with a yield of 70% following identical procedure. The incorporation of xanthate functionality was further confirmed through ^1H NMR spectra where appearance of sulfur attached methyl protons at 2.56 ppm and 2.57 ppm corresponding to compounds **4.3a** and **4.4a** respectively was noticeable. The appearance of m/z peak at 427.1230 for $[\text{M} + \text{H}]^+$ in HRMS further confirmed the formation of the required product. Similar spectral observation was also persistent in **4.3b** and **4.4b**.

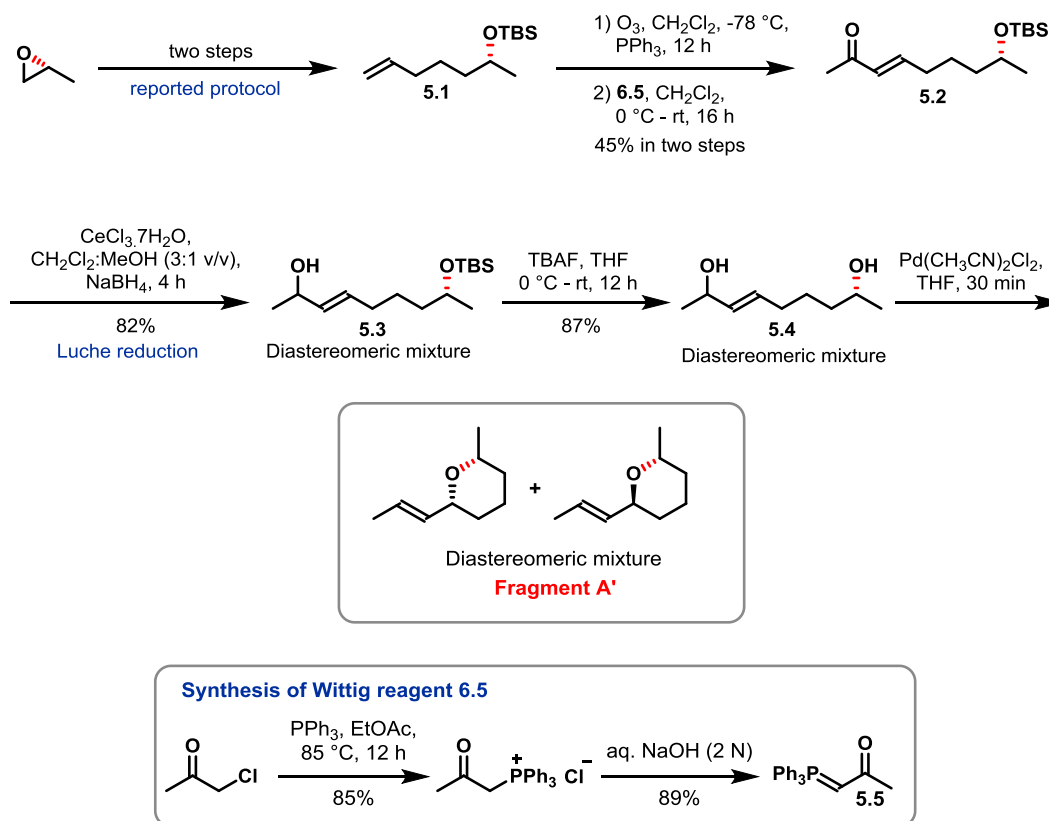
The four diastereomeric xanthates thus obtained were separately subjected to Barton–McCombie reaction to furnish compounds **4.5a**, **4.6a**, **4.5b**, and **4.6b** in moderate yields ($\sim 60\%$). The formation of product was confirmed by NMR spectral analysis where the disappearance of proton peaks at ~ 6.00 ppm corresponding to xanthate attached proton and at ~ 2.5 ppm corresponding to sulfur attached methyl protons was observed. Besides the appearance of m/z peak at 321.1691 corresponding to $[\text{M} + \text{H}]^+$ further confirms the product formation. After complete characterization of all the chiral pure precursors, they were subjected to aluminum triiodide-mediated exhaustive demethylation³⁰ to furnish cladosporin (**CLADO-1**) and three of its stereoisomers, i.e.; **CLADO-2**, **3** and **4** (Scheme 4). The use of completely dry benzene as the reaction solvent and maintaining the reaction temperature between 5-7 °C is significantly crucial for a better yield of the reaction. Among the four synthesized stereoisomers, spectral data for cladosporin (**CLADO-1**) are available in the literature¹⁹ which is in complete agreement with our synthesized compound **CLADO-1**. Besides, the spectral data (^1H NMR and ^{13}C NMR) of all these compounds (**CLADO-1**, **2**, **3** and **4**) are in complete agreement with the assigned structures.^{19, 20}

1.1.2.3. Synthesis of key fragment A' from (*R*)-propylene oxide

After successfully synthesizing and thoroughly characterizing cladosporin and three of its stereoisomers (**CLADO-1**, **2**, **3** and **4**) we directed our efforts toward the synthesis of the remaining four stereoisomers. For the same, we synthesized fragment A' starting from (*R*)-propylene oxide, following similar procedure as depicted in scheme 5.

Chapter 1 (Section A): Synthesis of Entire Stereoisomeric Set of Anti-malarial Natural Product Cladosporin, their Biological Evaluation and Co-crystallization

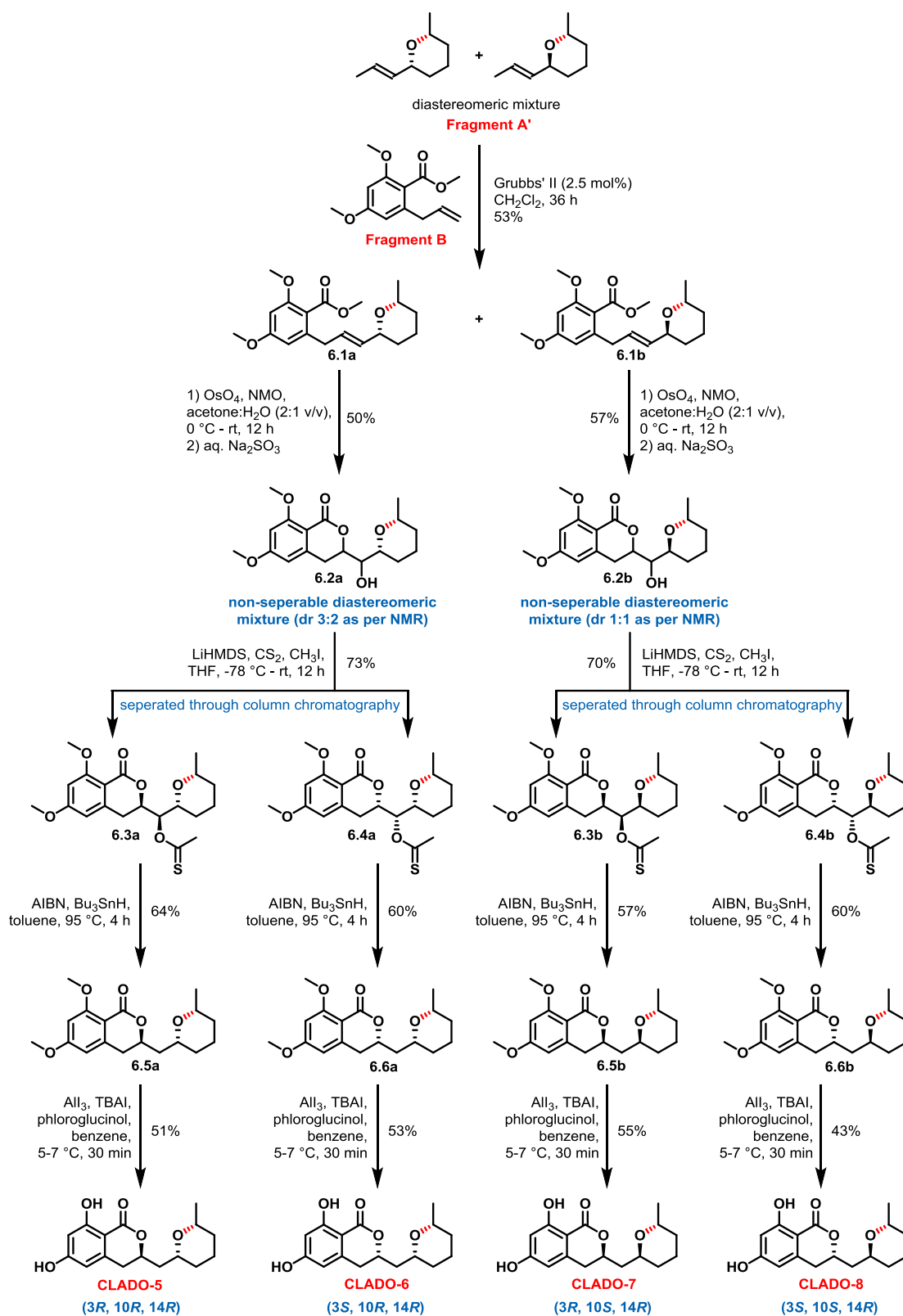
Starting from (*R*)-propylene oxide as the chiral source, through relevant functional group incorporation and organic transformations we synthesized the required fragment A' as 1:1 diastereomeric mixture (Scheme 5).



Scheme 5. Synthesis of Fragment A'.

After synthesizing fragment A', it was further forwarded following similar procedure as depicted in scheme 4 to access the rest of the four stereoisomers of cladosporin (**CLADO-5**, **6**, **8**, and **8**) (Scheme 6). As these four stereoisomers maintain an exact enantiomeric relationship with the previously synthesized stereoisomers (**CLADO-1**, **2**, **3** and **4**) from (*S*)-propylene oxide, the ¹H and ¹³C NMR spectral data were in complete co-relation with each other. Besides, the absolute stereochemistry of this four isomers (**CLADO-5**, **6**, **7** and **8**) were also determined using single crystal X-ray diffraction (Figure 8), thus leaving no space for structural and functional ambiguity. Besides, NMR spectral data of **CLADO-5** and **CLADO-6** were in complete agreement with reported data. ¹H and ¹³C NMR spectra of selected compounds are provided at the end of this chapter.

Chapter 1 (Section A): Synthesis of Entire Stereoisomeric Set of Anti-malarial Natural Product Cladosporin, their Biological Evaluation and Co-crystallization



Scheme 6. Synthesis of four stereoisomers of cladosporin from (*R*)-propylene oxide.

Chapter 1 (Section A): Synthesis of Entire Stereoisomeric Set of Anti-malarial Natural Product Cladosporin, their Biological Evaluation and Co-crystallization

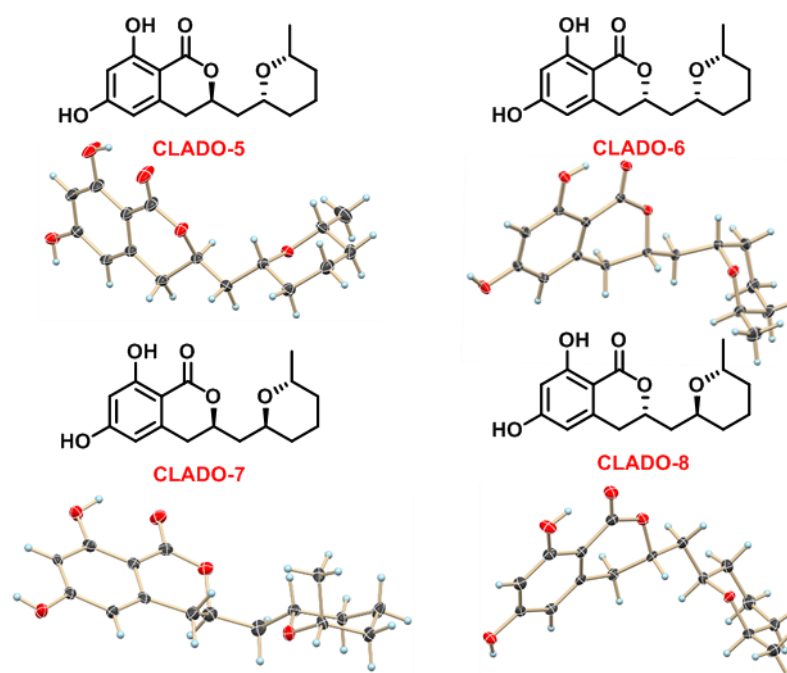


Figure 8. Single crystal structure (*ORTEP*) of **CLADO-5**, **6**, **7** and **8**.

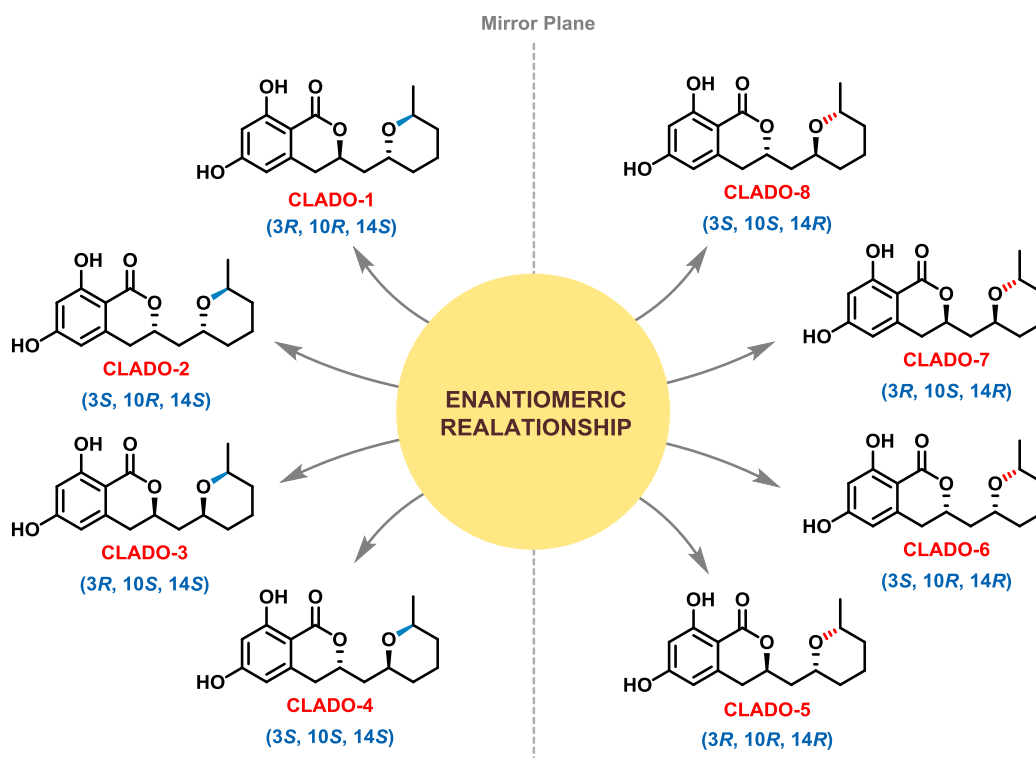


Figure 9. Structures of the eight stereoisomers of cladosporin.

Chapter 1 (Section A): Synthesis of Entire Stereoisomeric Set of Anti-malarial Natural Product Cladosporin, their Biological Evaluation and Co-crystalization

In collaboration with Prof. Bifulco from the University of Salerno, we developed a methodological approach based on the comparison of QM (quantum mechanics) calculated set of NMR data with experimentally obtained set (Table 1), that can assist the correct assignment of a group of stereoisomers.³¹

CLADO-1 (in CDCl ₃)	CLADO-2 (in CDCl ₃)	CLADO-3 (in MeOD)	CLADO-4 (in MeOD)
169.9	170.0	171.7	171.7
164.3	164.4	166.4	166.4
163.1	163.0	165.8	165.8
141.8	141.6	143.6	143.7
106.7	106.7	108.1	108.0
102.0	102.0	102.3	102.3
101.5	101.6	101.8	101.7
76.3	76.6	78.0	77.6
68.0	67.4	75.5	75.3
66.6	67.2	75.2	74.8
39.3	37.3	42.2	43.0
33.6	32.6	34.5	34.6
30.9	31.5	33.8	34.5
29.7	29.8	32.5	33.1
18.9	19.7	24.7	24.8
18.1	18.1	22.6	22.5

Table 1. ¹³C NMR values (in ppm) of all cladologs.

Chapter 1 (Section A): Synthesis of Entire Stereoisomeric Set of Antimalarial Natural Product Cladosporin, their Biological Evaluation and Co-crystalization

1.1.2.4. Biological assessment of synthesized cladologs (In collaboration with Dr. Amit Sharma, ICGEB, New Delhi and Dr. Dhanasekaran Shanmugam, CSIR-NCL, Pune)

1.1.2.4.1. Thermal shift assay (TSA):

All the synthesized cladologs were initially screened under thermal shift assay (TSA) so as to decipher the extent of their thermodynamic binding with *Pf*KRS (Figure 10). A higher magnitude of ΔT_m (obtained from TSA) indicates a strong enzyme-drug complex in a comparative scenario. Our TSA data for cladolog-*Pf*KRS complexes reflected a thermal shift range of ~ 7.9 to 17.3 °C, with a striking ΔT_m value of 17.3 and 16.2 °C for **CLADO-1** and **CLADO-5**, respectively (Figure 10b, Table 2). Based on the TSA data of the eight cladologs, we successfully assigned **CLADO-1** and **CLADO-5** as strong binders to *Pf*KRS, **CLADO-2**, **CLADO-3** and **CLADO-7** as moderate binders and **CLADO-4**, **CLADO-6** and **CLADO-8** as poor (Table 2). It was quite fascinating and striking to see such spectrum of low to high binding affinity of cladologs with target enzyme *Pf*KRS. After collecting similar data on *Hs*KRS we observed a very low magnitude of thermal shifts with a range of ~ 0.14 – 1.1 °C, indicating a retainment of overall selectivity for all the cladologs against human KRS (Figure 10a and 10b).

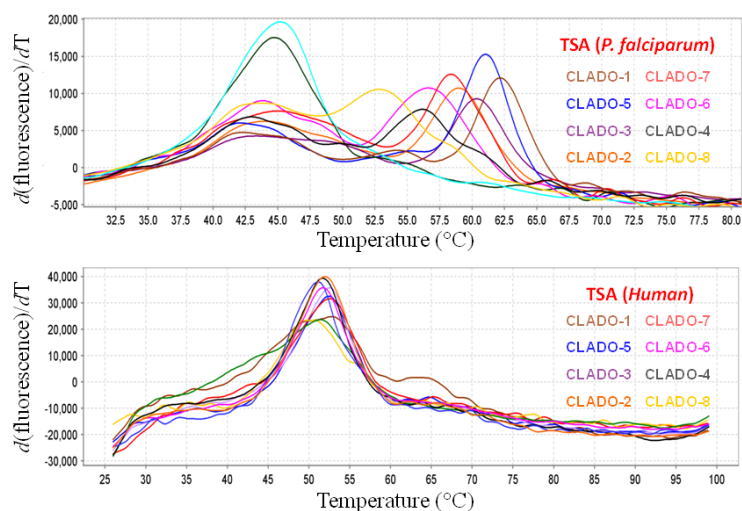


Figure 10a. Thermal shift assay of cladologs with *Pf*KRS and *Hs*KRS.

Chapter 1 (Section A): Synthesis of Entire Stereoisomeric Set of Antimalarial Natural Product Cladosporin, their Biological Evaluation and Co-crystalization

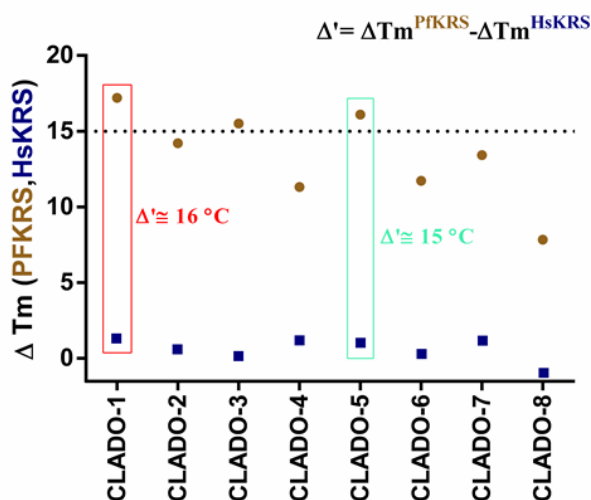


Figure 10b. Thermal shift profiles of *PfKRS* and *HsKRS* at 2 μ M and 4 μ M, respectively, in the presence of L-lysine.

1.1.2.4.2. Aminoacylation assay (enzyme inhibition assay):

The classification of the eight synthesized cladologs into three distinct classes of potency intrigued us to conduct further studies on the same. As a part of which, we addressed the enzyme inhibition activity of all the cladologs in both *Plasmodium falciparum* (*PfKRS*) as well as human counterpart (*HsKRS*) through standard aminoacylation assays. The obtained IC_{50} values for eight cladologs showed a trend similar to thermal shift data (Figure 10b, Table 2). **CLADO-1** and **CLADO-5** reflected highest inhibition potency with IC_{50} values of 0.125 μ M and 0.29 μ M respectively against *PfKRS*. **CLADO-2**, **CLADO-3** and **CLADO-7** turned out to be moderately active with IC_{50} values ranging from ~ 4 to 7 μ M. **CLADO-4**, **CLADO-6** and **CLADO-8** displayed an IC_{50} range of ~ 21 to 50 μ M (Figure 11a, Table 2) indicating poor enzyme inhibitory potency. It was very intriguing to see a striking difference of ~ 500 fold in the IC_{50} values between the best (**CLADO-1**) and the poorest stereoisomer (**CLADO-8**).

To assess the target specificity of the cladologs, we determined the IC_{50} values against *HsKRS* as well. All the synthesized stereoisomers (cladologs) essentially turned out to be inert (Figure 11a). These data sets further provided us with a possibility to evaluate

Chapter 1 (Section A): Synthesis of Entire Stereoisomeric Set of Anti-malarial Natural Product Cladosporin, their Biological Evaluation and Co-crystalization

the selectivity indices of each cladolog, wherein **CLADO-5** (3*R*, 10*R*, and 14*R*) with a score of ~965 turned out to be even better than cladosporin (**CLADO-1**) (3*R*, 10*R*, and 14*S*), which had a score of ~840 (Figure 12b).

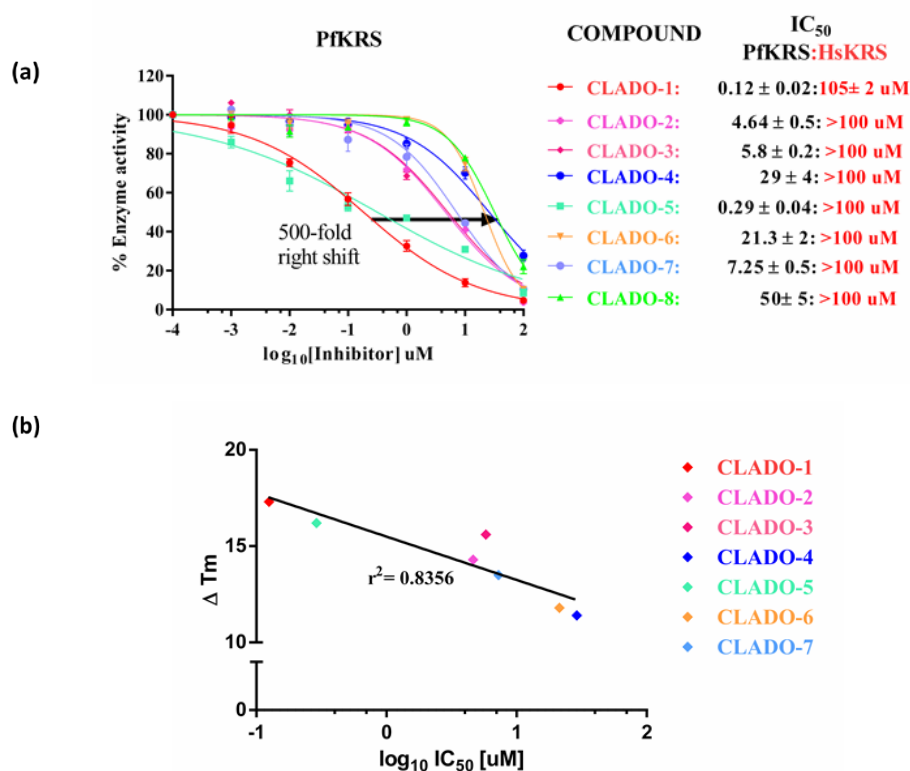


Figure 11. (a) Aminoacylation activity inhibition assays of synthesized cladologs. (b) Linear regression: thermal shift (ΔT_m) versus \log_{10} IC₅₀ obtained through the data collected from enzyme, thermal shift and parasite inhibition assays.

1.1.2.4.3. Parasite growth inhibition assay:

The observed thermal shift profile and IC₅₀ values reflected a consistent trend of anti-malarial potency in the cladolog series, thus provided us with a firm ground to evaluate the corresponding EC₅₀ values through parasite growth inhibition assays using in vitro *P. falciparum* cultures (Figure 12a). To our surprise, the experimental EC₅₀ values of the entire stereoisomeric set were in accordance to the observed thermal shift and enzyme inhibition profile. **CLADO-1** and **CLADO-5** outperformed the rest with an EC₅₀ value of 0.04 μ M and 0.27 μ M respectively. **CLADO-2**, **CLADO-3** and

Chapter 1 (Section A): Synthesis of Entire Stereoisomeric Set of Antimalarial Natural Product Cladosporin, their Biological Evaluation and Co-crystalization

CLADO-7 demonstrated moderate potency in their EC_{50} values ranging from 1.1 μM to 1.6 μM . On the other hand, CLADO-4, CLADO-6 and CLADO-8 turned out to be the least potent ones (Figure 13, Table 2).

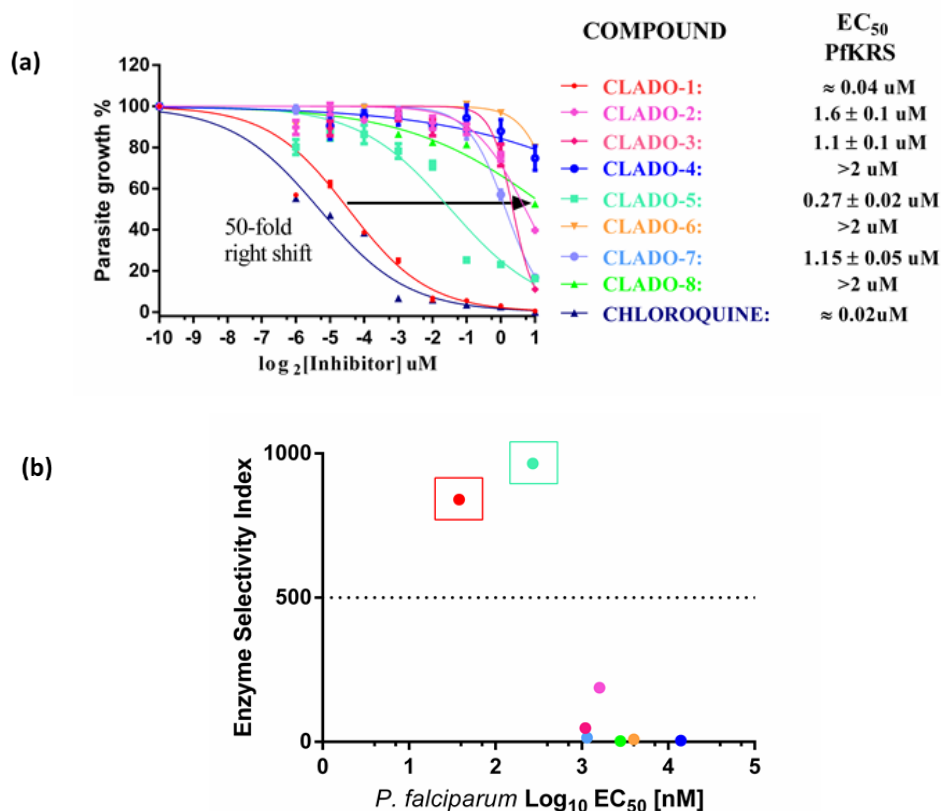
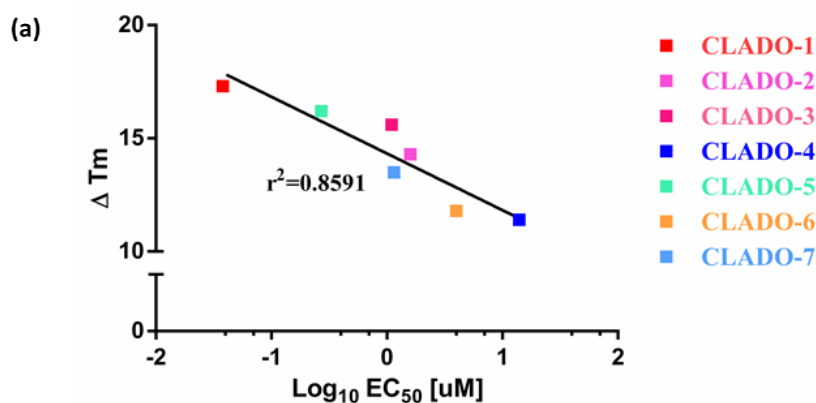


Figure 12. (a) Blood stage *P. falciparum* growth inhibition assays of the synthesized cladologs. (b) Selectivity profile (scattered plots).



Chapter 1 (Section A): Synthesis of Entire Stereoisomeric Set of Antimalarial Natural Product Cladosporin, their Biological Evaluation and Co-crystalization

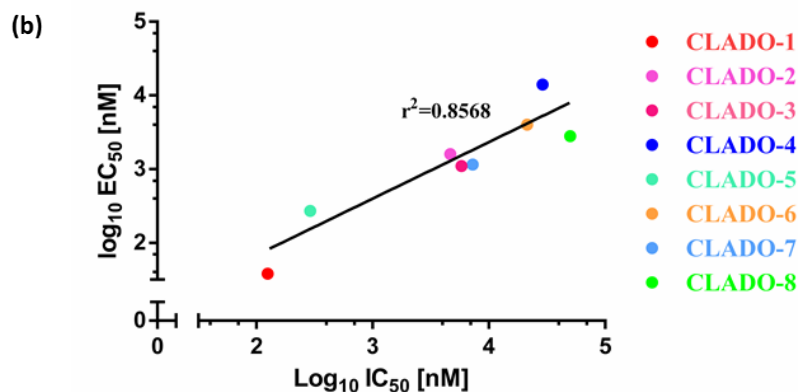


Figure 13. (a) Linear regression plot: thermal shift (ΔT_m) versus $\log_{10} EC_{50}$ obtained through the data collected from enzyme and cell-based assays for malaria parasites.

(b) Linear regression plot: $\log_{10} IC_{50}$ and $\log_{10} EC_{50}$ for malarial parasites.

All the data sets and observations from these assays led us to classify the entire stereochemical library of cladosporin (cladologs) into three distinct categories.

- **Class A:** Most potent (**CLADO-1** and **CLADO-5**)
- **Class B:** Moderately potent (**CLADO-2**, **CLADO-3** and **CLADO-7**)
- **Class C:** Non-potent (**CLADO-4**, **CLADO-6** and **CLADO-8**)

(The above categorical distribution of the set of isomers is also depicted in Table 2)

It is noteworthy to observe that the most potent isomer **CLADO-1** and least potent **CLADO-8** maintain an exact enantiomeric relationship with each other with exactly opposite chirality at all the positions of C3, C10 and C14 (Figure 9). It is also noteworthy to observe that **CLADO-1** and **CLADO-5** are the most potent compounds in the cladolog series despite change in the stereochemistry of C14 center which clearly makes the absolute stereochemistry at C14 center as a non-detrimental factor for anti-malarial potency. All other cladologs, namely **CLADO-2**, **CLADO-3**, **CLADO-4**, **CLADO-6**, **CLADO-7**, **CLADO-8** have stereoisomeric modifications at C3/C10 or both (Figure 9). Therefore, it is very evident that these stereochemical differences are crucial in determining the drug potency of the synthesized stereoisomers (cladologs) against *Plasmodium falciparum*.

Chapter 1 (Section A): Synthesis of Entire Stereoisomeric Set of Anti-malarial Natural Product Cladosporin, their Biological Evaluation and Co-crystalization

	Compounds	<i>Plasmodium falciparum</i>			Human	
		IC ₅₀ (μM)	EC ₅₀ (μM)	ΔT _m	IC ₅₀ (μM)	ΔT _m
Class A	CLADO-1	0.12 ± 0.0	~0.04	17.3 ± 0.5	105 ± 2	1.3
	CLADO-5	0.29 ± 0.00	0.27 ± 0.0	16.2 ± 0.5	>100	1.0
Class B	CLADO-2	4.64 ± 0.5	1.6 ± 0.1	14.3 ± 1.0	>100	0.5
	CLADO-3	5.8 ± 0.2	1.1 ± 0.1	15.6 ± 1.0	>100	0.1
	CLADO-7	7.25 ± 0.5	1.15 ± 0.0	13.5 ± 1.0	>100	1.1
Class C	CLADO-4	29.0 ± 4	>2	11.4 ± 1.0	>100	1.1
	CLADO-6	21.3 ± 2	>2	11.8 ± 0.4	>100	0.3
	CLADO-8	50.0 ± 5	>2	7.9 ± 1.0	>100	-0.9

Table 2. Classification of Cladologs.

1.1.2.5. Structural bases for cladolog-KRS binding

Through successfully assessment of anti-malarial potency of all the stereoisomers of cladosporin through enzyme and cell based assay, we demonstrated significant and crucial dependency of potency on the chirality of the isomers. Being intrigued with this, we further planned to decipher the structural bases of cladolog engagement with *Pf*KRS through X-ray co-crystals of selected cladologs with the target enzyme *Pf*KRS. Previously, the co-crystal structure of **CLADO-1** (cladosporin) with *Pf*KRS have been determined and analyzed in the literature.^{15, 16, 17} To further investigate the structural the cladolog selectivity on structural basis, we tried to co-crystallize six stereoisomers (**CLADO-2**, **CLADO-3**, **CLADO-4**, **CLADO-5**, **CLADO-6** and **CLADO-7**) and an enantiomer (**CLADO-8**) with *Pf*KRS in presence of L-lysine. We successfully obtained co-crystals of all the compounds except for **CLADO-8**. *Pf*KRS-CLADO-2/5/6/7

Chapter 1 (Section A): Synthesis of Entire Stereoisomeric Set of Antimalarial Natural Product Cladosporin, their Biological Evaluation and Co-crystalization

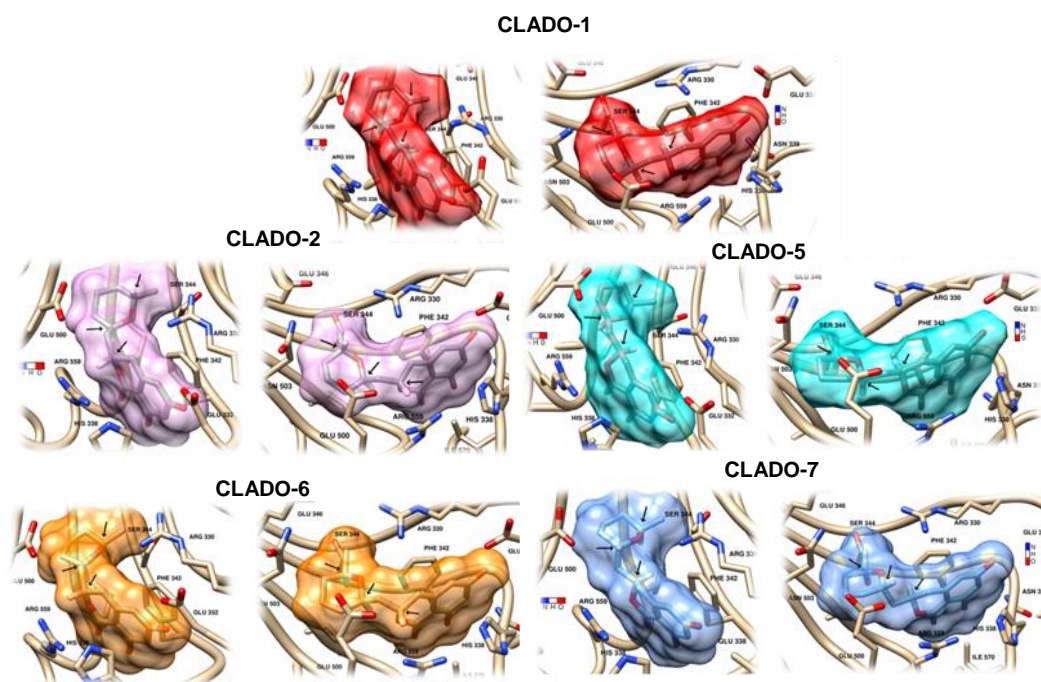


Figure 14. Co-crystal structures of the eight stereoisomers of cladosporin with *PfKRS*.

complex cocrystals, diffracted at ~ 3 Å resolution, whereas *PfKRS*-CLADO-3/4 cocrystals, showed comparably poor diffraction with >3.5 Å resolution. A clear electron density was observed for both L-lysine and the specific cladologs (CLADO-2/5/6/7; Figures 14) On the other hand, in the case of CLADO-3 and CLADO-4 no electron densities were observed for either Lys or the cladologs. The models were refined for *PfKRS*-CLADO-2/5/6/7 cocrystals and superimposed on *PfKRS*-CLADO-1 for further in depth analyses (Figure 15).

All five cladologs were found to have similar binding modes (Figure 15). In each isomers, the aromatic dihydroisocoumarin moiety of the cladolog stacks between the residues Arg559 and Phe342 (Figures 14, 15). As the chiral center at C3 of the dihydroisocoumarin moiety sterically clashes into the the carbon atoms of Phe343 and guanidium group of Arg559, an *R*-stereochemistry is most suitable for this center (Figure 15). Moreover, the C10 position also seems to favour an *R*-configuration, as apparent from the structural data of *PfKRS* bound CLADO-1, CLADO-2 and

Chapter 1 (Section A): Synthesis of Entire Stereoisomeric Set of Antimalarial Natural Product Cladosporin, their Biological Evaluation and Co-crystalization

CLADO-5 (Figures 14, 15, 16a). In the case of C14 center, stereochemistry is not a defining factor for potency as both *R*- and *S*-configurations are favorable.

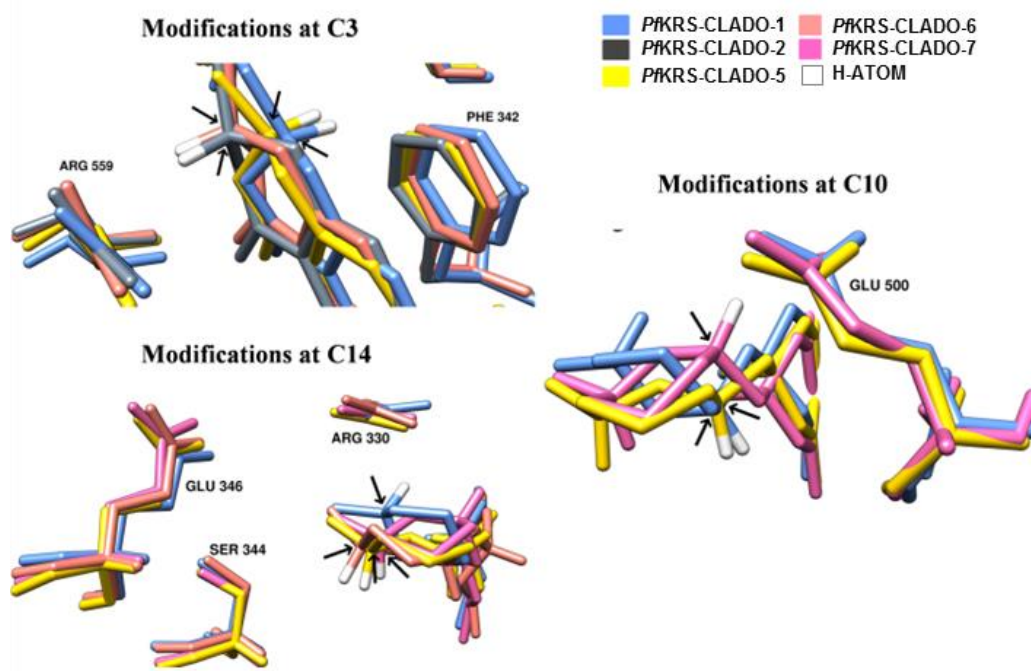


Figure 15. Structural comparison among the most potent cladolog (**CLADO-1**, **CLADO-5**) and other co-crystal structures of (**CLADO-2**, **CLADO-6**, **CLADO-7**).

In the above figure (Figure 15) the chiral centers of the superimposed cladologs are indicated with an arrow. For C3 chiral center the interacting side chain residues of Arg 559 and Phe 342 are shown. For C10 stereocenter the residue Glu500 is depicted and for C14, side chain residues of Ser 344, Arg 330 and Glu346 are shown. In **CLADO-1** and **CLADO-5** (*3R*), the C3 H atom is more accessible to Phe342 as compared to **CLADO-2** and **CLADO-6** (*3S*). C10 H atom in **CLADO-7** (*10S*) as compared to **CLADO-1** and **CLADO-5** (*3R*) stacks proximately to Glu500 side chain. As compared to **CLADO-5**, **CLADO-6** and **CLADO-7**, C14 H atom in **CLADO-1** is adjacent to Arg330.

The cladologs with *S*-configurations at positions C3/C10 (**CLADO-4** and **CLADO-8**) and at C10/C14 (**CLADO-3**) are not conformationally favorable on steric grounds. The presentation of the THP ring in the active site of *PfKRS* is affected by the

Chapter 1 (Section A): Synthesis of Entire Stereoisomeric Set of Antimalarial Natural Product Cladosporin, their Biological Evaluation and Co-crystallization

stereoisomeric alterations at either C3/C10/C14 or its combination (Figure 14). In comparison to the most potent cladologs (**CLADO-1** and **CLADO-5**) the binding of **CLADO-2**, **CLADO-6** and **CLADO-7** to the active site of *PfKRS* induced rotameric rearrangements of amino acid side chain of Phe342, Arg559, and Glu500 (Figure 15). Furthermore, it was also noted that the atomic arrangement at C10 is pivotal for cladolog binding, since out of four cladologs (**CLADO-3**, **CLADO-4**, **CLADO-7** and **CLADO-8**) having *S* conformation at C10, only one (**CLADO-7**) was successfully crystallized, while two failed (**CLADO-3** and **CLADO-4**). Besides, it appears that stereoisomeric alterations at C14 alone (**CLADO-5**) are not crucial for potency as both isomers (natural *S* and synthetic *R*) are highly potent (**CLADO-1** and **CLADO-5**). Hence, this analysis concludes that both *R*-C3 and *R*-C10 might serve as key enantiomeric determinants in enzyme inhibition.

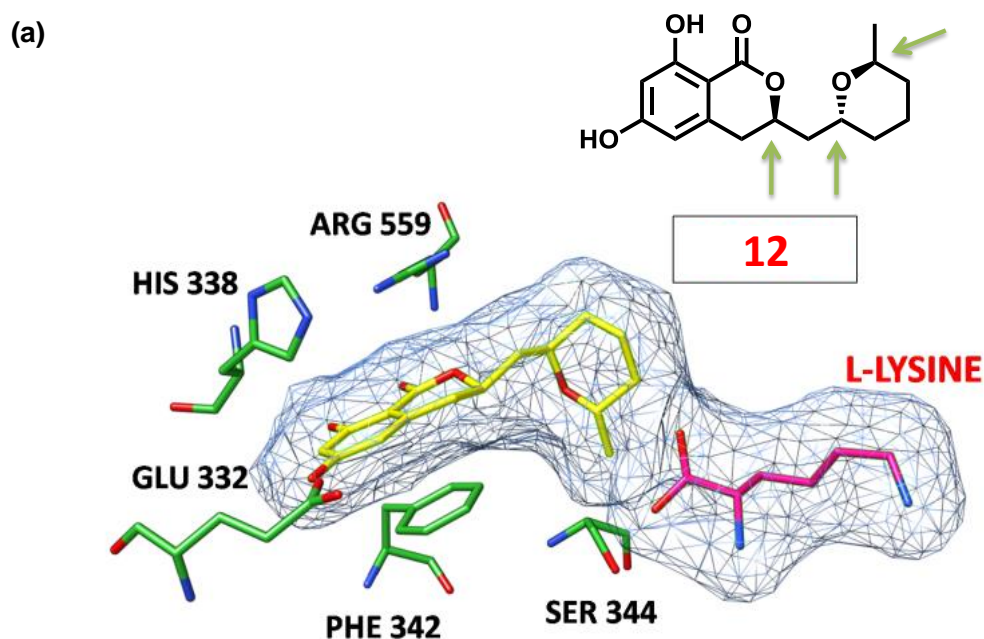


Figure 16. (a) Cladolog-induced rotameric changes in *PfKRS* side chains. Molecule surfaces for L-lysine and **CLADO-1** are as in the published crystal structure of *PfKRS*-K-**CLADO-1**.²¹

Chapter 1 (Section A): Synthesis of Entire Stereoisomeric Set of Anti-malarial Natural Product Cladosporin, their Biological Evaluation and Co-crystallization

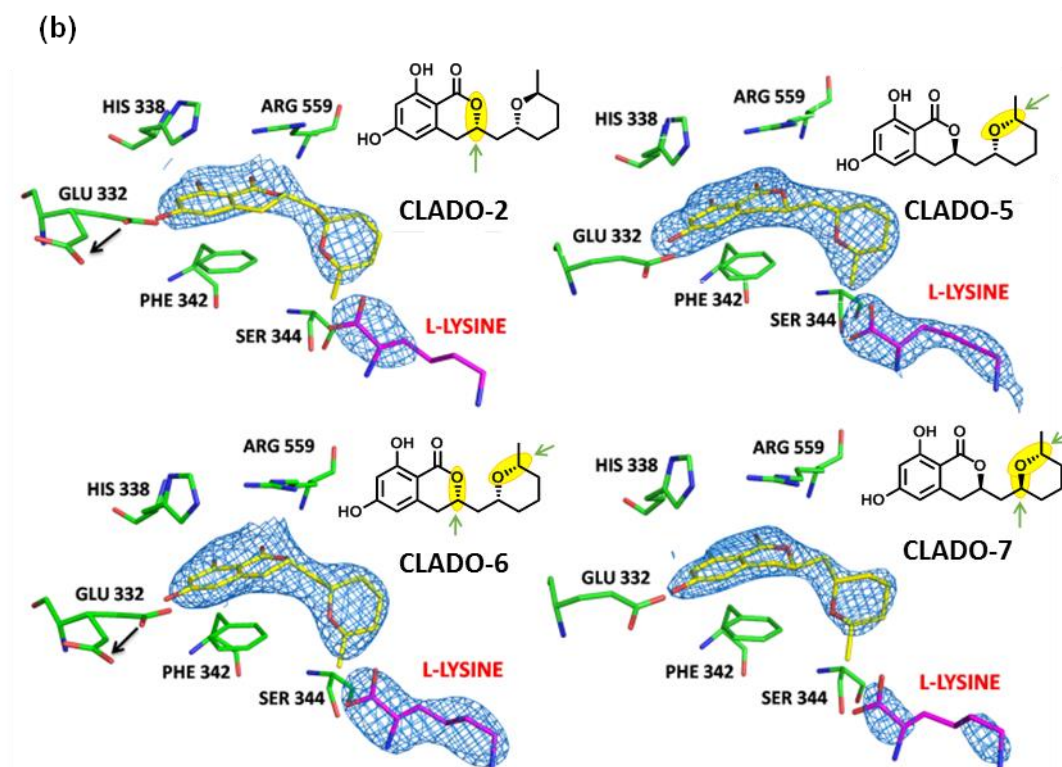


Figure 16. (b) Simulated annealing omit maps are shown for cladologs and L-lysine in the new *PfKRS*-K-cladolog complexes.

1.1.3. Conclusions from stereochemical structure activity relationship (S-SAR) studies

After thorough biological screening of all the eight possible stereoisomers of cladosporin in cell based and enzyme based assay we classified the entire stereoisomeric set in to three discrete categories comprising of most potent (**CLADO-1** and **CLADO-5**), moderately potent (**CLADO-2**, **CLADO-3** and **CLADO-7**) and non-potent (**CLAD-4**, **CLADO-6** and **CLADO-8**). The structural bases of *PfKRS*-cladolog binding was also deciphered through X-ray analysis of co-crystals of selected cladologs and *PfKRS*. The overall conclusion of the following studies are as follows.

- An “*R*” stereochemistry at C3 center of cladosporin scaffold in crucial for its anti-malarial potency.

Chapter 1 (Section A): Synthesis of Entire Stereoisomeric Set of Anti-malarial Natural Product Cladosporin, their Biological Evaluation and Co-crystalization

- An “*R*” stereochemistry at C10 center is also vital for bio-activity.
- The stereochemistry at C14 center is not a detrimental factor for exhibiting anti-malarial activity.

Conclusions from stereochemical SAR are also depicted in Figure 17.

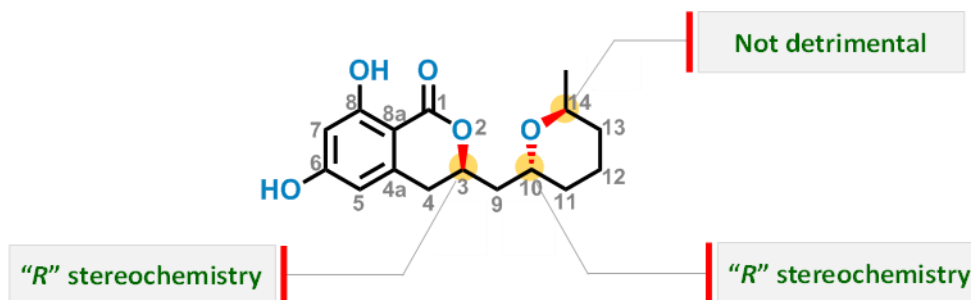


Figure 17. Conclusions from stereochemical Structure Activity Relationship.

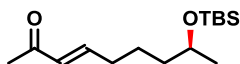
In summary, we have developed a novel divergent synthetic route for accessing all the possible stereoisomers of cladosporin. Similar synthetic approach can also be applied to access stereoisomeric sets of bio-active natural products and synthetic molecule with multiple chiral centers, which will in turn be valuable for Stereochemical Structure Activity Relationship (S-SAR) studies. This work also highlights the possibility of fine tuning the relevant functional groups in a bio-active molecule to produce large number of closely related analogues around the active scaffold. Such advancements will eventually pave a way for better understanding and application of stereochemical attributes in drug discovery and medicinal chemistry programs. These in turn can deliver more potent and selective lead molecules for drug development. We have demonstrated that enantioselectivity within KRS-cladologs serves as a key facet for these compounds as anti-malarial agents. Besides, our exploration further provides a striking example of the importance of chiral awareness in drug discovery and development. This work also lays the foundation of a promising scope for cladologs for the development of lead molecules against KRSs of other eukaryotic parasites where the active site residue is conserved.^{15, 16, 18}

Chapter 1 (Section A): Synthesis of Entire Stereoisomeric Set of Anti-malarial Natural Product Cladosporin, their Biological Evaluation and Co-crystalization

1.1.4. Experimental section

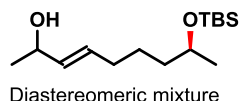
Synthesis of eight isomers of cladosporin

(*S,E*)-8-((*tert*-butyldimethylsilyl)oxy)non-3-en-2-one (2.2)



A solution of compound **2.1** (18 g, 78.809 mmol) in 500 mL of CH₂Cl₂ was stirred at -78 °C as ozone was passed through the same. Once blue colour was observed oxygen was passed to remove the excess ozone until the solution became colourless. Triphenyl phosphine (30.9 g, 118.188 mmol) was added and the reaction mixture was allowed to reach room temperature and stirred for an additional 12 h. The resulting solution of aldehyde was cooled to 0°C and 1-(triphenyl-15-phosphanylidene)propan-2-one **2.5** (62.723 g, 197.021 mmol) was added portion wise in one pot and left to stir for 16 h. The resultant solution was concentrated under *vacuo* and filtered through silica and forwarded to next step without further purification.

(*8S,E*)-8-((*tert*-butyldimethylsilyl)oxy)non-3-en-2-ol (2.3):



To a solution of **2.2** (10 g, 36.968 mmol) in CH₂Cl₂ (150 mL) and CH₃OH (50 mL) (3:1 v/v) was added CeCl₃·7H₂O (16.5 g, 44.362 mmol) at 0 °C and stirred for 30 minutes. NaBH₄ (1.5 g, 40.667 mmol) was added portion wise to the stirring solution at the same temperature and the reaction mixture was allowed to reach room temperature and stirred for 12 h. Reaction mixture was cooled to 0 °C and saturated aqueous solution of sodium potassium tartarate (50 mL) was added to the reaction flask and stirred for 15 mins followed by evaporation of CH₃OH and CH₂Cl₂ under *vacuo*. To the remaining aqueous mixture was added 1N HCl (100 mL) and extracted with ethyl acetate. The collected organic parts were dried over sodium sulphate, concentrated under *vacuo* and purified through column chromatography (silica gel 230-400 mesh 10% ethyl acetate – pet

Chapter 1 (Section A): Synthesis of Entire Stereoisomeric Set of Antimalarial Natural Product Cladosporin, their Biological Evaluation and Co-crystalization

ether) to afford compound **2.3** (8.9 g, 88 %) as a colourless oil (1:1 diastereomeric mixture).

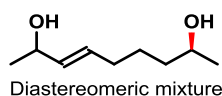
IR ν_{\max} (film): cm^{-1} 1728, 3431, 2938, 1250;

^1H NMR (400 MHz, CDCl_3): δ 5.62 (dd, $J = 14.2, 7.6$ Hz, 1H), 5.51 (dd, $J = 15.4, 6.5$ Hz, 1H), 4.26 (q, $J = 6.3$ Hz, 1H), 3.82 – 3.74 (m, 1H), 2.01 (dd, $J = 13.3, 6.6$ Hz, 2H), 1.42 (tdd, $J = 18.0, 8.7, 4.1$ Hz, 4H), 1.26 (d, $J = 6.0$ Hz, 3H), 1.12 (d, $J = 6.0$ Hz, 4H), 0.89 (s, 9H), 0.05 (s, 6H).

^{13}C NMR (100 MHz, CDCl_3): δ 134.2, 131.0, 68.9, 68.4, 39.1, 32.1, 25.9, 25.3, 23.8, 23.4, 18.1, -4.4, -4.7.

HRMS calculated for $\text{C}_{15}\text{H}_{32}\text{O}_2\text{Si}$ $[\text{M} + \text{Na}]^+$ 295.2062, observed 295.2064.

(8*S*,*E*)-non-3-ene-2,8-diol (2.4):



To a solution of compound **2.3** (8.9 g, 32.660 mmol) in THF (50 mL) was added tetrabutylammonium fluoride solution (1 M in THF) (65 mL, 65.32 mmol) at 0 °C. After stirring for 12 h at room temperature reaction mixture was cooled to 0 °C saturated aqueous NH_4Cl (40 mL) was added to the same extracted with excess ethyl acetate several times. The collected organic layers were dried over sodium sulphate, concentrated under *vacuo* and purified via column chromatography (silica gel 230-400 mesh 50% ethyl acetate – pet ether) to give compound **2.4** (4.4 g, 85 %) as a pale-yellow oil (1:1 diastereomeric mixture);

IR ν_{\max} (film): cm^{-1} 1719, 3020, 1217, 1369;

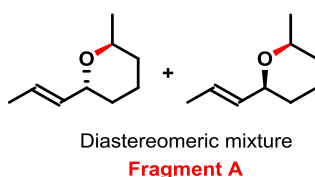
^1H NMR (400MHz, CDCl_3): δ 5.65 – 5.48 (m, 1H), 5.50 (dd, $J = 15.4, 6.4$ Hz, 1H), 4.23 (dd, $J = 12.5, 6.2$ Hz, 1H), 3.79 – 3.66 (m, 1H), 2.11 (s, 2H), 2.03 – 2.00 (m, 2H), 1.47 – 1.40 (m, 4H), 1.23 (d, $J = 6.3$ Hz, 3H), 1.17 (d, $J = 6.1$ Hz, 4H).

Chapter 1 (Section A): Synthesis of Entire Stereoisomeric Set of Antimalarial Natural Product Cladosporin, their Biological Evaluation and Co-crystalization

^{13}C NMR (100 MHz, CDCl_3): δ 134.5, 130.5, 68.8, 67.9, 67.8, 38.6, 31.9, 31.9, 25.2, 23.4, 23.4.

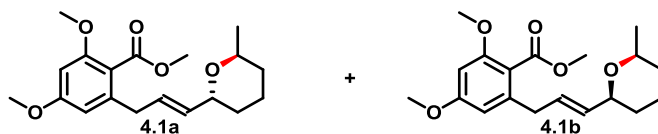
HRMS calculated for $\text{C}_9\text{H}_{18}\text{O}_2$ $[\text{M} + \text{Na}]^+$ 181.1198, observed 181.1199.

Fragment A:



Bis(acetonitrile)dichloropalladium(II) (0.72 g, 2.78 mmol) was added to a solution of compound **2.4** (4.4 g, 27.806 mmol) in THF at 0 °C and stirred for 30 mins at the same temperature. After completion of the reaction which was monitored through TLC, resultant reaction mixture was filtered through a pad of celite to furnish fragment A and concentrated via rotary evaporation at low temperature to afford a colourless oil (1:1 diastereomeric mixture) which was forwarded to next step without further purification. HRMS calculated for $\text{C}_9\text{H}_{17}\text{O}$ $[\text{M} + \text{H}]^+$ 141.1274, observed 141.1269.

methyl 2,4-dimethoxy-6-((E)-3-((2R,6S)-6-methyltetrahydro-2H-pyran-2-yl)allyl)benzoate (4.1a) and methyl 2,4-dimethoxy-6-((E)-3-((2S,6S)-6-methyltetrahydro-2H-pyran-2-yl)allyl)benzoate (4.1b)



A solution of fragment B (2.0 g, 8.465 mmol) in CH_2Cl_2 (50 mL) was degassed with argon for 15 minutes. Solution of fragment A in CH_2Cl_2 was added in the same followed by addition of 5 mol% of the Grubbs' 2nd generation catalyst. The reaction mixture was stirred at room temperature for 36 h. It was then filtered through a short pad of celite and concentrated under reduced pressure to remove excess CH_2Cl_2 and. Careful purification by silica gel chromatography (silica gel 230-400 mesh 25 % ethyl acetate

Chapter 1 (Section A): Synthesis of Entire Stereoisomeric Set of Antimalarial Natural Product Cladosporin, their Biological Evaluation and Co-crystalization

– pet ether) allowed the separation of two diastereomers **4.1a** (0.570g) and **4.1b** (0.540g) with a combined yield of 53 %.

Compound 4.1a

$[\alpha]_{\text{D}}^{25} = -5.09$ ($c = 1.6$, CHCl_3);

IR ν_{max} (film): cm^{-1} 1712, 1215, 3020, 1604;

$^1\text{H NMR}$ (400 MHz, CDCl_3): δ 6.34 (s, 2H), 5.74 – 5.61 (m, 2H), 4.33 (d, $J = 4.2$ Hz, 1H), 3.88 (s, 1H), 3.86 (s, 3H), 3.79 (s, 6H), 3.35 (d, $J = 5.7$ Hz, 2H), 1.70 (dd, $J = 12.0$, 4.7 Hz, 1H), 1.62 – 1.60 (m, 3H), 1.53 – 1.51 (m, 1H), 1.27 (dd, $J = 15.6$, 7.5 Hz, 1H), 1.15 (d, $J = 6.3$ Hz, 3H).

$^{13}\text{C NMR}$ (100 MHz, CDCl_3): δ 168.5, 161.5, 158.2, 140.6, 132.4, 129.6, 116.2, 106.0, 96.6, 71.7, 67.1, 55.9, 55.3, 52.0, 36.8, 32.2, 29.4, 20.6, 18.6

HRMS calculated for $\text{C}_{19}\text{H}_{27}\text{O}_5$ $[\text{M} + \text{H}]^+$ 335.1853, observed 335.1839.

Compound 4.1b:

$[\alpha]_{\text{D}}^{25} = -3.14$ ($c = 1.6$, CHCl_3); IR ν_{max} (film): cm^{-1} 1782, 1214, 1332, 3020;

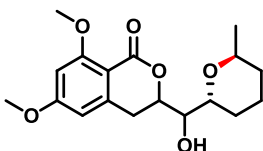
$^1\text{H NMR}$ (400 MHz, CDCl_3): δ 6.33 (s, 2H), 5.76 – 5.69 (m, 1H), 5.55 (dd, $J = 15.2$, 6.5 Hz, 1H), 3.86 (s, 3H), 3.80 (d, $J = 0.5$ Hz, 7H), 3.46 (td, $J = 10.9$, 5.7 Hz, 1H), 3.33 (d, $J = 6.6$ Hz, 2H), 1.83 – 1.79 (m, 1H), 1.59 – 1.45 (m, 4H), 1.29 (dd, $J = 11.7$, 3.8 Hz, 1H), 1.18 (d, $J = 6.2$ Hz, 3H).

$^{13}\text{C NMR}$ (100 MHz, CDCl_3): δ 168.4, 161.5, 158.2, 140.5, 133.3, 128.9, 116.2, 106.1, 96.5, 78.0, 73.7, 55.9, 55.3, 52.0, 36.8, 33.0, 31.4, 23.5, 22.2

HRMS calculated for $\text{C}_{19}\text{H}_{27}\text{O}_5$ $[\text{M} + \text{H}]^+$ 335.1853, observed 335.1840.

Chapter 1 (Section A): Synthesis of Entire Stereoisomeric Set of Antimalarial Natural Product Cladosporin, their Biological Evaluation and Co-crystallization

3-(hydroxy((2*R*,6*S*)-6-methyltetrahydro-2*H*-pyran-2-yl)methyl)-6,8-dimethoxyisochroman-1-one (4.2a):



Non-seperable diastereomeric mixture (dr 3:2 as per NMR)

To a solution of compound **4.1a** (0.714 g, 2.135 mmol) in acetone (12 mL) and water (6 mL) was added 4-Methylmorpholine N-oxide (0.749 g, 6.405 mmol) followed by the careful addition of catalytic amount of 2.5 % OsO₄ (*tert*-butanol solution) at 0 °C. After stirring for 12 h at room temperature saturated aqueous solution of Na₂SO₃ (15 mL) was added and further stirred for 6 h at room temperature. Excess acetone was removed under *vacuo* and the remaining aqueous part was extracted with ethyl acetate (3 x 30 mL). The combined organic parts were dried over sodium sulphate and concentrated under *vacuo*. Purification through column chromatography (silica gel 100-200 mesh 10% ethyl acetate – pet ether) afforded compound **4.2a** (0.382 g) (3:2 diastereomeric mixture) as colourless oil with a yield of 53%;

IR ν_{\max} (film): cm⁻¹ 3021, 1722, 1599, 1217;

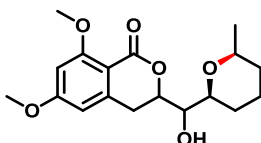
¹H NMR (400 MHz, CDCl₃): δ 6.39 (s, 1H), 6.33 (s, 1H), 4.69 – 4.40 (m, 1H), 4.13 – 3.98 (m, 1H), 3.91 – 3.90 (m, 4H), 3.85 (s, 3H), 3.69 – 3.55 (m, 1H), 3.35 – 3.21 (m, 1H), 2.75 - 2.65 (m, 1H), 2.33 (br. s, 1H), 1.87 - 1.63 (m, 4H), 1.56 - 1.51 (m, 1H), 1.35 - 1.32 (m, 1H), 1.25 – 1.16 (m, 3H).

¹³C NMR (100 MHz, CDCl₃): δ 164.5, 164.4, 163.1, 163.0, 162.3, 162.2, 144.2, 144.1, 106.6, 104.0, 103.9, 97.7, 76.8, 75.8, 73.5, 73.1, 68.9, 68.8, 68.6, 68.4, 56.1, 55.5, 31.8, 31.1, 30.7, 30.0, 27.0, 26.6, 18.7, 18.1, 17.8

HRMS calculated for C₁₈H₂₅O₆ [M + H]⁺ 337.1646, observed 337.1635.

Chapter 1 (Section A): Synthesis of Entire Stereoisomeric Set of Antimalarial Natural Product Cladosporin, their Biological Evaluation and Co-crystallization

3-(hydroxy((2*S*,6*S*)-6-methyltetrahydro-2H-pyran-2-yl)methyl)-6,8-dimethoxyisochroman-1-one (4.2b):



Non-separable diastereomeric mixture (dr 1:1 as per NMR)

Compound **8.2b** (0.432 g) with a yield of 60 % was synthesized as 1:1 diastereomeric mixture from compound **8.1b** using similar procedure for the synthesis of compound **8.2a**.

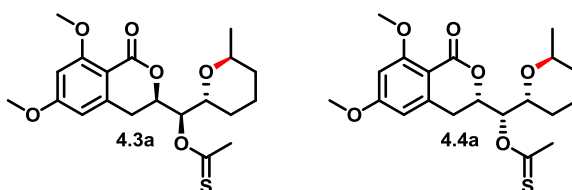
IR ν_{\max} (film): cm^{-1} 3021, 2403, 1721, 1601, 1216;

^1H NMR (400MHz, CDCl_3): δ 6.40 (s, 1 H), 6.34 (s, 1 H), 4.77 – 4.44 (m, 1H), 3.91 (d, $J = 5.5$ Hz, 3H), 3.86 (s, 3H), 3.75 – 3.71 (m, 1H), 3.59 - 3.25 (m, 3H), 2.76 - 2.64 (m, 1H), 2.12 – 1.79 (m, 3H), 1.62 - 1.49 (m, 2 H), 1.41 – 1.32 (m, 1H), 1.18 – 1.09 (m, 3 H).

^{13}C NMR (100MHz, CDCl_3): δ 164.5, 164.4, 163.0, 162.2, 144.4, 144.2, 106.7, 104.0, 103.9, 97.7, 76.5, 76.3, 76.0, 75.5, 75.1, 74.5, 74.1, 73.9, 56.1, 55.5, 33.3, 33.0, 31.7, 31.1, 28.1, 26.7, 23.1, 23.0, 22.1, 22.0

HRMS calculated for $\text{C}_{18}\text{H}_{25}\text{O}_6$ $[\text{M} + \text{H}]^+$ 337.1646, observed 337.1632.

O-((*S*)-((*S*)-6,8-dimethoxy-1-oxoisochroman-3-yl)((2*R*,6*S*)-6-methyltetrahydro-2H-pyran-2-yl)methyl) *S*-methyl carbonodithioate (4.3a) and O-((*R*)-((*R*)-6,8-dimethoxy-1-oxoisochroman-3-yl)((2*R*,6*S*)-6-methyltetrahydro-2H-pyran-2-yl)methyl) *S*-methyl carbonodithioate (4.4a):



Chapter 1 (Section A): Synthesis of Entire Stereoisomeric Set of Antimalarial Natural Product Cladosporin, their Biological Evaluation and Co-crystallization

To a solution of **4.2a** (0.382 g, 1.136 mmol) (1:1 diastereomeric mixture) in THF (30 mL) was added LiHMDS (1 M in THF) (1.2 mL) at 0 °C. After 15 minutes CS₂ (137 μ l, 2.271 mmol) was added, which was followed by the addition of CH₃I (283 μ l, 4.542 mmol). After stirring the reaction mixture for 12 h, H₂O (10 mL) was added to the same and extracted with ethyl acetate. The combined organic layers were dried over sodium sulphate and concentrated under *vacuo*. Purification through flash chromatography 28% ethyl acetate – pet ether gave clean separation of the two diastereomers **4.3a** (0.227 g) and **4.4a** (0.151 g) as foamy solids with an overall yield of 78%.

Compound 4.3a:

$[\alpha]^{25}_{\text{D}} = +15.99$ ($c = 1.6$, CHCl₃);

IR ν_{max} (film): cm⁻¹ 3024, 1640, 1430, 1217, 766;

¹H NMR (400 MHz, CDCl₃): δ 6.39 (s, 1H), 6.30 (s, 1H), 6.20 (d, $J = 9.6$ Hz, 1H), 4.87 (d, $J = 11.7$ Hz, 1H), 4.42 (dd, $J = 11.7, 5.3$ Hz, 1H), 3.92 (s, 4H), 3.84 (s, 3H), 3.00 (dd, $J = 15.8, 12.6$ Hz, 1H), 2.75 (dd, $J = 16.0, 2.4$ Hz, 1H), 2.57 (s, 3H), 1.69 – 1.66 (m, 4H), 1.35 (dt, $J = 12.6, 7.3$ Hz, 2H), 1.21 (d, $J = 6.5$ Hz, 3H).

¹³C NMR (100 MHz, CDCl₃): δ 217.2, 164.4, 163.0, 161.9, 143.5, 106.9, 103.8, 97.9, 80.6, 74.2, 68.6, 66.9, 56.1, 55.5, 31.7, 30.9, 26.1, 19.2, 18.2

HRMS calculated for C₂₀H₂₇O₆S₂ [M + H]⁺ 427.1244, observed 427.1230.

Compound 4.4a:

$[\alpha]^{25}_{\text{D}} = -18.78$ ($c = 1.5$, CHCl₃); ν_{max} (film): cm⁻¹ 3025, 1639, 1431, 1218, 769;

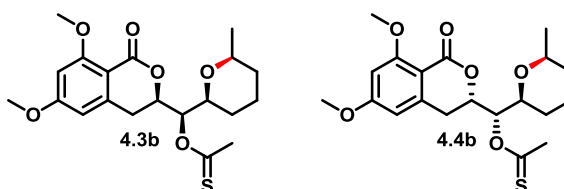
¹H NMR (400 MHz, CDCl₃): δ 6.40 (s, 1H), 6.31 (s, 1H), 6.22 (dd, $J = 6.8, 3.3$ Hz, 1H), 4.71 – 4.67 (m, 1H), 4.35 (dd, $J = 10.5, 6.7$ Hz, 1H), 4.05 (d, $J = 3.1$ Hz, 1H), 3.91 (s, 3H), 3.85 (s, 3H), 3.09 (dd, $J = 16.0, 11.6$ Hz, 1H), 2.90 – 2.80 (m, 1H), 2.58 (s, 3H), 1.71 (dt, $J = 16.6, 10.1$ Hz, 2H), 1.62 – 1.57 (m, 2H), 1.30 – 1.25 (m, 2H), 1.17 (d, $J = 6.4$ Hz, 3H).

Chapter 1 (Section A): Synthesis of Entire Stereoisomeric Set of Antimalarial Natural Product Cladosporin, their Biological Evaluation and Co-crystallization

^{13}C NMR (100 MHz, CDCl_3): δ 217.2, 164.5, 163.1, 161.6, 143.3, 106.7, 103.9, 98.0, 82.1, 75.4, 69.5, 68.5, 56.2, 55.6, 31.5, 30.6, 26.5, 19.0, 18.9, 18.4;

HRMS calculated for $\text{C}_{20}\text{H}_{27}\text{O}_6\text{S}_2$ $[\text{M} + \text{H}]^+$ 427.1244, observed 427.1231.

O-((R)-((R)-6,8-dimethoxy-1-oxoisochroman-3-yl)((2S,6S)-6-methyltetrahydro-2H-pyran-2-yl)methyl) S-methyl carbonodithioate (**4.3b**) and O-((S)-((S)-6,8-dimethoxy-1-oxoisochroman-3-yl)((2S,6S)-6-methyltetrahydro-2H-pyran-2-yl)methyl) S-methyl carbonodithioate (**4.4b**):



Compound **4.3b** (0.195 g) and **4.4b** (0.190 g) with an overall yield of 70% was synthesized from compound **4.2b** as a semi solid by following similar procedure for the synthesis of compound **4.3a** and **4.4a**.

Compound **4.3b**:

$[\alpha]_{\text{D}}^{25} = +95.92$ ($c = 0.6$, CHCl_3);

IR ν_{max} (film): cm^{-1} 3023, 1640, 1431, 1218, 768;

^1H NMR (400 MHz, CDCl_3): δ 6.40 (s, 1H), 6.32 (s, 1H), 6.01 (t, $J = 4.6$ Hz, 1H), 4.77 (dt, $J = 11.3, 3.0$ Hz, 1H), 3.96 – 3.86 (m, 4H), 3.86 (s, 3H), 3.45 (dd, $J = 10.4, 5.7$ Hz, 1H), 3.14 (dd, $J = 16.1, 11.5$ Hz, 1H), 2.87 (dd, $J = 16.2, 2.4$ Hz, 1H), 2.58 (s, 3H), 1.87 – 1.83 (m, 1H), 1.67 – 1.63 (m, 2H), 1.57 – 1.49 (m, 1H), 1.40 (ddd, $J = 15.3, 12.6, 3.3$ Hz, 1H), 1.20 (dd, $J = 11.0, 3.4$ Hz, 1H), 1.13 (d, $J = 6.1$ Hz, 3H).

^{13}C NMR (100 MHz, CDCl_3): δ 217.1, 164.5, 163.1, 161.7, 143.4, 106.8, 103.9, 97.9, 83.0, 75.8, 75.0, 74.3, 56.2, 55.6, 32.9, 31.5, 26.7, 23.2, 22.0, 19.0

HRMS calculated for $\text{C}_{20}\text{H}_{27}\text{O}_6\text{S}_2$ $[\text{M} + \text{H}]^+$ 427.1244, observed 427.1228.

Chapter 1 (Section A): Synthesis of Entire Stereoisomeric Set of Antimalarial Natural Product Cladosporin, their Biological Evaluation and Co-crystallization

Compound 4.4b:

$[\alpha]_{\text{D}}^{25} = -146.8$ ($c = 0.5$, CHCl_3);

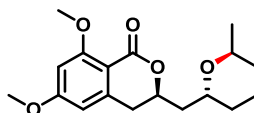
IR ν_{max} (film): cm^{-1} 3022, 1640, 1430, 1217, 768;

^1H NMR (400 MHz, CDCl_3): δ 6.39 (s, 1H), 6.29 (s, 1H), 5.97 (d, $J = 9.4$ Hz, 1H), 4.95 (d, $J = 11.7$ Hz, 1H), 4.09 (t, $J = 10.1$ Hz, 1H), 3.93 (s, 3H), 3.84 (s, 3H), 3.52 (dd, $J = 10.6, 5.8$ Hz, 1H), 3.02 – 2.95 (m, 1H), 2.77 – 2.73 (m, 1H), 2.57 (s, 3H), 1.83 (d, $J = 12.9$ Hz, 1H), 1.56 (ddd, $J = 23.7, 16.4, 12.1$ Hz, 3H), 1.20 – 1.17 (m, 2H), 1.12 (d, $J = 6.0$ Hz, 3H).

^{13}C NMR (100 MHz, CDCl_3): δ 217.3, 164.5, 163.0, 162.3, 143.6, 106.9, 103.8, 97.9, 82.6, 74.0, 73.3, 56.2, 55.5, 33.2, 31.6, 27.5, 22.8, 22.0, 19.3

HRMS calculated for $\text{C}_{20}\text{H}_{27}\text{O}_6\text{S}_2$ $[\text{M} + \text{H}]^+$ 427.1244, observed 427.1230.

(*R*)-6,8-dimethoxy-3-(((2*R*,6*S*)-6-methyltetrahydro-2H-pyran-2-yl)methyl)isochroman-1-one (4.5a):



Compound **4.3a** (0.227 g, 0.532 mmol) was dissolved in toluene which was followed by the addition of AIBN (8.7 mg, 0.053 mmol) and tributyltin hydride (430 μl , 1.596 mmol). The reaction mixture was stirred at 95°C for 4 h. After completion of the reaction toluene was evaporated under *vacuo* and the crude was purified by column chromatography which afforded compound **4.5a** (0.106 mg) as a foamy solid with 62 % yield.

$[\alpha]_{\text{D}}^{25} = +36.76$ ($c = 1.5$, CHCl_3);

IR ν_{max} (film): cm^{-1} 3014, 2852, 1713, 1599, 1220;

^1H NMR (400 MHz, CDCl_3): δ 6.39 (s, 1H), 6.29 (s, 1H), 4.57 (dd, $J = 10.9, 8.7$ Hz, 1H), 4.07 (t, $J = 8.2$ Hz, 1H), 3.91 (s, 4H), 3.85 (s, 3H), 2.84 (ddd, $J = 18.3, 15.9, 7.0$

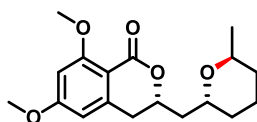
Chapter 1 (Section A): Synthesis of Entire Stereoisomeric Set of Antimalarial Natural Product Cladosporin, their Biological Evaluation and Co-crystallization

Hz, 2H), 1.85 (dtd, $J = 16.3, 14.2, 2.6$ Hz, 2H), 1.72 – 1.56 (m, 4H), 1.31 (dd, $J = 15.6, 7.4$ Hz, 2H), 1.19 (d, $J = 6.5$ Hz, 3H).

^{13}C NMR (100 MHz, CDCl_3): δ 164.3, 163.0, 162.8, 144.0, 107.1, 103.8, 97.7, 74.4, 67.6, 66.1, 56.1, 55.5, 39.6, 35.5, 31.0, 30.8, 18.8, 18.2.

HRMS calculated for $\text{C}_{18}\text{H}_{25}\text{O}_5$ $[\text{M} + \text{H}]^+$ 321.1697, observed 321.1691.

(S)-6,8-dimethoxy-3-(((2R,6S)-6-methyltetrahydro-2H-pyran-2-yl)methyl)isochroman-1-one (4.6a):



Compound **4.6a** (69 mg) with a yield of 61 % was synthesized as a semi solid from compound **4.4a** using similar procedure for the synthesis of compound **4.5a**.

$[\alpha]_{\text{D}}^{25} = -10.88$ ($c = 1.8$, CHCl_3);

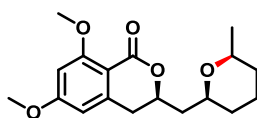
IR ν_{max} (film): cm^{-1} 3015, 2853, 1709, 1599, 1219;

^1H NMR (400 MHz, CDCl_3): δ 6.40 (s, 1H), 6.31 (s, 1H), 4.55 - 4.49 (m, 1 H), 4.04 (dd, $J = 4.3, 9.2$ Hz, 1H), 3.92 (s, 4H), 3.86 (s, 3H), 2.97 - 2.88 (m, 2H), 2.41 - 2.34 (m, 1H), 1.74 - 1.61 (m, 5H), 1.36 - 1.29 (m, 2 H), 1.16 (d, $J = 6.1$ Hz, 3 H).

^{13}C NMR (100 MHz, CDCl_3): δ 164.3, 163.1, 162.7, 144.0, 107.0, 103.9, 97.8, 74.6, 66.9, 66.9, 56.1, 55.5, 37.5, 34.3, 31.4, 29.9, 19.7, 18.2;

HRMS calculated for $\text{C}_{18}\text{H}_{25}\text{O}_5$ $[\text{M} + \text{H}]^+$ 321.1697, observed 321.1690;

(R)-6,8-dimethoxy-3-(((2S,6S)-6-methyltetrahydro-2H-pyran-2-yl)methyl)isochroman-1-one (4.5b):



Chapter 1 (Section A): Synthesis of Entire Stereoisomeric Set of Antimalarial Natural Product Cladosporin, their Biological Evaluation and Co-crystallization

Compound **4.5b** (88 mg) with a yield of 60% was synthesized from compound **4.3b** as a foamy solid using similar procedure for the synthesis of **4.5a** and **4.6a**.

$[\alpha]^{25}_{\text{D}} = +78.26$ ($c = 1.0$, CHCl_3);

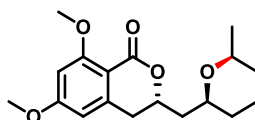
IR ν_{max} (film): cm^{-1} 3015, 2931, 1704, 1598, 1218;

^1H NMR (400 MHz, CDCl_3): δ 6.40 (s, 1H), 6.32 (s, 1H), 4.57 (qd, $J = 6.4, 2.9$ Hz, 1H), 3.92 (s, 3H), 3.86 (s, 3H), 3.64 (dt, $J = 11.1, 5.7$ Hz, 1H), 3.46 – 3.40 (m, 1H), 2.98 (dd, $J = 16.0, 11.3$ Hz, 1H), 2.84 (dd, $J = 16.1, 2.6$ Hz, 1H), 2.10 (dt, $J = 14.0, 7.0$ Hz, 1H), 1.83 – 1.73 (m, 2H), 1.64 – 1.50 (m, 4H), 1.28 – 1.18 (m, 3H), 1.14 (d, $J = 6.2$ Hz, 4H).

^{13}C NMR (100 MHz, CDCl_3): δ 164.3, 163.1, 162.8, 144.1, 107.0, 103.9, 97.7, 74.4, 73.8, 73.4, 56.1, 55.5, 40.8, 34.7, 33.1, 30.9, 23.5, 22.2.

HRMS calculated for $\text{C}_{18}\text{H}_{24}\text{O}_5\text{Na}$ $[\text{M} + \text{Na}]^+$ 343.1516, observed 343.1510.

(S)-6,8-dimethoxy-3-(((2S,6S)-6-methyltetrahydro-2H-pyran-2-yl)methyl)isochroman-1-one (4.6b):



Compound **4.6b** (83 mg) with a yield of 58% was synthesized as a yellowish oil from compound **4.4b** following similar procedure for the synthesis of compound **4.5a**, **4.6a** and **4.5b**.

$[\alpha]^{25}_{\text{D}} = -121.78$ ($c = 0.3$, CHCl_3);

IR ν_{max} (film): cm^{-1} 3015, 2931, 1704, 1598, 1218;

^1H NMR (400 MHz, CDCl_3): δ 6.39 (s, 1H), 6.28 (s, 1H), 4.69 - 4.64 (m, 1H), 3.91 (s, 3H), 3.84 (s, 3H), 3.70 (t, $J = 10.7$ Hz, 1H), 3.46 - 3.39 (m, 1H), 2.90 - 2.75 (m, 2H),

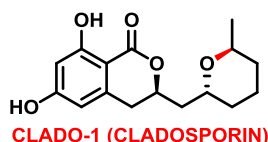
Chapter 1 (Section A): Synthesis of Entire Stereoisomeric Set of Anti-malarial Natural Product Cladosporin, their Biological Evaluation and Co-crystalization

1.88 - 1.77 (m, 2H), 1.72 - 1.66 (m, 2H), 1.57 - 1.51 (m, 3H), 1.19 - 1.16 (m, 1H), 1.11 (d, $J = 6.1$ Hz, 3H);

^{13}C NMR (100 MHz, CDCl_3): δ 164.3, 163.0, 144.2, 107.1, 103.8, 97.7, 73.8, 73.7, 73.0, 56.1, 55.5, 41.7, 35.5, 33.2, 31.6, 23.6, 22.1;

HRMS calculated for $\text{C}_{18}\text{H}_{24}\text{O}_5\text{Na}$ $[\text{M} + \text{Na}]^+$ 343.1516, observed 343.1510.

Cladosporin (CLADO-1):



A suspension of Aluminium powder (106 mg, 0.331 mmol) in dry benzene (5 mL) was treated with I_2 (1.3 g, 5.293 mmol) under argon, and the violet mixture was stirred under reflux for 30 min until the violet colour disappeared. After the mixture was cooled to 0 °C, few crystals of TBAI (10.6 mg, 0.033 mmol) and phloroglucinol (208.6 mg, 1.654 mmol) were added before a solution of compound **4.5a** (106 mg, 0.331 mmol) in dry benzene (3 mL) was added in one portion. The resulting green-brown suspension was stirred for 30 min at 5 °C before saturated $\text{Na}_2\text{S}_2\text{O}_3$ solution (8 mL) and ethyl acetate (8 mL) were added. After separation of the layers, the aqueous phase was extracted with ethyl acetate. The combined organic layers were washed with brine, dried over Na_2SO_4 , filtered, and concentrated in *vacuo*. Purification by column chromatography to afford cladosporin (CLADO-1) (0.052 g) as a white solid with a yield of 54 %.

Melting point: 171-173 °C;

$[\alpha]_D^{25} = -15.75$ ($c = 0.6$, EtOH);

IR ν_{max} (film): cm^{-1} 3416, 3022, 1656, 1218;

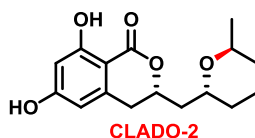
Chapter 1 (Section A): Synthesis of Entire Stereoisomeric Set of Antimalarial Natural Product Cladosporin, their Biological Evaluation and Co-crystallization

¹H NMR (400 MHz, CDCl₃): δ 11.09 (s, 1H), 6.30 (s, 1H), 6.17 (s, 1H), 4.68 (t, *J* = 9.8 Hz, 1H), 4.12 (s, 1H), 4.01 (s, 1H), 2.90 - 2.77 (m, 2H), 2.00 - 1.94 (m, 1H), 1.87 - 1.82 (m, 1H), 1.72 - 1.64 (m, 4H), 1.37-1.35 (m, 2H), 1.24 (d, *J* = 6.7 Hz, 3H);

¹³C NMR (100 MHz, CDCl₃): δ 169.9, 164.3, 163.1, 141.8, 106.7, 102.0, 101.5, 76.3, 68.0, 66.6, 39.3, 33.6, 30.9, 29.7, 18.9, 18.1;

HRMS calculated for C₁₆H₂₁O₅ [M + H]⁺ 293.1384, observed 293.1379.

(S)-6,8-dihydroxy-3-(((2R,6S)-6-methyltetrahydro-2H-pyran-2-yl)methyl)isochroman-1-one (CLADO-2):



CLADO-2 (0.031 g) with a yield of 49% was synthesized as a white solid from compound **4.6a** following similar procedure for the synthesis of **CLADO-1**.

Melting point: 134-138 °C

[α]²⁵_D = -100.7 (*c* = 0.5, CHCl₃);

IR ν_{max}(film): cm⁻¹ 3413, 3023, 1657, 1218;

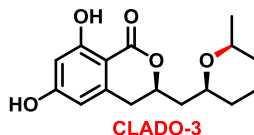
¹H NMR (400 MHz, CDCl₃): δ 11.12 (s, 1H), 7.20 (br. s.; 1H), 6.32 (s, 1H), 6.18 (s, 1H), 4.68 (s, 1H), 4.10 (s, 1H), 3.96 (s.; 1H), 2.93 - 2.92 (m, 2H), 2.44 - 2.36 (m, 1H), 1.83 - 1.70 (m, 5H), 1.40 - 1.34 (m, 2H), 1.20 (d, *J* = 6.1 Hz, 3H);

¹³C NMR (100 MHz, CDCl₃): δ 170.0, 164.4, 163.0, 141.6, 106.7, 102.0, 101.6, 76.6, 67.4, 67.2, 37.3, 32.6, 31.4, 29.8, 19.7, 18.1;

HRMS calculated for C₁₆H₂₁O₅ [M + H]⁺ 293.1384, observed 293.1379.

Chapter 1 (Section A): Synthesis of Entire Stereoisomeric Set of Antimalarial Natural Product Cladosporin, their Biological Evaluation and Co-crystalization

(R)-6,8-dihydroxy-3-(((2S,6S)-6-methyltetrahydro-2H-pyran-2-yl)methyl)isochroman-1-one (CLADO-3):



CLADO-3 (0.043 g) was synthesized with a yield of 57 % as a white solid from compound **4.5b** using similar procedure for the synthesis of **CLADO-1** and **CLADO-2**.

Melting point: 194-199 °C;

$[\alpha]^{25}_{\text{D}} = +46.44$ ($c = 0.5$, EtOH);

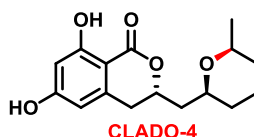
IR ν_{max} (film): cm^{-1} 3416, 3022, 1656, 1218;

^1H NMR (400 MHz, CD_3OD): δ 6.23 (s, 1H), 6.20 (s, 1H), 4.72 - 4.68 (m, 1H), 3.61 (s, 1H), 3.50 - 3.46 (m, 1H), 2.97 - 2.86 (m, 2H), 2.07 - 2.00 (m, 1H), 1.84 - 1.77 (m, 2H), 1.67 - 1.53 (m, 3H), 1.28 - 1.18 (m, 2H), 1.13 (d, $J = 6.1$ Hz, 3H);

^{13}C NMR (101MHz, CD_3OD): δ 171.7, 166.4, 165.8, 143.6, 108.1, 102.3, 101.8, 78.0, 75.5, 75.2, 42.2, 34.5, 33.8, 32.5, 24.7, 22.6.

HRMS calculated for $\text{C}_{16}\text{H}_{21}\text{O}_5$ $[\text{M} + \text{H}]^+$ 293.1384, observed 293.1379.

(S)-6,8-dihydroxy-3-(((2S,6S)-6-methyltetrahydro-2H-pyran-2-yl)methyl)isochroman-1-one (CLADO-4):



CLADO-4 (0.037 g) was synthesized from compound **4.4b** with a yield of 49% as a white solid using similar procedure for the synthesis of **CLADO-1**, **CLADO-2** and **CLADO-3**.

Chapter 1 (Section A): Synthesis of Entire Stereoisomeric Set of Anti-malarial Natural Product Cladosporin, their Biological Evaluation and Co-crystalization

Melting point: 154-157 °C;

$[\alpha]_{\text{D}}^{25} = -5.0$ ($c = 0.4$, CHCl_3);

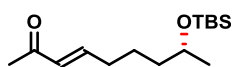
IR ν_{max} (film): cm^{-1} 3422, 3020, 1659, 1630, 1216;

^1H NMR (400 MHz, CD_3OD): δ 6.21 (s, 1H), 6.20 (s, 1H), 4.77 - 4.71 (m, 1H), 3.69 - 3.64 (m, 1H), 3.52 - 3.45 (m, 1H), 2.94 - 2.81 (m, 2H), 1.91 - 1.72 (m, 4H), 1.61 - 1.55 (m, 3H), 1.22 - 1.17 (dd, $J = 4.3, 11.6\text{Hz}$, 1H), 1.14 (d, $J = 6.7\text{ Hz}$, 3H).

^{13}C NMR (100 MHz, CD_3OD): δ 171.7, 166.4, 165.8, 143.7, 108.0, 102.3, 101.7, 77.6, 75.3, 74.8, 43.0, 34.6, 34.5, 33.1, 24.8, 22.5.

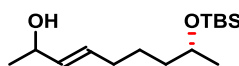
HRMS calculated for $\text{C}_{16}\text{H}_{21}\text{O}_5[\text{M} + \text{H}]^+$ 293.1384, observed 293.1382.

(*R,E*)-8-((*tert*-butyldimethylsilyl)oxy)non-3-en-2-one (5.2):



Compound **5.2** was synthesized from compound **5.1** as a colourless liquid by following similar procedure for the synthesis of **2.2**. The compound was filtered through silica and forwarded to next step without further characterization.

(8*R,E*)-8-((*tert*-butyldimethylsilyl)oxy)non-3-en-2-ol (5.3):



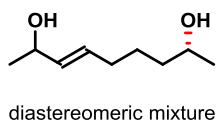
Diastereomeric mixture

The compound **5.3** (8 g, 82%) was synthesized (1:1 diastereomeric mixture) from compound **5.2** as a white colourless oil by following similar procedure for the synthesis of compound **2.3**.

^1H NMR (200 MHz, CDCl_3) δ 5.70 - 5.44 (m, 2H), 4.29 - 4.23 (m, 1H), 3.78 (dd, $J = 11.6, 5.7\text{ Hz}$, 1H), 2.01 (q, $J = 6.6\text{ Hz}$, 1H), 1.61 (s, 1H), 1.49 - 1.34 (m, 4H), 1.25 (d, $J = 6.3\text{ Hz}$, 2H), 1.11 (d, $J = 6.1\text{ Hz}$, 2H), 0.88 (s, 9H), 0.04 (s, 6H).

Chapter 1 (Section A): Synthesis of Entire Stereoisomeric Set of Anti-malarial Natural Product Cladosporin, their Biological Evaluation and Co-crystallization

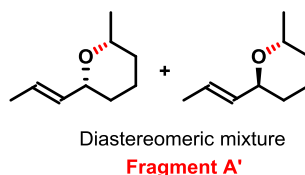
(8*R*,*E*)-non-3-ene-2,8-diol (**5.4**):



The compound **5.4** (3.7 g, 87%) was synthesized from compound **5.3** as a colourless oil by following similar procedure for the synthesis of compound **2.3**.

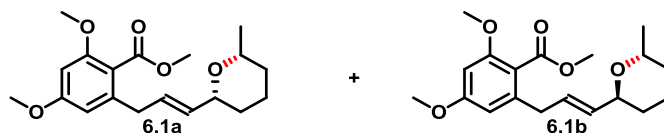
¹H NMR (200 MHz, CDCl₃) δ 5.70 – 5.45 (m, 2H), 4.25 (p, *J* = 6.1 Hz, 1H), 3.79 (dd, *J* = 11.8, 5.9 Hz, 1H), 2.05 – 2.02 (m, 2H), 1.61 (s, 2H), 1.49 – 1.40 (m, 4H), 1.24 (d, *J* = 6.3 Hz, 3H), 1.18 (d, *J* = 6.2 Hz, 3H).

Fragment A':



Fragment A' was synthesized from compound **5.4** as a pale yellow oil by following similar procedure for the synthesis of fragment A.

Methyl 2,4-dimethoxy-6-((*E*)-3-((2*R*,6*R*)-6-methyltetrahydro-2H-pyran-2-yl)allyl)benzoate (**6.1a**) and methyl 2,4-dimethoxy-6-((*E*)-3-((2*S*,6*R*)-6-methyltetrahydro-2H-pyran-2-yl)allyl)benzoate (**6.1b**):



The compound **6.1a** (0.55 g) and **6.1b** (0.52 mg) was synthesized with an overall yield of 53% from fragment A' and fragment B as a yellowish oil by following similar procedure for the synthesis of compound **4.1a** and **4.1b**.

Chapter 1 (Section A): Synthesis of Entire Stereoisomeric Set of Antimalarial Natural Product Cladosporin, their Biological Evaluation and Co-crystalization

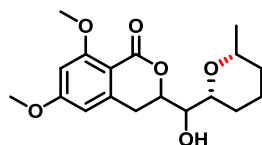
Compound 6.1a:

$^1\text{H NMR}$ (200 MHz, CDCl_3): δ 6.33 (s, 2H), 5.80 – 5.66 (m, 1H), 5.53 (dd, $J = 6.1$, 15.5 Hz, 1H), 3.85 (s, 3H), 3.79 (s, 7H), 3.51 - 3.42 (m, 1H), 3.32 (d, $J = 6.3$ Hz, 2H), 1.82 – 1.76 (m, 1H), 1.61 - 1.25 (m, 5H), 1.17 (d, $J = 6.2$ Hz, 3H).

Compound 6.1b:

$^1\text{H NMR}$ (200 MHz, CDCl_3) δ 6.33 (s, 1H), 5.70 – 5.65 (m, 2H), 4.33 (q, $J = 3.7$ Hz, 1H), 3.86 (s, 4H), 3.79 (s, 3H), 3.35 (d, $J = 4.3$ Hz, 2H), 2.41 (dt, $J = 11.3, 7.2$ Hz, 1H), 1.68 – 1.54 (m, 5H), 1.15 (d, $J = 6.4$ Hz, 3H).

3-(hydroxy((2*R*,6*R*)-6-methyltetrahydro-2H-pyran-2-yl)methyl)-6,8-dimethoxyisochroman-1-one (6.2a):

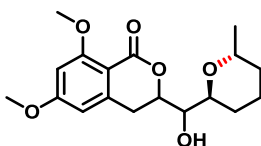


Non-seperable diastereomeric mixture (dr 3:2 as per NMR)

The compound **6.2a** (0.389 g, 50%) was synthesized from compound **6.1a** as a foamy solid by following similar procedure for the synthesis of compound **4.2a**.

$^1\text{H NMR}$ (400 MHz, CDCl_3): δ 6.39 (s.; 1H), 6.33 (s.; 1H), 4.76 – 4.43 (m, 1H), 3.91 (d, $J = 5.5$ Hz, 3H), 3.85 (s, 3H), 3.74 – 3.70 (m, 1H), 3.58 – 3.24 (m, 3H), 2.75 - 2.63 (m, 1H), 2.11 – 1.94 (m, 1H), 1.85 – 1.78 (m, 2H), 1.61 - 1.48 (m, 2H), 1.40 – 1.31 (m, 1H), 1.17 – 1.08 (m, 3H).

3-(hydroxy((2*S*,6*R*)-6-methyltetrahydro-2H-pyran-2-yl)methyl)-6,8-dimethoxyisochroman-1-one (6.2b):



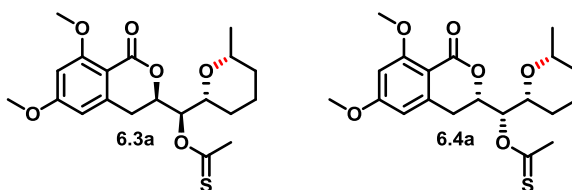
Non-seperable diastereomeric mixture (dr 1:1 as per NMR)

Chapter 1 (Section A): Synthesis of Entire Stereoisomeric Set of Anti-malarial Natural Product Cladosporin, their Biological Evaluation and Co-crystalization

Compound **6.2b** (0.397 g, 57%) was synthesized from compound **6.1b** as a yellowish oil by following similar procedure for the synthesis of compound **4.2b**.

$^1\text{H NMR}$ (400 MHz, CDCl_3): δ 6.38 (s, 1H), 6.32 (s, 1H), 4.68 – 4.39 (m, 1H), 4.12 – 3.97 (m, 1H), 3.89 (d, $J = 3.9$ Hz, 4H), 3.84 (s, 3H), 3.68 – 3.54 (m, 1H), 3.34 - 3.20 (m, 1H), 2.74 - 2.64 (m, 1H), 2.32 (br. s, 1H), 1.86 - 1.82 (m, 1H), 1.72 – 1.62 (m, 3H), 1.55 - 1.50 (m, 1H), 1.34 - 1.31 (m, 1H), 1.24 – 1.15 (m, 3H).

O-((S)-((S)-6,8-dimethoxy-1-oxisochroman-3-yl)((2R,6R)-6-methyltetrahydro-2H-pyran-2-yl)methyl) S-methyl carbonodithioate (6.3a) and O-((R)-((R)-6,8-dimethoxy-1-oxisochroman-3-yl)((2R,6R)-6-methyltetrahydro-2H-pyran-2-yl)methyl) S-methyl carbonodithioate (6.4a):



The compound **6.3a** (0.187 g) and **6.4a** (0.18 g) was synthesized with a yield of 73% from compound **6.2a** as foamy solids by following similar procedure for the synthesis of compound **4.3a** and **4.4a**.

Compound 6.3a:

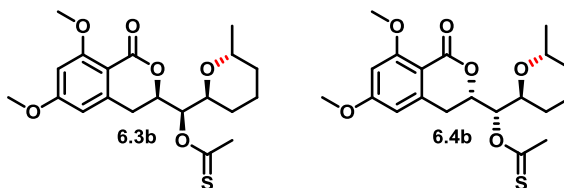
$^1\text{H NMR}$ (400 MHz, CDCl_3): δ 6.38 (s, 1H), 6.28 (s, 1H), 5.96 (d, $J = 9.2$ Hz, 1H), 4.94 (d, $J = 11.6$ Hz, 1H), 4.08 (t, $J = 10.1$ Hz, 1H), 3.91 (s, 3H), 3.83 (s, 3H), 3.58 – 3.45 (m, 1H), 3.01 - 2.94 (m, 1H), 2.76 - 2.72 (m, 1H), 2.56 (s, 3H), 1.82 (d, $J = 12.8$ Hz, 1H), 1.67 - 1.40 (m, 4H), 1.19 - 1.16 (m, 1H), 1.11 (d, $J = 5.5$ Hz, 3H).

Compound 6.4a:

$^1\text{H NMR}$ (400 MHz, CDCl_3) δ 6.39 (s, 1H), 6.31 (s, 1H), 6.00 (t, $J = 4.6$ Hz, 1H), 4.76 (dt, $J = 11.3, 3.0$ Hz, 1H), 3.90 (s, 4H), 3.85 (s, 3H), 3.44 (dd, $J = 10.4, 5.7$ Hz, 1H), 3.13 (dd, $J = 16.1, 11.5$ Hz, 1H), 2.86 (dd, $J = 16.2, 2.4$ Hz, 1H), 2.57 (s, 3H), 1.86 – 1.82 (m, 1H), 1.66 – 1.35 (m, 4H), 1.21 – 1.17 (m, 1H), 1.12 (d, $J = 6.1$ Hz, 3H).

Chapter 1 (Section A): Synthesis of Entire Stereoisomeric Set of Antimalarial Natural Product Cladosporin, their Biological Evaluation and Co-crystallization

O-((*R*)-((*R*)-6,8-dimethoxy-1-oxisochroman-3-yl)((*2S,6R*)-6-methyltetrahydro-2H-pyran-2-yl)methyl) S-methyl carbonodithioate (**6.3b**) and O-((*S*)-((*S*)-6,8-dimethoxy-1-oxisochroman-3-yl)((*2S,6R*)-6-methyltetrahydro-2H-pyran-2-yl)methyl) S-methyl carbonodithioate (**6.4b**):



The compound **6.3b** (0.215 g) and **6.4b** (0.135 g) was synthesized from compound **6.2b** with 70% yield as foamy solids by following similar procedure for the synthesis of **4.3b** and **4.4b**.

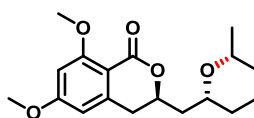
Compound **6.3b**:

$^1\text{H NMR}$ (500 MHz, CDCl_3): δ 6.39 (s, 1H), 6.31 (s, 1H), 6.21 (dd, $J = 3.4, 6.9$ Hz, 1H), 4.68 (td, $J = 2.8, 11.6$ Hz, 1H), 4.36 - 4.32 (m, 1H), 4.05 - 4.04 (m, 1H), 3.91 (s, 3H), 3.84 (s, 3H), 3.09 (dd, $J = 11.8, 16.0$ Hz, 1H), 2.87 (dd, $J = 2.3, 16.0$ Hz, 1H), 2.57 (s, 3H), 1.74 - 1.66 (m, 3H), 1.60 - 1.55 (m, 2H), 1.35 - 1.30 (m, 1H), 1.17 (d, $J = 6.5$ Hz, 3H).

Compound **6.4b**:

$^1\text{H NMR}$ (400 MHz, CDCl_3): δ 6.38 (s, 1H), 6.29 (s, 1H), 6.19 (d, $J = 9.8$ Hz, 1H), 4.86 (d, $J = 11.6$ Hz, 1H), 4.44 - 4.39 (m, 1H), 3.91 (s, 4H), 3.83 (s, 3H), 2.99 (dd, $J = 12.5, 15.6$ Hz, 1H), 2.74 (dd, $J = 2.4, 15.9$ Hz, 1H), 2.56 (s, 3H), 1.68 - 1.65 (m, 4H), 1.40 - 1.30 (m, 2H), 1.20 (d, $J = 6.7$ Hz, 3H).

(*R*)-6,8-dimethoxy-3-(((*2R,6R*)-6-methyltetrahydro-2H-pyran-2-yl)methyl)isochroman-1-one (**6.5a**):

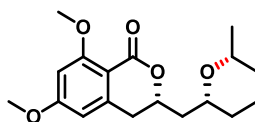


Chapter 1 (Section A): Synthesis of Entire Stereoisomeric Set of Anti-malarial Natural Product Cladosporin, their Biological Evaluation and Co-crystalization

The compound **6.5a** (0.087 g, 64%) was synthesized from compound **6.3a** as a yellowish oil by following similar procedure for the synthesis of compound **4.5a**.

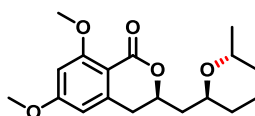
¹H NMR (400 MHz, CDCl₃): δ 6.39 (s, 1H), 6.28 (s, 1H), 4.69 - 4.64 (m, 1H), 3.91 (s, 3H), 3.84 (s, 3H), 3.70 (t, *J* = 10.7 Hz, 1H), 3.45 - 3.41 (m, 1H), 2.90 - 2.75 (m, 2H), 1.89 - 1.77 (m, 2H), 1.72 - 1.66 (m, 2H), 1.57 - 1.47 (m, 3H), 1.19 - 1.16 (m, 1H), 1.10 (d, *J* = 6.1 Hz, 3H).

(S)-6,8-dimethoxy-3-(((2R,6R)-6-methyltetrahydro-2H-pyran-2-yl)methyl)isochroman-1-one (6.6a):



The compound **6.6a** (0.079 g, 60%) was synthesized from compound **6.4a** as a foamy solid by following similar procedure for the synthesis of **4.6a**.

(R)-6,8-dimethoxy-3-(((2S,6R)-6-methyltetrahydro-2H-pyran-2-yl)methyl)isochroman-1-one (6.5b):

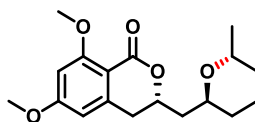


The compound **6.5b** (0.103 g, 57%) was synthesized from compound **6.3b** as a semi solid by following similar procedure for the synthesis of compound **4.5b**.

¹H NMR (400 MHz, CDCl₃): δ 6.39 (s, 1H), 6.31 (s, 1H), 4.55 - 4.52 (m, 1H), 4.04 - 4.03 (m, 1H), 3.91 (s, 3H), 3.85 (s, 3H), 2.96 - 2.81 (m, 2H), 2.41 - 2.34 (m, 1H), 1.72 - 1.66 (m, 4H), 1.36 - 1.28 (m, 3H), 1.15 (d, *J* = 6.1 Hz, 3H).

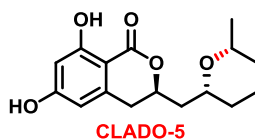
Chapter 1 (Section A): Synthesis of Entire Stereoisomeric Set of Antimalarial Natural Product Cladosporin, their Biological Evaluation and Co-crystallization

(*S*)-6,8-dimethoxy-3-(((2*S*,6*R*)-6-methyltetrahydro-2H-pyran-2-yl)methyl)isochroman-1-one (**6.6b**):



The compound **6.6b** (0.087 g, 60%) was synthesized from compound **6.4b** as a white solid by following similar procedure for the synthesis of **4.6b**.

(*R*)-6,8-dihydroxy-3-(((2*R*,6*R*)-6-methyltetrahydro-2H-pyran-2-yl)methyl)isochroman-1-one (**CLADO-5**):



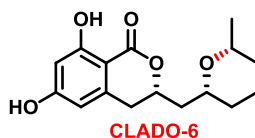
CLADO-5 (0.034 g, 51%) was synthesized from compound **6.5a** as a white solid by following similar procedure for the synthesis of **CLADO-1**.

Melting point: 155-158 °C;

$[\alpha]^{25D} = +5.6$ ($c = 0.4$, CHCl_3);

$^1\text{H NMR}$ (400 MHz, CD_3OD): d 6.21 (s, 1H), 6.20 (s, 1H), 4.74 (t, $J = 9.8$ Hz, 1H), 3.69 - 3.64 (m, 1H), 3.49 - 3.46 (m, 1H), 2.93 - 2.81 (m, 2H), 1.91 - 1.73 (m, 3H), 1.60 (d, $J = 10.4$ Hz, 3H), 1.29 - 1.18 (m, 2H), 1.14 (d, $J = 6.1$ Hz, 3H).

(*S*)-6,8-dihydroxy-3-(((2*R*,6*R*)-6-methyltetrahydro-2H-pyran-2-yl)methyl)isochroman-1-one (**CLADO-6**):



Chapter 1 (Section A): Synthesis of Entire Stereoisomeric Set of Antimalarial Natural Product Cladosporin, their Biological Evaluation and Co-crystalization

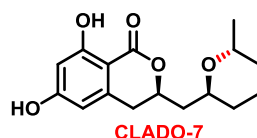
CLADO-6 (0.017 g, 53%) was synthesized from compound **6.6aa** as a white solid by following similar procedure for the synthesis of **CLADO-2**.

Melting point: 195-197 °C;

$[\alpha]^{25D} = -45.23$ ($c = 0.5$, EtOH);

$^1\text{H NMR}$ (400 MHz, CD_3OD): δ 6.23 (s, 1H), 6.20 (s, 1H), 4.74 - 4.67 (m, 1H), 3.63 - 3.58 (m, 1H), 3.52 - 3.46 (m, 1H), 2.98 - 2.86 (m, 2H), 2.07 - 2.00 (m, 1H), 1.84 - 1.77 (m, 2H), 1.67 - 1.53 (m, 3H), 1.28 - 1.18 (m, 2H), 1.13 (d, $J = 6.1$ Hz, 3H).

(R)-6,8-dihydroxy-3-(((2S,6R)-6-methyltetrahydro-2H-pyran-2-yl)methyl)isochroman-1-one (CLADO-7):



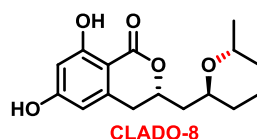
CLADO-7 (0.021 g, 55%) was synthesized from compound **6.5b** as a white solid by following similar procedure for the synthesis of **CLADO-3**.

Melting point: 135-139 °C;

$[\alpha]^{25D} = +104.19$ ($c = 0.2$, CHCl_3);

$^1\text{H NMR}$ (400 MHz, CDCl_3): δ 11.11 (s, 1H), 6.31 (s, 1H), 6.17 (s, 1H), 4.68 - 4.65 (m, 1H), 4.09 - 4.08 (m, 1H), 3.95 (s, 1H), 2.92 - 2.81 (m, 2H), 2.46 - 2.35 (m, 1H), 1.76 - 1.69 (m, 5H), 1.41 - 1.30 (m, 2H), 1.19 (d, $J = 6.1$ Hz, 3H).

(S)-6,8-dihydroxy-3-(((2S,6R)-6-methyltetrahydro-2H-pyran-2-yl)methyl)isochroman-1-one (CLADO-8):



Chapter 1 (Section A): Synthesis of Entire Stereoisomeric Set of Antimalarial Natural Product Cladosporin, their Biological Evaluation and Co-crystalization

CLADO-8 (0.023 g, 43%) was synthesized from compound **6.6b** as a white solid by following similar procedure for the synthesis of **CLADO-4**.

Melting point: 174-177 °C;

$[\alpha]^{25D} = +16.57$ ($c = 0.5$, EtOH);

$^1\text{H NMR}$ (400 MHz, CDCl_3): δ 11.06 (s, 1H), 6.29 (s, 1H), 6.15 (s, 1H), 4.69 (t, $J = 9.8$ Hz, 1H), 4.12 (s, 1H), 4.01 (s, 1H), 2.88 - 2.75 (m, 2H), 1.99 - 1.94 (m, 1H), 1.87 - 1.81 (m, 1H), 1.69 - 1.63 (m, 4H), 1.36 - 1.34 (m, 2H), 1.23 (d, $J = 6.7$ Hz, 3H).

Single crystal X- ray diffraction:

X-ray intensity data measurements of compounds CLADO-5, CLADO-6, CLADO-7 and CLADO-8 were carried out on a Bruker D8 VENTURE Kappa Duo PHOTON II CPAD diffractometer equipped with Incoatech multilayer mirrors optics. The intensity measurements were carried out at 100(2) K temperature with Mo micro-focus sealed tube diffraction source ($\text{MoK}\alpha = 0.71073 \text{ \AA}$) on compounds CLADO-6, CLADO-7 and CLADO-8 whereas for compound CLADO-5 the Cu micro-focus sealed tube diffraction source ($\text{CuK}\alpha = 1.54178 \text{ \AA}$) was used. The X-ray generator was operated at 50 kV and 1.1 mA (for Cu source) and 50 kV and 1.4 mA (for Mo source). A preliminary set of cell constants and an orientation matrix were calculated from three sets of 36 frames for compounds CLADO-6, CLADO-7 and CLADO-8 whereas two sets of 40 frames for compound CLADO-5. Data were collected with ω scan width of 0.5° at different settings of φ and 2θ with a frame time of 10-20 secs (depending on the diffraction power of the crystal) keeping the sample-to-detector distance fixed at 5.00 cm. The X-ray data collection was monitored by APEX3 program.³² All the data were corrected for Lorentzian, polarization and absorption effects using SAINT and SADABS programs.³² SHELX-97 was used for structure solution and full matrix least-squares refinement on F^2 .³³ All the hydrogen atoms were placed in a geometrically idealized positions and constrained to ride on its parent atoms An *ORTEP* III³⁴ view of compounds was

Chapter 1 (Section A): Synthesis of Entire Stereoisomeric Set of Antimalarial Natural Product Cladosporin, their Biological Evaluation and Co-crystalization

drawn with 50% probability displacement ellipsoids and H atoms are shown as small spheres of arbitrary radii.

Crystal data of CLADO-5:

$C_{16}H_{20}O_5$, $M = 292.32$, colorless needle, $0.24 \times 0.08 \times 0.05 \text{ mm}^3$, orthorhombic, chiral space group $P2_12_12_1$, $a = 7.5165(16) \text{ \AA}$, $b = 8.0959(17) \text{ \AA}$, $c = 24.661(9) \text{ \AA}$, $V = 1500.7(7) \text{ \AA}^3$, $Z = 4$, $T = 100(2) \text{ K}$, $2\theta_{\text{max}} = 144^\circ$, $D_{\text{calc}} (\text{g cm}^{-3}) = 1.294$, $F(000) = 624$, $\mu (\text{mm}^{-1}) = 0.792$, 25100 reflections collected, 2929 unique reflections ($R_{\text{int}} = 0.0342$, $R_{\text{sig}} = 0.0215$), 2901 observed ($I > 2\sigma(I)$) reflections, multi-scan absorption correction, $T_{\text{min}} = 0.833$, $T_{\text{max}} = 0.961$, 193 refined parameters, Good of Fit = $S = 1.110$, $R1 = 0.0307$, $wR2 = 0.0788$ (all data $R = 0.0310$, $wR2 = 0.0785$), maximum and minimum residual electron densities; $\Delta\rho_{\text{max}} = 0.230$, $\Delta\rho_{\text{min}} = -0.160$ (e \AA^{-3}). The absolute configuration for compound CLADO-5 was established by the structure determination of a compound containing a chiral reference molecule of known absolute configuration and confirmed by anomalous dispersion effects in diffraction measurements on the crystal (Flack parameter, $0.05(4)$). The single crystal X-ray diffraction data analysis clearly established that our synthesized compound has *R*, *R*, and *R*, configurations at C8, C11, and C15 positions respectively for compound CLADO-5.

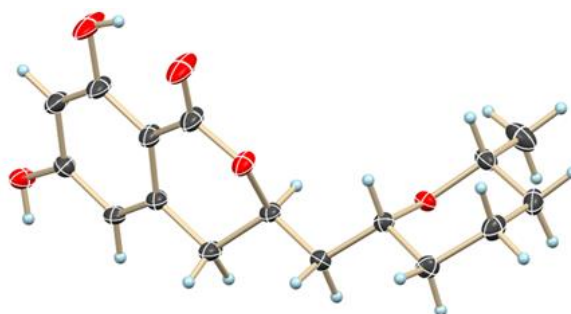


Figure 1: ORTEP diagram of CLADO-5.

Chapter 1 (Section A): Synthesis of Entire Stereoisomeric Set of Antimalarial Natural Product Cladosporin, their Biological Evaluation and Co-crystalization

Crystal data of CLADO-6:

$C_{16}H_{20}O_5$, $M = 292.32$, colorless needle, $0.27 \times 0.09 \times 0.07 \text{ mm}^3$, monoclinic, chiral space group $P2_1$, $a = 7.7904(6) \text{ \AA}$, $b = 11.4929(11) \text{ \AA}$, $c = 16.2869(15) \text{ \AA}$, $\beta = 103.739(3)$, $V = 1416.5(2) \text{ \AA}^3$, $Z = 4$, $T = 100(2) \text{ K}$, $2\theta_{\max} = 50^\circ$, $D_{\text{calc}} (\text{g cm}^{-3}) = 1.371$, $F(000) = 624$, $\mu (\text{mm}^{-1}) = 0.101$, 14984 reflections collected, 4894 unique reflections ($R_{\text{int}} = 0.0519$, $R_{\text{sig}} = 0.0549$), 4416 observed ($I > 2\sigma(I)$) reflections, multi-scan absorption correction, $T_{\min} = 0.973$, $T_{\max} = 0.993$, 386 refined parameters, Good of Fit = $S = 1.049$, $R1 = 0.0389$, $wR2 = 0.0784$ (all data $R = 0.0457$, $wR2 = 0.0808$), maximum and minimum residual electron densities; $\Delta\rho_{\max} = 0.235$, $\Delta\rho_{\min} = -0.178 (\text{e \AA}^{-3})$.

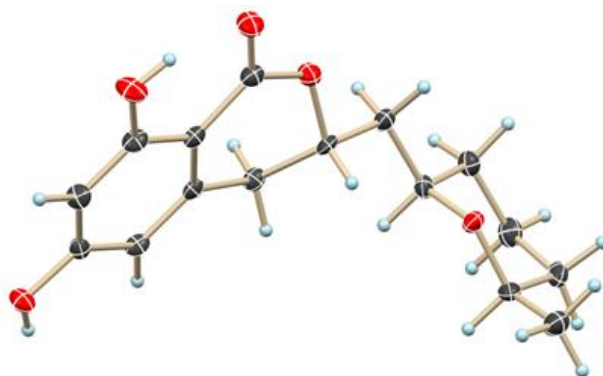


Figure 2: ORTEP diagram of CLADO-6.

Crystal data of CLADO-7:

$C_{16}H_{20}O_5$, $M = 292.32$, colorless needle, $0.15 \times 0.07 \times 0.03 \text{ mm}^3$, orthorhombic, chiral space group $P2_12_12_1$, $a = 6.9288(8) \text{ \AA}$, $b = 7.9172(9) \text{ \AA}$, $c = 52.844(6) \text{ \AA}$, $V = 2898.9(6) \text{ \AA}^3$, $Z = 4$, $T = 100(2) \text{ K}$, $2\theta_{\max} = 52.8^\circ$, $D_{\text{calc}} (\text{g cm}^{-3}) = 1.340$, $F(000) = 1248$, $\mu (\text{mm}^{-1}) = 0.099$, 39126 reflections collected, 5904 unique reflections ($R_{\text{int}} = 0.1157$, $R_{\text{sig}} = 0.1067$), 4006 observed ($I > 2\sigma(I)$) reflections, multi-scan absorption correction, $T_{\min} = 0.985$, $T_{\max} = 0.997$, 431 refined parameters, no of restraints = 108, Good of Fit = $S = 1.163$, $R1 = 0.1018$, $wR2 = 0.1704$ (all data $R = 0.1524$, $wR2$

Chapter 1 (Section A): Synthesis of Entire Stereoisomeric Set of Anti-malarial Natural Product Cladosporin, their Biological Evaluation and Co-crystalization

= 0.1864), maximum and minimum residual electron densities; $\Delta\rho_{\max} = 0.331$, $\Delta\rho_{\min} = -0.342$ ($e \text{ \AA}^{-3}$).

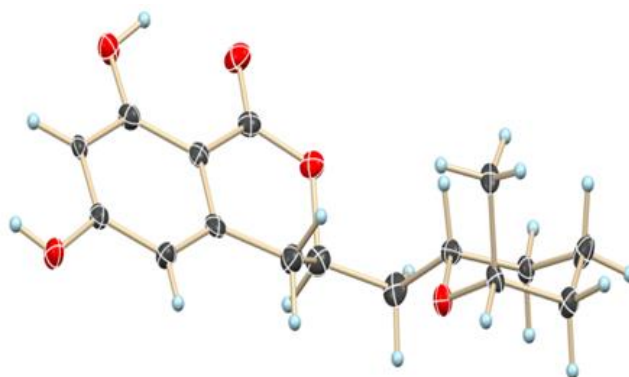


Figure 3: ORTEP diagram of CLADO-7.

Crystal data of CLADO-8:

$C_{16}H_{20}O_5$, $M = 292.32$, colorless plate, $0.33 \times 0.11 \times 0.05 \text{ mm}^3$, tetragonal, chiral space group $P4_32_12$, $a = 8.0784(3) \text{ \AA}$, $c = 45.237(2) \text{ \AA}$, $V = 2952.2(3) \text{ \AA}^3$, $Z = 8$, $T = 100(2) \text{ K}$, $2\theta_{\max} = 56^\circ$, $D_{\text{calc}} (\text{g cm}^{-3}) = 1.315$, $F(000) = 1248$, $\mu (\text{mm}^{-1}) = 0.097$, 58733 reflections collected, 3539 unique reflections ($R_{\text{int}} = 0.0234$, $R_{\text{sig}} = 0.0087$), 3519 observed ($I > 2\sigma(I)$) reflections, multi-scan absorption correction, $T_{\min} = 0.969$, $T_{\max} = 0.995$, 193 refined parameters, Good of Fit = $S = 1.084$, $R1 = 0.0301$, $wR2 = 0.0803$ (all data $R = 0.0303$, $wR2 = 0.0805$), maximum and minimum residual electron densities; $\Delta\rho_{\max} = 0.289$, $\Delta\rho_{\min} = -0.136$ ($e \text{ \AA}^{-3}$). The absolute configuration was established by the structure determination of a compound containing a chiral reference molecule of known absolute configuration and confirmed by anomalous dispersion effects in diffraction measurements on the crystal (Flack parameter, 0.09(10)). The single crystal X-ray diffraction data analysis clearly established that our synthesized compound has *S*, *S*, and *R*, configurations at C8, C11, and C15 positions respectively for compound CLADO-8.

Chapter 1 (Section A): Synthesis of Entire Stereoisomeric Set of Anti-malarial Natural Product Cladosporin, their Biological Evaluation and Co-crystallization

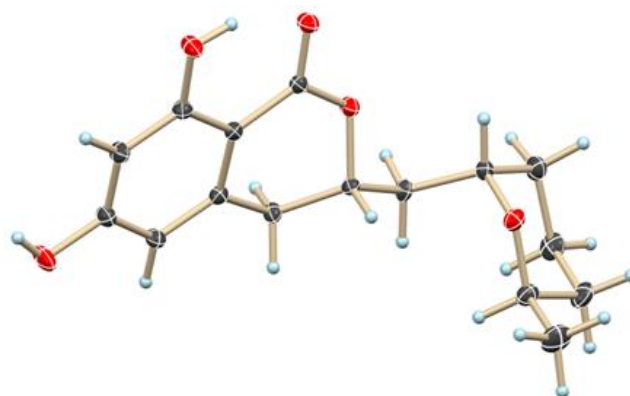


Figure 4: ORTEP diagram of CLADO-8.

Biological assay (in collaboration with Dr. Amit Sharma, ICGEB, New Delhi and Dr. Dhanasekaran Shanmugam, CSIR-NCL, Pune)

Detailed experimental procedure for protein expressions and purifications, thermal shift assays, aminoacylation assays, *P. falciparum* culture and co-crystallization could be found at *J. Med. Chem.* **2018**, *61*, 5664-5678.

Data collection and structure determination of KRS-cladolog complexes.

X-ray diffraction data were collected using multiple beam-lines at Diamond Light Source (DLS) and Synchrotron SOLEIL at 100 K with 0.1° increments per image, for a total of 3600 images. The data were auto-processed using X-ray Detector Software (XDS)/XSCALE,³⁵ diffraction integration for advanced light sources.³⁶ The structures were solved by molecular replacement in PHASER using *Pf*KRS-apo structure (PDB code: 4TWA) as the template. All models were initially refined using REFMAC5³⁷ and completed with *phenix.refine* in PHENIX.³⁸ Cladologs and water molecules were added into the electron density maps using COOT.³⁹ X-ray refinement restraint parameters were generated for cladologs using COOT34 and Sketcher program in CCP4 Suite.⁴⁰ The quality of the final models and bound ligands was verified using composite simulated annealing omit (SA-omit) maps. The occupancies of bound ligands and alternate conformations of protein residues were refined and confirmed using omit maps. The final model quality was analyzed using MolProbity.⁴¹ Statistics for data collection and structure refinements are given in Table 3. All structural

Chapter 1 (Section A): Synthesis of Entire Stereoisomeric Set of Antimalarial Natural Product Cladosporin, their Biological Evaluation and Co-crystalization

superposition and preparation of figures was done using UCSF Chimera⁴² and PyMOL (<http://www.pymol.org>).

1.1.5. References

1. Ratnayake, A. S.; Davis, R. A.; Harper, M. K.; Veltri, C. A.; Andjelic, C. D.; Barrows, L. R.; Ireland, C. M. Theopapuamide: a Cyclic Depsipeptide from a Papua New Guinea Lithistid Sponge *Theonella swinhoei*. *J. Nat. Prod.*; **2005**, *68*, 104–107.
2. Lee, M. L.; Schneider, G. Scaffold architecture and pharmacophoric properties of natural products and trade drugs: application in the design of natural product-based combinatorial libraries. *J. Comb. Chem.* **2001**, *3*, 284–289.
3. Henkel, T.; Brunne, R. M.; Müller, H.; Reichel, F. Statistical investigation into the structural complementarity of natural products and synthetic compounds. *Angew. Chem. Int. Ed.* **1999**, *38*, 643–647.
4. Wizemann, T.; Robinson, S.; Giffin, R. Breakthrough Business Models: Drug Development for Rare and Neglected Diseases and Individualized Therapies: Workshop Summary. National Academies Press (US).
5. <https://www.who.int/news-room/fact-sheets/detail/malaria>
6. Slater, A. F. Chloroquine: mechanism of drug action and resistance in *Plasmodium falciparum*. *Pharmacol. Ther.* **1993**, *57*, 203–235.
7. Jiang, S.; Zeng, Q.; Gettayacamin, M.; Tungtaeng, A.; Wannaying, S.; Lim, A.; Hansukjariya, P.; O. Okunji, C. O.; Zhu, S.; Fang, D. Antimalarial Activities and Therapeutic Properties of Febrifugine Analogs. *Antimicrob Agents Chemother.* **2005**, *49*, 1169–1176.
8. Krafts, K.; Hempelmann, E.; Skorska-Stania, A. From methylene blue to chloroquine: a brief review of the development of an antimalarial therapy. *Parasitol. Res.* **2012**, *111*, 1-6.
9. <https://www.mmv.org/malaria-medicines/history-antimalarials>

Chapter 1 (Section A): Synthesis of Entire Stereoisomeric Set of Anti-malarial Natural Product Cladosporin, their Biological Evaluation and Co-crystalization

10. Gaillard, T.; Madamet, M.; Tsombeng, F. F.; Dormoi, J.; Pradines, B. Antibiotics in malaria therapy: which antibiotics except tetracyclines and macrolides may be used against malaria? *Malar. J.* **2016**, *15*, 556-566.
11. https://www.who.int/malaria/media/artemisinin_resistance_qa/en/
12. Springer, J. P.; Cutler, H. G.; Crumley, F. G.; Cox, R. H.; Davis, E. E.; Thean, J. E. Plant growth regulatory effects and stereochemistry of cladosporin. *J. Agric. Food Chem.* **1981**, *29*, 853–855.
13. Scott, P. M.; Van Walbeek, W.; Maclean, W. M. Cladosporin, a new antifungal metabolite from *Cladosporium cladosporioides*. *J. Antibiot.* **1971**, *24*, 747–755.
14. Hoepfner, D.; McNamara, C. W.; Lim, C. S.; Studer, C.; Riedl, R.; Aust, T.; McCormack, S. L.; Plouffe, D. M.; Meister, S.; Schuierer, S.; Plikat, U.; Hartmann, N.; Staedtler, F.; Cotesta, S.; Schmitt, E. K.; Petersen, F.; Supek, F.; Glynn, R. J.; Tallarico, J. A.; Porter, J. A.; Fishman, M. C.; Bodenreider, C.; Diagana, T. T.; Movva, N. R.; Winzeler, E. A. Selective and specific inhibition of the *Plasmodium falciparum* lysyl-tRNA synthetase by the fungal secondary metabolite cladosporin. *Cell Host Microbe* **2012**, *11*, 654–663.
15. Khan, S.; Garg, A.; Camacho, N.; Van Rooyen, J.; Kumar Pole, A.; Belrhali, H.; Ribas de Pouplana, L.; Sharma, V.; Sharma, A. Structural analysis of malaria-parasite lysyl-tRNA synthetase provides a platform for drug development. *Acta Crystallogr.; Sect. D: Biol. Crystallogr.* **2013**, *69*, 785–795.
16. Khan, S.; Sharma, A.; Belrhali, H.; Yogavel, M.; Sharma, A. Structural basis of malaria parasite lysyl-tRNA synthetase inhibition by cladosporin. *J. Struct. Funct. Genomics* **2014**, *15*, 63–71.
17. Fang, P.; Han, H.; Wang, J.; Chen, K.; Chen, X.; Guo, M. Structural basis for specific inhibition of tRNA synthetase by an ATP competitive inhibitor. *Chem. Biol.* **2015**, *22*, 734–744.
18. Sharma, A.; Sharma, M.; Yogavel, M.; Sharma, A. Protein translation enzyme lysyl-trna synthetase presents a new target for drug development against causative agents of *loiasis* and *schistosomiasis*. *PLoS Neglected Trop. Dis.* **2016**, *10*, 1–19.

Chapter 1 (Section A): Synthesis of Entire Stereoisomeric Set of Antimalarial Natural Product Cladosporin, their Biological Evaluation and Co-crystalization

19. Zheng, H.; Zhao, C.; Fang, B.; Jing, P.; Yang, J.; Xie, X.; She, X. Asymmetric total synthesis of cladosporin and isocladosporin. *J. Org. Chem.* **2012**, *77*, 5656–5663.
20. Mohapatra, D. K.; Maity, S.; Rao, T. S.; Yadav, J. S.; Sridhar, B. An efficient formal total synthesis of cladosporin. *Eur. J. Org. Chem.* **2013**, *2013*, 2859–2863.
21. Mohapatra, D.K.; Maity, S.; Banoth, S.; Gonnade, R.G.; Yadav, J.S.; Total synthesis of isocladosporin and 3-*epi*-isocladosporin. *Tetrahedron Letters*, **2016**, *57*, 53–55.
22. Reddy, B. V. S.; Reddy, P. J.; Reddy, C. S. The stereoselective total synthesis of isocladosporin. *Tetrahedron Lett.* **2013**, *54*, 5185–5187.
23. McConathy, J.; Owens, M. J. Stereochemistry in drug action. Primary Care Companion. *J. Clin Psychiatry* **2003**, *5*, 70–73.
24. Brocks, D. R.; Mehvar, R. Stereoselectivity in the pharmacodynamics and pharmacokinetics of the chiral antimalarial drugs. *Clin. Pharmacokinet.* **2003**, *42*, 1359–1382.
25. Nguyen, L. A.; He, H.; Pham-Huy, C. Chiral drugs: an overview. *Int. J. Biomed. Sci.* **2006**, *2*, 85–100.
26. Vargesson, N. Thalidomide-induced limb defects: resolving a 50- year-old puzzle. *BioEssays* **2009**, *31*, 1327–1336.
27. Evans, A. M. Comparative pharmacology of *S*(+)-Ibuprofen and (*RS*)-Ibuprofen. *Clin. Rheumatol.* **2001**, *20*, 9–14.
28. Allu, S. R.; Banne, S.; Jiang, J.; Qi, N.; Guo, J.; He, Y. A Unified Synthetic Approach to Optically Pure Curvularin-Type Metabolites. *J. Org. Chem.* **2019**, *84*, *11*, 7227–7237
29. Chatterjee, A. K.; Choi, T. L.; Sanders, D. P.; Grubbs, R. H. A general model for selectivity in olefin cross metathesis. *J. Am. Chem. Soc.* **2003**, *125*, 11360–11370.
30. Tian, J.; Sang, D. Application of aluminum triiodide in organic synthesis. *ARKIVOC* **2015**, *ark.5550190*, 446–493.

Chapter 1 (Section A): Synthesis of Entire Stereoisomeric Set of Antimalarial Natural Product Cladosporin, their Biological Evaluation and Co-crystalization

31. Lauro, G.; Das, P.; Riccio, R.; Reddy, D. S.; Bifulco, G. *J. Org. Chem.* **2020**, *85*, 3297-3306.
32. Bruker (2016). APEX2, SAINT and SADABS. Bruker AXS Inc.; Madison, Wisconsin, USA.
33. Sheldrick, G. M. A short history of SHELX. *Acta Crystallogr.*; **2007**, *A64*, 112.
34. Barnes, C. L. ORTEP -3 for Window. *J. Appl. Crystallogr.* **1997**, *30*, 568–568.
35. Kabsch, W. *Acta Cryst.* 2010, *D66*, 125–132.
36. Waterman, D.G.; Winter, G.; Gildea, R.J.; Parkhurst, J. M.; Brewster, A. S.; Sauter, N. K.; Evans, G. Diffraction-geometry refinement in the DIALS framework. *G. Acta Crystallogr D Struct Biol.* **2016**, *72*, 558–575.
37. Murshudov, G. N.; Skubak, P.; Lebedev, A. A.; Pannu, N. S.; Steiner, R. A. REFMAC5 for the refinement of macromolecular crystal structures. *Acta Crystallogr. D Biol. Crystallogr.* **2011**, *67*, 355–367.
38. Adams, P. D.; Afonine, P. V.; Bunkoczi, G.; Chen, V. B.; Davis, I. W. PHENIX: a comprehensive Python-based system for macromolecular structure solution. *Acta Crystallogr. D Biol. Crystallogr.* **2010**, *66*, 213–221.
39. Emsley, P.; Lohkamp, B.; Scott, W. G.; Cowtan, K. Features and development of Coot. *Acta Crystallogr. D Biol. Crystallogr.* **2010**, *66*, 486–501.
40. Winn, M. D.; Ballard, C. C.; Cowtan, K. D.; Dodson, E. J.; Emsley, P.; Evans, P. R.; Keegan, R. M.; Krissinel, E. B.; Leslie, A. G. W.; McCoy, A.; McNicholas, S. J.; Murshudov, G. N.; Pannu, N. S.; Potterton, E. A.; Powell, H. R.; Read, R. J.; Vagin, A.; Wilson, K. S. *Acta Crystallogr. D Biol. Crystallogr.* **2011**, *67*, 235.
41. Chen, V. B.; Arendall, W. B.; Headd, J. J.; Keedy, D. A.; Immormino, R. M.; Kapral, G. J.; Murray, L. W.; Richardson, J. S.; Richardson, D. C. *Acta Crystallogr. D Biol. Crystallogr.* **2010**, *66*, 12.
42. Pettersen, E. F.; Goddard, T. D.; Huang, C. C.; Couch, G. S.; Greenblatt, D. M.; Meng, E. C.; Ferrin, T. E. UCSF Chimera—A visualization system for exploratory research and analysis. *J. Comput. Chem.* **2004**, *25*, 1605–1612.

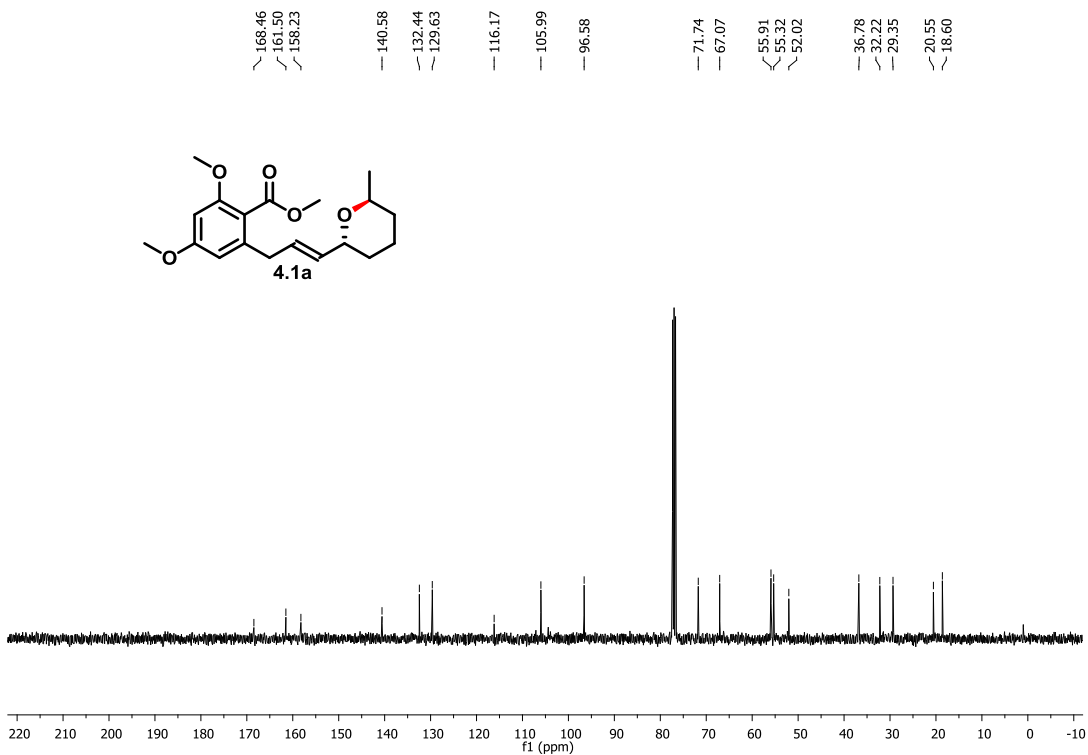
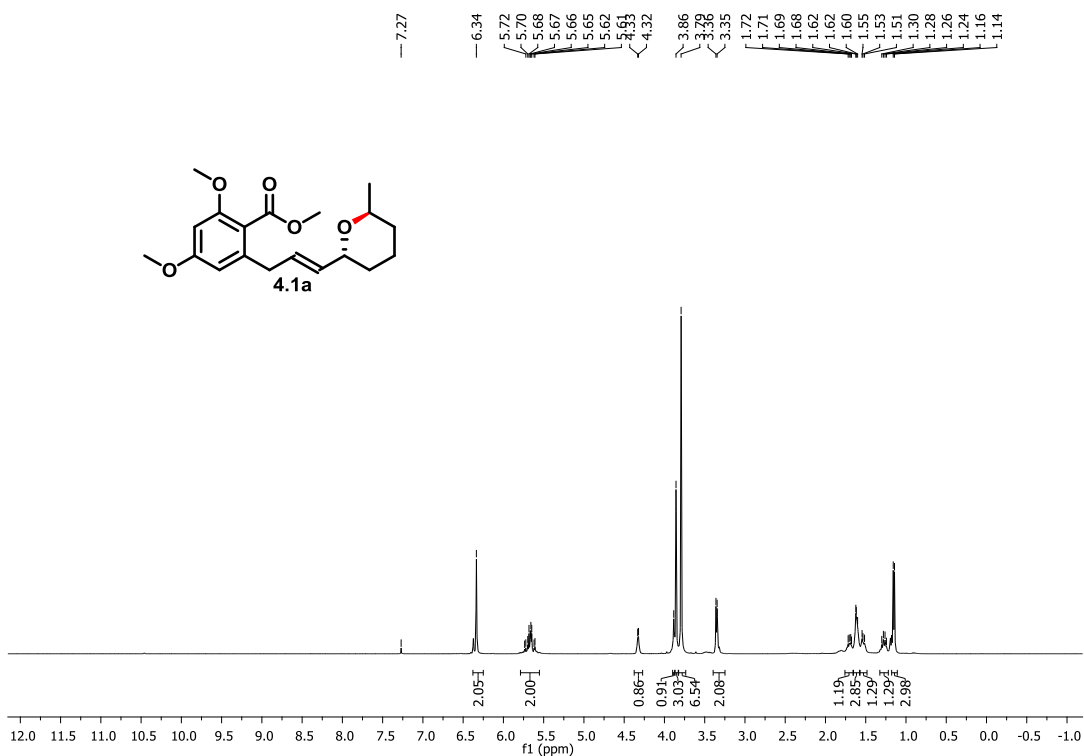
Chapter 1 (Section A): Synthesis of Entire Stereoisomeric Set of Anti-malarial Natural Product Cladosporin, their Biological Evaluation and Co-crystalization



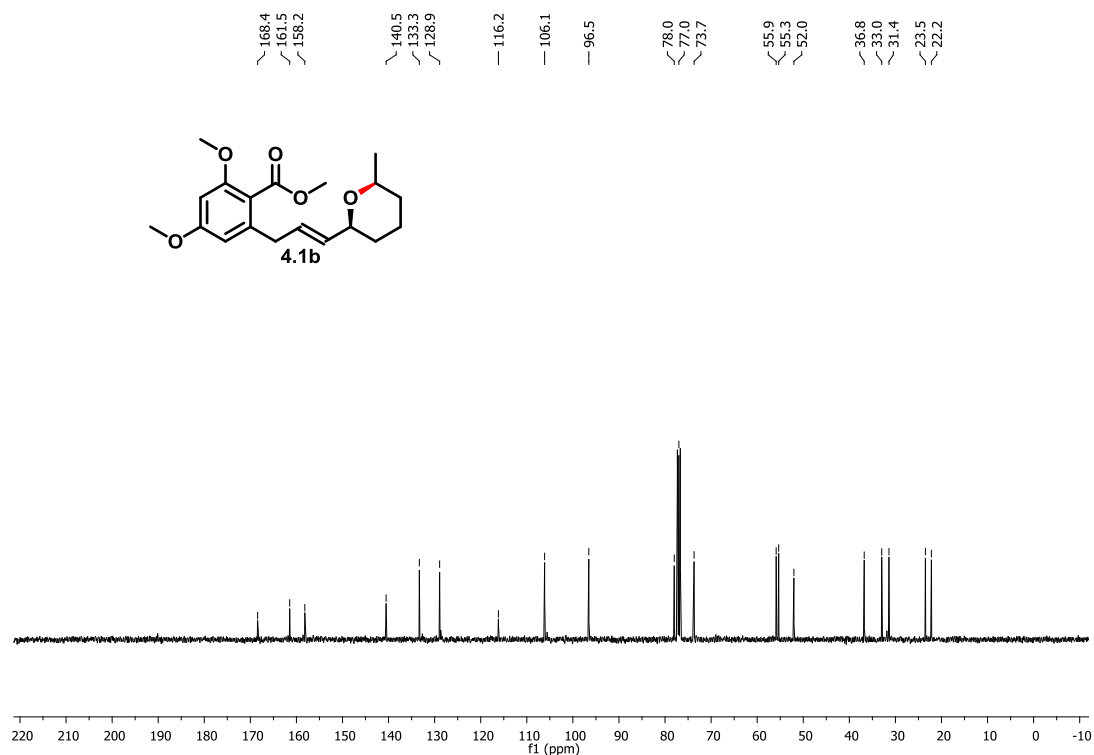
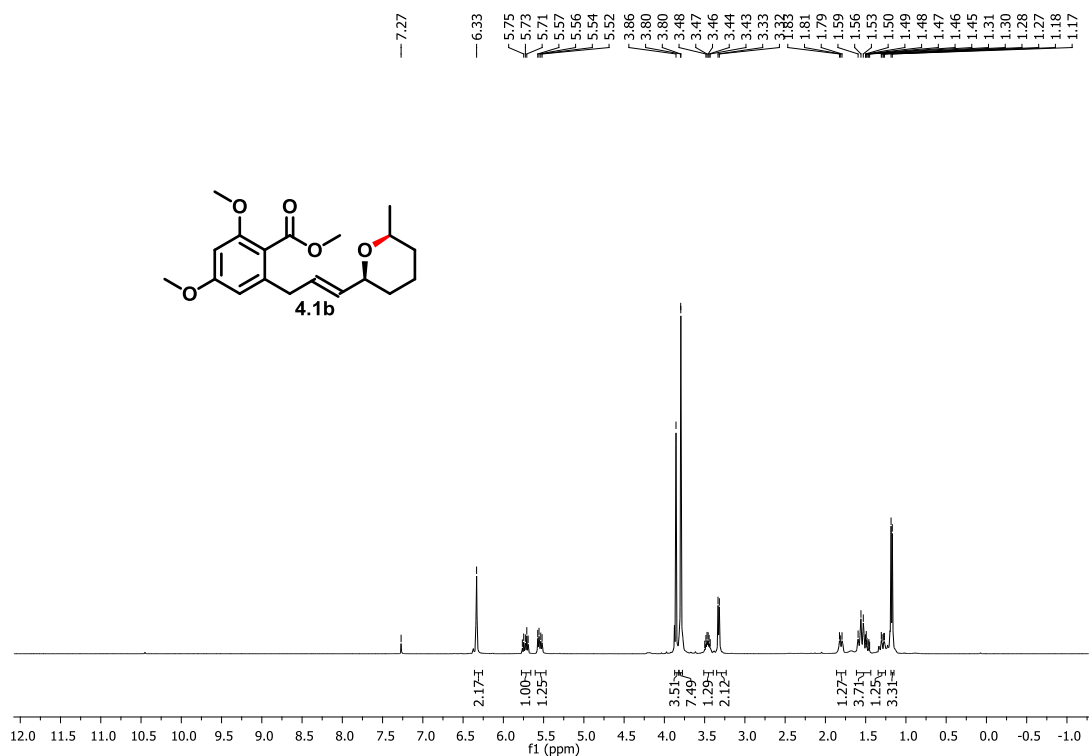
**Copies of
 ^1H and ^{13}C NMR Spectra of Selected
Compounds**



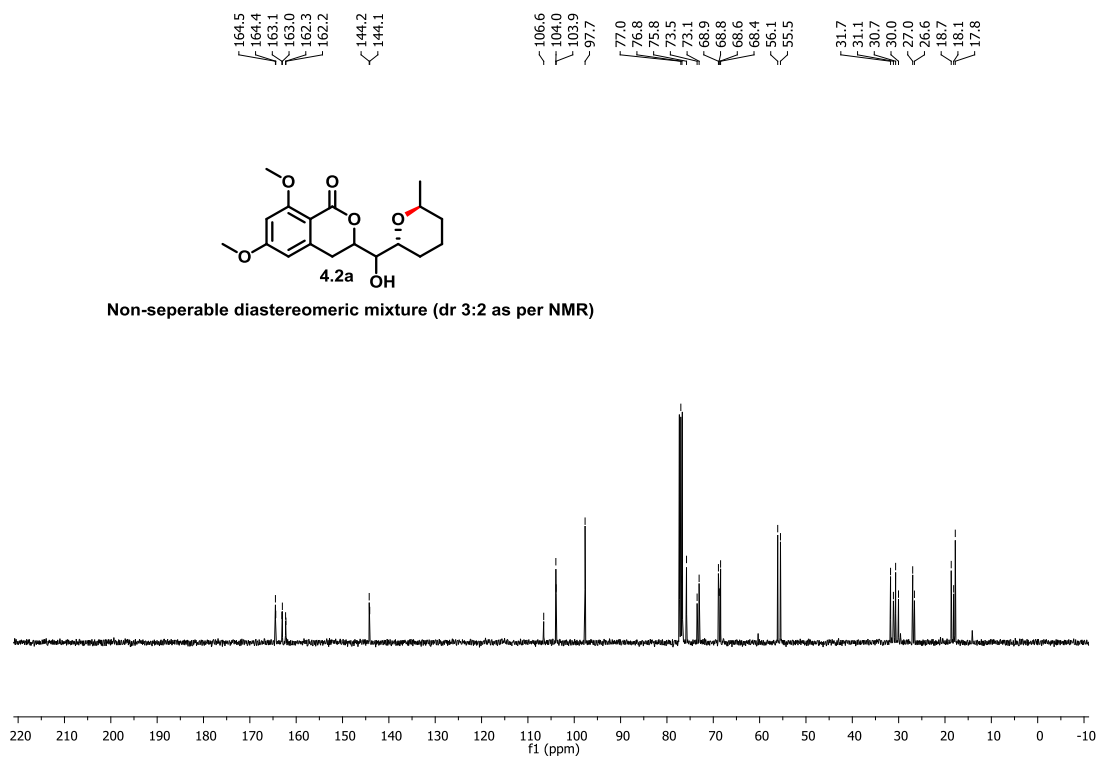
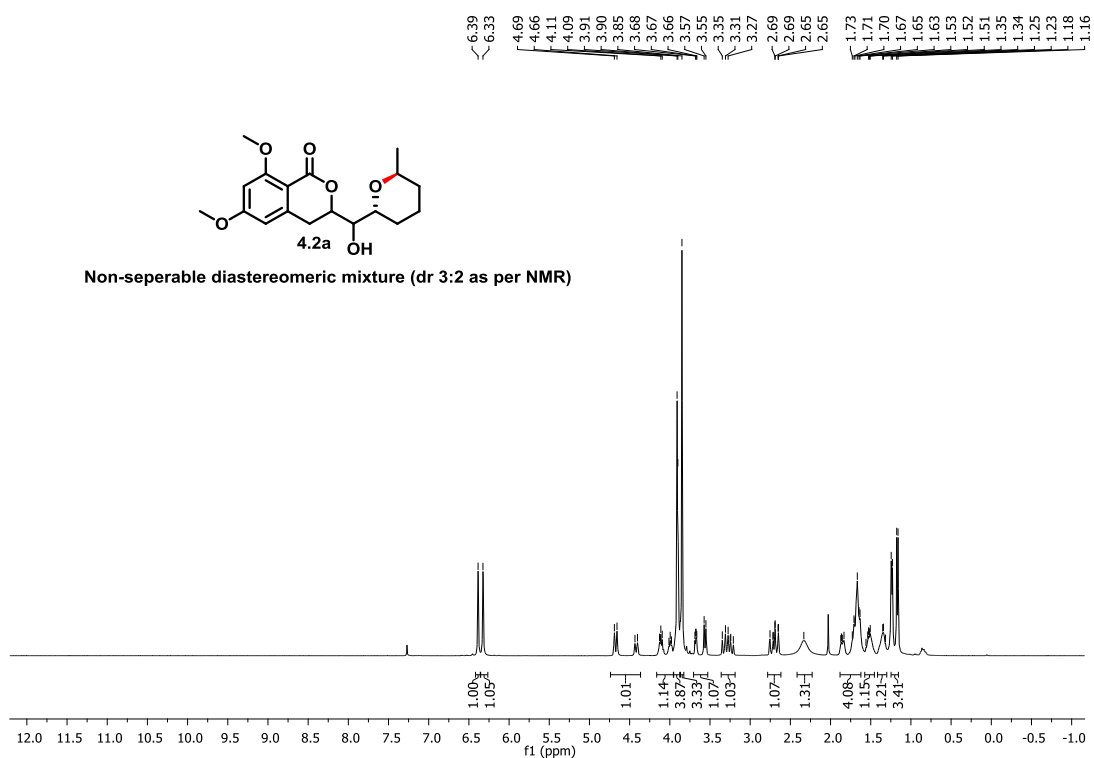
Chapter 1 (Section A): Synthesis of Entire Stereoisomeric Set of Anti-malarial Natural Product Cladosporin, their Biological Evaluation and Co-crystalization



Chapter 1 (Section A): Synthesis of Entire Stereoisomeric Set of Anti-malarial Natural Product Cladosporin, their Biological Evaluation and Co-crystallization



Chapter 1 (Section A): Synthesis of Entire Stereoisomeric Set of Anti-malarial Natural Product Cladosporin, their Biological Evaluation and Co-crystallization



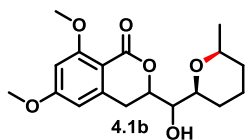
Chapter 1 (Section A): Synthesis of Entire Stereoisomeric Set of Anti-malarial Natural Product Cladosporin, their Biological Evaluation and Co-crystallization

164.5
164.4
163.1
163.0
162.3
162.2
144.2
144.1

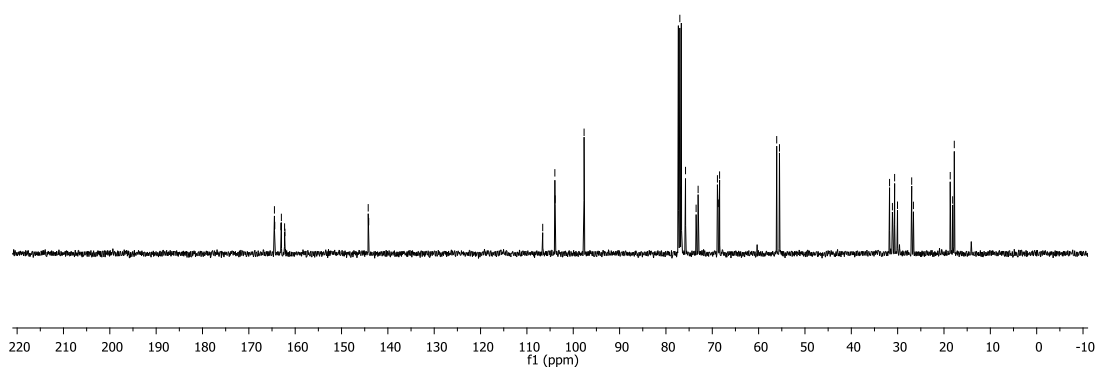
106.6
104.0
103.9
97.7

77.0
76.8
76.5
75.8
73.5
73.1
68.9
68.8
68.6
68.4
56.1
55.5

31.7
31.1
30.7
30.0
27.0
26.6
18.7
18.1
17.8



Non-seperable diastereomeric mixture (dr 1:1 as per NMR)

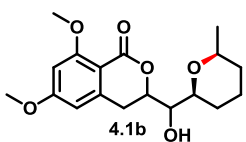


164.5
164.4
163.0
162.2
144.4
144.2

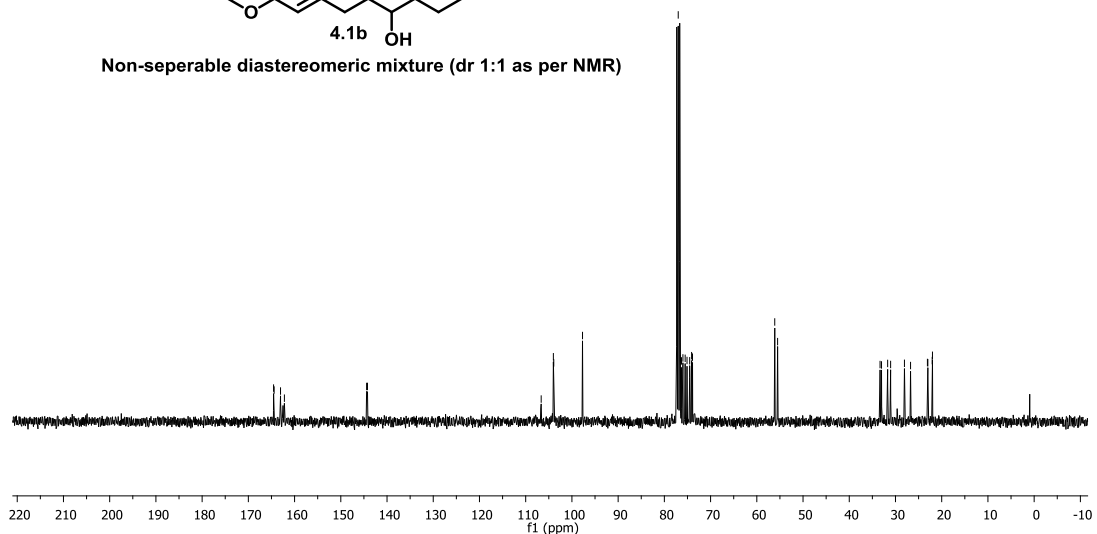
106.6
104.0
103.9
97.7

77.0
76.5
76.3
76.0
75.5
75.1
74.5
74.1
73.9
56.1
55.5

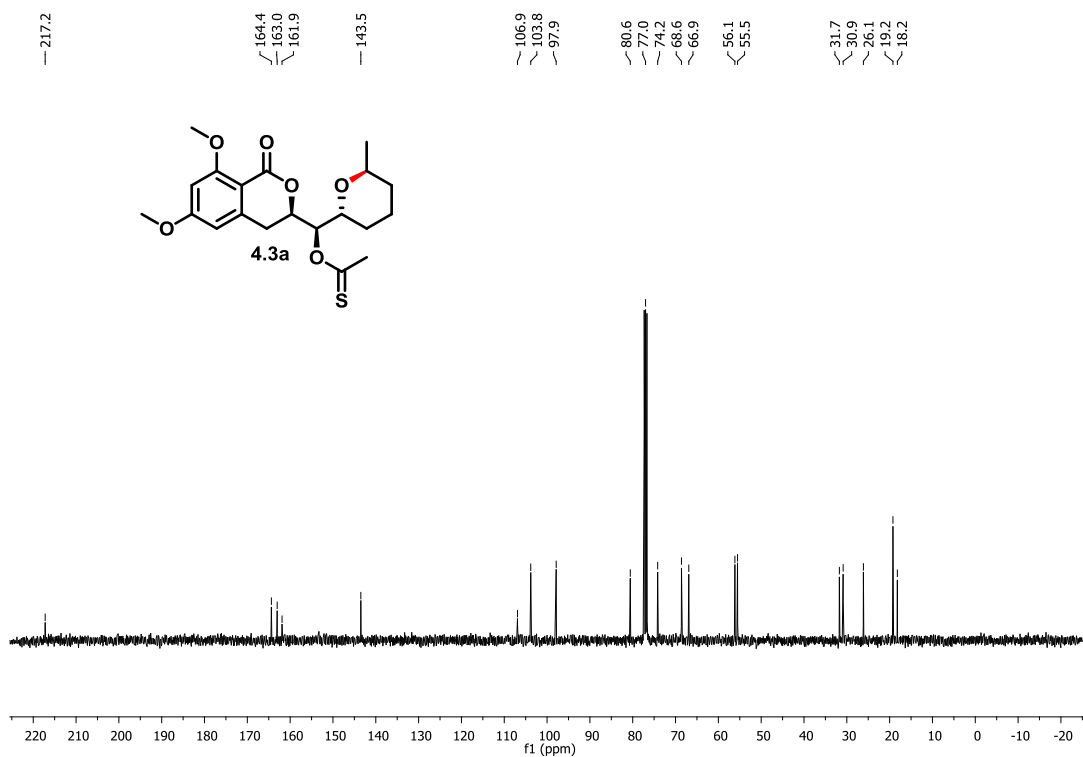
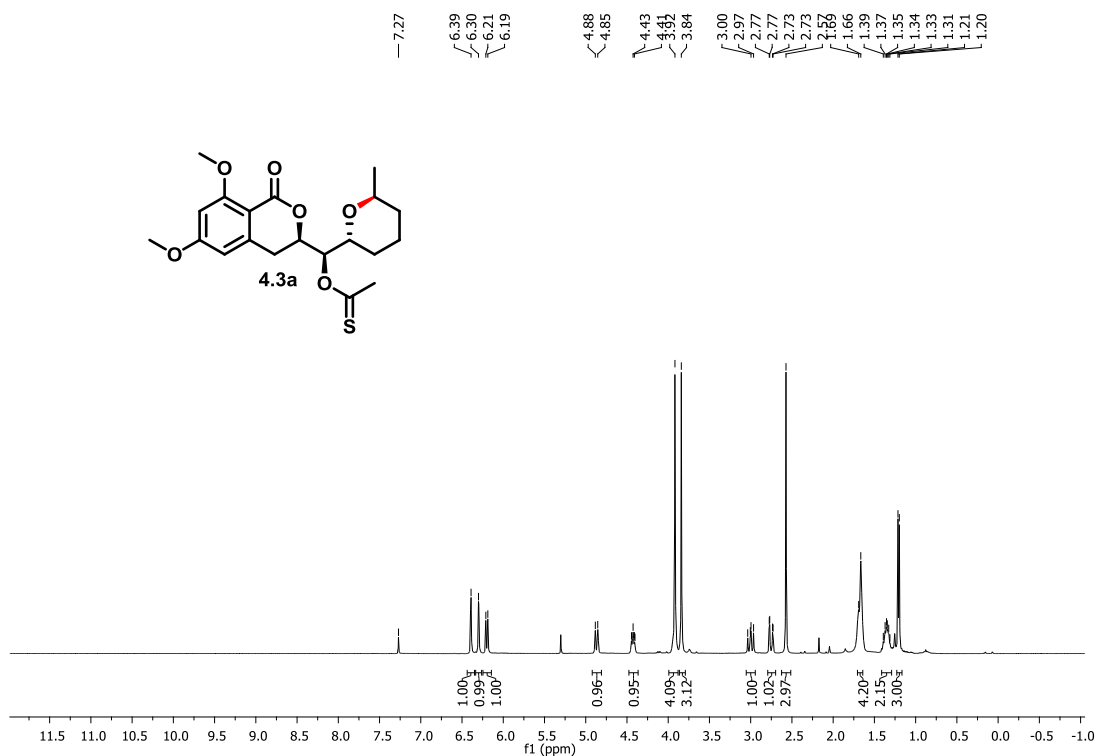
33.3
33.0
31.7
31.1
28.1
26.7
23.1
23.0
22.1
22.0



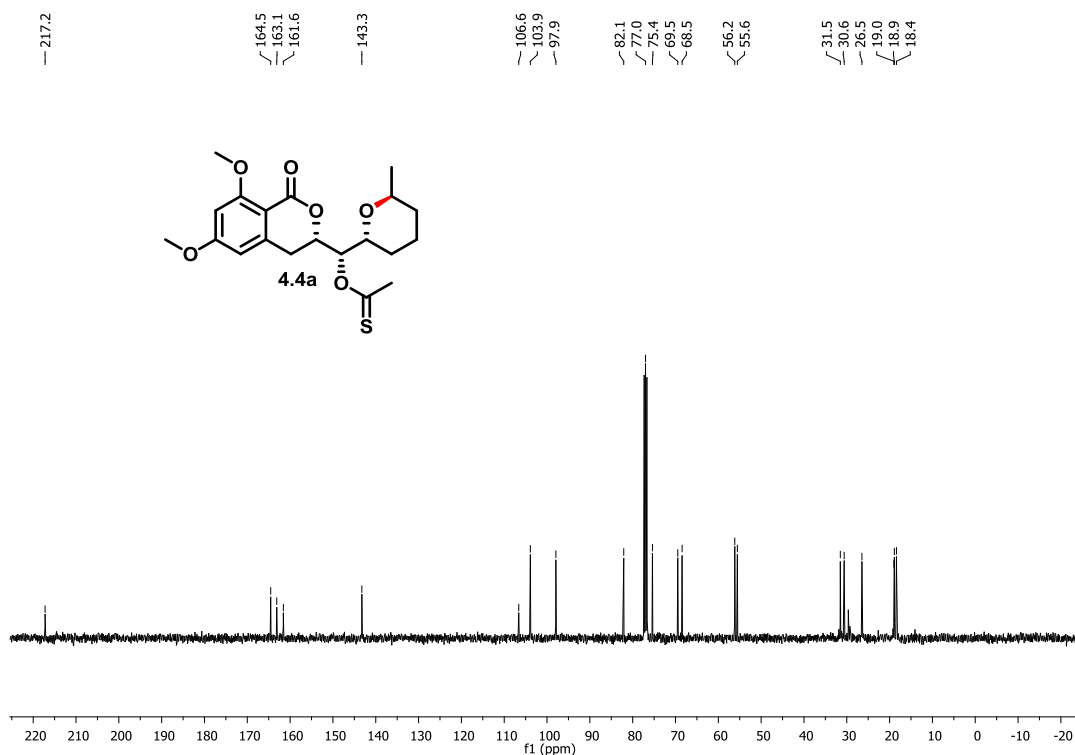
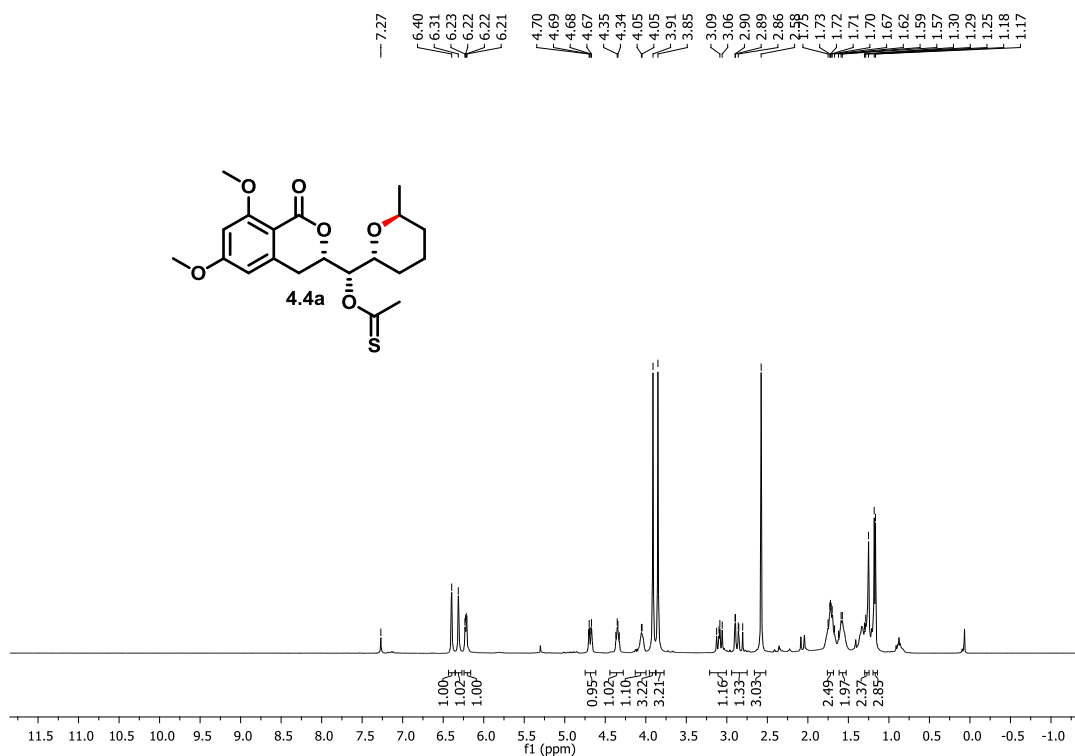
Non-seperable diastereomeric mixture (dr 1:1 as per NMR)



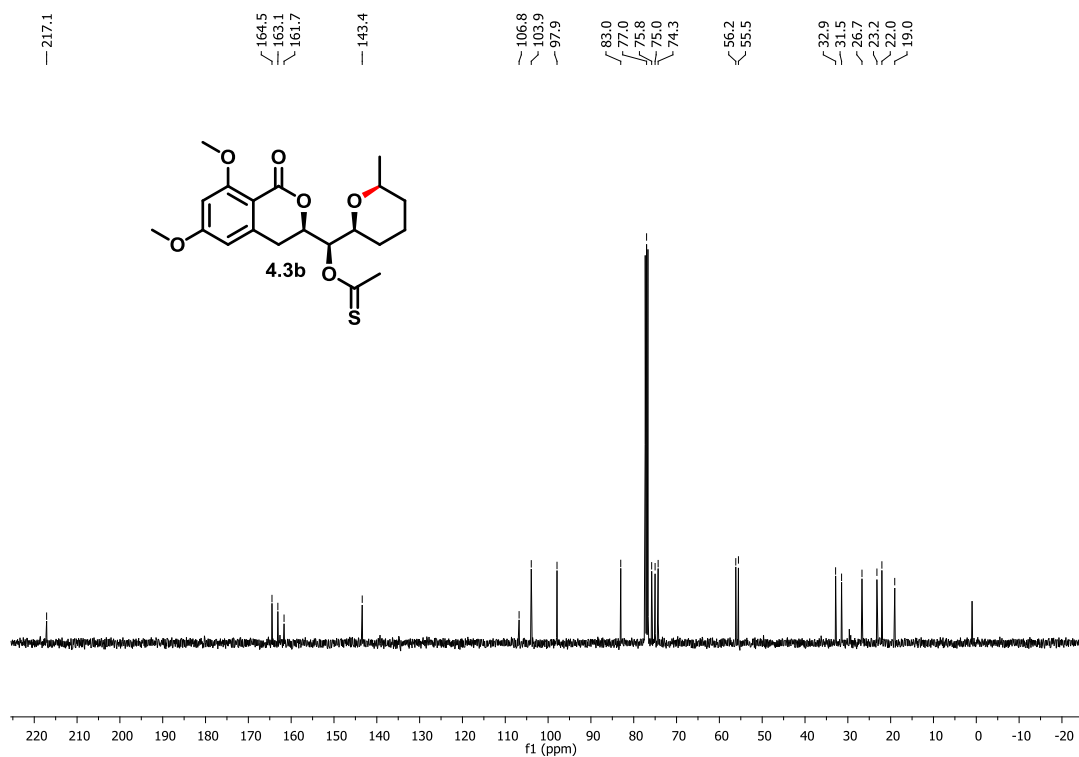
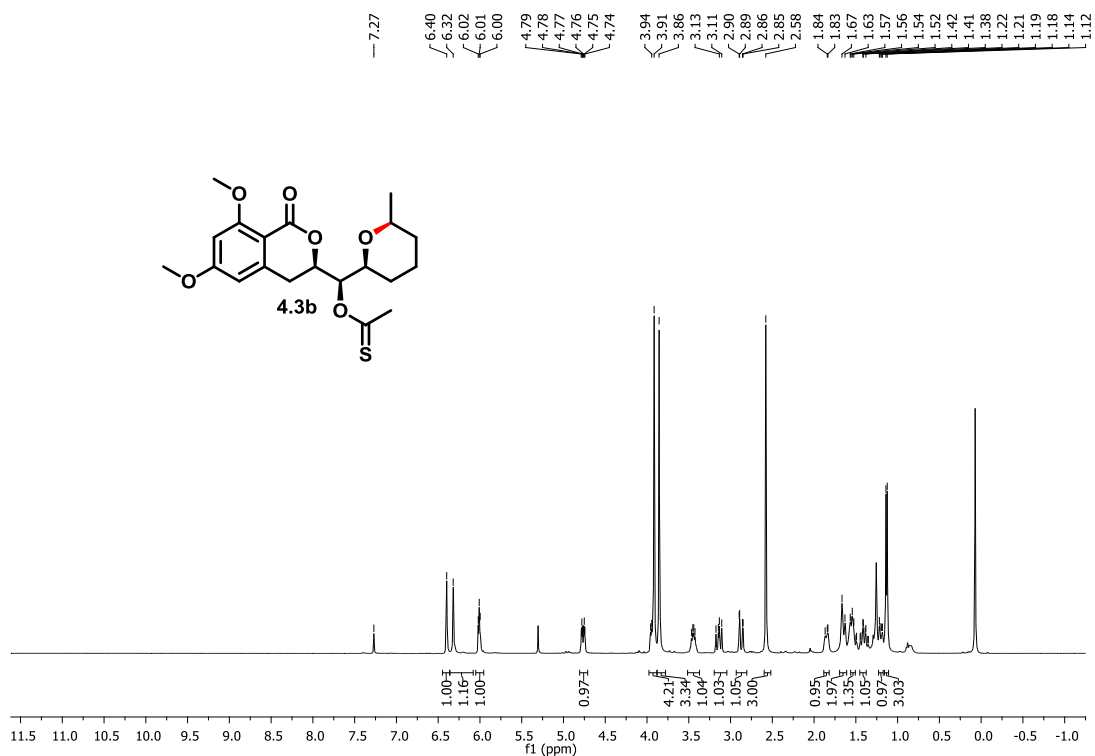
Chapter 1 (Section A): Synthesis of Entire Stereoisomeric Set of Anti-malarial Natural Product Cladosporin, their Biological Evaluation and Co-crystallization



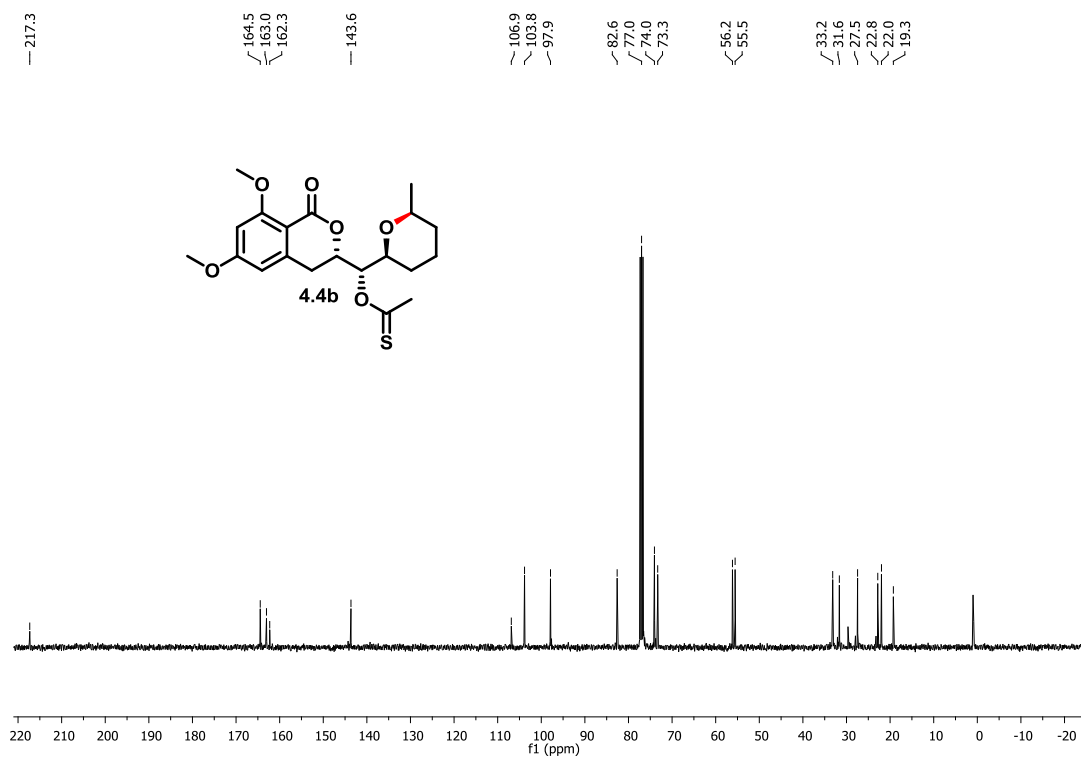
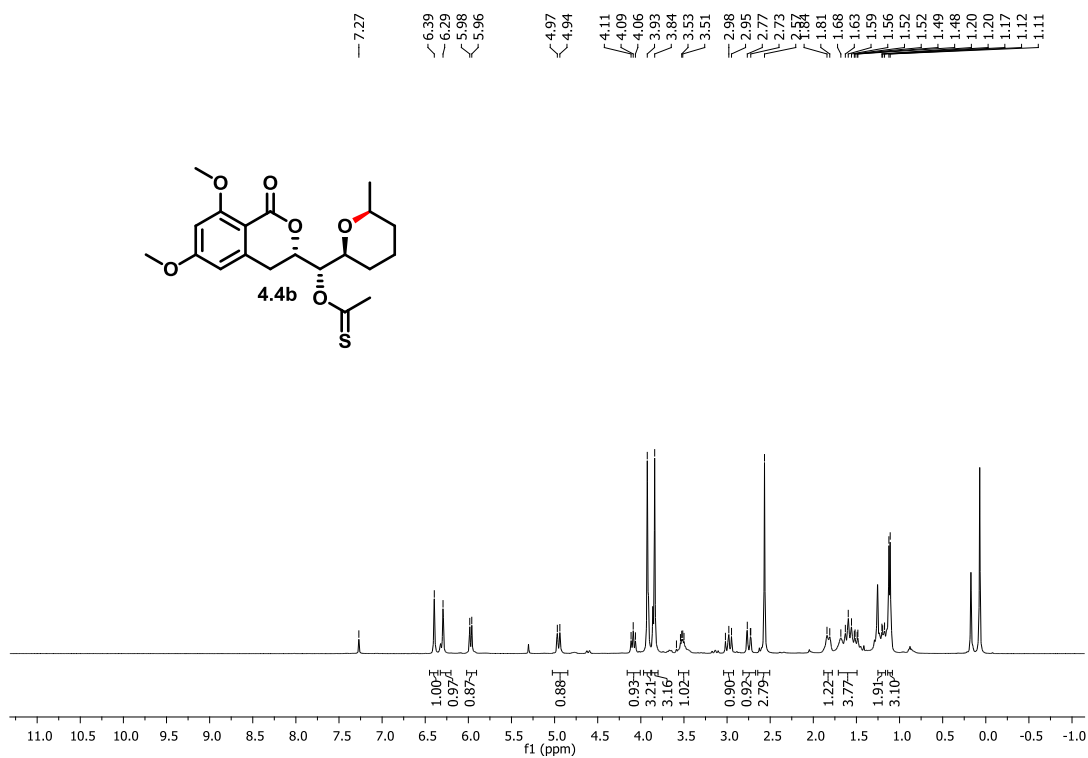
Chapter 1 (Section A): Synthesis of Entire Stereoisomeric Set of Anti-malarial Natural Product Cladosporin, their Biological Evaluation and Co-crystallization



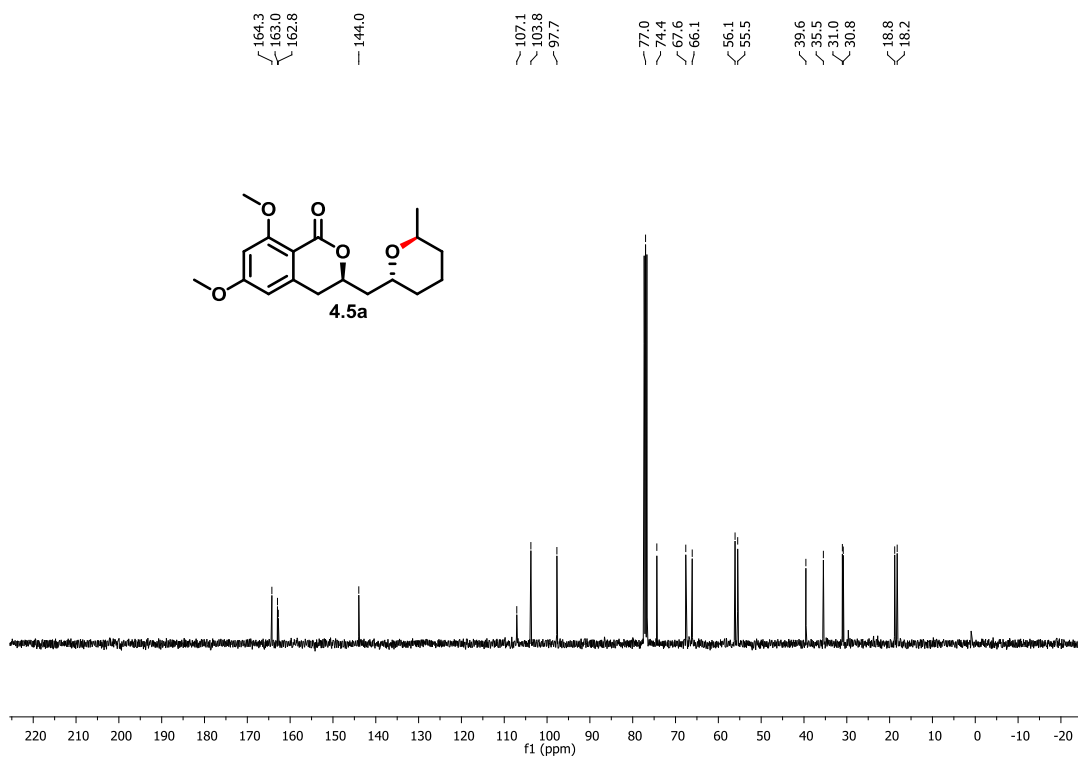
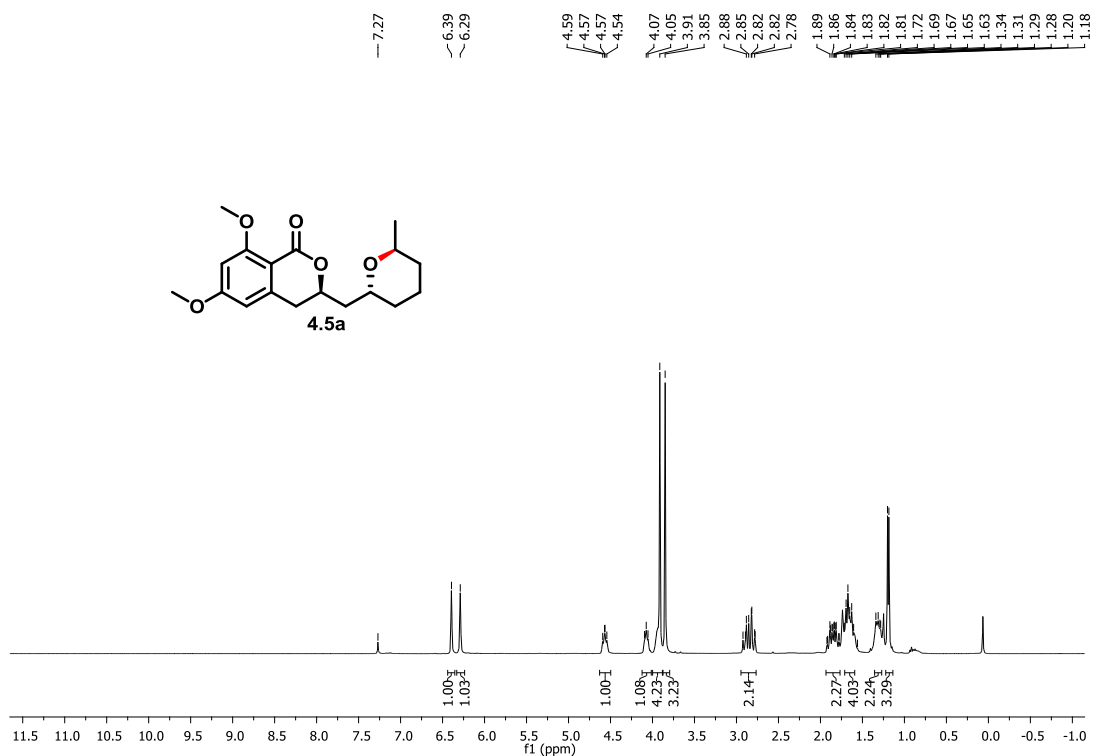
Chapter 1 (Section A): Synthesis of Entire Stereoisomeric Set of Anti-malarial Natural Product Cladosporin, their Biological Evaluation and Co-crystallization



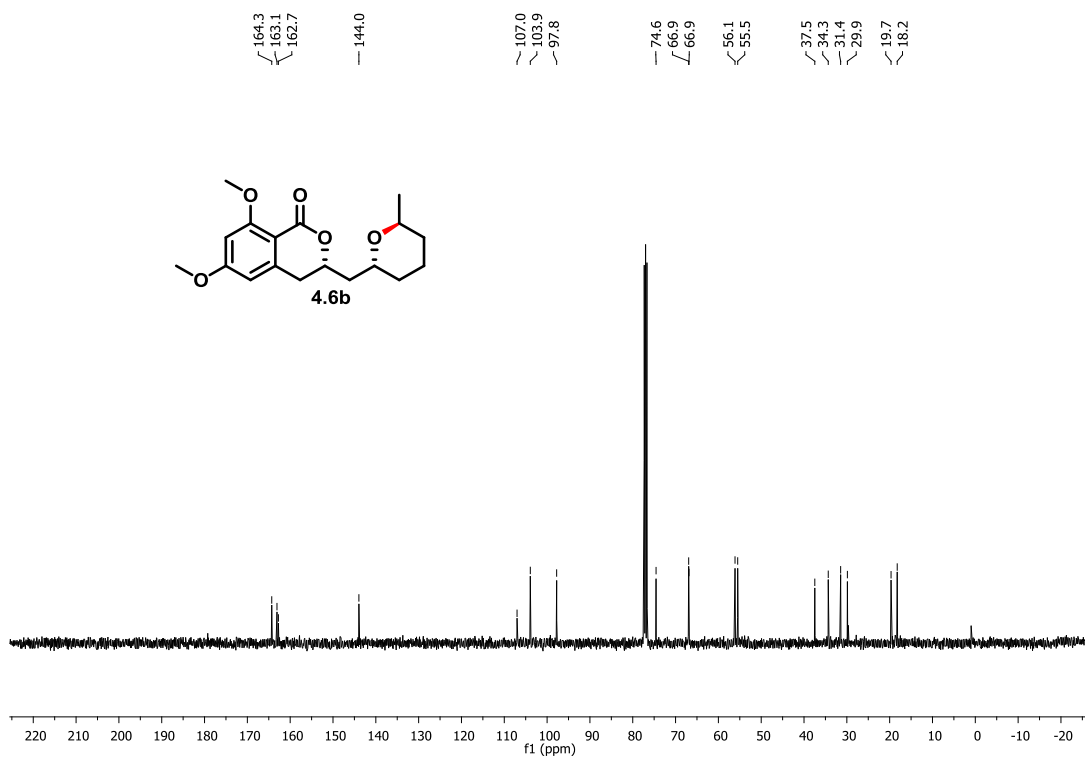
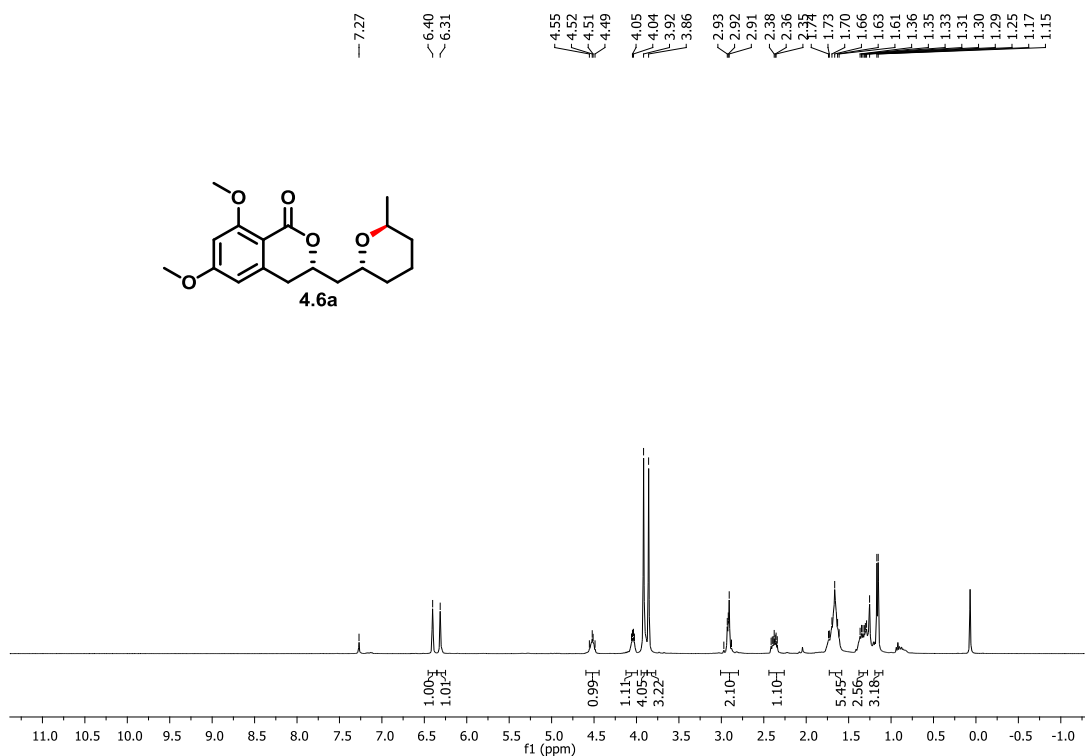
Chapter 1 (Section A): Synthesis of Entire Stereoisomeric Set of Anti-malarial Natural Product Cladosporin, their Biological Evaluation and Co-crystallization



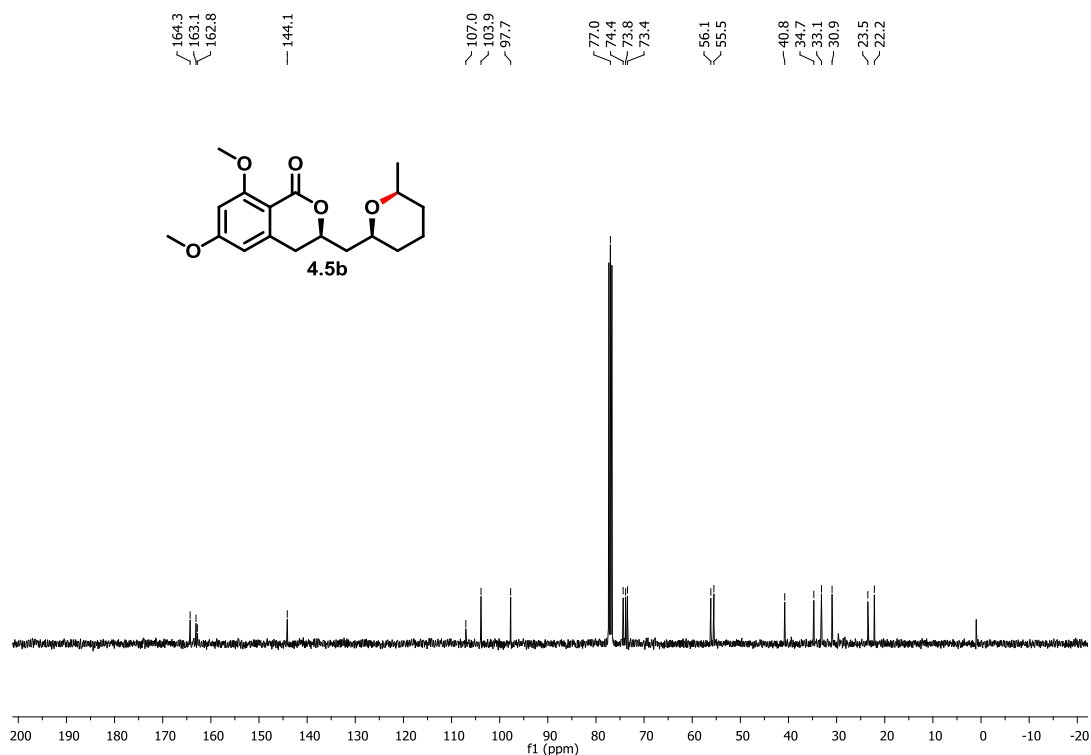
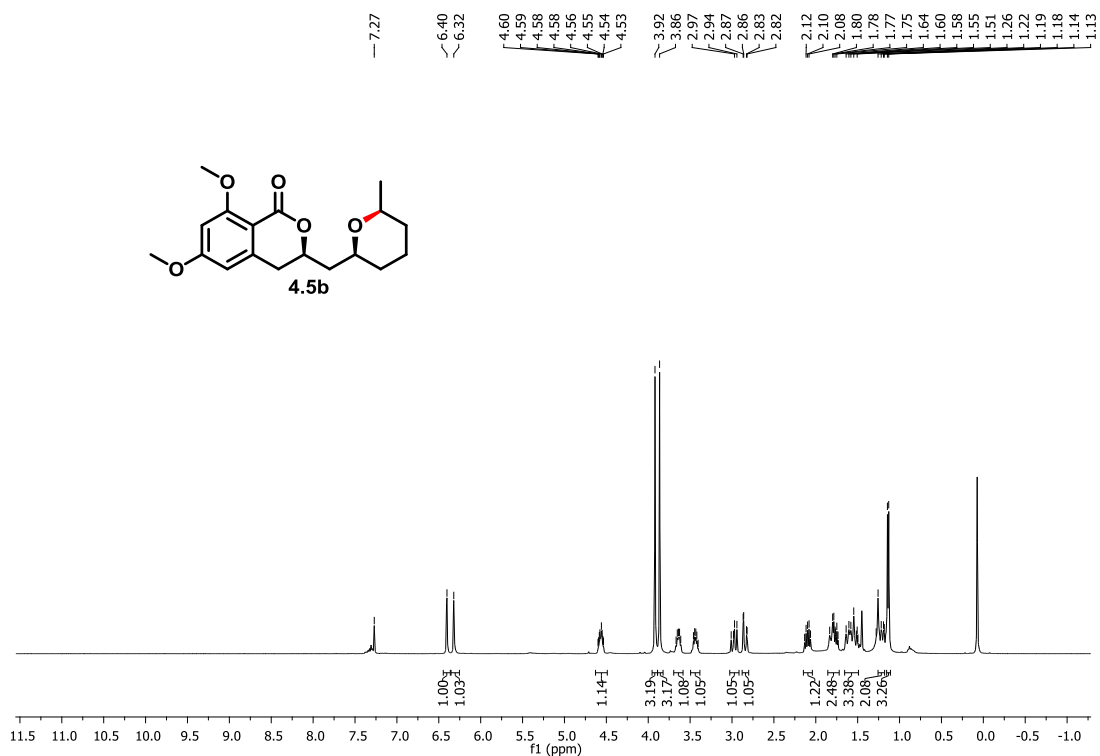
Chapter 1 (Section A): Synthesis of Entire Stereoisomeric Set of Anti-malarial Natural Product Cladosporin, their Biological Evaluation and Co-crystallization



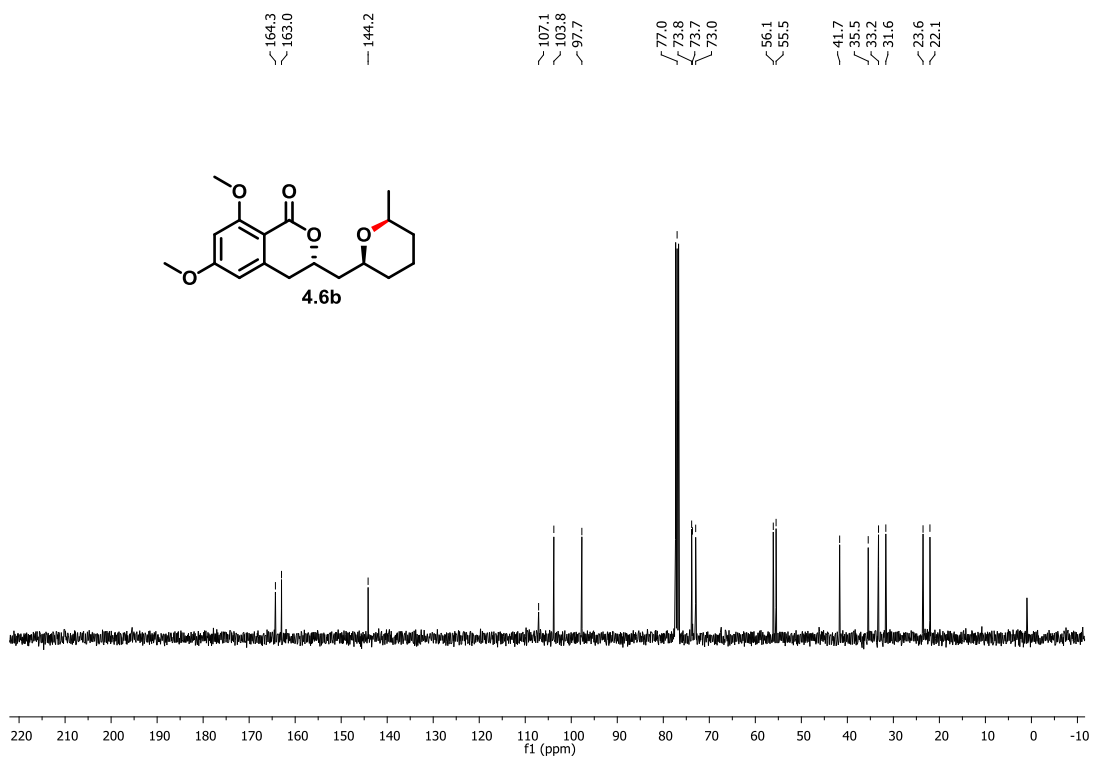
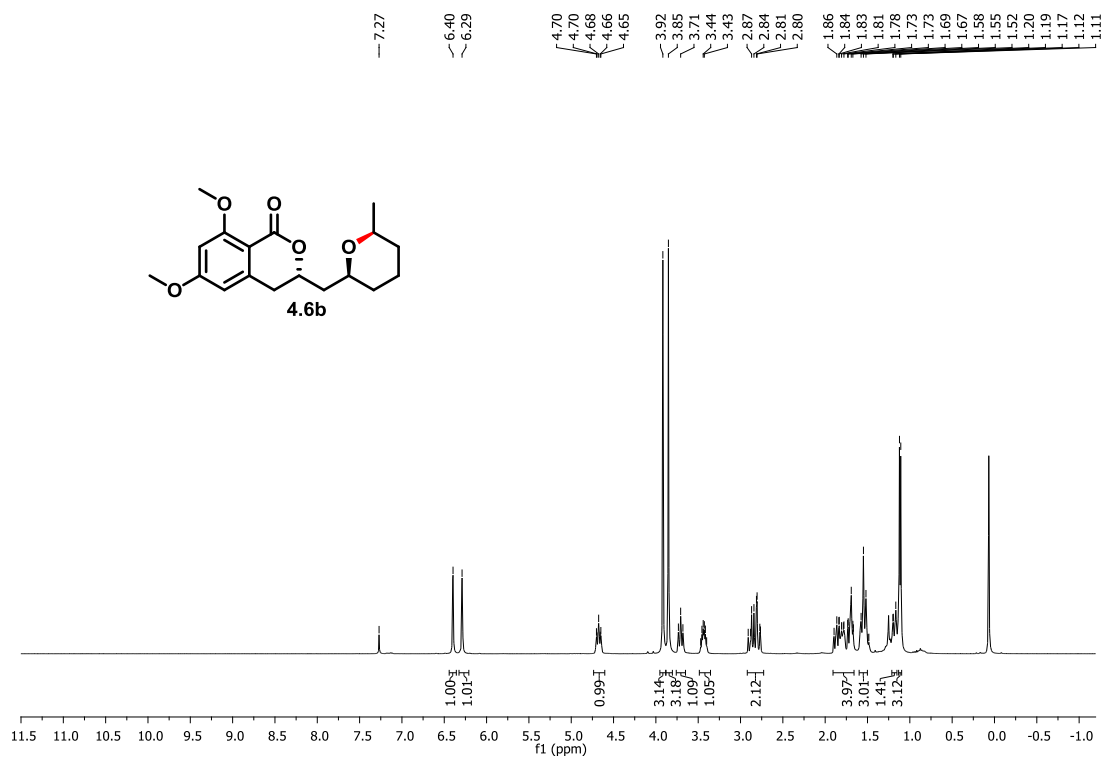
Chapter 1 (Section A): Synthesis of Entire Stereoisomeric Set of Anti-malarial Natural Product Cladosporin, their Biological Evaluation and Co-crystallization



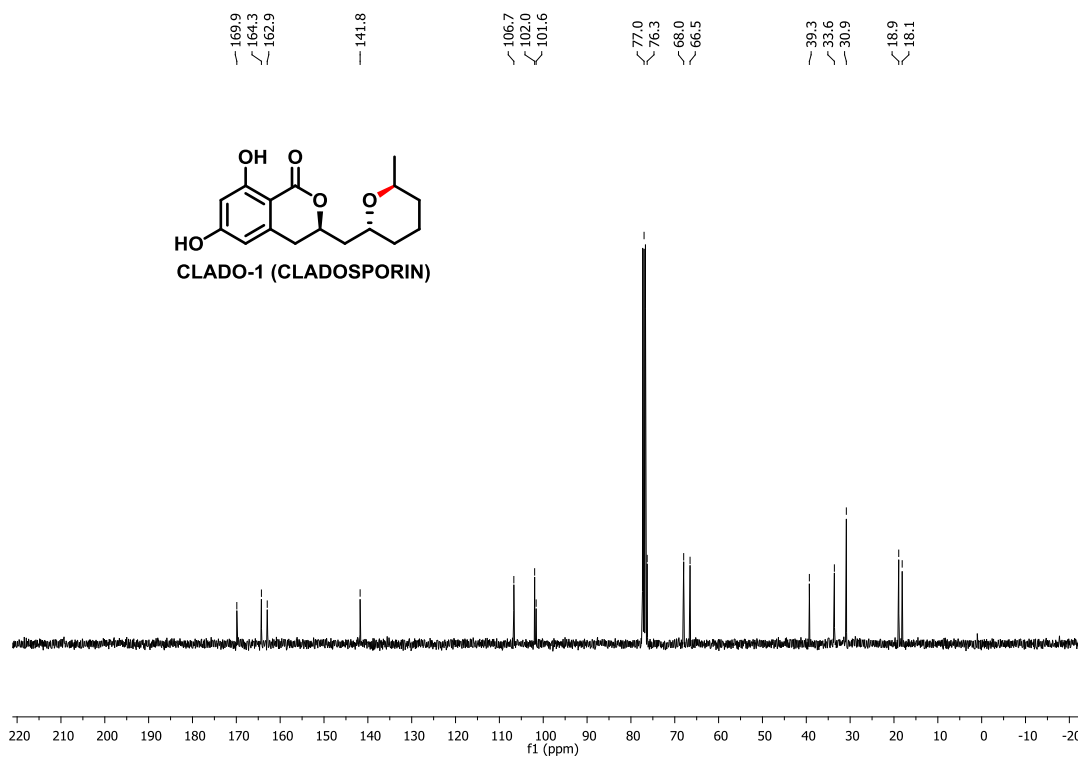
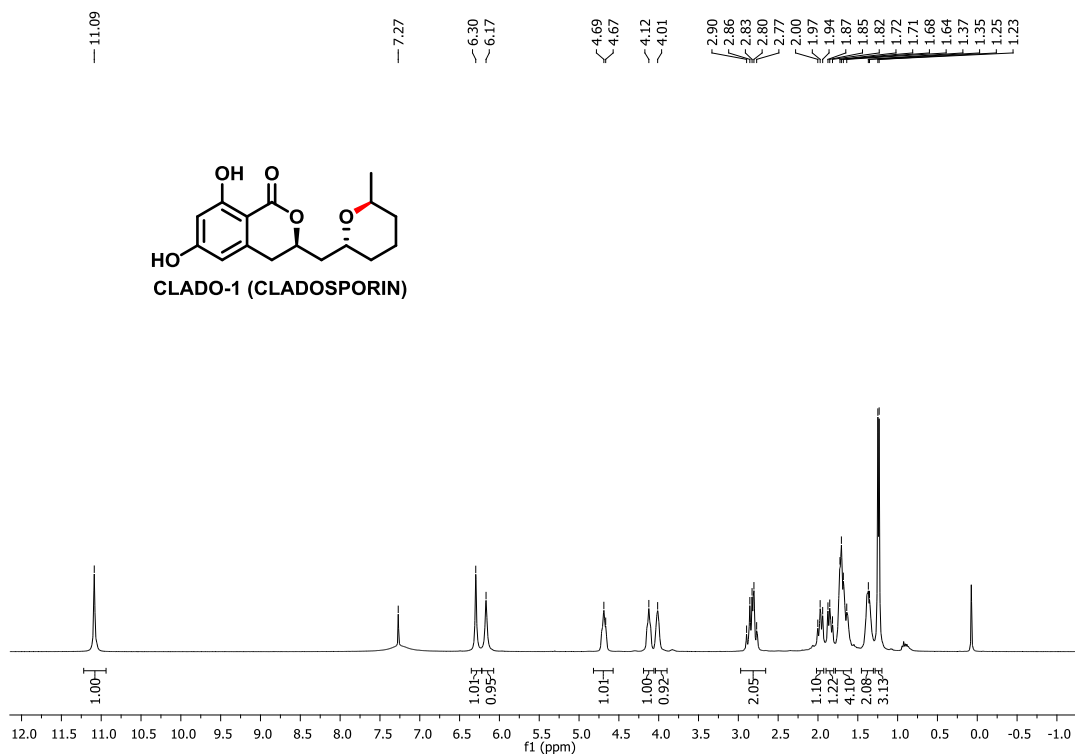
Chapter 1 (Section A): Synthesis of Entire Stereoisomeric Set of Anti-malarial Natural Product Cladosporin, their Biological Evaluation and Co-crystallization



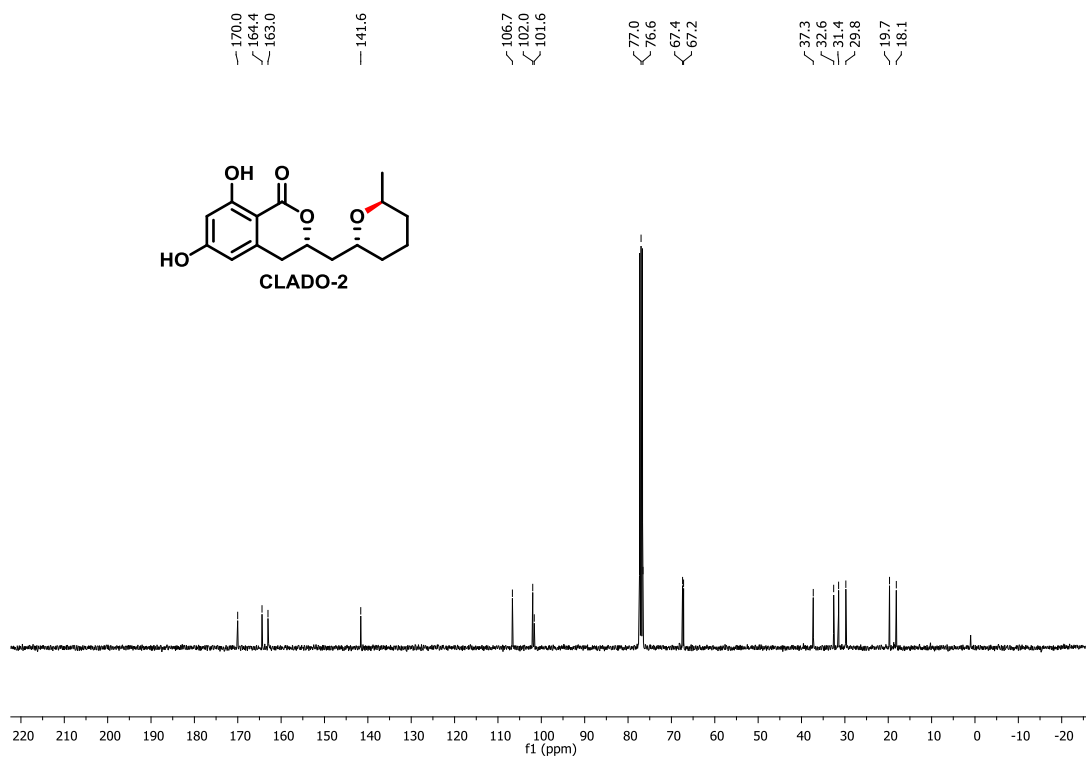
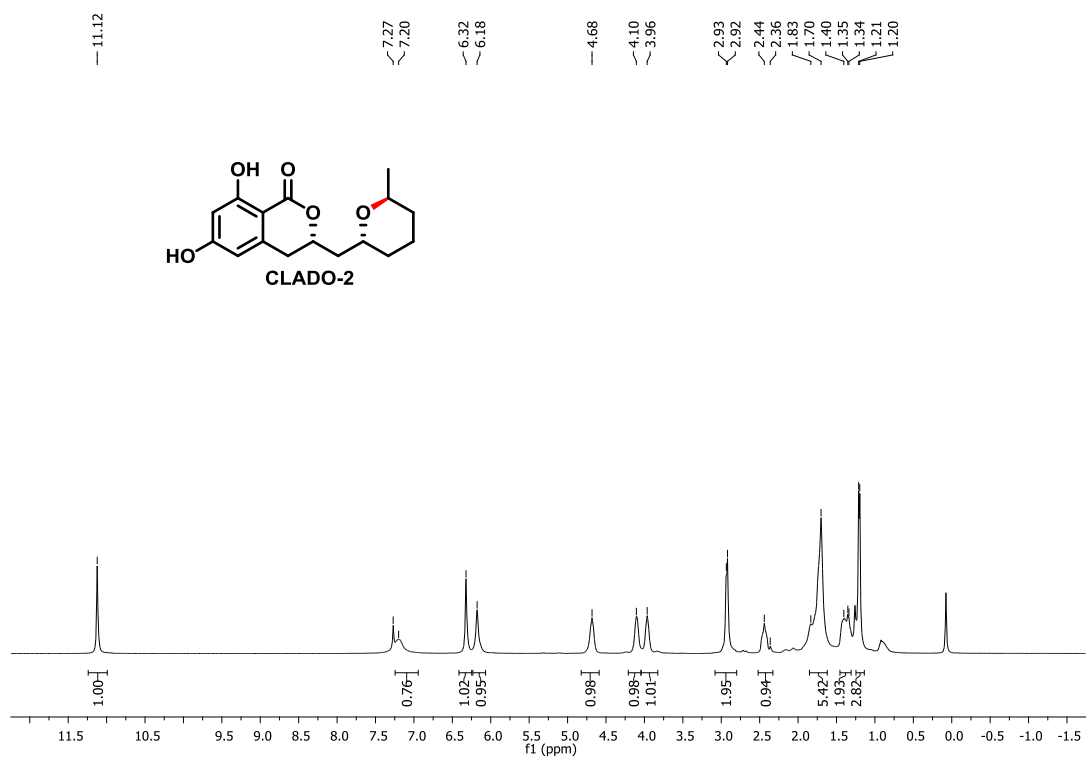
Chapter 1 (Section A): Synthesis of Entire Stereoisomeric Set of Anti-malarial Natural Product Cladosporin, their Biological Evaluation and Co-crystallization



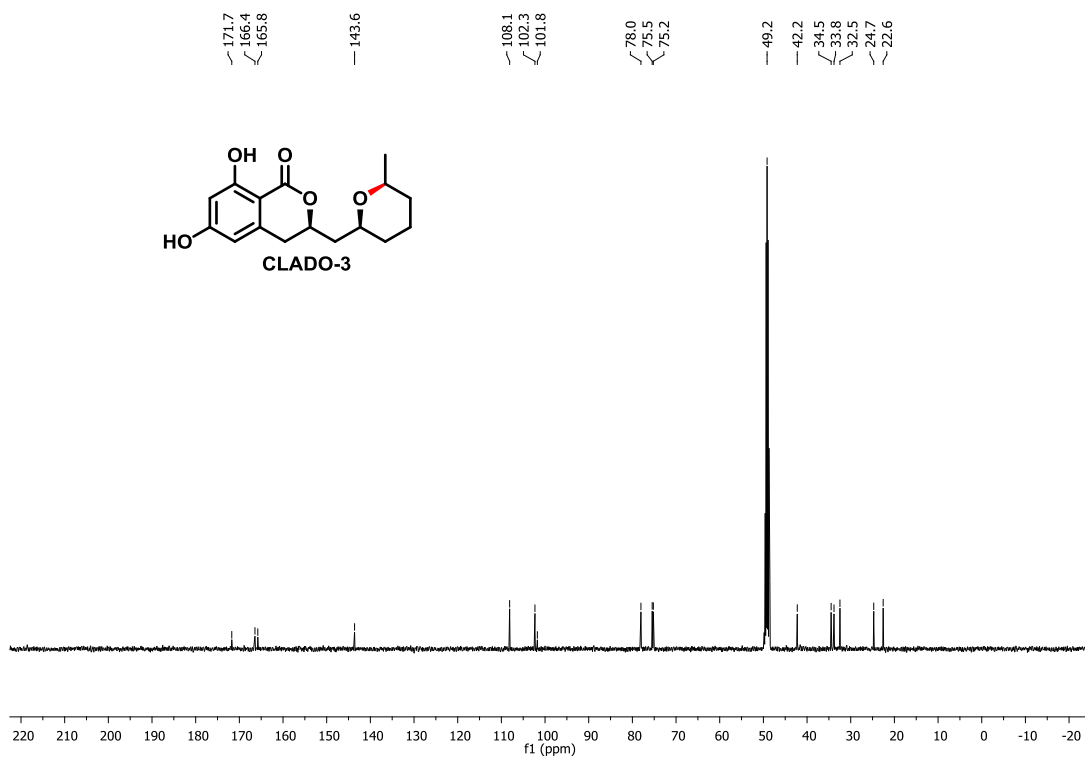
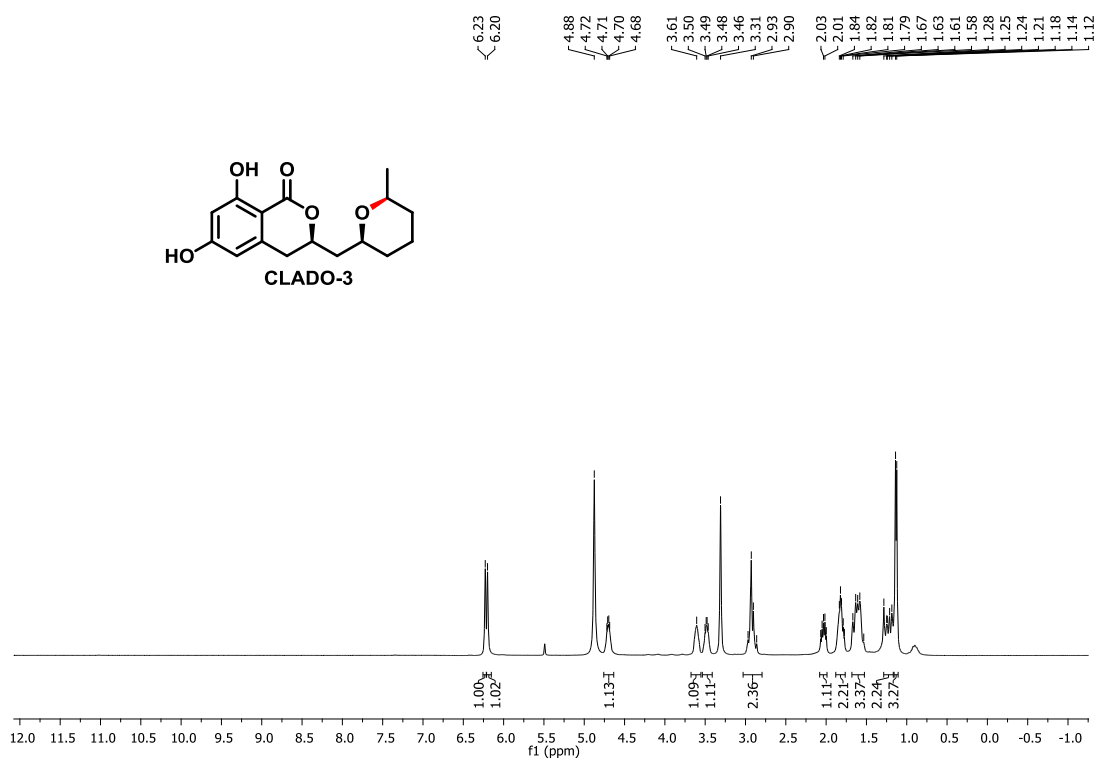
Chapter 1 (Section A): Synthesis of Entire Stereoisomeric Set of Anti-malarial Natural Product Cladosporin, their Biological Evaluation and Co-crystallization



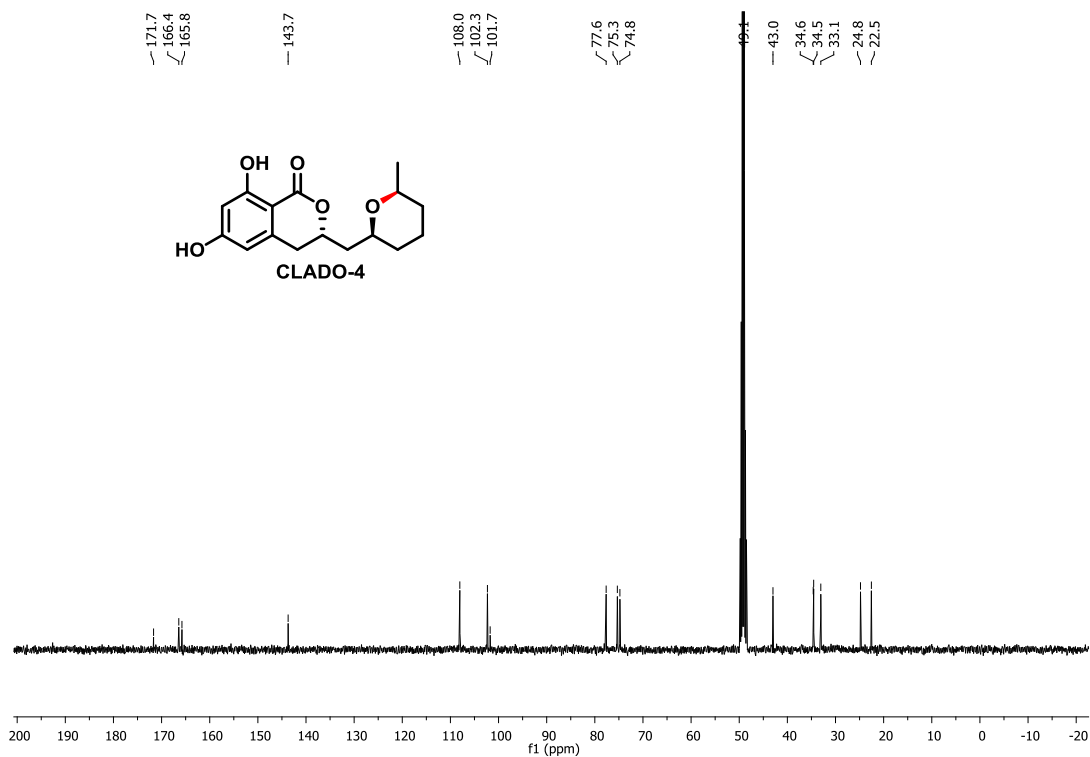
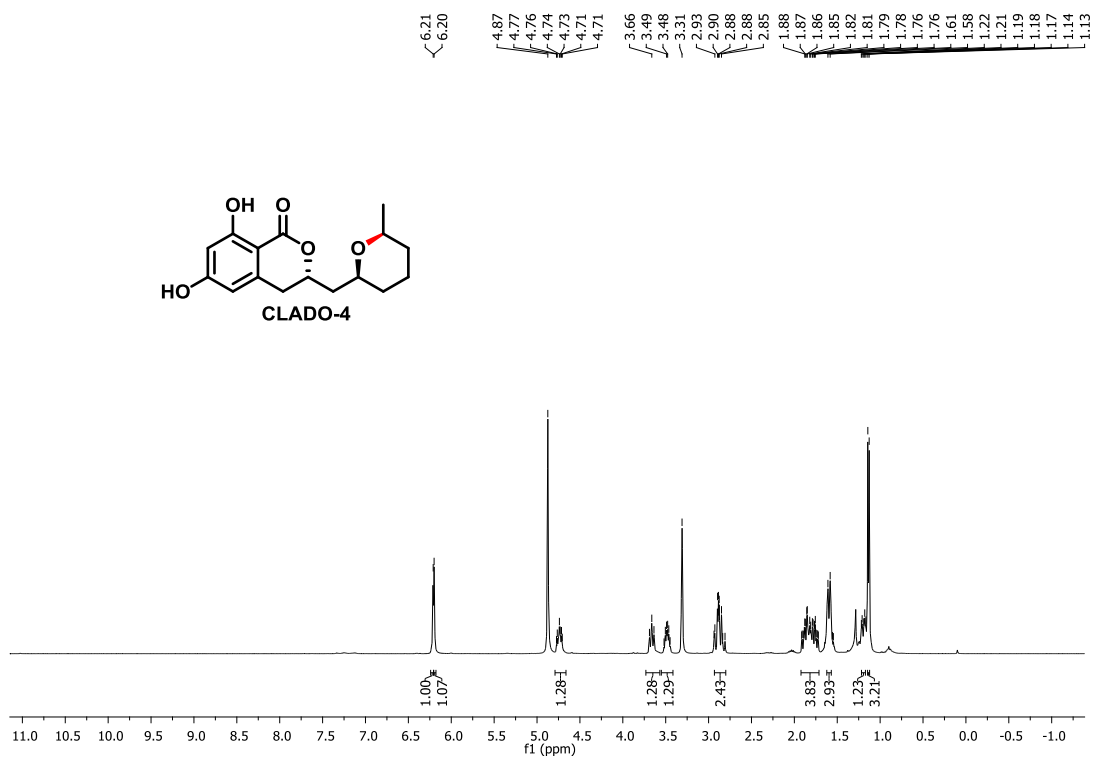
Chapter 1 (Section A): Synthesis of Entire Stereoisomeric Set of Antimalarial Natural Product Cladosporin, their Biological Evaluation and Co-crystallization



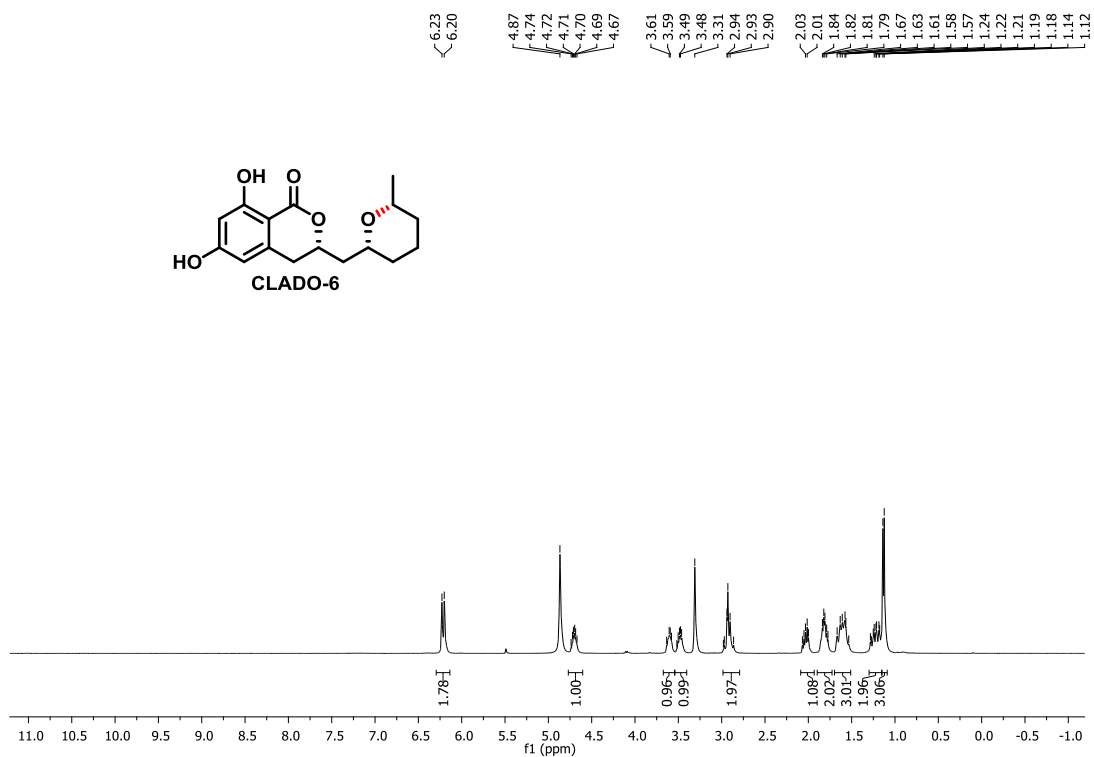
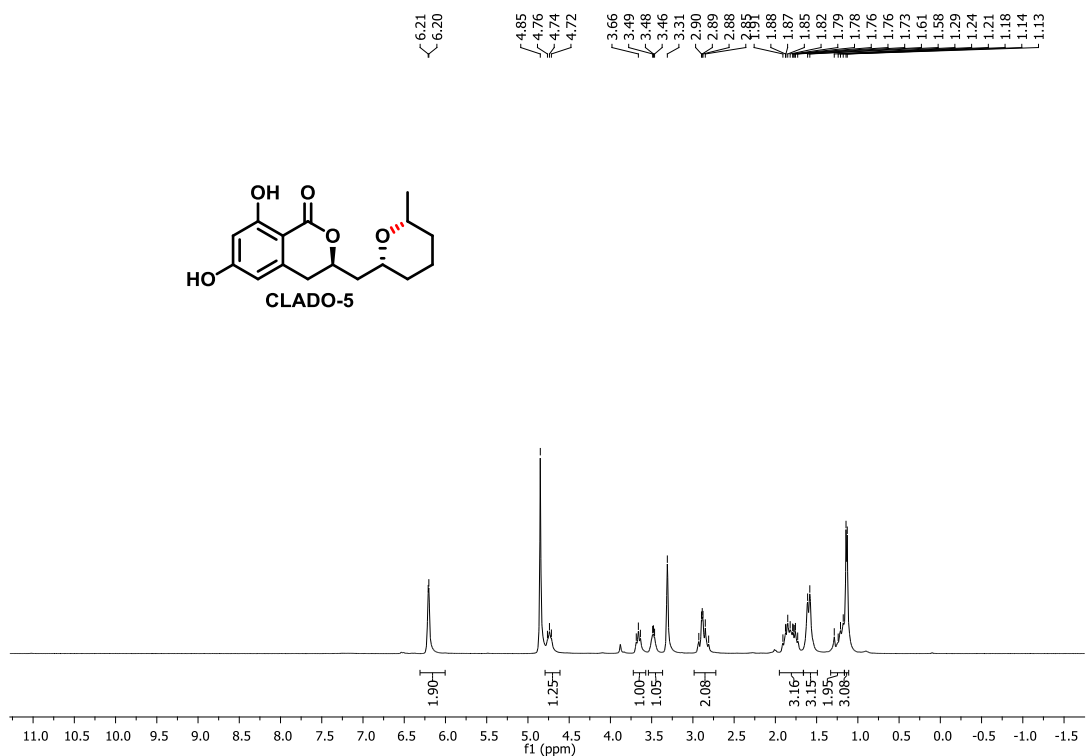
Chapter 1 (Section A): Synthesis of Entire Stereoisomeric Set of Anti-malarial Natural Product Cladosporin, their Biological Evaluation and Co-crystallization



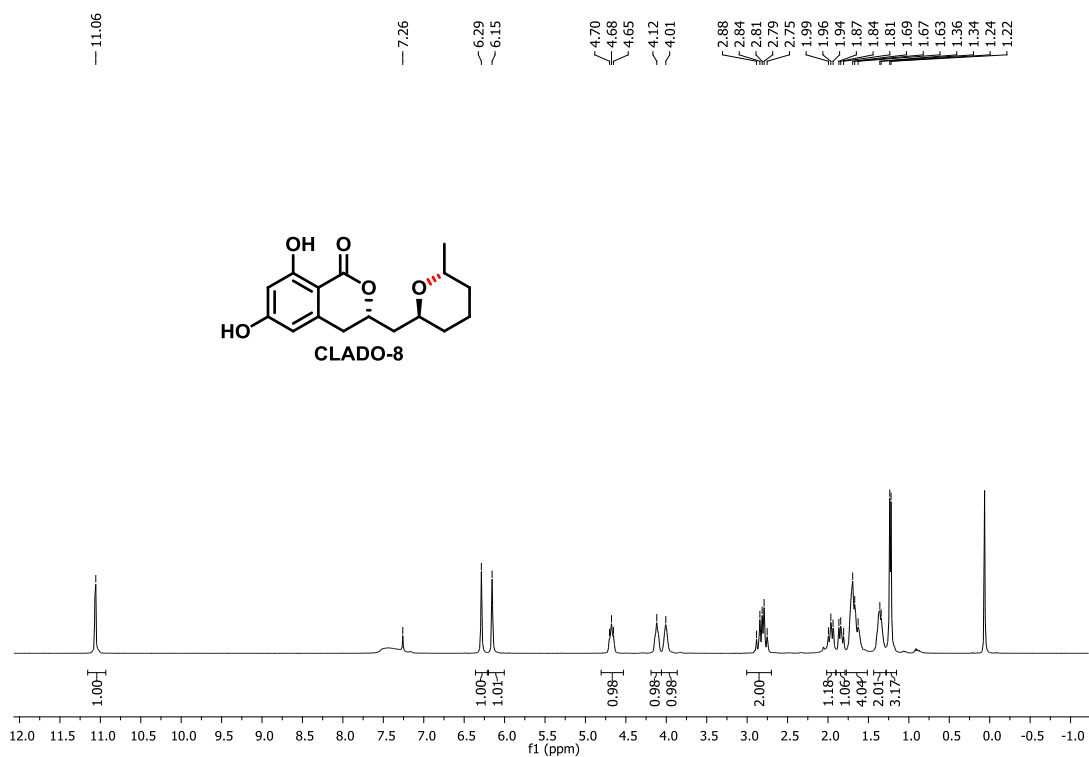
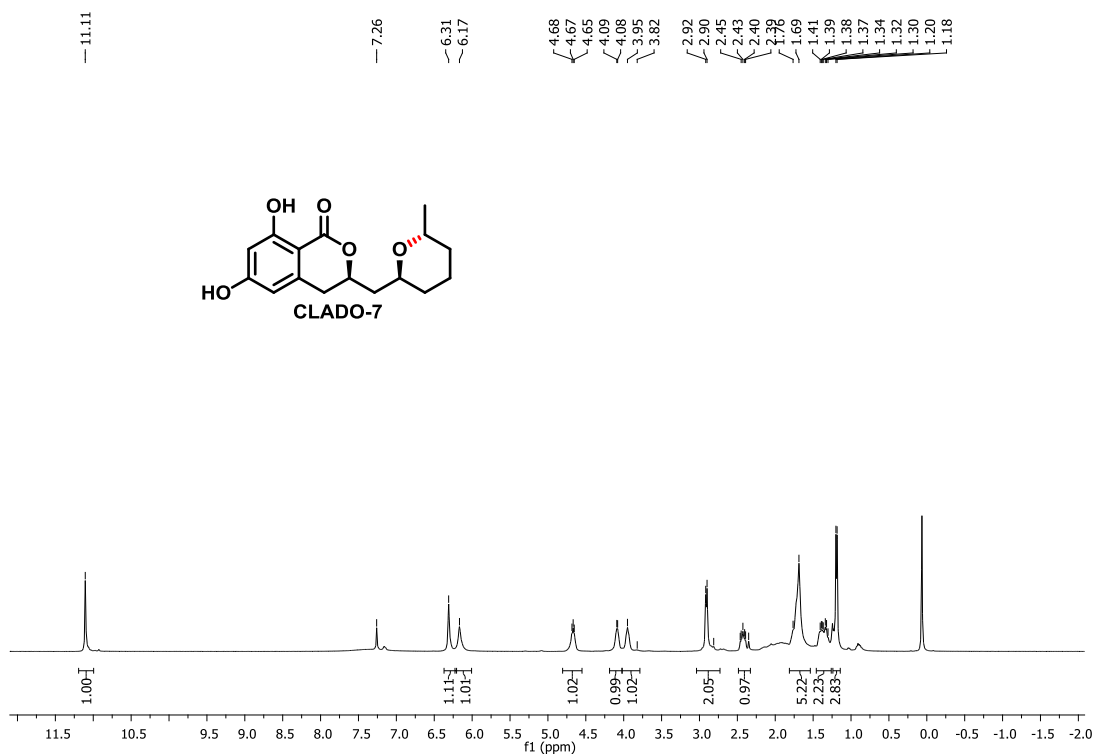
Chapter 1 (Section A): Synthesis of Entire Stereoisomeric Set of Anti-malarial Natural Product Cladosporin, their Biological Evaluation and Co-crystallization



Chapter 1 (Section A): Synthesis of Entire Stereoisomeric Set of Anti-malarial Natural Product Cladosporin, their Biological Evaluation and Co-crystallization



Chapter 1 (Section A): Synthesis of Entire Stereoisomeric Set of Anti-malarial Natural Product Cladosporin, their Biological Evaluation and Co-crystalization





FIRST CHAPTER

Section B

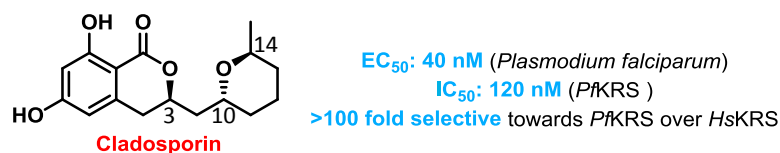


Gram Scale Synthesis of Cladosporin

Chapter 1 (Section B): Gram Scale Synthesis of Cladosporin

1.2.1. Introduction

Pharmacokinetics (PK) and pharmacodynamics (PD) play a key role in determining the therapeutic potential and toxicological profile of any drug. Hence assessment of the same becomes crucial in a drug development program. Besides, a thorough profiling of a bio-active scaffold required several in vivo studies which demands adequate amount of the active material. The paucity of NPs from natural sources seldom poses a challenge in this aspect. Hence development of advanced synthetic protocols to access bio-active NPs becomes a necessary task. In the context of anti-malarial drug development, natural product cladosporin holds a promising potential.^{1, 2} Details regarding the anti-malarial potency of cladosporin has been thoroughly described in the previous section of the thesis (Chapter 1, Section I).



Parasites		Fungus			
	IC_{50} (μ M)	<i>Penicillium</i> sp.	% inhibition	<i>Aspergillus</i> sp.	% inhibition
<i>Plasmodium yoeli</i>	0.04	<i>viridicatum</i>	100 (20 μ g/mL)	<i>niger</i>	95 (20 μ g/mL)
<i>Trypanosoma brucei</i>	2.05	<i>expansum</i>	85 (20 μ g/mL)	<i>ochraceus</i>	97 (20 μ g/mL)
<i>Leishmania donovani</i>	2.56	<i>obscurans</i>	22.1 (30 μ g/mL)	<i>versicolor</i>	<50 (20 μ g/mL)
<i>Toxoplasma gondii</i>	2.63	<i>viticola</i>	79.9 (30 μ g/mL)	<i>clavatus</i>	<50 (20 μ g/mL)
				<i>nidulans</i>	<50 (20 μ g/mL)

<i>Colletotrichum</i> sp. (Fungus)	% inhibition
<i>acutatum</i>	92.7 (30 μ g/mL)
<i>fragariae</i>	90.1 (30 μ g/mL)
<i>gloeosporioides</i>	95.4 (30 μ g/mL)

Figure 1. Spectrum of cladosporin bio-activity.

Cladosporin is found to inhibit *PfKRS*, an enzyme central to protein bio-synthesis in *plasmodium falciparum*, thus leading to parasitic death.² Apart from *PfKRS*, cladosporin is also known to inhibit KRSs from other species, which includes helminth parasites such as *Loa loa* (*Ll*) and *Schistosomamansoni* (*Sm*).³ Besides anti-malarial potency, cladosporin is also found to exhibit a broad spectrum of biological activities like antifungal,¹ insecticidal, plant growth inhibition^{4, 5} and antibacterial,⁶ as well as

Chapter 1 (Section B): Gram Scale Synthesis of Cladosporin

anti-inflammatory activity (Figure 1).⁷ Considering the promising anti-malarial potential of cladosporin we initially developed a divergent synthetic route for the synthesis of all the possible eight stereoisomers (cladologs) of cladosporin.⁸ In collaboration with Sharma et al.; we successfully deciphered the stereochemical basis of cladologs' interaction with *Pf*KRS through cladolog-*Pf*KRS co-crystallization.⁸ The impressive anti-malarial profile and a broad spectrum of bio-activity of cladosporin undoubtedly make it a promising scaffold for further development. In-depth biological assessment and proper quantification of its PK/PD properties through in vivo studies requires an adequate quantity of the natural product (cladosporin) which has limited access from natural sources. Hence the development of a scalable synthetic route for the same is worth exploring.

Till date, one asymmetric total synthesis⁹ followed by a formal synthesis¹⁰ of cladosporin are documented in the literature, following which, we further developed a divergent route to access its entire stereoisomeric set (Figure 2).⁸ The first total synthesis of cladosporin was published by She et al. in the year 2012 where they utilized Hydrolytic Kinetic Resolution (HKR) using (*S,S*)-Co^{II}-salen catalyst.⁹ Kinetic resolution techniques like HKR lead to the oxidation of one specific stereoisomer from the diastereoisomeric mixture of epoxide to its corresponding chiral diol leaving the unreacted isomer of the epoxide as such. But in techniques like this one has to encounter an inevitable loss of 50% of the concerned material with undesired chirality (Figure 2). In the following year, 2013 one formal synthesis of cladosporin appeared in the literature from Mohapatra et al.¹⁰ In this elegant synthesis, the use of Hoveyda Grubbs' catalyst at a very early stage makes it less cost-effective for gram scale operations. Besides, the use of AD-mix- α for asymmetric dihydroxylation also leads to a decrease in cost-effectiveness considering the bulk amount of AD-mix- α required for a gram scale operation (Figure 2). In the year 2018, we published an elegant divergent route for synthesizing all the possible stereoisomers of cladosporin.⁸ Considering the highly divergent nature of the scheme, and diastereoisomeric separations encountered, it is very unlikely to be amenable for scale-up (Figure 2).

Chapter 1 (Section B): Gram Scale Synthesis of Cladosporin

Previous work on synthesis:

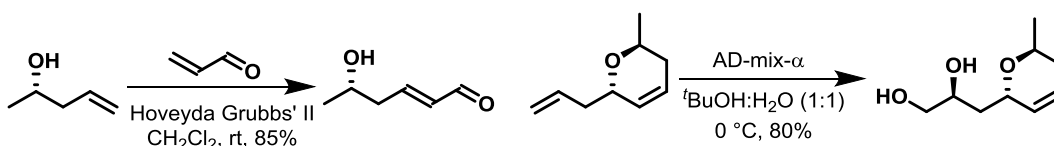
Two total syntheses and one formal synthesis have been achieved till date

1. (*J. Org. Chem.* **2012**, 77, 5656-5663) (*Total synthesis*)



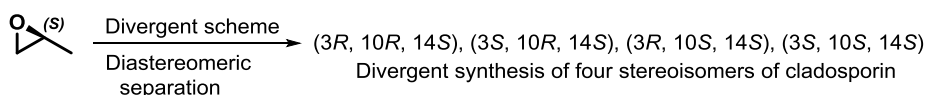
Drawback for scale up: Use of hydrolytic kinetic resolution results in a loss of 50% of chiral material

2. (*Eur. J. Org. Chem.* **2013**, 2859-2863) (*Formal synthesis*)



Drawback for scale up: Use of Hoveyda Grubbs' II catalyst at a very early stage and AD-mix- α makes it less cost effective in a scale up protocol

3. (*J. Med. Chem.* **2018**, 61, 5664-5678) (*Total synthesis*)



Drawback for scale up: Highly divergent scheme with diastereomeric separation. Not amenable for scale up.

Figure 2. Reported synthetic approaches towards cladosporin.

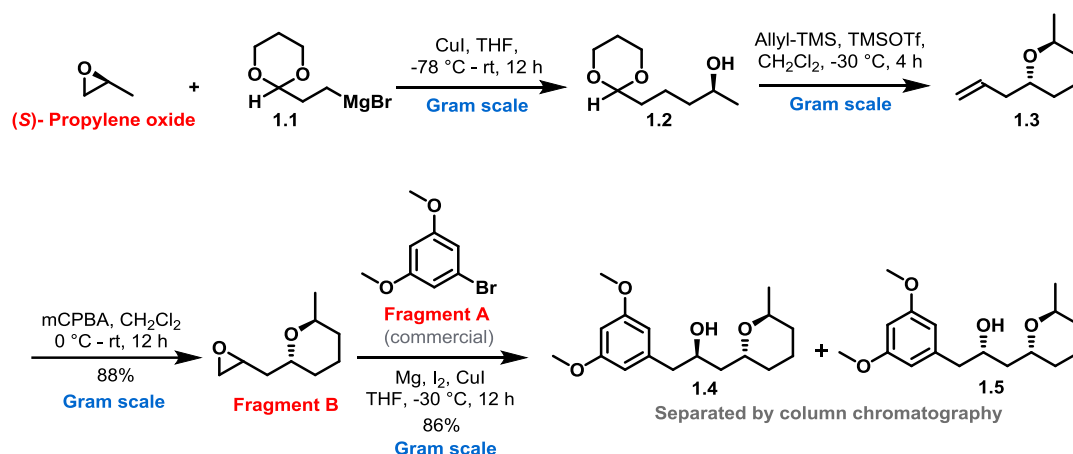
1.2.2. Results and discussion

Considering the above facts, we needed an optimized route that can furnish sufficient quantities of the active natural product for further biological profiling and relevant studies. We also needed the synthetic route to be efficient in respect to production cost, synthetic efforts, and time consumption. Considering the requirements, herein we discuss a modified approach to access cladosporin in “gram-scale” (Scheme 1).

Chapter 1 (Section B): Gram Scale Synthesis of Cladosporin

1.2.2.1. Synthesis of key alcohol fragment

Our synthesis commenced with the known intermediate **1.3** (prepared through a reported protocol⁹) which was subjected to epoxidation using mCPBA reagent to furnish its corresponding epoxide (fragment B) as an inseparable diastereomeric mixture (1:1 dr). The formation of epoxide was confirmed through analysis of the ¹H NMR spectrum where the appearance of a multiplet at 3.99-3.88 ppm for two protons is visible. Besides, the presence of m/z peak at 179.1040 correspondings to [M+Na]⁺ in HRMS further confirms the formation of the required compound. The epoxide thus obtained, on Grignard reaction with commercially available 1-bromo-3,5-dimethoxybenzene (fragment A) gave a 1:1 diastereomeric mixture of alcohols (**1.4** and **1.5**) with an excellent overall yield of 86% (Table 1).



Scheme 1. Synthesis of key alcohol fragment.

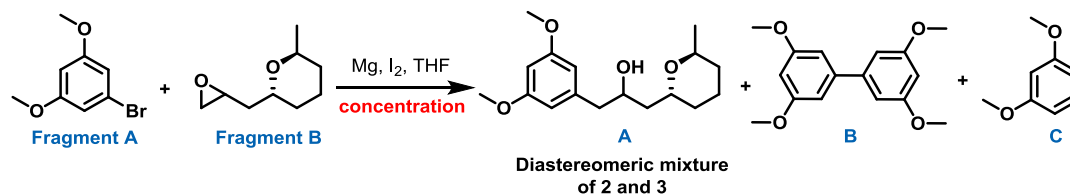
1.2.2.2. Optimization of Grignard reaction

Generation of Grignard reagent from commercially available 1-bromo-3,5-dimethoxybenzene (**fragment A**) was initially conducted under 1 M concentration. The addition of the concerned electrophile (**fragment B**) in presence of CuI did not lead to the formation of required alcohol **1.4** and **1.5**; instead, two major products **B** and **C** were isolated where a major amount of **fragment A** got dimerized to form compound **B** along with debromination to afford compound **C**. It is worth mentioning that maintaining a low concentration of Grignard reagent (< 0.5 M) is a key factor for a

Chapter 1 (Section B): Gram Scale Synthesis of Cladosporin

successful generation of the Grignard reagent. Higher concentrations of Grignard reagent results in an unrequired dimerized product (Table 1).

The diastereoisomeric mixture of alcohols **1.4** and **1.5** was effectively separated using simple silica gel column chromatography to obtain multigram quantities of each in a single batch operation.



Concentration	% yield		
	A	B	C
~ 1M	very low	65	23
less than 0.5 M	86	7	12

Table 1. Optimization of Grignard reaction.

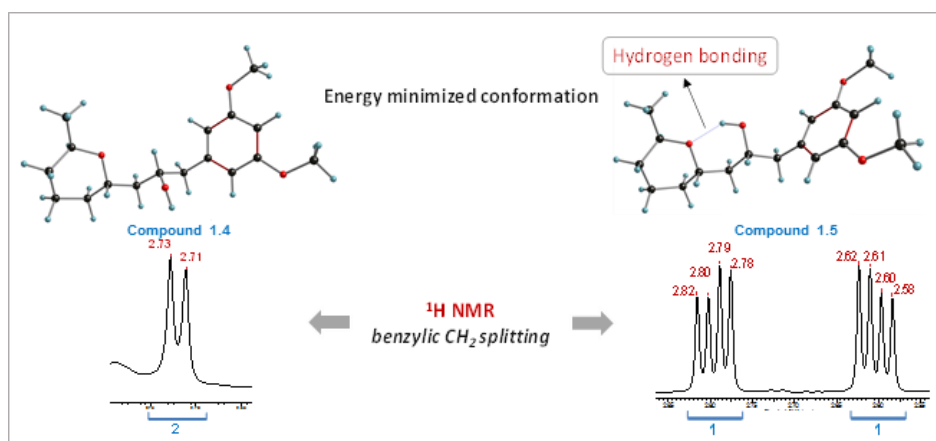
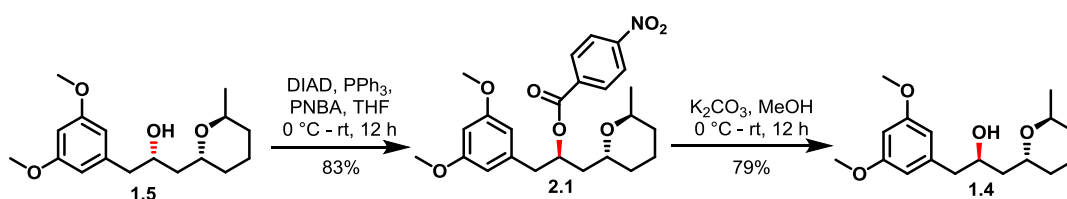


Figure 3. Difference in $^1\text{H NMR}$ splitting in compound **2** and **3**.

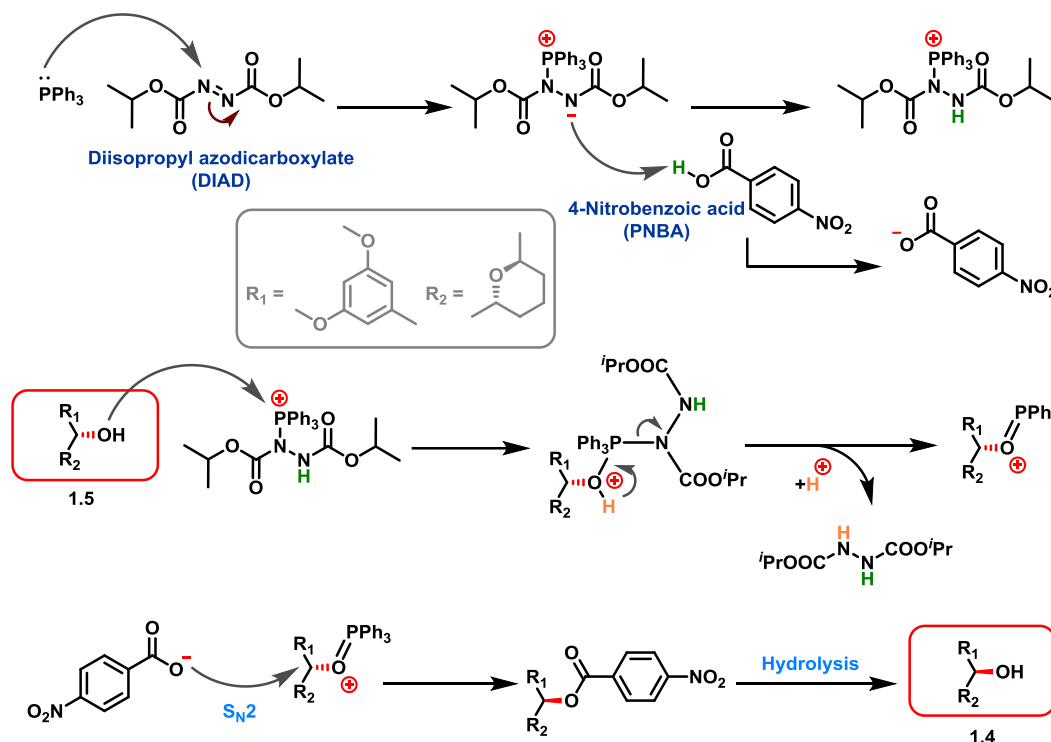
In this context, we made interesting observations while analyzing $^1\text{H NMR}$ data of compound **1.4** and **1.5**. The nature and chemical shifts of all the concerned protons for both the diastereomers were identical except the benzylic protons which showed a major difference, especially in the splitting pattern. Compound **1.4** showed a clean doublet at 2.72 ppm whereas an AB quartet pattern was observed for the benzylic protons of compound **1.5**. To understand the significant difference in the $^1\text{H NMR}$

Chapter 1 (Section B): Gram Scale Synthesis of Cladosporin

spectra we generated the energy minimized conformer for both diastereomers (**1.4** and **1.5**) using Gaussian. Unlike compound **1.4**, compound **1.5** was found to exhibit hydrogen bonding between the secondary alcohol functionality and the tetrahydropyran (THP) oxygen. This H-bonding interaction inevitably leads to a more constrained conformational rigidity in the case of compound **1.5** which in turn might have manifested in an AB quartet type splitting for the benzylic protons (Figure 3).



Mechanism:

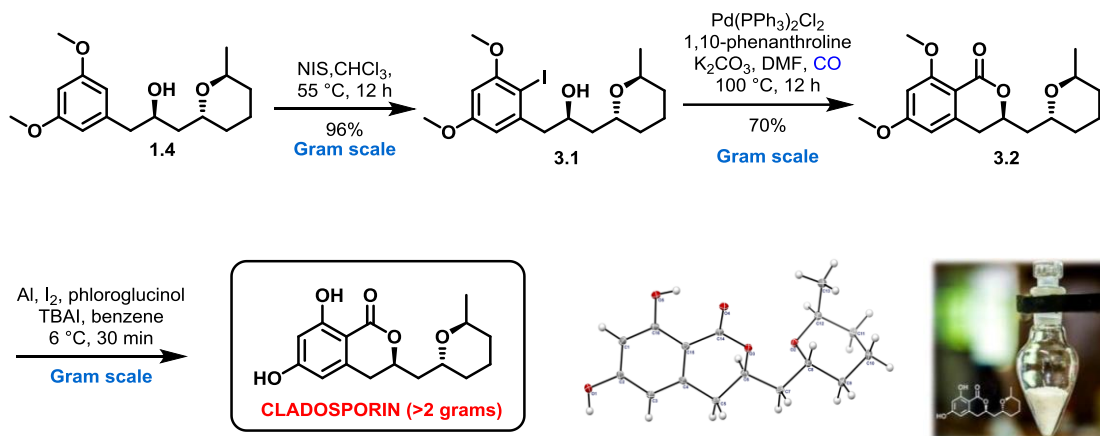


Scheme 2. Mitsunobu inversion of compound **1.5**.

Compound **1.4** holds the required stereochemical arrangements for the synthesis of cladosporin. Hence, to utilize the undesired diastereomer, compound **1.5** was subjected to Mitsunobu reaction followed by ester hydrolysis which led to the complete inversion

Chapter 1 (Section B): Gram Scale Synthesis of Cladosporin

of the secondary alcohol center in **1.5** to furnish the required diastereomeric alcohol **1.4** in good yields (Scheme 2). After having multi-gram quantities of the required alcohol **1.4** our next task was to effectively construct the lactone moiety, which after several trials, was planned to be synthesized using palladium catalyzed carbon monoxide insertion reaction. As per the plan, compound **1.4** was converted to its corresponding iodo compound **3.1** using *N*-iodosuccinimide (NIS) and catalytic *p*TSA in chloroform. The iodo-compound **3.1** was treated with Pd(PPh₃)₂Cl₂, potassium carbonate, and 1,10-phenanthroline in presence in DMF at 100 °C under a blanket of carbon monoxide to obtain the desired compound **3.2** in 70% yield.¹¹ After complete characterization and confirmation of compound **3.2**, we subjected the same to aluminium triiodide mediated exhaustive demethylation¹² to afford cladosporin in more than two gram scale (**Scheme 3**). The spectral data of the synthesized natural product was in complete accordance with the documented values in literature.^{9, 10} Besides, the structure and relative stereochemistry of the synthesized compound was further confirmed by single-crystal X-ray diffraction analysis for an unambiguous assignment of its stereocenters.

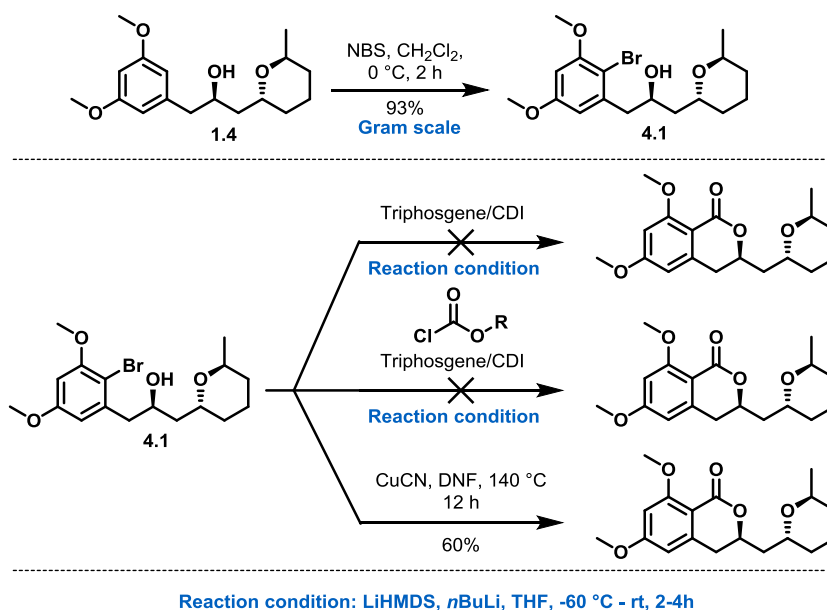


Scheme 3. Gram scale synthesis of cladosporin.

Herein, we would also like to document a few attempts that were initially tried to construct the six-membered lactone moiety (Scheme 4). For the same, alcohol **1.4** was treated with *N*-bromosuccinimide (NBS) in CH₂Cl₂ to afford bromo-compound **3.1** in excellent yield. In this context, it is worth mentioning that the addition of an exact 1 equivalent of NBS is crucial to avoid the di-bromination of the starting material.

Chapter 1 (Section B): Gram Scale Synthesis of Cladosporin

Besides, maintaining a temperature of 0 °C and a high dilution of the reaction also assists in avoiding unwanted di-bromination. The obtained bromo compound **4.1** was then treated with *n*BuLi, LiHMDS to generate the corresponding dianion which was in turn quenched with electrophiles like carboxydiimidazole (CDI), triphosgene, methyl chloroformate, and ethyl chloroformate which did not lead to any fruitful result (Scheme 4). Besides, we also tried to construct the lactone moiety through copper insertion in the carbon-halogen bond followed by protodecupration (copper-mediated tandem cyanation-lactonization).¹³ For the same we treated bromo compound **4.1** with CuCN in DMF at 140 °C for 12 hours, which led to the formation of the required lactone **2.2** with a decent yield of 60%. But the same was not reproducible when conducted in a single batch gram scale operation.



Scheme 4. Alternatives towards lactonization.

1.2.3. Conclusion

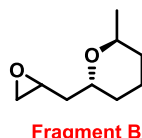
We have accomplished a scalable synthesis for potent anti-malarial natural product cladosporin. Gram-scale operations, Mitsunobu inversion to convert undesired alcohol to required one, and palladium-catalyzed carbon monoxide insertion reaction to construct six-membered lactone ring are the highlights of the work discussed herein.

Chapter 1 (Section B): Gram Scale Synthesis of Cladosporin

Presently we have more than two grams of cladosporin which is sufficient enough for a proper and an in-depth assessment of its pharmacokinetics and pharmacodynamics.

1.2.4. Experimental section

(2S,6R)-2-methyl-6-(oxiran-2-ylmethyl)tetrahydro-2H-pyran (fragment B).



To a solution of compound **1.3** (3.5 g, 24.96 mmol) in CH_2Cl_2 (35 mL) at 0 °C was added 55% mCPBA (11.6 g, 67.246 mmol) in one portion. The reaction mixture was warmed to room temperature and stirred for 12 h. After completion, the reaction mixture was quenched with a saturated solution of $\text{Na}_2\text{S}_2\text{O}_3$ followed by a saturated solution of NaHCO_3 and extracted with CH_2Cl_2 (25 mL x 3). The organic layer was dried over anhydrous Na_2SO_4 , filtered, and concentrated under *vacuo* to give a yellow oil which was purified by column chromatography on (SiO_2 , pet ether/ ethyl acetate 9:1) to afford the corresponding diastereomeric mixture (1:1) of epoxide as a colorless oil (**fragment B**) (3.45 g, 88%):

IR (film) $\nu_{\text{max}} = \text{cm}^{-1}$ 2931, 1444, 1380, 1038 cm^{-1} .

^1H NMR (400 MHz, CDCl_3): δ 3.99 – 3.88 (m, 2H), 3.03 – 3.00 (m, 1H), 2.75 (dt, $J = 12.1, 4.5$ Hz, 1H), 2.47 (ddd, $J = 8.0, 4.9, 2.7$ Hz, 1H), 2.02 – 1.91 (m, 1H), 1.67 – 1.64 (m, 4H), 1.55 – 1.42 (m, 1H), 1.36 – 1.29 (m, 2H), 1.17 (m, 3H, diastereomeric mixture) ppm.

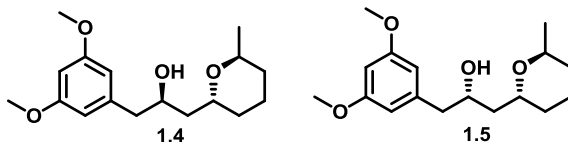
^{13}C NMR (100 MHz, CDCl_3): $\delta = 68.9, 68.6, 67.3, 50.2, 50.0, 47.3, 46.9, 36.9, 36.3, 31.5, 30.5, 30.0, 19.6, 18.4$ ppm.

HRMS (ESI) m/z : $[\text{M} + \text{Na}]^+$ calcd. for $\text{C}_9 \text{H}_{16}\text{O}_2\text{Na}$ 179.1043, found 179.1040.

(R)-1-(3,5-dimethoxyphenyl)-3-((2R,6S)-6-methyltetrahydro-2H-pyran-2-yl)propan-2-ol (compound 1.4) & (3-((S)-2-hydroxy-3-((2R,6S)-6-

Chapter 1 (Section B): Gram Scale Synthesis of Cladosporin

methyltetrahydro-2H-pyran-2-yl)propyl)-5-methoxyphenoxy)methylum
(compound 1.5).



To an oven-dried two-neck round-bottomed flask equipped with a magnetic stir bar was added activated magnesium metal (2.34 g, 97.379 mmol) under argon atmosphere. THF (200 mL) was added followed by the addition of a pinch of I₂ and was stirred vigorously for 30 min. 1-bromo-3,5-dimethoxy benzene (**fragment A**) (20.59 g, 94.853 mmol) dissolved in THF (50 mL) was added dropwise to the stirring solution. The onset of exothermic reaction was characterized by decolorization of I₂. The resulting mixture was stirred for 2 h. The freshly prepared Grignard reagent was cooled to -30 °C followed by the addition of Copper (I) iodide (1.05 g, 25 mol%). A solution of fragment B (3.45 g, 22.084 mmol) in THF (15 mL) was added dropwise and left to stir for 16 h at -30°C. The reaction mixture was quenched with saturated aqueous NH₄Cl (30 mL) and extracted with diethyl ether (30 mL x 3). The combined organic layers were dried over anhydrous Na₂SO₄ and concentrated under *vacuo*. The resulting mixture of diastereomers thus obtained as yellowish oil was purified and separated by column chromatography (SiO₂, pet ether/ ethyl acetate 8:2) to afford corresponding alcohols **1.4** (2.67 g) and **1.5** (2.93 g) as yellowish oil with an overall yield of 86%.

Compound 1.4:

IR (film) ν_{\max} = cm⁻¹ 3422, 2933, 1594, 1147 cm⁻¹.

$[\alpha]_{\text{D}}^{25}$ = -20.3 (*c* = 0.6, CHCl₃).

¹H NMR (400 MHz, CDCl₃): δ = 6.38 (d, *J* = 1.9 Hz, 2H), 6.33 (d, *J* = 1.9 Hz, 1H), 4.08 (m, 2H), 3.96 (dd, *J* = 11.6, 4.9 Hz, 1H), 3.77 (s, 6H), 2.78 (s, 1H), 2.71 (d, *J* = 6.6 Hz, 2H), 1.85 (ddd, *J* = 14.2, 9.3, 2.7 Hz, 1H), 1.64 (m, 4H), 1.47 (ddd, *J* = 14.3, 8.6, 3.2 Hz, 1H), 1.39 – 1.30 (m, 2H), 1.20 (d, *J* = 6.6 Hz, 3H) ppm.

Chapter 1 (Section B): Gram Scale Synthesis of Cladosporin

¹³C NMR (100 MHz, CDCl₃): δ = 160.7, 141.2, 107.3, 98.2, 69.6, 67.6, 55.2, 44.3, 39.6, 30.8, 30.5, 18.7, 18.3 ppm.

HRMS (ESI) *m/z*: [M + Na]⁺calcd for C₁₇ H₂₆O₄Na⁺ 317.1723, found 317.1716.

Compound 1.5:

IR (film) ν_{\max} = cm⁻¹ 3458, 2934, 1594, 1147 cm⁻¹;

[α]_D²⁵ = -12.2 (*c* = 2.7, CHCl₃);

¹H NMR (500 MHz, CDCl₃) δ 6.38 (d, *J* = 1.7 Hz, 2H), 6.32 (s, 1H), 4.04 (ddd, *J* = 12.2, 10.3, 3.8 Hz, 2H), 3.94 (dd, *J* = 10.2, 7.9 Hz, 1H), 3.77 (s, 6H), 2.79 (dd, *J* = 13.4, 6.5 Hz, 1H), 2.59 (dd, *J* = 13.4, 6.6 Hz, 1H), 1.78 – 1.57 (m, 5H), 1.45 – 1.42 (m, 1H), 1.34 – 1.29 (m, 2H), 1.20 (d, *J* = 6.6 Hz, 3H);

¹³C NMR (125 MHz, CDCl₃) δ 160.7, 141.1, 107.4, 98.1, 73.3, 71.8, 67.7, 55.2, 44.2, 39.4, 31.1, 30.6, 18.8, 18.1;

HRMS (ESI)*m/z*: [M + Na]⁺calcd for C₁₇ H₂₆O₄Na 317.1723, found 317.1716.

Mitsunobu Inversion of compound 1.5 to compound 1.4.

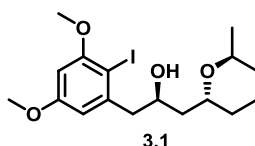
Compound **1.5** (2.93 g, 9.953 mmol) was dissolved in THF (25 mL) followed by the addition of triphenylphosphine (5.2 g, 19.825 mmol), 4-nitrobenzoic acid (1.97 g, 11.789 mmol) at 0 °C. A solution of diisopropyl azodicarboxylate (DIAD) (4.02 mL, 19.301 mmol) in THF (15 mL) was added dropwise to the stirring solution. The reaction mixture was allowed to warm to room temperature and stirred overnight. The solvent was removed under rotary evaporation and the crude was forwarded without further purification.

To a methanolic solution of this ester (3.6 g, 8.664 mmol) was added K₂CO₃ (2.4 g, 17.329 mmol) and stirred at room temperature for 4 h. After completion of the reaction, methanol was removed under *vacuo* and the product was extracted with ethyl acetate (20 mL x 3). The combined organic layers were dried over anhydrous Na₂CO₃ and concentrated under reduced pressure. The crude thus obtained was purified through column chromatography to afford compound **2** as a yellowish oil (2.45 g, 83% in two

Chapter 1 (Section B): Gram Scale Synthesis of Cladosporin

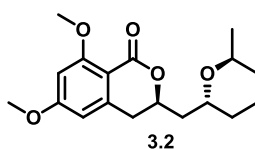
steps). The spectral data of the product is in complete agreement with compound **1.4** synthesized in the Grignard reaction step.

(R)-1-(2-iodo-3,5-dimethoxyphenyl)-3-((2R,6S)-6-methyltetrahydro-2H-pyran-2-yl)propan-2-ol (compound 2.1).



To a solution of compound **1.4** (5.12 g, 17.391 mmol) in CHCl_3 (20 mL) was added catalytic pTSA followed by the addition of *N*-iodosuccinimide (4.3 g, 19.130 mmol). The reaction mixture was heated at 55 °C for 16 h. After completion of reaction, the reaction mixture was quenched with saturated aqueous NaHCO_3 (35 mL) and extracted with CH_2Cl_2 (20 mL x 3). The collected organic fractions were dried over anhydrous Na_2SO_4 and concentrated under *vacuo* to afford a brown sticky compound **2.1** which was forwarded to the next step without further purification and characterization.

(R)-6,8-dimethoxy-3-(((2R,6S)-6-methyltetrahydro-2H-pyran-2-yl)methyl)isochroman-1-one (compound 2.2).



Compound **2.1** (7.04 g, 16.750 mmol) was dissolved in DMF (35 mL) followed by the addition of K_2CO_3 (4.6 g, 33.5 mmol), 1,10-phenanthroline (1.5 g, 8.375 mmol) and $\text{Pd}(\text{PPh}_3)_2\text{Cl}_2$ (1.2 g, 1.71 mmol). The mixture was stirred for 5 min, purged with carbon monoxide, and stirred at 100 °C under carbon monoxide for 12 h. After completion of reaction, the reaction mixture was extracted with ethyl acetate (20 mL x 3). The collected organic layers were dried over anhydrous Na_2SO_4 and concentrated under *vacuo* to afford a brown sticky mass which was purified by column chromatography (SiO_2 , pet ether/ ethyl acetate 1:1) to furnish lactone **2.2** as a foamy solid (3.75 g, 70%).

IR (film) $\nu_{\text{max}} = \text{cm}^{-1}$ 2932, 1713, 1601, 1159, 1077 cm^{-1} .

Chapter 1 (Section B): Gram Scale Synthesis of Cladosporin

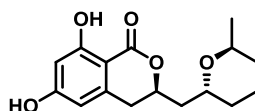
$[\alpha]_D^{25} = +36.76$ ($c = 1.2$, CHCl_3).

$^1\text{H NMR}$ (400 MHz, CDCl_3): $\delta = 6.38$ (s, 1H), 6.28 (s, 1H), 4.56 (dd, $J = 11.0, 8.7$ Hz, 1H), 4.06 (t, $J = 8.3$ Hz, 1H), 3.92 (s, 1H), 3.90 (s, 3H), 3.84 (s, 3H), 2.91 – 2.77 (m, 2H), 1.91 – 1.80 (m, 2H), 1.69 – 1.60 (m, 4H), 1.33 – 1.27 (m, 2H), 1.18 (d, $J = 6.5$ Hz, 3H) ppm.

$^{13}\text{C NMR}$ (100 MHz, CDCl_3): $\delta = 164.3, 163.0, 162.8, 144.0, 107.1, 103.8, 97.7, 74.4, 67.6, 66.1, 56.1, 55.5, 39.6, 35.5, 31.0, 30.8, 18.8, 18.2$ ppm.

HRMS (ESI) m/z [$\text{M} + \text{Na}$] $^+$ calcd for $\text{C}_{18}\text{H}_{24}\text{O}_5\text{Na}^+$ 343.1516, found 343.1508.

Cladosporin.



A suspension of Al powder (15.9 g, 588.889 mmol) in dry benzene (65 mL) was treated with I_2 (55.5 g, 201.706 mmol) under Ar and the violet mixture was stirred under reflux for 30 min until the color had changed to a colorless mixture. After the mixture was cooled to 6 °C, a few crystals of TBAI (177.8 mg, 0.551 mmol) and phloroglucinol (7.4 g, 58.524 mmol) were added before a solution of lactone **2.2** (3.75 g, 11.705 mmol) in dry benzene (12 mL) was added in one portion. The resulting green-brown suspension was stirred for 30 min at 6 °C before saturated $\text{Na}_2\text{S}_2\text{O}_3$ solution (20 mL) and ethyl acetate (45 mL) were added. After separation of the layers, the aqueous phase was extracted with ethyl acetate (35 mL x 3). The combined organic layers were washed with brine, dried over Na_2SO_4 , filtered, and concentrated under *vacuo*. Purification by column chromatography (SiO_2 , pet ether/ ethyl acetate 17:3) afforded cladosporin (2.1 g, 62%) as a white solid.

Melting point: 172-173 °C.

IR (film) $\nu_{\text{max}} = \text{cm}^{-1}$ 3416, 3022, 1656, 1218 cm^{-1} .

$[\alpha]_D^{25} = -15.24$ ($c = 0.5$, EtOH).

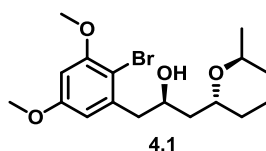
Chapter 1 (Section B): Gram Scale Synthesis of Cladosporin

$^1\text{H NMR}$ (400 MHz, CDCl_3): δ = 11.08 (s, 1H), 6.29 (s, 1H), 6.16 (s, 1H), 4.68 (t, J = 9.5 Hz, 1H), 4.11 (s, 1H), 4.00 (s, 1H), 2.89 – 2.76 (m, 2H), 1.99 – 1.93 (m, 1H), 1.86 – 1.81 (m, 1H), 1.71 – 1.63 (m, 4H), 1.36 – 1.34 (m, 2H), 1.23 (d, J = 6.5 Hz, 3H) ppm.

$^{13}\text{C NMR}$ (100 MHz, CDCl_3): δ = 169.9, 164.3, 163.0, 141.8, 106.7, 102.0, 101.6, 76.3, 68.0, 66.5, 39.3, 33.6, 30.9, 18.9, 18.1 ppm.

HRMS (ESI) m/z $[\text{M} + \text{H}]^+$ calcd for $\text{C}_{16}\text{H}_{21}\text{O}_5^+$ 293.1384, found 293.1379.

(R)-1-(2-bromo-3,5-dimethoxyphenyl)-3-((2R,6S)-6-methyltetrahydro-2H-pyran-2-yl)propan-2-ol (compound 3.1).



To a solution of compound **1.4** (5.1 g, 17.391 mmol) in CH_2Cl_2 (300 mL) was added *N*-bromosuccinimide (3.1 g, 17.391 mmol) at 0 °C and stirred for 1 h at the same temperature. The reaction mixture was quenched with saturated aqueous NaHCO_3 (55 mL) and extracted with CH_2Cl_2 (50 mL x 3). The collected organic fractions were dried over anhydrous Na_2SO_4 and concentrated under *vacuoto* afford a yellowish sticky mass (compound **3.1**) which was forwarded to next step without further purification.

X-ray crystal structure of cladosporin (ORTEP diagram)

X-ray intensity data measurements of all sulphonamides were carried out on a Bruker D8 VENTURE Kappa Duo PHOTON II CPAD diffractometer equipped with Incoatech multilayer mirrors optics. The intensity measurements were carried out with Mo micro-focus sealed tube diffraction source ($\text{Cu-K}\alpha = 1.543 \text{ \AA}$) at 100(2) K temperature. The X-ray generator was operated at 50 kV and 1.4 mA. A preliminary set of cell constants and an orientation matrix were calculated from two sets of 20 frames. Data were collected with ω scan width of 0.5° at different settings of φ and 2θ with a frame time of 40 seconds keeping the sample-to-detector distance fixed at 4.00 cm. The X-ray data collection was monitored by APEX3 program (Bruker, 2016). All the data were corrected for Lorentzian, polarization and absorption effects using SAINT and

Chapter 1 (Section B): Gram Scale Synthesis of Cladosporin

SADABS programs (Bruker, 2016). SHELX-97 was used for structure solution and full matrix least-squares refinement on F2. Molecular diagrams were generated using ORTEP-33 and Mercury programs. Geometrical calculations were performed using SHELXTL and PLATON. All the hydrogen atoms were placed in geometrically idealized position and constrained to ride on their parent atoms. An ORTEP III view of both compounds were drawn with 50% probability displacement ellipsoids and H-atoms are shown as small spheres of arbitrary radii.

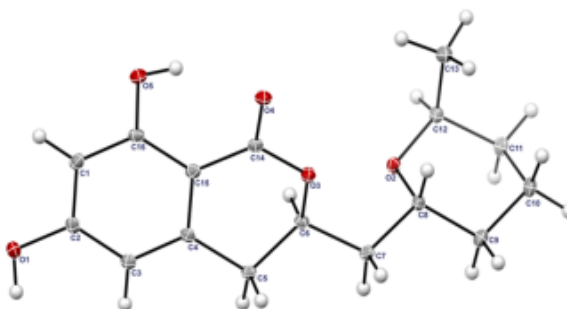


Figure 4. ORTEP diagram of cladosporin.

Crystallographic data for cladosporin (C₁₆H₂₀O₅): M = 292.32, Crystal dimensions 0.440 x 0.230 x 0.120 mm³, Orthorhombic, space group P2₁2₁2₁, a = 8.5341(7) Å, b = 11.6093(10) Å, c = 14.2508(12) Å, α = 90° β = 90° γ = 90°, V = 1411.9(2) Å³, Z = 4, ρ_{calcd} = 1.375 Mg/m³, μ (Cu-Kα) = 0.842 mm⁻¹, F(000) = 624, 2θ_{max} = 77.493°, T = 100(2) K, 28190 reflections collected, 2796 unique reflections (R(int) = 0.0336), 2796 observed (I > 2σ(I)) reflections, multi-scan absorption correction, T_{min} = 0.793, T_{max} = 0.904, refined parameters, No. of restraints 0, S = 0.753, R₁ = 0.0282, wR₂ = 0.095 (all data R₁ = 0.0287, wR₂ = 0.0945), maximum and minimum residual electron densities; Δρ_{max} = 0.272, Δρ_{min} = -0.218 (e⁻Å⁻³). Crystallographic data for compound intermediate deposited with the Cambridge Crystallographic Data Centre as supplementary publication no CCDC 1862372.

1.2.5. References

1. Scott, P. M.; Van Walbeek, W.; Maclean, W. M. Cladosporin, a new antifungal metabolite from *Cladosporium cladosporioides*. *J. Antibiot.* **1971**, *24*, 747–755.

Chapter 1 (Section B): Gram Scale Synthesis of Cladosporin

2. Hoepfner, D.; McNamara, C. W.; Lim, C. S.; Studer, C.; Riedl, R.; Aust, T.; McCormack, S. L.; Plouffe, D. M.; Meister, S.; Schuierer, S.; Plikat, U.; Hartmann, N.; Staedtler, F.; Cotesta, S.; Schmitt, E. K.; Petersen, F.; Supek, F.; Glynne, R. J.; Tallarico, J. A.; Porter, J. A.; Fishman, M. C.; Bodenreider, C.; Diagona, T. T.; Movva, N. R.; Winzeler, E. A. Selective and specific inhibition of the *Plasmodium falciparum* lysyl-tRNA synthetase by the fungal secondary metabolite cladosporin. *Cell Host Microbe* **2012**, *11*, 654–663.
3. Sharma, A.; Sharma, M.; Yogavel, M.; Sharma, A. Protein Translation Enzyme lysyl-tRNA Synthetase Presents a New Target for Drug Development against Causative Agents of Loiasis and Schistosomiasis *PLoS Neglected Trop. Dis.* **2016**, *10*, 1–19.
4. Springer, J. P.; Cutler, H. G.; Crumley, F. G.; Cox, R. H.; Davis, E. E.; Thean, J. E. Plant growth regulatory effects and stereochemistry of cladosporin. *J. Agric. Food Chem.* **1981**, *29*, 853–855.
5. Kimura, Y.; Shimomura, N.; Tanigawa, F.; Fujioka, S.; Shimada, A. Plant Growth Activities of Aspyran, Asperentin, and its Analogues Produced by the Fungus *Aspergillus* sp. *Z Naturforsch C.* **2012**, *67*, 587–593.
6. Anke, H. *J. Antibiot. (Tokyo)* Metabolic products of microorganisms. **1979**, *32*, 952–958.
7. Miller, J. D.; Sun, M.; Gilyan, A.; Roy, J.; Rand, T. G. Inflammation-associated gene transcription and expression in mouse lungs induced by low molecular weight compounds from fungi from the built environment. *ChemBiol Interact.* **2010**, *183*, 113–124.
8. Das, P.; Babbar, P.; Malhotra, N.; Sharma, M.; Jachak, G. R.; Gonnade, R. G.; Shanmugam, D.; Harlos, K.; Yogavel, M.; Sharma, A.; Reddy, D. S. *J. Med. Chem.* **2018**, *61*, 5664–5678.
9. Zheng, H.; Zhao, C.; Fang, B.; Jing, P.; Yang, J.; Xie, X.; She, X. Asymmetric Total Synthesis of Cladosporin and Isocladosporin. *J. Org. Chem.* **2012**, *77*, 13, 5656–5663.
10. Mohapatra, D. K.; Maity, S.; Rao, T. S.; Yadav, J. S.; Sridhar, B. An efficient formal total synthesis of cladosporin. *Eur. J. Org. Chem.* **2013**, *2013*, 2859–2863.

Chapter 1 (Section B): Gram Scale Synthesis of Cladosporin

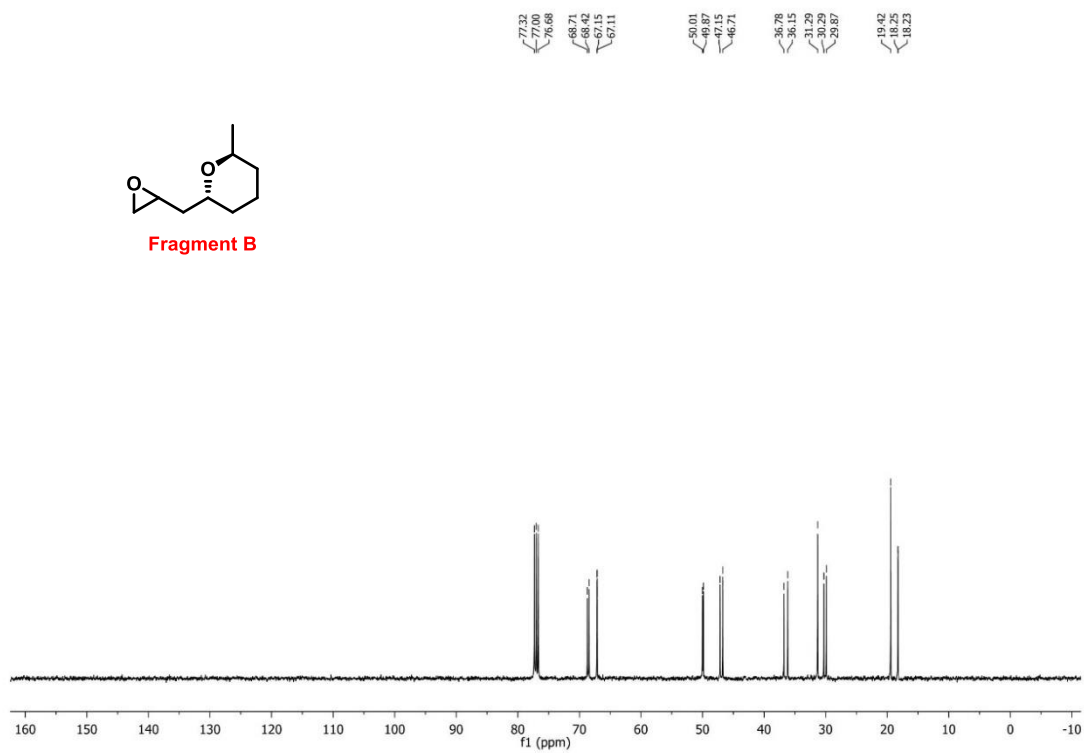
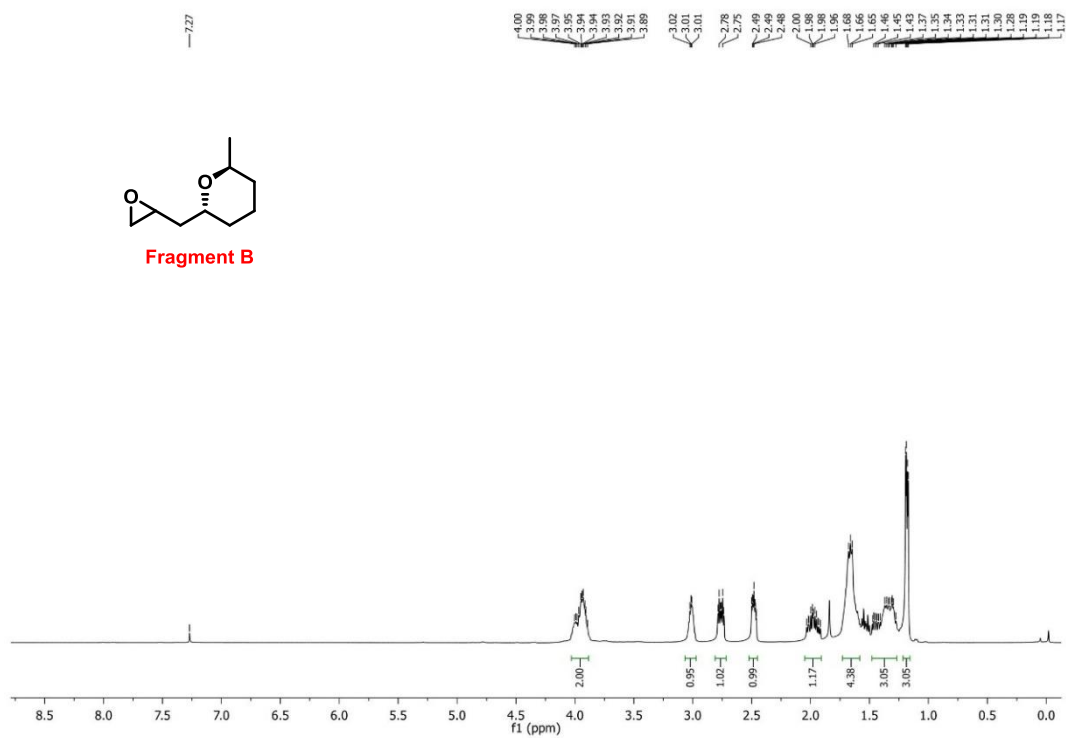
11. Srinivas, B. T. V.; Maadhur, A. R.; Bojja, S. Total synthesis of racemic, natural (+) and unnatural (–) scorzocreticin. *Tetrahedron*, **2014**, 70, 8191–8167.
12. Tian, J.; Sang, D. Application of aluminum triiodide in organic synthesis. *ARKIVOC*, **2015**, ark.5550190, 446–493.
13. Nookraju, U.; Begari, E.; Kumar, P. Total synthesis of (+)-monocerin via tandem dihydroxylation-SN₂ cyclization and a copper mediated tandem cyanation–lactonization approach. *Org. Biomol. Chem.* **2014**, 12, 5973–5980.



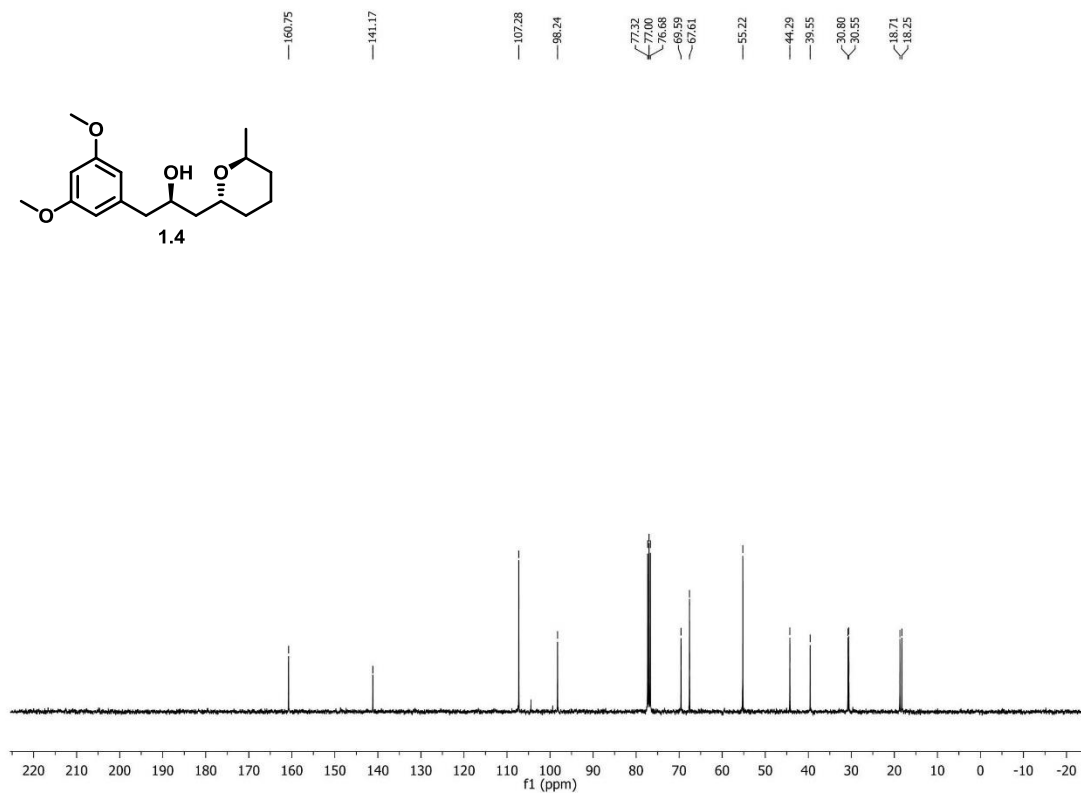
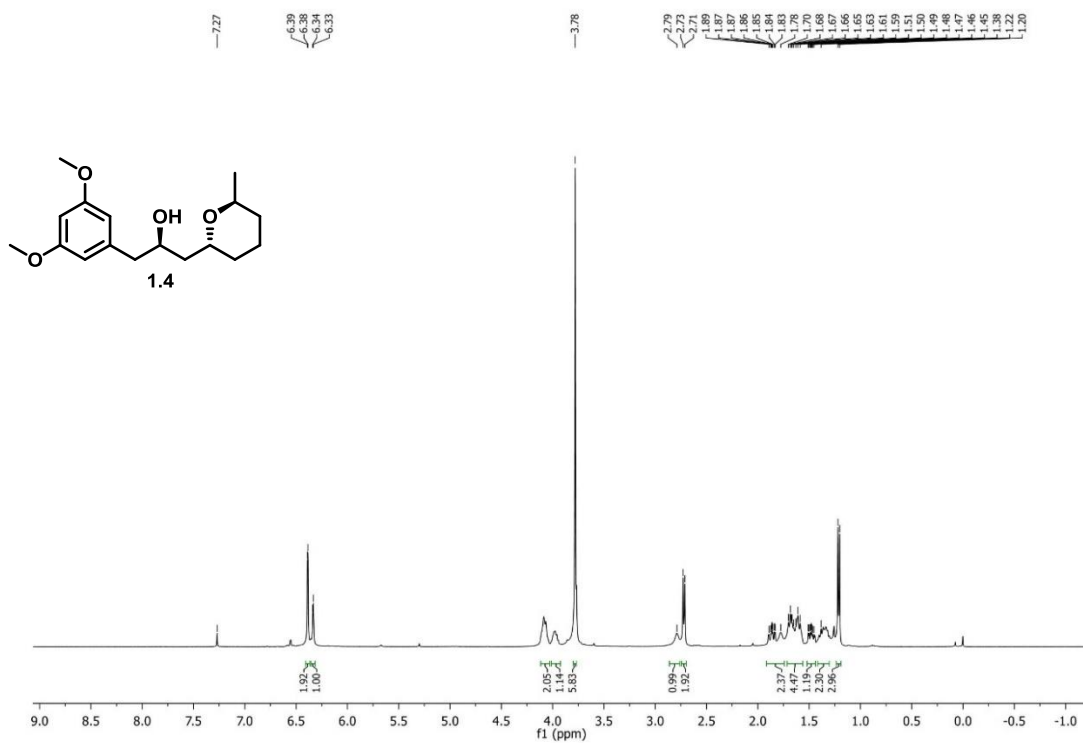
**Copies of
 ^1H and ^{13}C NMR Spectra of Selected
Compounds**



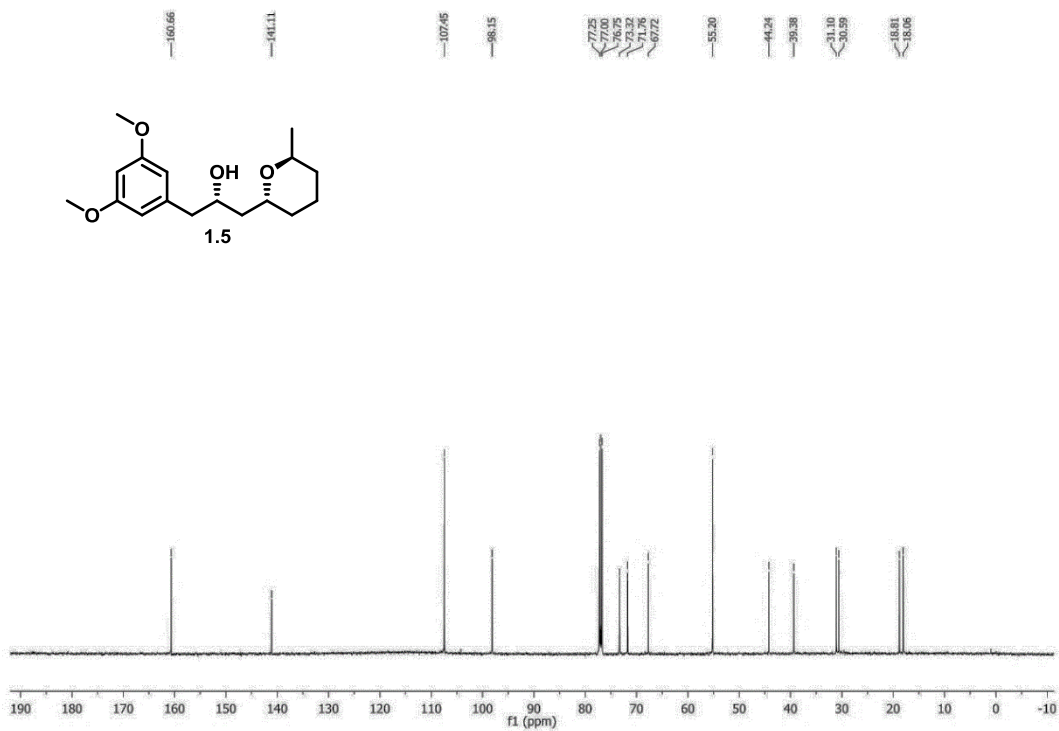
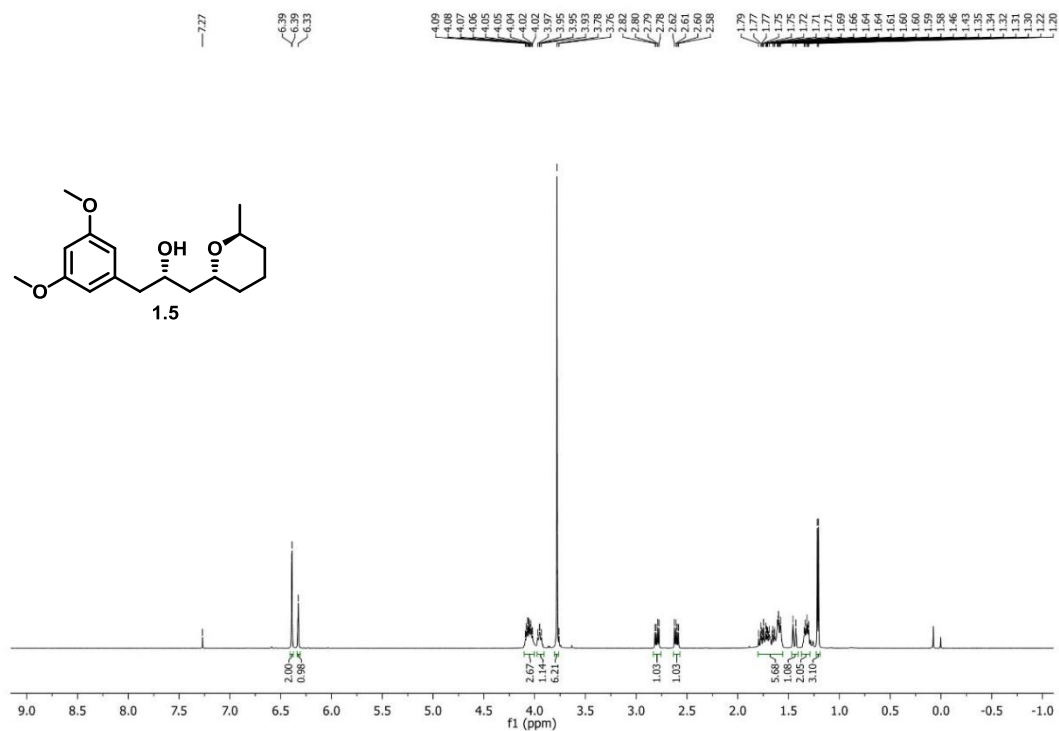
Chapter 1 (Section B): Gram Scale Synthesis of Cladosporin



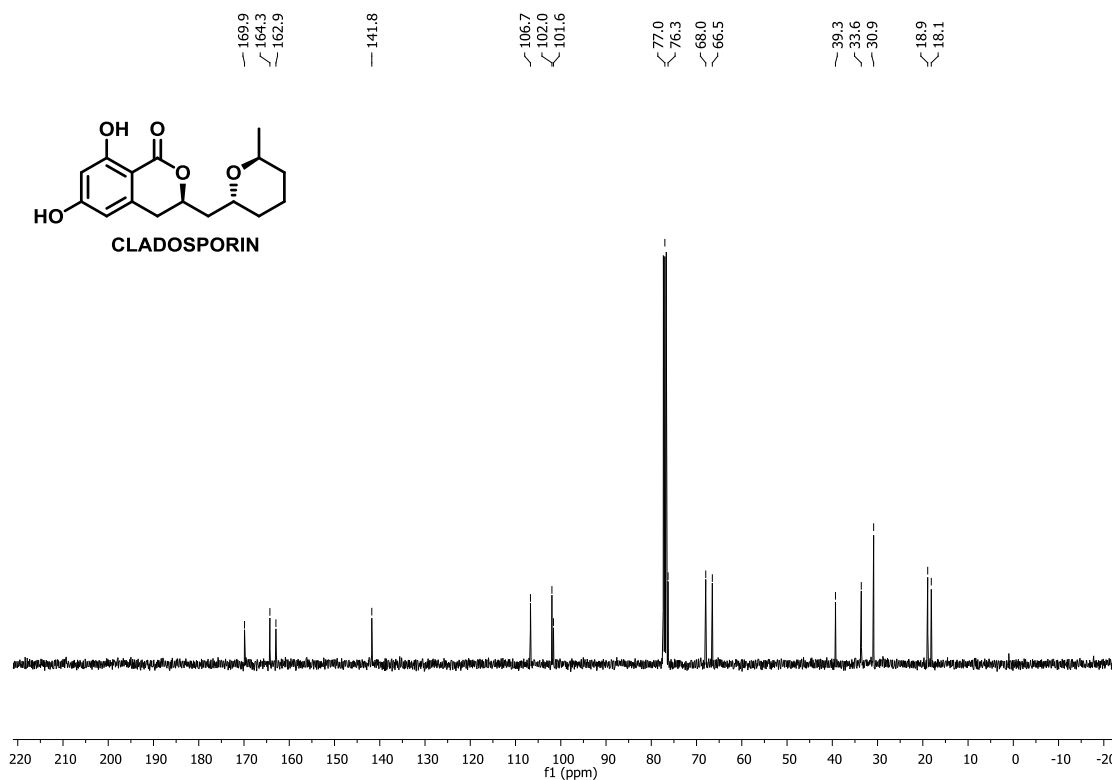
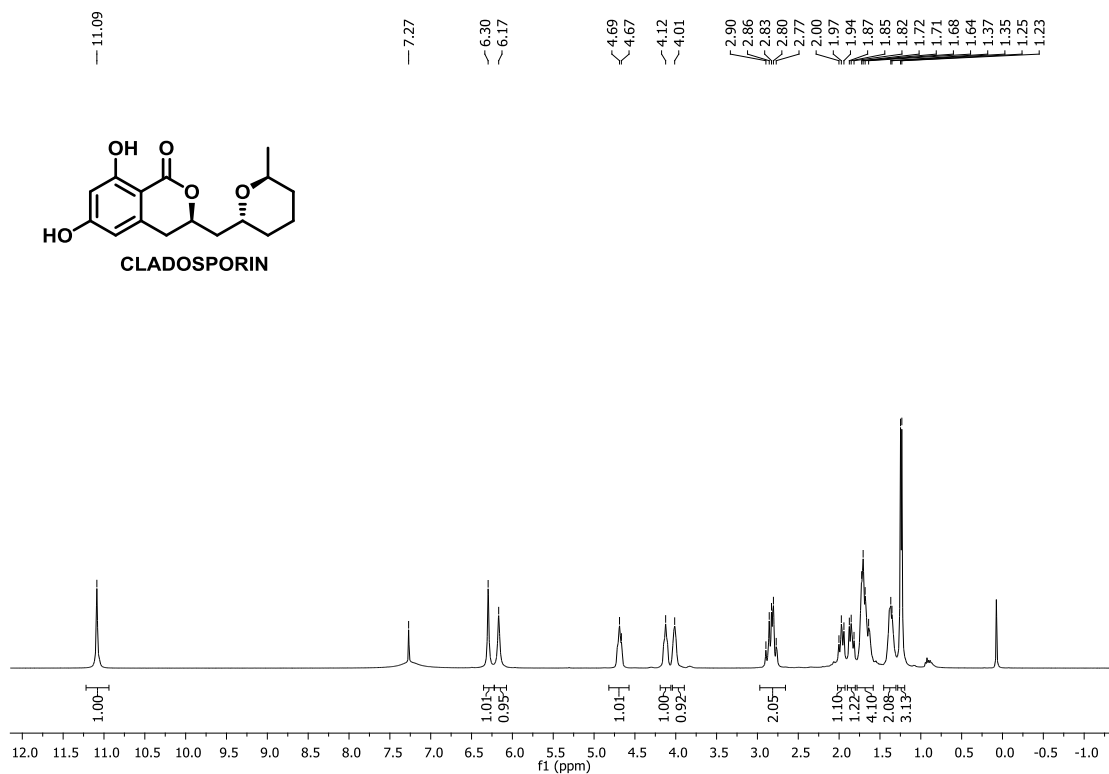
Chapter 1 (Section B): Gram Scale Synthesis of Cladosporin



Chapter 1 (Section B): Gram Scale Synthesis of Cladosporin



Chapter 1 (Section B): Gram Scale Synthesis of Cladosporin





FIRST CHAPTER

Section C



**Design, Synthesis, Biological Evaluation of lysyl
tRNA synthetase (KRS) Inhibitors based on
Cladosporin Scaffold towards Identification of
Antimalarial Leads**

Chapter 1 (Section C): Design, Synthesis, Biological Evaluation of Lysyl tRNA synthetase (KRS) Inhibitors based on Cladosporin Scaffold towards Identification of Antimalarial Leads

1.3.1 Introduction

Protein bio-synthesis is a core biological process which is crucial for the maintenance of life form. From the perspective of drug development and medicinal chemistry, proteins as enzymes have been a popular class of drug targets for several marketed drugs. In this context, aminoacyl-tRNA synthetases (AARSs), a specific class of enzymes responsible for the covalent attachment of specific amino acids to their cognate tRNAs,¹ deserves special mention. This pivotal role of AARSs in protein bio-synthesis has made them an interesting drug target in present times. For instance, popular antibacterial drug Mupirocin, used for treating *Staphylococcus aureus* infections, acts through the inhibition of isoleucyl-tRNA synthetase (IleRS) of gram-positive bacteria.^{2,3} Likewise, Indolmycin was discovered to be highly selective against prokaryotic tryptophanyl (TrpRS) and targets human pathogens like *Helicobacter pylori* and *Staphylococcus aureus*.^{4,5,6} Halofuginone, a halogen derivative of natural product febrifugine further acts on prolyl tRNA synthetase (ProRS)^{7,8} Its piperidine ring occupies the amino-acid pocket whereas its quinazolinone part colonizes the 3' end of the tRNA binding pocket. The drug is FDA approved to treat coccidiosis in poultry caused by *Eimeria tenella* and cryptosporidiosis in cattle caused by *Cryptosporidium parvum*. Due to its mammalian toxicity it could not be used as an antimalarial drug (Figure 1).^{9,10}

In this very context of anti-malarial drug discovery, cladosporin deserves a special mention. It is a potent anti-malarial natural product that targets parasitic cytosolic lysyl tRNA synthetase or *PfKRS* (a class of aminoacyl-tRNA synthetase) in *Plasmodium falciparum*, which happens to be one of the prominent causative pathogen of malaria, and hence terminating the protein bio-synthesis process inside the parasite, thus leading to parasitic death.^{11, 12, 13} Speaking on structural basis, cladosporin, an anti-fungal antibiotic and plant growth regulator isolated from *Cladosporin cladosporioides* and *Aspergillus flavus* in 1971,^{14, 15} is a complex chiral molecule bearing a 6,8-dihydroxyl isocoumarin ring joined to tetrahydropyran group with a methyl moiety, which together mimics the adenosine moiety of ATP (natural substrate of *PfKRS*) and thereby inhibits

Chapter 1 (Section C): Design, Synthesis, Biological Evaluation of Lysyl tRNA synthetase (KRS) Inhibitors based on Cladosporin Scaffold towards Identification of Antimalarial Leads

the enzyme by competing with ATP.^{12, 13} This specific enzyme inactivation leads to the termination of parasitic protein bio-synthesis and leads to parasitic death. More interestingly, cladosporin restricts parasitic growth in both liver and blood stage infection with activity in nano-molar range. Besides, it demonstrates an impressive selectivity of >100 folds for parasitic KRS (*Pf*KRS) over human counterpart (*Hs*KRS).^{12, 13} This exquisite species specific selectivity of cladosporin has been attributed to residues val329 and ser346 which seem to be sterically crucial for accommodating the methyl moiety of THP ring in case of *Plasmodium falciparum*.^{12, 13} Apart from malarial cladosporin has also proved to be effective by targeting KRSs of several other species like *Cryptosporidium parvum*, *Loa loa* and *Schistosoma mansoni*.^{16, 17}

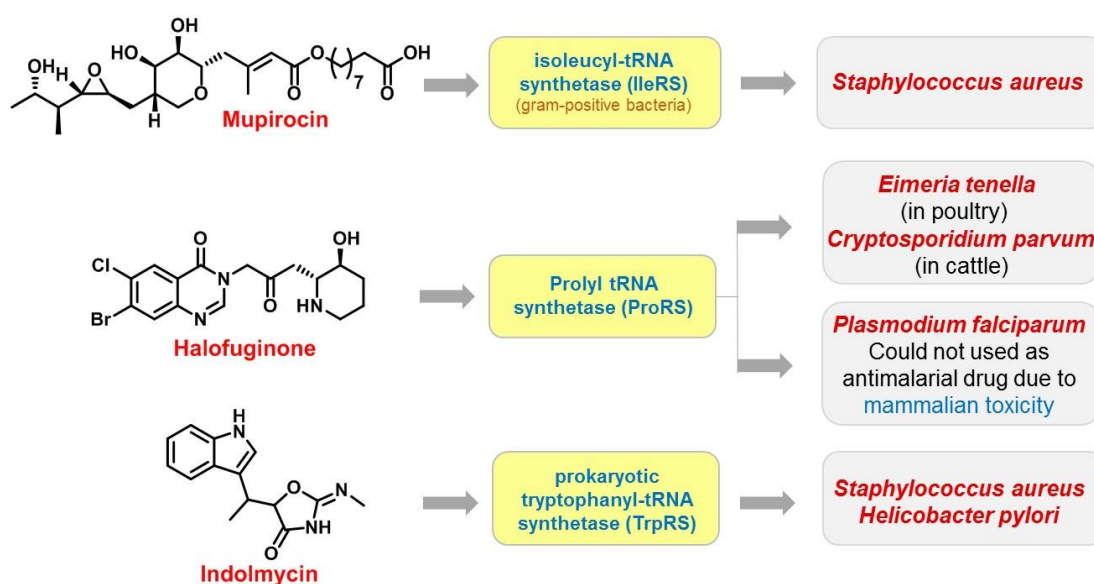


Figure 1. Aminoacyl-tRNA synthetases (AARSs) as drug targets.

In spite of having such impressive biological profile, cladosporin is not compliant to be developed as a drug lead owing to its low bio-availability and high metabolic instability. As efforts to increase the metabolic stability of cladosporin research has been ongoing along with peer reviewed publications from our group and other groups around the world where it has been demonstrated how proposed inhibitors inspired from cladosporin targets the universal conserved ATP pocket.¹⁸ As a part of our previous

Chapter 1 (Section C): Design, Synthesis, Biological Evaluation of Lysyl tRNA synthetase (KRS) Inhibitors based on Cladosporin Scaffold towards Identification of Antimalarial Leads

work, we have deciphered the effect of stereochemical modifications of cladosporin scaffolds on its anti-malarial potency, where we have synthesized all the possible stereoisomers of cladosporin and evaluated their anti-plasmodial potency through enzyme and cell based assays.¹⁹ Our study revealed that out of three chiral centers of cladosporin, two are prerequisite for anti-malarial action.¹⁹ (Chapter 1, Section A)

In this very section of the thesis, we will be discussing the Structural Activity Relationship (SAR) studies on a broad library of compounds which were designed and synthesized based on cladosporin core scaffold, so as to come up with a potent and modified anti-malarial lead with enhanced drug-like properties. The entire library of analogues was tested in vitro against *Plasmodium falciparum* and *Homo sapiense* KRS enzyme (*PfKRS* and *HsKRS*) along with in vivo parasite inhibition assay. Besides, the metabolic stability of selected potent compounds were also tested in human and liver microsomes. The top lead compound **CL-2** was further studied for interaction with its target KRS wherein the *PfKRS*-CL-2 co-crystal structure revealed new features of enzyme-drug interaction. This work hence provides a valuable lead compound with enhanced metabolically stability, equal selectivity and potent as that of cladosporin.

1.3.2. Synthesis of analogue library around cladosporin scaffold

After gaining valuable information from high-resolution X-ray data from co-crystal of cladosporin and *PfKRS*,^{15, 19} we synthesized a library of compounds by varying different substitutions around the cladosporin core structure. All the variations are grouped in to four categories (Figure 2). Major structural variations have been incorporated in the aromatic dihydroisocoumarin moiety and the tetrahydropyran counterpart of the natural product. Functional group variations have also been conducted in the methylene functionality of the linker. Besides, related analogues with major variations, modifications and combinations have also been highlighted herein. (Figure 2).

Chapter 1 (Section C): Design, Synthesis, Biological Evaluation of Lysyl tRNA synthetase (KRS) Inhibitors based on Cladosporin Scaffold towards Identification of Antimalarial Leads

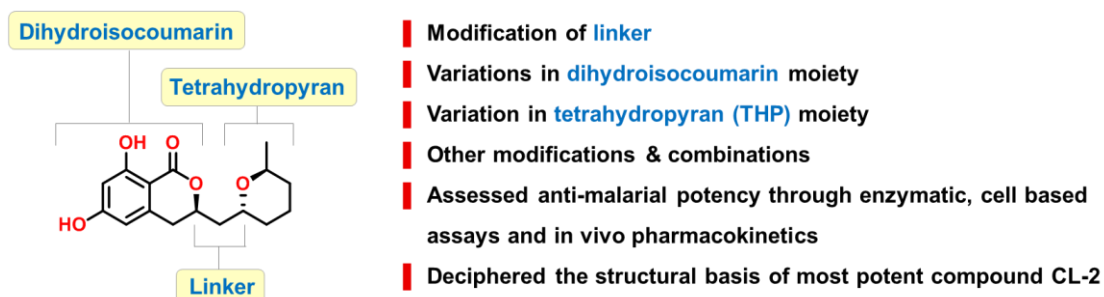
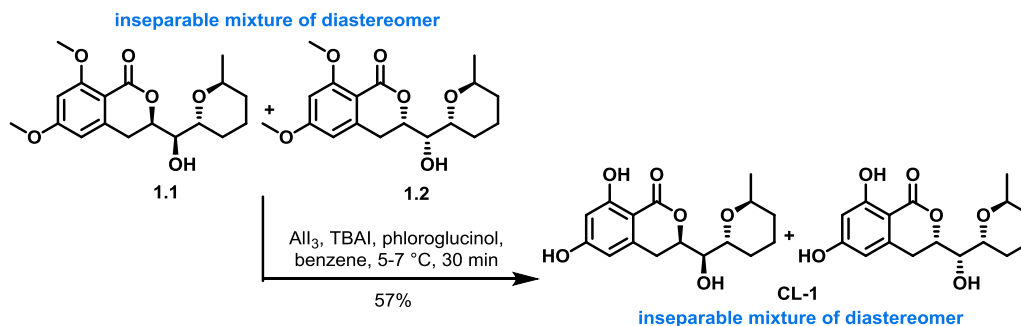


Figure 2. Planned variations around cladosporin scaffold.

1.3.2.1. Modification at linker

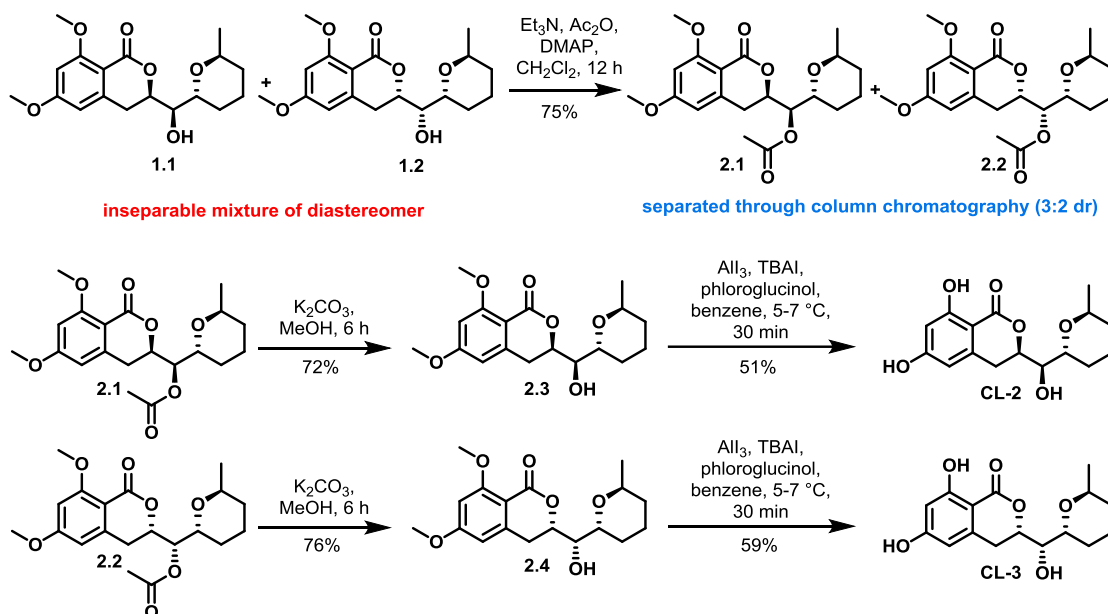
Hydrogen bonding interaction is one of the crucial interaction that defines the binding of a drug molecule with the target protein (enzyme). In this context, the importance of hydroxyl (-OH) functionality is of crucial significance. This very functional group can engage into relevant hydrogen bonding interaction within the active site of the target protein/enzyme. This interaction in turn can result in a better binding of the drug molecule to the target enzyme which can eventually lead to an increased therapeutic efficiency. Alongside, the inherent polarity of the -OH group can further increase the hydrophilicity or aqueous solubility of the molecule leading to an improved bio-availability. Based on this hypothesis, we envisioned to introduce an extra -OH functionality in the linker region of the natural product so as to have an increased hydrophilicity and an enhanced binding of the same with the active site of the parasitic target enzyme (*PfKRS*).



Scheme 1. Synthesis of racemic hydroxyl-cladosporin (CL-1).

Chapter 1 (Section C): Design, Synthesis, Biological Evaluation of Lysyl tRNA synthetase (KRS) Inhibitors based on Cladosporin Scaffold towards Identification of Antimalarial Leads

Initially we planned to synthesize racemic version of the planned analogue (**CL-1**, inseparable mixture of diastereomers). Our synthesis started with diastereomeric mixture of compound **1.1** and **1.2**,¹⁹ which upon exhaustive demethylation furnished **CL-1** as a mixture of diastereomer (Scheme 1).



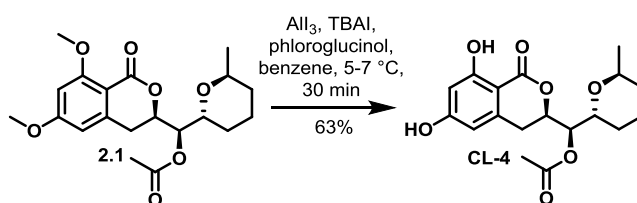
Scheme 2. Synthesis of both diastereomers (**CL-2** and **CL-3**) of **CL-1**.

Biological evaluation of the racemic hydroxy cladosporin through enzymatic and cell-based assay revealed impressive potency (explained in results and discussion) as compared to cladosporin. The impressive activity of the analogue (**CL-1**) intrigued us to synthesize both the diastereomers (**CL-2** and **CL-3**) of **CL-1** in chiral pure forms (Scheme 2). For this purpose, we treated dimethoxy protected racemic hydroxy-cladosporin (compound **1.1** and **1.2**) with acetic anhydride and Et₃N which led to the acetylation of the secondary –OH group. While monitoring the progress of reaction through TLC, we found a clean separation of the diastereoisomers under 50% EtOAc/pet ether mobile phase. Both the acetylated diastereomers were then cleanly separated through column chromatography. After successful separation, both the isomers were characterized completely using NMR and IR spectroscopy along with HRMS. The appearance of a singlet peak at 2.07 ppm and 2.13 ppm in the ¹H NMR spectrum of compound **2.1** and **2.2** respectively further confirmed a successful

Chapter 1 (Section C): Design, Synthesis, Biological Evaluation of Lysyl tRNA synthetase (KRS) Inhibitors based on Cladosporin Scaffold towards Identification of Antimalarial Leads

acetylation. Besides the presence of mass peak at 379.1751 corresponding to $[M+H]^+$ further supports the success of the reaction. Having synthesized these chiral pure diastereomers, they were deacetylated using K_2CO_3 and methanol, followed by AlI_3 mediated exhaustive demethylation to afford both the diastereomers of hydroxy-cladosporin (**CL-2** and **CL-3**) in chiral pure form (Scheme 2).

To, further strengthen our hypothesis and experimental data of correlation, between hydrogen bonding and potency of the compound, we planned to synthesize an analogue (**CL-4**) where the linker $-OH$ group is protected with an acetate functionality. This will in turn nullify the possibility of any hydrogen bonding interaction between the concerned analogue and active site of *Pf*KRS. As a part of our synthesis, we took previously synthesized compound **2.1** and subjected the same to AlI_3 mediated exhaustive demethylation which in turn furnished the final analogue **CL-2**. The disappearance of the peaks at 3.91 ppm and 3.84 ppm in the 1H NMR of **CL-4** corresponding to the two aromatic methoxy functionality confirmed a successful demethylation. Besides the appearance of peaks at 11.05 ppm and 7.11 ppm in the 1H NMR spectrum corresponding to the phenolic $-OH$ groups also confirms the formation of the required product. Presence of $[M+H]^+$ peak at 351.1438 in HRMS also adds to the successful formation of **CL-4** (Scheme 3).



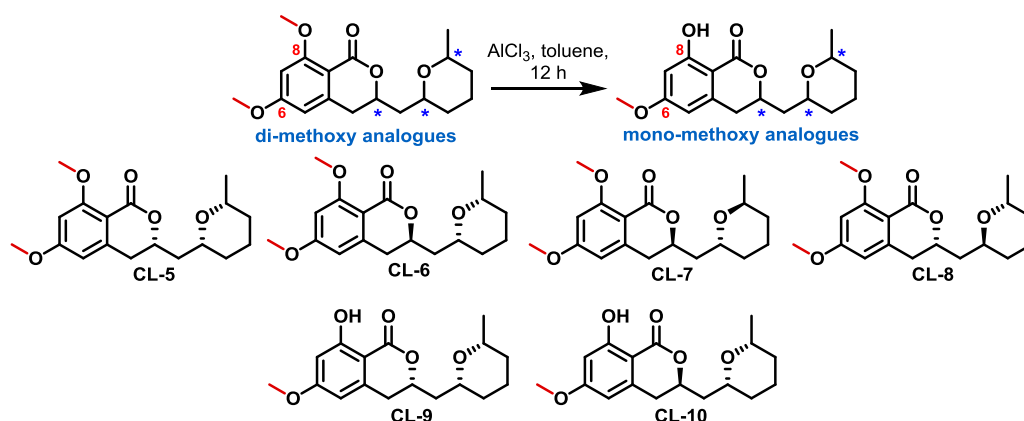
Scheme 3. Synthesis of **CL-4**.

1.3.2.2. Modifications at dihydroisocoumarin moiety

As mentioned earlier, $-OH$ functional group is of significance importance in the context of medicinal chemistry and drug development, as this polar functional group can efficiently engage itself in relevant and crucial hydrogen bonding interaction in the active site of the biological target. In this case, cladosporin consists of two phenolic $-$

Chapter 1 (Section C): Design, Synthesis, Biological Evaluation of Lysyl tRNA synthetase (KRS) Inhibitors based on Cladosporin Scaffold towards Identification of Antimalarial Leads

OH groups *meta* to each other. To decipher, whether these –OH groups are responsible for active hydrogen bonding interaction within the active site of *PfKRS*, we successfully synthesized analogues where both the –OH groups remain protected as methyl ethers so as to nullify any possible hydrogen bonding interaction within the active site of *PfKRS*. We also synthesized analogues where only C6-OH group remains selectively protected. As a part of synthesis, we utilized dimethoxy protected analogues and treated the same with AlCl_3 in toluene, which led to selective demethylation of C8-OMe group to furnish 6-methoxy analogues of cladosporin. (Scheme 4)

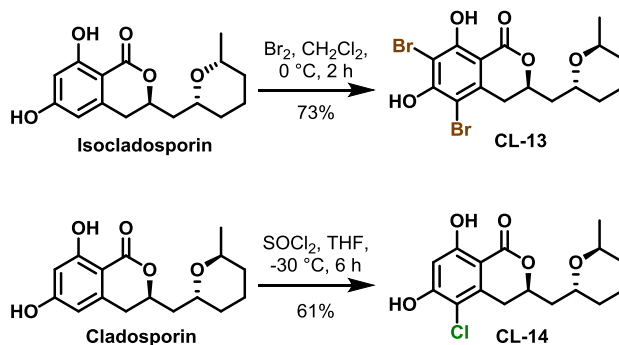


Scheme 4. Synthesis of hydroxyl group protected analogues.

As discussed earlier (Chapter 1, Section A), we have synthesized all the eight possible stereoisomers of cladosporin, and in depth biological evaluation of the entire stereoisomeric set led to the identification of two active stereochemical scaffold (cladosporin/**CLADO-1** and isocladosporin/**CLADO-5**) that exhibited promising anti-malarial potency against *Plasmodium falciparum*.¹⁹ In the present work, we analysed the effect of halogen substitution in the aromatic counter part of the two active stereoisomers. For the same, we treated isocladosporin (**CLADO-5**) with bromine in CH_2Cl_2 at 0 °C for 2 h which furnished di-bromo analogue **CL-13** in good yield. The loss of aromatic protons in the region of 6.00 ppm to 6.5 ppm in ^1H NMR spectrum confirmed the di-bromo substitution. Besides, other relevant peaks in the ^1H and ^{13}C NMR spectrum were also in accordance with the structure of **CL-13** (Scheme 5).

Chapter 1 (Section C): Design, Synthesis, Biological Evaluation of Lysyl tRNA synthetase (KRS) Inhibitors based on Cladosporin Scaffold towards Identification of Antimalarial Leads

We further envisioned to decipher the role of chloride substitution in the aromatic counter part of the active scaffold. Treatment of cladosporin (**CLADO-1**) with SOCl_2 in THF at $-30\text{ }^\circ\text{C}$ led to regioselective chlorination of the same to afford **CL-14** (Scheme 5). The disappearance of one of the two aromatic protons in the ^1H NMR confirmed the the mono-substitution. Besides, other relevant peaks in ^1H and ^{13}C NMR further confirmed the structure of the chlorinated analogue (**CL-14**).

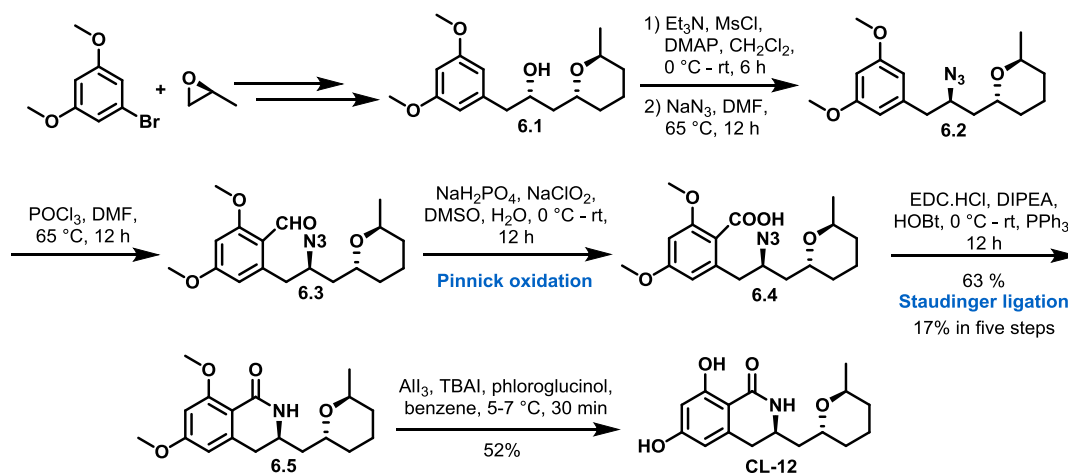


Scheme 5. Synthesis of halogenated analogues, **CL-13** and **CL-14**.

The core structure of cladosporin consists of a dihydroisocoumarin moiety which bears a lactone core. Now, looking from a medicinal chemistry perspective, lactone functional group is often labile in biological conditions, as it can readily get hydrolysed by specific classes of enzymes present in the biological system.²⁰ This metabolic instability might often lead to a reduced efficacy as well. Hence, we planned to switch the lactone functionality with corresponding lactam as the later is comparatively more stable as compared to the lactone congener. As a part of synthesis, we commenced with a known alcohol intermediate **6.1**²¹ which was converted to corresponding mesylated intermediate using triethylamine and methanesulfonyl chloride in presence of catalytic DMAP.²² The obtained mesylated intermediate was then subjected to $\text{S}_\text{N}2$ reaction with sodium azide in DMF to afford azide intermediate **6.2**²³ with a complete inversion of stereochemistry at the azide attached carbon. Intermediate **6.2** was then further subjected to Vilsmeier Haack reaction with DMF and POCl_3 to obtain required aldehyde **6.3** which was in turn treated with NaH_2PO_4 and NaClO_2 in DMSO and water (Pinnick oxidation) to afford acid intermediate **6.4**. The next step was to incorporate the

Chapter 1 (Section C): Design, Synthesis, Biological Evaluation of Lysyl tRNA synthetase (KRS) Inhibitors based on Cladosporin Scaffold towards Identification of Antimalarial Leads

lactam functionality in the core scaffold. Staudinger ligation²⁴ reaction on the same led to the conversion of azide to amine followed by one-pot amide coupling leading to the formation of the final precursor **6.5**. ¹H and ¹³C NMR spectra were in complete correlation with the assigned structure of the intermediate. Beside the presence of mass peak of 320.1856 corresponding to [M+H]⁺ further supports the formation of **6.5**. The next task was to demethylate the aromatic methoxy (-OMe) groups, which was achieved through AlI₃ mediated exhaustive demethylation to furnish aza-cladosporin (**CL-12**). The disappearance of ¹H NMR peaks at 3.92-3.83 ppm corresponding to the aromatic -OMe group in **CL-12** confirms a successful demethylation. Besides appearance of mass peak at 314.1363 corresponding to [M+Na]⁺ further confirms the formation of **CL-12** (Scheme 6).



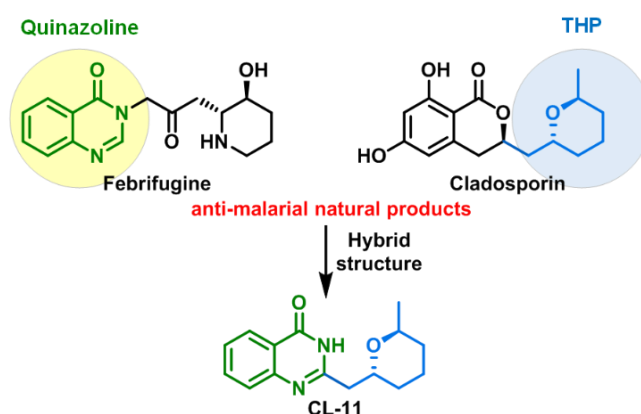
Scheme 6. Synthesis of aza-cladosporin (**CL-12**).

Hybridization of bio-active molecules is a powerful and efficient technique in drug discovery and is often used to target a variety of diseases.²⁵ Based on this concept we designed a hybrid analogue of two potent anti-malarial natural products, namely cladosporin and febrifugine (mentioned in Introduction) where the quinazoline moiety of febrifugine is fused with the tetrahydropyran moiety of cladosporin (Scheme 7).

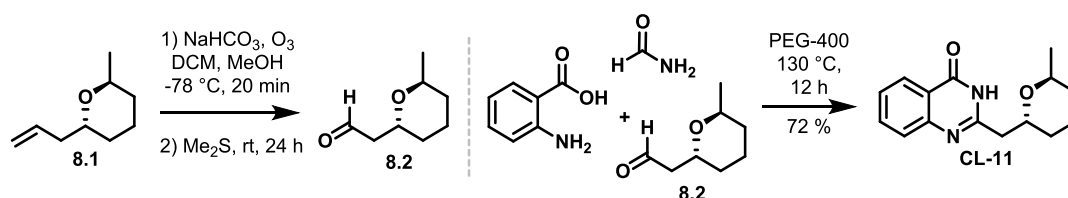
Our synthesis commenced with known THP fragment **8.1**²¹ (synthesized from (*S*)-propylene oxide through relevant functional group interconversion) which was converted to its corresponding aldehyde **8.2** through ozonolysis, followed by

Chapter 1 (Section C): Design, Synthesis, Biological Evaluation of Lysyl tRNA synthetase (KRS) Inhibitors based on Cladosporin Scaffold towards Identification of Antimalarial Leads

condensation with 2-aminobenzoic acid and formamide in PEG-400 to afford the required hybrid analogue **CL-11** (Scheme 8). The presence of ^1H NMR peak at 8.26-7.44 and 3.81-3.55 ppm corresponding to aromatic protons and oxygen attached protons in the THP counterpart respectively confirms the formation of the desired product. Besides a doublet at 1.28 ppm corresponding to the methyl group of THP moiety further adds to the structural confirmation.



Scheme 7. Hybrid analogue of febrifugine and cladosporin.



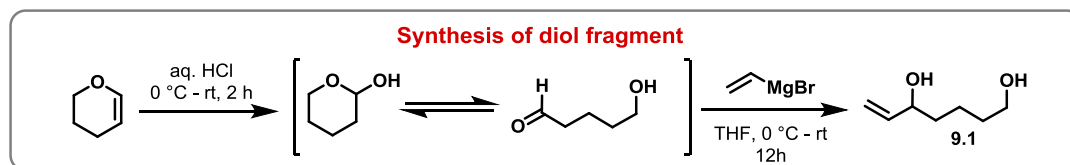
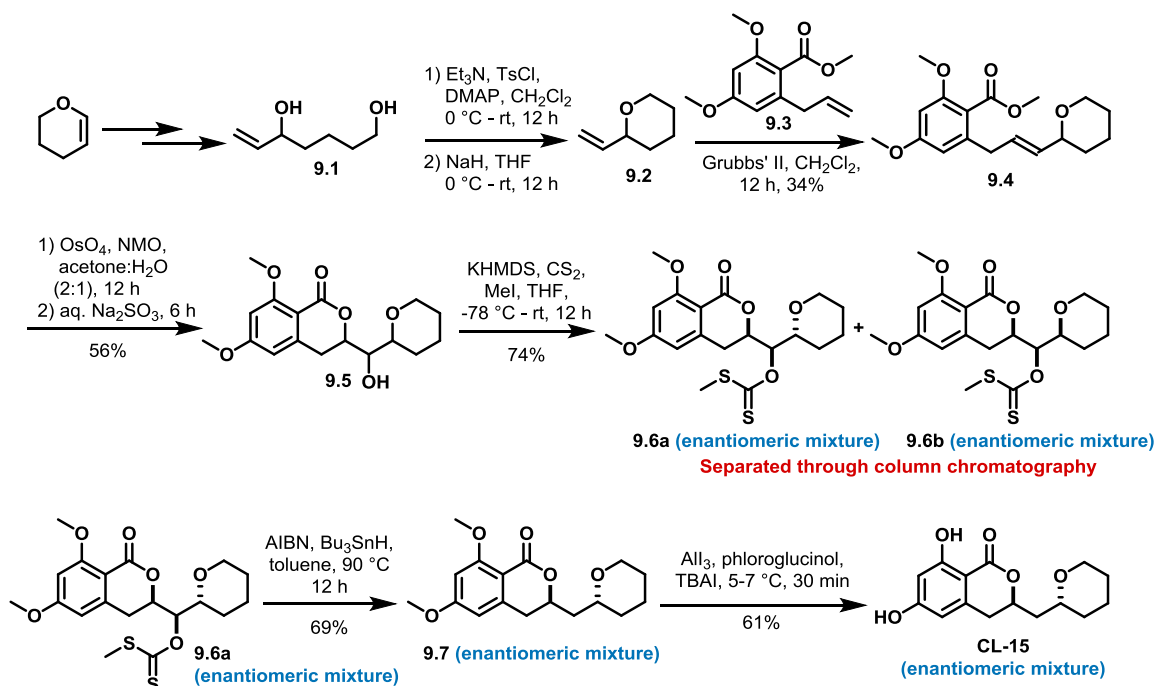
Scheme 8. Synthesis of hybrid analogue (**CL-11**).

1.3.2.3. Modifications at tetrahydropyran moiety

As a part of our analogue synthesis, we planned to incorporate structural variations in the tetrahydropyran moiety of cladosporin as well. In this context, we initially planned to decipher the role of the methyl group residing on C-14 of the tetrahydropyran (THP) moiety of cladosporin. Besides generating an analogue, it will also lead to a simplified cladosporin core structure by eliminating one among the three chiral centers present in the natural product.

Chapter 1 (Section C): Design, Synthesis, Biological Evaluation of Lysyl tRNA synthetase (KRS) Inhibitors based on Cladosporin Scaffold towards Identification of Antimalarial Leads

As a part of synthesis, the diol compound **9.1** was synthesized from 3,4-dihydro-2H-pyran following reported protocol²⁶ which was selectively tosylated using TsCl and Et₃N to furnish corresponding tosylated intermediate. In this step, to ensure mono-tosylation, 0.9 equivalent of TsCl was added and the reaction mixture was monitored frequently through thin layer chromatography (TLC). After accessing the mono-tosylated intermediate, treatment of the same with NaH in THF led to the formation of



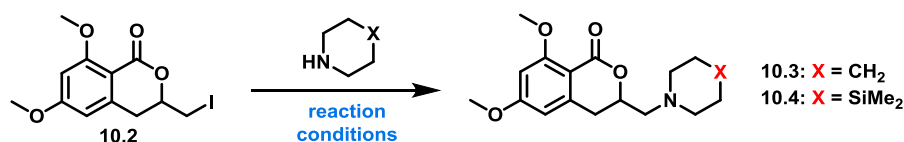
Scheme 9. Synthesis of des-methyl cladosporin (CL-15).

required THP fragment **9.2**, which was further subjected to cross metathesis with fragment **9.3** (synthesized following reported protocol¹⁹) to furnish compound **9.4**. The presence of peaks at 5.76-5.50 ppm in the ¹H NMR corresponding to alkene functionality confirms a successful cross metathesis. Besides, the presence of mass peak at 343.1516 in HRMS corresponding to [M+Na]⁺ further adds up to the structural confirmation. The obtained intermediate **9.4** was then subjected to OsO₄ mediated

Chapter 1 (Section C): Design, Synthesis, Biological Evaluation of Lysyl tRNA synthetase (KRS) Inhibitors based on Cladosporin Scaffold towards Identification of Antimalarial Leads

dihydroxylation and quenching with aq. Na₂SO₃ led to an in situ lactonization of the diol to afford compound **9.5**. Presence of ¹H NMR peak at 4.71 ppm corresponding to the proton attached to the lactone functionality, and HRMS peak at 323.1489 corresponding to [M+H]⁺ confirms the product formation. Compound **9.5** thus obtained, was further converted to its corresponding xanthate ester using KHMDS, CS₂ and MeI to afford diastereomers **9.6a** and **9.6b** which were separated through careful column chromatography with **9.6a** being the major isomer. In our previous work while synthesizing the entire stereoisomeric set of cladosporin, we performed similar reactions to synthesize xanthate esters where the *trans* diastereomer was formed as the major product.¹⁹ Hence, tentatively considering **9.6a** (major diastereomer) as the required *trans* isomer, we subjected the same to Barton McCombie reaction to afford final precursor **9.7**, which was in turn subjected to AlI₃ mediated exhaustive demethylation¹⁹ to furnish the required analogue **CL-15** as enantiomeric mixture (Scheme 9).

To identify the role of tetrahydropyran ring in the antimalarial potency of cladosporin we planned to modify and replace the same with hetero atom containing six membered rings, namely piperazine and 4,4-dimethyl-1,4-azasilinane (Scheme 10). For this purpose, we initially synthesized iodolactone **10.2** from known acid intermediate **10.1**.²⁷ The next step was to knock out the iodo functionality, for which we tried few conditions which did not lead to any fruitful results (Table 1).

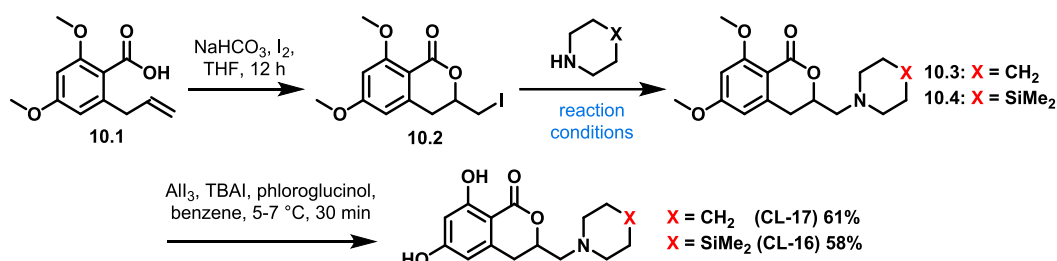


Choice of base	Reaction condition	Yield of product
K ₂ CO ₃	DMF, rt	No reaction progress
K ₂ CO ₃	DMF, 80 °C	No reaction progress
Cs ₂ CO ₃	DMF, 130 °C, Microwave	~26%
Et ₃ N	AcN, 150 °C, Microwave	~67%

Table 1. Optimization of iodo-displacement reaction (S_N2).

Chapter 1 (Section C): Design, Synthesis, Biological Evaluation of Lysyl tRNA synthetase (KRS) Inhibitors based on Cladosporin Scaffold towards Identification of Antimalarial Leads

Finally, treatment of iodolactone **10.2** and the required nucleophile with Et_3N and heating the same at $150\text{ }^\circ\text{C}$ under microwave irradiation furnished the the required intermediate **10.3** and **10.4**. Exhaustive demethylation of the same using AlI_3 afforded the analogues **CL-16** and **CL-17**. (Scheme 10). The presence of lactone attached proton peak at 5.19 ppm, and nitrogen attached proton peak at 3.73-3.38 ppm in ^1H NMR spectrum confirmed the formation of **CL-17**. The presence of lactone attached proton at 5.20 ppm, and nitrogen attached proton at 3.51 ppm confirmed the formation of **CL-16** as well. Besides the appearance of silicon attached methyl peaks at 0.18 ppm and 0.12 ppm in the ^1H NMR further contributes to the structural confirmation of **CL-16**.

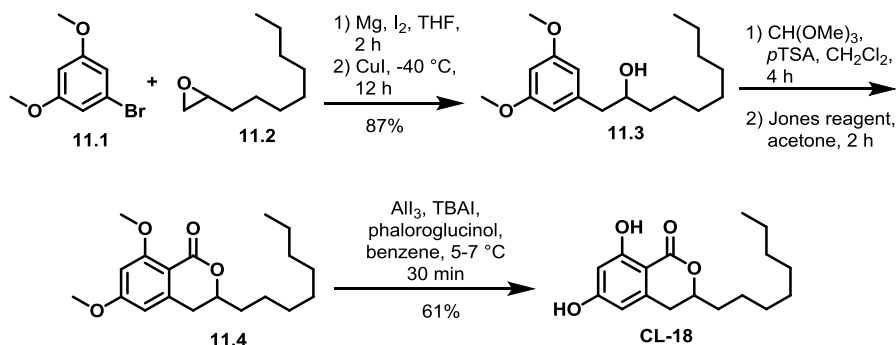


Scheme 10. Synthesis of **CL-16** and **CL-17**.

We also wanted to notice the effect in anti-malarial potency of cladosporin after complete replacement of its tetrahydropyran (THP) moiety. For the same we planned to replace the THP moiety with an eight carbon, saturated, aliphatic long chain. Our synthesis started with known epoxide **11.2** which was reacted with Grignard reagent generated from 1-bromo-3,5-dimethoxybenzene (**11.1**) in presence of CuI to furnish alcohol **11.3**. The presence of three aromatic proton peaks at 6.37-6.34 ppm and seven protons corresponding to one $-\text{OH}$ attached proton and two aromatic $-\text{OMe}$ at 3.82-3.73 ppm confirmed the formation of alcohol **11.3**. Besides the presence of HRMS peak at 295.2268 corresponding to $[\text{M}+\text{H}]^+$ further confirmed a successful Grignard reaction. The obtained alcohol **11.3** was further treated with trimethyl orthoformate in presence of $p\text{TSA}$ followed by Jones oxidation to afford precursor **11.4**. AlI_3 mediated exhaustive demethylation of compound **11.4** afforded the final analogue **CL-18** (Scheme 11). The presence of ^1H NMR peak at 11.15 ppm and 6.70 ppm corresponding

Chapter 1 (Section C): Design, Synthesis, Biological Evaluation of Lysyl tRNA synthetase (KRS) Inhibitors based on Cladosporin Scaffold towards Identification of Antimalarial Leads

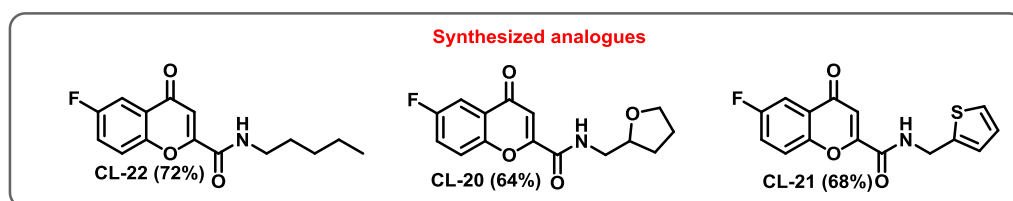
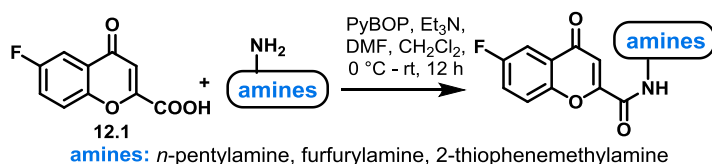
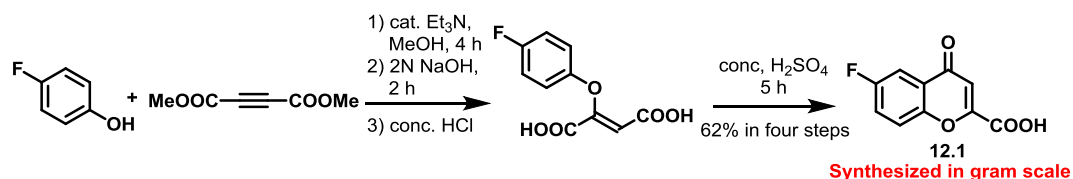
to aromatic hydroxyl (-OH) groups and lactone attached proton at 4.51 ppm confirmed the formation of **CL-18**.



Scheme 11. Synthesis of **CL-18**.

1.3.2.4. Other modifications

After all the systematic structural and functional tweakings in the core structure of cladosporin, we planned to incorporate some major changes in the same by replacing the dihydroisocoumarin moiety with similar counterparts like chromen and isochromen. Besides, the simple methylene linker was also replaced by an amide bond and the THP moiety was switched with aromatic and aliphatic counterparts.

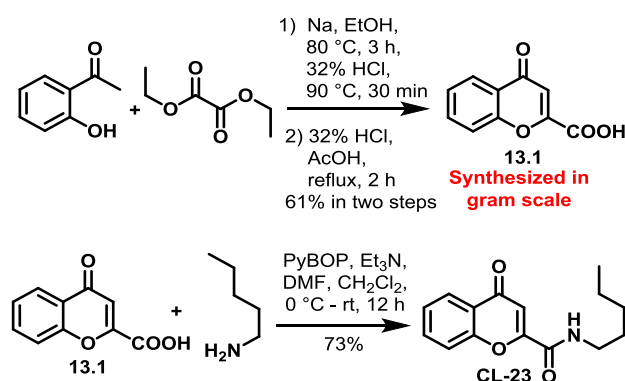


Scheme 12. Synthesis of analogues with chromen moiety.

Chapter 1 (Section C): Design, Synthesis, Biological Evaluation of Lysyl tRNA synthetase (KRS) Inhibitors based on Cladosporin Scaffold towards Identification of Antimalarial Leads

As a part of our plan, we first synthesized chromen carboxylic acid **12.1** in gram scale using known protocol²⁸ starting from 4-fluoro phenol and dimethylacetylenedicarboxylate. Without further purification of the acid intermediate **12.1**, it was then coupled directly with different amines namely, *n*-pentylamine, tetrahydrofurfurylamine and 2-thiophenemethylamine in presence of PyBOP and Et₃N to furnish the following analogues as depicted in scheme 12.

We also synthesized an analogue structurally similar to **CL-22** but without the aromatic halogen (fluorine). This analogue was synthesized to decipher whether the aromatic fluorine atom has any significant role in the anti-plasmodial activity of the analogue. For synthesizing the same, we initially synthesized acid fragment **13.1** starting from 2-hydroxyacetophenon and diethyl oxalate in presence of freshly prepared sodium ethoxide²⁹. The required acid **13.1** was then coupled with *n*-pentylamine using similar protocol to afford **CL-23** (Scheme 13). The presence of four aromatic protons was evident from the appearance of four proton peaks at 7.5 ppm to 8.5 ppm in the ¹H NMR spectrum. Besides the appearance of HRMS peak at 260.1281 corresponding to [M+H]⁺ further confirms the formation of the required product.

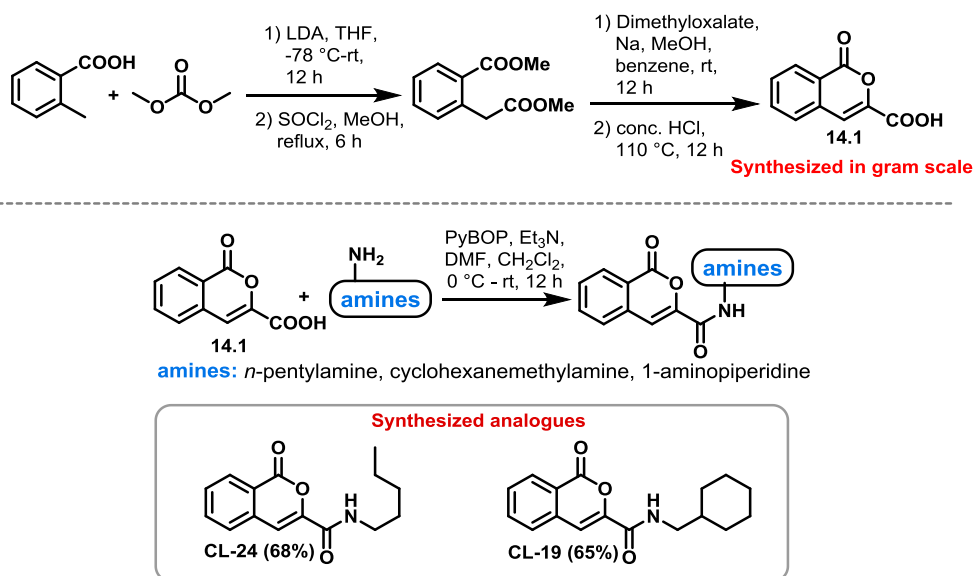


Scheme 13. Synthesis of **CL-23**.

Following the line, we also synthesized few analogues where the isocoumarin moiety has been replaced with isochromen. For the same we initially synthesized isochromen acid **14.1** using synthetic protocol documented in the literature³⁰. After having synthesized the required acid fragment in gram scale starting from 2-methylbenzoic

Chapter 1 (Section C): Design, Synthesis, Biological Evaluation of Lysyl tRNA synthetase (KRS) Inhibitors based on Cladosporin Scaffold towards Identification of Antimalarial Leads

acid and dimethyl carbonate as the starting materials we coupled the same with amines, namely, *n*-pentylamine and cyclohexanemethylamine in the presence of PyBOP and Et₃N to access the following analogues as depicted in scheme 14.



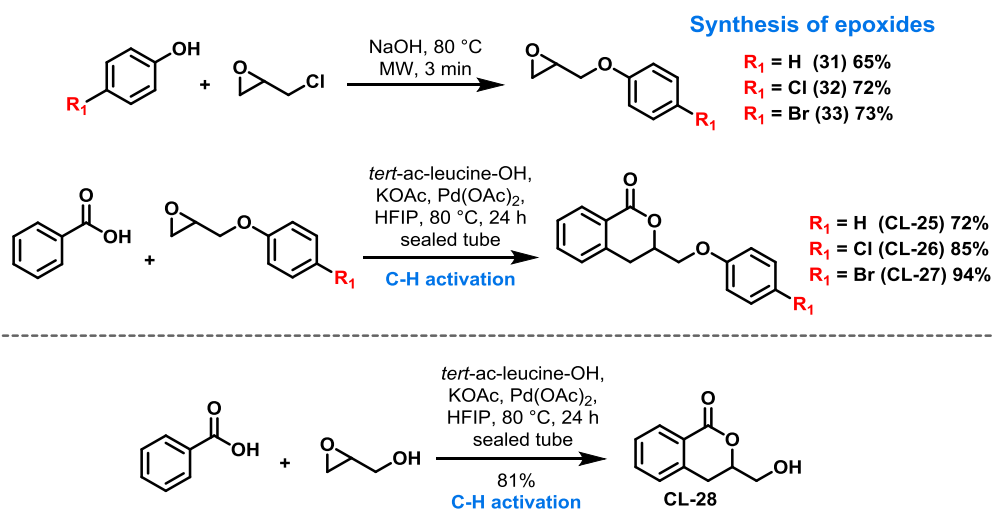
Scheme 14. Synthesis of CL-24 and CL-19.

As a part of analogue synthesis, we next planned to replace the tetrahydropyran (THP) moiety of cladosporin with aliphatic substitutions as well as aromatic and substituted aromatic counterparts. For the following purpose we adopted a novel palladium catalyzed C-H activation protocol³¹ (Scheme 15) where Pd(II)-catalyzed ortho-alkylation of benzoic acids with both terminal and internal epoxides affords 3,4-dihydroisocoumarins in one step. As per the optimized protocol we used potassium acetate as base along with tert-ac-leucine-OH as ligand, Pd(OAc)₂ as the catalyst and hexafluoro-2-propanol (HFIP) as the solvent. In this case we prepared several substituted epoxides following reported procedure³² which were subjected to the above-mentioned C-H activation protocol to furnish the following analogues as demonstrated in scheme 15.

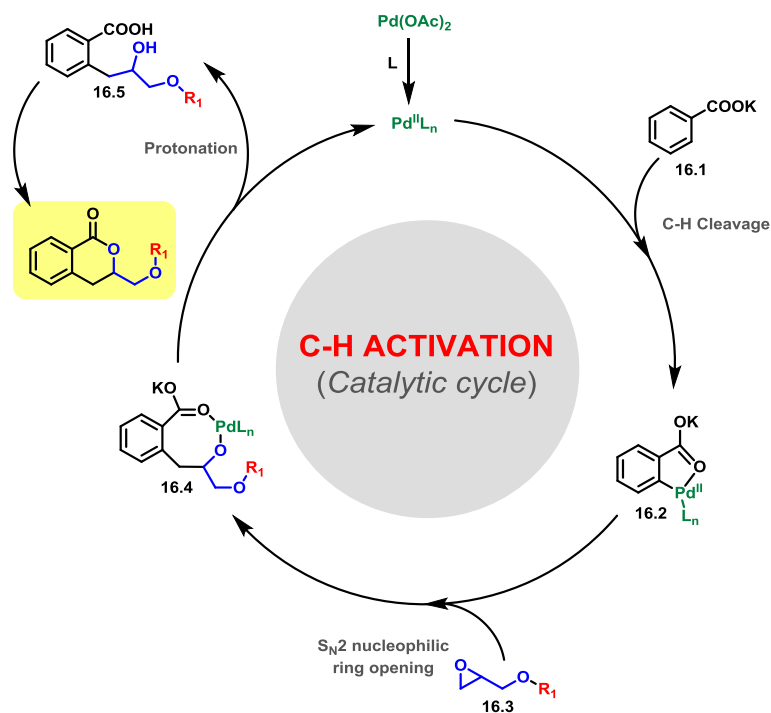
Mechanism of C-H activation: Mechanistically speaking, the potassium salt of benzoic acid **16.1** undergoes C-H cleavage in the presence of Pd(II) catalyst to form

Chapter 1 (Section C): Design, Synthesis, Biological Evaluation of Lysyl tRNA synthetase (KRS) Inhibitors based on Cladosporin Scaffold towards Identification of Antimalarial Leads

weakly co-ordinated arylpalladium intermediate **16.2** which in turn reacts with the epoxide **16.3** via redox neutral S_N2 ring opening process to generate intermediate **16.4** which upon subsequent protonation and catalyst regeneration gives free alcohol intermediate **16.5** which readily gets lactonized to afford the required lactone analogues (Scheme 16).³¹



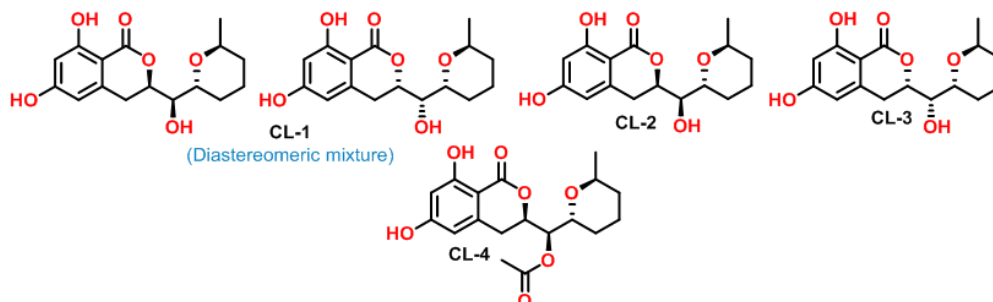
Scheme 15. Synthesis of analogues with modified and replaced THP moiety.



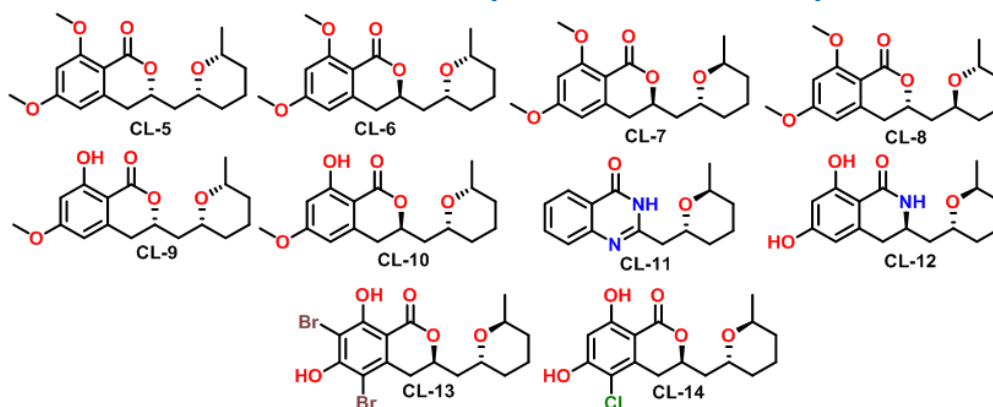
Scheme 16. Catalytic cycle of C-H activation.³¹

Chapter 1 (Section C): Design, Synthesis, Biological Evaluation of Lysyl tRNA synthetase (KRS) Inhibitors based on Cladosporin Scaffold towards Identification of Antimalarial Leads

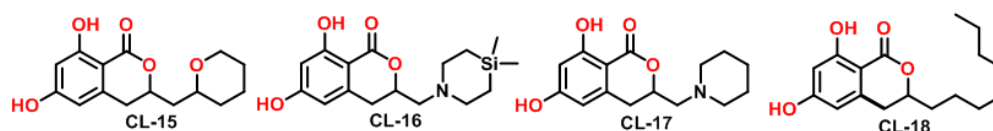
1. Modifications at linker



2. Variations in dihydroisocoumarin moiety



3. Variations in tetrahydropyran moiety



4. Other modifications and combinations

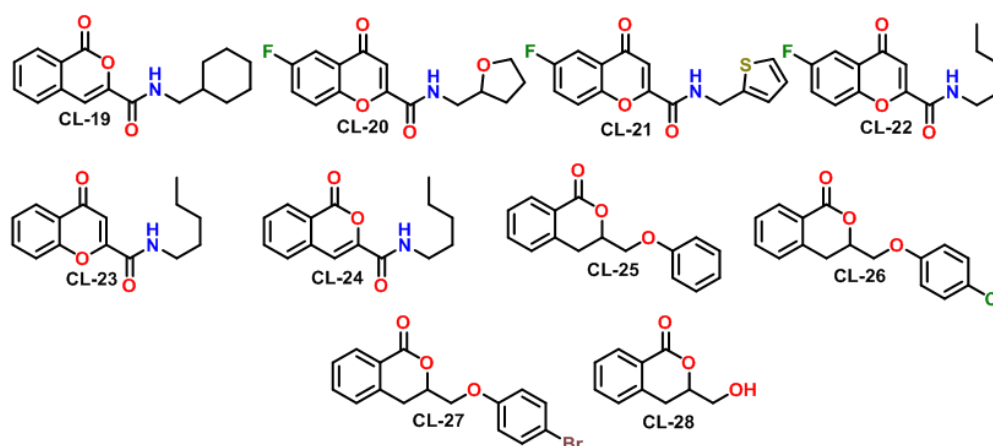


Figure 3. Chemical structures of the synthesized compounds that form cladosporin inspired library.

Chapter 1 (Section C): Design, Synthesis, Biological Evaluation of Lysyl tRNA synthetase (KRS) Inhibitors based on Cladosporin Scaffold towards Identification of Antimalarial Leads

1.3.3. Biological assessment of synthesized analogues

(in collaboration with Dr. Amit Sharma, ICGEB, New Delhi)

1.3.3.1. Structure activity relationship (SAR) study

To investigate the activity and target specificity, all the synthesized analogues were screened under relevant biological assays. We initially performed thermal shift assay (TSA) to explore the compound-induced stabilization of the target proteins, *PfKRS* as well as its human counter-part, *HsKRS*, which was followed by aminoacylation assays to understand the enzymatic inhibition activity of *PfKRS* and *HsKRS*, and to calculate the half-maximal inhibitory concentration (IC_{50}) of the synthesized compounds. *PfKRS* and *HsKRS* efficiently catalysed aminoacylation reaction which was quantitatively measured by the amount of pyrophosphate released. Bio-Mol reagent was used to study the amount of pyrophosphate released. We further investigated the in vitro dose dependent cell-based parasite growth inhibition assays in presence of the synthesized analogues to calculate the half-maximal effective concentration (EC_{50}).

Among the analogues with modifications at linker, **CL-1** (diastereomeric mixture) was found to bind to *PfKRS* tightly with a shift of $\sim 14.5^{\circ}C$ in TSA, similar to that of cladosporin (Figure 5b). *PfKRS* enzyme and parasite growth inhibition assays for **CL-1** also showed an impressive activity (IC_{50} value of $0.17 \mu M$ and EC_{50} value of $0.1 \mu M$) in consistence to the TSA results. Such promising activity of this compound (**CL-1**) intrigued us to resolve its structural interactions with *PfKRS* via co-crystallization with L-lysine. The crystal diffracted at 2.6 \AA resolution and was solved by molecular replacement using *PfKRS*-L-lysine-CL as a template (PDB: 4PG3). A clear electron density was observed for one of the diastereomers of **CL-1** (named **CL-2** in the current series) bound to the adenosine pocket of *PfKRS* (Figure 4). This prompted us to synthesize both the diastereomers of **CL-1** (**CL-2** and **CL-3**) in chiral pure form and independently assess their potency. **CL-2** was found to bind to *PfKRS* tightly, similar to cladosporin and **CL-1**, with a thermal shift of $14.5^{\circ}C$, whereas the other diastereomer **CL-3** displayed a weaker binding with a thermal shift of $9.6^{\circ}C$. Similar results were also obtained in the ATP hydrolysis assay where **CL-2** and **CL-3** showed

Chapter 1 (Section C): Design, Synthesis, Biological Evaluation of Lysyl tRNA synthetase (KRS) Inhibitors based on Cladosporin Scaffold towards Identification of Antimalarial Leads

an IC_{50} value of $0.1 \mu\text{M}$ and $5.0 \mu\text{M}$ respectively. Similarly, the EC_{50} values for **CL-2** and **CL-3** were $0.08 \mu\text{M}$ and $4.0 \mu\text{M}$ respectively (Table 2) thus concluding diastereomer **CL-3** to be a moderate inhibitor (Table 2). The experimental data thus suggests **CL-2** to be potent and better than the diastereomeric mixture **CL-1** (and comparable to cladosporin). On the other hand, **CL-4**, where the linker hydroxyl group is protected as acetate functionality, turned out to be a moderate inhibitor of *PfKRS* with an IC_{50} of $3.2 \mu\text{M}$ and EC_{50} of $4.3 \mu\text{M}$ (Figure 5d). Hence, the biological data clearly suggests that the linker hydroxyl in **CL-2** adds to the potency of the compound.

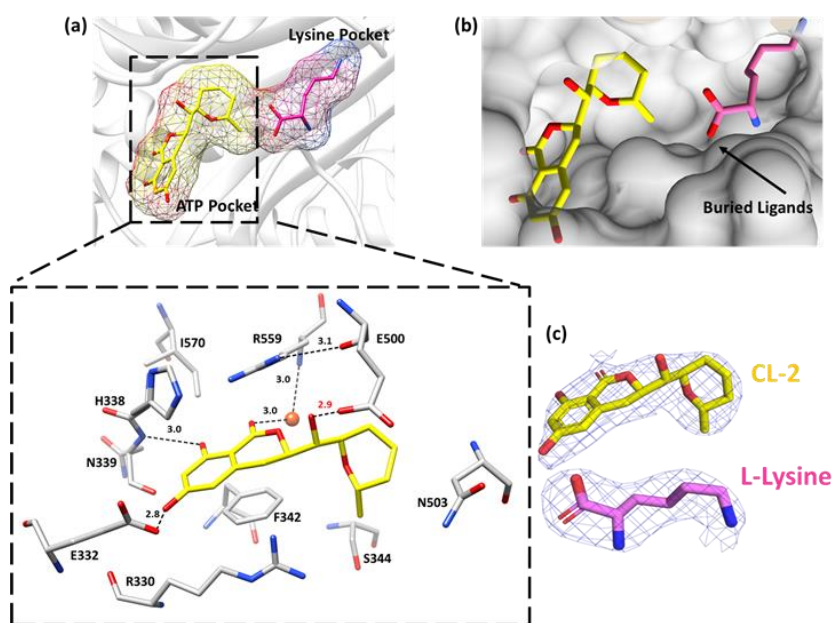


Figure 4. Crystal structure of *PfKRS*+**CL-2**+**L-Lys** (PDB ID 6M0T). **(a)** A close-up view of the binding pockets of *PfKRS* (grey cartoon) with ligands. **CL-2** (yellow) in the adenosine pocket and **L-Lys** (purple) are shown in ball-and-stick with mesh. Zoomed view shows the bound **CL-2** (yellow) with hydrogen bond interactions (dashed line) and the distances (\AA) are marked. The important hydrogen bond interaction between **CL-2** and protein residue Glu500 is marked in red. The water molecule (orange sphere) involved in the interaction is also shown. **(b)** Surface representation of active site pocket of *PfKRS* with **CL-2** and **L-Lys**. **(c)** Simulated annealing omit (SA-omit) map counteracted at 1σ level for **CL-2** and **L-Lys**.

Chapter 1 (Section C): Design, Synthesis, Biological Evaluation of Lysyl tRNA synthetase (KRS) Inhibitors based on Cladosporin Scaffold towards Identification of Antimalarial Leads

Compounds with modifications at dihydroisocoumarin moiety were also studied (Figure 2 and 3). **CL-5, 6, 7** and **8** where both the phenolic hydroxyl groups are protected as methyl ethers turned out to be inactive in TSA, enzyme and parasitic inhibition assay (Table 3) suggesting the significant and crucial importance of the phenolic hydroxyl groups in anti-malarial potency. **CL-10** with only one of the hydroxyl groups (C6-OH) protected showed weak inhibition with an IC_{50} of 3.6 μ M and an EC_{50} of 5.5 μ M (Figure 5d) whereas its diastereomer **CL-9** was inactive (Table 3). **CL-13** and **14** with halogen (Cl and Br) incorporation in the dihydroisocoumarin moiety showed no inhibitory activity in enzyme or parasite inhibition assays (Table 3), hence suggesting a loss in anti-malarial activity on incorporation of halogen. On the other hand, the lactam incorporated analogue **CL-12** showed moderate inhibition with an IC_{50} of 3.0 μ M and an EC_{50} of 2.5 μ M (Figure 5d). Unfortunately, the hybrid analogue of cladosporin and febrifugine (**CL-11**), was surprisingly found to be inactive with no enzyme and parasite inhibition (Table 3).

Analogues with modifications at tetrahydropyran ring were also studied (Figure 2 and 3). **CL-16, 17** and **18** turned out to be inactive with no enzyme and parasite inhibition (Table 3), thus suggesting the importance of the tetrahydropyran moiety in anti-plasmodial activity of cladosporin. **CL-15**, where the methyl functionality in tetrahydropyran ring was removed, was moderately active with thermal shift of 13.2 °C, IC_{50} and an EC_{50} value of 1.5 μ M and 1.2 μ M respectively. This compound turned out to be the second best among the synthesized library of analogues (Figure 5d).

The set of analogues (**CL-19** to **CL-24**) with major modifications and combinations were effectively found to be inert after experimental assessment (Table 3) except for **CL-22** and **CL-23** which showed moderate enzyme and parasite inhibition with IC_{50} of 2.0 μ M and 3.1 μ M respectively and an EC_{50} of 4.3 μ M each (Figure 5d). Both analogues are structurally similar except for the presence of fluorine in the phenyl ring (at C-7) of **CL-22**, indicating no prominent role of fluorine. Compounds synthesized through C-H activation (**CL-25** to **28**) were found to be effectively inert as well (Table 3).

Chapter 1 (Section C): Design, Synthesis, Biological Evaluation of Lysyl tRNA synthetase (KRS) Inhibitors based on Cladosporin Scaffold towards Identification of Antimalarial Leads

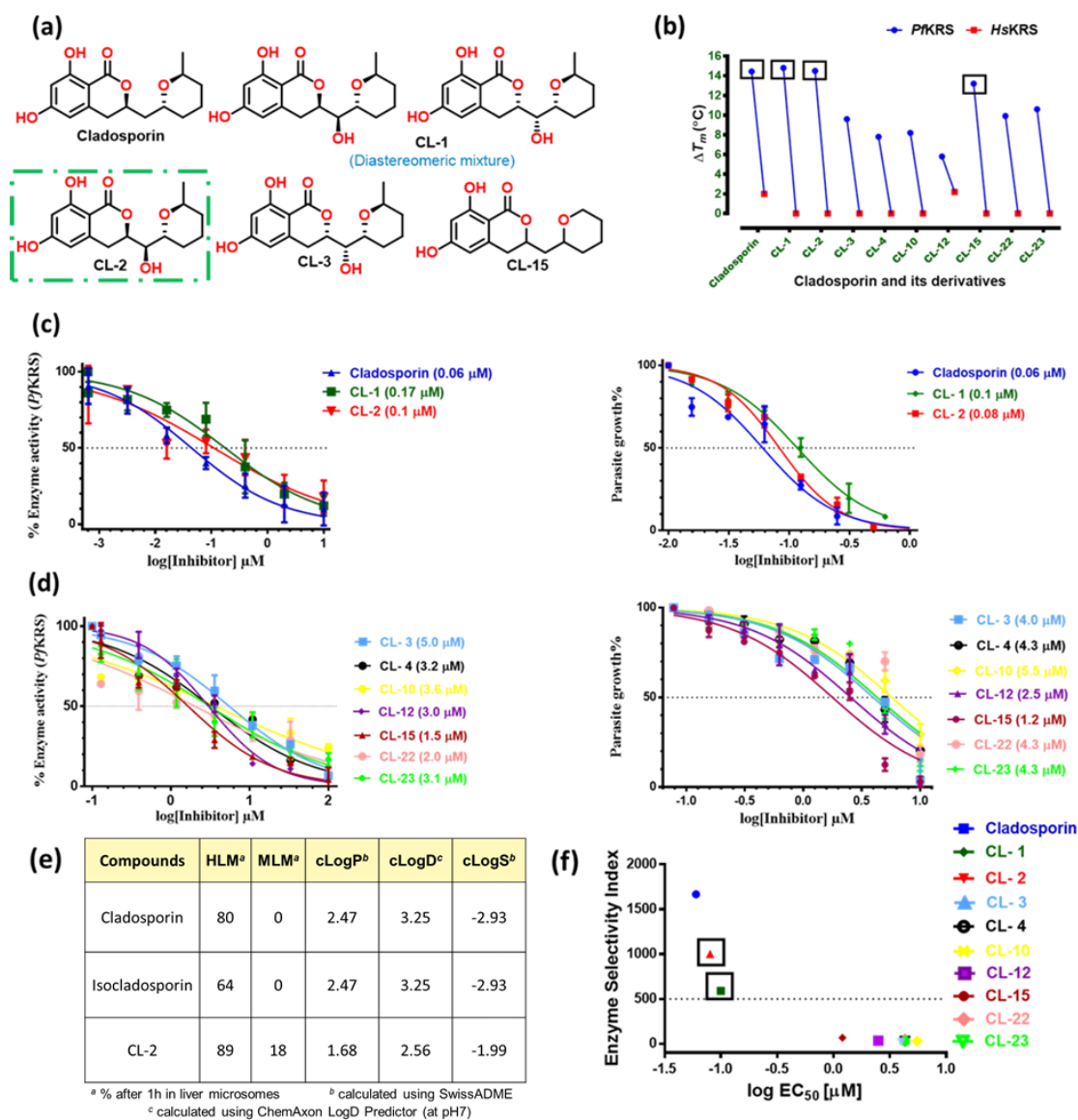


Figure 5. (a) Structures of potent compounds like cladosporin, diastereomer **CL-1** and its chirally pure enantiomers **CL-2**, **CL-3** and **CL-15**. (b) Protein thermal shift profiles of *Pf*KRS and *Hs*KRS (at 2 μ M protein respectively) in the presence of 2 mM L-lysine for the potent compounds in our library. (c) Aminoacylation activity inhibition assays and blood stage *Plasmodium falciparum* growth inhibition assays in presence of cladosporin, **CL-1** and its potent enantiomer **CL-2**. For aminoacylation assays the concentration for compound ranged from 10 to 0.01 μ M and for parasite inhibition assays it ranged from 1 to 0.0078 μ M. (d) Same for **CL-3**, **CL-4**, **CL-10**, **CL-12**, **CL-**

Chapter 1 (Section C): Design, Synthesis, Biological Evaluation of Lysyl tRNA synthetase (KRS) Inhibitors based on Cladosporin Scaffold towards Identification of Antimalarial Leads

15, CL-22 and CL-23. For aminoacylation assays the concentration for compounds ranged from 100 to 0.01 μM and for parasite inhibition assays it ranged from 10 to 0.078 μM . (e) Metabolic stability using liver microsomes from human (HLM) and mice (MLM) along with cLogP, cLogD at pH 7.0 and cLogS values for CL-2, cladosporin, and isocladosporin. (f) Selectivity profile (scatter plots) for each active compound based on enzyme selectivity index and parasite inhibition.

Conclusions from Structure Activity Relationship (SAR) study

After thorough and in depth analysis of the structure activity relationships, **CL-2** was identified to be the most potent compound among the entire set with a thermal shift of 14.5 $^{\circ}\text{C}$, IC_{50} value of 0.1 μM and an EC_{50} of 0.08 μM (Figure 5b and 5c, Table 3). **CL-15**, on the other hand, turned out to be the second best with a thermal shift profile of 13.2 $^{\circ}\text{C}$, an IC_{50} and EC_{50} values of 1.5 and 1.2 μM respectively (Figure 5b and 5d, Table 3). The other moderately active compounds among the synthesized library were **CL-3, CL-4, CL-10, CL-12, CL-22 and CL-23** with thermal shifts ranging from 5.8 - 9.9 $^{\circ}\text{C}$, IC_{50} of 2 - 5.0 μM and EC_{50} ranging from 2.5 - 5.5 μM (Figure 5d).

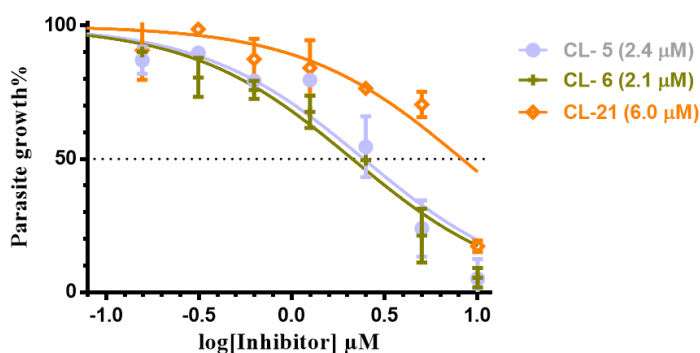


Figure 6. Parasitic growth inhibition assay for **CL-5, CL-6 and CL-21** indicating a different cellular target.

While analyzing these sets of data, we found out that though **CL-5, CL-6, and CL-21** did not bind to or inhibit *PfKRS*, they did lead to a weak parasitic inhibition with EC_{50} values in the range of 2.1- 6.0 μM suggesting possible alternate cellular targets (Figure 6). Finally, after the assessment of selectivity indices for each inhibitor based on the

Chapter 1 (Section C): Design, Synthesis, Biological Evaluation of Lysyl tRNA synthetase (KRS) Inhibitors based on Cladosporin Scaffold towards Identification of Antimalarial Leads

above data, compound **CL-2** with a value of ~1000 scored better than the diastereomeric mixture **CL-1** which had a value of ~588 (Figure 5f).

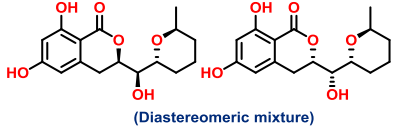
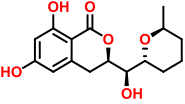
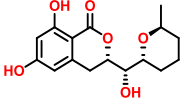
Compounds	Structure	ΔT_m (°C)		<i>Plasmodium falciparum</i> (Pf)	
		Pf	Hs	IC ₅₀ (μM)	EC ₅₀ (μM)
CL-1	 (Diastereomeric mixture)	14.8	NB	0.17	0.1
CL-2		14.5	NB	0.1	0.08
CL-3		9.6	NB	5.4	4.0

Table 2. Potency of diastereomeric mixture **CL-1** and its chirally pure versions **CL-2** and **CL-3**. (NB- No Binding)

1.3.3.2. In vitro pharmacokinetics

To evaluate the metabolic stability of cladosporin, isocladosporin and our best compound **CL-2**, in vivo clearance was investigated using liver microsomes from human (HLM) and mice (MLM). The test compounds were incubated for one hour with microsomes in the presence and absence of the cofactor NADPH and the reaction was quenched by the addition of ice-cold acetonitrile containing an internal standard. The disappearance of the test compounds with time was monitored using LC-MS/MS. The experimental values suggests **CL-2** to be more metabolically stable than cladosporin and isocladosporin (Figure 5e).

Other physicochemical properties (cLogP, cLogD, cLogS) were also calculated for the entire set of synthesized analogues along with cladosporin and isocladosporin. Among

Chapter 1 (Section C): Design, Synthesis, Biological Evaluation of Lysyl tRNA synthetase (KRS) Inhibitors based on Cladosporin Scaffold towards Identification of Antimalarial Leads

the entire set compounds, **CL-2** reflected an increase in hydrophilicity with a cLogP and cLogD value of 1.68 and -1.99 respectively whereas both cladosporin and isocladosporin showed a cLogP of 2.47 and cLogD of 3.25 (Figure 5e, Table 3). In case of **CL-2**, a cLogS value of -1.99 was observed as compared to cladosporin with a cLogS of -2.93, indicating an increased hydrophilicity of **CL-2** which might possibly lead to a better bio-availability of the active compound (Figure 5e, Table 3).

1.3.3.3. Structural interactions in the CL-2-KRS complex

Identical structure were observed for **CL-2** and cladosporin bound *Pf*KRS enzymes with a root-mean-square deviation (RMSD) of 0.7 Å. Both the molecules bind to the adenosine binding pocket and the surrounding waters are mostly conserved. Both the structures showed well-defined electron density for a disulphide bond (Cys517–Cys540).

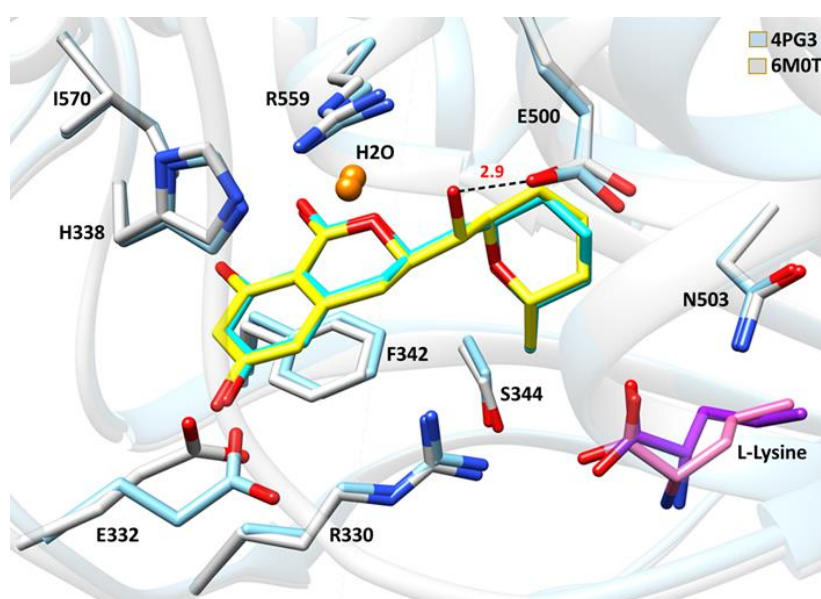


Figure 7. The superimposition of **CL-2** bound structure (*Pf*KRS+**CL-2**+L-Lys; PDB ID 6M0T) onto cladosporin (**CL**) bound structure (*Pf*KRS+**CL**+L-Lys; PDB ID 4PG3). In both structures, the heterocyclic ring in the dihydroisocoumarin moiety and tetrahydropyran ring of the bound ligands **CL** and **CL-2** adopt half-chair and chair conformations. The additional OH group present in the linker of ligand **CL-2** makes

Chapter 1 (Section C): Design, Synthesis, Biological Evaluation of Lysyl tRNA synthetase (KRS) Inhibitors based on Cladosporin Scaffold towards Identification of Antimalarial Leads

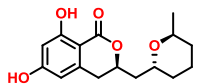
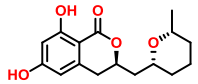
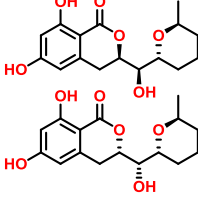
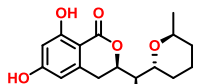
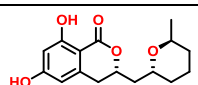
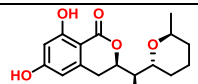
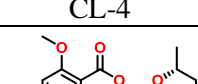
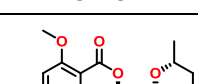
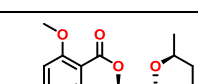
hydrogen bond interactions with Glu500 when compared to cladosporin (shown as dashed line). The conserved water molecule (orange sphere) present in both structures are shown.

Similar to cladosporin, the isocoumarin moiety of **CL-2** stacks between the side chain of Phe342, His338, and Arg559 and the two hydroxyl groups form hydrogen bonds with the side chain of Glu332 and Asn339. The carbonyl group on the other hand forms H-bond with the highly coordinated water, just like with cladosporin. The THP ring of ligand **CL-2** accommodates itself in the ribose recognizing pocket of *Pf*KRS formed by the side chains of Arg330, Ser344, and Asn503, identical to cladosporin (Figure 4 and 7). **CL-2** has an extra hydroxyl group at the linker region as compared to cladosporin. This extra –OH group forms a strong hydrogen bond with the side chain of Glu500 creating a new interaction between drug and the protein.

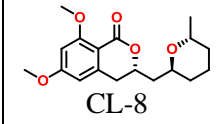
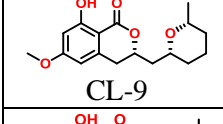
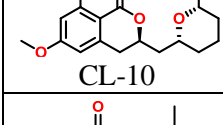
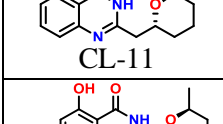
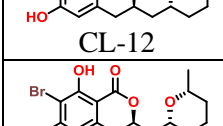
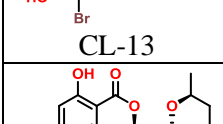
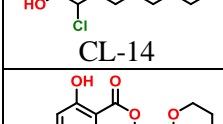
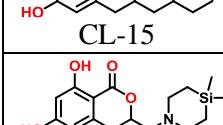
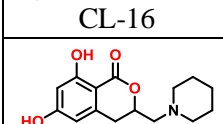
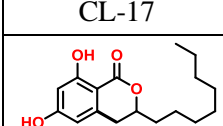
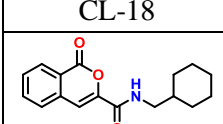
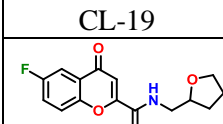
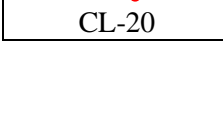
1.3.4. Conclusion

The entire library of compounds were synthesized using a variety of chemical reactions including strategic functional group incorporation and interconversion. All the analogues thus synthesized were purified and characterized, leaving no structural and functional ambiguity. The enzyme-based binding and enzyme/cell-based inhibition assays along with in vitro pharmacokinetics studies led us to identify a potent lead compound for further development. We resolved the co-crystal structure of the most potent compound **CL-2** and show that it forms an additional hydrogen bond in the *Pf*KRS active site. This study provides new insights on how even the slightest stereochemical or functional modification can play an important role in potency of the compound. Such advances will pave the way for more potent and selective lead molecules in future.

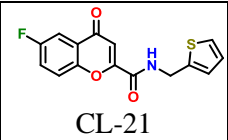
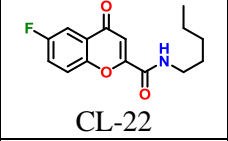
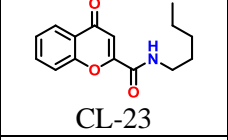
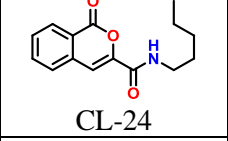
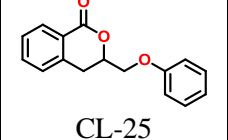
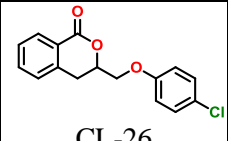
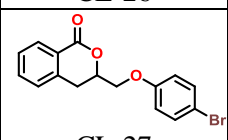
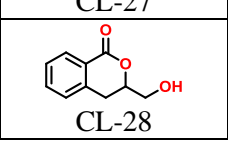
Chapter 1 (Section C): Design, Synthesis, Biological Evaluation of Lysyl tRNA synthetase (KRS) Inhibitors based on Cladosporin Scaffold towards Identification of Antimalarial Leads

Compound	ΔT_m (°C) (KRS)		<i>Pf</i>		cLog <i>P</i> ^a	cLog <i>D</i> ^b (pH 7)	cLog <i>S</i> ^a	<i>H-bond</i> ^a	
	<i>Pf</i>	<i>Hs</i>	IC ₅₀ (μM)	EC ₅₀ (μM)				Donor	Acceptor
 Cladosporin	14.5	2.0	0.06	0.06	2.47	3.25	-2.93	2	5
 Isocladosporin	16.2	1.0	0.27	0.29	2.47	3.25	-2.93	2	5
 CL-1 (Diastereomeric mixture)	14.8	NB	0.17	0.1	1.68	2.56	-1.99	3	6
 CL-2	14.5	NB	0.1	0.08	1.68	2.56	-1.99	3	6
 CL-3	9.6	NB	5.0	4.0	1.68	2.56	-1.99	3	6
 CL-4	7.8	NB	3.2	4.3	2.13	3.00	-2.62	2	7
 CL-5	1.6	NB	NI	2.4	3.52	2.9	-4.32	0	5
 CL-6	NB	NB	NI	2.1	3.52	2.9	-4.32	0	5
 CL-7	NB	NB	NI	NI	3.52	2.9	-4.32	0	5

Chapter 1 (Section C): Design, Synthesis, Biological Evaluation of Lysyl tRNA synthetase (KRS) Inhibitors based on Cladosporin Scaffold towards Identification of Antimalarial Leads

 CL-8	NB	NB	NI	NI	3.52	2.9	-4.32	0	5
 CL-9	6.0	NB	NI	NI	2.99	3.4	-3.62	1	5
 CL-10	8.2	NB	3.6	5.5	2.99	3.4	-3.62	1	5
 CL-11	NB	NB	NI	NI	3.50	2.17	-4.70	1	3
 CL-12	5.8	NB	3.0	2.5	2.15	2.49	-3.24	3	4
 CL-13	NB	NB	NI	NI	3.81	3.7	-4.51	2	5
 CL-14	6.0	NB	NI	NI	3.10	2.58	-3.53	2	5
 CL-15	13.2	3.0	1.5	1.2	2.39	2.83	-2.78	2	5
 CL-16	NB	NB	NI	NI	1.01	1.62	-3.18	2	5
 CL-17	2.5	NB	NI	NI	1.91	1.6	-2.60	2	5
 CL-18	NB	NB	NI	NI	4.05	5.45	-4.69	2	4
 CL-19	7.0	NB	NI	NI	3.57	3.21	-5.45	1	3
 CL-20	3.3	NB	NI	NI	3.11	1.28	-4.91	1	5

Chapter 1 (Section C): Design, Synthesis, Biological Evaluation of Lysyl tRNA synthetase (KRS) Inhibitors based on Cladosporin Scaffold towards Identification of Antimalarial Leads

 CL-21	7.2	NB	NI	NI	4.51	2.49	-6.07	1	4
 CL-22	9.9	2.39	2.0	4.3	3.88	2.63	-5.90	1	4
 CL-23	9.9	NB	3.1	4.3	3.45	2.48	-5.62	1	3
 CL-24	1.3	NB	NI	NI	3.45	2.87	-5.62	1	3
 CL-25	NB	NB	NI	NI	3.43	3.52	-5.29	0	3
 CL-26	NB	NB	NI	NI	4.05	4.12	-5.90	0	3
 CL-27	NB	NB	NI	NI	4.09	4.29	-6.11	0	3
 CL-28	NB	NB	NI	NI	1.82	1.19	-2.41	1	3

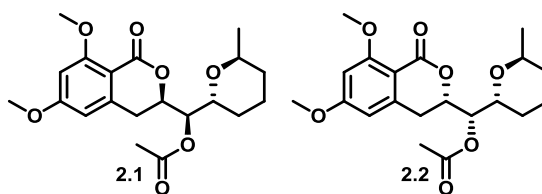
*NB- No Binding, NI- No Inhibition, CL- Cladosporin, ICLA- Isocladosporin
^a calculated using SwissADME ^b calculated using ChemAxon LogD Predictor

Table 3. Compiled data of synthesized analogues.

Chapter 1 (Section C): Design, Synthesis, Biological Evaluation of Lysyl tRNA synthetase (KRS) Inhibitors based on Cladosporin Scaffold towards Identification of Antimalarial Leads

1.3.5. Experimental section

Synthesis of compound (*R*)-((*R*)-6,8-dimethoxy-1-oxisochroman-3-yl)((2*R*,6*S*)-6-methyltetrahydro-2H-pyran-2-yl)methyl acetate (**2.1**) and (*S*)-((*S*)-6,8-dimethoxy-1-oxisochroman-3-yl)((2*R*,6*S*)-6-methyltetrahydro-2H-pyran-2-yl)methyl acetate(**2.2**)



separated through column chromatography (3:2 dr)

Inseparable diastereomeric mixture (0.17 g, 0.505 mmol) of compound **1.1** and **1.2** was dissolved in dry CH₂Cl₂ (25 mL) and cooled to 0 °C. Triethylamine (0.14 mL, 1.01 mmol) was added followed by the addition of acetic anhydride (0.113 mL, 1.16 mmol). Catalytic DMAP (5 mg) was added to the reaction mixture and was stirred at room temperature for 12 h. After completion of the reaction, it was further diluted with CH₂Cl₂ (10 mL) and washed thoroughly with H₂O (10 mL x 3). The combined organic layers were dried over Na₂SO₄ and concentrated under vacuo. The obtained diastereomeric mixture was purified and separated using column chromatography to afford compound **2.1** (0.05 g) and compound **2.2** (0.035 g) with an overall yield of 75%.

Compound **2.1**:

$[\alpha]_D^{25} = +67.4$ (c 0.7, CHCl₃).

IR ν_{\max} (film): cm⁻¹ 1228, 1602, 1729, 2938.

¹H NMR (400 MHz, CDCl₃): δ 6.39 (s, 1H), 6.29 (s, 1H), 5.14 (d, *J* = 9.6 Hz, 1H), 4.76 (d, *J* = 11.7 Hz, 1H), 4.21 (t, *J* = 8.2 Hz, 1H), 3.91 (s, 3H), 3.91 (overlap, 1H), 3.84 (s, 3H), 2.95 – 2.88 (m, 1H), 2.69 (d, *J* = 15.9 Hz, 1H), 2.07 (s, 3H), 1.65 (dd, *J* = 13.1, 8.0 Hz, 4H), 1.29 (dd, *J* = 18.1, 11.3 Hz, 2H), 1.19 (d, *J* = 6.2 Hz, 3H).

Chapter 1 (Section C): Design, Synthesis, Biological Evaluation of Lysyl tRNA synthetase (KRS) Inhibitors based on Cladosporin Scaffold towards Identification of Antimalarial Leads

^{13}C NMR (100 MHz, CDCl_3): δ 170.6, 164.4, 163.0, 162.0, 143.5, 107.0, 103.8, 97.8, 73.9, 72.5, 68.4, 66.7, 56.1, 55.5, 31.7, 30.8, 26.4, 20.7, 19.0, 17.8.

HRMS calculated for $\text{C}_{20}\text{H}_{26}\text{O}_7$ $[\text{M} + \text{H}]^+$ 379.1752, observed 379.1751.

Compound 2.2:

$[\alpha]^{25}_{\text{D}} = -71.3$ (c 0.5, CHCl_3).

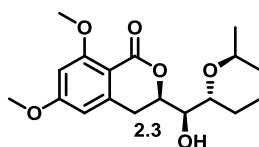
IR ν_{max} (film): cm^{-1} 1229, 1603, 1730, 2939.

^1H NMR (400 MHz, CDCl_3): δ 6.39 (s, 1H), 6.29 (s, 1H), 5.26 – 5.23 (m, 1H), 4.58 – 4.55 (m, 1H), 4.12 (s, 1H), 4.03 (s, 1H), 3.90 (s, 3H), 3.85 (s, 3H), 3.01 (dd, $J = 15.7$, 11.6 Hz, 1H), 2.78 (d, $J = 16.0$ Hz, 1H), 2.13 (s, 3H), 1.72 – 1.65 (m, 3H), 1.48 – 1.42 (m, 1H), 1.35 – 1.29 (m, 2H), 1.18 (d, $J = 6.4$ Hz, 3H).

^{13}C NMR (100 MHz, CDCl_3): δ 170.9, 164.5, 163.2, 161.7, 143.2, 106.7, 103.9, 97.8, 75.3, 73.5, 69.0, 68.2, 56.2, 55.5, 31.3, 30.4, 26.5, 20.9, 18.6, 18.2.

HRMS calculated for $\text{C}_{20}\text{H}_{26}\text{O}_7$ $[\text{M} + \text{H}]^+$ 379.1755, observed 379.1751.

Synthesis of compound (*R*)-3-((*R*)-hydroxy((2*R*,6*S*)-6-methyltetrahydro-2H-pyran-2-yl)methyl)-6,8-dimethoxyisochroman-1-one (2.3)

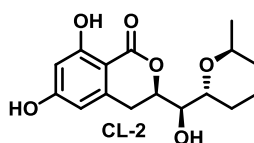


K_2CO_3 (0.037 mg, 0.264 mmol) was added to a methanolic solution of compound **2.1** (0.05 g, 0.132 mmol) at 0 °C. The reaction mixture was then warmed to room temperature and stirred for 6 h. After completion of the reaction, methanol was removed using rotary evaporation, following which it was diluted with ethyl acetate (15 mL) and washed with saturated aqueous NaHCO_3 solution (10 mL x 3). The collected organic layers were further washed with H_2O (15 mL x 3), brine (15 mL), then dried over

Chapter 1 (Section C): Design, Synthesis, Biological Evaluation of Lysyl tRNA synthetase (KRS) Inhibitors based on Cladosporin Scaffold towards Identification of Antimalarial Leads

Na₂SO₄ and concentrated under vacuo to afford compound **2.3** which was forwarded as such without further purification.

Synthesis of (*R*)-6,8-dihydroxy-3-((*R*)-hydroxy((2*R*,6*S*)-6-methyltetrahydro-2H-pyran-2-yl)methyl)isochroman-1-one (CL-2)



A suspension of aluminium powder (0.11 g, 4.09 mmol) in dry benzene (5 mL) was treated with I₂ (0.39 g, 1.52 mmol) under argon, and the violet mixture was stirred under reflux for 30 min until the violet color disappeared. After the mixture was cooled to 0 °C, few crystals of TBAI (0.002 g, 0.01 mmol) and phloroglucinol (0.06 g, 0.476 mmol) were added before a solution of compound **2.3** (0.032 mg, 0.095 mmol) in dry benzene (3 mL) was added in one portion. The resulting green-brown suspension was stirred for 30 min at 5 °C before saturated Na₂S₂O₃ solution (8 mL) and ethyl acetate (8 mL) were added. After separation of the layers, the aqueous phase was extracted with ethyl acetate. The combined organic layers were washed with brine, dried over Na₂SO₄, filtered, and concentrated in vacuo. Purification by column chromatography afforded **CL-2** (0.015 g) in 51% yield.

$[\alpha]_{28}^D = +1.5$ (c 0.9, MeOH).

IR ν_{\max} (film): cm⁻¹ 1247, 1642, 2934, 3300.

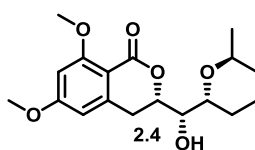
¹H NMR (400 MHz, MeOD) δ 6.25 (s, 1H), 6.20 (d, *J* = 2.1 Hz, 1H), 4.76 (ddd, *J* = 13.1, 3.0, 1.5 Hz, 1H), 3.98 (ddd, *J* = 9.8, 5.7, 4.2 Hz, 1H), 3.88 (ddd, *J* = 9.0, 6.1, 2.7 Hz, 1H), 3.74 (d, *J* = 9.5 Hz, 1H), 3.32 – 3.24 (m, 1H), 2.72 (dd, *J* = 16.4, 3.0 Hz, 1H), 1.81 (dt, *J* = 7.8, 4.1 Hz, 1H), 1.75 – 1.62 (m, 4H), 1.36 – 1.28 (m, 1H), 1.17 (d, *J* = 6.4 Hz, 3H).

Chapter 1 (Section C): Design, Synthesis, Biological Evaluation of Lysyl tRNA synthetase (KRS) Inhibitors based on Cladosporin Scaffold towards Identification of Antimalarial Leads

^{13}C NMR (100 MHz, MeOD) δ 171.7, 166.3, 165.7, 144.2, 108.0, 102.1, 101.7, 79.0, 72.2, 70.8, 69.5, 32.7, 30.7, 27.5, 20.1, 19.1

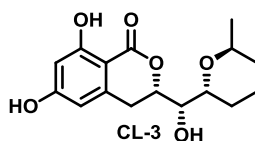
HRMS calculated for $\text{C}_{16}\text{H}_{21}\text{O}_6$ $[\text{M} + \text{H}]^+$ 309.1334, observed 309.1333.

Synthesis of compound (S)-3-((S)-hydroxy((2R,6S)-6-methyltetrahydro-2H-pyran-2-yl)methyl)-6,8-dimethoxyisochroman-1-one (2.4)



Compound **2.4** was synthesized using similar procedure as that of compound **2.3**.

Synthesis of (S)-6,8-dihydroxy-3-((S)-hydroxy((2R,6S)-6-methyltetrahydro-2H-pyran-2-yl)methyl)isochroman-1-one (CL-3)



CL-3 was synthesized using similar procedure as that of **CL-2**.

$[\alpha]^{28}_{\text{D}} = -34.25$ (c 0.6, MeOH).

IR ν_{max} (film): cm^{-1} 1244, 1635, 2935, 3311.

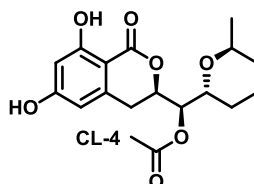
^1H NMR (400 MHz, MeOD) δ 6.23 (s, 1H), 6.19 (d, $J = 1.6$ Hz, 1H), 4.89 – 4.58 (m, 1H), 4.09 (dt, $J = 14.3, 5.3$ Hz, 1H), 3.99 – 3.95 (m, 1H), 3.70 (dd, $J = 6.1, 4.1$ Hz, 1H), 3.19 (dd, $J = 16.3, 12.6$ Hz, 1H), 2.79 (dd, $J = 16.5, 3.0$ Hz, 1H), 1.78 – 1.65 (m, 3H), 1.64 – 1.57 (m, 2H), 1.38 (dd, $J = 13.2, 4.7$ Hz, 1H), 1.26 (d, $J = 6.6$ Hz, 3H).

^{13}C NMR (100 MHz, MeOD): δ 171.5, 166.4, 165.7, 143.8, 108.0, 102.2, 101.6, 80.9, 74.3, 71.4, 69.7, 31.7, 30.6, 27.8, 19.2, 18.6.

HRMS calculated for $\text{C}_{16}\text{H}_{21}\text{O}_6$ $[\text{M} + \text{H}]^+$ 309.1334, observed 309.1333.

Chapter 1 (Section C): Design, Synthesis, Biological Evaluation of Lysyl tRNA synthetase (KRS) Inhibitors based on Cladosporin Scaffold towards Identification of Antimalarial Leads

Synthesis of (R)-((R)-6,8-dihydroxy-1-oxoisochroman-3-yl)((2R,6S)-6-methyltetrahydro-2H-pyran-2-yl)methyl acetate (CL-4)



CL-4 was synthesized using similar procedure as that of CL-2.

$[\alpha]^{25}_{\text{D}} = +9.4$ (c 0.6, CHCl_3).

IR ν_{max} (film): cm^{-1} 1234, 1633, 1743, 2931.

^1H NMR (400 MHz, CDCl_3): δ 11.05 (s, 1H), 7.11 (s, 1H), 6.31 (d, $J = 1.3$ Hz, 1H), 6.20 (s, 1H), 5.21 (dd, $J = 9.7, 1.4$ Hz, 1H), 4.98 – 4.94 (m, 1H), 4.20 – 4.16 (m, 1H), 3.94 (dd, $J = 6.2, 3.8$ Hz, 1H), 2.94 – 2.78 (m, 2H), 2.04 (s, 3H), 1.70 – 1.60 (m, 4H), 1.36 – 1.30 (m, 2H), 1.21 (d, $J = 6.5$ Hz, 3H).

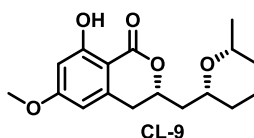
^{13}C NMR (100 MHz, CDCl_3): δ 171.0, 169.3, 164.2, 163.0, 141.1, 106.8, 101.9, 101.6, 75.4, 72.6, 68.6, 66.9, 30.8, 29.8, 26.2, 20.6, 19.2, 17.8.

HRMS calculated for $\text{C}_{18}\text{H}_{23}\text{O}_7$ $[\text{M} + \text{H}]^+$ 351.1440, observed 351.1438.

Synthesis of CL-5, CL-6, CL-7, CL-8

All these compounds have been synthesized using literature protocol.¹⁹

Synthesis of (S)-8-hydroxy-6-methoxy-3-(((2R,6R)-6-methyltetrahydro-2H-pyran-2-yl)methyl)isochroman-1-one (CL-9)



Compound CL-5 (0.05 g, 0.163 mmol) was dissolved in dry toluene (8 ml) under argon following which anhydrous AlCl_3 (0.039 g, 0.294 mmol) was added to the same at 0 °C. The reaction mixture was stirred for 12h at room temperature. After completion of the reaction as monitored by TLC, the reaction was quenched with ice cold water and extracted with ethyl acetate (15 mL x 3). The combined organic layers were dried over

Chapter 1 (Section C): Design, Synthesis, Biological Evaluation of Lysyl tRNA synthetase (KRS) Inhibitors based on Cladosporin Scaffold towards Identification of Antimalarial Leads

Na₂SO₄ and concentrated under vacuo. Purification through column chromatography afforded **CL-9** as a foamy solid (0.029 g) in 58% yield.

$[\alpha]^{25}_{\text{D}} = -5.4$ (c 0.5, CHCl₃).

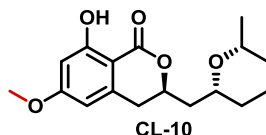
IR ν_{max} (**film**): cm⁻¹ 1248, 1665, 2851, 2930.

¹H NMR (400 MHz, CDCl₃): δ 11.22 (s, 1H), 6.36 (s, 1H), 6.26 (s, 1H), 4.73 (td, $J = 10.1, 6.1$ Hz, 1H), 3.82 (s, 3H), 3.63 – 3.57 (m, 1H), 3.43 (dd, $J = 10.7, 5.3$ Hz, 1H), 2.93 (ddd, $J = 19.6, 16.3, 7.4$ Hz, 2H), 2.12 (dt, $J = 14.0, 6.9$ Hz, 1H), 1.84 – 1.78 (m, 2H), 1.63 – 1.48 (m, 4H), 1.20 (s, 1H), 1.14 (d, $J = 6.1$ Hz, 3H).

¹³C NMR (100 MHz, CDCl₃): δ 169.9, 165.8, 164.5, 141.2, 106.2, 101.8, 99.4, 76.4, 73.9, 73.3, 55.5, 40.9, 33.1, 32.9, 31.1, 23.5, 22.14.

HRMS calculated for C₁₇H₂₃O₅ [M + H]⁺ 307.1545, observed 307.1540.

Synthesis of (R)-8-hydroxy-6-methoxy-3-(((2R,6R)-6-methyltetrahydro-2H-pyran-2-yl)methyl)isochroman-1-one (CL-10)



The concerned compound **CL-10** was synthesized using similar protocol as that of **CL-9**.

$[\alpha]^{25}_{\text{D}} = +48.90$ (c, CHCl₃).

IR ν_{max} (**film**): cm⁻¹ 1374, 1665, 1743, 2852, 2931.

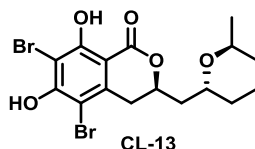
¹H NMR (400 MHz, CDCl₃): δ 11.22 (s, 1H), 7.26 (s, 1H), 6.35 (d, $J = 1.5$ Hz, 1H), 6.23 (s, 1H), 4.83 (td, $J = 9.8, 2.7$ Hz, 1H), 3.81 (s, 3H), 3.69 (t, $J = 10.6$ Hz, 1H), 3.48 – 3.42 (m, 1H), 2.86 (d, $J = 7.3$ Hz, 2H), 1.89 – 1.75 (m, 4H), 1.57 (dd, $J = 16.6, 6.2$ Hz, 4H), 1.13 (d, $J = 6.2$ Hz, 3H).

¹³C NMR (100 MHz, CDCl₃): δ 169.9, 165.8, 164.5, 141.2, 106.1, 101.8, 99.4, 75.9, 73.7, 72.9, 55.5, 42.0, 33.8, 33.2, 31.7, 23.5, 22.1.

Chapter 1 (Section C): Design, Synthesis, Biological Evaluation of Lysyl tRNA synthetase (KRS) Inhibitors based on Cladosporin Scaffold towards Identification of Antimalarial Leads

HRMS calculated for C₁₇H₂₃O₅ [M + H]⁺ 307.1545, observed 307.1540.

Synthesis of (*R*)-5,7-dibromo-6,8-dihydroxy-3-(((2*R*,6*S*)-6-methyltetrahydro-2H-pyran-2-yl)methyl)isochroman-1-one (CL-13)



Br₂ was added dropwise to a solution of isocladosporin (0.015 g, 0.051 mmol) in CH₂Cl₂ (10 mL) at 0 °C. Following which the reaction mixture was quenched with Na₂S₂O₃ and extracted with CH₂Cl₂ (10 mL x 3). The combined organic layers were dried over Na₂SO₄ and concentrated under vacuo to furnish **CL-13** (0.017 g) in 73% yield.

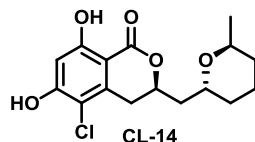
[α]²⁵_D = +11.8 (c 0.7, CHCl₃).

IR ν_{max} (film): cm⁻¹ 1645, 1822, 2920, 3330.

¹H NMR (400 MHz, MeOD): δ 4.86 – 4.74 (m, 1H), 3.64 (t, *J* = 10.4 Hz, 1H), 3.48 – 3.45 (m, 1H), 3.32 (overlap, 1H), 2.80 (dd, *J* = 17.1, 11.6 Hz, 1H), 1.96 – 1.90 (m, 1H), 1.85 – 1.78 (m, 2H), 1.59 (d, *J* = 10.4 Hz, 3H), 1.23 – 1.20 (m, 2H), 1.14 (d, *J* = 6.1 Hz, 3H).

¹³C NMR (100 MHz, MeOD): δ 170.94, 161.2, 159.4, 141.0, 103.8, 102.8, 98.5, 77.5, 75.3, 74.9, 42.9, 35.4, 34.5, 33.0, 24.8, 22.6.

Synthesis of (*R*)-5-chloro-6,8-dihydroxy-3-(((2*R*,6*S*)-6-methyltetrahydro-2H-pyran-2-yl)methyl)isochroman-1-one (CL-14)



Cladosporin (0.05 g, 0.171 mmol) was dissolved in THF (5 mL) and cooled to -30°C. SOCl₂ (18 mL, 0.257 mmol) was added at the same temperature and stirred for 6 h.

Chapter 1 (Section C): Design, Synthesis, Biological Evaluation of Lysyl tRNA synthetase (KRS) Inhibitors based on Cladosporin Scaffold towards Identification of Antimalarial Leads

After completion of the reaction as monitored by TLC, the reaction mixture was diluted with ethyl acetate (15 mL) and washed with saturated aqueous solution of NaHCO₃ (10 mL x 3). The combined organic layers were dried over Na₂SO₄ and concentrated under vacuo. Purification through column chromatography afforded **CL-14** (0.034 g) in 61% yield.

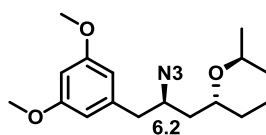
$[\alpha]^{25}_{\text{D}} = +17.2$ (c 1.2, CHCl₃).

IR ν_{max} (film): cm⁻¹ 1246, 1662, 1793, 2930.

¹H NMR (400 MHz, CDCl₃): δ 11.19 (s, 1H), 6.91 (s, 1H), 6.53 (s, 1H), 4.72 (ddt, $J = 12.1, 8.9, 3.3$ Hz, 1H), 4.12 (td, $J = 7.4, 3.6$ Hz, 1H), 3.98 – 3.95 (m, 1H), 3.19 (dd, $J = 17.0, 3.4$ Hz, 1H), 2.79 (dd, $J = 17.0, 11.8$ Hz, 1H), 2.04 (ddd, $J = 14.0, 10.5, 3.4$ Hz, 1H), 1.85 (ddd, $J = 14.7, 8.9, 2.6$ Hz, 1H), 1.73 – 1.62 (m, 4H), 1.34 (dd, $J = 14.1, 6.6$ Hz, 2H), 1.22 (d, $J = 6.4$ Hz, 4H).

¹³C NMR (100 MHz, CDCl₃): δ 169.3, 162.7, 158.1, 138.1, 109.9, 102.7, 102.7, 75.8, 67.7, 66.3, 39.2, 31.3, 30.9, 30.8, 19.0, 18.2.

Synthesis of compound (2*R*,6*S*)-2-((*R*)-2-azido-3-(3,5-dimethoxyphenyl)propyl)-6-methyltetrahydro-2*H*-pyran (6.2)

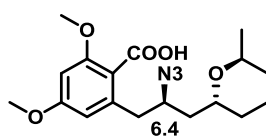


Compound **6.1** (0.5 g, 1.69 mmol) was dissolved in CH₂Cl₂ (12 mL) and cooled to 0 °C, following which Et₃N (0.47 mL, 3.4 mmol) was added at the same temperature. After 15 mins methanesulfonyl chloride (0.2 mL, 2.55 mmol) and cat. DMAP (10 mg) was added to the same. The reaction mixture was allowed to reach room temperature and was stirred for 6 h. Upon completion of the reaction as monitored by TLC, it was diluted with DCM (10 mL x 3) and washed with saturated aqueous solution of NaHCO₃ (7 mL x 3). The combined organic layers were dried over Na₂SO₄, concentrated under vacuo and forwarded to next step without further purification. The obtained mesylated compound was dissolved in dry DMF (6 mL), following which NaN₃ (0.55 g, 8.483

Chapter 1 (Section C): Design, Synthesis, Biological Evaluation of Lysyl tRNA synthetase (KRS) Inhibitors based on Cladosporin Scaffold towards Identification of Antimalarial Leads

mmol) was added to the same and stirred at 65 °C for 12 h. The reaction mixture was diluted with ethyl acetate (18 mL) and washed with ice. The organic layer was dried over Na₂SO₄, concentrated under vacuo and forwarded as such without further purification.

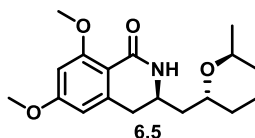
Synthesis of compound 2-((*R*)-2-azido-3-((2*R*,6*S*)-6-methyltetrahydro-2H-pyran-2-yl)propyl)-4,6-dimethoxybenzoic acid (6.4)



POCl₃ (0.476 mL, 5.09 mmol) was added dropwise to an ice cold solution of the obtained azide intermediate **6.2** in DMF (7 ml). The reaction mixture was heated at 65 °C for 12 h. After completion of the reaction as monitored by TLC, the reaction mixture was poured in to ice and saturated aqueous solution of NaHCO₃ was added until basic. The reaction mixture was then extracted with ethyl acetate (15 mL x 2) was washed with ice. The organic layers were dried over Na₂SO₄, concentrated under vacuo to afford formylated intermediate which was forwarded to next step without further purification. The obtained formylated intermediate (0.679 g, 1.688 mmol) was dissolved in DMSO (20 mL) and cooled to 5-7 °C followed by addition of aqueous solution (5 ml) of NaH₂PO₄ (0.506 g, 4.22 mmol) at the same temperature. 2-methyl-2-butene (15 mL) was added to the reaction mixture, following which aqueous solution (5 mL) of NaClO₂ (0.382 g, 4.22 mmol) was added dropwise and left to stir at room temperature for 12 h. The reaction mixture was diluted with saturated aqueous NaHCO₃ until basic and washed with ethyl acetate (10 mL x 3). The collected aqueous layers were combined, acidified with 1N HCl and extracted with ethyl acetate (10 mL x 3). The organic layer thus obtained was dried over Na₂SO₄ and concentrated under vacuo to afford acid **9** which was used in next step as such.

Chapter 1 (Section C): Design, Synthesis, Biological Evaluation of Lysyl tRNA synthetase (KRS) Inhibitors based on Cladosporin Scaffold towards Identification of Antimalarial Leads

Synthesis of compound (*R*)-6,8-dimethoxy-3-(((2*R*,6*S*)-6-methyltetrahydro-2H-pyran-2-yl)methyl)-3,4-dihydroisoquinolin-1(2H)-one (6.5)



DIPEA (0.738 ml, 4.238 mmol) was added to a solution of acid **6.4** (0.706 g, 1.695 mmol) in THF (10 mL) at 0 °C followed by the addition of EDC.HCl (0.65 g mg, 3.39 mmol) and HOBT (0.458 g, 3.39 mmol). After 15 minutes triphenylphosphine (0.667 g, 2.543 mmol) was added to the reaction mixture and was left to stir for 12 h at room temperature. The reaction mixture was then diluted with ethyl acetate (10 mL x 2) and washed with 1N HCl followed by saturated aqueous NaHCO₃. The combined organic layers were dried over Na₂SO₄, concentrated under vacuo and purified by column chromatography to afford compound **6.5** (0.094 g) in 17% yield in 5 steps.

$[\alpha]^{25}_{\text{D}} = -22.81$ (1.5, CHCl₃).

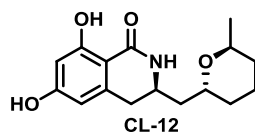
IR ν_{max} (film): cm⁻¹ 1297, 1605, 1654, 1932.

¹H NMR (400 MHz, CDCl₃): δ 6.38 (d, $J = 2.2$ Hz, 1H), 6.28 (d, $J = 2.2$ Hz, 1H), 6.12 (s, 1H), 3.99 – 3.95 (m, 1H), 3.92 – 3.86 (m, 4H), 3.83 (s, 3H), 3.76 (ddd, $J = 10.1, 7.9, 3.9$ Hz, 1H), 2.98 (dd, $J = 15.3, 4.6$ Hz, 1H), 2.70 (dd, $J = 15.3, 8.1$ Hz, 1H), 1.79 – 1.66 (m, 4H), 1.59 – 1.53 (m, 2H), 1.33 – 1.26 (m, 2H), 1.19 (d, $J = 6.6$ Hz, 3H).

¹³C NMR (100 MHz, CDCl₃): δ 164.6, 163.0, 161.8, 142.6, 110.5, 104.4, 97.5, 67.7, 66.9, 56.1, 55.3, 47.0, 38.5, 36.6, 30.6, 30.5, 18.6, 18.2.

HRMS calculated for C₁₈H₂₆O₄N [M + H]⁺ 320.1861, observed 320.1856.

Synthesis of (*R*)-6,8-dihydroxy-3-(((2*R*,6*S*)-6-methyltetrahydro-2H-pyran-2-yl)methyl)-3,4-dihydroisoquinolin-1(2H)-one (CL-12)



Chapter 1 (Section C): Design, Synthesis, Biological Evaluation of Lysyl tRNA synthetase (KRS) Inhibitors based on Cladosporin Scaffold towards Identification of Antimalarial Leads

A suspension of aluminium powder (0.365 g, 13.54 mmol) in dry benzene (5 mL) was treated with I₂ (1.2 g, 4.71 mmol) under argon, and the violet mixture was stirred under reflux for 30 min until the violet color disappeared. After the mixture was cooled to 0 °C, few crystals of TBAI (7.7 mg, 0.029 mmol) and phloroglucinol (0.186 g, 1.47 mmol) were added before a solution of compound **6.5** (0.094 g, 0.294 mmol) in dry benzene (3 mL) was added in one portion. The resulting green-brown suspension was stirred for 30 min at 5 °C before saturated Na₂S₂O₃ solution (8 mL) and ethyl acetate (8 mL) were added. After separation of the layers, the aqueous phase was extracted with ethyl acetate. The combined organic layers were washed with brine, dried over Na₂SO₄, filtered, and concentrated in vacuo. Purification by column chromatography afforded **CL-12** in 52% yield.

$[\alpha]_{\text{D}}^{25} = -25.1$ (c 1.5, CHCl₃).

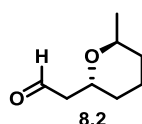
IR ν_{max} (**film**): cm⁻¹ 1295, 1653, 1346, 1643, 3416.

¹H NMR (400 MHz, MeOD): δ 6.18 (d, $J = 2.2$ Hz, 1H), 6.13 (d, $J = 2.3$ Hz, 1H), 4.03 – 3.92 (m, 2H), 3.76 (tt, $J = 8.2, 5.1$ Hz, 1H), 3.00 (dd, $J = 15.7, 5.1$ Hz, 1H), 2.73 (dd, $J = 15.7, 7.9$ Hz, 1H), 1.96 (ddd, $J = 14.4, 9.4, 5.1$ Hz, 1H), 1.71 – 1.59 (m, 5H), 1.37 – 1.31 (m, 2H), 1.22 (d, $J = 6.5$ Hz, 3H).

¹³C NMR (100 MHz, MeOD): δ 171.4, 164.6, 164.4, 142.2, 107.7, 104.4, 101.9, 69.5, 68.5, 38.7, 35.0, 32.6, 31.2, 19.8, 19.3.

HRMS calculated for C₁₆H₂₁O₄NNa [M + Na]⁺ 314.1360, observed 314.1363.

Synthesis of compound 2-((2R,6S)-6-methyltetrahydro-2H-pyran-2-yl)acetaldehyde (8.2)

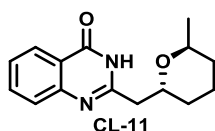


Compound **8.1** (0.18 g, 1.3 mmol) was dissolved in a mixture of 3:1 CH₂Cl₂ : MeOH (20 mL) and the solution was then cooled to -78 °C. Solid NaHCO₃ (1.0 g) was added

Chapter 1 (Section C): Design, Synthesis, Biological Evaluation of Lysyl tRNA synthetase (KRS) Inhibitors based on Cladosporin Scaffold towards Identification of Antimalarial Leads

then ozone was bubbled until the solution turned blue. Argon was bubbled till complete disappearance of blue color, then dimethyl sulphide (x mL) was added and the mixture allowed to warm to room temperature and stirred for 16 h. The solvent and excess Me₂S were removed in vacuo and the residue was taken up with CH₂Cl₂ (3 x 10 mL). The solution was then filtered and concentrated in vacuo to afford aldehyde **8.2** which was forwarded to next step without further purification.

Synthesis of 2-(((2*R*,6*S*)-6-methyltetrahydro-2*H*-pyran-2-yl)methyl)quinazolin-4(3*H*)-one (CL-11)



Anthranilic acid (0.231 g, 1.69 mmol), formamide (67 mL, 1.69 mmol) and compound **8.2** (0.12 g, 0.845 mmol) was dissolved in PEG-400 (8 mL) and was stirred at 130 °C for 12 h. The reaction mixture was then cooled to room temperature and diluted with ethyl acetate (15 mL), following which it was washed with H₂O. The combined organic layers were dried over Na₂SO₄, concentrated under vacuo and purified through column chromatography to afford **CL-11** (0.156 g) in 72% yield as a foamy solid.

$[\alpha]^{25}_{\text{D}} = -0.4$ (c 0.5, CHCl₃).

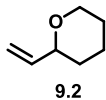
IR ν_{max} (film): cm⁻¹ 1257, 1613, 1657, 2853, 2917.

¹H NMR (400 MHz, CDCl₃): δ 10.3 (s, 1H), 8.26 (d, $J = 7.4$ Hz, 1H), 7.74 – 7.70 (m, 1H), 7.63 (d, $J = 8.1$ Hz, 1H), 7.44 (t, $J = 7.4$ Hz, 1H), 3.81 – 3.77 (m, 1H), 3.55 (dd, $J = 10.8, 4.8$ Hz, 1H), 2.91 – 2.81 (m, 2H), 1.86 – 1.83 (m, 1H), 1.67 – 1.50 (m, 4H), 1.41 – 1.33 (m, 1H), 1.28 (d, $J = 6.1$ Hz, 3H).

¹³C NMR (100 MHz, CDCl₃): δ 161.6, 154.8, 148.8, 134.4, 126.9, 126.4, 121.4, 75.6, 74.6, 41.6, 32.7, 30.8, 23.2, 22.1

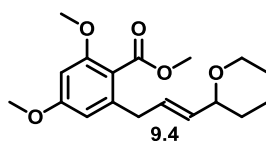
Chapter 1 (Section C): Design, Synthesis, Biological Evaluation of Lysyl tRNA synthetase (KRS) Inhibitors based on Cladosporin Scaffold towards Identification of Antimalarial Leads

Synthesis of compound 2-vinyltetrahydro-2H-pyran (9.2)



Triethylamine (2.1 mL, 15.00 mmol) was added to a solution of diol 5 (1.5 g, 11.52 mmol) in CH₂Cl₂ (30 mL) at 0 °C. After 15 minutes methanesulfonyl chloride (0.8 mL, 10.37 mmol) was added to the same followed by the addition of catalytic DMAP (15 mg). The reaction mixture was warmed to room temperature and stirred for 12 h. After completion of the reaction it was diluted with DCM (15 mL) and washed with saturated aqueous NaHCO₃. The combined organic layers were washed with brine, dried over Na₂SO₄, filtered, and concentrated in vacuo to afford corresponding mesylated compound which was forwarded to next step without further purification. The obtained mesylated compound was dissolved in dry THF (35 mL) and NaH (~55%) (0.654 g, 14.98 mmol) was added at 0 °C. The reaction mixture was warmed to room temperature and stirred for 12 h. After completion of the reaction as monitored by TLC, the reaction mass cooled to 0 °C was quenched with saturated aqueous NH₄Cl solution (15 mL). The reaction mixture was then extracted with diethyl ether (15 mL x 3) dried over Na₂SO₄ and the resultant reaction mixture was filtered through a pad of celite and concentrated via rotary evaporation at low temperature to afford compound **9.2**.

Synthesis of compound methyl (*E*)-2,4-dimethoxy-6-(3-(tetrahydro-2H-pyran-2-yl)allyl)benzoate (9.4)



A solution of compound **9.2** (0.831 g, 7.41 mmol) in CH₂Cl₂ (50 mL) was degassed with argon for 15 min. Solution of Compound **9.3** (0.7 g, 2.96 mmol) in CH₂Cl₂ was added in the same followed by addition of 5 mol % of the Grubbs' second generation catalyst. The reaction mixture was stirred at room temperature for 36 h. It was then filtered through a short pad of Celite and concentrated under reduced pressure to remove excess CH₂Cl₂. The crude thus obtained was purified through column chromatography to afford compound **9.4** (0.322 g) in 34 % yield.

Chapter 1 (Section C): Design, Synthesis, Biological Evaluation of Lysyl tRNA synthetase (KRS) Inhibitors based on Cladosporin Scaffold towards Identification of Antimalarial Leads

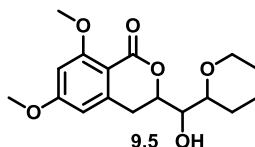
IR ν_{\max} (film): cm^{-1} 1458, 1600, 1722, 2935.

^1H NMR (400 MHz, CDCl_3): δ 6.32 (s, 2H), 5.76 – 5.69 (m, 1H), 5.50 (dd, $J = 15.4$, 5.9 Hz, 1H), 3.97 (d, $J = 9.4$ Hz, 1H), 3.85 (s, 3H), 3.85-3.72 (m, 7H), 3.44 (t, $J = 11.2$ Hz, 1H), 3.31 (d, $J = 6.4$ Hz, 2H), 1.83 – 1.81 (m, 1H), 1.61 (dd, $J = 24.6$, 12.1 Hz, 2H), 1.50 (dd, $J = 16.3$, 7.7 Hz, 2H), 1.36 (dd, $J = 23.1$, 11.6 Hz, 1H).

^{13}C NMR (100 MHz, CDCl_3): δ 168.4, 161.5, 158.2, 140.5, 133.1, 128.9, 116.1, 106.1, 96.5, 77.9, 68.3, 55.9, 55.3, 52.0, 36.7, 32.0, 25.8, 23.3.

HRMS calculated for $\text{C}_{18}\text{H}_{24}\text{O}_5\text{Na}$ $[\text{M} + \text{Na}]^+$ 343.1517, observed 343.1516.

Synthesis of compound 3-(hydroxy(tetrahydro-2H-pyran-2-yl)methyl)-6,8-dimethoxyisochroman-1-one (9.5)



To a solution of compound **9.4** (0.322 g, 1.005 mmol) in acetone (12 mL) and water (6 mL) was added 4-methylmorpholine N-oxide (0.353 g, 3.015 mmol) followed by the careful addition of catalytic amount of 2.5% OsO_4 (tert-butanol solution) at 0 °C. After stirring for 12 h at room temperature saturated aqueous solution of Na_2SO_3 (15 mL) was added and further stirred for 6 h at room temperature. Excess acetone was removed under vacuo, and the remaining aqueous part was extracted with ethyl acetate (3×20 mL). The combined organic parts were dried over sodium sulfate and concentrated under vacuo. Purification through column chromatography afforded compound **9.5** (0.181 g) in 56 % yield.

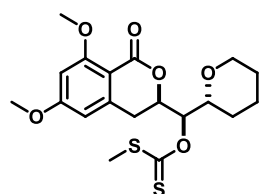
IR ν_{\max} (film): cm^{-1} 1247, 1374, 1662, 2929.

^1H NMR (400 MHz, CDCl_3): δ 6.39 (s, 1H), 6.33 (s, 1H), 4.71 (d, $J = 12.9$ Hz, 1H), 3.92-3.89 (m, 4H), 3.86-3.80 (m, 4H), 3.52 (t, $J = 9.3$ Hz, 1H), 3.44 – 3.28 (m, 3H), 2.66 – 2.62 (m, 1H), 2.04 – 1.88 (m, 3H), 1.37 – 1.25 (m, 3H).

Chapter 1 (Section C): Design, Synthesis, Biological Evaluation of Lysyl tRNA synthetase (KRS) Inhibitors based on Cladosporin Scaffold towards Identification of Antimalarial Leads

^{13}C NMR (100 MHz, CDCl_3): δ 164.6, 163.1, 162.5, 144.3, 106.6, 104.0, 97.7, 76.1, 75.6, 75.1, 68.5, 56.16, 55.6, 31.7, 28.6, 26.1, 22.9. HRMS calculated for $\text{C}_{17}\text{H}_{23}\text{O}_6$ [$\text{M} + \text{H}$] $^+$ 323.1493, observed 31323.1489.

Synthesis of compound O-((6,8-dimethoxy-1-oxoisochroman-3-yl)(tetrahydro-2H-pyran-2-yl)methyl) S-methyl carbonodithioate (9.6a)



9.6a (enantiomeric mixture)

To a solution of compound **9.5** (0.181 g, 0.561 mmol) in THF (20 mL) was added KHMDS (1 M in THF) (0.7 mL, 0.73 mmol) at 0 °C. After 15 min CS_2 (68 ml, 1.12 mmol) was added, which was followed by the addition of CH_3I (105 mL, 1.68 mmol). After stirring the reaction mixture for 12 h, H_2O (10 mL) was added to the same and extracted with ethyl acetate. The combined organic layers were dried over Na_2SO_4 and concentrated under vacuo. Purification through flash chromatography gave clean separation of the two diastereomer **18a** (0.095 g) and **18b** (0.056 g) as foamy solids with an overall yield of 71% and **9.6a** as the major diastereomer.

IR ν_{max} (film): cm^{-1} 1210, 1598, 1722, 2937.

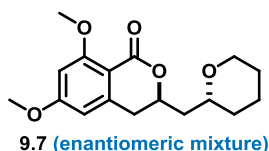
^1H NMR (400 MHz, CDCl_3): δ 6.38 (d, $J = 2.2$ Hz, 1H), 6.28 (d, $J = 1.9$ Hz, 1H), 5.96 (dd, $J = 9.2, 1.5$ Hz, 1H), 4.89 (ddd, $J = 12.3, 2.8, 1.5$ Hz, 1H), 4.02 (ddd, $J = 11.2, 7.0, 2.1$ Hz, 1H), 3.91 (s, 4H), 3.83 (s, 3H), 3.48 (td, $J = 11.1, 3.8$ Hz, 1H), 3.00 – 2.93 (m, 1H), 2.72 (dd, $J = 16.2, 2.8$ Hz, 1H), 2.56 (s, 3H), 1.85 – 1.82 (m, 1H), 1.57 – 1.45 (m, 3H), 1.30 (ddd, $J = 12.6, 10.5, 3.5$ Hz, 1H).

^{13}C NMR (100 MHz, CDCl_3): δ 217.3, 164.4, 163.0, 162.2, 143.6, 106.9, 103.8, 97.9, 82.5, 74.1, 73.5, 68.5, 56.1, 55.5, 31.6, 28.0, 25.9, 22.6, 19.3.

HRMS calculated for $\text{C}_{19}\text{H}_{25}\text{O}_6\text{S}_2$ [$\text{M} + \text{Na}$] $^+$ 413.1087, observed 413.1087.

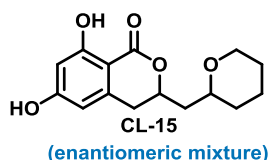
Chapter 1 (Section C): Design, Synthesis, Biological Evaluation of Lysyl tRNA synthetase (KRS) Inhibitors based on Cladosporin Scaffold towards Identification of Antimalarial Leads

Synthesis of compound **6,8-dimethoxy-3-((tetrahydro-2H-pyran-2-yl)methyl)isochroman-1-one (9.7)**



Compound **9.6a** (0.095 g, 0.23 mmol) was dissolved in toluene (12 mL) which was followed by the addition of AIBN (3.8 mg, 0.023 mmol) and tributyltin hydride (0.186 mL, 0.69 mmol). The reaction mixture was stirred at 95 °C for 4 h. After completion of the reaction as monitored by TLC, it was washed with brine (15 ml x 3) and then with 30% aqueous KF (30 mL) solution to precipitate the unwanted tin impurities. The solid precipitate was filtered off and the process was repeated five times. The obtained organic layers were washed with water (20 mL x 3) and dried over Na₂SO₄ and concentrated under vacuo to obtain the final product which was forwarded as such.

Synthesis of **6,8-dihydroxy-3-((tetrahydro-2H-pyran-2-yl)methyl)isochroman-1-one (CL-15)**



CL-15 was synthesized using similar protocol as that of **CL-2**.

IR ν_{\max} (film): cm⁻¹ 1251, 1636, 2856, 2930.

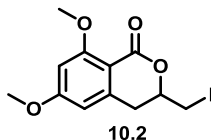
¹H NMR (400 MHz, CDCl₃): δ 11.07 (s, 1H), 7.83 (s, 1H), 6.30 (s, 1H), 6.09 (s, 1H), 4.76 (t, *J* = 10.0 Hz, 1H), 4.01 (d, *J* = 10.6 Hz, 1H), 3.74 (t, *J* = 10.1 Hz, 1H), 3.51 (t, *J* = 9.1 Hz, 1H), 2.85 – 2.78 (m, 1H), 2.62 (d, *J* = 15.8 Hz, 1H), 1.92 – 1.86 (m, 2H), 1.74 – 1.68 (m, 1H), 1.62 – 1.57 (m, 3H), 1.37 – 1.24 (m, 2H).

¹³C NMR (100 MHz, CDCl₃): δ 169.9, 164.4, 163.3, 141.7, 106.4, 102.2, 101.5, 75.7, 73.8, 68.7, 41.7, 33.6, 32.0, 25.8, 23.2.

HRMS calculated for C₁₅H₁₉O₅ [M + H]⁺ 279.1230, observed 279.1227.

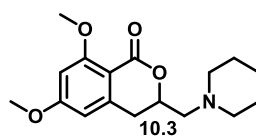
Chapter 1 (Section C): Design, Synthesis, Biological Evaluation of Lysyl tRNA synthetase (KRS) Inhibitors based on Cladosporin Scaffold towards Identification of Antimalarial Leads

Synthesis of compound 3-(iodomethyl)-6,8-dimethoxyisochroman-1-one (10.2)



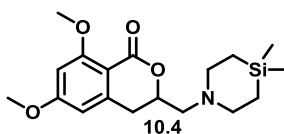
Acid **10.1** (2.5 g, 11.25 mmol) was dissolved in THF (18 mL) and cooled to 0 °C, following which NaHCO₃ (1.89 g, 22.5 mmol) and I₂ (3.43 g, 13.5 mmol) was added one after the other. The reaction mixture was stirred for 12 h at room temperature. After complete consumption of the starting material, the reaction mass was diluted with ethyl acetate (20 mL) and washed with saturated aqueous NH₄Cl solution (10 mL x 3). The combined organic layers were dried over Na₂SO₄, concentrated under vacuo and forwarded as such without further purification.

Synthesis of compound 6,8-dimethoxy-3-(piperidin-1-ylmethyl)isochroman-1-one (10.3)



Compound **10.2** (0.2 g, 0.574 mmol) and piperidine (113 ml, 1.15 mmol) was dissolved in acetonitrile (7 mL) following which triethylamine (0.2 ml, 1.44 mmol) was added the reaction mixture was heated at 150 °C under micro wave irradiation. After complete conversion of the starting material, the reaction mixture was diluted with ethyl acetate (20 mL) and washed thoroughly with H₂O (15 mL x 4). The collected organic layers were washed with brine, dried over Na₂SO₄ and concentrated under vacuo. The crude was passed through a short pad of silica to afford compound **10.3** which was forwarded to next step without further purification.

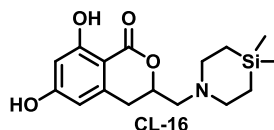
Synthesis of compound 3-((4,4-dimethyl-1,4-azasilinan-1-yl)methyl)-6,8-dimethoxyisochroman-1-one (10.4)



Compound **10.4** was synthesized following similar procedure as that of compound **10.3**.

Chapter 1 (Section C): Design, Synthesis, Biological Evaluation of Lysyl tRNA synthetase (KRS) Inhibitors based on Cladosporin Scaffold towards Identification of Antimalarial Leads

Synthesis of 3-((4,4-dimethyl-1,4-azasilinan-1-yl)methyl)-6,8-dihydroxyisochroman-1-one (CL-16)



CL-16 was synthesized following similar procedure as that of CL-2.

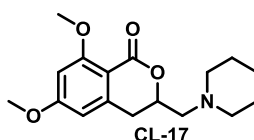
IR ν_{\max} (film): cm^{-1} 1245, 1669, 1821, 3651, 3771.

$^1\text{H NMR}$ (400 MHz, DMSO- d_6): δ 10.87 (s, 1H), 10.13 (s, 1H), 6.30 (s, 1H), 6.26 (s, 1H), 5.20 (d, $J = 6.8$ Hz, 1H), 3.59 – 3.39 (m, 6H), 2.96 (d, $J = 7.1$ Hz, 2H), 1.17 – 0.96 (m, 4H), 0.18 (s, 3H), 0.12 (s, 3H).

$^{13}\text{C NMR}$ (100 MHz, DMSO- d_6): δ 167.9, 164.8, 163.4, 141.0, 107.1, 101.2, 100.0, 73.1, 56.7, 52.3, 51.3, 30.2, 9.5, -3.3, -4.3.

HRMS calculated for $\text{C}_{16}\text{H}_{24}\text{NSi}$ $[\text{M} + \text{H}]^+$ 322.1476, observed 322.1469.

Synthesis of 6,8-dimethoxy-3-(piperidin-1-ylmethyl)isochroman-1-one (CL-17)



CL-17 was synthesized following similar procedure as that of CL-2.

IR ν_{\max} (film): cm^{-1} 1241, 1622, 1671, 2658, 3138.

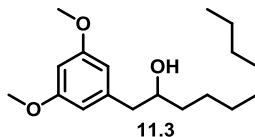
$^1\text{H NMR}$ (400 MHz, DMSO- d_6): δ 10.87 (s, 1H), 9.83 (s, 1H), 6.30 (s, 1H), 6.25 (s, 1H), 5.21 – 5.17 (m, 1H), 3.73 – 3.43 (m, 6H), 2.96 – 2.94 (m, 2H), 1.80 – 1.68 (m, 5H), 1.39 (s, 1H).

$^{13}\text{C NMR}$ (100 MHz, DMSO- d_6): δ 167.8, 164.8, 163.4, 140.9, 107.1, 101.2, 100.0, 72.6, 58.1, 53.6, 51.9, 29.9, 22.2, 22.1, 21.1.

HRMS calculated for $\text{C}_{15}\text{H}_{20}\text{O}_4\text{N}$ $[\text{M} + \text{H}]^+$ 278.1389, observed 278.1387.

Chapter 1 (Section C): Design, Synthesis, Biological Evaluation of Lysyl tRNA synthetase (KRS) Inhibitors based on Cladosporin Scaffold towards Identification of Antimalarial Leads

Synthesis of compound 1-(3,5-dimethoxyphenyl)decan-2-ol (11.3)



To an oven dried two neck round bottomed flask equipped with a magnetic stir bar was added activated magnesium metal (1.00 g, 42.27 mmol) under argon atmosphere. THF (100 mL) was added followed by the addition of a pinch of I₂ and was stirred vigorously for 30 min. 1-bromo-3,5-dimethoxy benzene (**11.1**) (8.33 g, 38.4 mmol) dissolved in THF (30 mL) was added drop wise to the stirring solution. The onset of exothermic reaction was characterized by decolorization of I₂. The resulting mixture was stirred for 2 h. The freshly prepared Grignard reagent was cooled to -30 °C followed by the addition of Copper (I) iodide (0.366 g, 1.92 mol%). Solution of epoxide **11.2** (1.5 g, 9.6 mmol) in THF (10 mL) was added drop wise and left to stir for 16 h at -30°C. The reaction mixture was quenched with saturated aqueous NH₄Cl (30 mL) and extracted with diethyl ether (30 mL x 3). The combined organic layers were dried over anhydrous Na₂SO₄, and concentrated under vacuo. The resulting mixture thus obtained as yellowish oil was purified by column chromatography to afford corresponding alcohols **11.3** (2.5 g) as yellowish oil with an overall yield of 87%.

IR ν_{\max} (film): cm⁻¹ 1154, 1463, 1600, 2853, 2925.

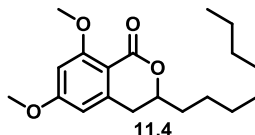
¹H NMR (400 MHz, CDCl₃): δ 6.37 (d, *J* = 2.2 Hz, 2H), 6.35-6.34 (m, 1H), 3.82 – 3.73 (m, 7H), 2.77 (dd, *J* = 13.5, 4.0 Hz, 1H), 2.57 (dd, *J* = 13.5, 8.6 Hz, 1H), 1.58 – 1.50 (m, 4H), 1.36 – 1.27 (m, 10H), 0.88 (t, *J* = 6.9 Hz, 3H).

¹³C NMR (100 MHz, CDCl₃): δ 160.9, 141.0, 107.3, 98.4, 72.5, 55.3, 44.4, 36.9, 31.9, 29.7, 29.6, 29.3, 25.8, 22.7, 14.1.

HRMS calculated for C₁₈H₃₁O₃ [M + H]⁺ 295.2265, observed 295.2268.

Chapter 1 (Section C): Design, Synthesis, Biological Evaluation of Lysyl tRNA synthetase (KRS) Inhibitors based on Cladosporin Scaffold towards Identification of Antimalarial Leads

Synthesis of compound 6,8-dimethoxy-3-octylisochroman-1-one (11.4)



To a solution of compound **11.3** (1.00 g, 3.396 mmol) and trimethyl orthoformate (8 mL) in DCM (15 mL) was added *p*TSA (58 mg, 0.34 mmol). After being stirred for 1 h, the reaction mixture was quenched with addition of saturated aqueous NaHCO₃ solution, and the resulting mixture was diluted with Et₂O (20 mL). The layers were separated, and the aqueous layer was extracted with Et₂O. The combined organic layers were dried over anhydrous Na₂SO₄ and concentrated in vacuo to obtain a brownish oil. To a cooled (0 °C) solution of the obtained brownish oil in acetone (12 mL) was added 3.0 M Jones oxidant (2.4 mL). The reaction mixture was then warmed to room temperature and stirred for 1 h. After quenching by addition of water, the resulting mixture was diluted with ethyl acetate (20 mL). The layers were separated, and the aqueous layer was further extracted with ethyl acetate (15 mL). The combined organic layers were dried over anhydrous Na₂SO₄ and concentrated under vacuo. The residue was purified by column chromatography to afford compound **11.4** as a brownish oil.

IR ν_{\max} (film): cm⁻¹ 1235, 1599, 1719, 2926.

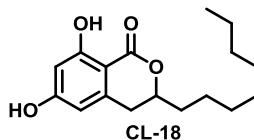
¹H NMR (400 MHz, CDCl₃): δ 6.39 (d, *J* = 2.2 Hz, 1H), 6.29 (d, *J* = 2.1 Hz, 1H), 4.33 (tdd, *J* = 10.8, 5.2, 3.2 Hz, 1H), 3.91 (s, 3H), 3.85 (s, 3H), 2.82 (qd, *J* = 16.0, 7.1 Hz, 2H), 1.82 (dddd, *J* = 12.3, 10.1, 7.4, 4.9 Hz, 1H), 1.68 – 1.59 (m, 1H), 1.56 – 1.47 (m, 1H), 1.40 (ddd, *J* = 18.3, 10.4, 5.4 Hz, 1H), 1.28 – 1.26 (m, 10H), 0.87 (t, *J* = 6.9 Hz, 3H).

¹³C NMR (100 MHz, CDCl₃): δ 164.3, 163.1, 162.8, 144.0, 107.1, 103.8, 97.7, 77.3, 56.1, 55.5, 34.9, 34.7, 31.8, 29.4, 29.4, 29.2, 24.9, 22.6, 14.1.

HRMS calculated for C₁₉H₂₉O₄ [M + H]⁺ 321.2063, observed 321.2060.

Chapter 1 (Section C): Design, Synthesis, Biological Evaluation of Lysyl tRNA synthetase (KRS) Inhibitors based on Cladosporin Scaffold towards Identification of Antimalarial Leads

Synthesis of 6,8-dihydroxy-3-octylisochroman-1-one (CL-18)



CL-18 was synthesized following similar procedure as that of CL-2.

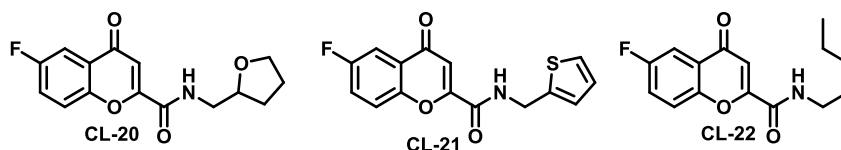
IR ν_{\max} (film): cm^{-1} 1249, 1632, 2856, 2923, 3243.

$^1\text{H NMR}$ (400 MHz, CDCl_3): δ 11.15 (s, 1H), 6.70 (s, 1H), 6.33 (s, 1H), 6.22 (s, 1H), 4.51 (ddt, $J = 10.2, 7.4, 5.0$ Hz, 1H), 2.91 – 2.79 (m, 2H), 1.90 – 1.81 (m, 1H), 1.73 – 1.64 (m, 1H), 1.56 – 1.49 (m, 1H), 1.44 – 1.39 (m, 1H), 1.31 – 1.26 (m, 10H), 0.88 (t, $J = 6.8$ Hz, 3H).

$^{13}\text{C NMR}$ (100 MHz, CDCl_3): δ 170.3, 164.3, 162.8, 141.8, 106.7, 101.9, 101.7, 79.4, 34.7, 33.1, 31.8, 29.4, 29.3, 29.2, 24.8, 22.6, 14.0.

HRMS calculated for $\text{C}_{17}\text{H}_{25}\text{O}_4$ $[\text{M} + \text{H}]^+$ 293.1750, observed 293.1747.

General procedure for the synthesis of 6-fluoro-4-oxo-N-((tetrahydrofuran-2-yl)methyl)-4H-chromene-2-carboxamide (CL-20), 6-fluoro-4-oxo-N-(thiophen-2-ylmethyl)-4H-chromene-2-carboxamide (CL-21) and 6-fluoro-4-oxo-N-pentyl-4H-chromene-2-carboxamide (CL-22)



Chromen carboxylic acid **12.1** was dissolved in dry DMF following which triethylamine (1.5 equivalent) was added at 0 °C. Corresponding amine (1.3 equivalent) was added to the reaction which was followed by dropwise addition a solution of PyBOP (2.0 equivalent) in DCM at the same temperature. The reaction mixture was allowed to stir at room temperature for 12 h. After completion of reaction, it was diluted with ethyl acetate and washed with ice to remove the excess DMF. The ethyl acetate layer thus obtained was further washed with 1N HCl, saturated aqueous NaHCO_3 and

Chapter 1 (Section C): Design, Synthesis, Biological Evaluation of Lysyl tRNA synthetase (KRS) Inhibitors based on Cladosporin Scaffold towards Identification of Antimalarial Leads

water. The collected organic layer was dried over Na₂SO₄, concentrated under vacuo and purified through column chromatography to afford the final amide analogue (**CL-20**, **CL-21** and **CL-22**).

CL-22:

IR ν_{\max} (**film**): cm⁻¹ 1469, 1645, 2935, 3314.

¹H NMR (500 MHz, CDCl₃): δ 7.84 (dd, *J* = 8.0, 3.1 Hz, 1H), 7.54 (dd, *J* = 9.2, 4.1 Hz, 1H), 7.46 (ddd, *J* = 9.2, 7.5, 3.1 Hz, 1H), 7.15 (s, 1H), 6.91 (s, 1H), 3.48 (dd, *J* = 14.0, 6.5 Hz, 2H), 1.66 (p, *J* = 7.4 Hz, 2H), 1.37 (dq, *J* = 7.2, 3.7 Hz, 4H), 0.96 – 0.81 (m, 3H).

¹³C NMR (125 MHz, CDCl₃): δ 177.4, 160.9, 158.9, 155.0, 151.4, 125.6, 125.5, 122.8, 122.6, 120.2, 120.1, 111.3, 111.2, 111.0, 40.1, 29.1, 29.0, 22.3, 13.9.

HRMS calculated for C₁₅H₁₇O₃NF [M + H]⁺ 278.1192, observed 278.1187.

CL-20:

IR ν_{\max} (**film**): cm⁻¹ 1079, 1504, 1672, 2925.

¹H NMR (400 MHz, CDCl₃): δ 7.85 (dd, *J* = 8.0, 2.9 Hz, 1H), 7.57 (dd, *J* = 9.1, 4.0 Hz, 1H), 7.48 – 7.43 (m, 1H), 7.15 (s, 1H), 4.11 – 4.07 (m, 1H), 3.93 (dd, *J* = 14.8, 6.9 Hz, 1H), 3.82 (dd, *J* = 14.4, 6.9 Hz, 2H), 3.37 – 3.31 (m, 1H), 2.08 (dt, *J* = 12.5, 6.7 Hz, 1H), 1.96 (dt, *J* = 13.7, 6.9 Hz, 2H), 1.61 (td, *J* = 15.5, 7.6 Hz, 1H).

¹³C NMR (100 MHz, CDCl₃): δ 177.4, 161.1, 159.1, 158.7, 154.9, 151.4, 125.6, 122.9, 122.6, 120.4, 120.3, 111.4, 111.2, 110.9, 68.3, 43.7, 28.8, 25.8.

HRMS calculated for C₁₅H₁₄O₄NF [M + H]⁺ 291.0914, observed 291.0910.

CL-21:

IR ν_{\max} (**film**): cm⁻¹ 1521, 1641, 2924, 3306.

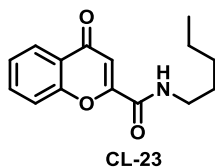
Chapter 1 (Section C): Design, Synthesis, Biological Evaluation of Lysyl tRNA synthetase (KRS) Inhibitors based on Cladosporin Scaffold towards Identification of Antimalarial Leads

¹H NMR (400 MHz, CDCl₃): δ 7.84 (dd, *J* = 8.0, 3.0 Hz, 1H), 7.52 (dd, *J* = 9.2, 4.1 Hz, 1H), 7.47 – 7.42 (m, 1H), 7.29 (dd, *J* = 5.2, 1.0 Hz, 1H), 7.22 (s, 1H), 7.18 (s, 1H), 7.10 (d, *J* = 3.2 Hz, 1H), 7.00 (dd, *J* = 5.1, 3.4 Hz, 1H), 4.85 (d, *J* = 5.6 Hz, 2H).

¹³C NMR (100 MHz, CDCl₃): δ 177.2, 161.2, 158.7, 154.6, 151.4, 139.1, 127.2, 127.0, 126.0, 125.6, 125.6, 122.9, 122.7, 120.3, 120.2, 111.6, 111.2, 111.0, 38.6.

HRMS calculated for C₁₅H₁₁O₃NFS [M + H]⁺ 304.0442, observed 304.0438.

Synthesis of 4-oxo-N-pentyl-4H-chromene-2-carboxamide (CL-23)



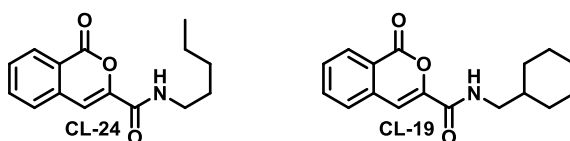
After synthesizing acid fragment **13.1** using known protocol it was further coupled with *n*-pentylamine following similar procedure as that of **CL-20**, **CL-21** and **CL-22** to afford **CL-23**.

¹H NMR (400 MHz, CDCl₃): δ 8.20 (dd, *J* = 8.0, 1.6 Hz, 1H), 7.73 (ddd, *J* = 8.7, 7.2, 1.7 Hz, 1H), 7.53 – 7.51 (m, 1H), 7.47 – 7.42 (m, 1H), 7.16 (d, *J* = 1.2 Hz, 1H), 7.02 (s, 1H), 3.49 (dd, *J* = 13.9, 6.7 Hz, 2H), 1.67 (p, *J* = 7.3 Hz, 2H), 1.38 (td, *J* = 7.1, 3.6 Hz, 4H), 0.92 (t, *J* = 7.0 Hz, 3H).

¹³C NMR (100 MHz, CDCl₃): δ 178.2, 159.1, 155.2, 154.8, 134.5, 126.0, 125.9, 124.3, 118.0, 112.0, 40.0, 29.1, 29.0, 22.3, 13.9.

HRMS calculated for C₁₅H₁₈O₃N [M + H]⁺ 260.1284, observed 260.1281.

General procedure for the synthesis of 1-oxo-N-pentyl-1H-isochromene-3-carboxamide (CL-19) and N-(cyclohexylmethyl)-1-oxo-1H-isochromene-3-carboxamide (CL-24)



Chapter 1 (Section C): Design, Synthesis, Biological Evaluation of Lysyl tRNA synthetase (KRS) Inhibitors based on Cladosporin Scaffold towards Identification of Antimalarial Leads

CL-19 and CL-24 was synthesized using similar protocol as that of CL-20, CL-21 and CL-22.

CL-24:

IR ν_{\max} (film): cm^{-1} 1465, 1644, 1713, 1940, 3314.

$^1\text{H NMR}$ (400 MHz, CDCl_3): δ 8.32 (d, $J = 8.1$ Hz, 1H), 7.78 (dd, $J = 10.9, 4.2$ Hz, 1H), 7.61 (t, $J = 8.2$ Hz, 2H), 7.49 (s, 1H), 6.93 (s, 1H), 3.44 (dd, $J = 13.7, 6.8$ Hz, 2H), 1.65 – 1.58 (m, 2H), 1.37 – 1.34 (m, 4H), 0.91 (t, $J = 6.9$ Hz, 3H).

$^{13}\text{C NMR}$ (100 MHz, CDCl_3): δ 160.8, 159.1, 145.9, 135.8, 135.4, 130.0, 130.0, 127.6, 121.9, 108.6, 39.7, 29.1, 29.0, 22.3, 13.9.

HRMS calculated for $\text{C}_{15}\text{H}_{18}\text{O}_3\text{N}$ $[\text{M} + \text{H}]^+$ 260.1284, observed 260.1281

CL-19:

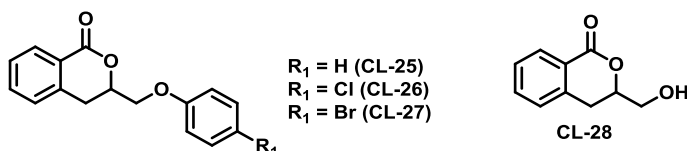
IR ν_{\max} (film): cm^{-1} 1527, 1667, 1734, 2919, 3372.

$^1\text{H NMR}$ (400 MHz, CDCl_3): δ 8.32 (d, $J = 7.8$ Hz, 1H), 7.79 (td, $J = 7.6, 1.3$ Hz, 1H), 7.64 – 7.60 (m, 2H), 7.50 (s, 1H), 6.96 (s, 1H), 3.29 (t, $J = 6.6$ Hz, 2H), 1.80 – 1.54 (m, 6H), 1.30 – 1.15 (m, 3H), 1.04 – 0.95 (m, 2H).

$^{13}\text{C NMR}$ (100 MHz, CDCl_3): δ 160.8, 159.2, 145.9, 135.8, 135.4, 130.0, 130.0, 127.6, 121.9, 108.6, 45.9, 37.9, 30.8, 26.3, 25.7.

HRMS calculated for $\text{C}_{17}\text{H}_{20}\text{O}_3\text{N}$ $[\text{M} + \text{H}]^+$ 286.1439, observed 286.1438.

General procedure of CH-activation

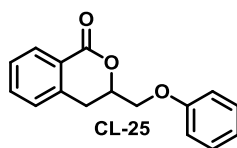


Benzoic acid (1.0 equivalent) and required epoxide (2.0 equivalent) was dissolved in HFIP in an oven dried sealed tube. *tert*-ac-leucine-OH (5 mol%), KOAc (1.0

Chapter 1 (Section C): Design, Synthesis, Biological Evaluation of Lysyl tRNA synthetase (KRS) Inhibitors based on Cladosporin Scaffold towards Identification of Antimalarial Leads

equivalent) and Pd(OAc)₂ (2.5 mol %) was added sequentially and the reaction mixture was heated at 80 °C for 24 h. The reaction mass was diluted with ethyl acetate and washed with saturated NH₄Cl solution three times. The combined organic layers were washed with brine, dries over Na₂SO₄ and concentrated under vacuo. Purification using column chromatography afforded the final products as foamy solids.

3-(phenoxymethyl)isochroman-1-one (CL-25):



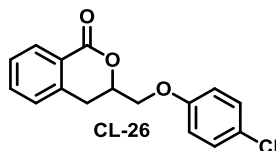
IR ν_{\max} (film): cm⁻¹ 1235, 1494, 1598, 1722, 2928.

¹H NMR (400 MHz, CDCl₃): δ 8.12 (d, J = 7.7 Hz, 1H), 7.57 (t, J = 7.4 Hz, 1H), 7.42 (t, J = 7.6 Hz, 1H), 7.31 (t, J = 6.7 Hz, 3H), 7.01 – 6.92 (m, 3H), 4.91 (dt, J = 10.3, 4.5 Hz, 1H), 4.31 (dd, J = 9.9, 4.5 Hz, 1H), 4.22 (dd, J = 9.9, 5.9 Hz, 1H), 3.28 (dd, J = 16.2, 11.3 Hz, 1H), 3.14 (dd, J = 16.4, 3.3 Hz, 1H).

¹³C NMR (100 MHz, CDCl₃): δ 164.7, 158.1, 138.4, 134.0, 130.4, 129.6, 127.8, 127.6, 124.9, 121.4, 114.5, 76.1, 68.6, 30.2.

HRMS calculated for C₁₆H₁₅O₃ [M + H]⁺ 255.1014, observed 255.1016.

3-((4-chlorophenoxy)methyl)isochroman-1-one (CL-26):



IR ν_{\max} (film): cm⁻¹ 1235, 1490, 1721, 2930.

¹H NMR (400 MHz, CDCl₃): δ 8.14 (dd, J = 7.8, 0.9 Hz, 1H), 7.59 (td, J = 7.5, 1.3 Hz, 1H), 7.44 (t, J = 7.6 Hz, 1H), 7.32 (d, J = 7.6 Hz, 1H), 7.29 – 7.27 (m, 1H), 7.27 – 7.24

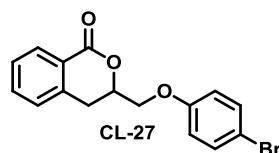
Chapter 1 (Section C): Design, Synthesis, Biological Evaluation of Lysyl tRNA synthetase (KRS) Inhibitors based on Cladosporin Scaffold towards Identification of Antimalarial Leads

(m, 1H), 6.90 – 6.88 (m, 1H), 6.87 – 6.86 (m, 1H), 4.91 (dtd, $J = 11.4, 4.9, 3.5$ Hz, 1H), 4.28 (dd, $J = 10.0, 4.6$ Hz, 1H), 4.22 (dd, $J = 10.0, 5.4$ Hz, 1H), 3.30 (dd, $J = 16.4, 11.5$ Hz, 1H), 3.12 (dd, $J = 16.4, 3.4$ Hz, 1H).

^{13}C NMR (100 MHz, CDCl_3): δ 164.6, 156.8, 138.3, 134.0, 130.4, 129.4, 127.9, 127.6, 126.3, 124.8, 115.8, 76.0, 69.0, 30.0.

HRMS calculated for $\text{C}_{16}\text{H}_{14}\text{O}_3\text{Cl}$ $[\text{M} + \text{H}]^+$ 289.0629, observed 289.0626.

3-((4-bromophenoxy)methyl)isochroman-1-one (CL-27):



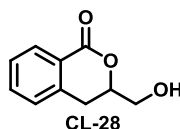
IR ν_{max} (film): cm^{-1} 1235, 1493, 1722, 2931.

^1H NMR (400 MHz, CDCl_3): δ 8.12 (dd, $J = 7.8, 1.1$ Hz, 1H), 7.57 (td, $J = 7.5, 1.4$ Hz, 1H), 7.44 – 7.38 (m, 3H), 7.30 (d, $J = 7.4$ Hz, 1H), 6.83 – 6.79 (m, 2H), 4.92 – 4.86 (m, 1H), 4.23 (ddd, $J = 15.4, 9.9, 5.0$ Hz, 2H), 3.28 (dd, $J = 16.4, 11.4$ Hz, 1H), 3.10 (dd, $J = 16.4, 3.4$ Hz, 1H).

^{13}C NMR (100 MHz, CDCl_3): δ 164.6, 157.2, 138.3, 134.0, 132.4, 130.4, 127.9, 127.6, 124.8, 116.3, 113.7, 76.0, 69.0, 30.0.

HRMS calculated for $\text{C}_{16}\text{H}_{14}\text{O}_3\text{Br}$ $[\text{M} + \text{H}]^+$ 333.0126, observed 333.0121.

3-(hydroxymethyl)isochroman-1-one (CL-28):



IR ν_{max} (film): cm^{-1} 1279, 1713, 2931, 3421.

Chapter 1 (Section C): Design, Synthesis, Biological Evaluation of Lysyl tRNA synthetase (KRS) Inhibitors based on Cladosporin Scaffold towards Identification of Antimalarial Leads

$^1\text{H NMR}$ (400 MHz, CDCl_3): δ 8.09 (d, $J = 7.4$ Hz, 1H), 7.55 (td, $J = 7.4, 1.1$ Hz, 1H), 7.40 (t, $J = 7.6$ Hz, 1H), 7.27 (d, $J = 9.1$ Hz, 1H), 4.68 – 4.62 (m, 1H), 3.97 (dd, $J = 12.2, 2.9$ Hz, 1H), 3.85 (dd, $J = 12.2, 5.0$ Hz, 1H), 3.23 (dd, $J = 16.4, 12.4$ Hz, 1H), 2.86 (dd, $J = 16.4, 3.1$ Hz, 1H), 2.46 (s, 1H).

$^{13}\text{C NMR}$ (100 MHz, CDCl_3): δ 165.2, 138.8, 134.0, 130.3, 127.7, 127.6, 124.7, 79.0, 64.2, 29.1.

HRMS calculated for $\text{C}_{10}\text{H}_{11}\text{O}_3$ $[\text{M} + \text{H}]^+$ 179.0701, observed 179.0703.

Biological Assay

(in collaboration with Dr. Amit Sharma, ICGEB, New Delhi, India)

Detailed experimental procedure for protein expressions and purifications, thermal shift assays, aminoacylation assays, *P. falciparum* culture and co-crystallization could be found at *J. Med. Chem.* **2018**, *61*, 5664-5678.

Crystallization:

Highly pure *PfKRS* was stored at 15 mg ml⁻¹ -80 °C. Before crystallization, 0.5 mM inhibitors along with 2 mM L-Lys were added to 13 mg ml⁻¹ protein solutions and incubated at 4 °C for 30 min. The *PfKRS*+CL-1+L-Lys crystals were obtained using hanging-drop vapour diffusion method at 20 °C. Initial screenings were carried out using nano-drop dispensing robot Mosquito (TTP Labtech) and the droplet size was a mixture of 100 nl of *PfKRS*+CL-1+L-Lys complex and 100 nl of well solutions from commercial crystal screens (Hampton Research and Molecular Dimensions). The crystallization drops were equilibrated against 75/100 mL well reservoir solutions using commercially available Morpheus screening reagents from Molecular Dimensions Ltd.

Data collection and structure determination

X-ray diffraction data were collected using beam-line I02 at Diamond Light Source (DLS), United Kingdom at a wavelength of 0.9688 Å. The data were processed by the xia2 auto-processing pipeline using DIALS^{32, 33} for integration. The initial model for

Chapter 1 (Section C): Design, Synthesis, Biological Evaluation of Lysyl tRNA synthetase (KRS) Inhibitors based on Cladosporin Scaffold towards Identification of Antimalarial Leads

*Pf*KRS-L-Lys-CL-2 was determined by the molecular-replacement (MR) method using Phaser³⁴ with PDB entry 4PG3 as the template. The structure was further refined by iterative cycles of refinement with Refmac³⁵ and Phenix³⁶ and model building with COOT³⁷. The stereo-chemical quality of the model was analysed using MolProbity³⁸. The atomic coordinates and structural factors have been deposited into Protein Data Bank with accession code **6M0T**. All structural superposition and preparation of figures was done using UCSF Chimera and PyMOL (<http://www.pymol.org>).

In vitro pharmacokinetics

The objective of the study was to evaluate the metabolic stability of test compounds in liver microsomes from human (HLM) and mice (MLM). This was accomplished by incubating test compounds with microsomes and monitoring disappearance with time using LC-MS/MS. Verapamil in HLM and imipramine in MLM were run as positive controls.

A microsomal mix (microsomes and Kphos buffer) was prepared at concentration of 0.357 mg mL⁻¹ in 2 mL tubes. To this microsomal mix 1.6 μ L (1 mM) of test compound and positive control were spiked, from this mix 70 μ L was transferred to 96 well plate and pre-incubated in a 37 °C water bath for 5 min. After pre-incubation zero-minute time point reaction was stopped using 100 μ L of ice-cold acetonitrile containing internal standard, to this 30 μ L of NADPH (3.33 mM in Kphos buffer) was added. For 60 min time point reaction was initiated by addition of 30 μ L of NADPH (3.33 mM in Kphos buffer) and incubated at 37 °C for 60 min, incubation reaction was stopped with 100 μ L of ice-cold acetonitrile containing internal standard (glipizide). The plates were centrifuged at 4000 RPM for 15 min and 100 μ L aliquots were submitted for analysis by LC-MS/MS. Samples were monitored for parent compound disappearance in MRM mode using LC-MS/MS. The peak area ratios of analyte versus internal standard were used to calculate the % remaining at the end of 1 h in presence NADPH. Metabolic stability of positive control compounds verapamil for HLM and imipramine for MLM used in the experiment was consistent with literature values. The above in vitro

Chapter 1 (Section C): Design, Synthesis, Biological Evaluation of Lysyl tRNA synthetase (KRS) Inhibitors based on Cladosporin Scaffold towards Identification of Antimalarial Leads

pharmacokinetic studies have been conducted in collaboration with Sai Life Sciences Limited.

1.3.6. References

1. Manickam, Y.; Chaturvedi, R.; Babbar, P.; Malhotra, N.; Jain, V.; and Sharma, A. Drug targeting of one or more aminoacyl-tRNA synthetase in the malaria parasite *Plasmodium falciparum*. *Drug Discovery Today* **2018**, *23*, 1233-1240.
2. Hughes, J.; and Mellows, G. Interaction of pseudomonic acid A with *Escherichia coli* B isoleucyl-tRNA synthetase. *Biochem. J.* **1980**, *191*, 209-219.
3. Silvan, L. F.; Wang, J.; and Steitz, T. A. Insights into editing from an ile-tRNA synthetase structure with tRNA^{ile} and mupirocin. *Science* **1999**, *285*, 1074-1077.
4. Werner, R.G.; Thorpe, L.F.; Reuter, W.; and Nierhaus, K. H. Indolmycin inhibits pro-karyotic tryptophanyl-tRNA ligase. *Eur. J. Biochem.* **1976**, *68*, 1-3.
5. Hurdle, J. G.; O'Neill, A. J.; Chopra, I. Anti-staphylococcal activity of indolmycin, a potential topical agent for control of staphylococcal infections. *J. Antimicrob. Chemother.* **2004**, *54*, 549–552.
6. Kanamaru, T.; Nakano, Y.; Toyoda, Y.; Miyagawa, K.; Tada, M.; Kaisho, T.; Nakao, M. In Vitro and In Vivo Antibacterial Activities of TAK-083, an Agent for Treatment of *Helicobacter pylori* Infection. *Antimicrob. Agents Chemother.* **2001**, *45*, 2455–2459.
7. Jain, V.; Yogavel, M.; Oshima, Y.; Kikuchi, H.; Touquet, B.; Hakimi, M.A.; and Sharma, A. Structure of prolyl-tRNA synthetase-halofuginone complex provides basis for development of drugs against malaria and toxoplasmosis. *Structure* **2015**, *23*, 819–829.
8. Jain, V.; Yogavel, M.; Kikuchi, H.; Oshima, Y.; Hariguchi, N.; Matsumoto, M.; Goel, P.; Touquet, B.; Jumani, R.S.; Tacchini-Cottier, F.; Harlos, K.; Huston, C.D.; Hakimi, M. A.; and Sharma, A. Targeting prolyl-tRNA synthetase to accelerate drug discovery against malaria, leishmaniasis, toxoplasmosis, cryptosporidiosis, and coccidiosis. *Structure* **2017**, *25*, 1495-1505.

Chapter 1 (Section C): Design, Synthesis, Biological Evaluation of Lysyl tRNA synthetase (KRS) Inhibitors based on Cladosporin Scaffold towards Identification of Antimalarial Leads

9. Committee for Veterinary Medicinal Products (1999) European Agency for the Evaluation of Medicinal Products. EMEA/CVMP/643/99 Halocur dossier submission, Brussels, Belgium.
10. Ningthoujam, S. S.; Talukdar, A. D.; Nath, D.; Basar, N.; Potsangbam, K. S.; Choudhury, M. D. Febrifugine and Its Analogs: Studies for Their Antimalarial and Other Therapeutic Properties. *Stud. Nat. Prod. Chem.* **2015**, *44*, 93-112.
11. Hoepfner, D.; McNamara, C.W.; Lim, C.S.; Studer, C.; Riedl, R.; Aust, T.; McCormack, S.L.; Plouffe, D.M.; Meister, S.; Schuierer, S.; Plikat, U.; Hartmann, N.; Staedtler, F.; Cotesta, S.; Schmitt, E.K.; Petersen, F.; Supek, F.; Glynn, R.J.; Tallarico, J.A.; Porter, J.A.; Fishman, M.C.; Bodenreider, C.; Diagana, T.T.; Movva, N.R.; and Winzeler, E.A. Selective and specific inhibition of the plasmodium falciparum lysyl-tRNA synthetase by the fungal secondary metabolite cladosporin. *Cell Host Microbe* **2012**, *11*, 654-663.
12. Khan, S.; Garg, A.; Camacho, N.; Van Rooyen, J.; Kumar, P. A.; Belrhali, H.; Ribas de Pouplana, L.; Sharma, V.; and Sharma, A. Structural analysis of malaria-parasite lysyl-tRNA synthetase provides a platform for drug development. *Acta. Crystallogr. D. Biol. Crystallogr.* **2013**, *69*, 785-795.
13. Khan, S.; Sharma, A.; Belrhali, H.; Yogavel, M.; and Sharma, A. Structural basis of malaria parasite lysyl-tRNA synthetase inhibition by cladosporin. *J. Struct. Funct. Genomics* **2014**, *15*, 63-71.
14. Springer, J. P.; Cutler, H.G.; Crumley, F.G.; Cox, R.H.; Davis, E.E.; and Thean, J.E. Plant Growth Regulatory Effects and Stereochemistry of Cladosporin. *J. Agric. Food Chem.* **1981**, *29*, 853-855.
15. Scott, P. M.; Van Walbeek, W.; and Maclean, W. M. Cladosporin, a new antifungal metabolite from *Cladosporium cladosporioides*. *J. Antibiot.* **1971**, *24*, 747-755.
16. Sharma, A.; Sharma, M.; Yogavel, M.; and Sharma, A. Protein Translation Enzyme lysyl-tRNA Synthetase Presents a New Target for Drug Development against Causative Agents of Loiasis and Schistosomiasis. *PLoS Negl. Trop. Dis.* **2016**, *10*, 1-19.

Chapter 1 (Section C): Design, Synthesis, Biological Evaluation of Lysyl tRNA synthetase (KRS) Inhibitors based on Cladosporin Scaffold towards Identification of Antimalarial Leads

17. Baragana, B.; Forte, B.; Choi, R.; Nakazawa Hewitt, S.; Bueren-Calabuig, J. A.; Pisco, J. P.; Peet, C.; Dranow, D. M.; Robinson, D. A.; Jansen, C.; Norcross, N. R.; Vinayak, S.; Anderson, M.; Brooks, C. F.; Cooper, C. A.; Damerow, S.; Delves, M.; Dowers, K.; Duffy, J.; Edwards, T. E.; Hallyburton, I.; Horst, B.G.; Hulverson, M. A.; Ferguson, L.; Jimenez-Diaz, M. B.; Jumani, R. S.; Lorimer, D. D.; Love, M. S.; Maher, S.; Matthews, H.; McNamara, C. W.; Miller, P.; O'Neill, S.; Ojo, K. K.; Osuna-Cabello, M.; Pinto, E.; Post, J.; Riley, J.; Rottmann, M.; Sanz, L. M.; Scullion, P.; Sharma, A.; Shepherd, S. M.; Shishikura, Y.; Simeons, F. R. C.; Stebbins, E. E.; Stojanovski, L.; Straschil, U.; Tamaki, F. K.; Tamjar, J.; Torrie, L.S.; Vantaux, A.; Witkowski, B.; Wittlin, S.; Yogavel, M.; Zuccotto, F.; Angulo-Barturen, I.; Sinden, R.; Baum, J.; Gamo, F. J.; Maser, P.; Kyle, D. E.; Winzeler, E. A.; Myler, P. J.; Wyatt, P. G.; Floyd, D.; Matthews, D.; Sharma, A.; Striepen, B.; Huston, C. D.; Gray, D. W.; Fairlamb, A. H.; Pisljakov, A. V.; Walpole, C.; Read, K. D.; Van Voorhis, W. C.; and Gilbert, I. H. Lysyl-tRNA synthetase as a drug target in malaria and cryptosporidiosis. *Proc. Natl. Acad. Sci. U. S. A.* **2019**, *116*, 7015-7020.
18. Rusch, M.; Thevenon, A.; Hoepfner, D.; Aust, T.; Studer, C.; Patoor, M.; Rollin, P.; Livendahl, M.; Ranieri, B.; Schmitt, E.; Spanka, C.; Gademann, K.; Bouchez, L. C. Design and Synthesis of Metabolically Stable tRNA Synthetase Inhibitors Derived from Cladosporin. *Chem Bio Chem.* **2018**, *20*, 644-649.
19. Das, P.; Babbar, P.; Malhotra, N.; Sharma, M.; Jachak, G. R.; Gonnade, R. G.; Shanmugam, D.; Harlos, K.; Yogavel, M.; Sharma, A.; and Reddy, D. S. Specific Stereoisomeric Conformations Determine the Drug Potency of Cladosporin Scaffold against Malarial Parasite. *J. Med. Chem.* **2018**, *61*, 5664-5678.
20. Kobayashi, M.; Shinohara, M.; Sakoh, C.; Kataoka, M.; Shimizu, S. Lactone-ring-cleaving enzyme: Genetic analysis, novel RNA editing, and evolutionary implications. *Proc. Natl. Acad. Sci.* **1998**, *95*, 12787-12792.
21. Das, P.; Mankad, Y.; Reddy, S. Scalable synthesis of cladosporin. *Tetrahedron lett.* **2019**, *12*, 831-833.

Chapter 1 (Section C): Design, Synthesis, Biological Evaluation of Lysyl tRNA synthetase (KRS) Inhibitors based on Cladosporin Scaffold towards Identification of Antimalarial Leads

22. Olivito, F.; Costanzo, P.; Di Gioia, M. L.; Nardi, M.; M.; Oliverio; Procopio, A. Efficient synthesis of organic thioacetates in water. *Org. Biomol. Chem.* **2018**, *16*, 7753-7759.
23. Liu, Zhen; Derosa, Joseph; Engle, Keary M. Palladium (II)-Catalyzed Regioselective syn-Hydroarylation of Disubstituted Alkynes Using a Removable Directing Group. *J. Am. Chem. Soc.* **2016**, *138*, 13076-13081.
24. Wang, Xiao; Nelson, Scott G.; Curran, Dennis P. The azido acid approach to β -peptides: parallel synthesis of a tri- β -peptide library by fluororous tagging. *Tetrahedron* **2007**, *63*, 6141-6145.
25. McLaughlin, N. P.; Evans, P.; Pines, M. The chemistry and biology of febrifugine and halofuginone. *Bioorg. Med. Chem.* **2014**, *22*, 1993-2004.
26. Chen, Y. G.; Shuai, B.; Ma, C.; Zhang, X, J.; Fang, P.; Mei, T. S. Regioselective Ni-Catalyzed Carboxylation of Allylic and Propargylic Alcohols with Carbon Dioxide. *Org. Lett.* **2017**, *19*, 2969-2972.
27. Mikula, H.; Hametner, C.; Froehlich, J. *Synth. Commun.* **2013**, *43*, 1939-1946.
28. Kashid, B. B.; Salunkhe, P. H.; Dongare, B. B.; More, K. R.; Khedkar, V. M.; Ghanwat, A. A. Synthesis of novel of 2, 5-disubstituted 1, 3, 4- oxadiazole derivatives and their in vitro anti-inflammatory, anti-oxidant evaluation, and molecular docking study. *Bioorganic & Medicinal Chemistry Letters* **2020**, *20*, 127136
29. Cagide, F.; Oliveira, C.; Reis, J.; Borges, F. Optimizing the synthetic route of chromone-2-carboxylic acids: a step forward to speed-up the discovery of chromone-based multitarget-directed ligands. **2009**, *Molecules* *24*, 4214.
30. Weerasinghe, M. S.; Karlson, S. T.; Lu, Y.; Wheeler, K. A. Crystal Photodimerization Reactions of Spatially Engineered Isocoumarin Assemblies. *Cryst. Growth Des.* **2016**, *16*, 1781-1785.
31. Cheng, G.; Li, T. J.; Yu, J. Q. Practical Pd(II)-Catalyzed C-H Alkylation with Epoxides: One-Step Syntheses of 3,4-Dihydroisocoumarins. *J. Am. Chem. Soc.* **2015**, *137*, 10950-10953.

Chapter 1 (Section C): Design, Synthesis, Biological Evaluation of Lysyl tRNA synthetase (KRS) Inhibitors based on Cladosporin Scaffold towards Identification of Antimalarial Leads

32. Winter, G.; Lobley, C. M.; and Prince, S. M. Decision making in xia2. *Acta Crystallogr.; Sect. D: Struct. Biol.* **2013**, *69*, 1260-1273.
33. Clabbers, M. T. B.; Gruene, T.; Parkhurst, J. M.; Abrahamsa, J. P.; Waterman, D. G. Electron diffraction data processing with DIALS. *Acta Crystallogr.; Sect. D: Struct. Biol.* **2018**, *74*, 506-518.
34. McCoy, A. J.; Kunstleve, R. W. G.; Adams, P. D.; Winn, M. D.; Storonia, L. C.; Read, R. J. Phaser crystallographic software. *J. Appl. Cryst.* **2007**, *40*, 658-674.
35. Murshudov, G. N.; Skubak, P.; Lebedev, A. A.; Pannu, N. S.; Steiner, R. A.; Nicholls, R. A.; Winn, M. D.; Long, F.; Vagin, A. A. REFMAC5 for the refinement of macromolecular crystal structures. *Acta Crystallogr. D Biol. Crystallogr.* **2011**, *67*, 355.
36. Adams, P. D.; Afonine, P. V.; Bunkoczi, G.; Chen, V. B.; Davis, I. W.; Echols, N.; Headd, J. J.; Hung, L. W.; Kapral, G. J.; Grosse-Kunstleve, R. W.; McCoy, A. J.; Moriarty, N. W.; Oeffner, R.; Read, R. J.; Richardson, D. C.; Richardson, J. S.; Terwilliger, T. C.; Zwart, P. H. PHENIX: a comprehensive Python-based system for macromolecular structure solution. *Acta Crystallogr.; Sect. D: Struct. Biol.* **2010**, *66*, 213-221.
37. Emsley, P.; Lohkamp, B.; Scott, W. G.; and Cowtan, K. Features and development of Coot. *Acta Crystallogr.; Sect. D: Struct. Biol.* **2010**, *66*, 486-501.
38. Chen, V. B.; Arendall, III, W. B.; Headd, J. J.; Keedy, D.A.; Immormino, R.M.; Kapral, G. J.; Murray, L.W.; Richardson, J. S. and Richardson, D. C. MolProbity: all-atom structure validation for macromolecular crystallography. *Acta Crystallogr. D Biol. Crystallogr.* **2010**, *66*, 12.

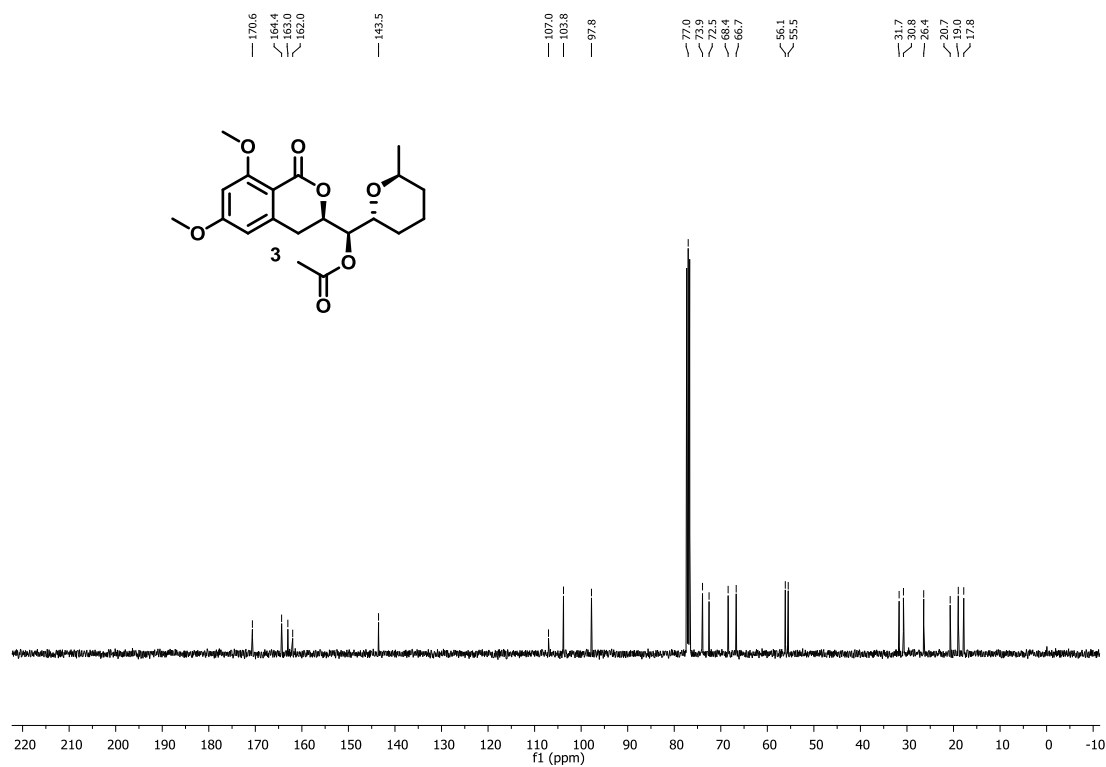
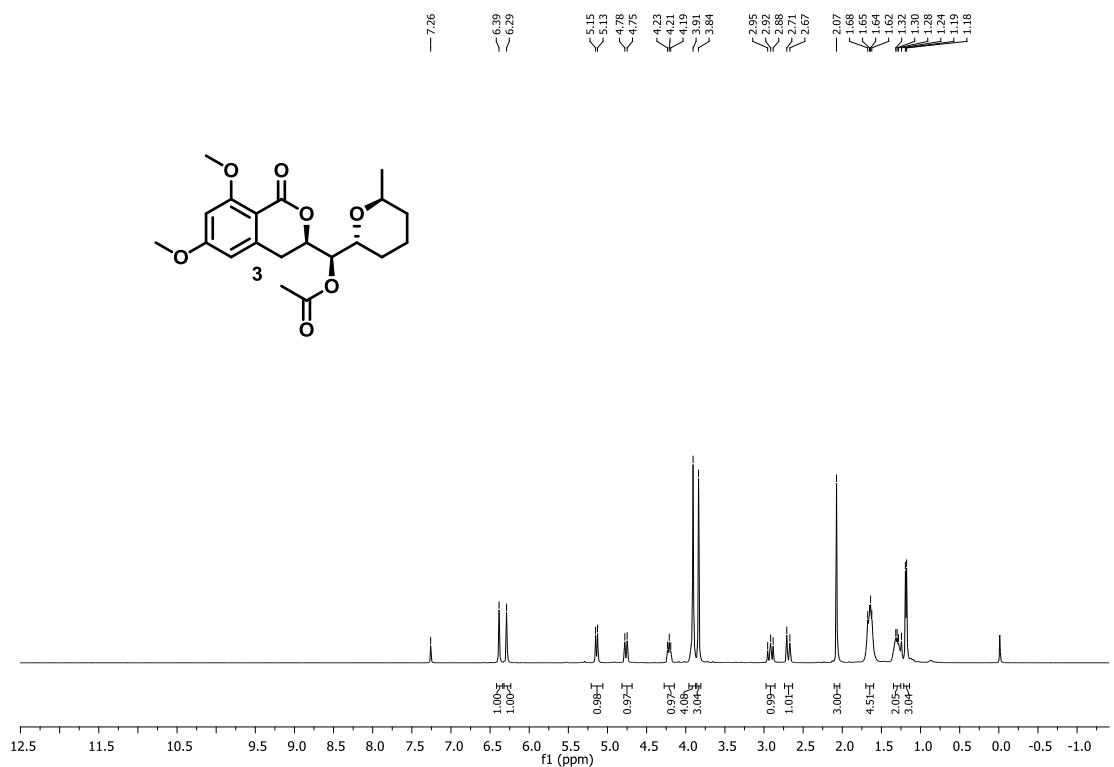
**Chapter 1 (Section C): Design, Synthesis, Biological Evaluation of Lysyl
tRNA synthetase (KRS) Inhibitors based on Cladosporin Scaffold
towards Identification of Antimalarial Leads**



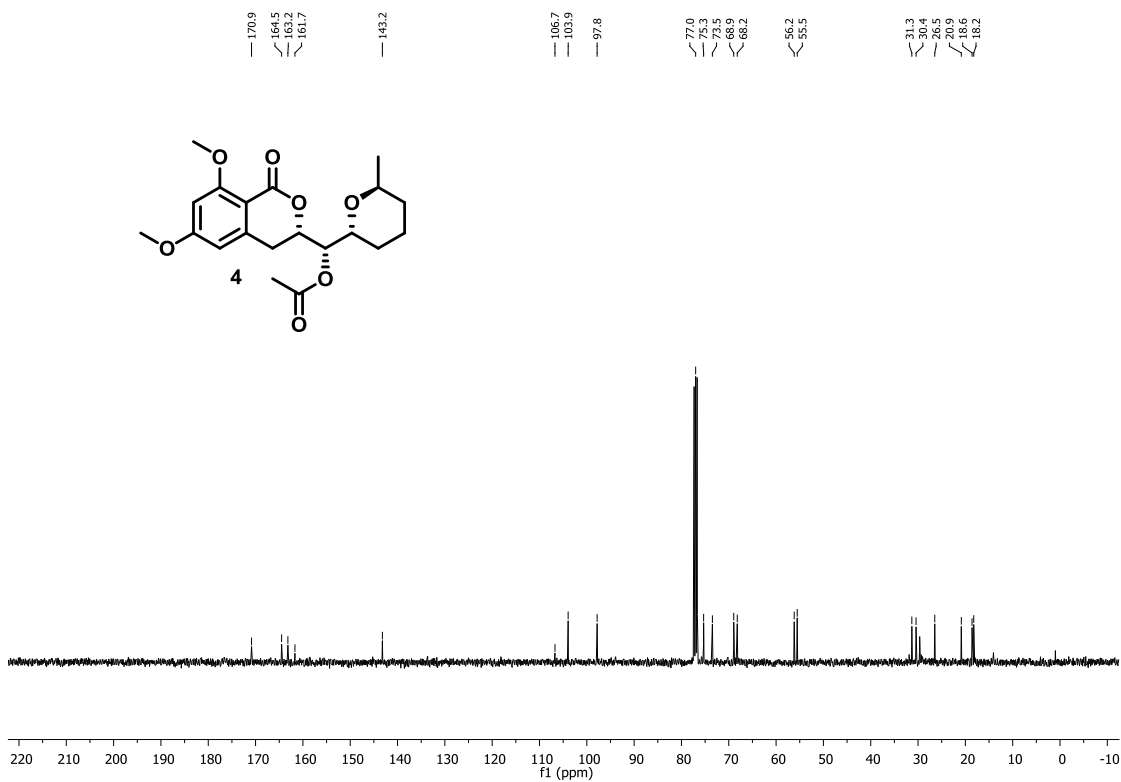
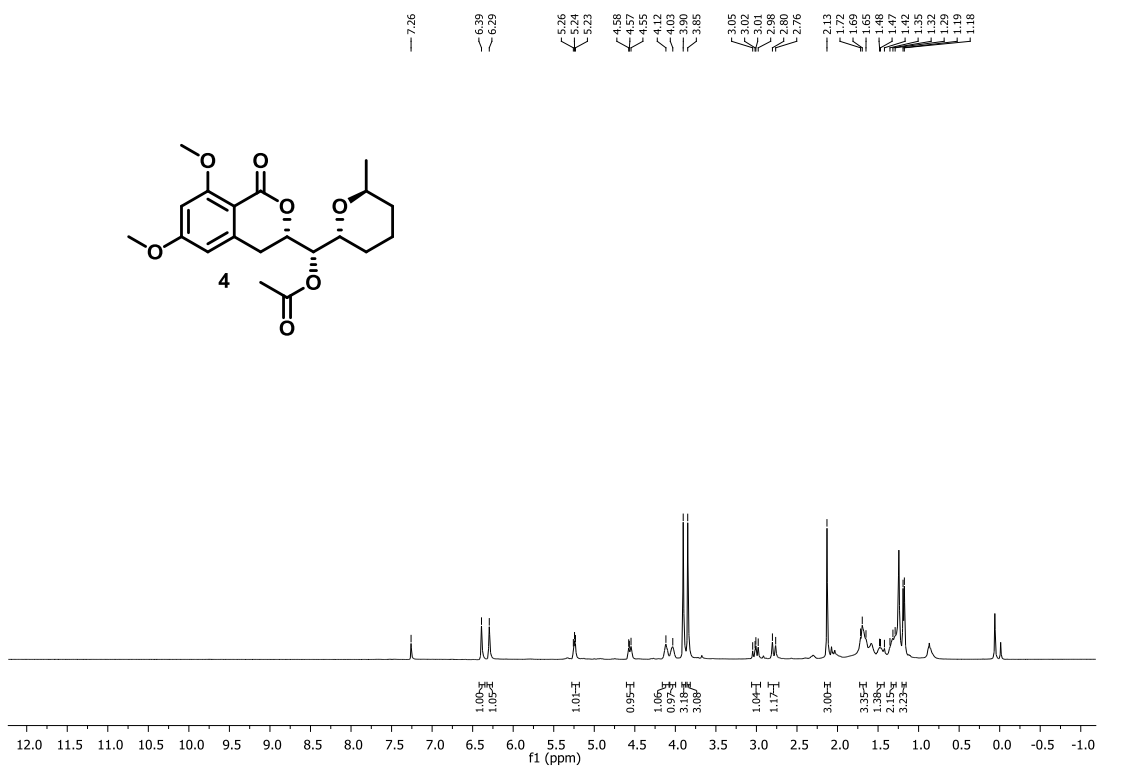
**Copies of
 ^1H and ^{13}C NMR Spectra of Selected
Compounds**



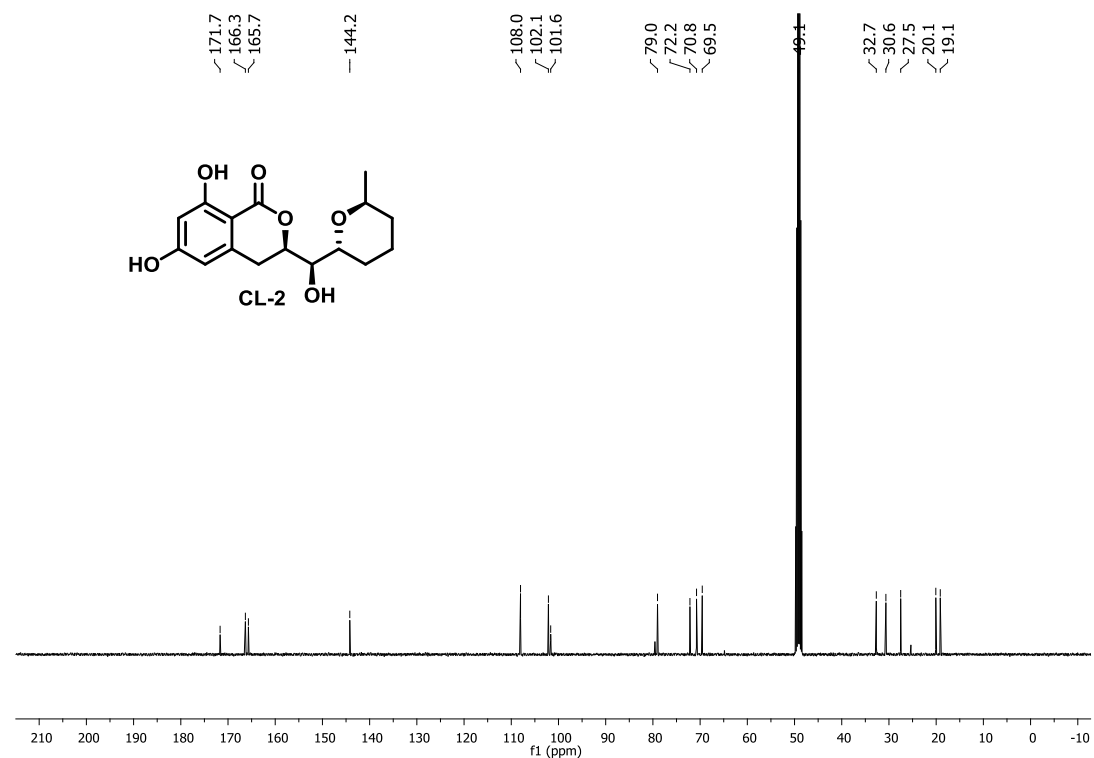
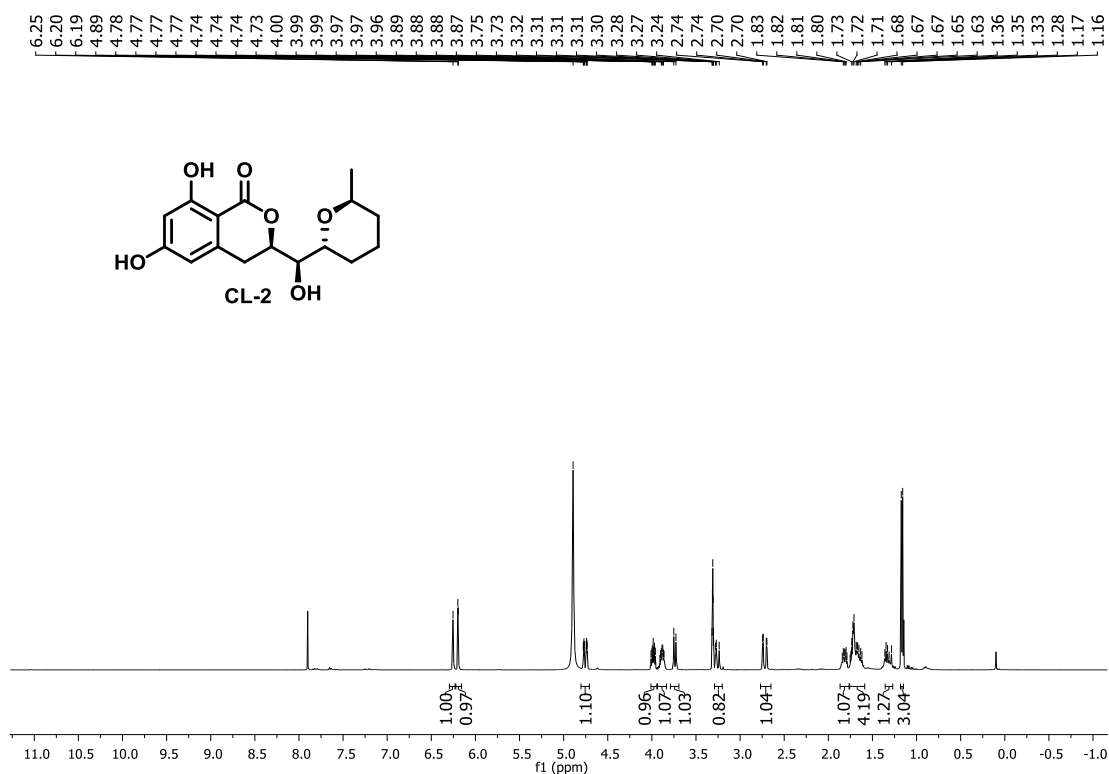
Chapter 1 (Section C): Design, Synthesis, Biological Evaluation of Lysyl tRNA synthetase (KRS) Inhibitors based on Cladosporin Scaffold towards Identification of Antimalarial Leads



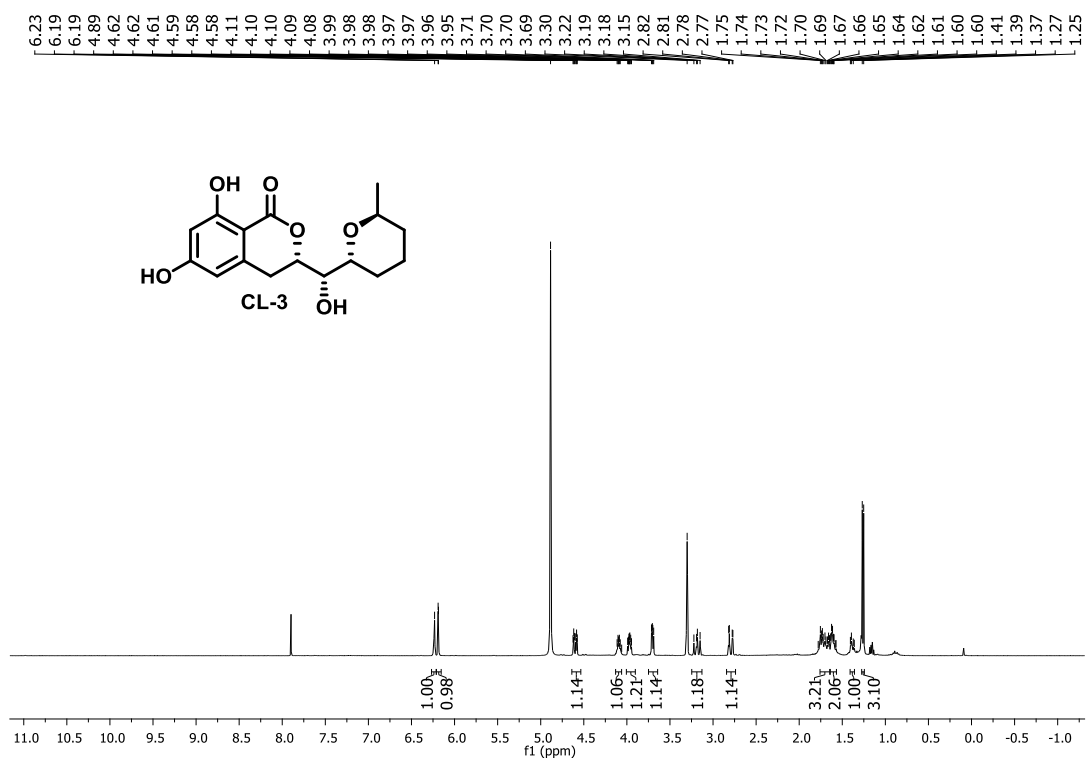
Chapter 1 (Section C): Design, Synthesis, Biological Evaluation of Lysyl tRNA synthetase (KRS) Inhibitors based on Cladosporin Scaffold towards Identification of Antimalarial Leads



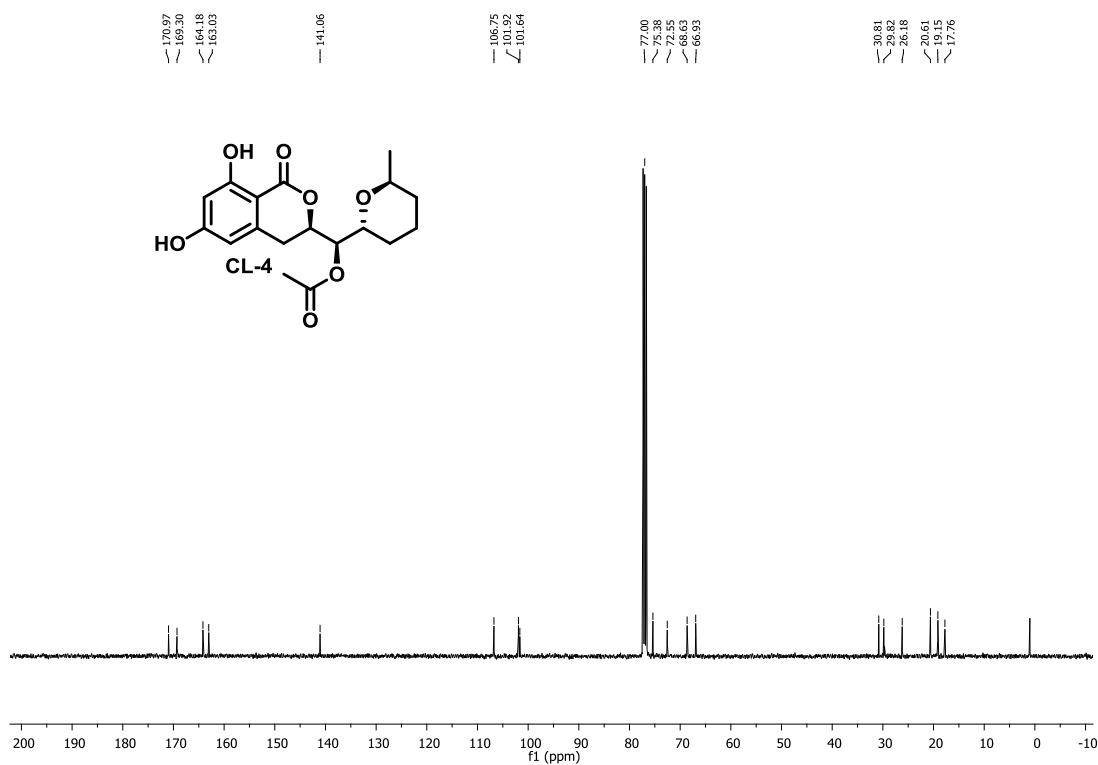
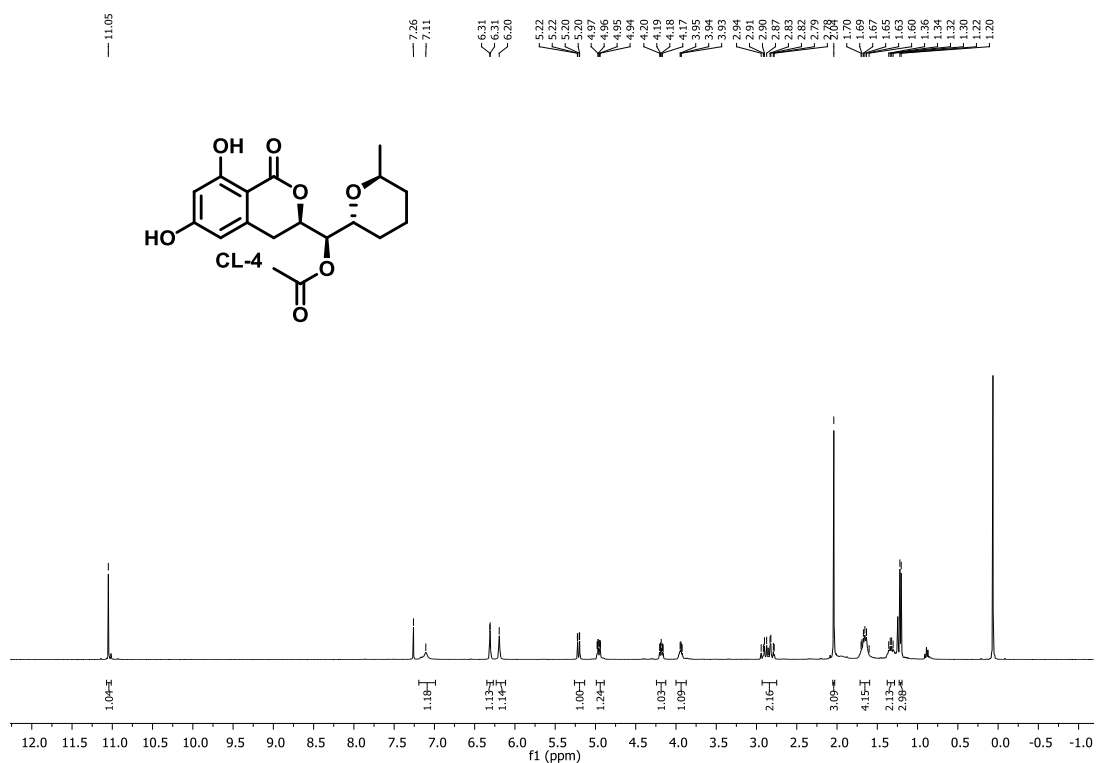
Chapter 1 (Section C): Design, Synthesis, Biological Evaluation of Lysyl tRNA synthetase (KRS) Inhibitors based on Cladosporin Scaffold towards Identification of Antimalarial Leads



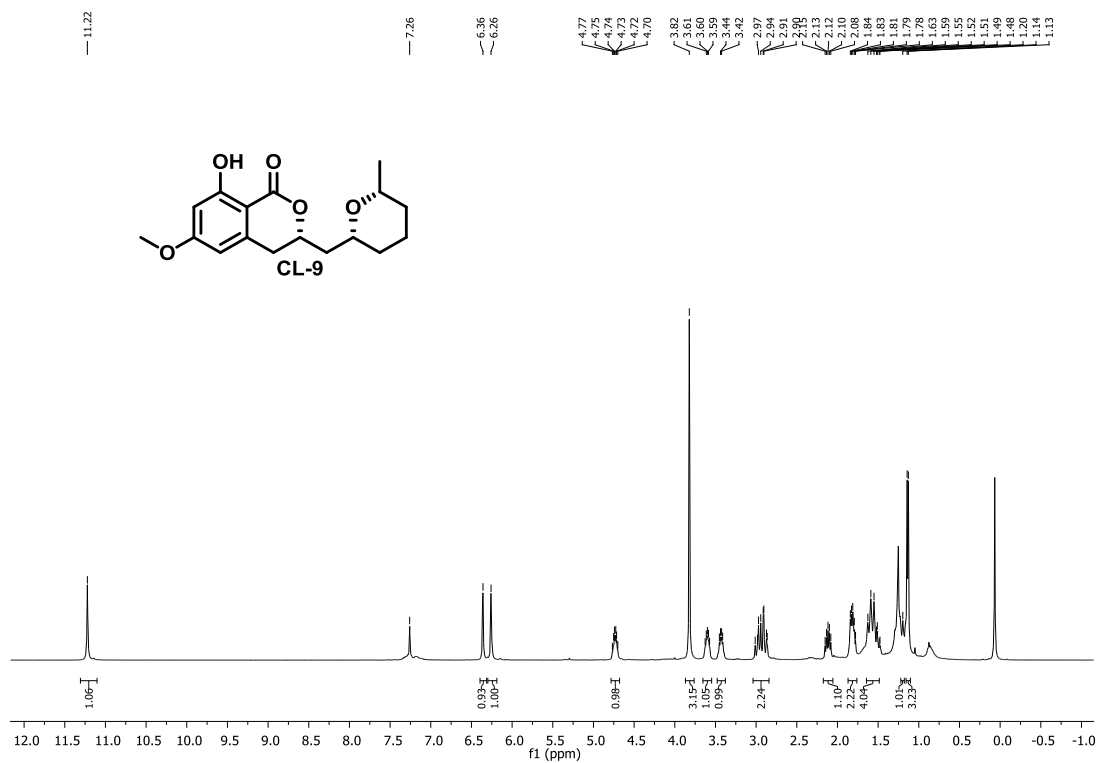
Chapter 1 (Section C): Design, Synthesis, Biological Evaluation of Lysyl tRNA synthetase (KRS) Inhibitors based on Cladosporin Scaffold towards Identification of Antimalarial Leads



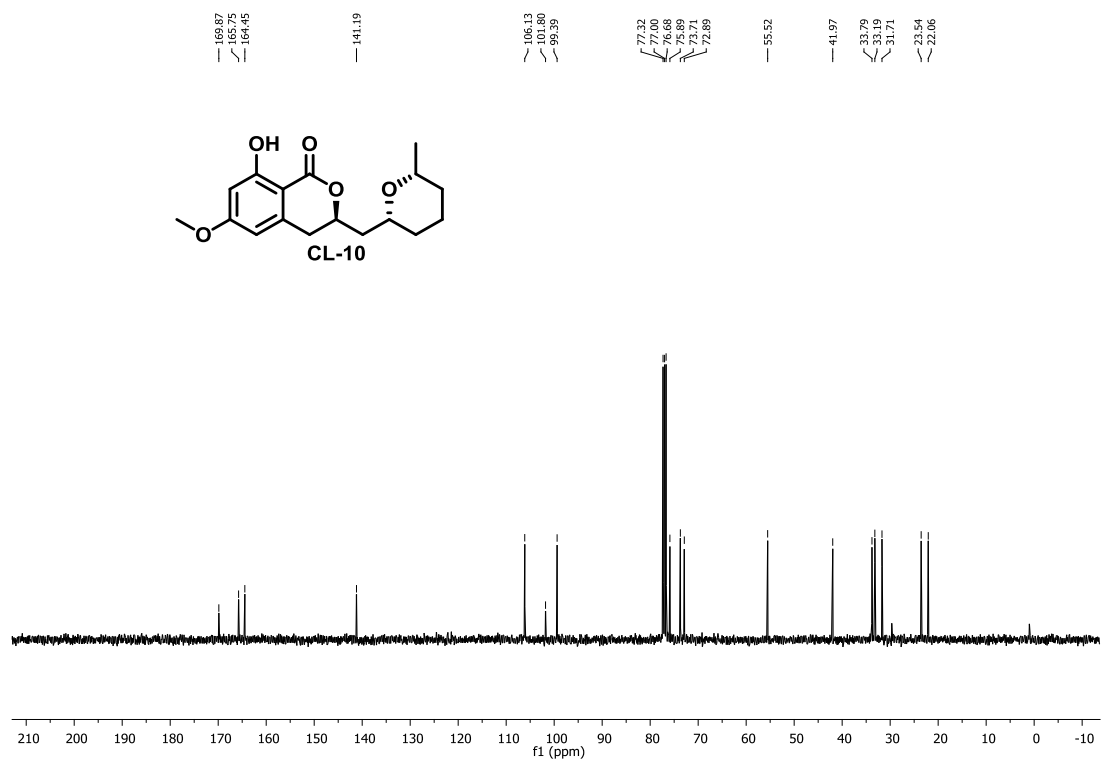
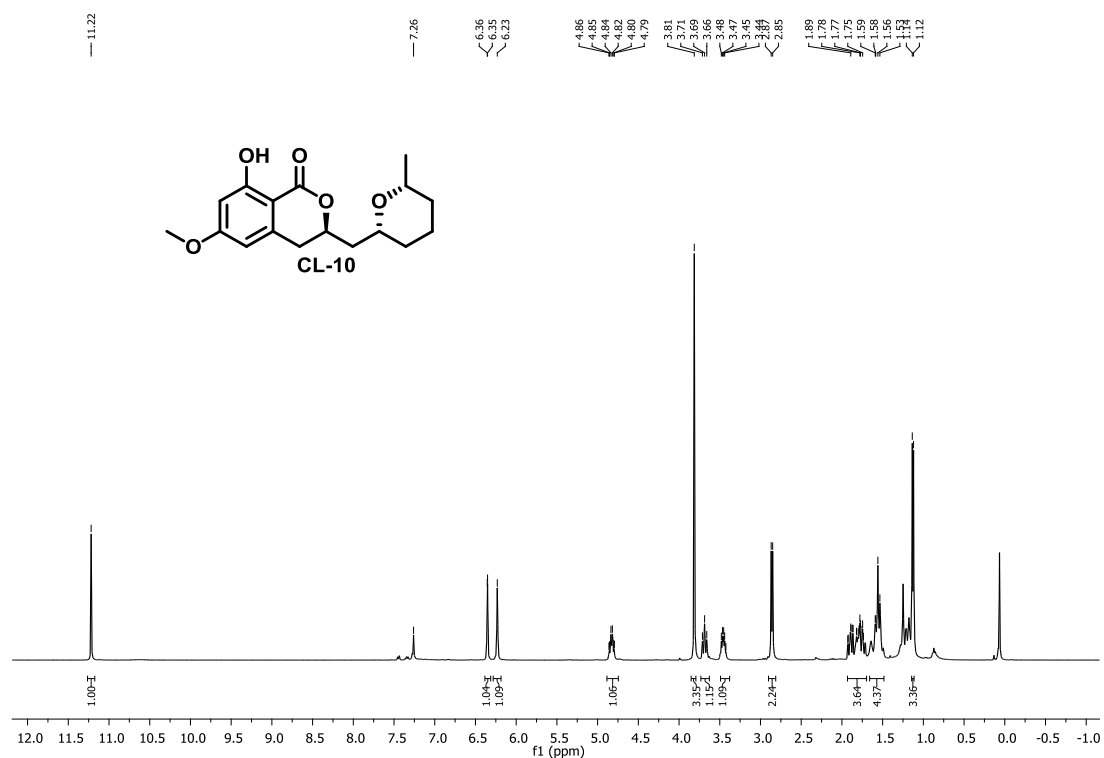
Chapter 1 (Section C): Design, Synthesis, Biological Evaluation of Lysyl tRNA synthetase (KRS) Inhibitors based on Cladosporin Scaffold towards Identification of Antimalarial Leads



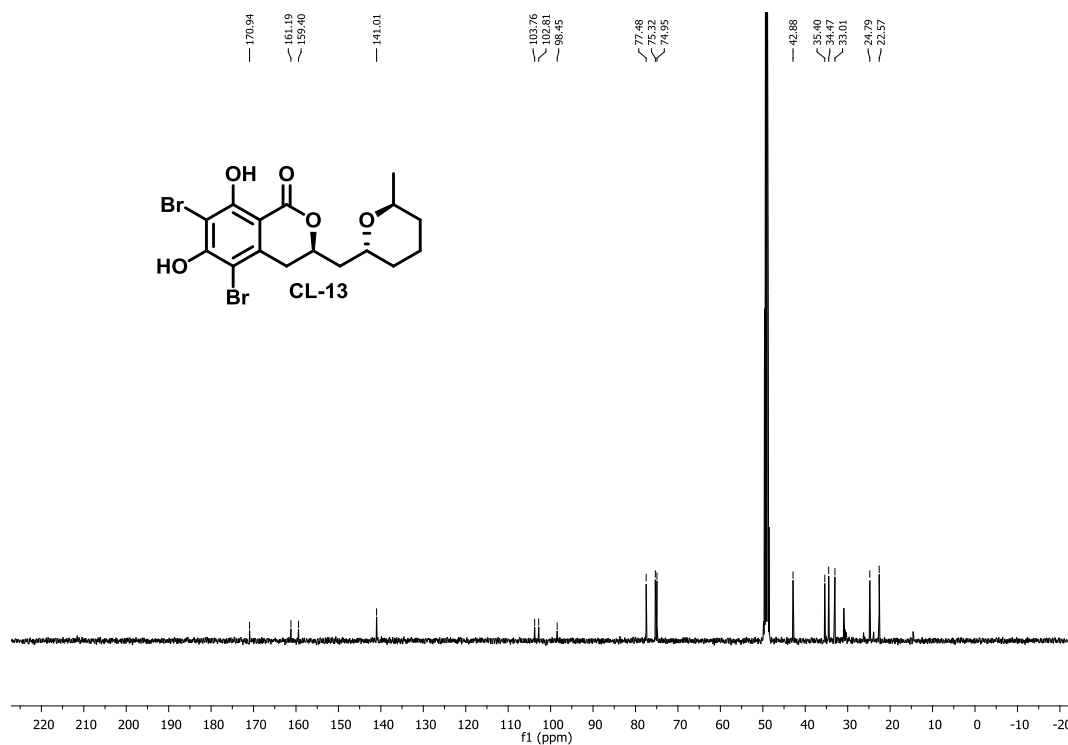
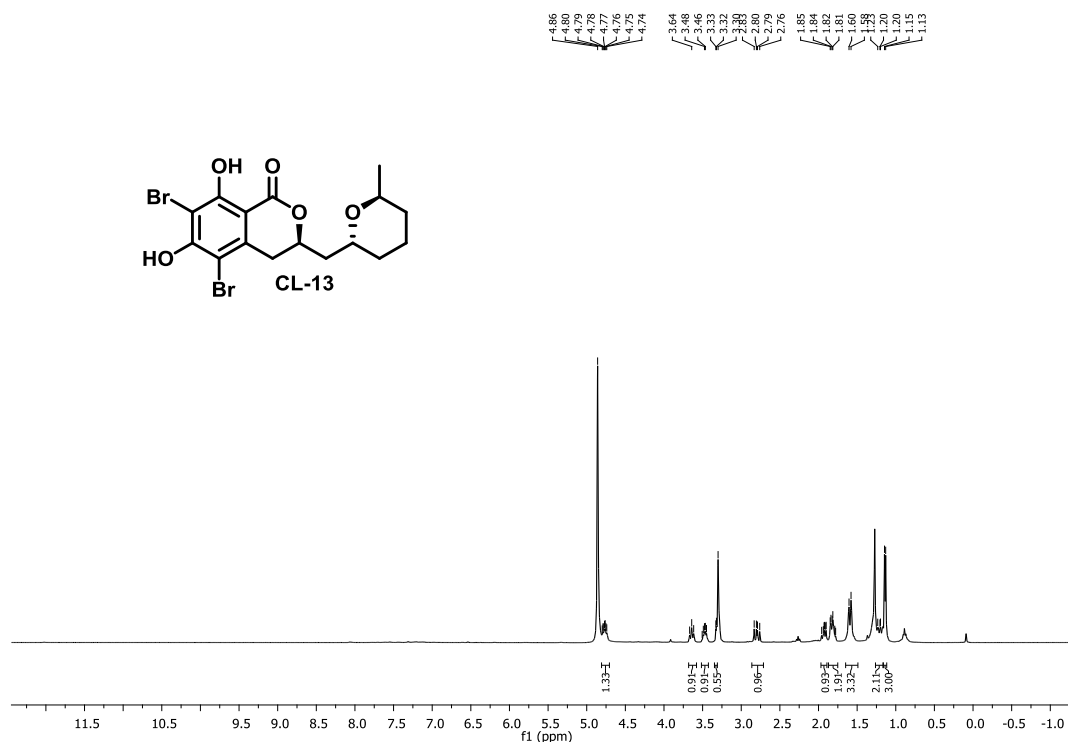
Chapter 1 (Section C): Design, Synthesis, Biological Evaluation of Lysyl tRNA synthetase (KRS) Inhibitors based on Cladosporin Scaffold towards Identification of Antimalarial Leads



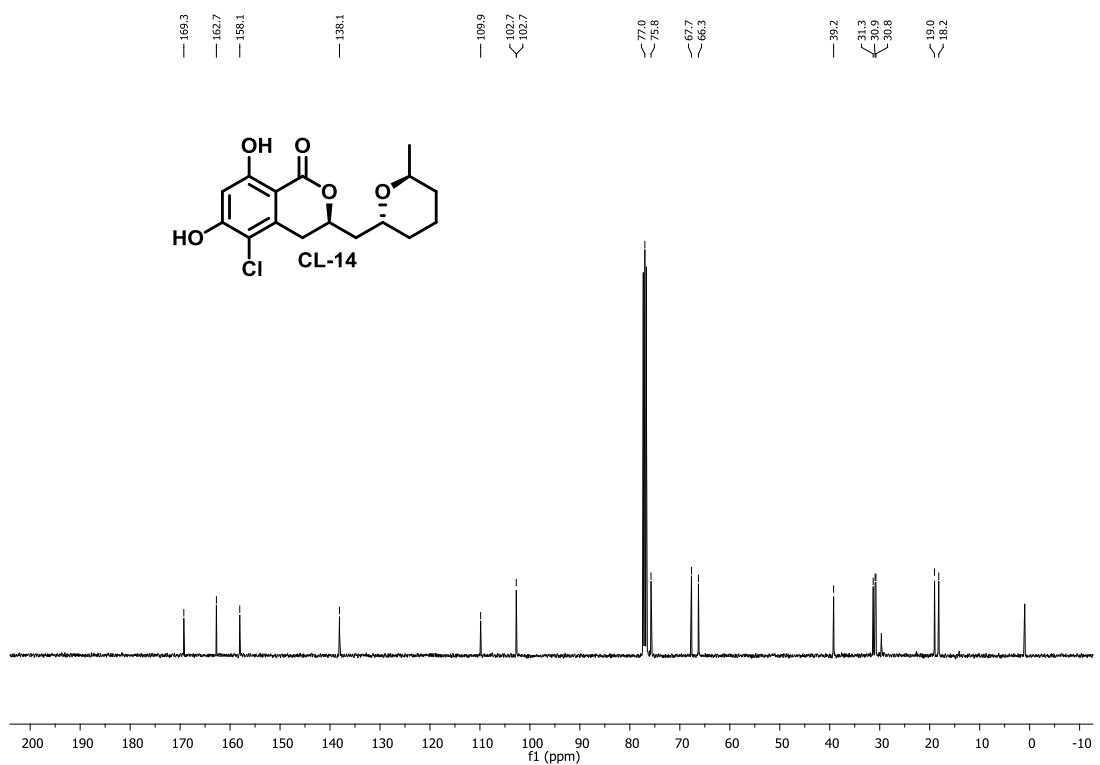
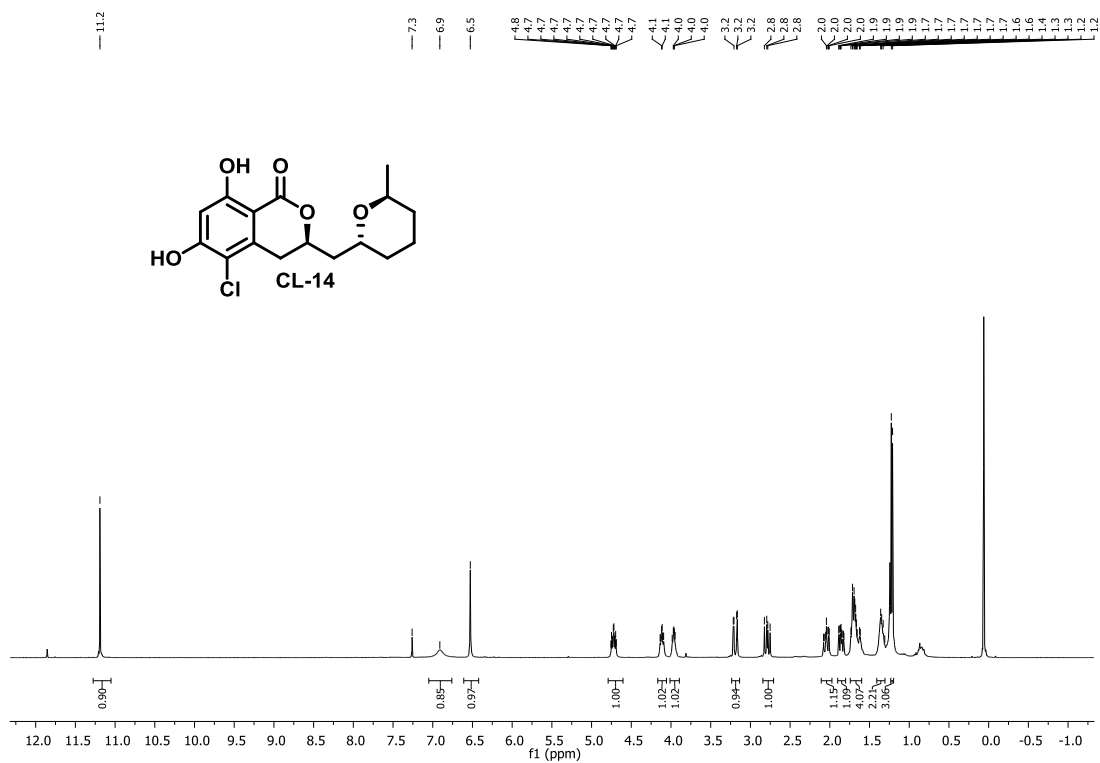
Chapter 1 (Section C): Design, Synthesis, Biological Evaluation of Lysyl tRNA synthetase (KRS) Inhibitors based on Cladosporin Scaffold towards Identification of Antimalarial Leads



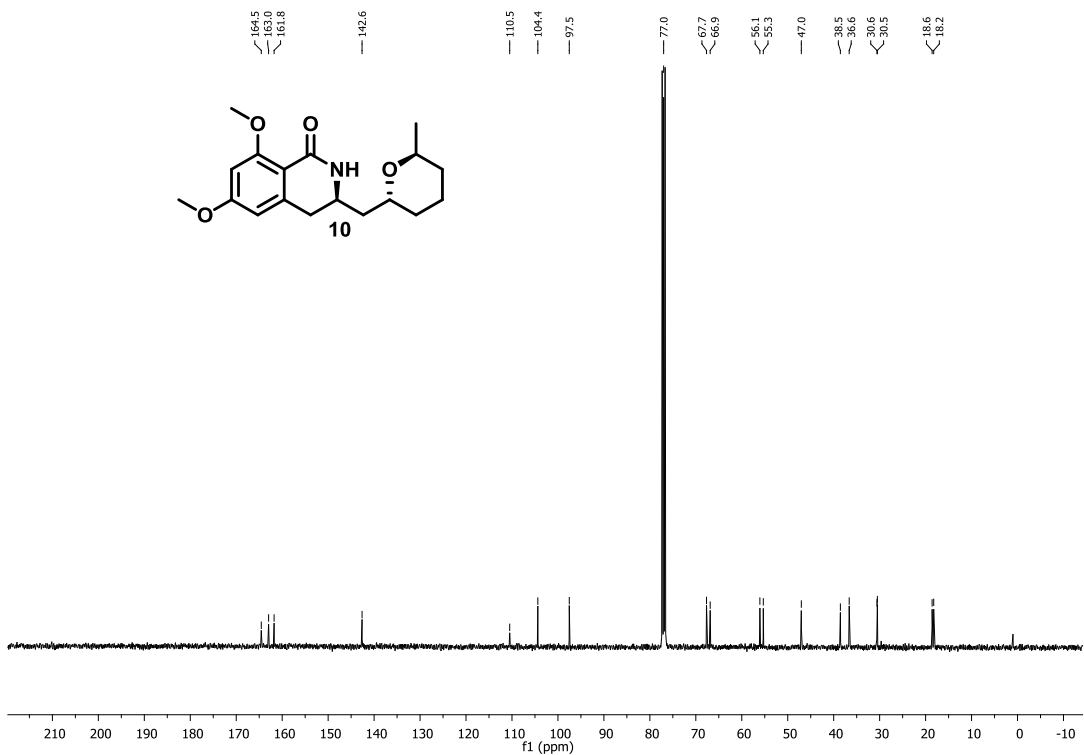
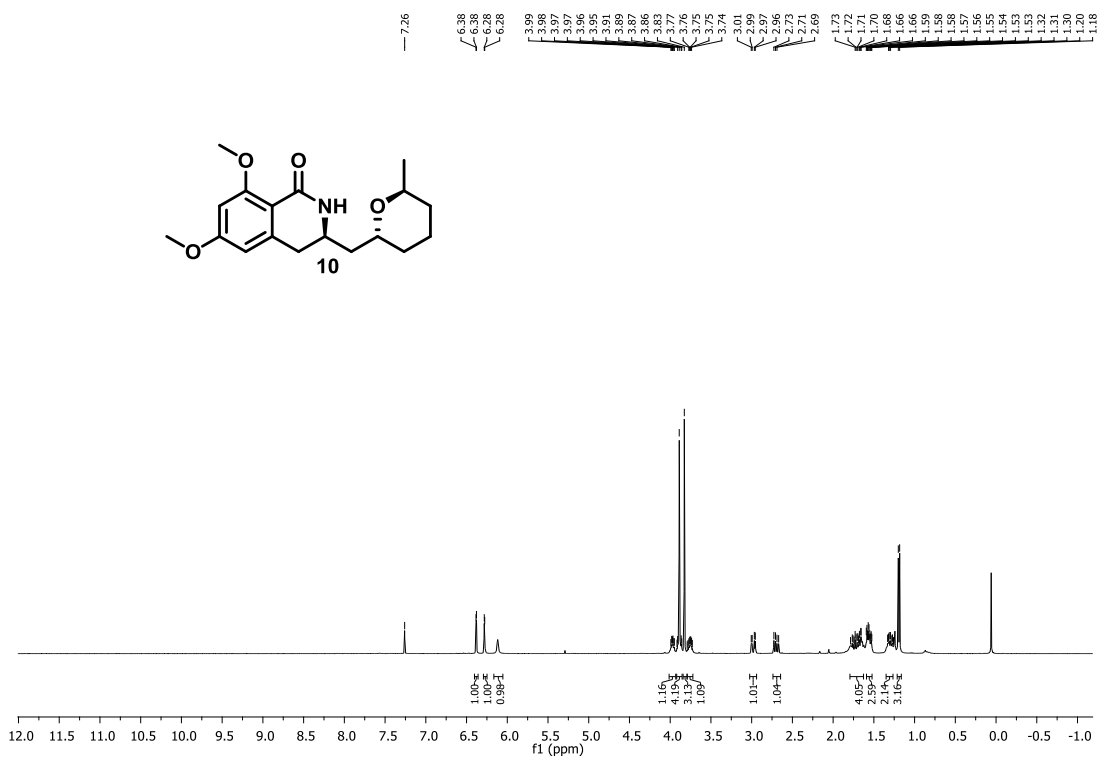
Chapter 1 (Section C): Design, Synthesis, Biological Evaluation of Lysyl tRNA synthetase (KRS) Inhibitors based on Cladosporin Scaffold towards Identification of Antimalarial Leads



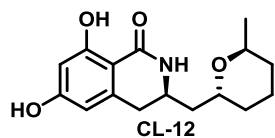
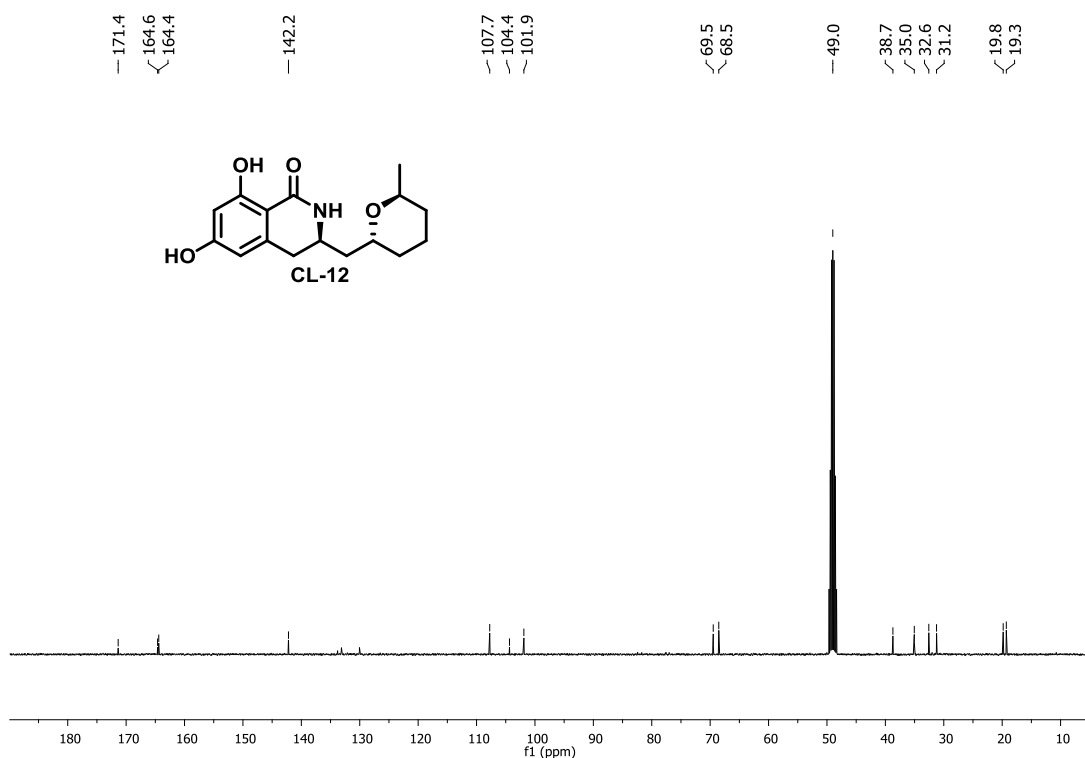
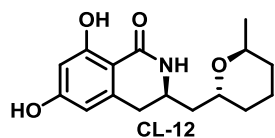
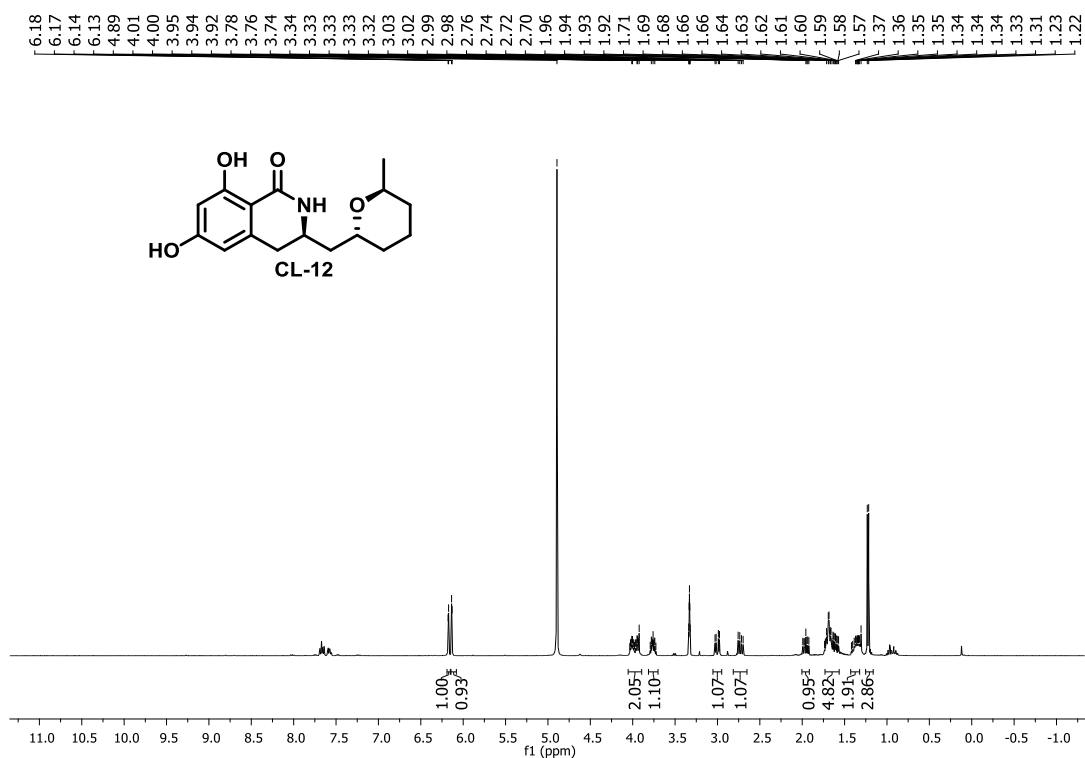
Chapter 1 (Section C): Design, Synthesis, Biological Evaluation of Lysyl tRNA synthetase (KRS) Inhibitors based on Cladosporin Scaffold towards Identification of Antimalarial Leads



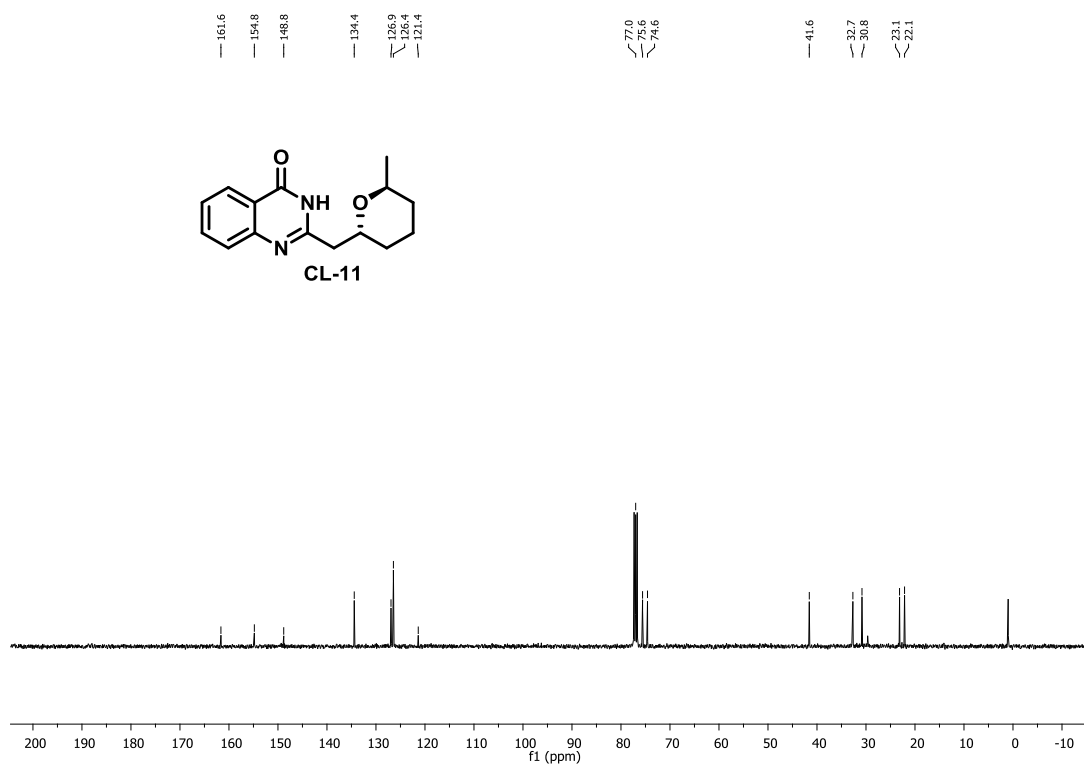
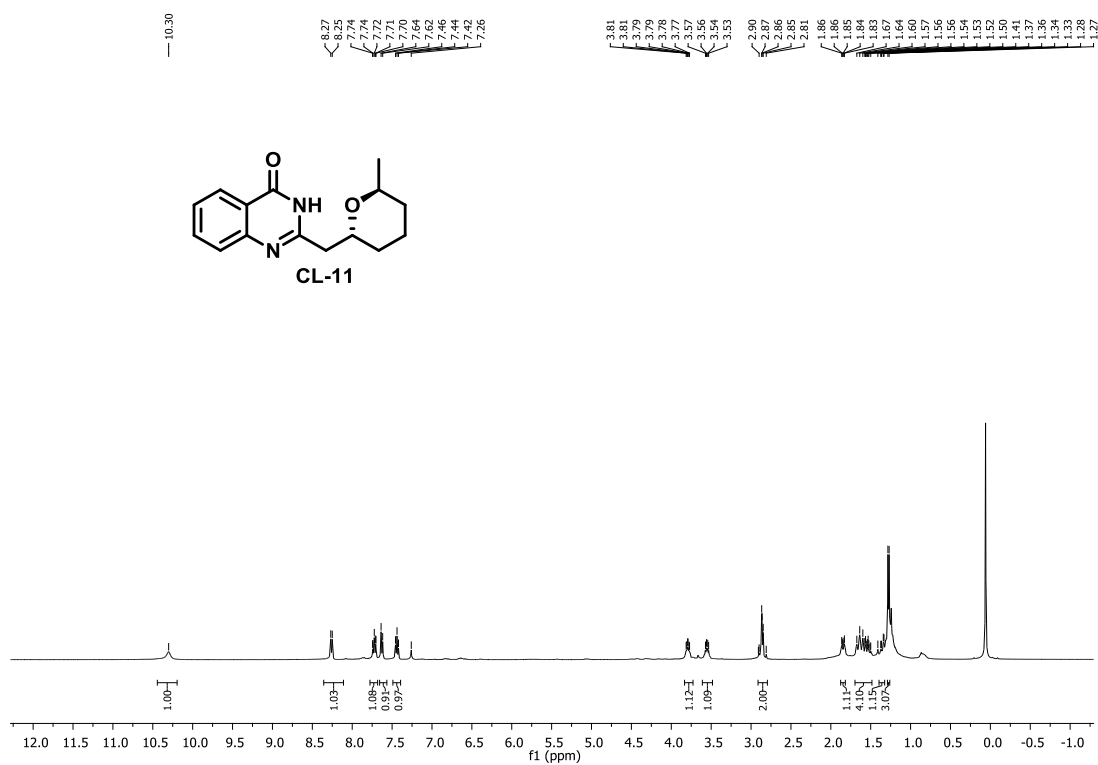
Chapter 1 (Section C): Design, Synthesis, Biological Evaluation of Lysyl tRNA synthetase (KRS) Inhibitors based on Cladosporin Scaffold towards Identification of Antimalarial Leads



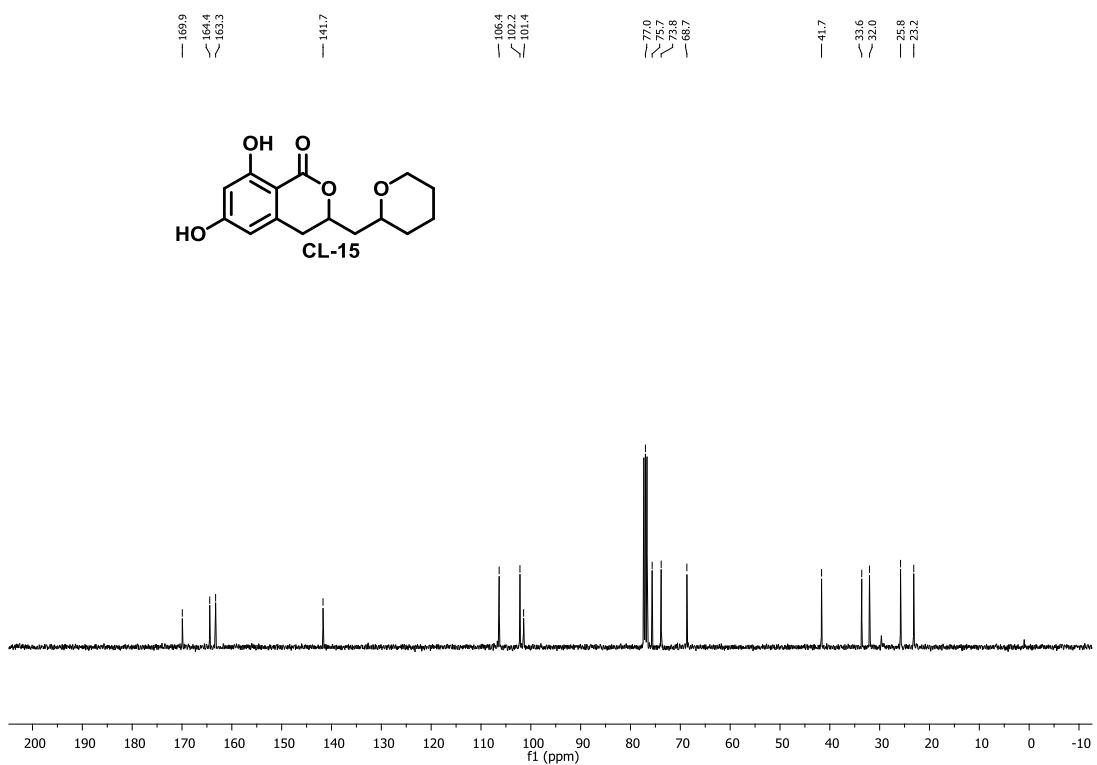
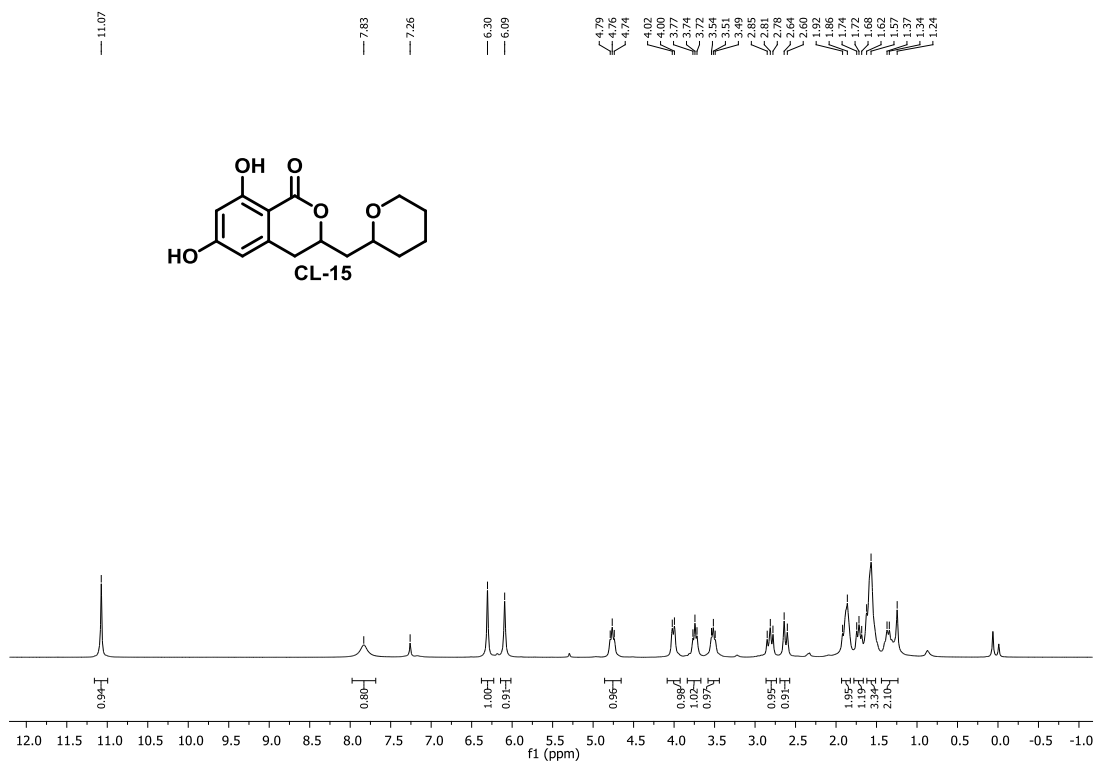
Chapter 1 (Section C): Design, Synthesis, Biological Evaluation of Lysyl tRNA synthetase (KRS) Inhibitors based on Cladosporin Scaffold towards Identification of Antimalarial Leads



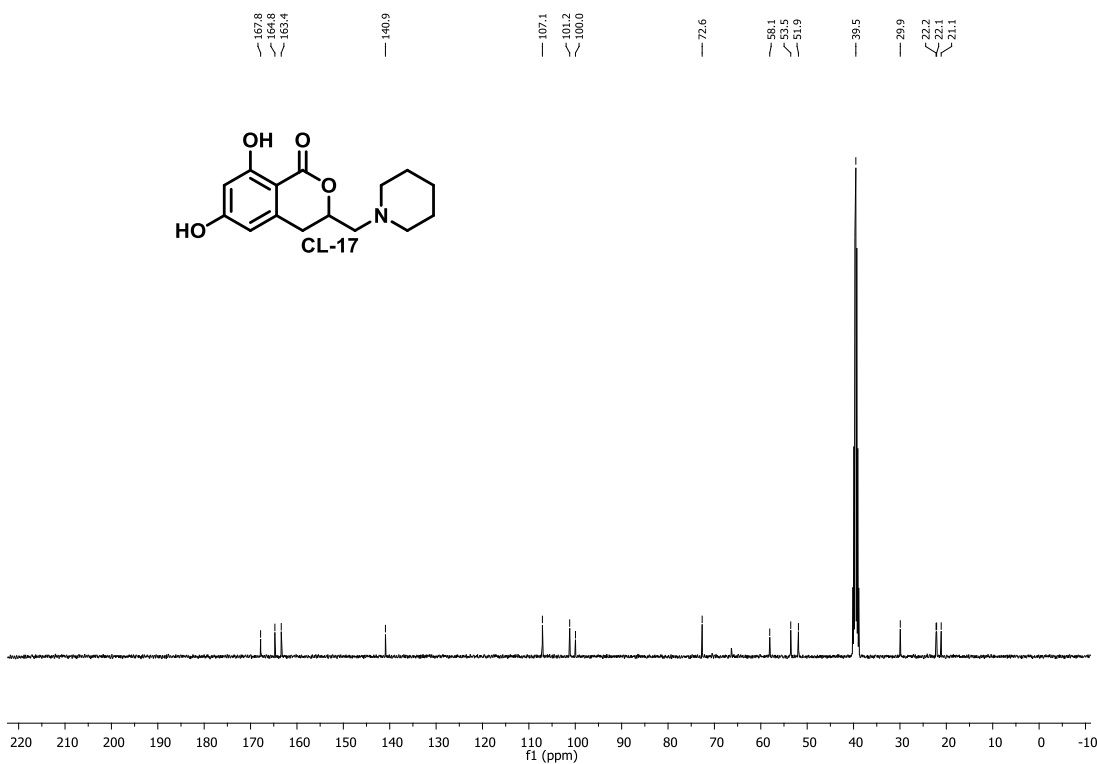
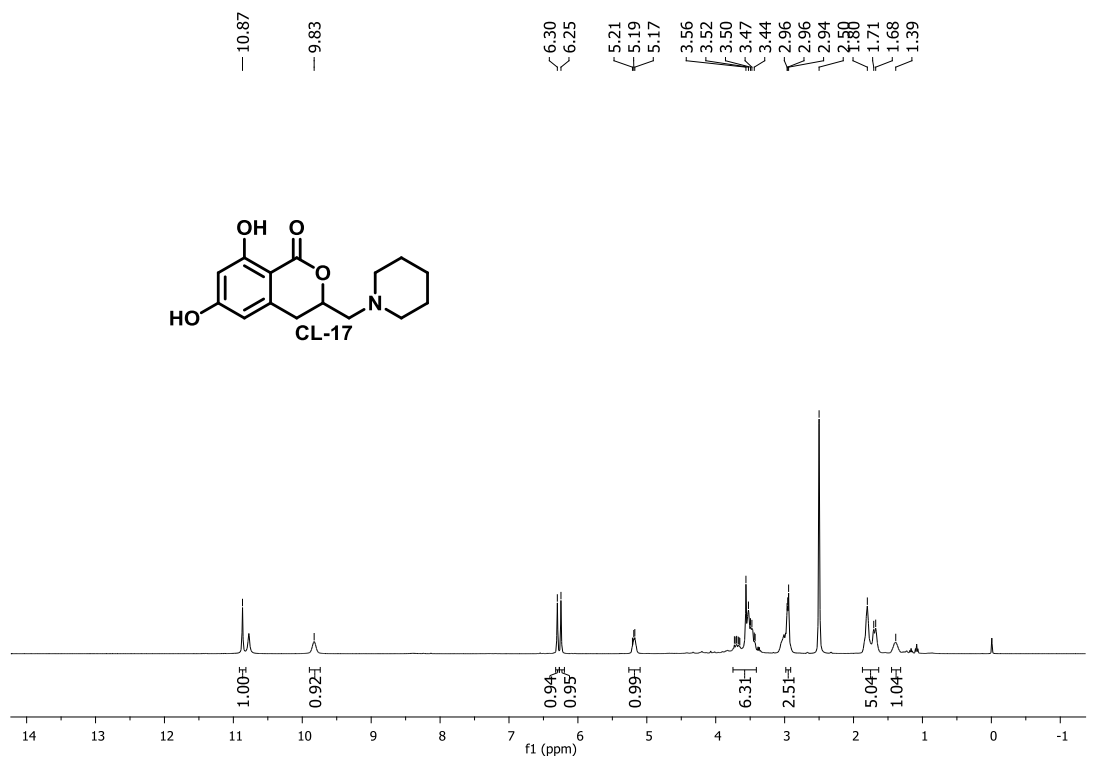
Chapter 1 (Section C): Design, Synthesis, Biological Evaluation of Lysyl tRNA synthetase (KRS) Inhibitors based on Cladosporin Scaffold towards Identification of Antimalarial Leads



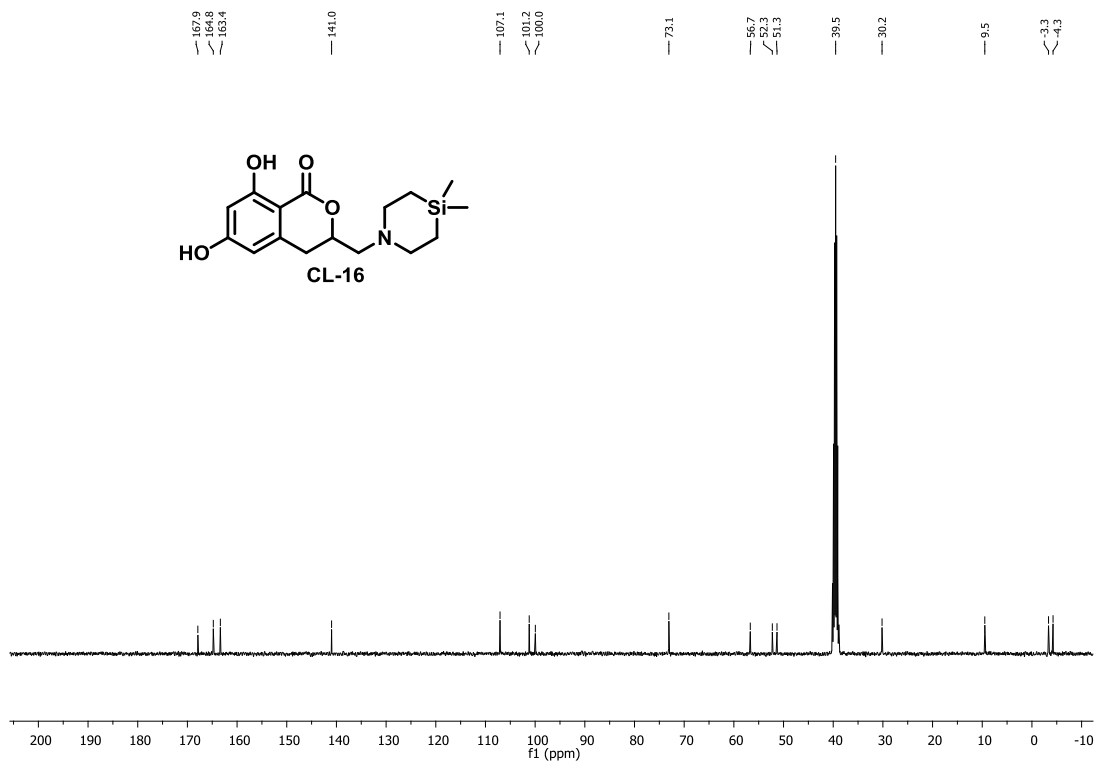
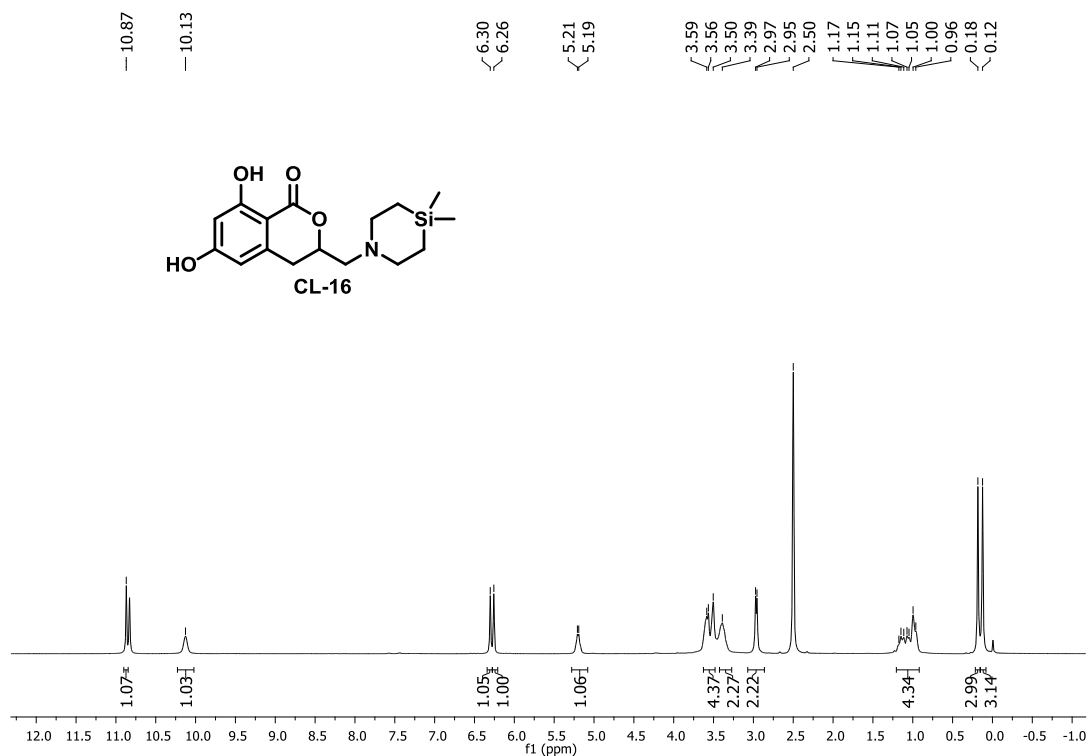
Chapter 1 (Section C): Design, Synthesis, Biological Evaluation of Lysyl tRNA synthetase (KRS) Inhibitors based on Cladosporin Scaffold towards Identification of Antimalarial Leads



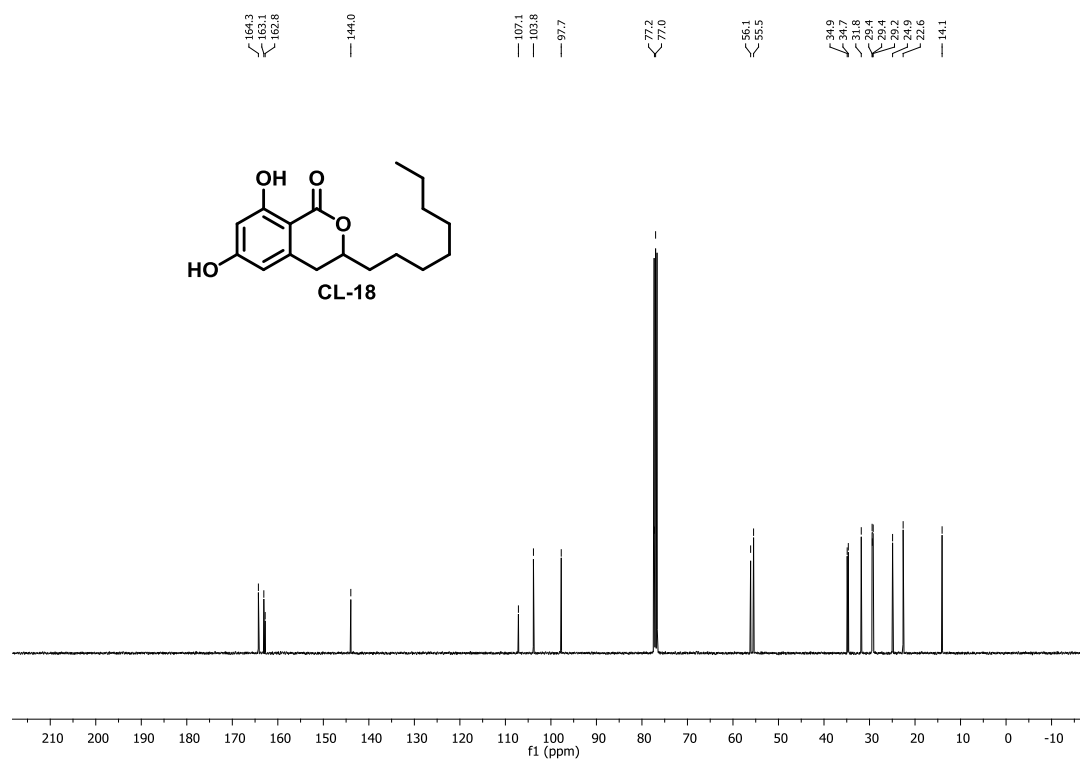
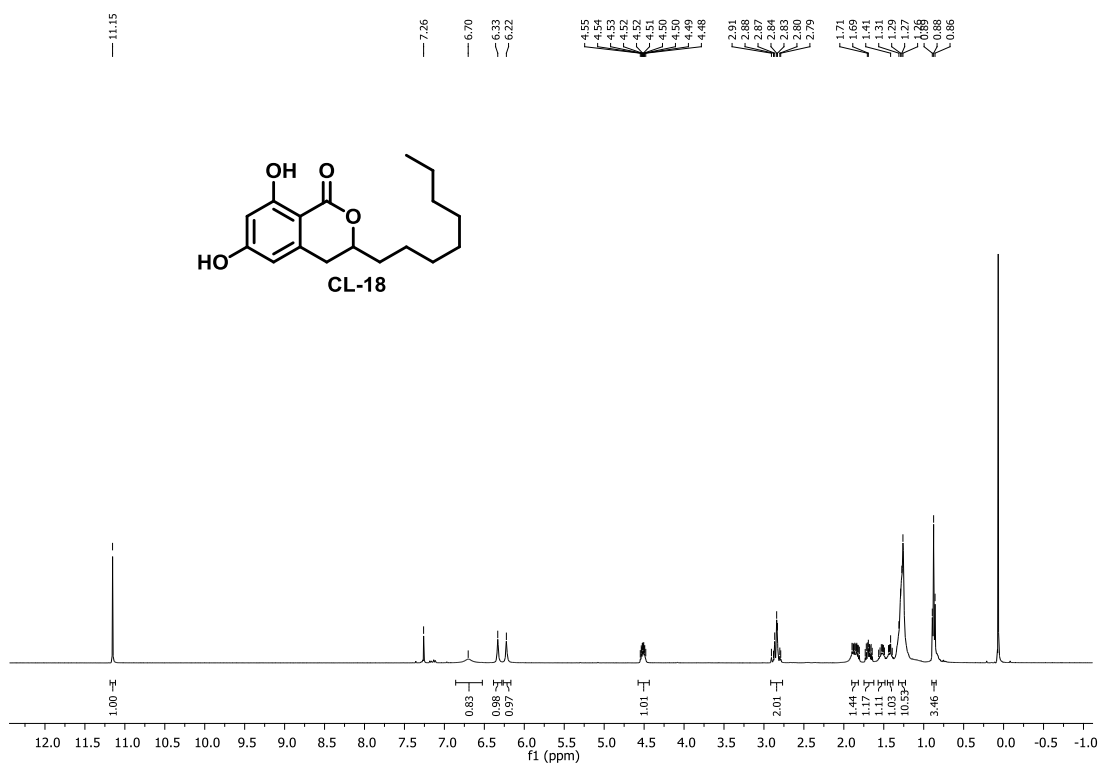
Chapter 1 (Section C): Design, Synthesis, Biological Evaluation of Lysyl tRNA synthetase (KRS) Inhibitors based on Cladosporin Scaffold towards Identification of Antimalarial Leads



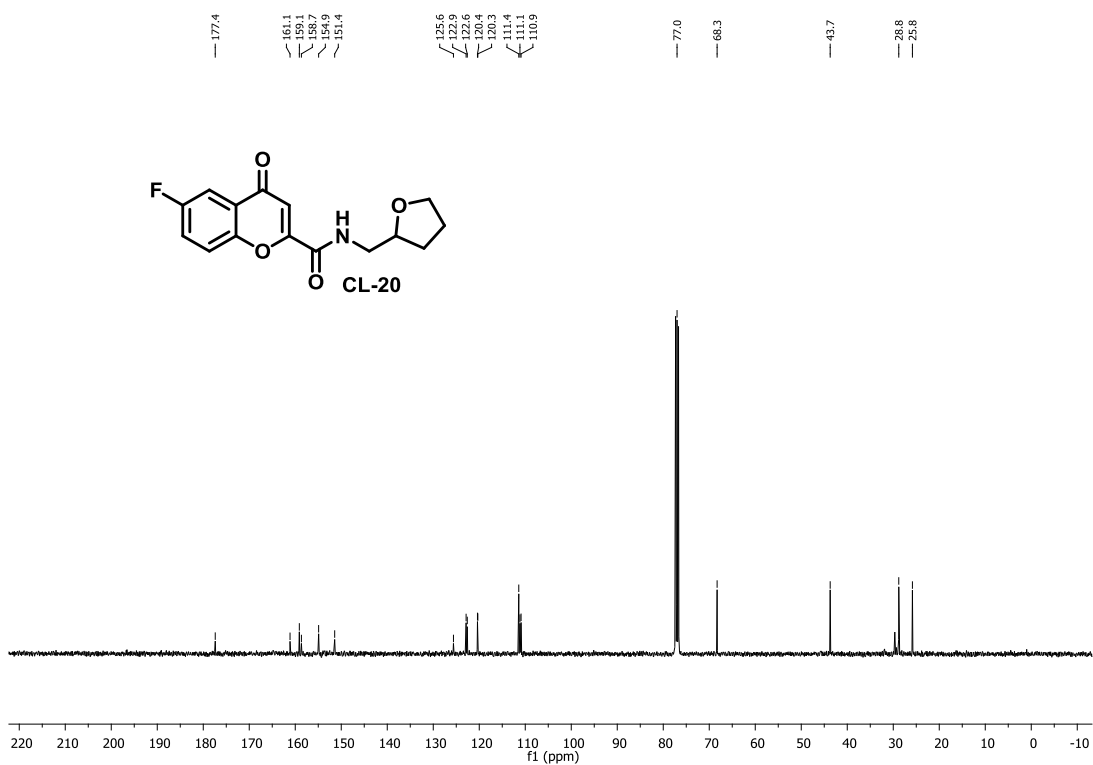
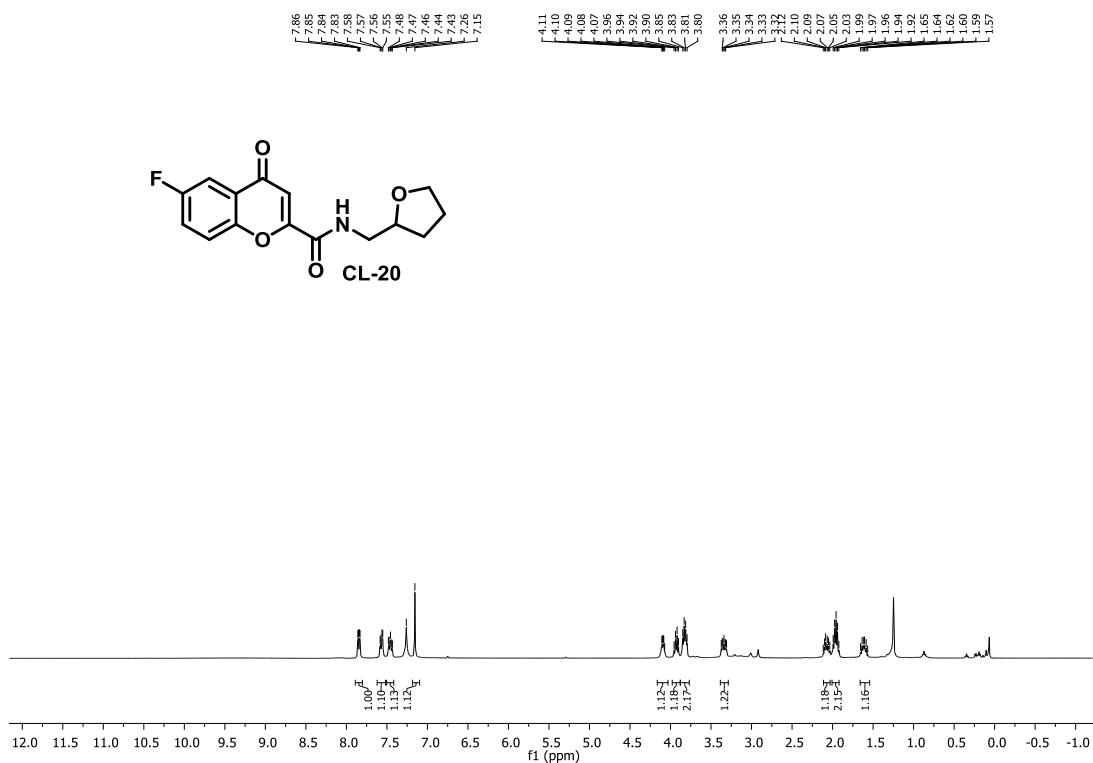
Chapter 1 (Section C): Design, Synthesis, Biological Evaluation of Lysyl tRNA synthetase (KRS) Inhibitors based on Cladosporin Scaffold towards Identification of Antimalarial Leads



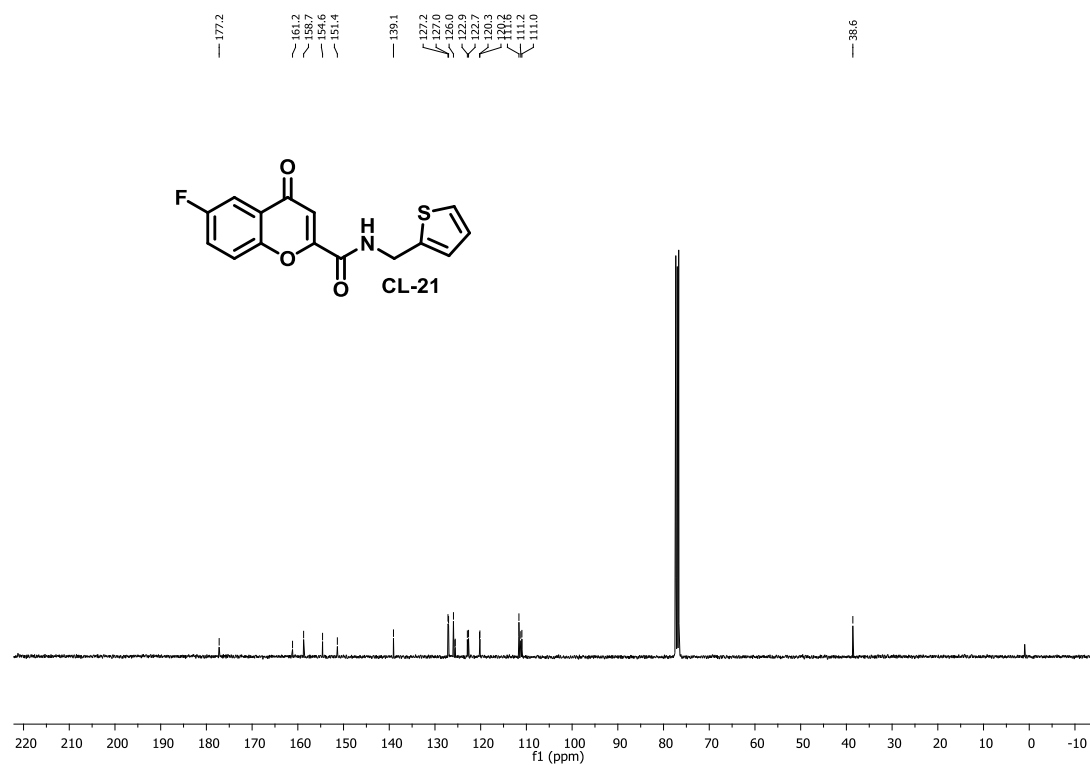
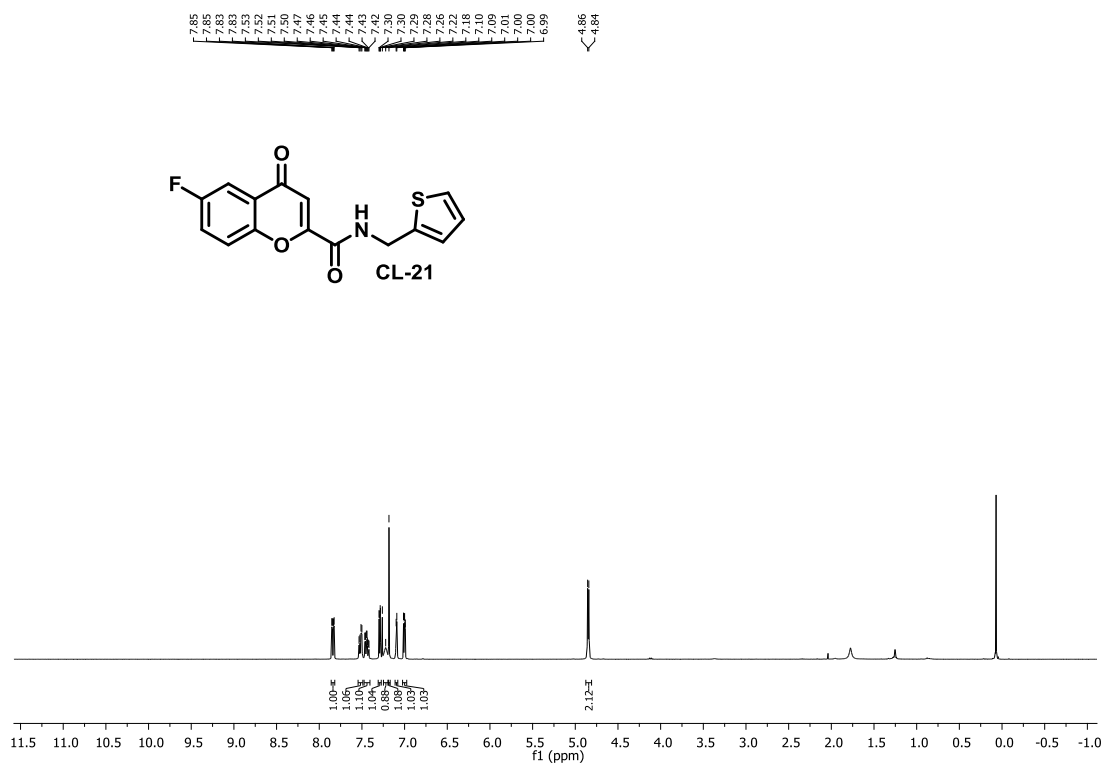
Chapter 1 (Section C): Design, Synthesis, Biological Evaluation of Lysyl tRNA synthetase (KRS) Inhibitors based on Cladosporin Scaffold towards Identification of Antimalarial Leads



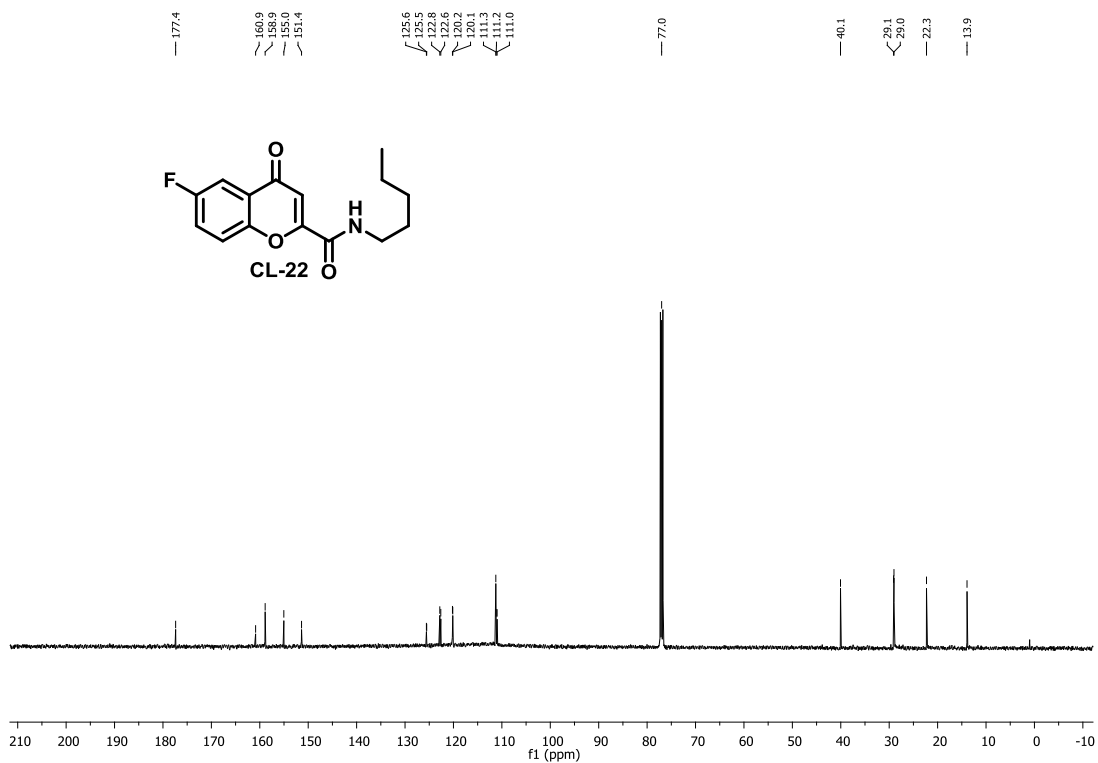
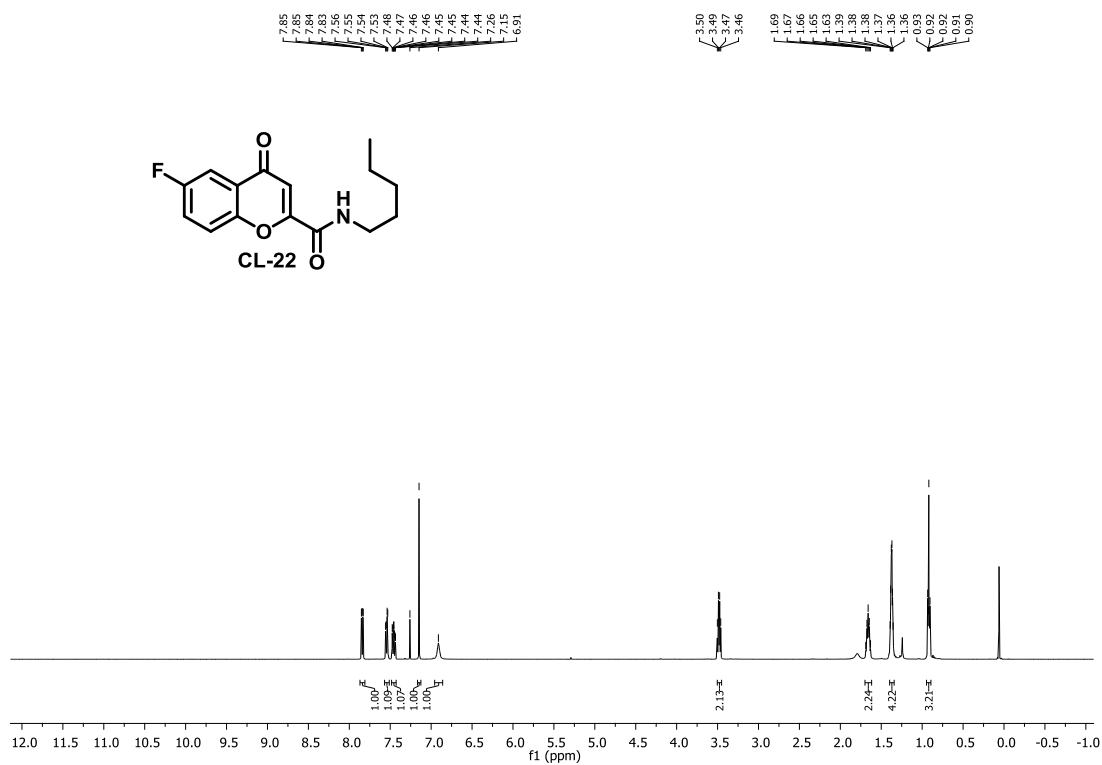
Chapter 1 (Section C): Design, Synthesis, Biological Evaluation of Lysyl tRNA synthetase (KRS) Inhibitors based on Cladosporin Scaffold towards Identification of Antimalarial Leads



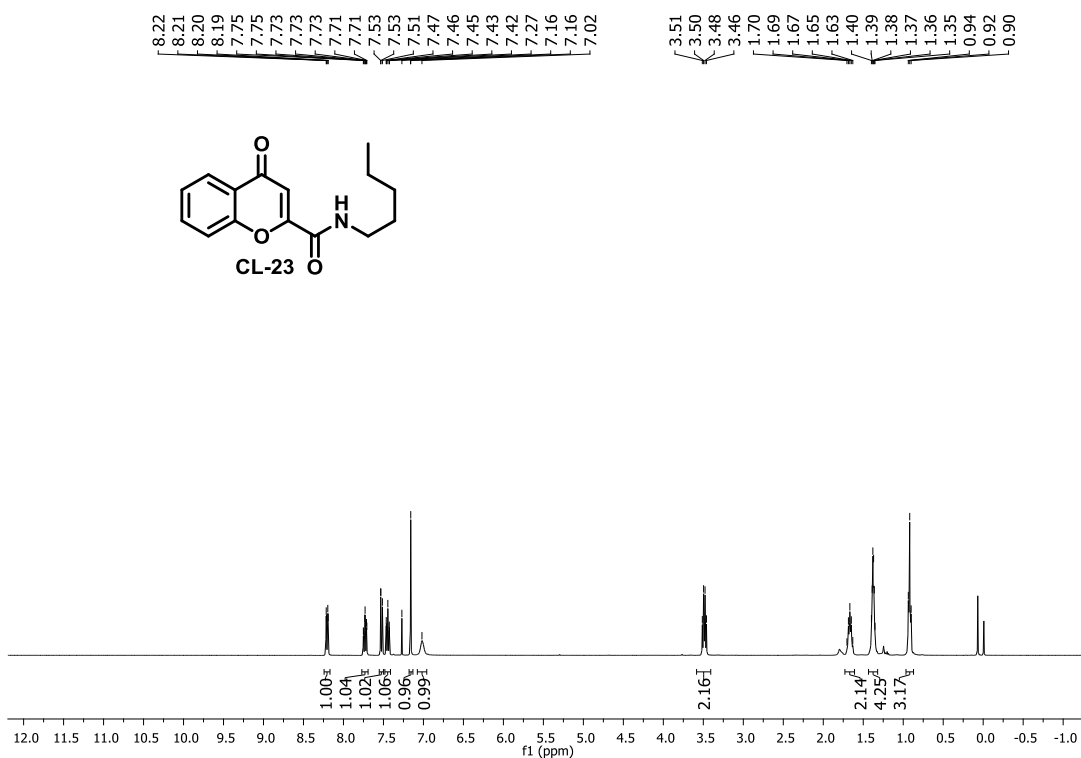
Chapter 1 (Section C): Design, Synthesis, Biological Evaluation of Lysyl tRNA synthetase (KRS) Inhibitors based on Cladosporin Scaffold towards Identification of Antimalarial Leads



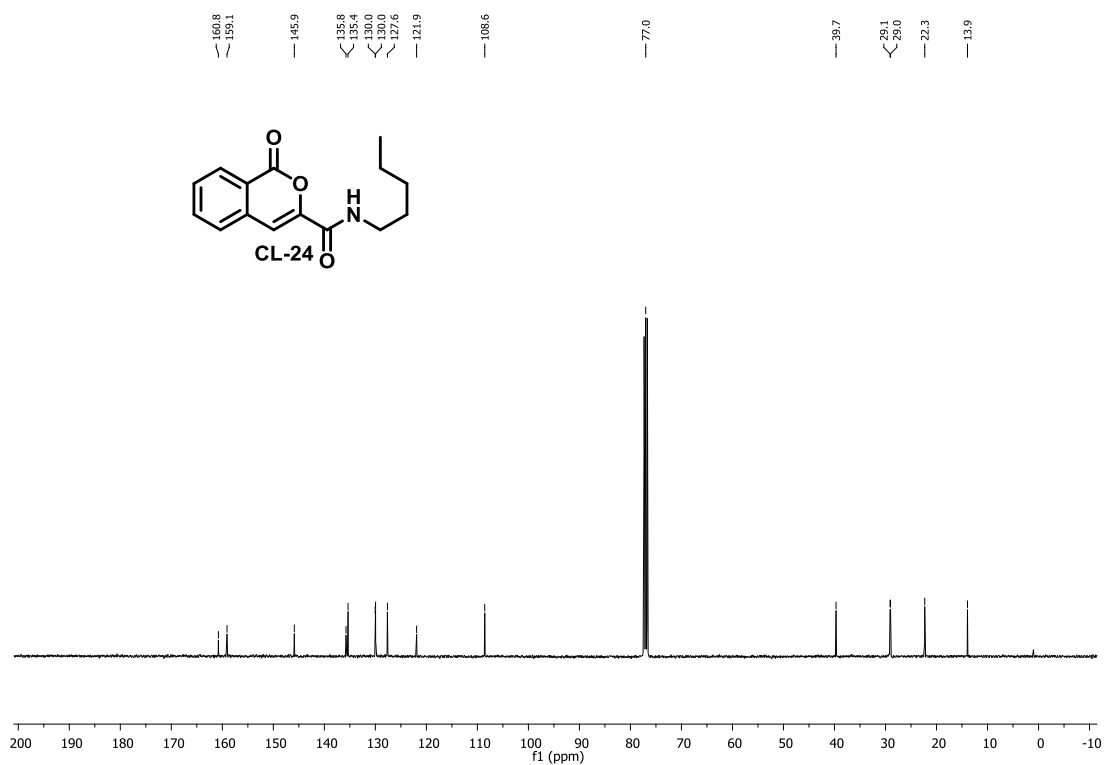
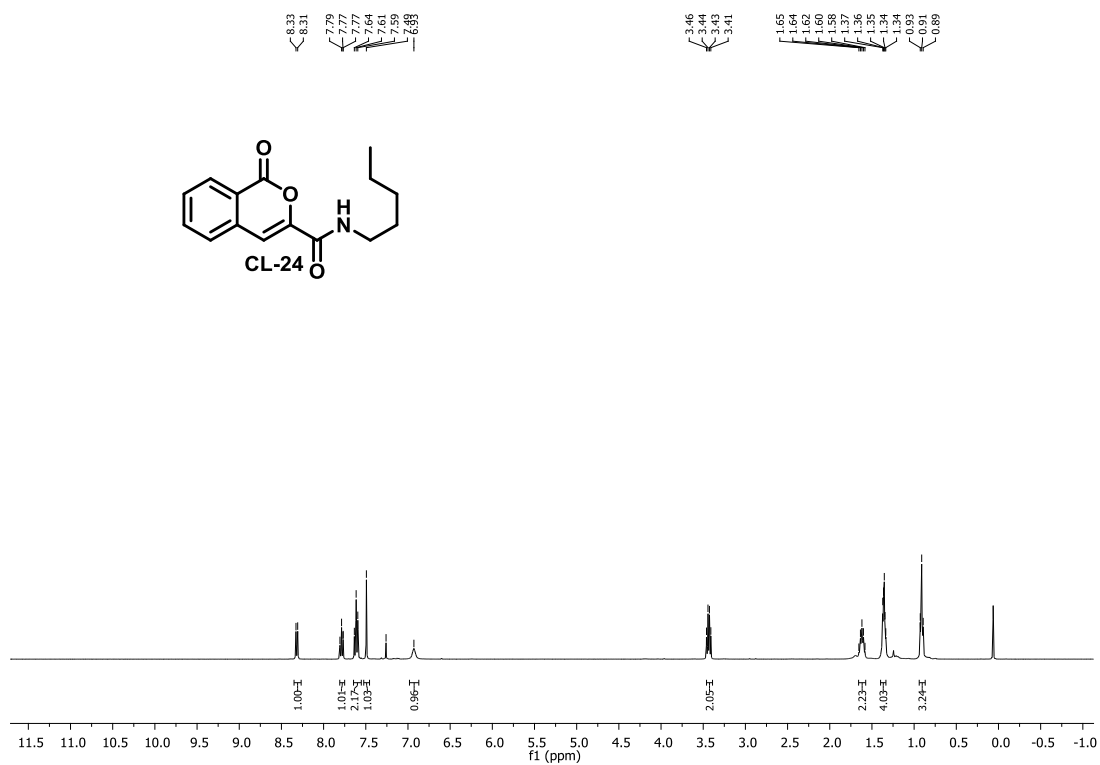
Chapter 1 (Section C): Design, Synthesis, Biological Evaluation of Lysyl tRNA synthetase (KRS) Inhibitors based on Cladosporin Scaffold towards Identification of Antimalarial Leads



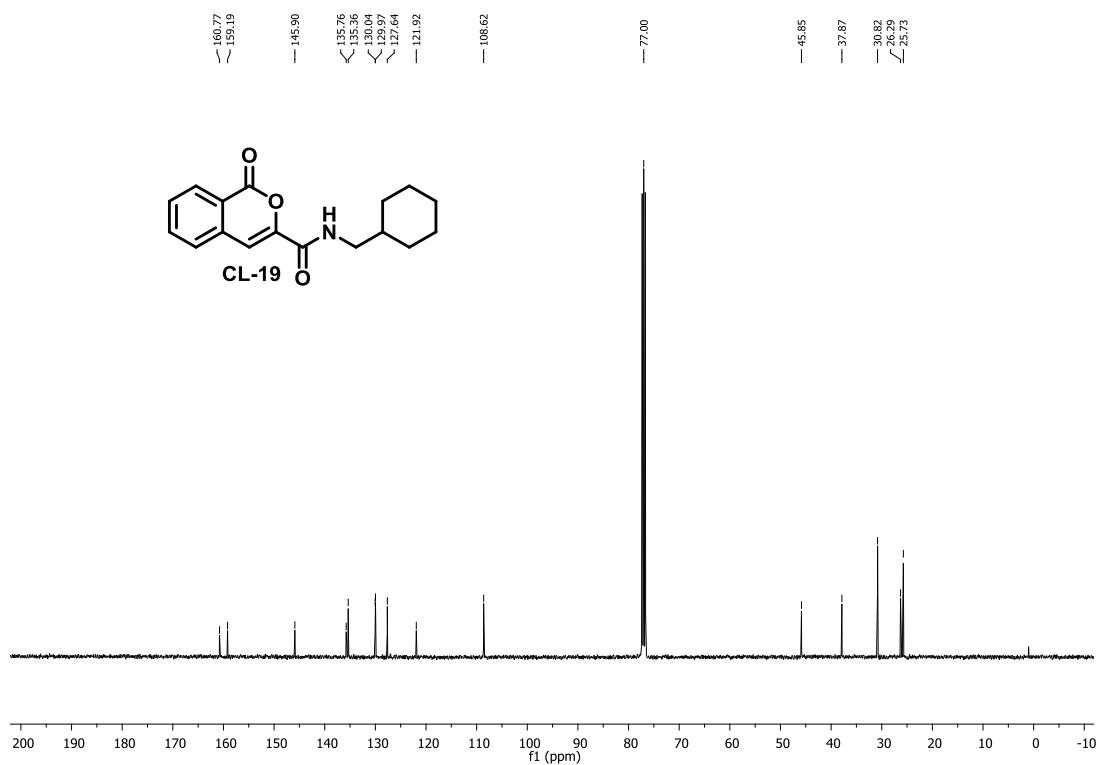
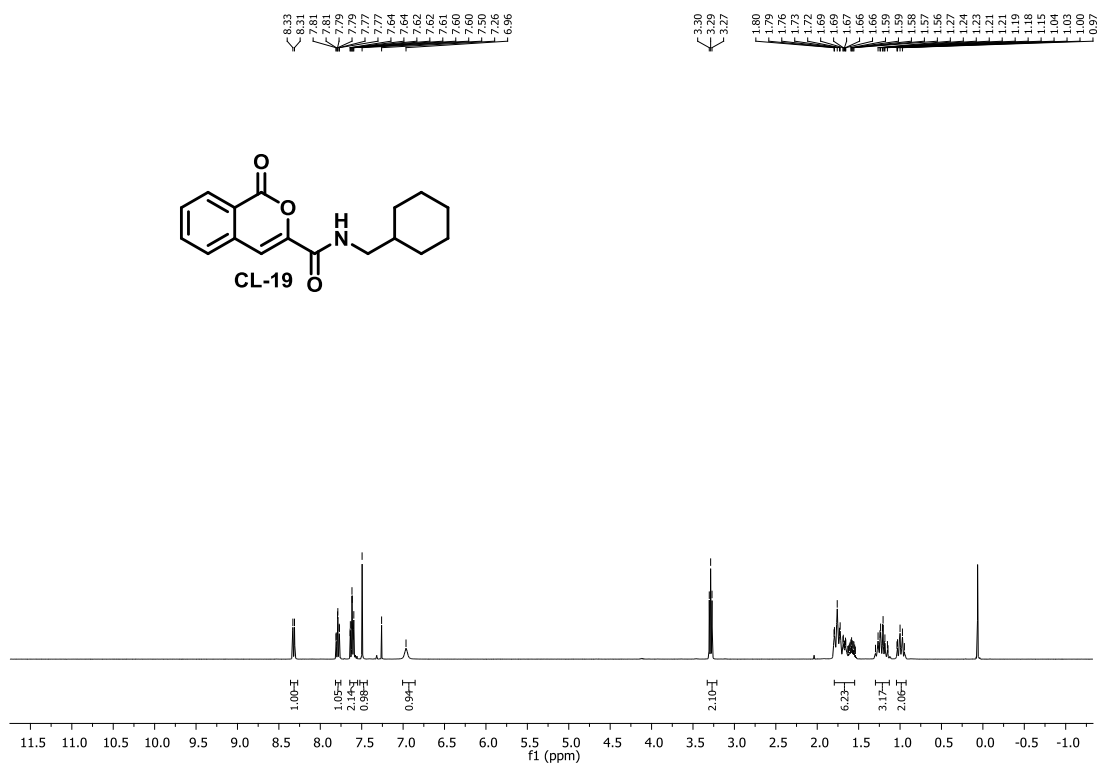
Chapter 1 (Section C): Design, Synthesis, Biological Evaluation of Lysyl tRNA synthetase (KRS) Inhibitors based on Cladosporin Scaffold towards Identification of Antimalarial Leads



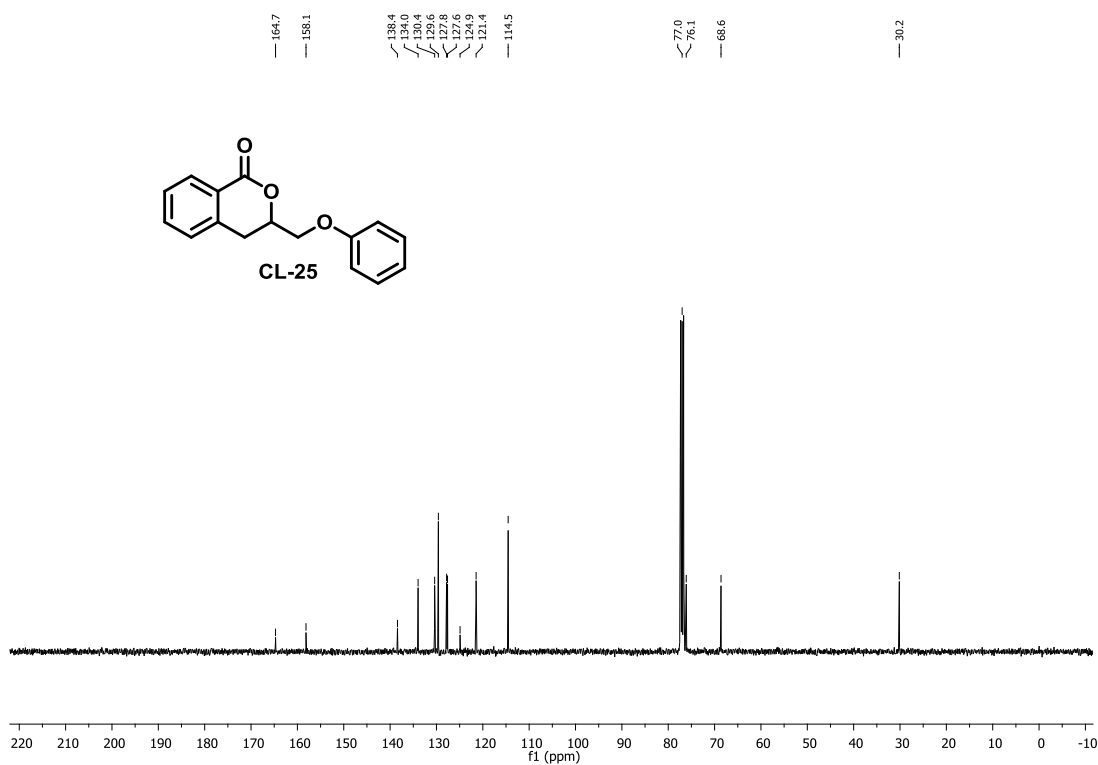
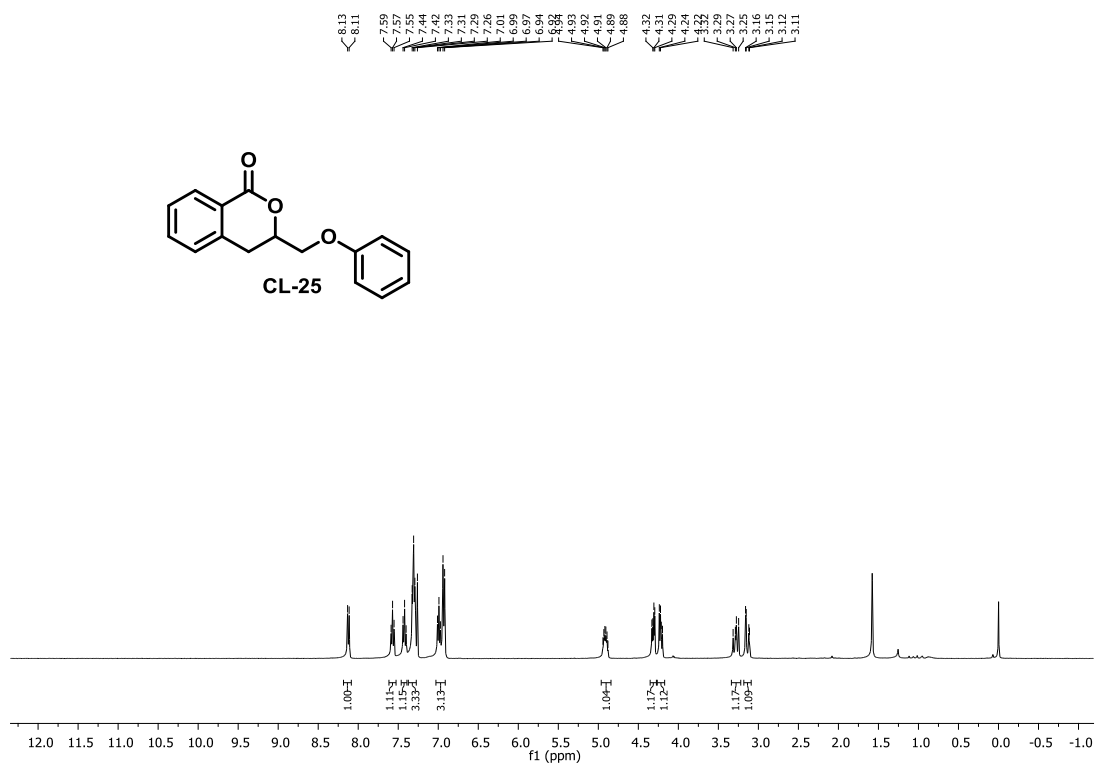
Chapter 1 (Section C): Design, Synthesis, Biological Evaluation of Lysyl tRNA synthetase (KRS) Inhibitors based on Cladosporin Scaffold towards Identification of Antimalarial Leads



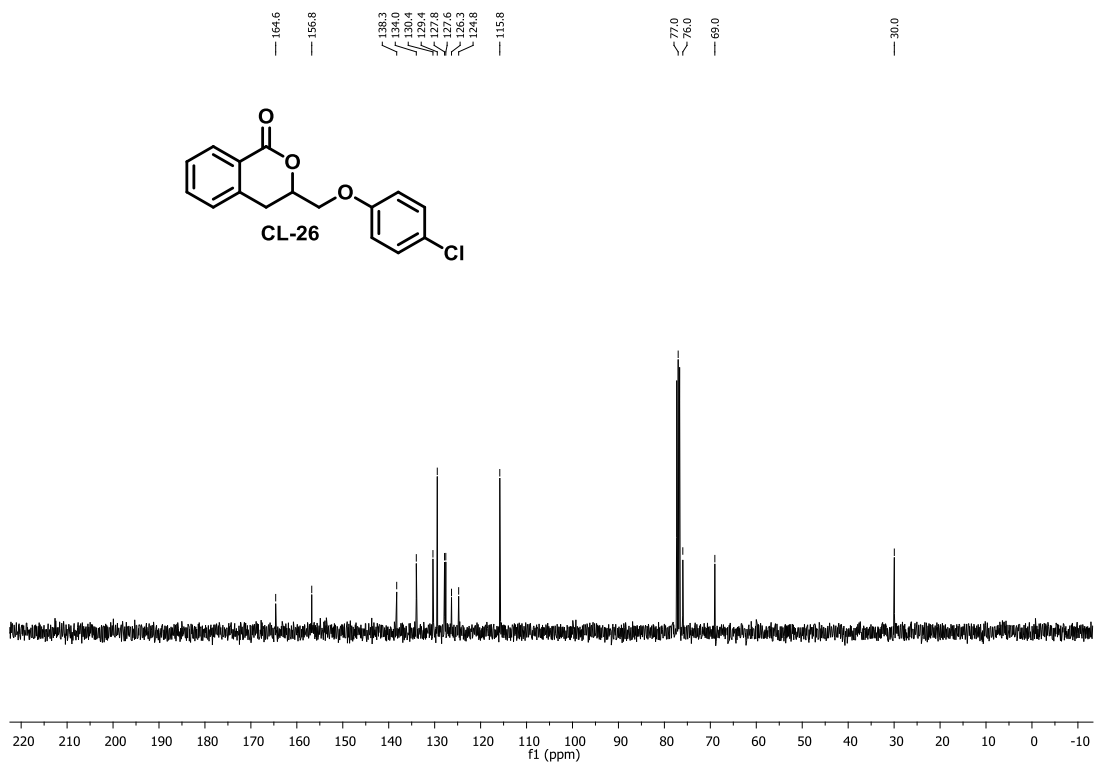
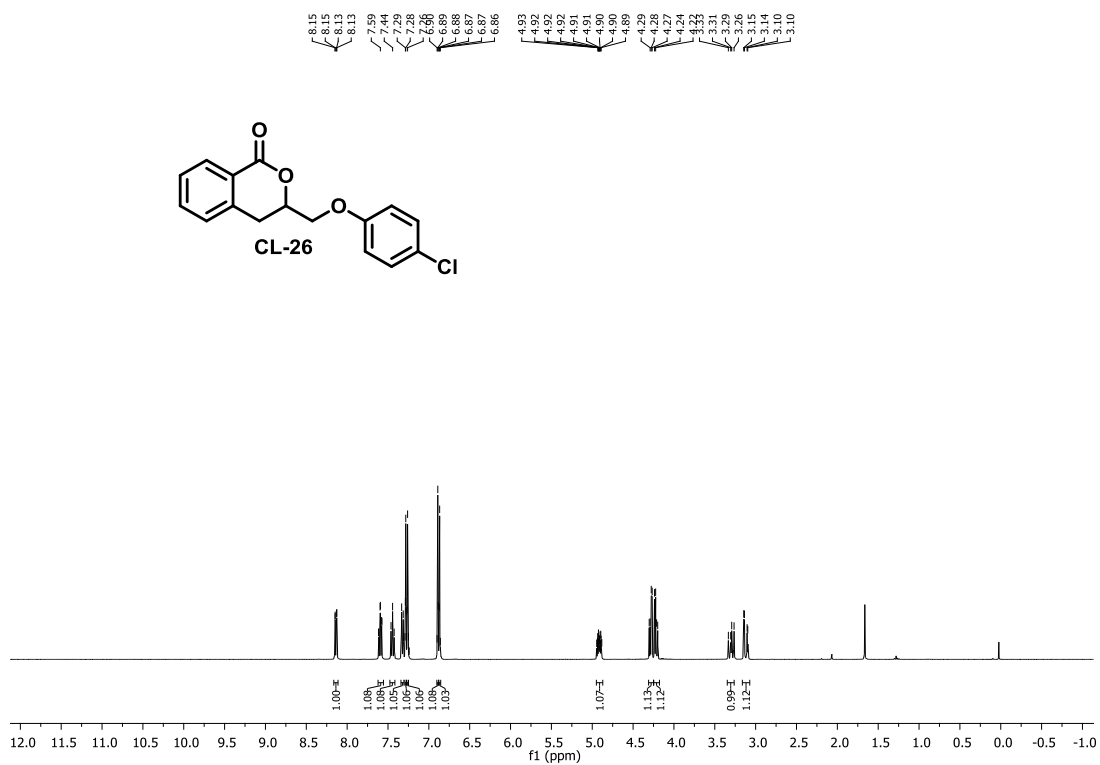
Chapter 1 (Section C): Design, Synthesis, Biological Evaluation of Lysyl tRNA synthetase (KRS) Inhibitors based on Cladosporin Scaffold towards Identification of Antimalarial Leads



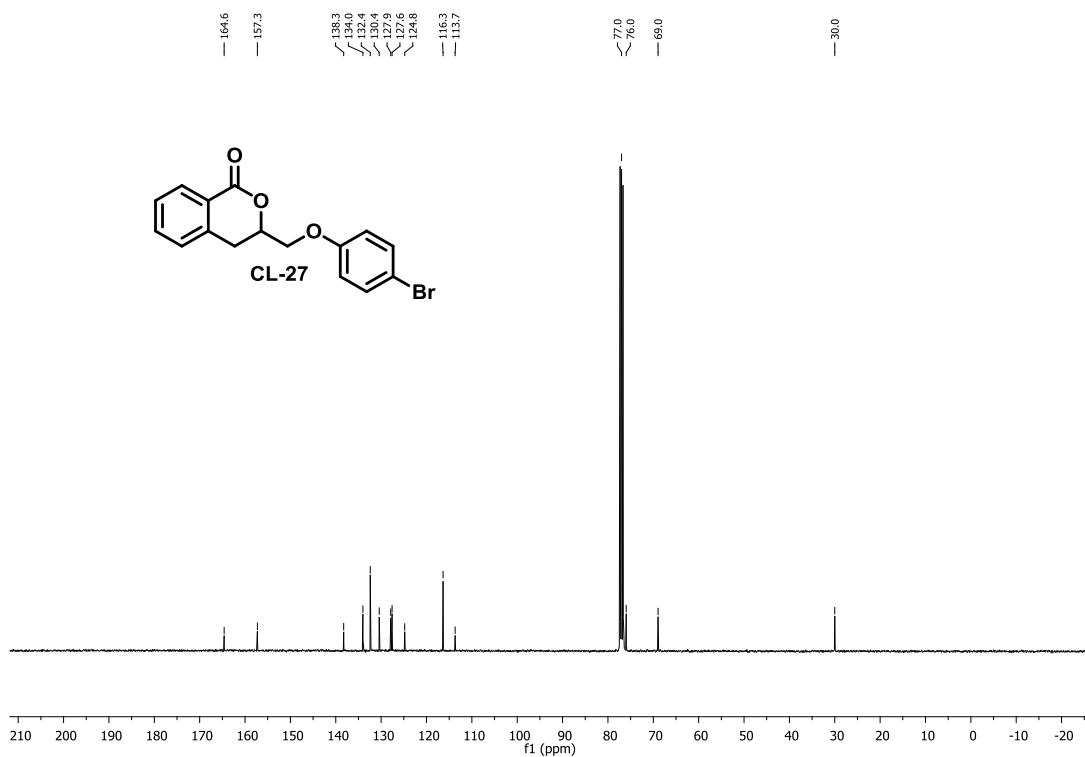
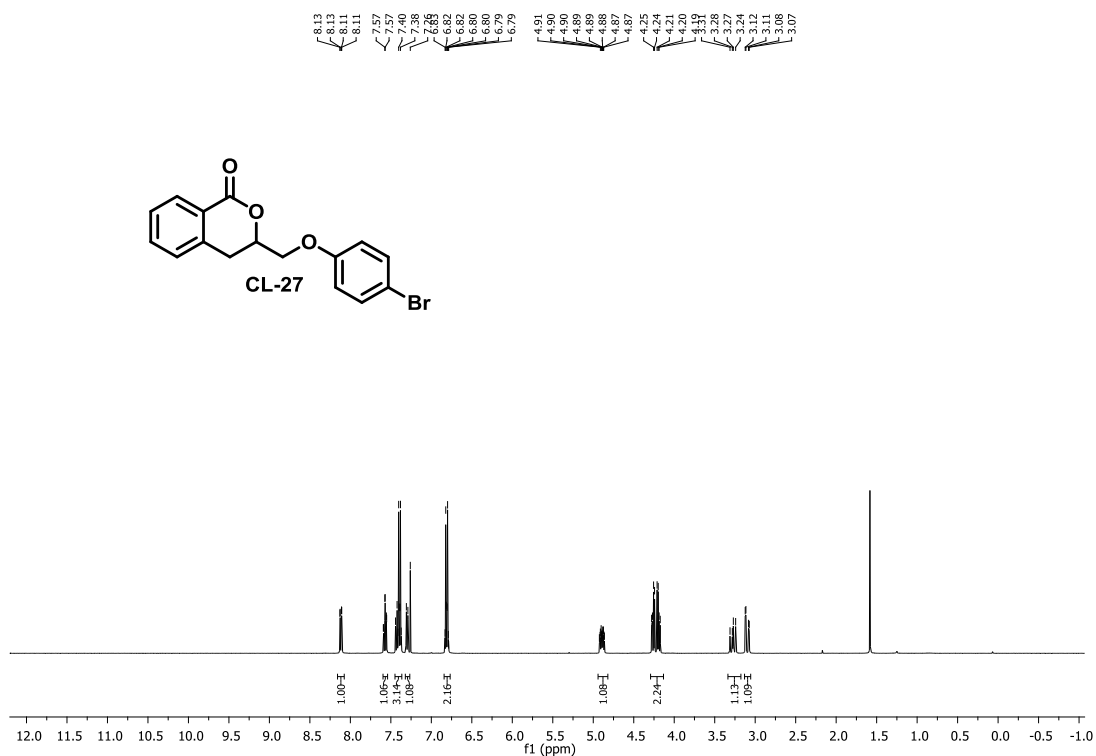
Chapter 1 (Section C): Design, Synthesis, Biological Evaluation of Lysyl tRNA synthetase (KRS) Inhibitors based on Cladosporin Scaffold towards Identification of Antimalarial Leads



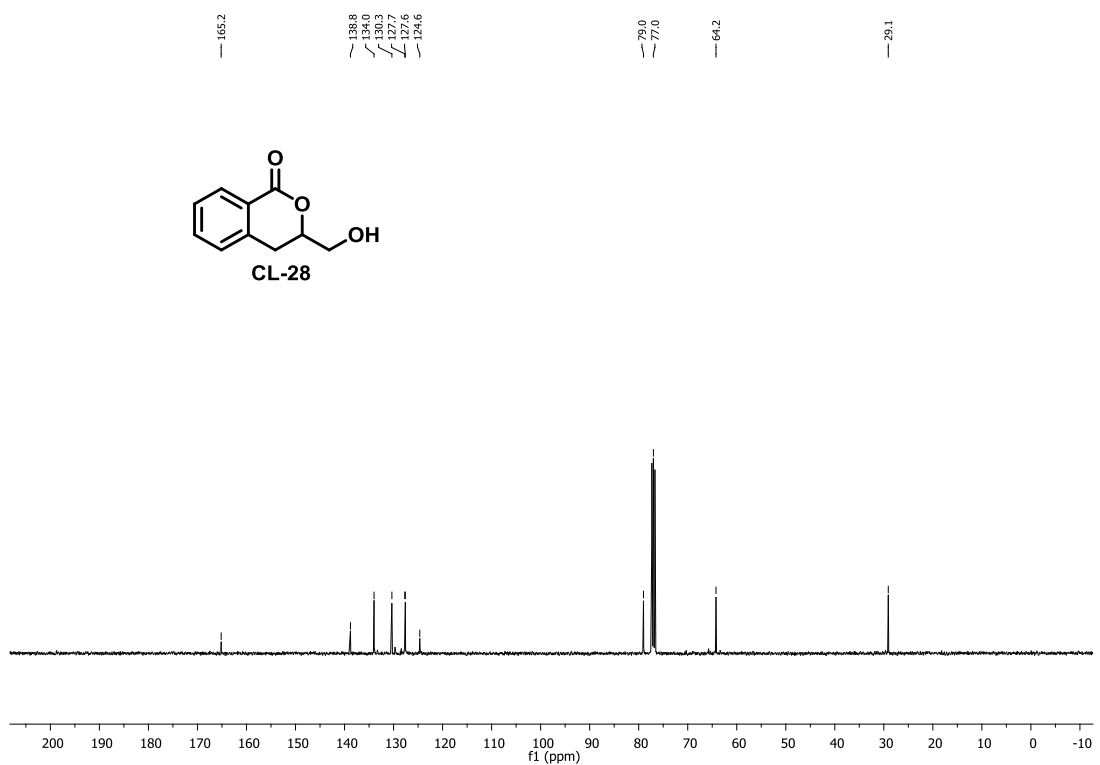
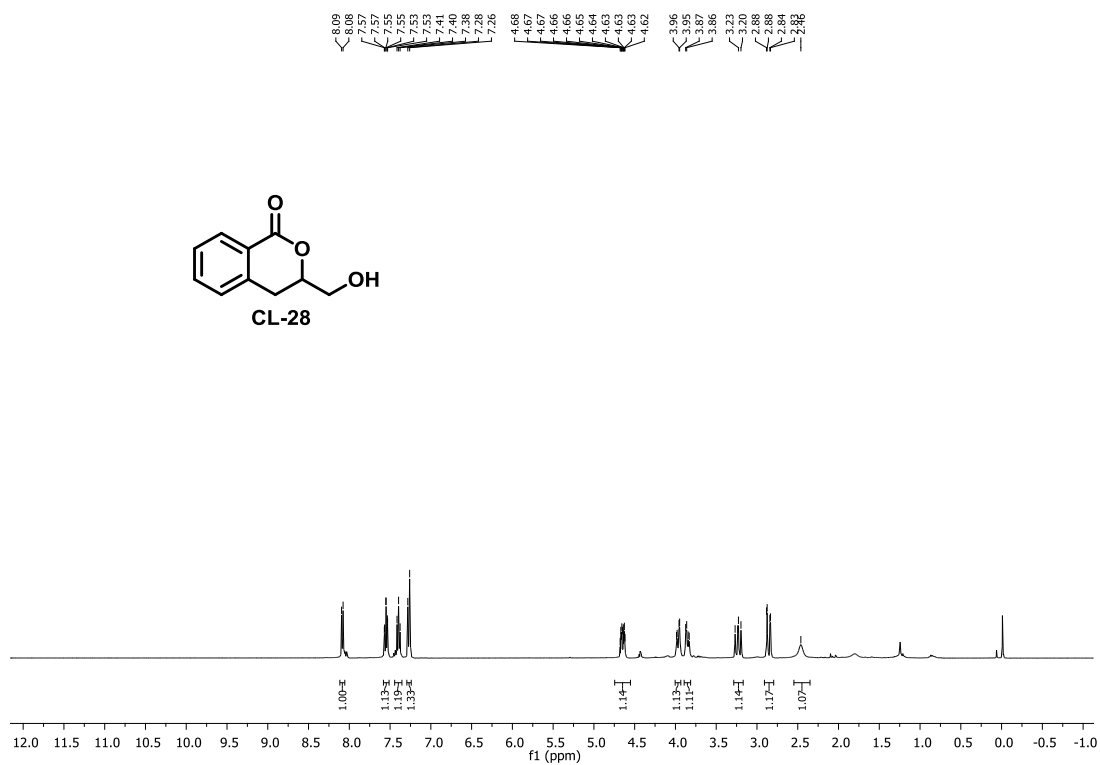
Chapter 1 (Section C): Design, Synthesis, Biological Evaluation of Lysyl tRNA synthetase (KRS) Inhibitors based on Cladosporin Scaffold towards Identification of Antimalarial Leads



Chapter 1 (Section C): Design, Synthesis, Biological Evaluation of Lysyl tRNA synthetase (KRS) Inhibitors based on Cladosporin Scaffold towards Identification of Antimalarial Leads



Chapter 1 (Section C): Design, Synthesis, Biological Evaluation of Lysyl tRNA synthetase (KRS) Inhibitors based on Cladosporin Scaffold towards Identification of Antimalarial Leads





SECOND CHAPTER



Total Synthesis of Cladosporin Related Twelve Membered Macrocyclic Natural Products

Chapter 2: Total Synthesis of Cladosporin Related Twelve Membered Macrocyclic Natural Products

2.1. Introduction

Fungal secondary metabolites are of significant synthetic interest and are often considered as privileged scaffolds in identification of lead molecules in medicinal chemistry and drug discovery program.¹ Fungal secondary metabolites can be categorized into four main classes, namely, polyketides, terpenoids, shikimic acid derived compounds, and non-ribosomal peptides. Besides, hybrid metabolites, composed of fused scaffolds from different classes are also prevalent, as in the case of meroterpenoids (fusion of terpenes and polyketides).² Specifically speaking, fungal polyketides demonstrate one of the most structurally diverse classes of natural product which includes simple aromatic metabolites as well as complex macrocyclic lactones.³⁻⁷ Among these fungal polyketide secondary metabolites, benzenediol lactone (BDL) represents a growing class of compounds consisting of 1,3-benzenediol moiety bridged by a macrocyclic lactone.⁸ This class of compounds represents a rich scaffold for structural variations, which are mainly reflected in the different degrees of unsaturation and positioning of oxidation in the macrolactone ring. The BDL family of natural products can further be categorized into resorcylic acid lactones (RALs) and dihydroxyphenylacetic acid lactones (DALs) based on the substituted resorcinol fragment fused to α , β -, and β , γ -positions of the macrolactone ring (Figure 1).

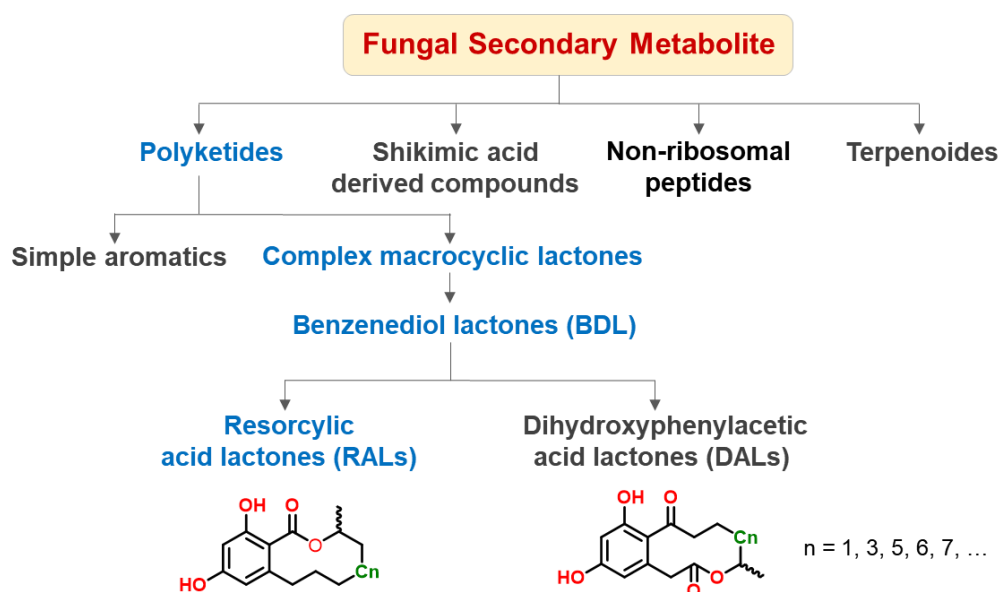


Figure 1. Broad categorical distribution of fungal secondary metabolites.

Chapter 2: Total Synthesis of Cladosporin Related Twelve Membered Macrocyclic Natural Products

Resorcylic acid lactones (RALs), a specific class of compounds belonging to the BDL family, consists of a substituted resorcinol fragment fused with the macrolactone (Figure 1).^{9, 10} This specific class of compounds reflects a broad spectrum of biological activity which includes anti-tumor, anti-bacterial, anti-malarial activities^{11, 8} and are produced by a variety of fungal strains, such as *Lasiodiplodia theobromae*, *Penicillium sp.*; *Syncephalastrum racemosum*, *Pyrenophora teres*, and *Acremonium zeae*.¹² Though several efforts have been invested in synthesizing twelve membered RALs (RAL₁₂), no synthetic reports on total synthesis have been documented for penicimenolide family of RAL₁₂ isolated from *Penicillium sp.* (NO. SYP-F-7919) in 2016.¹²

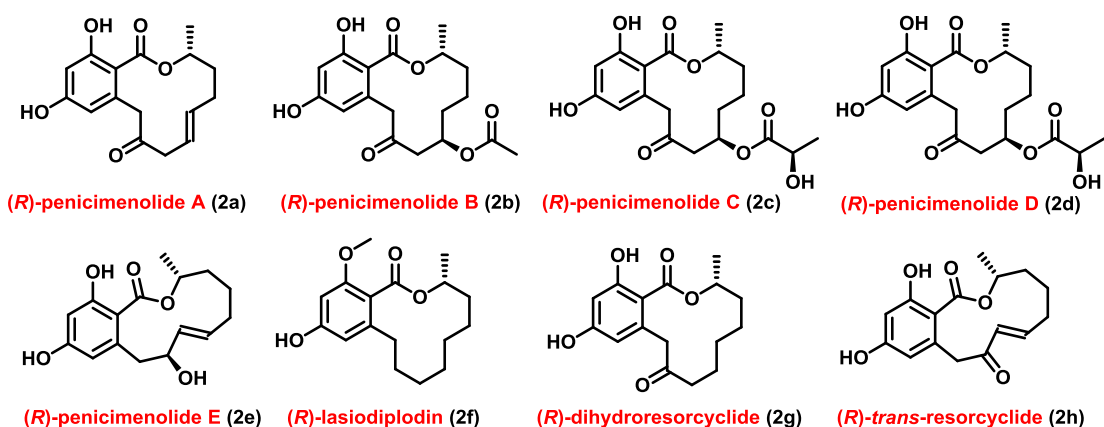


Figure 2. Structures of RAL₁₂ class of natural products.

2.1.1. Structural similarity between cladosporin and (R)-penicimenolide A

Following close scrutiny of the structural features of anti-malarial natural product cladosporin (discussed in Chapter 1) and (R)-penicimenolide A (**2a**) (RAL₁₂), we identified an underlying and interesting structural similarity between the two (Figure 3). A hypothetical acyl-oxygen cleavage of the lactone functionality of cladosporin converts the same to acid intermediate **3a**. Oxidation of the homobenzylic alcohol functionality in **3a** leads to intermediate **3b**, following which a C-O cleavage of the tetrahydropyran (THP) moiety in **3b** converts the same to intermediate **3c**. A hypothetical macrolactonization of **3c** could further generate the twelve membered macrolactone **3d** followed by the introduction of α,β -unsaturation to obtain (R)-penicimenolide A. Hence, we could observe a close structural compliance between

Chapter 2: Total Synthesis of Cladosporin Related Twelve Membered Macrocyclic Natural Products

cladosporin and (*R*)-penicimenolide A through hypothetical bond breaking and making as well as functional group interconversion and incorporation (Figure 3).

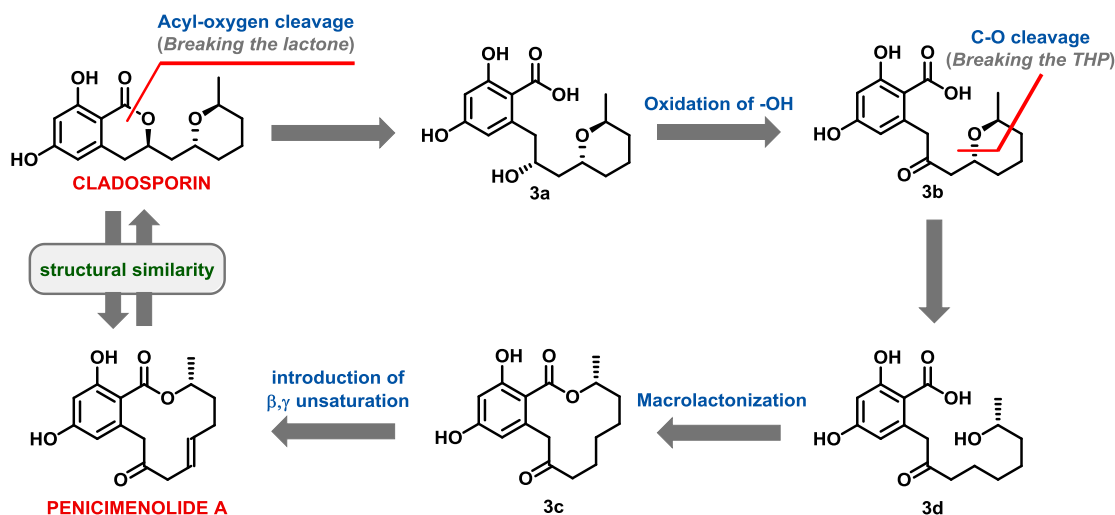


Figure 3. Structural similarity between cladosporin and (*R*)-penicimenolide A.

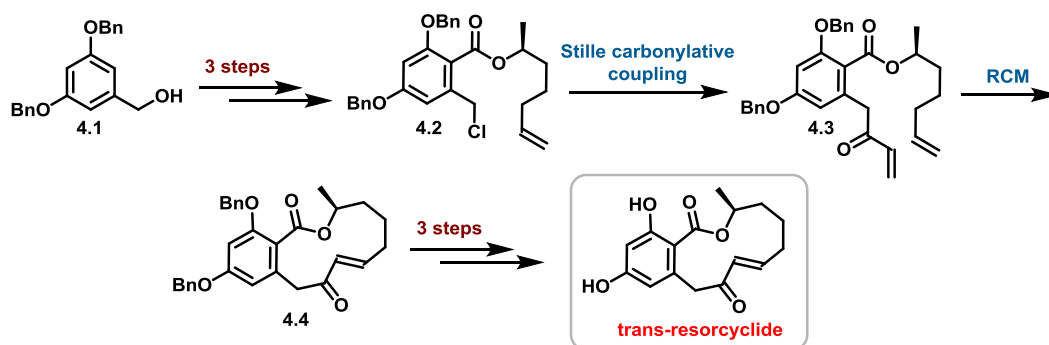
As mentioned earlier, no reports on the total synthesis of penicimenolide family of natural products have been documented in the literature to date except few synthetic approaches to related molecules. After identifying an interesting structural similarity between cladosporin and (*R*)-penicimenolide A (**2a**), we planned to accomplish the total synthesis of (*R*)-penicimenolide A (**2a**) for the first time along with two other RALs namely, (*R*)-dihydroresorcyclide (**2g**) and (*R*)-*trans*-resorcyclide (**2h**). The reported synthetic approach for related natural products are mentioned below (Figure 4 and 5).

2.1.2. Selected previous synthesis of related compounds

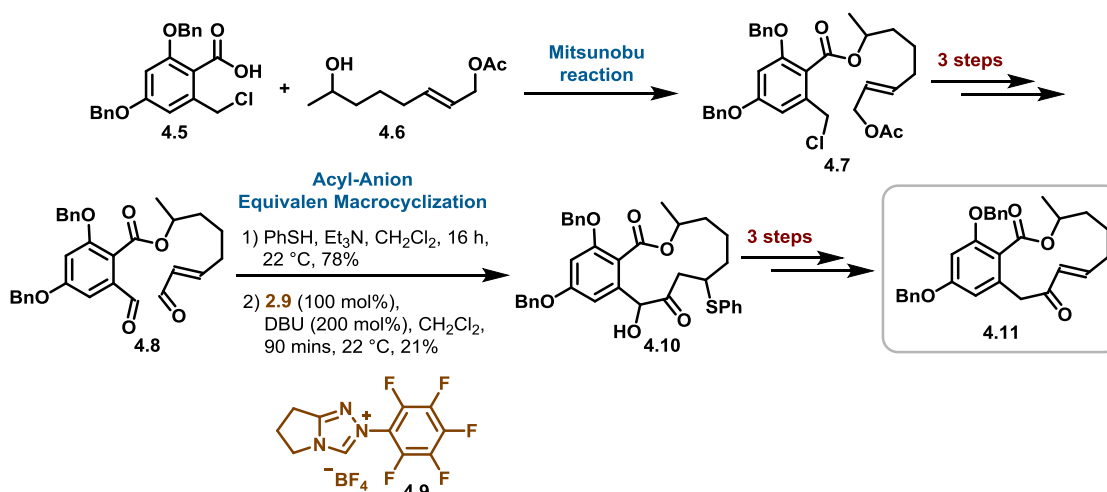
The first total synthesis of *trans*-resorcyclide was reported by Couladouros et al. in the year 2004. An unique eight-step linear synthesis has been utilized in this case where ring-closing metathesis and Stille carbonylative coupling were the key highlights¹³ (Figure 4). Following this, Miller et al. reported a nine-step formal synthesis of *trans*-resorcyclide in the year 2007.¹⁴ The synthesis highlights an elegant bio-inspired Acyl-Anion Equivalen Macrocyclization reaction as the key step in constructing the macrocyclic core (Figure 4).

Chapter 2: Total Synthesis of Cladosporin Related Twelve Membered Macrocylic Natural Products

Total synthesis of *trans*-resorcyclide by Couladouros et al. (8 step linear synthesis)



Formal synthesis of *trans*-resorcyclide by Miller et al. (9 step linear synthesis)



Total synthesis of *trans*-resorcyclide by Dai et al. (12 step synthesis)

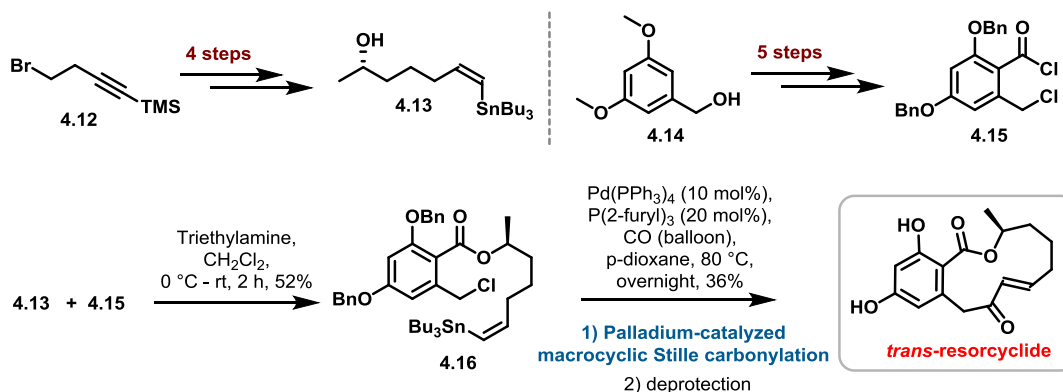


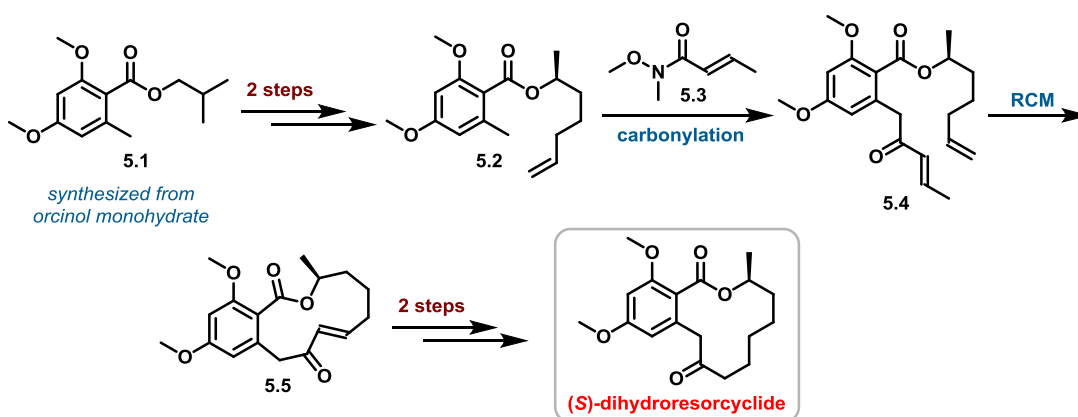
Figure 4. Reported synthesis of *trans*-resorcyclide.

Another report on the total synthesis of *trans*-resorcyclide appeared in the literature by Dai et al. in the year 2018, featuring a palladium-catalyzed macrocyclic Stille carbonylation as the key step in constructing the required macrocycle.¹⁵ The synthesis

Chapter 2: Total Synthesis of Cladosporin Related Twelve Membered Macrocyclic Natural Products

started with bromo compound **4.12**, which was converted to required vinylstannane **4.13** in four steps. On the other hand, required acid chloride **4.15** was synthesized from commercially available starting material **4.14** in five step sequence. The desired Stille carbonylation precursor **4.16** was obtained through coupling of intermediates **4.13** and **4.15**. Palladium-catalyzed macrocyclic Stille carbonylation reaction on **4.15** followed by debenzylation furnished (*R*)-*trans*-resorcyclide (Figure 4).

Total synthesis of dihydroresorcyclide by Guo et al. (9 step synthesis)



Total synthesis of (*R*)- and (*S*)-dihydroresorcyclide by Guo et al. (7 step synthesis)

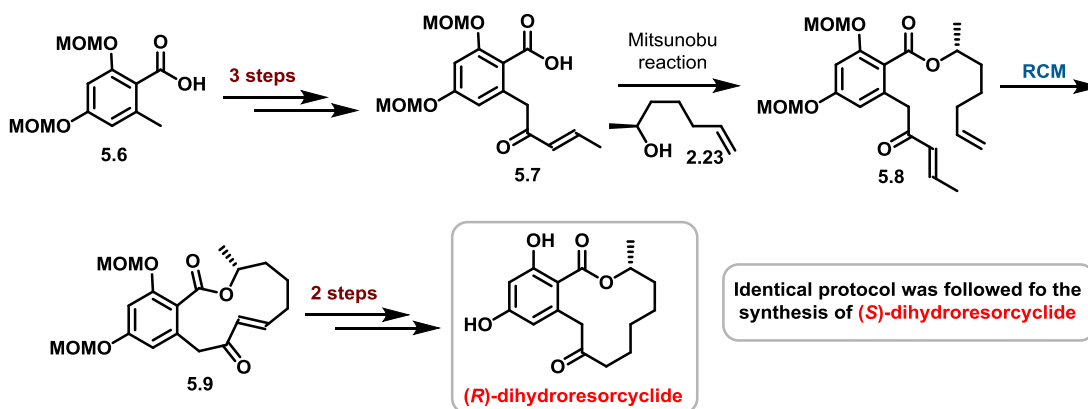


Figure 5. Reported synthesis of dihydroresorcyclide.

In the year 2013, Guo et al. reported an efficient synthesis of (*S*)-dihydroresorcyclide in nine linear steps from commercially available orcinol monohydrate using esterification, carbonylation, and ring-closing metathesis (RCM) as the key steps.¹⁶ Ring closing metathesis was used as the key step in constructing the core macrocyclic scaffold (Figure 4). Following the synthesis of (*S*)-dihydroresorcyclide in 2013, Guo et

Chapter 2: Total Synthesis of Cladosporin Related Twelve Membered Macrocyclic Natural Products

al. published yet another total synthesis of both (*R*)- and (*S*)-dihydroresorcyclide in an attempt to confirm the absolute stereochemistry of the molecule (Figure 4).¹⁷ In this effort, the absolute configuration of the natural product was revised from an *S* stereochemistry to *R* based on specific rotation values. Besides, (*R*)-version of the natural product was found to be a novel highly specific PTP1B inhibitor with an IC₅₀ value of 17.06 μM.

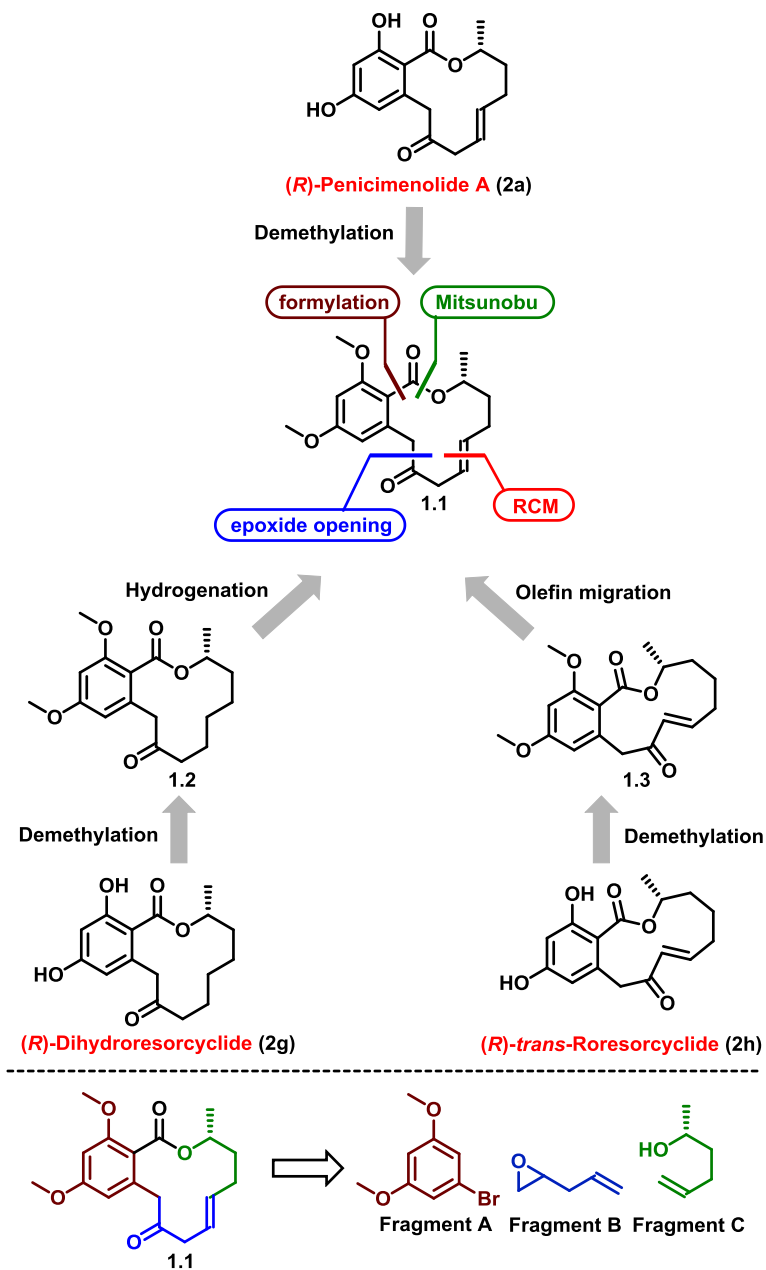
2.2. Results and discussion

Herein, we report the first total synthesis of (*R*)-penicimenolide A (**2a**), where we have used Ring Closing Metathesis (RCM) as the key step for constructing the macrocycle. Besides, we also did achieve the total synthesis of two other RAL₁₂ namely, (*R*)-dihydroresorcyclide (**2g**) and (*R*)-*trans*-resorcyclide (**2h**) (Figure 2). The strategy for synthesis discussed herein is amenable for further modifications to generate analogues of similar scaffold for a systematic structure activity relationship (SAR) study.

2.2.1. Retrosynthetic analysis of (*R*)-penicimenolide A , (*R*)-dihydroresorcyclide and (*R*)-*trans*-resorcyclide

Retrosynthetically, we envisioned the synthesis of (*R*)-penicimenolide A (**2a**), (*R*)-dihydroresorcyclide (**2g**) and (*R*)-*trans*-resorcyclide (**2h**), from the common macrocyclic intermediate **1.1**. Demethylation of macrocycle **1.1** would afford (*R*)-penicimenolide A (**2a**). Hydrogenation of compound **1.1** followed by demethylation of the saturated macrocycle **1.2** will furnish (*R*)-dihydroresorcyclide (**2g**). Lastly, olefin migration on macrocycle **1.1** followed by similar demethylation would in turn afford (*R*)-*trans*-resorcyclide (**2h**). Common macrocyclic intermediate **1.1** was planned to be procured from key fragments A, B and C through relevant functional group incorporation and interconversion (Scheme 1). The key macrolactone **1.1** was in turn planned to be synthesized using RCM as the key step (Scheme 1).

Chapter 2: Total Synthesis of Cladosporin Related Twelve Membered Macrocyclic Natural Products



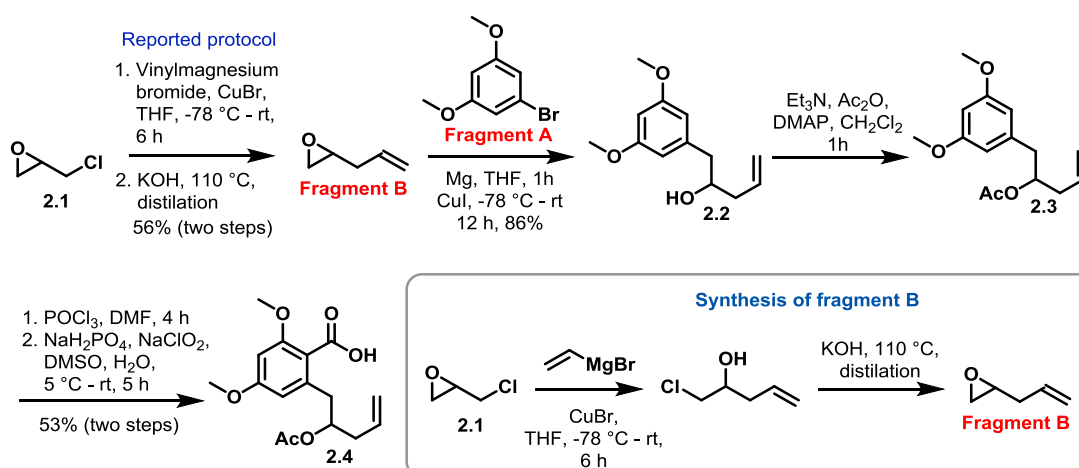
Scheme 1. Retrosynthetic analysis of (*R*)-penicimenolide A (**2.1**) (*R*)-*trans*-resorcyclide (**2.8**) and (*R*)-dihydroresorcyclide (**2.7**).

2.2.2. Total synthesis of (*R*)-penicimenolide A

(*R*)-penicimenolide A (**2a**) is a twelve membered resorcylic acid lactone (RAL₁₂) isolated from *Penicillium* sp. (NO. SYP-F-7919), a fungus obtained from the rhizosphere soil of *Panax notoginseng* collected from the Yunnan province of China.¹²

Chapter 2: Total Synthesis of Cladosporin Related Twelve Membered Macrocyclic Natural Products

Our synthesis commenced with the epoxide fragment B which was synthesized using a documented procedure from the literature,¹⁸ where racemic epichlorohydrin (**2.1**) was opened using vinyl magnesium bromide followed by an intramolecular S_N2 reaction to furnish fragment B. The epoxide fragment B was then further opened using Grignard reagent generated from commercially available 1-bromo-3,5-dimethoxybenzene (Fragment A) to afford alcohol intermediate **2.2** which was confirmed by the presence of ¹H NMR peak at 3.88 ppm corresponding to –OH attached proton. Besides, the presence of ¹H NMR peak at 3.78 ppm corresponding to the methoxy groups also supports the product formation. The secondary hydroxyl group in **2.2** was protected with acetate functionality to afford intermediate **2.3** which was forwarded as such without any purification. Vilsmeier Haack reaction on compound **2.3** followed by Pinnick oxidation furnished the required acid fragment **2.4** (Scheme 3).

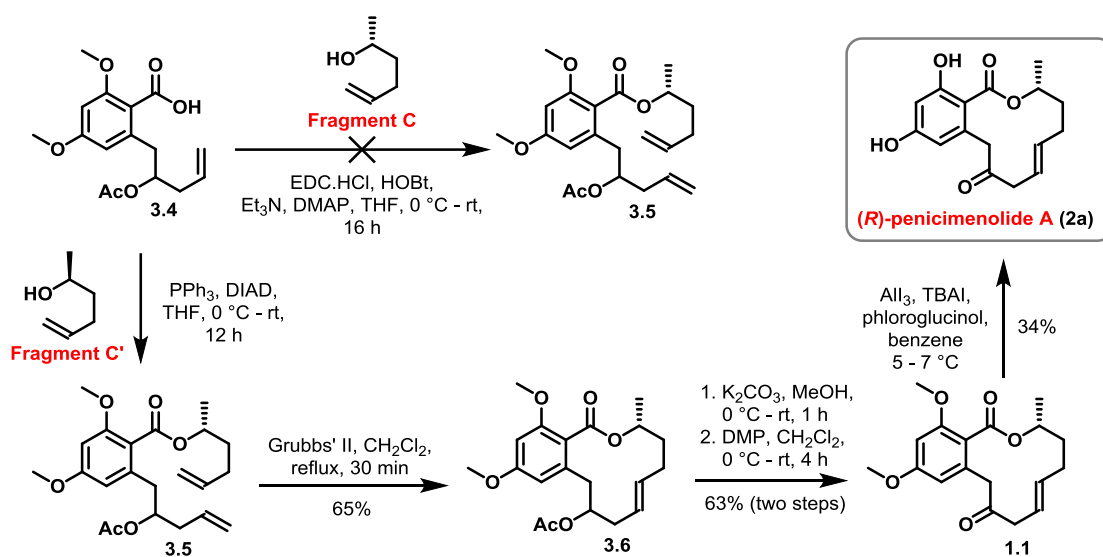


Scheme 2. Synthesis of acid fragment **2.4**.

We planned to utilize Steglich easterification reaction to couple acid **2.4** with (*R*)-hex-5-en-2-ol (Fragment C) for which we adopted standard reaction protocol using EDC.HCl and DMAP in CH₂Cl₂, but were unable to obtain the desired ester **3.5**. As an alternative, we performed Mitsunobu reaction on acid **2.4** in presence of (*S*)-hex-5-en-2-ol (Fragment C') to afford RCM precursor **3.5** as a diastereomeric mixture. The presence of two aromatic protons peaks at around 6.36 - 6.33 ppm, olefinic protons at 5.89 – 4.97 ppm with terminal olefinic pattern confirms the formation of the required

Chapter 2: Total Synthesis of Cladosporin Related Twelve Membered Macrocyclic Natural Products

product. Fragment C and Fragment C' used in this case were synthesized using reported procedure from Grignard reaction of allyl magnesium bromide and propylene oxide of appropriate chirality.¹⁹ Grubbs' II mediated RCM of compound **3.5** in refluxing CH₂Cl₂ furnished macrocycle intermediate **3.6**. The appearance of a multiplet pattern at 5.64 – 4.93 ppm corresponding to two alkene protons, one proton attached to the lactone functionality, and one attached to the acetate functionality confirms the success of the reaction. Besides, the disappearance of terminal olefinic pattern at 5.88 – 5.69 ppm in the ¹H NMR further supports the product formation.



Scheme 3. Total synthesis of (*R*)-penicimenolide A (**2a**).

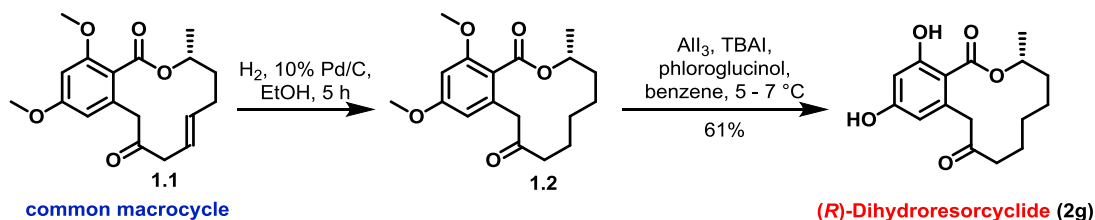
The removal of the acetate functionality in macrocycle **3.6** was achieved using K₂CO₃ in methanol, which was followed by Dess-Martin periodinane mediated oxidation of the secondary alcohol to afford chiral pure macrocycle **1.1**. The presence of ¹H NMR peak at 6.35 ppm corresponding to two aromatic protons, multiplet pattern of two olefinic protons at 5.57 – 5.43 ppm, and one proton attached to lactone functionality at 5.22 – 2.15 ppm confirms the formation of the required compound **1.1**. Besides the presence of ¹H NMR peak at 4.16 and 3.17 ppm characteristic to benzylic protons also adds up to the success of the reaction. The 1,3-phenolic methoxy groups in **1.1** were demethylated using AlI₃ mediated exhaustive demethylation, where the crude product was carefully purified through careful column chromatography (30% ethyl acetate/CHCl₃) to furnish (*R*)-penicimenolide A (**2a**) (Scheme 3). The reason behind an

Chapter 2: Total Synthesis of Cladosporin Related Twelve Membered Macrocyclic Natural Products

exceptional low yield of demethylation reaction in this case could possibly be cited to the formation of unwanted biproducts. All the spectral data of the synthesized (*R*)-penicimenolide A (**2a**) are in complete agreement with the documented data in the literature.¹²

2.2.3. Total synthesis of (*R*)-dihydroresorcyclide

(*R*)-dihydroresorcyclide (**2g**), a phytotoxic resorcinol-fused twelve-membered macrolide belonging to the class of RAL₁₂ fungal polyketide, was isolated from the fermentation extracts of an endophyte *Acremonium zeae* by Poling *et al.*²⁰ After successfully synthesizing (*R*)-penicimenolide A (**2a**), we further planned to utilize the common macrocycle intermediate **1.1** to access (*R*)-dihydroresorcyclide (**2g**) as well. For this purpose, we hydrogenated the macrocycle **1.1** under hydrogen atmosphere (balloon) in presence of 10% Pd/C to afford saturated macrocycle **1.2**. Disappearance of the olefinic proton peaks in ¹H NMR of the same confirms the formation of the required saturated macrocycle **1.2**. Besides the presence of a triplet in the ¹H NMR at 2.43 ppm corresponding to α -protons adjacent to the keto functionality further adds up to the success of the reaction. The presence of doublets in the ¹H NMR at 4.12 ppm and 3.55 ppm corresponding to benzylic methylene protons were also observed. Compound **1.2** was further subjected to AlI₃ mediated exhaustive demethylation to furnish (*R*)-dihydroresorcyclide (**2g**) in moderate yields (Scheme 4). The disappearance of the ¹H NMR peak corresponding to the phenolic methoxy groups confirms a successful demethylation. Besides, all the spectral data of the synthesized compound are in complete agreement with the documented data in the literature.^{16, 17}

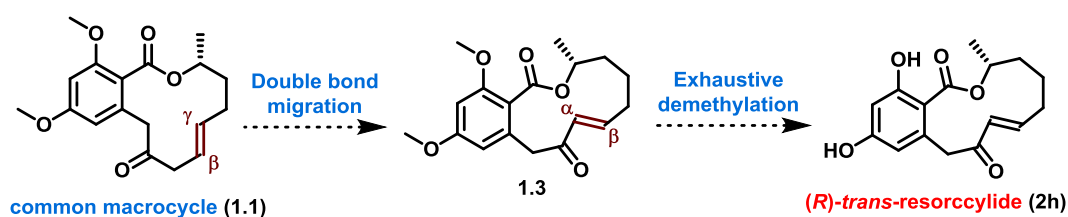


Scheme 4. Total synthesis of (*R*)-dihydroresorcyclide (**2g**).

2.2.4. Total synthesis of (*R*)-*trans*-resorcyclide

Chapter 2: Total Synthesis of Cladosporin Related Twelve Membered Macrocyclic Natural Products

(*R*)-*trans*-resorcyclide (**2h**) is a naturally occurring macrolide and a plant growth inhibitor isolated from different *Penicillium sp.*²¹ Structurally, this specific RAL₁₂ features an α,β -unsaturated keto functionality as a part of the macrocycle ring system. For a ready access to the natural product, we initially planned to utilize the common macrocycle intermediate **1.1**, and migrate the β,γ -olefin in the same to α,β -unsaturated keto functionality (**1.3**), followed by AlI₃ mediated exhaustive demethylation, to access (*R*)-*trans*-resorcyclide (Scheme 5).



Scheme 5. Planned synthetic scheme to access (*R*)-*trans*-resorcyclide (**2h**) from common macrocycle intermediate **1.1**.

2.2.4.1. Efforts towards olefin migration:

In an effort towards the synthesis of (*R*)-*trans*-resorcyclide (**2h**), we envisioned an initial olefin migration reaction on common macrocycle **1.1** to access the required α,β -unsaturated keto functionality in the macrocyclic scaffold. As a part of our efforts, we initially tried base mediated olefin migration on common macrocycle **1.1**. Our initial choice of base for the same was 1,8-Diazabicyclo[5.4.0]undec-7-ene (DBU), which was reacted with the substrate **1.1** in presence of acetonitrile solvent at room temperature. While monitoring the progress of reaction through thin layer chromatography (TLC), we did not observe any migrated product even after 12 h of reaction time. We even tried the same reaction condition with an elevated temperature of 80 °C for 12 h but were unable to obtain the required migrated product **1.3**. Next, we changed our choice of the base from DBU to Lithium diisopropylamide (LDA). In this case, we used freshly prepared LDA from diisopropylamine and *n*BuLi (1.6 M in THF) and conducted the migration reaction in THF at -78 °C for 12 h, but we were unable to obtain the required product. We further warmed the reaction mixture to room temperature which led to the

Chapter 2: Total Synthesis of Cladosporin Related Twelve Membered Macrocyclic Natural Products

decomposition of the starting material **1.1** as observed in TLC analysis. We also tried the olefin migration reaction using LiHMDS (1.0 M in THF) in THF as a solvent but did not observe any fruitful result. Being unable to obtain the required migrated product **1.3** though bases mediated migration condition we planned to utilize Lewis acid like $\text{BF}_3 \cdot \text{OEt}_2$ in THF for the same. In this case, as well, we did not observe any reaction progress (TLC analysis) even after 12 h of reaction time at room temperature.

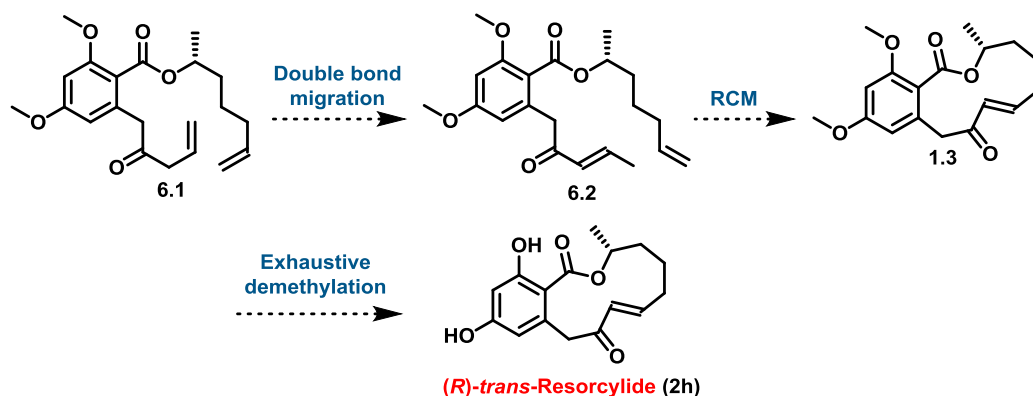
Entry	Reaction Condition	Observation
1	DBU, ACN, rt, 12 h	No migration
2	DBU, ACN, 80 °C, 12 h	No migration
3	LDA, THF, -78 °C, 12 h	No migration
4	LDA, THF, -78 °C – rt, 12 h	Compound decomposed
5	LiHMDS, THF, 0 °C – rt, 12 h	No migration
6	RhCl_3 , EtOH, reflux, 12 h	No migration
7	RhCl_3 , THF, reflux, 12 h	No migration
8	RhCl_3 , toluene, reflux, 12 h	No migration
9	$\text{BF}_3 \cdot \text{OEt}_2$, THF, rt, 12 h	No migration

Table 1. Conditions for olefin migration.

We next planned to use Rhodium (III) chloride (RhCl_3) as a reagent for the required olefin migration. Initially, we used ethanol as a solvent in reflux conditions for 12 h, but did not observe any progress in the reaction. We further changed the choice of solvent from polar protic (EtOH) to moderately polar aprotic solvent like THF, but could not obtain the required macrocycle (**1.3**) with α, β -unsaturated keto functionality. We also used non-polar aprotic solvent like toluene and refluxed the reaction mixture at 112 °C with RhCl_3 for 12 h but were unable to observe the desired result. In this case, we further purified the reaction mixture and spectral analysis (NMR) of the same revealed the presence of starting material **1.1** which was evident from the presence of olefinic proton peaks at 5.32 – 5.49 ppm corresponding to β, γ -olefin in the ^1H NMR spectrum (400 MHz, CD_3OD). All the conditions adopted for the required olefin migration are listed in table 1.

Chapter 2: Total Synthesis of Cladosporin Related Twelve Membered Macrocyclic Natural Products

After getting no fruitful results of olefin migration in the macrocycle **1.1**, the reason for which could be cited to a possibly more stable β,γ -olefin than the required α,β -unsaturated ketone in a constrained macrocyclic conformer, we planned to pre-conduct the migration reaction in an open chain macrocycle precursor **6.1** followed by RCM to afford the required macrocycle **1.3** which upon exhaustive demethylation will afford the required natural product (*R*)-*trans*-resorcylicide (**2h**) (Scheme 6).

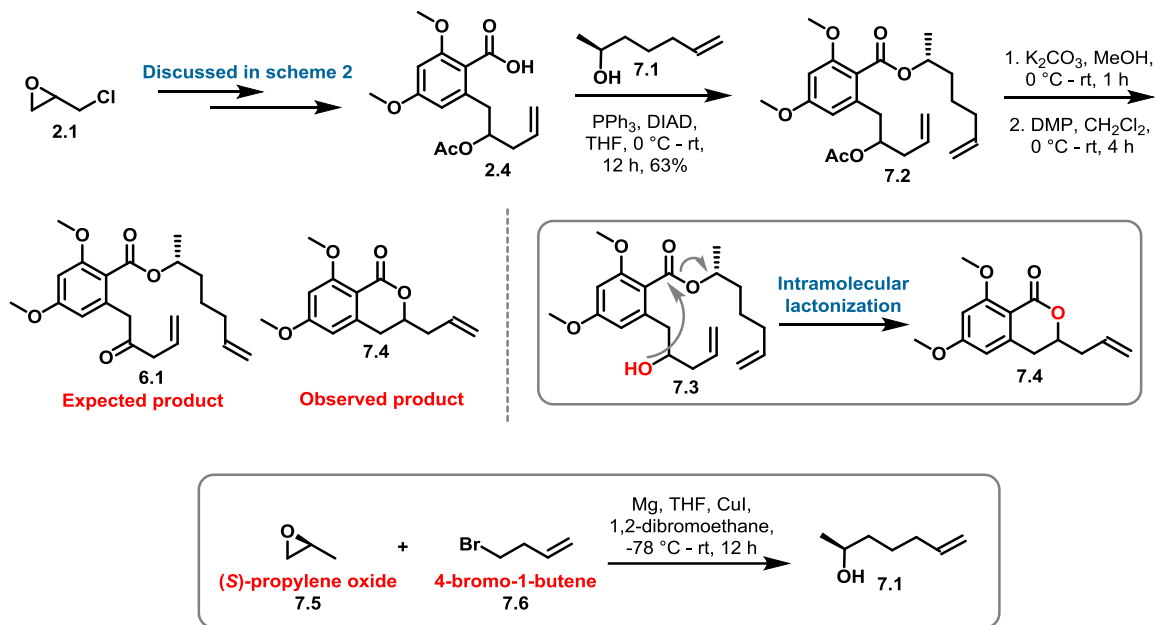


Scheme 6. Planned synthetic scheme to (*R*)-*trans*-resorcylicide (**2h**).

As a part of our synthesis, we used racemic epichlorohydrin (**2.1**) to synthesize the acid intermediate **2.4** utilizing identical protocol as described in scheme 2. Compound **2.4** was coupled with alcohol **7.1** under Mitsunobu reaction condition to afford diene **7.2**. Alcohol **7.1** used in this case was synthesized via the opening of (*S*)-propylene oxide (**7.5**) using Grignard reagent generated from commercially available 4-bromo-1-butene (**7.6**). Acetate functionality in compound **7.2** was deprotected using K_2CO_3 in methanol and to obtained alcohol **7.3** which was forwarded for Dess-martin periodinane mediated oxidation. Characterization of the acquired product revealed the formation of stable six-membered lactone **7.4** (Scheme 7) instead of required compound **6.1**. The presence of 1H NMR peak at 5.92 – 5.81 ppm and 5.19 – 5.13 ppm corresponding to one and two olefinic protons respectively confirms the presence of a single terminal olefin. Besides, a 1H NMR peak at 4.44 – 4.37 ppm corresponding to a single proton next to the lactone functionality further confirms the structure of **7.4**. The unexpected formation of compound **7.4** could be cited to a facile intra-molecular nucleophilic attack of the

Chapter 2: Total Synthesis of Cladosporin Related Twelve Membered Macrocyclic Natural Products

secondary hydroxyl (-OH) group in **7.3** on the lactone functionality to form stable six-membered lactone **7.4** (Scheme 7).



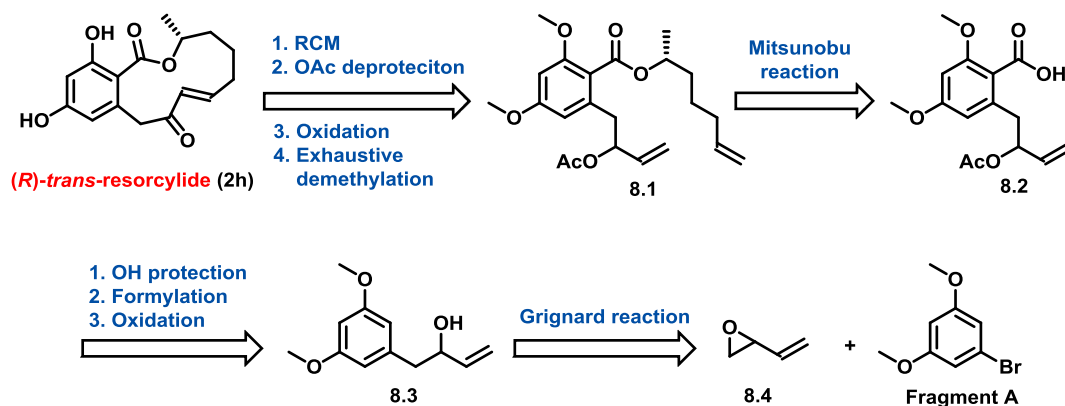
Scheme 7. Unwanted formation of lactone **7.4** through intra-molecular lactonization.

2.2.4.3. Revision of the retrosynthetic scheme for (*R*)-*trans*-resorcyclide (**2h**)

After identifying the unwanted formation of lactone **7.4**, we revised the entire retrosynthetic scheme for (*R*)-*trans*-resorcyclide (**2h**) and envisioned the same to be synthesized from diene **8.1** which in turn can be procured from acid intermediate **8.2**. Acid **8.2** was further planned to be synthesized from alcohol **8.3** which could be obtained from commercially available 2-vinyloxirane (**8.4**) and 1-bromo-3,5-dimethoxybenzene (fragment A) (Scheme 8).

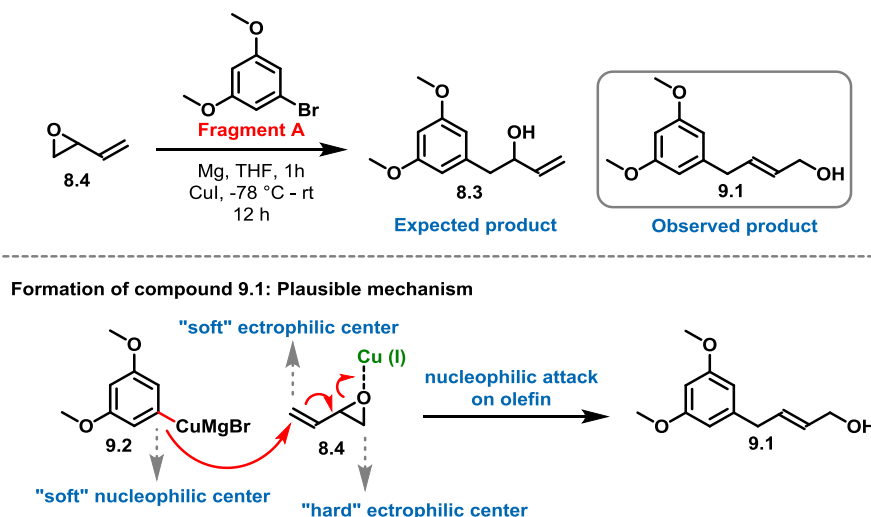
Reaction of commercially available 2-vinyloxirane (**8.4**) with Grignard reagent generated from fragment A was conducted to access key alcohol fragment **8.3**. Spectroscopic analysis (^1H and ^{13}C) of the obtained product revealed the formation of primary alcohol **9.1**. The presence of two protons corresponding to the internal olefin was evident from the appearance of a multiplet pattern at 5.82 – 5.65 ppm in the ^1H NMR spectrum.

Chapter 2: Total Synthesis of Cladosporin Related Twelve Membered Macrocyclic Natural Products



Scheme 8. Revised retrosynthetic scheme for (*R*)-*trans*-resorcyclide (**2h**).

Besides the presence of two doublets at 4.10 and 3.31 ppm in the ^1H NMR peak corresponds to the two methylene ($-\text{CH}_2-$) groups in **9.1**. The plausible explanation for the same could be cited to the formation of a soft nucleophilic centre in compound **9.2** which in turn led to a preferred attack on the terminal olefinic functionality of epoxide **8.4** which happens to be a soft electrophilic site. Besides, the coordination of Cu(I) to the epoxide functionality in **8.4** might have further facilitated the nucleophilic attack (Scheme 9).

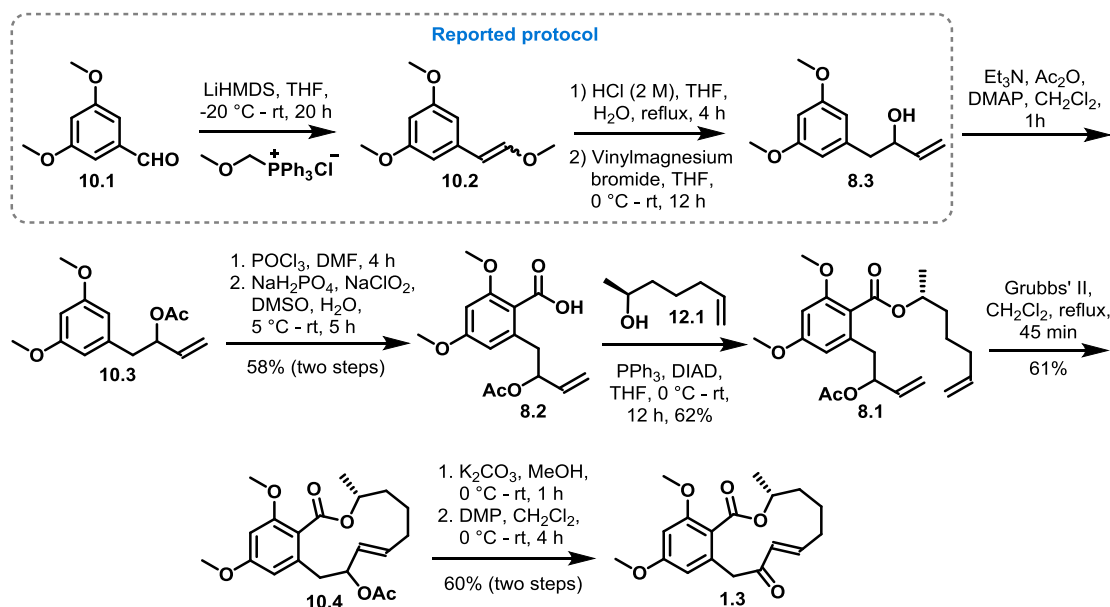


Scheme 9. Formation of compound **9.1** and its plausible mechanism.

Following this observation, we synthesized the required alcohol **8.3** using documented procedure in the literature²² starting from 3,5-dimethoxybenzaldehyde (**10.1**). The

Chapter 2: Total Synthesis of Cladosporin Related Twelve Membered Macrocyclic Natural Products

presence of a terminal olefinic pattern in the ^1H NMR with three olefinic protons appearing at 5.93, 5.27 and 5.13 ppm confirmed the structure of alcohol **8.3**. Alcohol **8.3** thus obtained was converted to its corresponding acetate intermediate **10.3**, which was then subjected to Vilsmeier Haack reaction followed by Pinnick oxidation to furnish acid **8.2**. After thorough work-up, the synthesized acid fragment **8.2** was forwarded as such for further reaction. Mitsunobu reaction of **8.2** with alcohol **7.1** afforded the formation of macrocycle precursor **8.1**. The presence of two aromatic protons peaks at around 6.36 - 6.33 ppm, olefinic protons at 5.85 – 4.93 with terminal olefinic patten confirms the formation of the required product. Compound **8.1** was then subjected to Grubbs' II mediated RCM in refluxing CH_2Cl_2 to afford macrocycle **10.4** as a diastereomeric mixture. The presence of a ^1H NMR peak at 5.72 – 4.94 ppm corresponding to two olefinic protons, one proton adjacent to lactone, and one adjacent to acetate functionality confirmed a successful RCM.



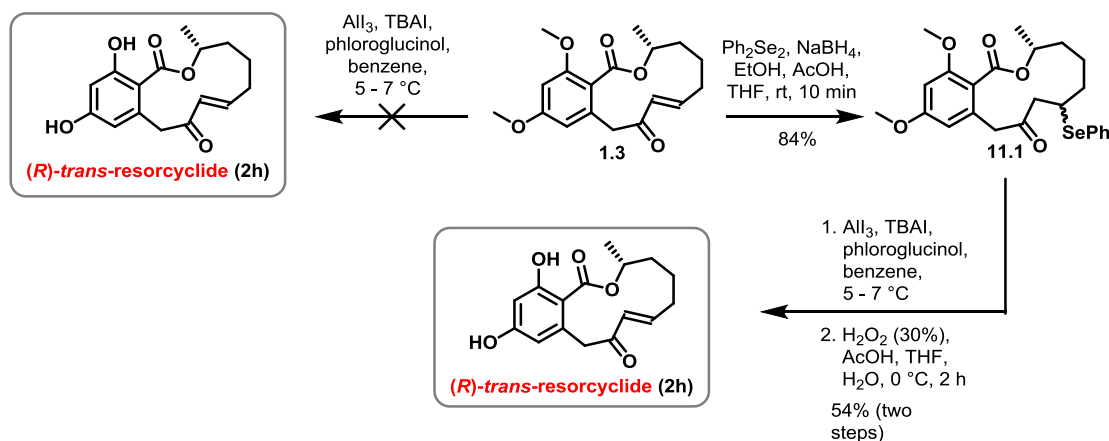
Scheme 10. Synthesis of compound required macrocycle **1.3**.

The acetate functionality in **10.4** was then deprotected using K_2CO_3 in methanol followed by Dess-Martin Periodinane mediated oxidation to furnish compound **1.3**. The appearance of ^1H NMR peak at 6.89 ppm and 5.92 ppm corresponding to the olefinic

Chapter 2: Total Synthesis of Cladosporin Related Twelve Membered Macrocyclic Natural Products

protons α and β to the keto functionality respectively confirmed the presence of α,β unsaturation in the macrocyclic ring system.

After having the required precursor **1.3**, we subjected the same to AlI_3 mediated exhaustive demethylation but were unable to access the required natural product **2h**. Hence, we masked the olefin through the formation of selenide intermediate **11.1**¹³ which was then subjected to AlI_3 mediated exhaustive demethylation followed by oxidation of the selenide and one-pot elimination to furnished (*R*)-*trans*-resorcyclide (**2h**) in excellent yield (Scheme 11). All the spectral data of the synthesized natural product are in complete accordance with values documented in the literature.



Scheme 11. Synthesis of (*R*)-*trans*-resorcyclide (**2h**).

2.3. Conclusion

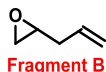
In this work, we have achieved the first total synthesis of a twelve membered RAL (RAL_{12}), (*R*)-penicimenolide A (**2a**). We have further achieved the synthesis of two more similar classes of macrocyclic natural products namely, (*R*)-dihydroresorcyclide (**2g**) and (*R*)-*trans*-resorcyclide (**2h**). In the synthesis of these natural products, we have utilized RCM as the key step in the construction of the core macrocycle. All the intermediates and final products have been thoroughly characterized using NMR, IR, and HRMS, and the ^1H and ^{13}C NMR spectrum of the natural products are in complete agreement with the documented values in the literature. Besides the synthetic scheme

Chapter 2: Total Synthesis of Cladosporin Related Twelve Membered Macrocyclic Natural Products

discussed herein is amenable to further modifications to access a library of analogues around the core macrocyclic scaffold.

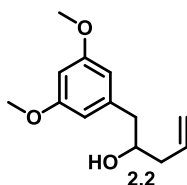
2.4. Experimental section

Synthesis of 2-allyloxirane (Fragment B)



Fragment B has been synthesized from racemic epichlorohydrin using reported protocol.

Synthesis of compound 1-(3,5-dimethoxyphenyl)pent-4-en-2-ol (2.2)



To an oven dried two-neck round-bottomed flask equipped with a magnetic stir bar was added activated magnesium metal (2.95 g, 121.26 mmol) under argon atmosphere. THF (200 mL) was added followed by the addition of a pinch of I_2 and was stirred vigorously for 30 min. 1-bromo-3,5-dimethoxy benzene (fragment A) (23.22 g, 107 mmol) dissolved in THF (20 mL) was added dropwise to the stirring solution. The onset of exothermic reaction was characterized by decolorization of I_2 . The resulting mixture was stirred for 2 h. The freshly prepared Grignard reagent was cooled to $-30\text{ }^\circ\text{C}$ followed by the addition of Copper (I) iodide (2.72 g, 20 mol %). Solution of fragment B (6.00 g, 71.33 mmol) in THF (10 mL) was added dropwise and left to stir for 16 h at $-30\text{ }^\circ\text{C}$. The reaction mixture was quenched with saturated aqueous NH_4Cl (30 mL) and extracted with diethyl ether (30 mL x 3). The combined organic layers were dried over anhydrous Na_2SO_4 , and concentrated under *vacuo*. The resulting mixture of diastereomers thus obtained as yellowish oil was purified and separated by column chromatography (SiO_2 , ethyl acetate/pet ether 1:4) to afford corresponding alcohols **2.2** (13.64 g) as a yellowish oil with an overall yield of 86%.

IR (film) ν_{max} : cm^{-1} 2925, 1596, 1459, 1201, 1149

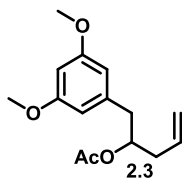
Chapter 2: Total Synthesis of Cladosporin Related Twelve Membered Macrocyclic Natural Products

¹H NMR (400 MHz, CDCl₃) δ 6.38 (d, $J = 2.3$ Hz, 2H), 6.35 (t, $J = 2.3$ Hz, 1H), 5.88 – 5.83 (m, 1H), 5.17 (dd, $J = 7.4, 1.4$ Hz, 1H), 5.14 (t, $J = 1.1$ Hz, 1H), 3.88 (dt, $J = 14.6, 7.3$ Hz, 1H), 3.78 (s, 6H), 2.76 (dd, $J = 13.5, 4.7$ Hz, 1H), 2.65 (dd, $J = 13.5, 8.1$ Hz, 1H), 2.36 – 2.31 (m, 1H), 2.27 – 2.22 (m, 1H)

¹³C NMR (100 MHz, CDCl₃) δ 160.9, 140.7, 134.6, 118.1, 107.4, 98.5, 71.5, 55.3, 43.6, 41.2

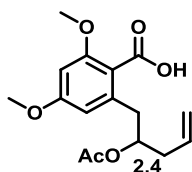
HRMS (ESI) calcd. for C₁₃H₁₉O₃ [M+H]⁺: 223.1334; found: 223.1333.

Synthesis of compound 1-(3,5-dimethoxyphenyl)pent-4-en-2-yl acetate (2.3)



To a solution of compound **2.2** (13.64 g, 61.36 mmol) in CH₂Cl₂ (50 mL) was added triethylamine (12.8 mL, 92.04 mmol) at 0 °C following acetic anhydride (8.7 mL, 92.04 mmol) was added at the same temperature. Catalytic DMAP was added to the reaction mixture and stirred for 1 h at room temperature. After complete conversion of the starting material, the reaction mixture was washed with saturated aqueous NaHCO₃ (30 mL x 3). The collected organic layers were washed with brine (30 mL x 2), extracted with CH₂Cl₂ (20 mL x 3) and dried over anhydrous Na₂SO₄. Excess solvent was then removed through rotary evaporation to afford compound **2.3** (15.2 g) as a pale yellow oil which was forwarded to next step without further purification.

Synthesis of compound 2-(2-acetoxypent-4-en-1-yl)-4,6-dimethoxybenzoic acid (2.4)

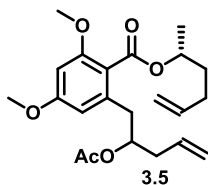


Chapter 2: Total Synthesis of Cladosporin Related Twelve Membered Macrocyclic Natural Products

POCl_3 (10.7 mL, 115.01 mmol) was added dropwise to an ice-cold solution of compound **2.3** (15.2 g, 57.51 mmol) in DMF (10 mL). The brown reaction mixture was stirred at room temperature for 4 h following which it was poured in-to crushed ice and the resulting mixture was diluted with ethyl acetate (30 mL) followed by addition of a saturated aqueous solution of sodium acetate until basic. The entire reaction mixture was then washed with cold water (30 mL x 3) to remove excess DMF. The collected organic layers were then dried over anhydrous Na_2SO_4 and concentrated under vacuo to afford a brown oil which was forwarded to next step without further purification.

The obtained formylated intermediate (16.3 mg, 55.76 mmol) was dissolved in DMSO (30 mL) and cooled to 0 °C. NaH_2PO_4 (16.72 g, 139.4 mmol) in water (15 mL), was added to the reaction mixture followed by the addition of 2-methyl-2-butene (29.5 mL, 278.79 mmol). Following which, NaClO_2 (12.6 g, 139.4 mmol) was dissolved in water (15 mL) and added dropwise at 0 °C. The reaction mixture was allowed to reach room temperature and was stirred for 5 h. Upon completion of the reaction as monitored by TLC, a saturated solution of NaHCO_3 was added to the reaction mixture at 0 °C until basic. The reaction mixture was then washed with ethyl acetate (40 mL x 3) and the collected aqueous layers were acidified with 2 N HCl. The acidified mixture was then extracted with ethyl acetate (30 mL x 3) and the collected organic fractions were dried over anhydrous Na_2SO_4 to furnish acid fragment **2.4** (11 g) as a yellow oil which used for next step without further purification.

Synthesis of compound (*R*)-hex-5-en-2-yl 2-(2-acetoxypent-4-en-1-yl)-4,6-dimethoxybenzoate (**3.5**) (Mitsunobu inversion of secondary alcohol)



Acid fragment **2.4** (10 g, 32.43 mmol) and alcohol key fragment C (3.57 g, 35.68 mmol) was dissolved in THF (40 mL) followed by the addition of triphenylphosphine (17.01 g, 64.87 mmol) at 0 °C. A solution of DIAD (7.64 mL, 38.92 mmol) in THF (10 mL)

Chapter 2: Total Synthesis of Cladosporin Related Twelve Membered Macrocyclic Natural Products

was then added dropwise to the reaction mixture at the same temperature, following which, the mixture was allowed to reach room temperature and was stirred for 12 h. After completion of the reaction, the mixture was extracted with ethyl acetate (40 mL x 3) and the collected organic layers were dried over anhydrous Na₂SO₄. The excess solvent was then removed via rotary evaporation and the crude reaction mixture was purified through column chromatography (SiO₂, ethyl acetate/ pet ether 3:22) to afford compound **3.5** (7.85 g) in 62% yield as pale yellow oil.

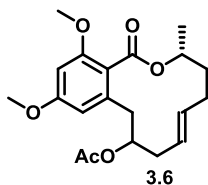
IR (film) ν_{\max} : cm⁻¹ 2932, 1725, 1597, 1238, 1036

¹H NMR (diastereomeric mixture) (400 MHz, CDCl₃) δ 6.36 (d, J = 2.1 Hz, 1H), 6.33 (d, J = 2.2 Hz, 1H), 5.89 – 5.69 (m, 2H), 5.16 (dddd, J = 9.7, 7.7, 5.5, 2.5 Hz, 2H), 5.09 – 4.97 (m, 4H), 3.79 (s, 3H), 3.77 (s, 3H), 2.91 – 2.77 (m, 2H), 2.39 – 2.25 (m, 2H), 2.24 – 2.12 (m, 1H), 1.97 (s, 3H), 1.86 – 1.76 (m, 1H), 1.73 – 1.60 (m, 2H), 1.35 (dd, J = 6.2, 3.9 Hz, 3H)

¹³C NMR (diastereomeric mixture) (100 MHz, CDCl₃) δ 170.4, 167.6, 161.1, 158.0, 137.9, 137.5, 133.5, 117.9, 114.9, 106.3, 97.1, 73.3, 71.4, 71.4, 55.7, 55.4, 38.6, 38.4, 37.5, 37.4, 35.2, 29.6, 21.1, 20.0

HRMS (ESI) calcd. for C₂₂H₃₁O₆ [M+H]⁺: 391.2120; found: 391.2119.

Synthesis of compound (3*R*,*E*)-12,14-dimethoxy-3-methyl-1-oxo-3,4,5,8,9,10-hexahydro-1H-benzo[*c*][1]oxacyclododecin-9-yl acetate (3.6) (Ring closing metathesis)



A dilute solution of macrocycle precursor **3.5** (500 mg, 1.255 mmol) in CH₂Cl₂ (450 mL) was degassed with argon for 15 mins. Grubbs' II catalyst (10 mol %) was then added and the reaction mixture was refluxed under argon for 30 mins. After completion

Chapter 2: Total Synthesis of Cladosporin Related Twelve Membered Macrocyclic Natural Products

of the reaction as monitored by TLC, the mixture was then concentrated under vacuo and purified through careful column chromatography (SiO₂, ethyl acetate/ pet ether 1:9) to furnish macrocycle **3.6** (diastereomeric mixture) (0.3 g) with a yield of 65% as pale brown oil.

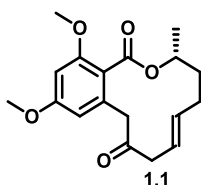
IR (film) ν_{\max} : cm⁻¹ 2924, 1720, 1598, 1245, 1027

¹H NMR (diastereomeric mixture) (400 MHz, CDCl₃) δ 6.57 – 6.32 (m, 2H), 5.45 – 4.94 (m, 4H), 3.81 – 3.77 (m, 6H), 3.12 – 2.75 (m, 2H), 2.40 – 2.24 (m, 2H), 2.10 – 2.08 (m, 3H), 2.05 – 1.68 (m, 4H), 1.34 – 1.32 (m, 3H)

¹³C NMR (diastereomeric mixture) (100 MHz, CDCl₃) δ 170.1, 167.5, 160.8, 158.3, 137.4, 135.4, 122.8, 121.2, 118.7, 108.9, 107.3, 105.1, 97.1, 73.8, 72.9, 56.0, 55.9, 55.2, 35.1, 34.2, 33.5, 31.5, 29.7, 21.5, 21.0

HRMS (ESI) calcd. for C₂₀H₂₇O₆ [M+H]⁺: 363.1801; found: 363.1806.

Synthesis of compound (*R,E*)-12,14-dimethoxy-3-methyl-3,4,5,8-tetrahydro-1H-benzo[*c*][1]oxacyclododecine-1,9(10H)-dione (1.1)



To a solution of diastereomeric mixture of macrocycle **3.6** (0.9 g, 2.48 mmol) in MeOH (30 mL) was added K₂CO₃ (514.8 mg, 3.72 mmol) at 0 °C. The reaction mixture was then allowed to reach room temperature and stirred for an additional 1 h. After completion of reaction, the same was diluted and extracted with ethyl acetate (40 mL x 3). The collected organic layers were then dried over anhydrous Na₂SO₄. The excess solvent was removed via rotary evaporation and the crude reaction mixture (780 mg) was used for further reaction.

The obtained acetate deprotected intermediate (780 mg, 2.43 mmol) was dissolved in CH₂Cl₂ (35 mL) which was followed by the addition of Dess-Martin periodinane (3.1

Chapter 2: Total Synthesis of Cladosporin Related Twelve Membered Macrocyclic Natural Products

mg, 7.304 mmol) at 0 °C. The reaction mixture was allowed to stir for 4 h at room temperature. After attaining reaction completion, a saturated aqueous solution of NaHCO₃ (30 mL) was added to the reaction mixture at 0 °C and was stirred for 15 mins. The reaction mixture was then extracted with CH₂Cl₂ (20 mL x 3) and the collected organic layers were dried over anhydrous Na₂SO₄. Purification through column chromatography (SiO₂, ethyl acetate/ pet ether 1:9) afforded the key macrocycle **1.1** (0.5 g) with 63% yield (in two steps) as a foamy solid.

$[\alpha]_D^{26}$ -125.5 (c 1.6, CHCl₃)

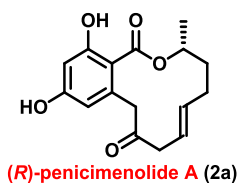
IR (film) ν_{\max} : cm⁻¹ 2929, 1710, 1597, 1276, 1156

¹H NMR (400 MHz, CDCl₃) δ 6.35 (dd, J = 6.2, 2.2 Hz, 2H), 5.57 – 5.43 (m, 2H), 5.22 – 5.15 (m, 1H), 4.16 (d, J = 15.1 Hz, 1H), 3.79 (s, 2H), 3.77 (s, 1H), 3.37 (d, J = 15.2 Hz, 1H), 2.96 (d, J = 5.6 Hz, 2H), 2.40 – 2.34 (m, 1H), 2.24 – 2.14 (m, 1H), 1.89 – 1.71 (m, 2H), 1.33 (d, J = 6.3 Hz, 2H)

¹³C NMR (100 MHz, CDCl₃) δ 206.4, 167.7, 161.2, 158.2, 137.4, 133.3, 120.0, 117.8, 106.5, 97.8, 73.0, 55.8, 55.4, 45.7, 44.5, 33.7, 31.3, 21.0

HRMS (ESI) calcd. for C₁₈H₂₃O₆ [M+H]⁺: 319.1545; found: 319.1543.

Synthesis of (*R*)-penicimenolide A (**2a**)



A suspension of aluminum powder (50 mg, 0.16 mmol) in dry benzene (4 mL) was treated with I₂ (637.8 mg, 2.51 mmol) under argon, and the violet mixture was stirred under reflux for 30 min until the color disappeared. After the mixture was cooled to 0 °C, few crystals of TBAI and phloroglucinol (297 mg, 2.36 mmol) were added before a solution of compound **1.1** (99 mg, 0.78 mmol) in dry benzene (2 mL) was added in one portion. The resulting green-brown suspension was stirred for 30 min at 5 °C before

Chapter 2: Total Synthesis of Cladosporin Related Twelve Membered Macrocyclic Natural Products

saturated $\text{Na}_2\text{S}_2\text{O}_3$ solution (10 mL) and ethyl acetate (15 mL) were added. After separation of the layers, the aqueous phase was extracted with ethyl acetate (15 mL x 3). The combined organic layers were washed with brine, dried over Na_2SO_4 , filtered, and concentrated in vacuo. Purification by column chromatography (SiO_2 , ethyl acetate/ CHCl_3 3:7) afforded (*R*)-penicimenolide A (**2a**) (15 mg) with a yield of 34% as a white solid.

$[\alpha]_D^{26} +65.3$ (c 0.4, MeOH)

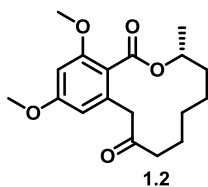
IR (film) ν_{max} : cm^{-1} 3346, 2923, 1703, 1633, 1260

^1H NMR (400 MHz, MeOD) δ 6.24 (dd, $J = 3.2, 1.7$ Hz, 1H), 6.13 (d, $J = 2.5$ Hz, 1H), 5.58 (dt, $J = 15.7, 6.5$ Hz, 2H), 5.38 (pd, $J = 6.5, 2.3$ Hz, 1H), 4.38 (d, $J = 17.1$ Hz, 1H), 3.99 (d, $J = 17.1$ Hz, 1H), 3.00 (d, $J = 6.1$ Hz, 2H), 2.48 – 2.37 (m, 1H), 2.22 (dddd, $J = 8.4, 4.4, 3.2, 2.2$ Hz, 1H), 2.01 – 1.93 (m, 1H), 1.85 (dddd, $J = 15.3, 7.5, 6.5, 3.2$ Hz, 1H), 1.35 (d, $J = 6.5$ Hz, 3H)

^{13}C NMR (100 MHz, MeOD) δ 208.0, 172.1, 165.2, 163.0, 139.0, 138.3, 122.3, 113.6, 107.7, 102.9, 74.6, 47.2, 46.1, 34.5, 29.5, 19.1

HRMS (ESI) calcd. for $\text{C}_{16}\text{H}_{19}\text{O}_5$ $[\text{M}+\text{H}]^+$: 291.1232; found: 291.1231.

Synthesis of compound (*R*)-12,14-dimethoxy-3-methyl-3,4,5,6,7,8-hexahydro-1H-benzo[*c*][1]oxacyclododecine-1,9(10H)-dione (1.2**)**



A solution of macrocycle **1.1** (50 mg, 0.16 mmol) in EtOH (10 mL) was degassed with argon for 10 mins, following with Pd/C (10 mol %) was added to the same. The reaction mixture was stirred under H_2 for 5 h, following which it was filtered through a bed of celite and the filtrate was concentrated under vacuo to afford saturated macrocycle **1.2**(49 mg).

Chapter 2: Total Synthesis of Cladosporin Related Twelve Membered Macrocyclic Natural Products

$[\alpha]_D^{26}$ -0.8 (c 1.0, CHCl_3)

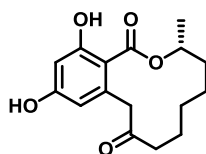
IR (film) ν_{max} : cm^{-1} 2933, 1714, 1599, 1457, 1272

^1H NMR (400 MHz, CDCl_3) δ 6.39 (d, $J = 2.2$ Hz, 1H), 6.29 (d, $J = 2.2$ Hz, 1H), 5.29 – 5.22 (m, 1H), 4.12 (d, $J = 17.2$ Hz, 1H), 3.80 (s, 3H), 3.79 (s, 3H), 3.55 (d, $J = 17.2$ Hz, 1H), 2.43 (t, $J = 6.4$ Hz, 2H), 1.84 – 1.64 (m, 3H), 1.61 – 1.49 (m, 2H), 1.45 – 1.32 (m, 3H), 1.29 (d, $J = 6.4$ Hz, 3H)

^{13}C NMR (100 MHz, CDCl_3) δ 208.3, 168.0, 161.3, 158.3, 133.9, 117.9, 107.8, 97.8, 72.3, 56.0, 55.6, 47.5, 41.5, 32.9, 27.2, 22.9, 22.5, 20.2

HRMS (ESI) calcd. for $\text{C}_{18}\text{H}_{25}\text{O}_5$ $[\text{M}+\text{H}]^+$: 321.1702; found: 321.1708.

Synthesis of (*R*)-dihydroresorcyclide (**2g**)



(*R*)-dihydroresorcyclide (**2g**)

(*R*)-dihydroresorcyclide (**2g**) was synthesized using similar procedure as that of (*R*)-penicimenolide A (**2a**).

$[\alpha]_D^{26}$ +9.3 (c 0.3, MeOH)

IR (film) ν_{max} : cm^{-1} 2930, 1640, 1453, 1258

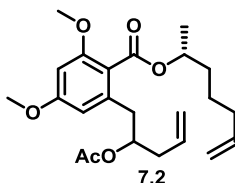
^1H NMR (400 MHz, MeOD) δ 6.25 (d, $J = 2.5$ Hz, 1H), 6.11 (d, $J = 2.5$ Hz, 1H), 5.12 (pd, $J = 6.2, 3.0$ Hz, 1H), 4.70 (d, $J = 18.7$ Hz, 1H), 3.80 (d, $J = 18.7$ Hz, 1H), 2.72 – 2.66 (m, 1H), 2.38 – 2.31 (m, 1H), 2.07 – 1.97 (m, 1H), 1.84 – 1.78 (m, 1H), 1.69 – 1.59 (m, 2H), 1.56 – 1.45 (m, 4H), 1.30 (d, $J = 6.3$ Hz, 3H)

^{13}C NMR (100 MHz, MeOD) δ 211.7, 172.4, 166.6, 163.8, 140.2, 113.7, 106.6, 102.9, 74.5, 51.7, 42.5, 32.7, 28.2, 22.2, 19.4

Chapter 2: Total Synthesis of Cladosporin Related Twelve Membered Macrocyclic Natural Products

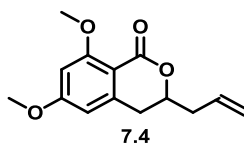
HRMS (ESI) calcd. for $C_{16}H_{21}O_5$ $[M+H]^+$: 293.1389; found: 293.1393.

Synthesis of compound (R)-hept-6-en-2-yl 2-(2-acetoxypent-4-en-1-yl)-4,6-dimethoxybenzoate (7.2)



Compound **7.2** was synthesized using similar protocol as that of compound **3.5**.

Synthesis of compound 3-allyl-6,8-dimethoxyisochroman-1-one (7.4)



Compound **7.4** was synthesized using similar protocol as that of compound **1.1**.

IR (film) ν_{\max} : cm^{-1} 1709, 1594, 1460, 1226, 1082

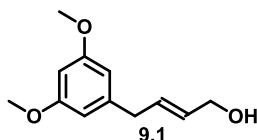
1H NMR (400 MHz, $CDCl_3$) δ 6.39 (d, $J = 2.2$ Hz, 1H), 6.29 (d, $J = 2.2$ Hz, 1H), 5.92 – 5.81 (m, 1H), 5.19 – 5.13 (m, 2H), 4.44 – 4.37 (m, 1H), 3.90 (s, 3H), 3.84 (s, 3H), 2.83 (qd, $J = 16.1, 7.1$ Hz, 2H), 2.64 – 2.57 (m, 1H), 2.45 (dt, $J = 14.3, 7.1$ Hz, 1H)

^{13}C NMR (100 MHz, $CDCl_3$) δ 164.4, 163.1, 162.6, 143.7, 132.6, 118.6, 106.9, 103.9, 97.8, 76.4, 56.1, 55.5, 38.9, 34.1

HRMS (ESI) calcd. for $C_{14}H_{17}O_4$ $[M+H]^+$: 249.1126; found: 249.1127.

Chapter 2: Total Synthesis of Cladosporin Related Twelve Membered Macrocyclic Natural Products

Synthesis of compound (*E*)-4-(3,5-dimethoxyphenyl)but-2-en-1-ol (9.1)



Compound **9.1** was synthesized using similar protocol as that of compound **2.2**.

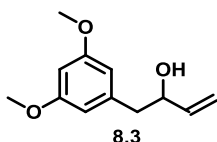
IR (film) ν_{\max} : cm^{-1} 2940, 2838, 1595, 1458, 1148

^1H NMR (400 MHz, CDCl_3) δ 6.34 (d, $J = 2.2$ Hz, 2H), 6.31 (t, $J = 2.2$ Hz, 1H), 5.82 (m, $J = 7.5, 6.6, 0.9$ Hz, 1H), 5.73 – 5.65 (m, 1H), 4.10 (d, $J = 5.7$ Hz, 1H), 3.77 (s, 6H), 3.31 (d, $J = 6.6$ Hz, 2H), 1.91 (bs, 1H)

^{13}C NMR (100 MHz, CDCl_3) δ 160.8, 142.4, 131.0, 130.5, 106.6, 98.0, 63.3, 55.2, 38.8

HRMS (ESI) calcd. for $\text{C}_{12}\text{H}_{17}\text{O}_3$ $[\text{M}+\text{H}]^+$: 209.1177; found: 209.1179.

Synthesis of compound 1-(3,5-dimethoxyphenyl)but-3-en-2-ol (8.3)



Compound **8.3** was synthesized using documented procedure in the literature.

IR (film) ν_{\max} : cm^{-1} 3463, 2939, 1596, 1459

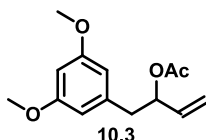
^1H NMR (400 MHz, CDCl_3) δ 6.39 (d, $J = 2.3$ Hz, 2H), 6.35 (t, $J = 2.3$ Hz, 1H), 5.93 (ddd, $J = 17.2, 10.5, 5.7$ Hz, 1H), 5.27 (dt, $J = 17.2, 1.4$ Hz, 1H), 5.13 (dt, $J = 10.5, 1.3$ Hz, 1H), 4.37 – 4.32 (m, 1H), 3.78 (s, 6H), 2.82 (dd, $J = 13.5, 4.9$ Hz, 1H), 2.71 (dd, $J = 13.5, 8.2$ Hz, 1H), 1.89 (bs, 1H)

^{13}C NMR (100 MHz, CDCl_3) δ 160.8, 140.0, 114.9, 107.5, 98.5, 73.3, 55.2, 44.1

Chapter 2: Total Synthesis of Cladosporin Related Twelve Membered Macrocyclic Natural Products

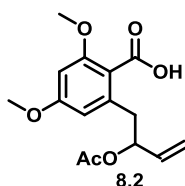
HRMS (ESI) calcd. for $C_{12}H_{17}O_3$ $[M+H]^+$: 209.1177; found: 209.1169.

Synthesis of compound 1-(3,5-dimethoxyphenyl)but-3-en-2-yl acetate (10.3)



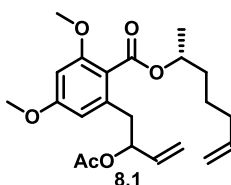
Compound 10.3 was synthesized using similar protocol as that of compound 2.3.

Synthesis of compound 2-(2-acetoxybut-3-en-1-yl)-4,6-dimethoxybenzoic acid (8.2)



Compound 8.2 was synthesized using similar protocol as that of compound 2.4.

Synthesis of compound (R)-hept-6-en-2-yl 2-(2-acetoxybut-3-en-1-yl)-4,6-dimethoxybenzoate (8.1)



Compound 8.1 was synthesized using similar protocol as that of compound 3.5.

IR (film) ν_{\max} : cm^{-1} 2935, 1723, 1599, 1233

1H NMR (diastereomeric mixture) (400 MHz, $CDCl_3$) δ 6.36 – 6.33 (m, 2H), 5.85 – 5.75 (m, 2H), 5.50 – 5.44 (m, 1H), 5.24 – 5.13 (m, 2H), 5.03 – 4.93 (m, 3H), 3.79 (s, 3H), 3.76 (s, 3H), 2.91 (dddd, $J = 17.7, 14.0, 11.6, 7.0$ Hz, 2H), 2.11 – 2.01 (m, 2H),

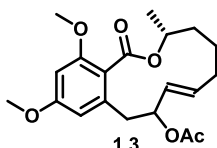
Chapter 2: Total Synthesis of Cladosporin Related Twelve Membered Macrocyclic Natural Products

2.01 – 2.00 (s, overlap, 3H), 1.74 – 1.66 (m, 2H), 1.60 – 1.49 (m, 2H), 1.33 (dd, $J = 6.3, 3.2$ Hz, 3H)

^{13}C NMR (diastereomeric mixture) (100 MHz, CDCl_3) δ 170.0, 167.6, 161.0, 158.0, 138.5, 136.9, 135.8, 135.7, 117.0, 116.9, 114.6, 106.6, 97.1, 74.5, 71.8, 55.7, 55.7, 55.3, 38.0, 38.0, 35.4, 33.5, 24.6, 21.1, 20.1, 20.0

HRMS (ESI) calcd. for $\text{C}_{22}\text{H}_{30}\text{O}_6\text{Na}$ $[\text{M}+\text{Na}]^+$: 413.1940; found: 413.1945.

Synthesis of compound (3R,E)-12,14-dimethoxy-3-methyl-1-oxo-3,4,5,6,9,10-hexahydro-1H-benzo[c][1]oxacyclododecin-9-yl acetate (10.4)



Compound **10.4** was synthesized using similar protocol as that of compound **3.6**.

IR (film) ν_{max} : cm^{-1} 2935, 1718, 1597, 1238

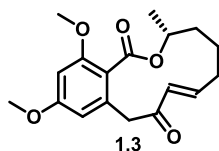
^1H NMR (diastereomeric mixture) (400 MHz, CDCl_3) δ 6.47 – 6.29 (m, 2H), 5.84 – 4.94 (m, 4H), 3.81 – 3.77 (m, 6H), 3.24 (dd, $J = 13.2, 7.1$ Hz, 1H), 2.85 (ddd, $J = 15.6, 14.2, 2.6$ Hz, 1H), 2.11 – 2.04 (m, 3H), 1.92 – 1.52 (m, 6H), 1.32 – 1.30 (m, 2H)

^{13}C NMR (diastereomeric mixture) (100 MHz, CDCl_3) δ 170.3, 170.1, 168.4, 168.1, 161.3, 160.7, 158.3, 158.1, 133.4, 130.2, 127.6, 127.4, 108.9, 107.0, 97.8, 97.3, 74.9, 74.1, 71.5, 71.3, 56.1, 56.0, 55.4, 55.3, 39.3, 37.9, 32.1, 30.3, 30.0, 21.4, 21.3, 21.2, 21.1

HRMS (ESI) calcd. for $\text{C}_{20}\text{H}_{26}\text{O}_6\text{Na}$ $[\text{M}+\text{Na}]^+$: 385.1627; found: 385.1622.

Chapter 2: Total Synthesis of Cladosporin Related Twelve Membered Macrocyclic Natural Products

Synthesis of compound (R,E)-12,14-dimethoxy-3-methyl-3,4,5,6-tetrahydro-1H-benzo[c][1]oxacyclododecine-1,9(10H)-dione (1.3)



Compound **1.3** was synthesized using similar protocol as that of compound **1.1**.

$[\alpha]_D^{26}$ -39.1 (c 0.5, CHCl₃)

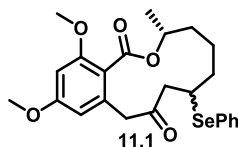
IR (film) ν_{\max} : cm⁻¹ 2929, 1707, 1597, 1284

¹H NMR (400 MHz, CDCl₃) δ 6.89 (ddd, J = 16.1, 8.8, 5.7 Hz, 1H), 6.54 (d, J = 2.2 Hz, 1H), 6.34 (d, J = 2.2 Hz, 1H), 5.92 (d, J = 16.2 Hz, 1H), 5.22 – 5.17 (m, 1H), 4.59 (d, J = 12.1 Hz, 1H), 3.80 (s, 3H), 3.76 (s, 3H), 3.28 (d, J = 12.2 Hz, 1H), 2.31 – 2.25 (m, 2H), 1.91 – 1.66 (m, 4H), 1.36 (d, J = 6.3 Hz, 3H)

¹³C NMR (100 MHz, CDCl₃) δ 199.1, 168.8, 161.5, 158.4, 150.2, 134.6, 130.8, 117.5, 106.5, 98.0, 72.4, 55.9, 55.5, 42.6, 34.0, 31.8, 24.7, 20.5

HRMS (ESI) calcd. for C₁₈H₂₂O₅ [M+Na]⁺: 341.1365; found: 341.1362.

Synthesis of compound (3R)-12,14-dimethoxy-3-methyl-7-(phenylselanyl)-3,4,5,6,7,8-hexahydro-1H-benzo[c][1]oxacyclododecine-1,9(10H)-dione (11.1)



To a stirred solution of diphenyl diselenide (666.7 mg, 2.14 mmol) in EtOH (5 mL), NaBH₄ (268.7 mg, 7.10 mmol) was added at 0 °C under argon. After decolorization of the reaction mixture, AcOH (528 μ L, 9.24 mmol) and a solution of enone compound **1.3** (170 mg, 0.53 mmol) in THF (10) was added and the reaction mixture was stirred for 10 mins at room temperature. After completion of reaction, as monitored by TLC,

Chapter 2: Total Synthesis of Cladosporin Related Twelve Membered Macrocyclic Natural Products

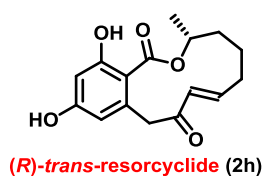
the mixture was extracted with ethyl acetate (15 mL x 3) and the combined organic layers were dried over Na₂SO₄ and concentrated under vacuo. Purification through column chromatography (SiO₂ ethyl acetate/pet ether 1:4) afforded selenide intermediate **11.1** (231 mg) with a yield of 84% as a foamy solid.

IR (film) ν_{\max} : cm⁻¹ 2929, 1707, 1667, 1597, 1284

¹H NMR (diastereomeric mixture) (400 MHz, CDCl₃) δ 7.57 – 7.52 (m, 2H), 7.30 – 7.26 (m, 3H), 6.39 (t, J = 2.1 Hz, 1H), 6.24 (dd, J = 12.0, 2.2 Hz, 1H), 5.34 – 5.13 (m, 1H), 4.04 (dd, J = 17.6, 14.2 Hz, 1H), 3.96 – 3.91 (m, 1H), 3.80 – 3.78 (m, 6H), 3.55 (d, J = 17.9 Hz, 1H), 2.89 (ddd, J = 24.3, 15.1, 10.4 Hz, 1H), 2.66 (ddd, J = 18.8, 15.2, 3.8 Hz, 1H), 1.88 – 1.77 (m, 1H), 1.74 – 1.65 (m, 3H), 1.56 – 1.41 (m, 2H), 1.28 (dd, J = 6.4, 1.7 Hz, 3H)

¹³C NMR (diastereomeric mixture) (100 MHz, CDCl₃) δ 205.7, 205.6, 168.0, 167.4, 161.4, 161.2, 158.7, 158.0, 135.0, 133.9, 133.6, 133.2, 129.3, 129.2, 127.9, 127.5, 117.7, 117.2, 107.8, 97.9, 97.7, 72.3, 71.5, 56.0, 55.8, 55.4, 48.8, 48.5, 46.8, 38.5, 37.2, 34.2, 33.8, 23.2, 20.8, 19.4

HRMS (ESI) calcd. for C₂₄H₂₈O₅SeNa [M+Na]⁺: 341.1365; found: 341.1365
Synthesis of compound (*R*)-trans-resorcyclide (2h)



The initial exhaustive demethylation step of compound **11.1** was conducted using similar procedure as that of compound (*R*)-penicimenolide A (**2a**).

To a solution of the obtained demethylated intermediate (50 mg, 0.11 mmol) in THF (15 mL) was added AcOH (6 μ L) followed by the addition of 30% aqueous H₂O₂ (32 μ L, 0.2820 mmol). After 2 h the reaction mixture was washed with saturated aqueous NaHCO₃ and extracted with diethyl ether (10 mL x 3). The combined organic layers

Chapter 2: Total Synthesis of Cladosporin Related Twelve Membered Macrocyclic Natural Products

were dried over anhydrous Na₂SO₄ and concentrated under vacuo. Purification through column chromatography (SiO₂ ethyl acetate/pet ether 1:9) afforded (*R*)-*trans*-resorcyclide (**2h**) (18 mg) with a yield of 54% (in two steps) as a white solid.

$[\alpha]_D^{26} +42.4$ (c 0.4, MeOH)

IR (film) ν_{\max} : cm⁻¹ 2927, 1714, 1598, 1459

¹H NMR (400 MHz, CDCl₃) δ 6.99 – 6.92 (m, 1H), 6.31 (d, *J* = 2.1 Hz, 1H), 6.22 (d, *J* = 2.2 Hz, 1H), 5.94 (d, *J* = 16.1 Hz, 1H), 5.17 – 5.11 (m, 1H), 4.43 (d, *J* = 12.7 Hz, 1H), 3.32 (d, *J* = 12.5 Hz, 1H), 2.28 (dt, *J* = 16.8, 8.1 Hz, 2H), 1.93 – 1.65 (m, 4H), 1.35 (d, *J* = 6.3 Hz, 3H)

¹³C NMR (100 MHz, CDCl₃) δ 201.8, 171.1, 161.1, 158.9, 152.1, 136.4, 131.3, 114.8, 110.4, 102.6, 73.7, 44.2, 35.0, 32.6, 25.5, 20.7

HRMS (ESI) calcd. for C₁₆H₁₉O₅ [M+H]⁺: 291.1232; found: 291.1229.

2.4. References

1. Shen, W.; Mao, H.; Huang, Q.; Dong, J. Benzenediol lactones: a class of fungal metabolites with diverse structural features and biological activities. *Eur. J. Med. Chem.* **2015**, *97*, 747–777.
2. Pusztahelyi, T.; Imre, H.; István, P. Secondary metabolites in fungus-plant interactions. *Front. Plant Sci.* **2015**, *6*, 573
3. Cichewicz, R. H. Epigenome manipulation as a pathway to new natural product scaffolds and their 9 congeners. *Nat. Prod. Rep.* 2001, *27*, 11-22.
4. Gao, J. M. New biologically active metabolites from Chinese higher fungi. *Curr. Org. Chem.* 2006, *10*, 849-871.
5. Gunatilaka, A. A. L. Natural products from plant-associated microorganisms: distribution, structural, diversity, bioactivity and implications of their occurrence. *J. Nat. Prod.* **2006**, *69*, 509-526.
6. Zhang, H. W.; Song, Y. C.; Tan, R. X. Biology and chemistry of endophytes. *Nat. Prod. Rep.* **2006**, *23*, 828-829.

Chapter 2: Total Synthesis of Cladosporin Related Twelve Membered Macrocyclic Natural Products

- Hoffmeister, D.; Keller, N. P. Natural products of filamentous fungi: enzymes, genes, and their regulation. *Nat. Prod. Rep.* **2007**, *24*, 393-416.
- Winssinger, N.; Barluenga, S. Chemistry and biology of resorcylic acid lactones. *Chem. Commun.* **2007**, *171*, 22–36.
- Thomas, R. A biosynthetic classification of fungal and streptomycete fused-ring aromatic polyketides. *ChemBioChem.* **2001**, *2*, 612–627.
- Xu, Y.; Zhou, T.; Zhou, Z.; Su, S.; Roberts, S. A.; Montfort, W. R.; Zeng, J.; Chen, M.; Zhang, W.; Zhan, J.; Molnár, I. Rational reprogramming of fungal polyketide first-ring cyclization, *Proc. Natl. Acad. Sci. U. S. A.* **2013**, *110*, 5398-5403.
- Jiang, C. S.; Liang, L. F.; Guo, Y. W. Natural products possessing protein tyrosine phosphatase 1B (PTP1B) inhibitory activity found in the last decades. *Acta Pharmacol. Sin.* **2012**, *33*, 1217–1245.
- An1, Y. N.; Zhang, X.; Zhang, T. Y.; Zhang, M. Y.; Zhang, Q.; Deng, X. Y.; Zhao, F.; Zhu, L. J.; Wang, G.; Zhang, J.; Zhang, Y. X.; Liu, B.; Yao1, X. S. Penicimenolides A-F, Resorcylic Acid Lactones from *Penicillium sp.*; isolated from the Rhizosphere Soil of *Panax notoginseng*. *Nature Sci. Rep.* **2016**, *6*, Article number: 27396.
- Couladouros, E. A.; Mihou, A. P.; Bouzas, E. A. First total synthesis of *trans*- and *cis*-resorcylic acid lactone: remarkable hydrogen-bond-controlled, stereospecific ring-closing metathesis. *Org Lett.* **2004**, *6*, 977–80.
- Mennen, S. M.; Miller, S. J. Development of a bio-inspired acyl-anion equivalent macrocyclization and synthesis of a *trans*-resorcylic acid lactone precursor. *J. Org. Chem.* **2007**, *72*, 5260–5269.
- Luo, Y.; Yin, X.; Dai, M. Total Synthesis of *trans*-Resorcylic acid lactone via Macrocyclic Stille Carbonylation. *J. Antibiot.* **2019**, *72*, 482–485.
- Zhang, Li.; Ma, W.; Xu, L.; Deng, F.; Guo, Y. Efficient Total Synthesis of (*S*)-Dihydroresorcylic acid lactone, a Bioactive Twelve-Membered Macrolide. *Chin. J. Chem.* **2013**, *31*, 339–343.
- Jiang, C. S.; Zhang, L.; Gong, J. X.; Li, J. Y.; Yao, L. G.; Li, J.; Guo, Y. W. Concise synthesis and PTP1B inhibitory activity of (*R*)- and (*S*)-

Chapter 2: Total Synthesis of Cladosporin Related Twelve Membered Macrocyclic Natural Products

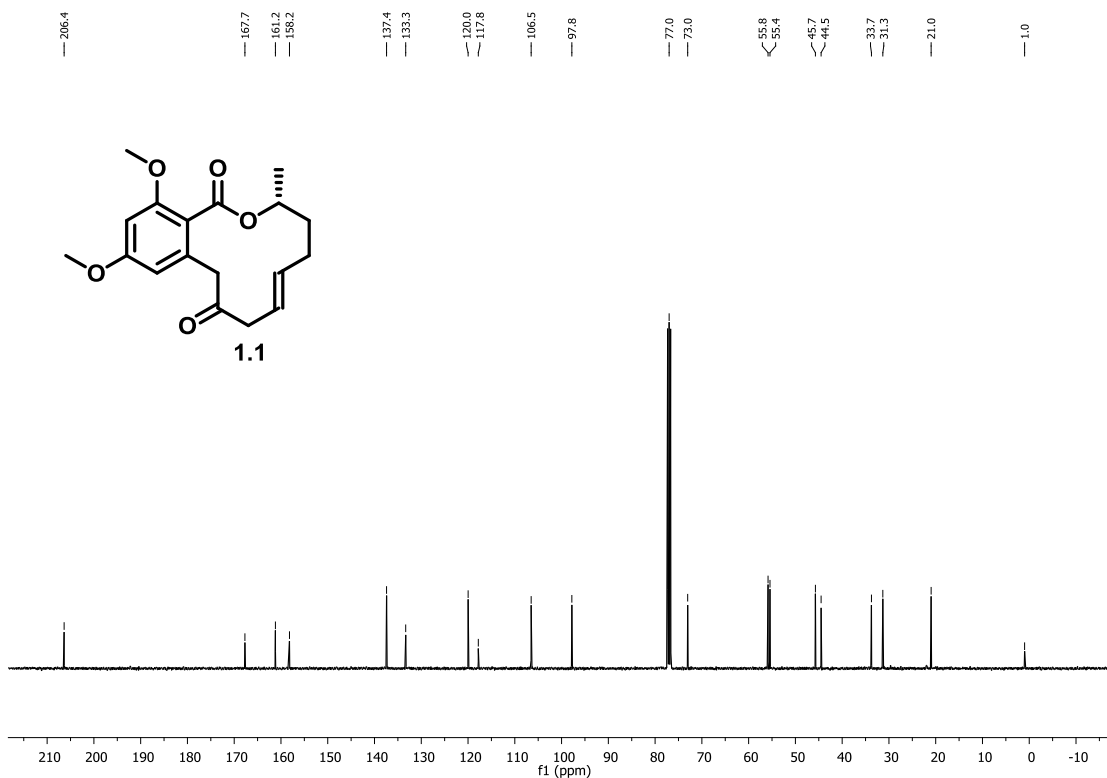
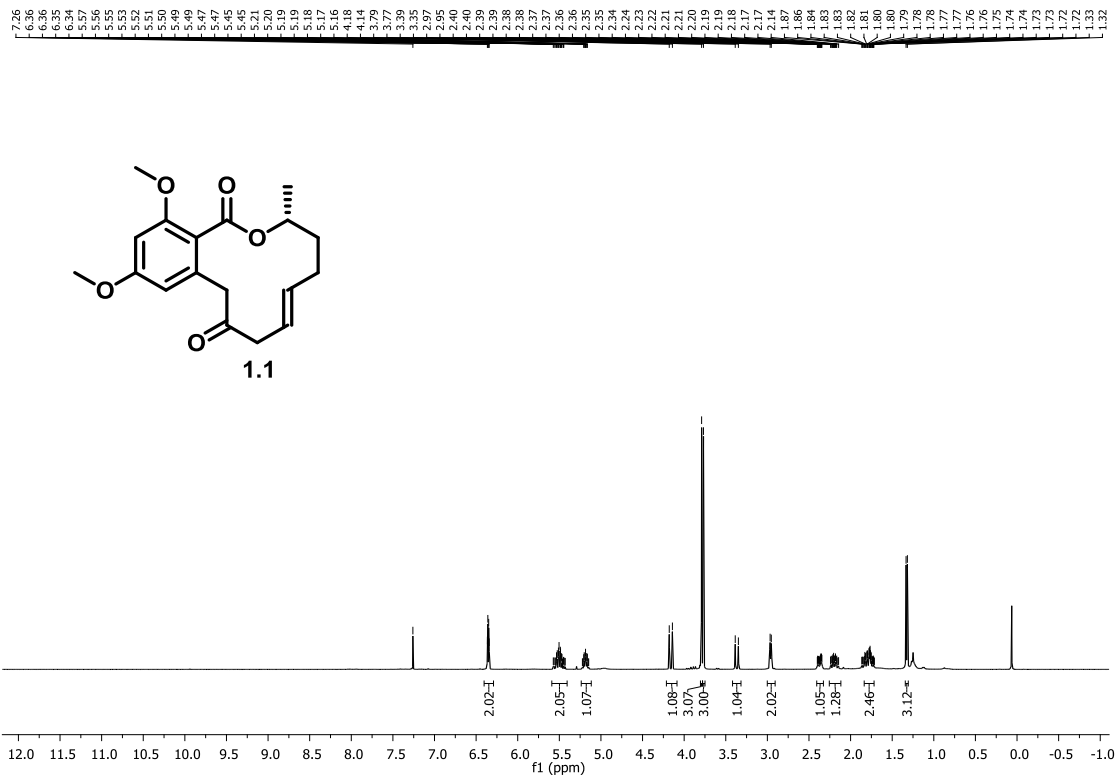
- dihydroresorcylide, *Journal of Asian Natural Products Research*, **2017**, *19*, 1204–1213.
18. Plummer, C. W.; Soheili, A.; Leighton, J. L. A Tandem Cross-Metathesis/Semipinacol Rearrangement Reaction. *Org. Lett.* **2012**, *14*, 2462–2464.
 19. Ma, B.; Zhong, Z.; Hu, H.; Li, H.; Zhao, C.; Xie, X.; She, X. Concise Enantioselective Synthesis of Cephalosporolide B, (4*R*)-4-OMe-Cephalosporolide C, and (4*S*)-4-OMe-Cephalosporolide C. *Chem. Asian J.* **2013**, *8*, 1391–1394.
 20. Poling, S. M.; Wicklow, D. T.; Rogers, K. D.; Gloer, J. B. *Acremonium zeae*, a Protective Endophyte of Maize, Produces Dihydroresorcylide and 7-Hydroxydihydroresorcylides. *J. Agric. Food. Chem.* **2008**, *56*, 3006–3009.
 21. (a) Oyama, H.; Sassa, T.; Ikeda, M. Structures of New Plant Growth Inhibitors, *trans*- and *cis*-Resorcylide. *Agric. Biol. Chem.* **1978**, *42*, 2407–2409.
(b) Barrow, C. J. New Macrocyclic Lactones from a *Penicillium* Species. *J. Nat. Prod.* **1997**, *60*, 1023–1025.
 22. Gualandi, A.; Canestrari, P.; Emer, E.; Cozzi, P. G. A Straightforward Organocatalytic Alkylation of 2-Arylacetaldehydes: An Approach towards Bisabolanes. *Adv. Synth. Catal.* **2014**, *356*, 528–536.



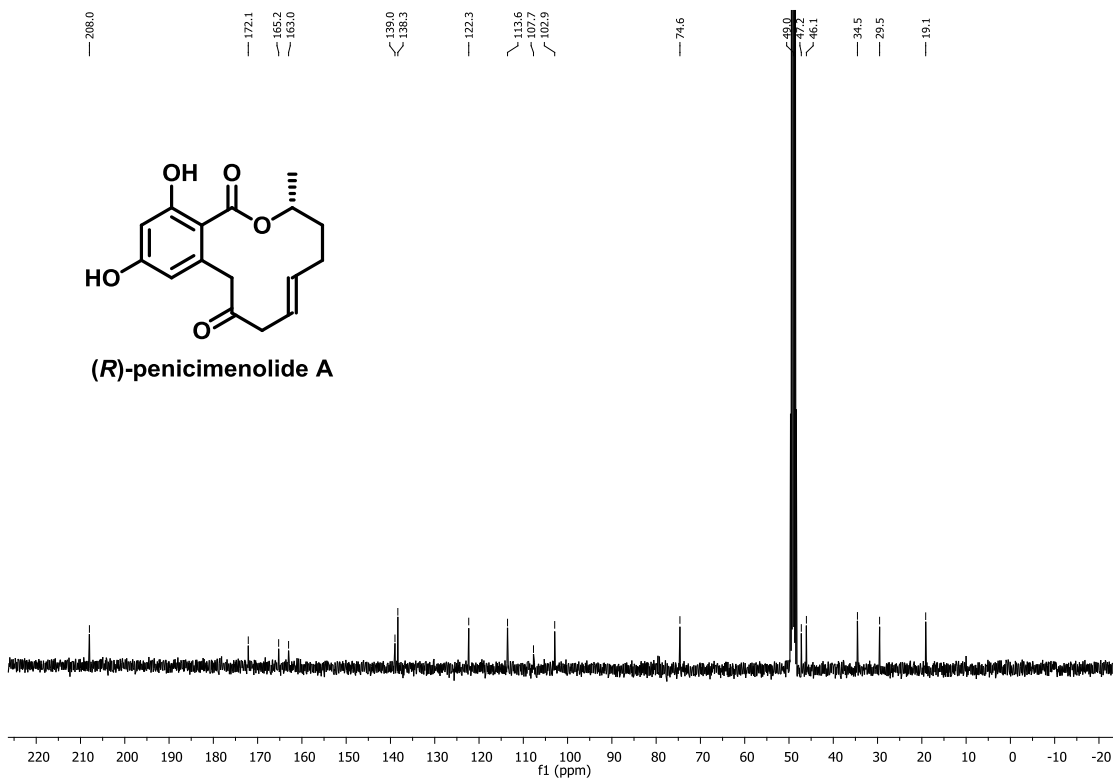
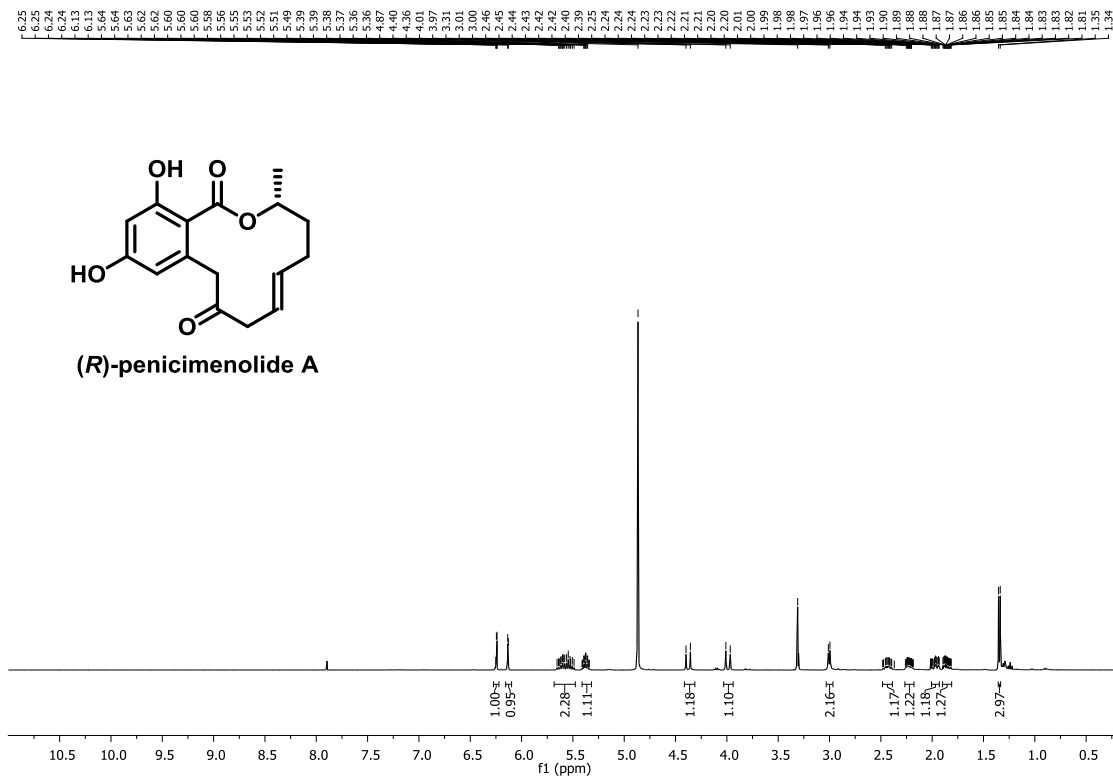
**Copies of
 ^1H and ^{13}C NMR Spectra of Selected
Compounds**



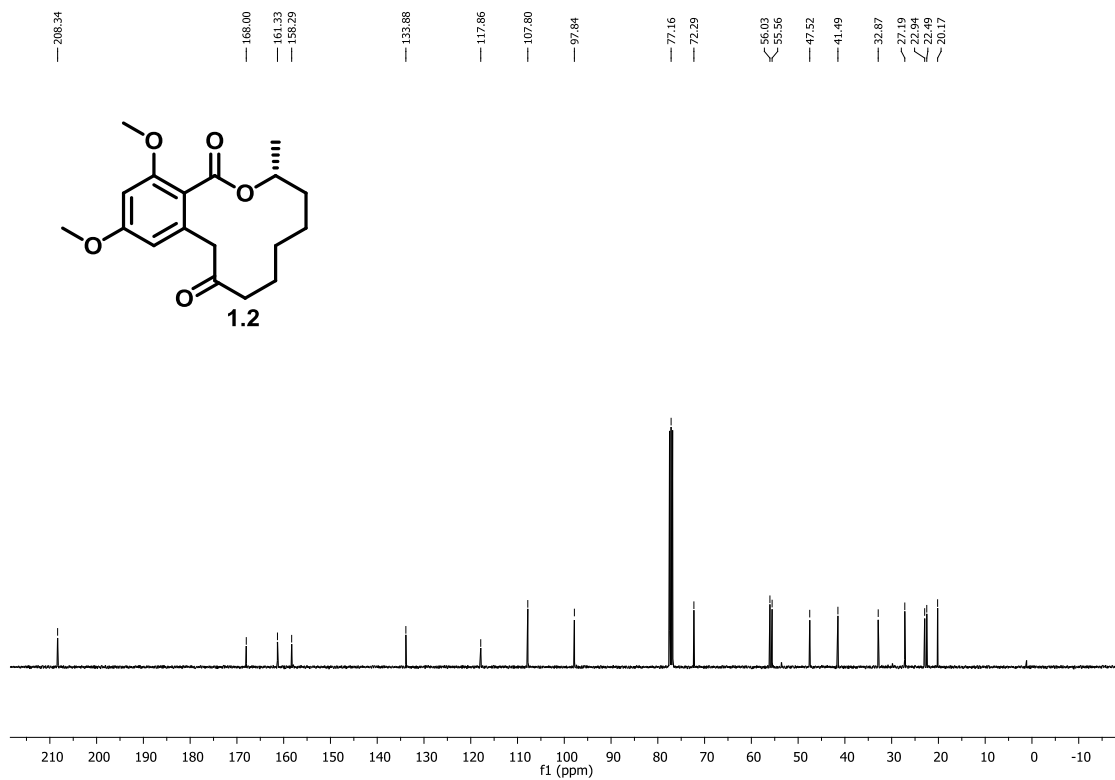
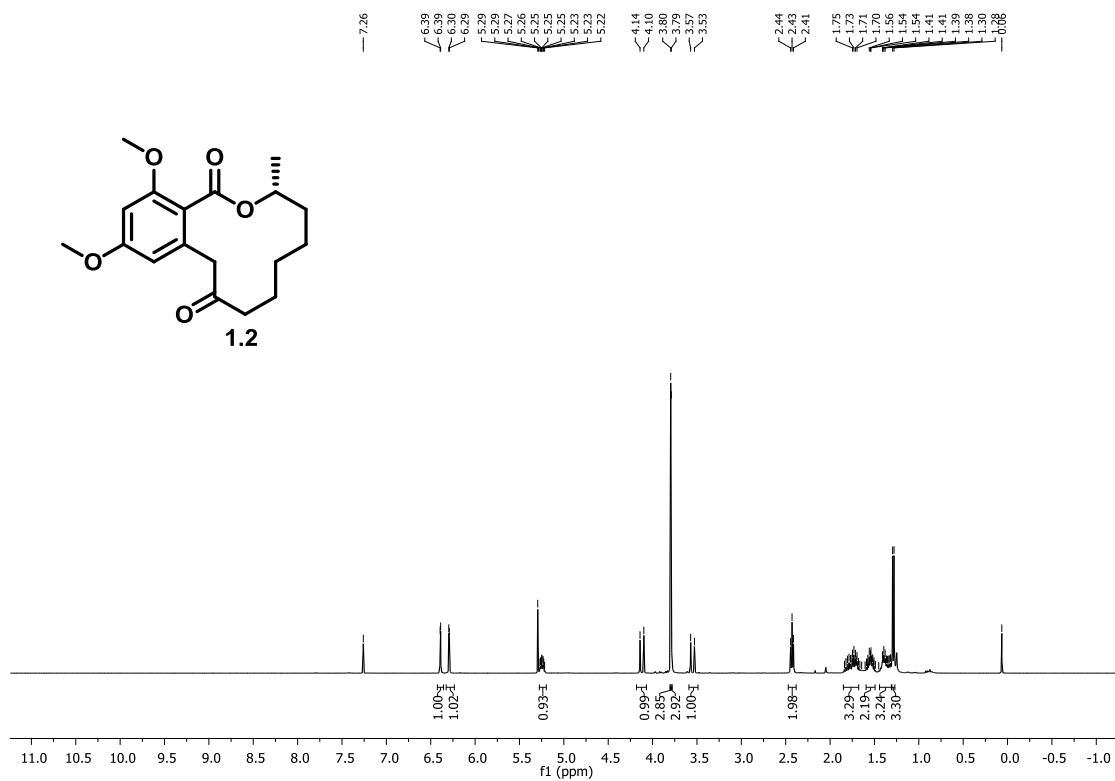
Chapter 2: Total Synthesis of Cladosporin Related Twelve Membered Macrocyclic Natural Products



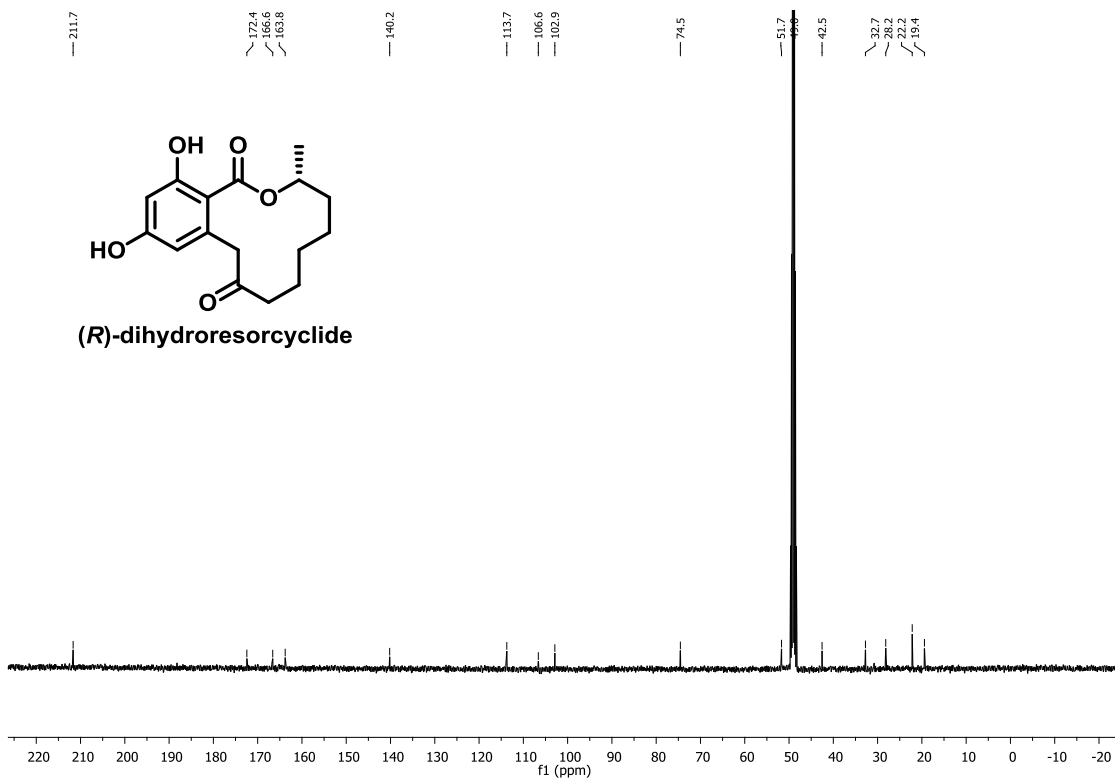
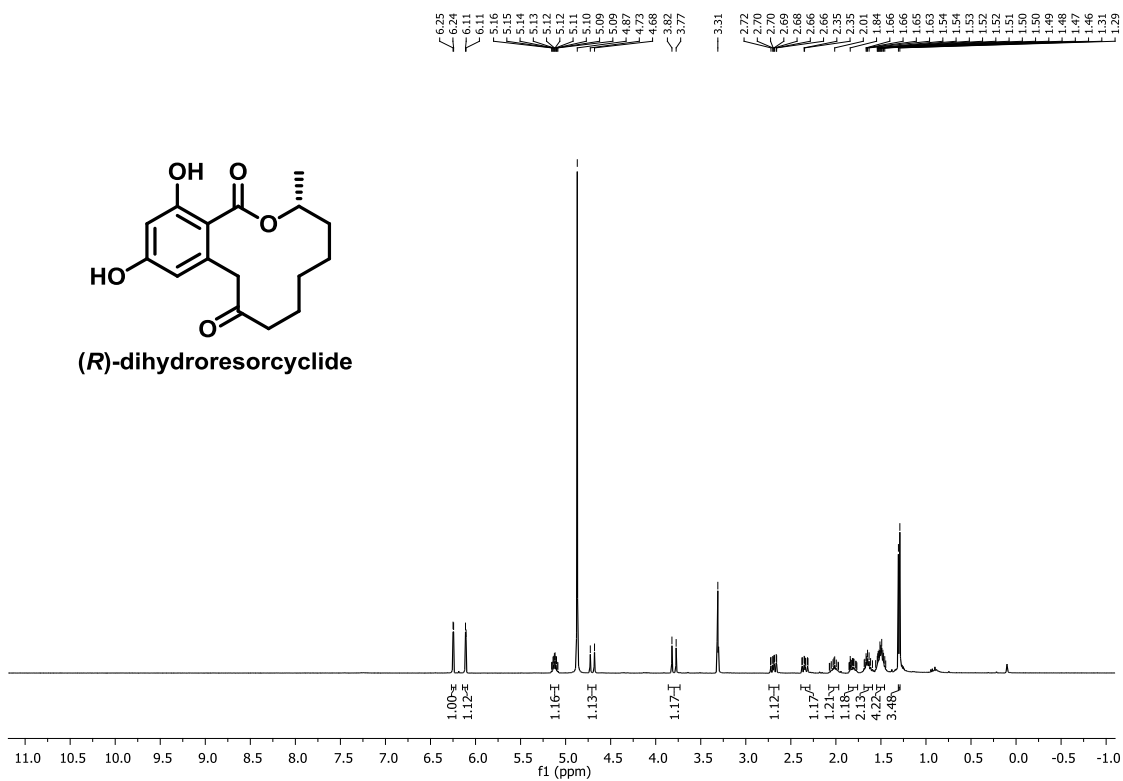
Chapter 2: Total Synthesis of Cladosporin Related Twelve Membered Macrocyclic Natural Products



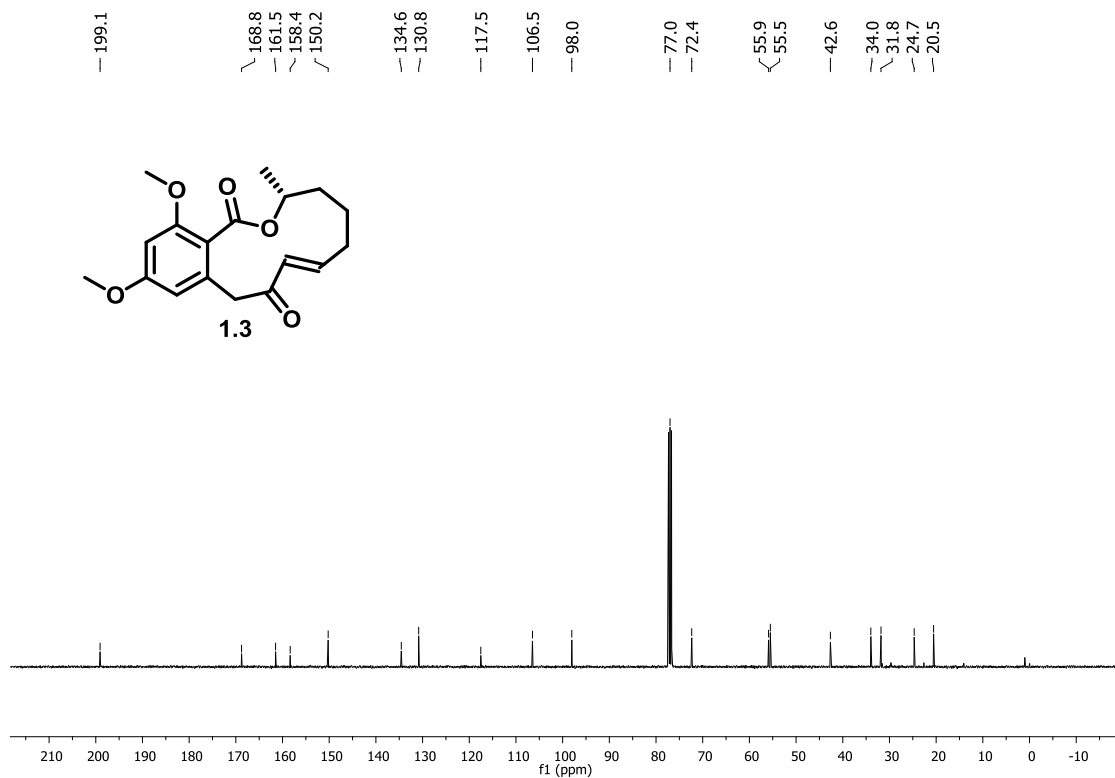
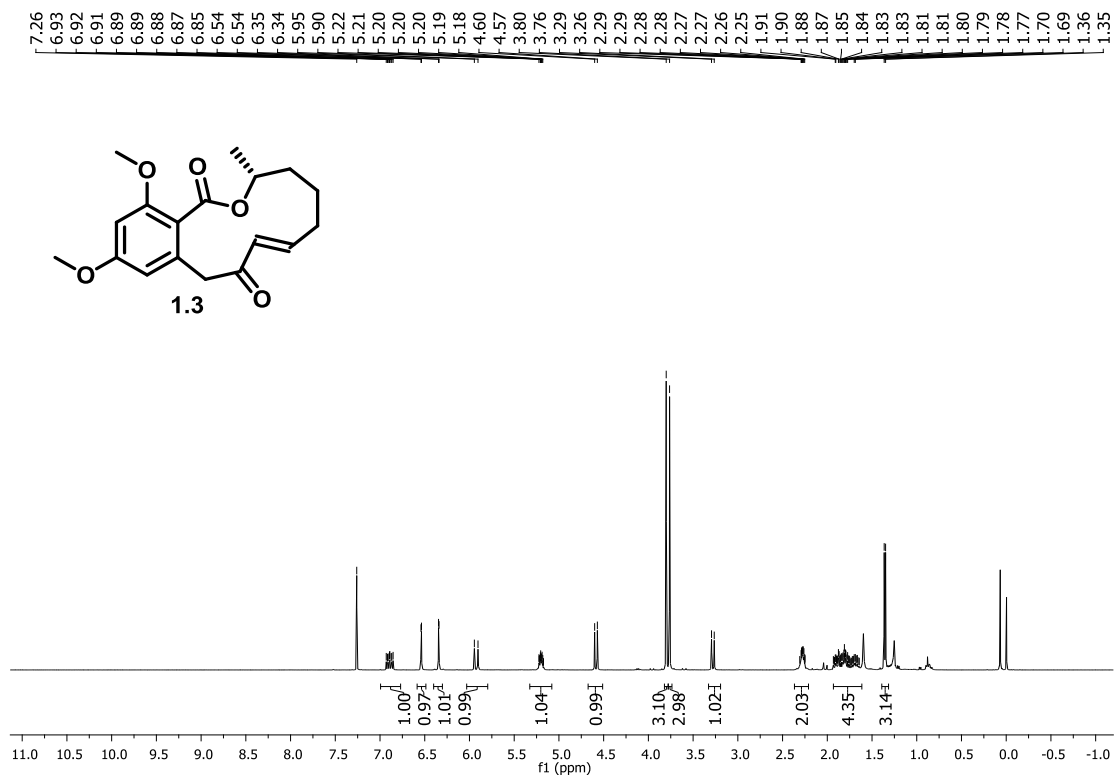
Chapter 2: Total Synthesis of Cladosporin Related Twelve Membered Macrocyclic Natural Products



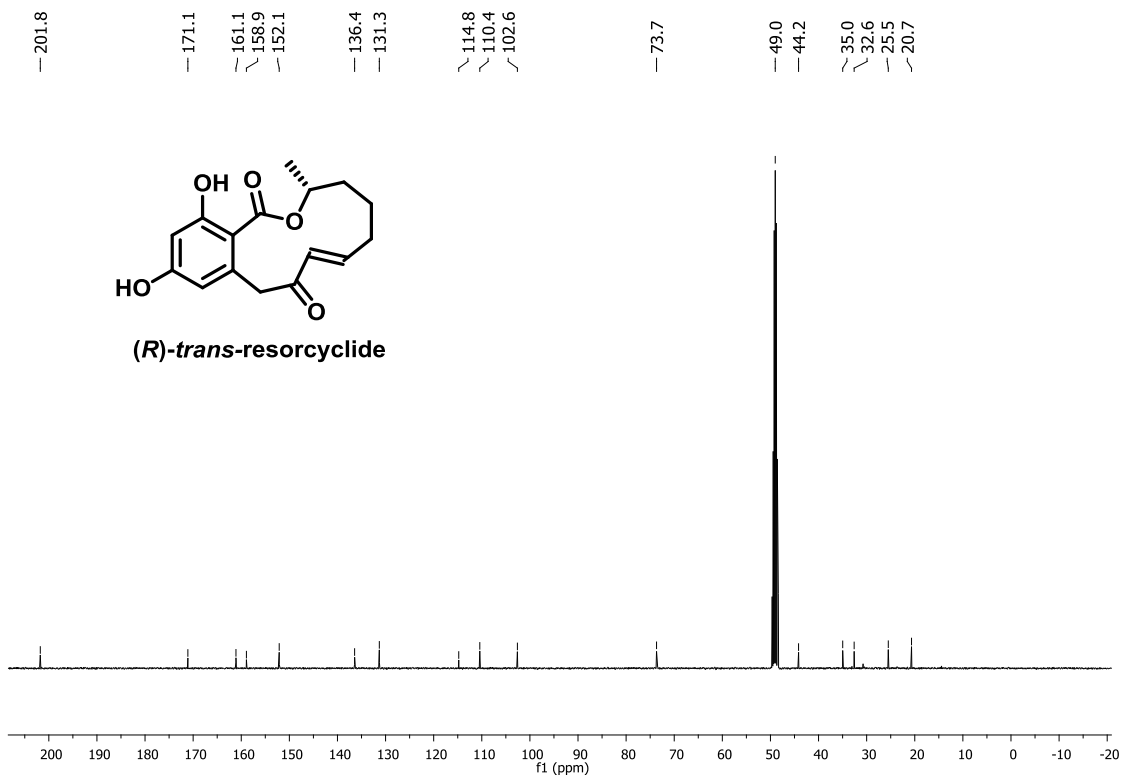
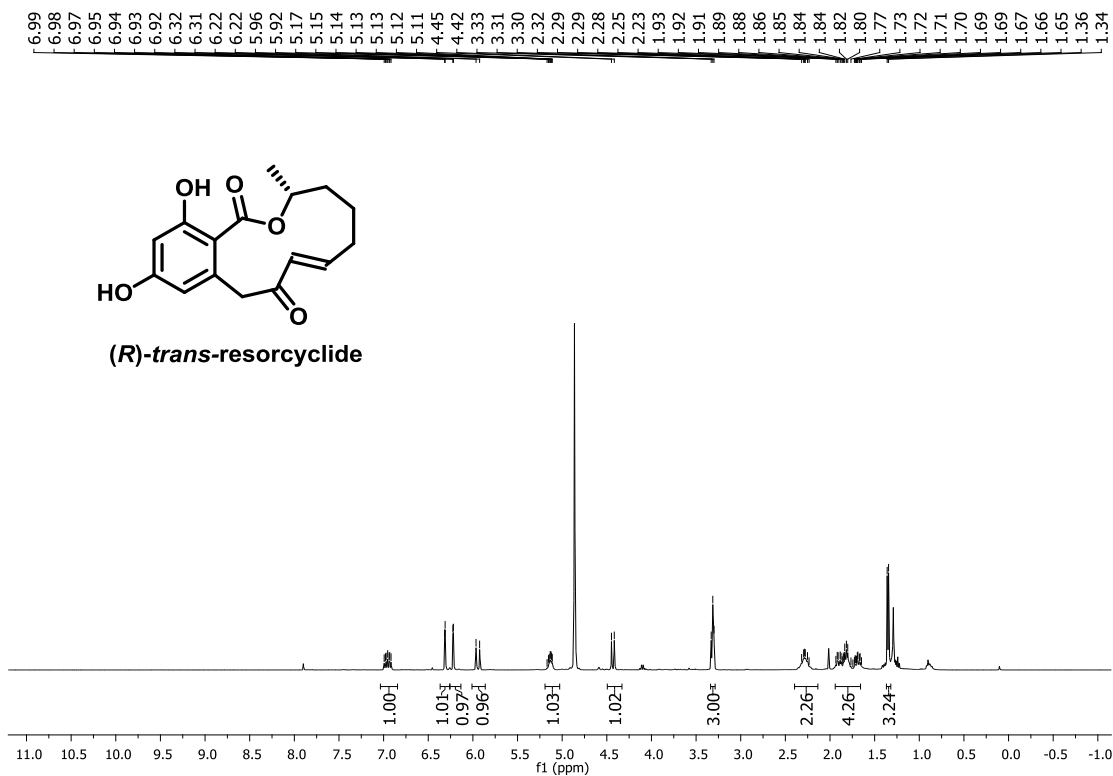
Chapter 2: Total Synthesis of Cladosporin Related Twelve Membered Macrocyclic Natural Products



Chapter 2: Total Synthesis of Cladosporin Related Twelve Membered Macrocyclic Natural Products



Chapter 2: Total Synthesis of Cladosporin Related Twelve Membered Macrocyclic Natural Products



ABSTRACT

Name of the Student: Pronay Das

Registration No. : 10CC15A26015

Faculty of Study: Chemical Sciences

Year of Submission: 2021

AcSIR academic centre/CSIR Lab: NCL, Pune

Name of the Supervisor (s): Dr. D. Srinivasa Reddy

Title of the thesis: Antimalarial Natural Product Cladosporin: Synthesis of Stereoisomeric Library, Lead Optimization, Co-Crystallization and Biological Evaluation and Synthesis of Related Macrocyclic Natural Products

The work incorporated in this thesis is mainly focused on “Medicinal chemistry” and “Total synthesis”. Herein we have developed a unique and divergent synthetic scheme to access all the possible stereoisomers of a potent anti-malarial natural product, cladosporin and assessed their inhibitory potency through parasite-, enzyme- and cell-based assays. Based on the scores from biological assays, we categorized the entire set of stereoisomers in to three different potency classes, two of them (including cladosporin) being the most potent ones. X-ray diffraction study of co-crystals of the stereoisomers with target protein, *PfKRS* further gave an insight about the structural bases of enzymatic binding of the isomers. This exercise collectively helped us to decipher the role of stereochemical modifications on anti-malarial potency of cladosporin.

Natural products are mostly procured in substantial low quantities from natural sources, which often hinders, and sometimes, even eliminates the possibility of in depth biological assessment (mainly in vivo). Hence, we adopted a modified synthetic protocol to access more than two grams of cladosporin in a single batch process. Besides, the scheme adopted herein is amenable to further scale-up.

In the later part of this work, we have studied a systematic structure activity relationship (SAR) of a library of analogues, designed and synthesized based on cladosporin scaffold in anti-malarial potency through parasite-, enzyme- and cell-based assays. In this effort, we identified a lead compound (**CL-2**) having similar potency to that of cladosporin, but with improved drug-like properties (increased metabolic stability and hydrophilicity). Besides, the co-crystal structure of the most active compound (**CL-2**) with target protein *PfKRS* reveals new features of enzyme drug interactions.

Lastly, we have accomplished the total synthesis of three bio-active twelve membered resorcyclic acid lactones (RAL₁₂) namely (*R*)-penicimenolide A, (*R*)-dihydroresorcyclide and (*R*)-*trans*-resorcyclide. These natural products bear an interesting structural compliance with cladosporin.

List of Publication(s) in SCI Journal(s) Emanating from the Thesis Work

List of publication (emanating from the thesis work)

- 1) **Das, P.**; Babbar, P.; Malhotra, N.; Sharma, M.; Jachak, G. R.; Gonnade, R. G.; Shanmugam, D.; Harlos, K.; Yogavel, M.; Sharma, A.; Reddy, D. S. Specific Stereoisomeric Conformations Determine the Drug Potency of Cladosporin Scaffold against Malarial Parasite. *J. Med. Chem.* **2018**, *61*, 5664-5678.
- 2) **Das, P.**; Mankad, Y.; Reddy, D. S. Scalable Synthesis of Cladosporin. *Tetrahedron Lett.* **2019**, *60*, 831-833.
- 3) **Das, P.**; Reddy, D. S. Total synthesis of twelve membered resorcylic acid lactones, (*R*)-penicimenolide A, (*R*)-resorcyclide and (*R*)-dihydroresorcyclide. *Tetrahedron*, **2020**, (Manuscript accepted) (<https://doi.org/10.1016/j.tet.2021.132059>).
- 4) Lauro, G.; **Das, P.**; Riccio, R.; Reddy, D. S.; Bifulco, G. *J. Org. Chem.* **2020**, *85*, 3297-3306.
- 5) Mankad, Y.; **Das, P.**; Pathan, E.; Deshpande, M. V.; Reddy, D. S. *J. Antibiot.* **2021**, (Manuscript accepted) (<https://doi.org/10.1038/s41429-020-00391-1>)

List of papers with abstract presented (oral or poster) at national or international conferences/seminars.

- 1) 21st International Conference on Organic Synthesis (ICOS), 2016 (*poster presented*)
- 2) Science Day Conference, 2017, CSIR-National Chemical Laboratory. (*poster presented*).
- 3) NCL-RF Annual Students' Conference, CSIR-National Chemical Laboratory, 2019 (*delivered oral presentation*).
- 4) Curious Minds: Academia-Industry Interaction, 2019, Indian Institute of Science and Education (IISER), Pune. (*poster presented*).
- 5) CSIR-Inter Institutional Student Conference on "Sustainable Chemistry for Health, Environment and Materials, 2019, Indian Institute of Chemical Technology, Hyderabad, India. (*poster Presented*).
- 6) XVI-JNOST-2020 (*oral Presentation delivered*).

Specific Stereoisomeric Conformations Determine the Drug Potency of Cladosporin Scaffold against Malarial Parasite

Pronay Das,^{†,‡,∇} Palak Babbar,^{§,∇} Nipun Malhotra,^{§,∇} Manmohan Sharma,[§] Goraknath R. Jachak,^{†,‡} Rajesh G. Gonnade,^{‡,||} Dhanasekaran Shanmugam,^{‡,⊥} Karl Harlos,[#] Manickam Yogavel,[§] Amit Sharma,^{*,§} and D. Srinivasa Reddy^{*,†,‡,||}

[†]Organic Chemistry Division, CSIR-National Chemical Laboratory, Dr. Homi Bhabha Road, Pune 411008, India

[‡]Academy of Scientific and Innovative Research (AcSIR), New Delhi 110025, India

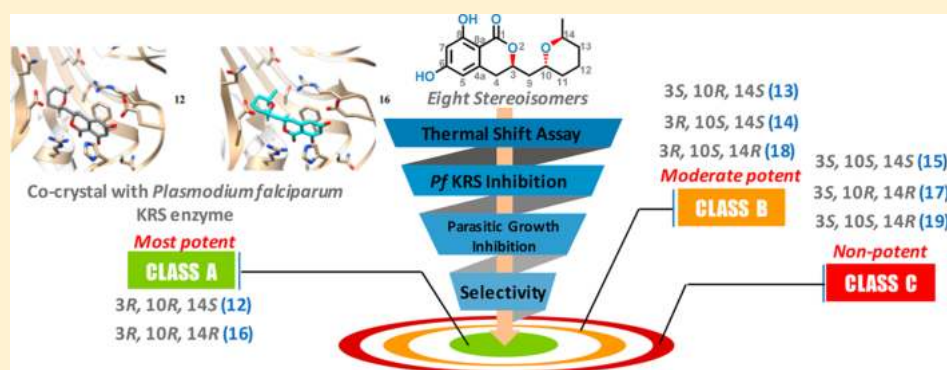
[§]Molecular Medicine Group, International Centre for Genetic Engineering and Biotechnology (ICGEB), New Delhi 110067, India

^{||}Center for Material Characterization, CSIR-National Chemical Laboratory, Dr. Homi Bhabha Road, Pune 411008, India

[⊥]Biochemical Sciences Division, CSIR-National Chemical Laboratory, Dr. Homi Bhabha Road, Pune 411008, India

[#]Division of Structural Biology, Wellcome Trust Centre for Human Genetics, The Nuffield Department of Medicine, University of Oxford, Oxford OX3 7BN, U.K.

Supporting Information



ABSTRACT: The dependence of drug potency on diastereomeric configurations is a key facet. Using a novel general divergent synthetic route for a three-chiral center antimalarial natural product cladosporin, we built its complete library of stereoisomers (cladologs) and assessed their inhibitory potential using parasite-, enzyme-, and structure-based assays. We show that potency is manifest via tetrahydropyran ring conformations that are housed in the ribose binding pocket of parasite lysyl tRNA synthetase (KRS). Strikingly, drug potency between top and worst enantiomers varied 500-fold, and structures of KRS-cladolog complexes reveal that alterations at C3 and C10 are detrimental to drug potency whereas changes at C3 are sensed by rotameric flipping of glutamate 332. Given that scores of antimalarial and anti-infective drugs contain chiral centers, this work provides a new foundation for focusing on inhibitor stereochemistry as a facet of antimicrobial drug development.

INTRODUCTION

Since the discovery of chirality in chemistry by Louis Pasteur, its significance in biology and in the pharmaceutical industry has been repeatedly emphasized. Chirality of natural biomolecules underpins molecular biology, while >50% of the marketed human drugs are chiral products, although many are administered as racemates of equimolar enantiomers. Intriguingly, artificial compounds may have chiral centers, but most natural small molecules appear in a solitary enantiomeric configuration. The pivotal role of chiral chemistry and separation of enantiomers was further highlighted with the recognition of 2001 Nobel Prize in Chemistry to Knowles, Sharpless, and Noyori for devising methodologies in asymmetric synthesis using chiral catalysts that lead to single enantiomers of high value in

pharmaceutical industry. A racemic formulation of a chiral drug molecule may be futile and can even cause undesired side effects.^{1,8} Along these lines, natural products (often produced in chirally pure form) have been serving as a priceless resource for the development of chiral drugs.² From a structural biology perspective, stereoisomers of drugs display differences in properties like pharmacology, toxicology, pharmacokinetics, and metabolism, despite possessing the same chemical connectivity of atoms.³ Therefore, in chiral drug synthesis, significant efforts are devoted to chiral separation.³ Given the potentially crucial differences in pharmacodynamics and pharmacokinetics between

Received: April 10, 2018

Published: May 21, 2018

diastereomers, it is not surprising that they display stereoselective toxicity; thalidomide⁴ and the pain killer ibuprofen⁵ serve as examples of this. Cladosporin, an antifungal antibiotic and plant growth regulator isolated from *Cladosporium cladosporioides* and *Aspergillus flavus* in 1971,^{6,7} is a chiral complex isocoumarin-based scaffold. It is a potential lead molecule with potent antimalarial activity against both liver and blood stage *Plasmodium falciparum* (Pf) and is known to target the parasite cytosolic lysyl-tRNA synthetase and terminating protein biosynthesis.^{9–11} The active scaffold is composed of a 6,8-dihydroxyisocoumarin ring joined to tetrahydropyran group with a methyl moiety, which together mimics an adenosine moiety and thereby inhibits enzyme activity by competing with ATP.¹⁰ Apart from PfKRS, cladosporin is known to inhibit KRSs from other species, including helminth parasites such as *Loa loa* (Ll) and *Schistosoma mansoni* (Sm).¹² Cladosporin (12) displays exquisite selectivity for the parasite lysyl-tRNA synthetase over human enzyme. This species specific selectivity of cladosporin has been previously described through comprehensive sequence alignment, where the residues val329 and ser346 seem to be sterically crucial for accommodating the methyl moiety of THP ring.¹⁰ The structural features of compound 12 clearly indicate the presence of three stereocenters, and therefore 2ⁿ (n = 3) i.e., eight, stereoisomers are possible (Figure 1). To date, only one asymmetric total

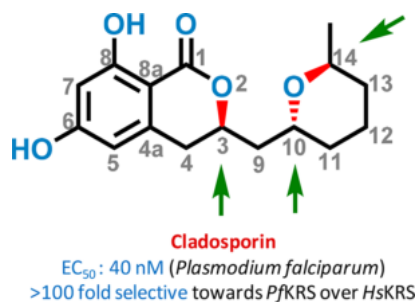


Figure 1. Structure of cladosporin.

synthesis of cladosporin¹³ has been achieved which was followed by another report of formal syntheses.¹⁴ Here, we have developed a general chemical synthesis route to synthetically access all the eight possible stereoisomers of compound 12. These eight cladologs were evaluated in enzyme- and cell-based inhibition assays. In addition, the structural basis for engagement of five of the eight cladologs was addressed via X-ray structures for cocrystal with the target enzyme PfKRS.

■ SYNTHESIS OF EIGHT STEREOISOMERS OF CLADOSPORIN (12)

We synthesized cladosporin (12) (Figure 1) and its isomers from fragment A and fragment B using cross metathesis protocol followed by relevant functional group interconversions (Scheme 1). Fragment A can be synthesized from an appropriate chiral propylene oxide, and fragment B can be obtained using known

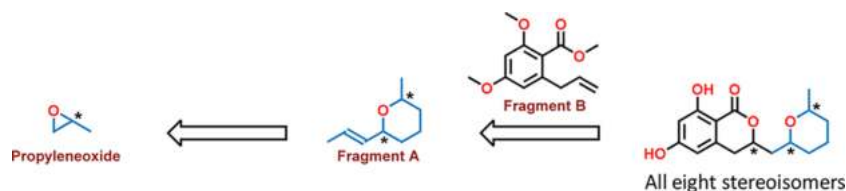
protocols.¹⁵ Our synthesis commenced with (*S*)-propylene oxide as the chiral source which was converted to its TBS ether 1 using reported procedure.¹⁶ As per the plan, compound 1 was then subjected to one-pot ozonolysis and Wittig reaction with 2 to give α,β -unsaturated ketone 3 in 47% yield which was further reduced under Luche condition (CeCl₃·7H₂O and NaBH₄) to give 1:1 diastereomeric mixture (by NMR) of an allylic alcohol 4 in 88% yield. Alcohol 4 was then treated with tetra-*n*-butylammonium fluoride to give diol 5 in 85% yield. Palladium-catalyzed intramolecular Tsuji–Trost type cyclization of the same afforded key fragment A as a 1:1 mixture of diastereomers. At this stage, cross metathesis¹⁷ of fragment A and fragment B was achieved by using 2.5 mol % of Grubbs'II catalyst in DCM to afford compounds 6a and 6b in 53% yield which were cleanly separated by column chromatography. Both compounds 6a and 6b were subjected to dihydroxylation conditions, independently, to have corresponding diols. However, to our surprise, the intermediate diols were in situ lactonized under the reaction conditions to furnish lactones 7a and 7b with a diastereomeric ratio of 3:2 and 1:1, respectively. The free hydroxy of compound 7a was then converted to its xanthate ester to afford diastereomeric mixture of compounds 8a and 9a with a yield of 78% which was then separated using flash chromatography. Following similar procedure, we also obtained xanthate esters 8b and 9b in 70% yield. Each of the four diastereomeric xanthates was separately subjected to Barton–McCombie condition to give compounds 10a, 11a, 10b, and 11b in moderate yields (~60%). Finally, all the phenolic hydroxy groups were liberated using aluminum triiodide-mediated exhaustive demethylation¹⁸ to furnish cladosporin (compound 12) and three of its stereoisomers, i.e., compound 13, compound 14, and compound 15 (Scheme 2). Among these, compound 12, i.e., cladosporin, is a known compound for which spectral data are available in the literature.¹³ The spectral data (¹H NMR and ¹³C NMR) of all these four compounds (compound 12, 13, 14, and 15) are in full agreement with the assigned structures (Figure 3). The remaining four stereoisomers were synthesized by repeating the above synthetic sequence from (*R*)-propylene oxide as the chiral building block (Scheme 3). The structures of compound 16, compound 17, compound 18, and compound 19 synthesized from (*R*)-propylene oxide were confirmed by using single crystal X-ray diffraction (Figures 2 and 3). Besides, spectral data (¹H and ¹³C NMR) of these four stereoisomers are also in complete agreement with the spectral data of their corresponding enantiomers (compound 12 to compound 15) synthesized from (*S*)-propylene oxide (Figure 3).

Spectral data of compound 16 and compound 17 are also in complete agreement with reported data^{13,19,20} (Figure 3).

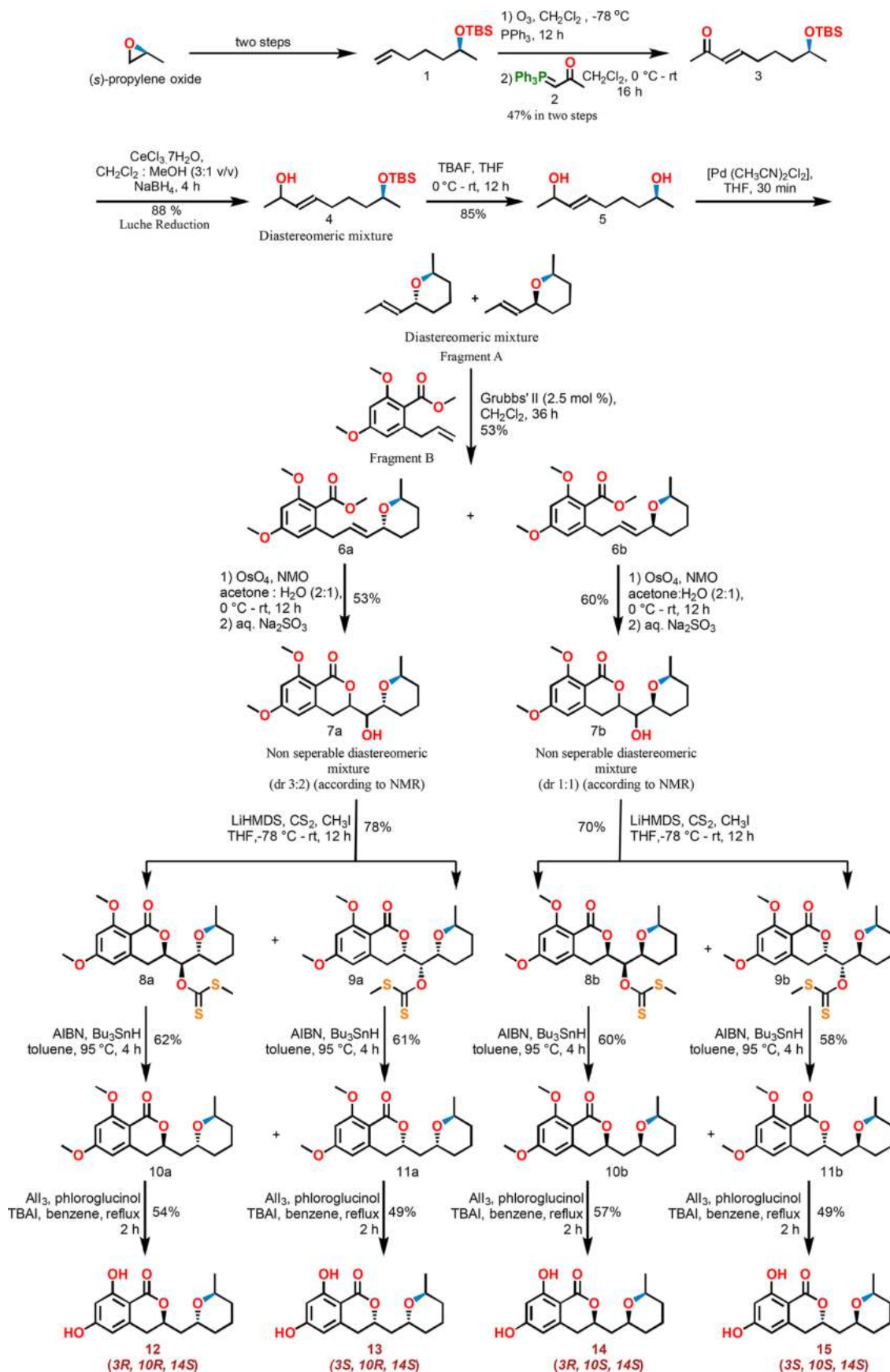
■ ASSESSMENT OF CLADOLOG POTENCY USING THERMAL SHIFT AND CELL- AND ENZYME-BASED ASSAYS

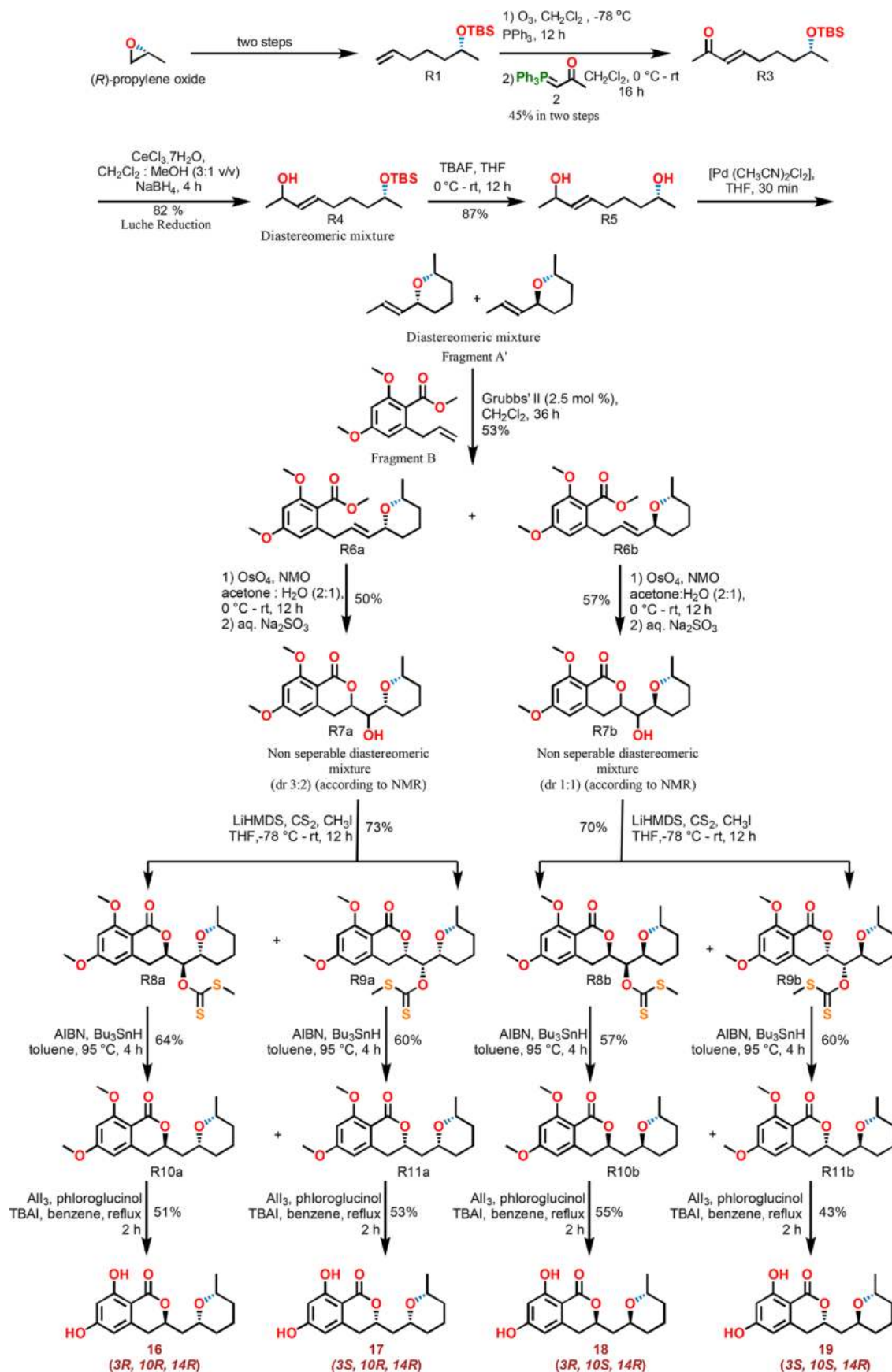
Enzyme–drug binding assays were performed to assess the potency of cladolog interactions with both *P. falciparum* KRS

Scheme 1. General Retrosynthetic Scheme of Cladosporin



Scheme 2. Synthesis of Cladosporin (12) and Three of Its Stereoisomers (Compounds 13–15) from (S)-Propylene Oxide



Scheme 3. Synthesis of Compounds 16–19 from (*R*)-Propylene Oxide

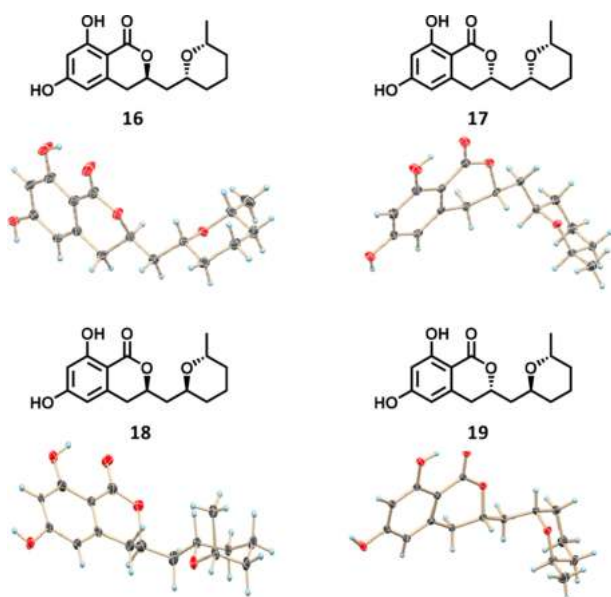


Figure 2. ORTEP diagrams of stereoisomers (compounds 16–19) based on their crystal structures.

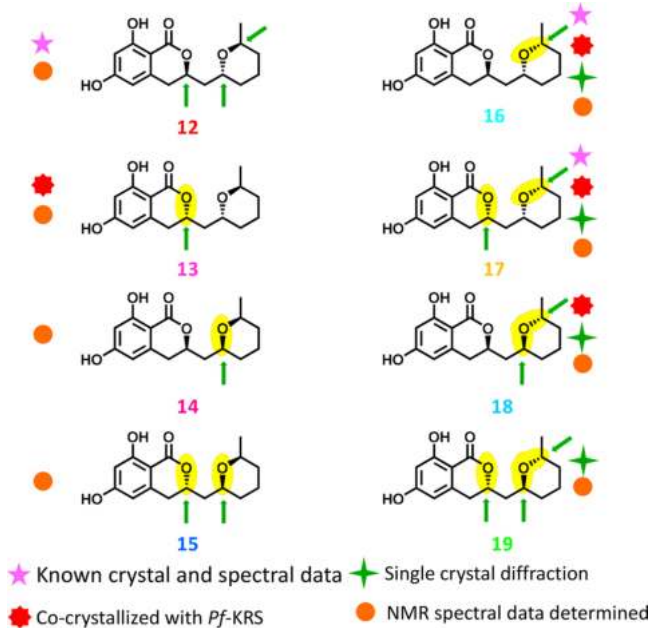


Figure 3. Chemical structures of the eight stereoisomers of cladosporin (12). The color used for each cladolog is mostly conserved in subsequent graphs and figures.

(*Pf*KRS) and its human counterpart *Hs*-KRS. These assays have been developed earlier to discriminate between strong and weak binders of KRS.^{10–12} Our data indicate that cladolog-*Pf*KRS complexes showed thermal shift values which ranged from ~ 7.9 to 17.3 °C, with a noticeable ΔT_m of 17.3 and 16.2 °C for compound 12 and compound 16, respectively (Figure 4c). On the basis of drug-binding characteristics of the eight cladologs, we were able to assign compound 12 and compound 16 as strong binders to *Pf*KRS, compound 13, compound 14, compound 18 as moderate binders, and compound 15, compound 17, compound 19 as poor (Figure 4c). This spectrum of high to low potency interactions of cladologs with *Pf*KRS was striking, and when identical data were collected on *Hs*-KRS, we observed very low/poor overall thermal shifts

(range of ~ 0.14 – 1.1 °C (Figure 4c) indicating that the cladologs retained their overall selectivity against the human KRS. The stratification of the eight cladologs into three discernible potency classes encouraged us to conduct further mechanistic studies. We then addressed the ability of cladologs to inhibit the enzymatic activity of *Pf*/*Hs*-KRSs in standard aminoacylation assays (Figure 4a). The evaluation of IC_{50} values for the eight cladologs revealed a trend consistent with that previously seen in thermal shift profiles (Figure 4d). Compound 12 and compound 16 displayed highest potency of inhibition (IC_{50} values of 0.125 μ M and 0.29 μ M against *Pf*KRS), while compounds 13, 3, and 7 showed moderate activity with IC_{50} values ranging from ~ 4 to 7 μ M. Compounds 15, 6, and 8 exhibited very poor activity with IC_{50} values ranging from ~ 21 to 50 μ M (Figure 4a,d). The IC_{50} range for the best (compound 12) to poorest stereoisomer (compound 19) spanned a striking ~ 500 -fold difference of their IC_{50} values (Figure 4b). To determine specificity, we assessed the IC_{50} values for *Hs*-KRS alongside, and all cladologs were found to be essentially inert (Figure 4b). These data also provided a window for assessing the selectivity indices for each cladolog (Figure 4g), wherein compound 16 (3*R*, 10*R*, and 14*R*) with a value of ~ 965 scored even better than the originally assessed conformation for compound 12 (3*R*, 10*R*, and 14*S*), which had a value of ~ 840 . In compound 16, the THP ring is in *cis* geometry and displays ~ 200 -fold difference when compared to compound 19. The consistent trends observed for antimalarial potency within the cladolog series provided grounds to assess the same in parasite growth inhibition assays using in vitro *P. falciparum* cultures (Figure 4b). Once again, the observed EC_{50} values were consistent with the observations from thermal shift and enzyme inhibition assays (Figure 4e,f). The EC_{50} value ranged from 0.04 to >2 μ M from best to worst, i.e., a 50-fold difference. Compounds 12 and 16 outperformed other enantiomers in their potency over the least potent ones, i.e., compounds 15, 17, and 19 (Figure 4b). Hence, together these above assays allowed us to classify the eight cladologs as class A (most potent, compounds 12, 16), class B (moderately potent, compounds 13, 14, and 18), and class C (nonpotent, compounds 15, 17, and 19) (Table 1). Note that compound 12 (best) and compound 19 (worst) have opposite chirality in all three positions of 3, 10, and 14 (Figure 3). It is also noteworthy that both compound 16 (14*R*) and compound 12 (14*S*) are the most potent compounds within cladologs despite changes in the C14 configuration (Figure 3). All other cladologs, i.e., compounds 13 (3*S*), 14 (10*S*), 15 (3*S*, 10*S*), 17 (3*S*, 14*R*), 18 (10*S*, 14*R*), 19 (3*S*, 10*S*, 14*R*), have stereoisomeric modifications at C3 or C10 or both (Figure 3). Therefore, it is apparent that these diastereomeric differences govern differential drug potency.

■ STRUCTURAL BASES FOR CLADOLOG-KRS BINDING

Previously, groups have determined the cocrystal structure of *Pf*KRS with compound 12.^{10,11,25} To further explore the structural basis of cladolog selectivity, we undertook the cocrystallization of six stereoisomers (compounds 13, 14, 15, 16, 17, 18) and one enantiomer (compound 19) with *Pf*KRS and L-lysine. We were successful in obtaining cocrystals for all compounds except for compound 19. For *Pf*KRS-compound 13/16/17/18 complex crystals, the diffractions were around ~ 3 Å resolution, while for *Pf*KRS-compound 14/15 crystals, the diffraction was poor (>3.5 Å resolution). A clear electron density was observed for both L-lysine and the specific

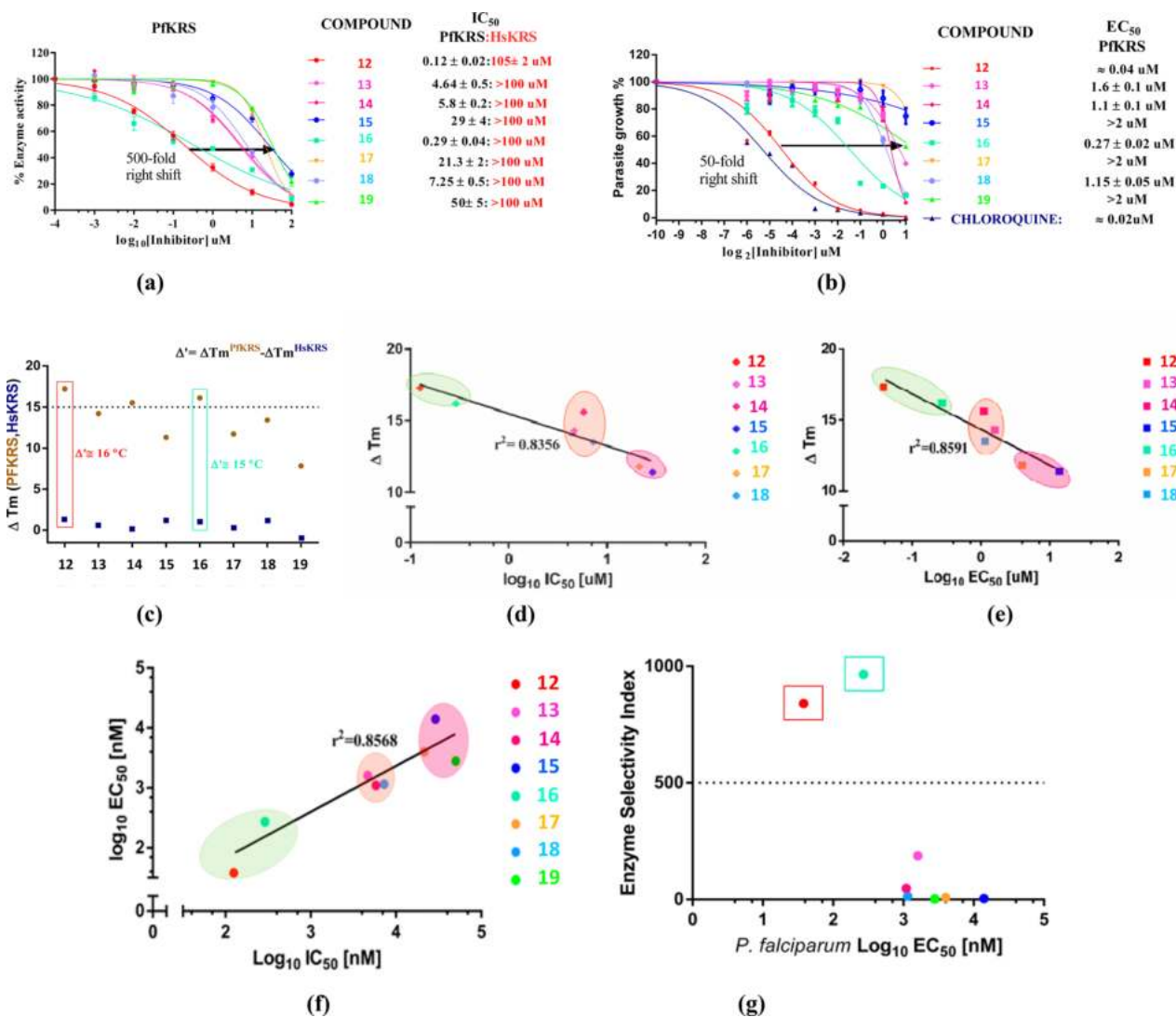


Figure 4. (a) Aminoacylation activity inhibition assays in the presence of cladologs 12–19. (b) Blood stage *Plasmodium falciparum* growth inhibition assays in the presence of compounds 12–19. (c) Protein thermal shift profiles of *PfKRS* and *Hs-KRS* (at 2 μ M and 4 μ M, respectively) in the presence of L-lysine. (d) Linear regression plot between thermal shift (ΔT_m) and $\log_{10} IC_{50}$ obtained through enzyme thermal shift and inhibition assays. (e) Linear regression plot between thermal shift (ΔT_m) and $\log_{10} EC_{50}$ obtained through enzyme and cell-based assays for malaria parasites. (f) Linear regression plot between $\log_{10} IC_{50}$ and $\log_{10} EC_{50}$ for malarial parasites, using equation $Y = mX + c$. (g) Selectivity profile (scatter plots) for each cladolog.

cladologs (compound 13/16/17/18; Figures 5, 6) and no electron densities were observed for either L-Lys or the drug for compound 14/15. The models were refined for *PfKRS*-compound 13/16/17/18 drug complexes and superimposed on *PfKRS*-compound 12 for further structural analyses (Figure 6). The binding modes for all five cladologs were similar (Figure 6). In each, the isocoumarin ring of the drug stacks between Phe342 and Arg559 (Figures 5, 6). As the chiral center (C3) in the isocoumarin moiety sterically bumps into carbon atoms (CE2) of Phe343 and the guanidum group of Arg559, an *R*-configuration is most favorable for this center (Figure 6). Both *S*- and *R*-configurations are favorable at C14 chiral center but again only *R*-configuration is favorable at C10 position, as evident from structural data for *PfKRS* bound compounds 12, 13, and 16 (Figures 5, 6, 7b). The side chain of *PfKRS* Glu332 adopts two conformations when the *R*-configuration of C3 is present (compounds 12, 13, 17; Figure 7b). The cladologs with *S*-configurations at positions C3/C10 (compounds 15 and 19) and at C10/C14 (compound 14) are not sterically

favorable. All cladologs have stereoisomeric alterations at either C3/C10/C14 or its combination; these affect the presentation of the THP ring (Figure 5). Amino acid side chain rotameric rearrangements for Phe342, Arg559, and Glu500 (Figure 6) were observed when compounds 13, 17, and 18 were bound in comparison to the most potent cladologs compounds 12 and 16. Furthermore, it is noteworthy, that the atomic arrangement at C10 is pivotal for cladolog binding, since out of four cladologs (compounds 14, 15, 18, 19) having *S* conformation at C10, only one crystallized (compound 18), while two failed to bind to *PfKRS* (compounds 14, 15). Moreover, it appears that stereomeric modifications at C14 alone (compound 16) are not crucial for potency as both its conformations (natural *S* and synthetic *R*) are highly potent (compounds 12 and 16). Therefore, peripheral yet crucial changes accommodate different drug scaffolds in its *R* conformation (Figure 6). Hence, this analysis substantiates that both *R*-C3 and *R*-C10 may serve as key enantiomeric determinants in enzyme inhibition.

Table 1. Classification of Cladologs

Compound	Plasmodium			Human	
	IC ₅₀ (uM)	EC ₅₀ (uM)	ΔTm	IC ₅₀ (uM)	ΔTm
12 Class A	0.12 ± 0.0	-0.04	17.3 ± 0.5	105 ± 2	1.3
16 Class A	0.29 ± 0.0	0.27 ± 0.0	16.2 ± 0.5	>100	1.0
13 Class B	4.64 ± 0.5	1.6 ± 0.1	14.3 ± 1.0	>100	0.5
14 Class B	5.8 ± 0.2	1.1 ± 0.1	15.6 ± 1.0	>100	0.1
18 Class B	7.25 ± 0.5	1.15 ± 0.0	13.5 ± 1.0	>100	1.1
15 Class C	29 ± 4	>2	11.4 ± 1.0	>100	1.1
17 Class C	21.3 ± 2	>2	11.8 ± 0.4	>100	0.3
19 Class C	50 ± 5	>2	7.9 ± 1.0	>100	-0.9

RESULTS AND DISCUSSION

The isocoumarin-based fungal metabolite compound **12** is synthesized in nature as a pure enantiomeric entity with an absolute configuration of 3*R*, 10*R*, 14*S*.^{9–11} But to interrogate role of its stereochemistry in antimalarial potency, we decided to undertake synthesis and assessment of eight stereoisomers. The cladologs consisted of two enantiomeric sets, each set containing four isomers. Given that the adoption of appropriate asymmetric synthetic routes for all eight isomers independently would have given the desired products but at a high cost, we devised a novel strategy for their synthesis via a single general route. Use of chiral starting material ((*S*)-propylene oxide) and incorporation of stereochemical divergence in two key chemical steps provided us with four stereoisomers (compounds **12**, **13**, **14**, **15**). The remaining four (compounds **16**, **17**, **18**, **19**) were synthesized by replacing the chiral starting material (*S*)-propylene oxide with (*R*)-propylene oxide and then following the entire synthetic sequence as for (*S*)-propylene oxide (Figure 8). The eight cladologs delivered by this stereodivergent route are functionally similar but spatially different, which made their individual characterization and stereochemical structure confirmation/assignment a very challenging task. Taking the knowledge of stereochemical transformations into consideration, scrutiny of the recorded NMR spectra led us to successfully assign the stereochemical outcomes for the divergent synthetic sequences adopted. We observed complete agreement of the recorded NMR data for this enantiomeric series. The assigned absolute structures of four compounds **16**, **17**, **18**, and **19** arising from (*R*)-propylene oxide were further confirmed unambiguously using single crystal X-ray structures. This type of divergent strategies can be developed and applied for the efficient delivery of an entire stereoisomeric set of a given bioactive natural product, and that would be valuable for stereostructure–activity relationship (S-SAR) studies. This achievement also highlights the possibility of fine-tuning of relevant functional groups within the starting materials and intermediates to produce a larger number of closely related analogues. Such advances will eventually pave the way toward better application of stereochemical attributes in therapeutic and drug safety studies and may ultimately deliver more potent and selective lead molecules. We have shown that enantioselectivity within KRS-cladologs plays a key role in tuning the potency of these

compounds as effective antimalarial agents. Our explorations of the stereoisomeric configurations within eight cladologs using binding-, enzyme-, cell-, and structure-based probes provide a striking example of the value of chiral awareness in drug development (Figure 8). The eight cladologs fall into three potency classes (A, B, and C), and their drug-like properties remain consistent when accessed via binding-, activity-, and cell-based analysis. The structural rationale for selective inhibitory potential of class A over other cladolog classes seems to rest on the criticality of chiral positions at C3, C10, and C14. This work hence lays a foundation for tailoring cladologs for the development of leads against KRSs from other eukaryotic parasites where active site residues are conserved.^{10–12} The remarkable discovery of cladosporin (compound **12**) as a nanomolar range drug that targets the malarial lysyl-tRNA synthetase^{9,21,28} and subsequent related studies on *Loa loa* and *Schistosoma mansoni*¹² relied on the active configuration of compound **12** with absolute stereochemistry of 3*R*, 10*R*, 14*S*. This work now reveals how fortuitous it was to have identified the fungal metabolite cladosporin (compound **12**) as a possible lead against malaria. Aside from compound **16**, all other enantiomers of compound **12** would likely have been rejected due to lack of potency in killing parasites in acceptable ranges used in high throughput phenotypic screenings (Figure 8). The justified attention on compound **12** therefore rests on its absolute stereoisomeric configuration, and most variations centered on its chiral centers seem to possess moderate to poor antimalarial activity.

Apart from compound **12**, there are several other currently used antimalarial drugs that have not yet been viewed in this present stereochemical perspective. Therefore, investigations centered on stereochemical screening will underpin stereostructure–activity relationship (S-SAR) and may assist in lead optimization. For instance, mefloquine, a chiral antimalarial agent with two chiral centers, is manufactured and marketed as a racemate of (11*R*, 12*S*) and (11*S*, 12*R*) enantiomers.²² Studies indicate that plasma concentration of mefloquine (–)-enantiomer (11*R*, 12*S*) is higher as compared to the (+)-enantiomer (11*S*, 12*R*) as a result of which the former has a shorter half-life than the other.^{8,22} Data suggest that the mefloquine (+)-enantiomer is responsible for treating malaria, whereas the (–)-enantiomer binds to the adenosine receptor in the central nervous system leading to psychotic effects.^{8,22,23} In this context, Hall et al. had accomplished the asymmetric synthesis of all four stereoisomers of mefloquine and showed that out of the four isomers three (11*R*, 12*S*), (11*S*, 12*R*), and (11*S*, 12*S*) are active against *Plasmodium falciparum*.²⁴

CONCLUSION

In short, identification of key chiral attributes in a pathogen drug discovery routine is therefore critical, as exemplified by our analyses. More significantly, the synthesis and production of all eight dissymmetric versions of compound **12**, as described in this work, will now allow rapid tinkering with the optimum scaffolds for enhancing the drug-like properties of these moieties. The extension of studies with compound **12** based enzyme inhibition to other eukaryotic parasite where KRS active sites are conserved is also feasible, especially in context of neglected tropical diseases.^{12,26–31} Our overall message of the centrality of chiral awareness in modern drug development will be valuable in efforts focused on drugging pressing infectious disease problems.

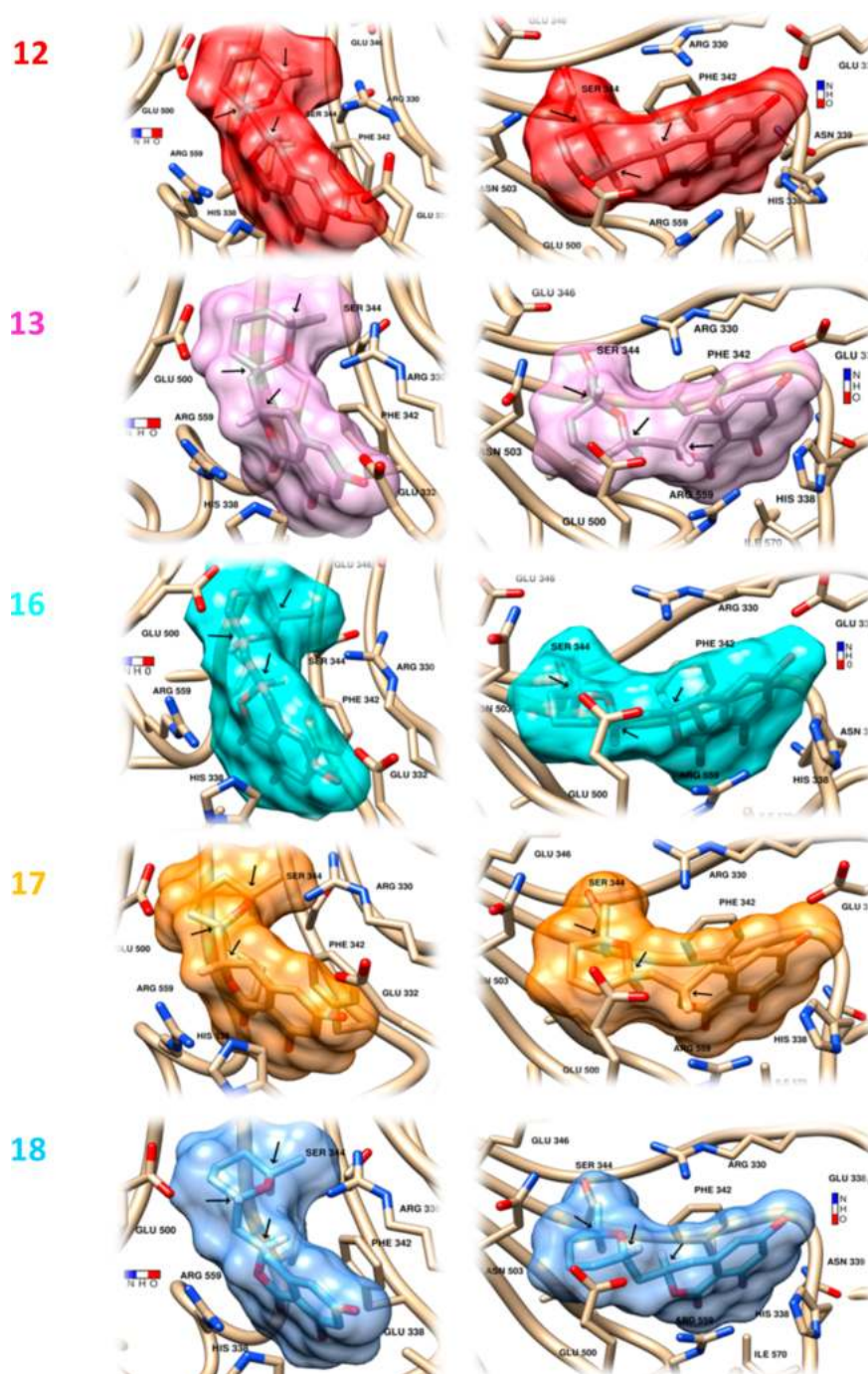


Figure 5. Two views for each cocrystal structure of *PfkRS* with a respective cladolog (compounds 12, 13, 16, 17, and 18). The mechanistically relevant binding modes are displayed; i.e., Arg559, Phe342, His338, Glu332, Arg330 stack with the isocoumarin ring, and Glu500, Glu346, Ser344 accommodate the THP fragment. Each cladolog along with relevant protein side chain residues are shown as sticks. PDB codes of compounds 12, 13, 16, 17, and 18 are 4HO2,¹¹ 5ZH5, 5ZH2, 5ZH3, and 5ZH4, respectively.

EXPERIMENTAL SECTION

General. All reactions were carried out in oven-dried glassware under a positive pressure of argon or nitrogen, unless otherwise mentioned, with magnetic stirring. Air sensitive reagents and solutions were transferred via syringe or cannula and were introduced to the apparatus via rubber septa. All reagents, starting materials, and solvents were obtained from commercial suppliers and used as such without further purification. Reactions were monitored by thin layer chromatography (TLC) with 0.25 mm precoated silica gel plates (60 F254). Visualization was accomplished with either UV light, iodine adsorbed on silica gel, or immersion in ethanolic solution of

phosphomolybdic acid (PMA), *p*-anisaldehyde, 2,4-DNP, KMnO₄ followed by heating with a heat gun for ~15 s. Column chromatography was performed on silica gel (100–200 or 230–400 mesh size). Deuterated solvents for NMR spectroscopic analyses were used as received. All ¹H NMR, ¹³C NMR spectra were obtained using a 400 MHz, 500 MHz spectrometer. Coupling constants were measured in hertz. All chemical shifts were quoted in ppm, relative to TMS, using the residual solvent peak as a reference standard. The following abbreviations were used to explain the multiplicities: s = singlet, d = doublet, t = triplet, q = quartet, m = multiplet, br = broad. HRMS (ESI) were recorded on ORBITRAP mass analyzer (Thermo Scientific, QExactive). Mass spectra were measured with ESI ionization

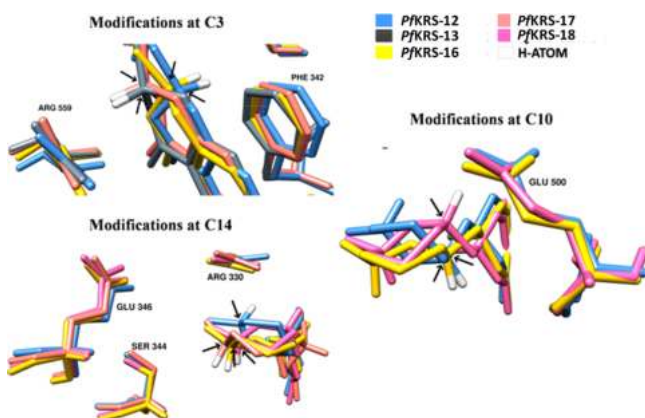


Figure 6. Structural analogy among most potent cladologs (compounds 12 and 16) and other cocrystallized ones (compounds 13, 17, and 18). The cladologs are superimposed and their chiral centers indicated with an arrow. For C3 the interacting residues of Arg 559 and Phe 342 are shown; for C10 the residue Glu500 is shown, and for C14 residues Glu346, Ser 344, and Arg 330 are shown. In compound 12/16 (3*R*), C3 H atom is more accessible to Phe342 as compared to compounds 13 and 17 (3*S*). C10 H atom in compound 18 (10*S*) as compared to compounds 12 and 16 (3*R*) stacks proximately to Glu500 side chain. As compared to compound 16/17/18, C14 H atom in compound 12 is adjacent to Arg330.

in MSQ LCMS mass spectrometer. Infrared (IR) spectra were recorded on a FT-IR spectrometer as a thin film. Chemical nomenclature was generated using ChemBiodraw Ultra 14.0. Melting points of solids were measured in melting point apparatus (Buchi S65). Optical rotation values were recorded on P-2000 polarimeter at 589 nm. All chemicals were used as received. THF, DCM, toluene, diethyl ether were used from SPS. All reactions under standard conditions were monitored by thin-layer chromatography (TLC) on gel F254 plates. The silica gel (200–300 meshes) was used for column chromatography, and the distillation range of petroleum was 60–90 °C. ¹H and ¹³C NMR spectral data were reported in ppm relative to tetramethylsilane (TMS) as internal standard. High-resolution mass spectra (HRMS) were recorded using a Fourier transform ion cyclotron resonance (FT-ICR) mass spectrometer. Purity of products was determined by reverse phase HPLC analysis using Agilent Technologies 1200 series. Column: ZORBAX Eclipse XBD-C-18 (4.6 mm × 250 mm, 5 μm). Flow rate 1.00 mL/min, UV 254 nm; using mobile phases, method 70/30 CH₃CN/H₂O for 10 min. Purity of all the final compounds is >95% as determined by the above method.

1. (5*E*)-8-((*tert*-Butyldimethylsilyloxy)non-3-en-2-one (3). A solution of compound 1 (18 g, 78.809 mmol) in 500 mL of CH₂Cl₂ was stirred at −78 °C as ozone was passed through the same. Once blue color was observed, oxygen was passed to remove the excess ozone until the solution became colorless. Triphenylphosphine (30.9 g, 118.188 mmol) was added, and the reaction mixture was allowed to reach room temperature and stirred for an additional 12 h. The resulting solution of aldehyde was cooled to 0 °C and 1-(triphenyl-1*S*-phosphanylidene)propan-2-one 2 (62.723 g, 197.021 mmol) was added portionwise in one pot and left to stir for 16 h. The resultant solution was concentrated under vacuo and filtered through silica and forwarded to next step without further purification.

2. (8*S,E*)-8-((*tert*-Butyldimethylsilyloxy)non-3-en-2-ol (4). To a solution of 3 (10 g, 36.968 mmol) in CH₂Cl₂ (150 mL) and CH₃OH (50 mL) (3:1 v/v) was added CeCl₃·7H₂O (16.5 g, 44.362 mmol) at 0 °C and stirred for 30 min. NaBH₄ (1.5 g, 40.667 mmol) was added portionwise to the stirring solution at the same temperature, and the reaction mixture was allowed to reach room temperature and stirred for 12 h. Reaction mixture was cooled to 0 °C, and saturated aqueous solution of sodium potassium tartarate (50 mL) was added to the reaction flask and stirred for 15 min followed by evaporation of CH₃OH and CH₂Cl₂ under vacuo. To the remaining

aqueous mixture was added 1 N HCl (100 mL) and extracted with ethyl acetate. The collected organic parts were dried over sodium sulfate, concentrated under vacuo, and purified through column chromatography (silica gel 230–400 mesh 10% ethyl acetate–pet ether) to afford compound 5 (8.9 g, 88%) as a colorless oil (1:1 diastereomeric mixture). IR ν_{max} (film): cm^{−1} 1728, 3431, 2938, 1250. ¹H NMR (400 MHz, CDCl₃): δ 5.65–5.58 (m, 1H), 5.53–5.47 (m, 1H), 4.27–4.22 (m, 1H), 3.79–3.75 (m, 1H), 2.03–2.00 (m, 2H), 1.44–1.37(m, 4H), 1.25 (d, *J* = 6.4 Hz, 3H), 1.11 (d, *J* = 5.9 Hz, 3H), 0.88 (s, 9H), 0.04 (s, 6H). ¹³C NMR (100 MHz, CDCl₃): δ 134.2, 130.9, 68.9, 68.4, 39.1, 32.1, 25.9, 25.3, 23.8, 23.4, 18.1, −4.4, −4.7. HRMS calculated for C₁₅H₃₂O₂Si [M + Na]⁺ 295.2062, observed 295.2064.

3. (8*S,E*)-Non-3-ene-2,8-diol (5). To a solution of compound 4 (8.9 g, 32.660 mmol) in THF (50 mL) was added tetrabutylammonium fluoride solution (1 M in THF) (65 mL, 65.32 mmol) at 0 °C. After stirring for 12 h at room temperature, reaction mixture was cooled to 0 °C, saturated aqueous NH₄Cl (40 mL) was added to the same and extracted with excess ethyl acetate several times. The collected organic layers were dried over sodium sulfate, concentrated under vacuo, and purified via column chromatography (silica gel 230–400 mesh, 50% ethyl acetate–pet ether) to give compound 5 (4.4 g, 85%) as a pale-yellow oil (1:1 diastereomeric mixture). IR ν_{max} (film): cm^{−1}1719, 3020, 1217, 1369. ¹H NMR (400 MHz, CDCl₃): δ 5.62–5.57 (m, 1H), 5.52–5.47 (m, 1H), 4.23 (t, *J* = 6.4 Hz, 1H), 3.79–3.75 (m, 1H), 2.10 (br s, 2H), 2.01 (d, *J* = 6.1 Hz, 2H), 1.50–1.39 (m, 4H), 1.23 (d, *J* = 6.1 Hz, 3H), 1.16 (d, *J* = 6.1 Hz, 3H). ¹³C NMR (100 MHz, CDCl₃): δ 134.5, 130.5, 68.8, 67.9, 38.6, 31.9, 25.2, 23.4, 23.4. HRMS calculated for C₉H₁₈O₂ [M + Na]⁺ 181.1198, observed 181.1199.

4. Fragment A. Bis(acetonitrile)dichloropalladium(II) (0.72 g, 2.78 mmol) was added to a solution of compound 5 (4.4 g, 27.806 mmol) in THF at 0 °C and stirred for 30 min at the same temperature. After completion of the reaction which was monitored through TLC, resultant reaction mixture was filtered through a pad of Celite and concentrated via rotary evaporation at low temperature to afford fragment A as a colorless oil (1:1 diastereomeric mixture) which was forwarded to next step without further purification. HRMS calculated for C₉H₁₇O [M + H]⁺ 141.1274, observed 141.1269.

5. Methyl 2,4-Dimethoxy-6-((*E*)-3-((2*R*,6*S*)-6-methyltetrahydro-2*H*-pyran-2-yl)allyl)benzoate (6a) and Methyl 2,4-Dimethoxy-6-((*E*)-3-((2*S*,6*S*)-6-methyltetrahydro-2*H*-pyran-2-yl)allyl)benzoate (6b). A solution of fragment B (2.0 g, 8.465 mmol) in CH₂Cl₂ (50 mL) was degassed with argon for 15 min. Solution of fragment A in CH₂Cl₂ was added in the same followed by addition of 5 mol % of the Grubbs' second generation catalyst. The reaction mixture was stirred at room temperature for 36 h. It was then filtered through a short pad of Celite and concentrated under reduced pressure to remove excess CH₂Cl₂. Careful purification by silica gel chromatography (silica gel 230–400 mesh, 25% ethyl acetate–pet ether) allowed the separation of two diastereomers 6a (0.570g) and 6b (0.540g) with a combined yield of 53%.

Compound 6a. [α]_D²⁵ −5.09 (*c* 1.6, CHCl₃). IR ν_{max} (film): cm^{−1}1712, 1215, 3020, 1604. ¹H NMR (400 MHz, CDCl₃): δ 6.32 (s, 2H), 5.73–5.60 (m, 2H), 4.32 (d, *J* = 3.9 Hz, 1H), 3.87 (s, 1H), 3.85 (s, 3H), 3.78 (s, 6H), 3.34 (d, *J* = 5.9 Hz, 2H), 1.74–1.67 (m, 1H), 1.61–1.59 (m, 3H), 1.53–1.50 (m, 1H), 1.31–1.23 (m, 1H), 1.14 (d, *J* = 6.4 Hz, 3H). ¹³C NMR (100 MHz, CDCl₃): δ 168.5, 161.5, 158.2, 140.6, 132.5, 129.6, 116.2, 106.0, 96.6, 71.7, 67.1, 55.9, 55.3, 52.0, 36.8, 32.2, 29.4, 20.6, 18.6. HRMS calculated for C₁₉H₂₇O₅ [M + H]⁺ 335.1853, observed 335.1839.

Compound 6b. [α]_D²⁵ −3.14 (*c* 1.6, CHCl₃). IR ν_{max} (film): cm^{−1}1782, 1214, 1332, 3020. ¹H NMR (400 MHz, CDCl₃): δ 6.32 (s, 2H), 5.74–5.68 (m, 1H), 5.54 (dd, *J* = 6.4, 15.2 Hz, 1H), 3.84 (s, 3H), 3.79 (m, 7H), 3.49–3.43 (m, 1H), 3.32 (d, *J* = 6.4 Hz, 2H), 1.81–1.78 (m, 1H), 1.58–1.47 (m, 4H), 1.28 (dd, *J* = 3.7, 11.5 Hz, 1H), 1.17 (d, *J* = 6.4 Hz, 3H). ¹³C NMR (100 MHz, CDCl₃): δ 168.4, 161.5, 158.2, 140.5, 133.3, 128.9, 116.2, 106.1, 96.5, 78.0, 73.7, 55.9, 55.3, 52.0, 36.8, 33.0, 31.4, 23.5, 22.2. HRMS calculated for C₁₉H₂₇O₅ [M + H]⁺ 335.1853, observed 335.1840.

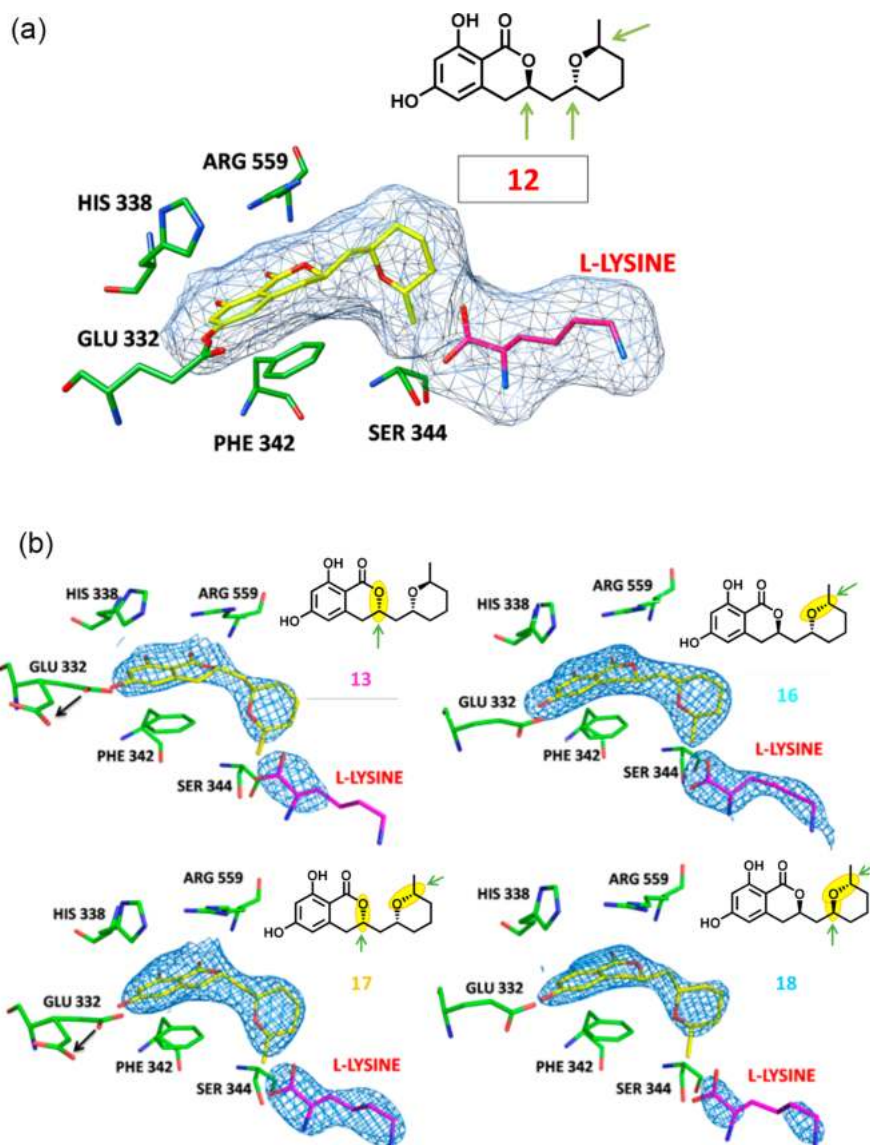


Figure 7. (a) Cladolog-induced rotameric changes in PfKRS side chains. Molecule surfaces for L-lysine and compound 12 are as in the published crystal structure of PfKRS-K-compound 12.¹¹ (b) Simulated annealing omit maps are shown for cladologs and L-lysine in the new PfKRS-K-cladolog complexes.

6. 3-(Hydroxy((2*R*,6*S*)-6-methyltetrahydro-2*H*-pyran-2-yl)-methyl)-6,8-dimethoxyisochroman-1-one (7a). To a solution of compound 6a (0.714 g, 2.135 mmol) in acetone (12 mL) and water (6 mL) was added 4-methylmorpholine *N*-oxide (0.749 g, 6.405 mmol) followed by the careful addition of catalytic amount of 2.5% OsO₄ (*tert*-butanol solution) at 0 °C. After stirring for 12 h at room temperature saturated aqueous solution of Na₂SO₃ (15 mL) was added and further stirred for 6 h at room temperature. Excess acetone was removed under vacuo, and the remaining aqueous part was extracted with ethyl acetate (3 × 30 mL). The combined organic parts were dried over sodium sulfate and concentrated under vacuo. Purification through column chromatography (silica gel 100–200 mesh 10% ethyl acetate–pet ether) afforded compound 7a (0.382 g) (3:2 diastereomeric mixture) as colorless oil with a yield of 53%. IR ν_{\max} (film): cm⁻¹ 3021, 1722, 1599, 1217. ¹H NMR (400 MHz, CDCl₃): δ 6.38 (s, 1H), 6.31 (s, 1H), 4.68–4.39 (m, 1H), 4.12–3.97 (m, 1H), 3.90–3.89 (m, 3H), 3.86 (s, 1H), 3.84 (s, 3H), 3.68–3.54 (m, 1H), 3.34–3.20 (m, 1H), 2.75–2.64 (m, 1H), 2.32 (br s, 1H), 1.86–1.82 (m, 1H), 1.70–1.62 (m, 3H), 1.55–1.49 (m, 1H), 1.34–1.31 (m, 1H), 1.24–1.15 (m, 3H). ¹³C NMR (100 MHz, CDCl₃): δ 164.5, 164.4, 163.1, 163.0, 162.3, 144.2, 144.1, 106.6, 104.0, 97.7, 76.7, 75.8, 73.1, 68.9, 68.8, 68.6, 68.4, 56.1, 55.5, 31.8, 31.1, 30.7, 30.0, 27.0, 26.6, 18.7, 18.1,

17.8. HRMS calculated for C₁₈H₂₅O₆ [M + H]⁺ 337.1646, observed 337.1635.

7. 3-(Hydroxy((2*S*,6*S*)-6-methyltetrahydro-2*H*-pyran-2-yl)-methyl)-6,8-dimethoxyisochroman-1-one (7b). Compound 7b (0.432 g) with a yield of 60% was synthesized as 1:1 diastereomeric mixture from compound 6b using similar procedure for the synthesis of compound 7a. IR ν_{\max} (film): cm⁻¹ 3021, 2403, 1721, 1601, 1216. ¹H NMR (400 MHz, CDCl₃): δ 6.39 (s, 1H), 6.33 (s, 1H), 4.76–4.43 (m, 1H), 3.91 (d, *J* = 5.5 Hz, 3H), 3.85 (s, 3H), 3.74–3.41 (m, 3H), 3.36–3.24 (m, 1H), 2.75–2.63 (m, 1H), 2.11–1.94 (m, 1H), 1.85–1.78 (m, 2H), 1.61–1.52 (m, 2H), 1.40–1.31 (m, 1H), 1.17–1.08 (m, 3H). ¹³C NMR (100 MHz, CDCl₃): δ 164.5, 164.4, 163.1, 163.0, 162.5, 162.2, 144.4, 144.2, 106.7, 106.7, 104.0, 103.9, 97.7, 76.5, 76.0, 75.5, 74.5, 74.1, 73.9, 56.1, 55.5, 33.3, 33.0, 31.7, 31.1, 28.1, 26.7, 23.1, 23.0, 22.1. HRMS calculated for C₁₈H₂₅O₆ [M + H]⁺ 337.1646, observed 337.1632.

8. *O*-((*S*)-((*S*)-6,8-Dimethoxy-1-oxoisochroman-3-yl))((2*R*,6*S*)-6-methyltetrahydro-2*H*-pyran-2-yl)methyl) *S*-Methyl Carbonodithioate (9a) and *O*-((*R*)-((*R*)-6,8-Dimethoxy-1-oxoisochroman-3-yl))((2*R*,6*S*)-6-methyltetrahydro-2*H*-pyran-2-yl)methyl) *S*-Methyl Carbonodithioate (8a). To a solution of 7a (0.382 g, 1.136 mmol) (1:1 diastereomeric mixture) in THF (30 mL) was added LiHMDS (1 M in THF) (1.2 mL) at 0 °C. After 15 min CS₂

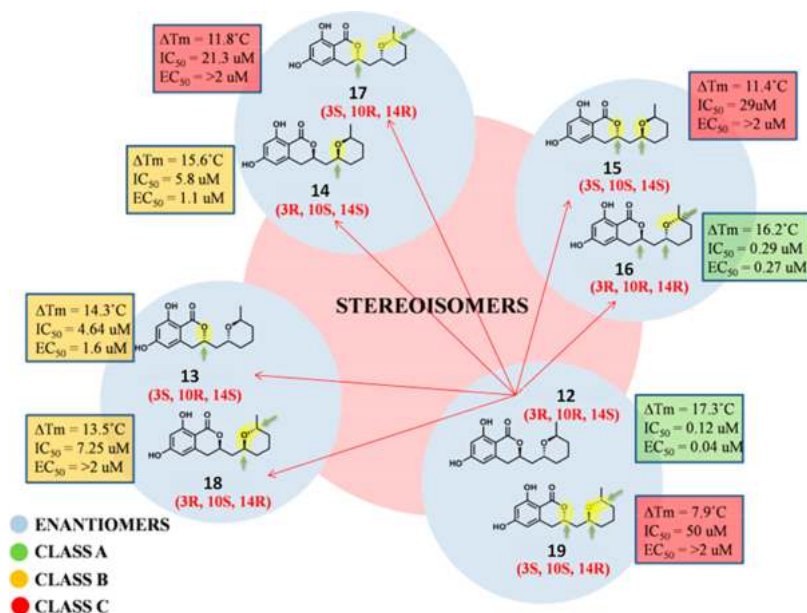


Figure 8. Overview of cladolog potency.

(137 μL , 2.271 mmol) was added, which was followed by the addition of CH_3I (283 μL , 4.542 mmol). After stirring the reaction mixture for 12 h, H_2O (10 mL) was added to the same and extracted with ethyl acetate. The combined organic layers were dried over sodium sulfate and concentrated under vacuo. Purification through flash chromatography 28% ethyl acetate–pet ether gave clean separation of the two diastereomers **8a** (0.227 g) and **9a** (0.151 g) as foamy solids with an overall yield of 78%.

Compound 8a. $[\alpha]_D^{25} +15.99$ (c 1.6, CHCl_3). IR ν_{max} (film): cm^{-1} 3024, 1640, 1430, 1217, 766. $^1\text{H NMR}$ (400 MHz, CDCl_3): δ 6.38 (s, 1H), 6.29 (s, 1H), 6.19 (d, $J = 9.8$ Hz, 1H), 4.86 (d, $J = 11.6$ Hz, 1H), 4.43–4.39 (m, 1H), 3.91 (s, 4H), 3.83 (s, 3H), 2.99 (dd, $J = 12.5$, 15.6 Hz, 1H), 2.74 (dd, $J = 2.4$, 15.9 Hz, 1H), 2.56 (s, 3H), 1.68–1.65 (m, 4H), 1.38–1.30 (m, 2H), 1.20 (d, $J = 6.7$ Hz, 3H). $^{13}\text{C NMR}$ (100 MHz, CDCl_3): δ 217.2, 164.4, 163.0, 161.9, 143.5, 106.9, 103.8, 97.9, 80.6, 74.2, 68.6, 66.9, 56.1, 55.5, 31.7, 30.9, 26.1, 19.2, 18.2. HRMS calculated for $\text{C}_{20}\text{H}_{27}\text{O}_6\text{S}_2$ $[\text{M} + \text{H}]^+$ 427.1244, observed 427.1230.

Compound 9a. $[\alpha]_D^{25} -18.78$ (c 1.5, CHCl_3). IR ν_{max} (film): cm^{-1} 3025, 1639, 1431, 1218, 769. $^1\text{H NMR}$ (400 MHz, CDCl_3): δ 6.39 (s, 1H), 6.31 (s, 1H), 6.21 (dd, $J = 3.1$, 6.7 Hz, 1H), 4.68 (td, $J = 2.8$, 11.4 Hz, 1H), 4.36–4.32 (m, 1H), 4.04–4.02 (m, 1H), 3.90 (s, 3H), 3.84 (s, 3H), 3.08 (dd, $J = 11.6$, 15.9 Hz, 1H), 2.89–2.80 (m, 1H), 2.57 (s, 3H), 1.71 (dd, $J = 4.3$, 7.9 Hz, 2H), 1.61–1.54 (m, 2H), 1.40–1.28 (m, 2H), 1.16 (d, $J = 6.1$ Hz, 3H). $^{13}\text{C NMR}$ (100 MHz, CDCl_3): δ 217.2, 164.5, 163.1, 161.6, 143.3, 106.7, 103.9, 98.0, 82.1, 75.4, 69.5, 68.5, 56.2, 55.6, 31.5, 30.6, 26.5, 19.0, 18.9, 18.4. HRMS calculated for $\text{C}_{20}\text{H}_{27}\text{O}_6\text{S}_2$ $[\text{M} + \text{H}]^+$ 427.1244, observed 427.1231.

9. O-((R)-6,8-Dimethoxy-1-oxoisochroman-3-yl)((2S,6S)-6-methyltetrahydro-2H-pyran-2-yl)methyl) S-Methyl Carbonodithioate (8b) and O-((S)-((S)-6,8-Dimethoxy-1-oxoisochroman-3-yl)((2S,6S)-6-methyltetrahydro-2H-pyran-2-yl)methyl) S-Methyl Carbonodithioate (9b). Compounds **8b** (0.195 g) and **9b** (0.190 g) with an overall yield of 70% was synthesized from compound **7b** as a semisolid by following similar procedure for the synthesis of compounds **8a** and **9a**.

Compound 8b. $[\alpha]_D^{25} +95.92$ (c 0.6, CHCl_3). IR ν_{max} (film): cm^{-1} 3023, 1640, 1431, 1218, 768. $^1\text{H NMR}$ (400 MHz, CDCl_3): δ 6.39 (s, 1H), 6.31 (s, 1H), 6.00 (t, $J = 4.9$ Hz, 1H), 4.76 (td, $J = 3.3$, 11.1 Hz, 1H), 3.94 (d, $J = 5.5$ Hz, 1H), 3.90 (s, 3H), 3.84 (s, 3H), 3.47–3.40 (m, 1H), 3.13 (dd, $J = 11.3$, 16.2 Hz, 1H), 2.86 (dd, $J = 2.4$, 16.5 Hz, 1H), 2.57 (s, 3H), 1.86–1.82 (m, 1H), 1.66–1.62 (m, 2H), 1.56–1.51 (m, 1H), 1.44–1.37 (m, 1H), 1.19 (dd, $J = 3.7$, 11.0 Hz, 1H), 1.12 (d, $J = 6.1$ Hz, 3H). $^{13}\text{C NMR}$ (100 MHz, CDCl_3): δ 217.1, 164.5,

163.1, 161.7, 143.4, 106.8, 103.9, 97.9, 83.0, 75.8, 75.0, 74.3, 56.2, 55.6, 32.9, 31.5, 26.7, 23.2, 22.1, 19.1. HRMS calculated for $\text{C}_{20}\text{H}_{27}\text{O}_6\text{S}_2$ $[\text{M} + \text{H}]^+$ 427.1244, observed 427.1228.

Compound 9b. $[\alpha]_D^{25} -146.8$ (c 0.5, CHCl_3). IR ν_{max} (film): cm^{-1} 3022, 1640, 1430, 1217, 768. $^1\text{H NMR}$ (400 MHz, CDCl_3): δ 6.38 (s, 1H), 6.28 (s, 1H), 5.96 (d, $J = 9.2$ Hz, 1H), 4.94 (d, $J = 11.6$ Hz, 1H), 4.08 (t, $J = 10.1$ Hz, 1H), 3.91 (s, 3H), 3.83 (s, 3H), 3.51 (dd, $J = 5.8$, 10.7 Hz, 1H), 3.01–2.94 (m, 1H), 2.76–2.71 (m, 1H), 2.56 (s, 3H), 1.82 (d, $J = 12.8$ Hz, 1H), 1.62–1.47 (m, 4H), 1.20–1.16 (m, 1H), 1.11 (d, $J = 5.5$ Hz, 3H). $^{13}\text{C NMR}$ (100 MHz, CDCl_3): δ 217.3, 164.5, 163.2, 162.3, 143.7, 106.9, 103.8, 103.8, 97.9, 82.6, 74.0, 73.3, 56.2, 55.5, 33.2, 31.6, 27.5, 22.8, 22.0, 19.3. HRMS calculated for $\text{C}_{20}\text{H}_{27}\text{O}_6\text{S}_2$ $[\text{M} + \text{H}]^+$ 427.1244, observed 427.1230.

10. (R)-6,8-Dimethoxy-3-((2R,6S)-6-methyltetrahydro-2H-pyran-2-yl)methyl)isochroman-1-one (10a). Compound **8a** (0.227 g, 0.532 mmol) was dissolved in toluene which was followed by the addition of AIBN (8.7 mg, 0.053 mmol) and tributyltin hydride (430 μL , 1.596 mmol). The reaction mixture was stirred at 95°C for 4 h. After completion of the reaction toluene was evaporated under vacuo and the crude was purified by column chromatography which afforded compound **10a** (0.106 mg) as a foamy solid with 62% yield. $[\alpha]_D^{25} +36.76$ (c 1.5, CHCl_3). IR ν_{max} (film): cm^{-1} 3014, 2852, 1713, 1599, 1220. $^1\text{H NMR}$ (400 MHz, CDCl_3): δ 6.38 (s, 1H), 6.28 (s, 1H), 4.58–4.53 (m, 1H), 4.06 (t, $J = 8.2$ Hz, 1H), 3.92 (s, 1H), 3.90 (s, 3H), 3.84 (s, 3H), 2.91–2.77 (m, 2H), 1.88–1.80 (m, 2H), 1.73–1.62 (m, 4H), 1.33–1.27 (m, 2H), 1.18 (d, $J = 6.1$ Hz, 3H). $^{13}\text{C NMR}$ (100 MHz, CDCl_3): δ 164.3, 163.0, 162.8, 144.0, 107.1, 103.8, 97.7, 77.4, 76.7, 66.1, 56.1, 55.5, 39.6, 35.5, 31.0, 30.8, 18.8, 18.2. HRMS calculated for $\text{C}_{18}\text{H}_{25}\text{O}_5$ $[\text{M} + \text{H}]^+$ 321.1697, observed 321.1691.

11. (S)-6,8-Dimethoxy-3-((2R,6S)-6-methyltetrahydro-2H-pyran-2-yl)methyl)isochroman-1-one (11a). Compound **11a** (69 mg) with a yield of 61% was synthesized as a semisolid from compound **9a** using similar procedure for the synthesis of compound **10a**. $[\alpha]_D^{25} -10.88$ (c 1.8, CHCl_3). IR ν_{max} (film): cm^{-1} 3015, 2853, 1709, 1599, 1219. $^1\text{H NMR}$ (400 MHz, CDCl_3): δ 6.39 (s, 1H), 6.30 (s, 1H), 4.55–4.48 (m, 1H), 4.03 (dd, $J = 4.3$, 9.2 Hz, 1H), 3.91 (s, 3H), 3.85 (s, 3H), 2.96–2.87 (m, 2H), 2.40–2.33 (m, 1H), 1.73–1.60 (m, 5H), 1.40–1.28 (m, 3H), 1.15 (d, $J = 6.1$ Hz, 3H). $^{13}\text{C NMR}$ (100 MHz, CDCl_3): δ 164.3, 163.1, 162.7, 144.0, 107.0, 103.9, 97.8, 74.6, 66.9, 56.1, 55.5, 37.5, 34.3, 31.5, 29.9, 19.7, 18.2. HRMS calculated for $\text{C}_{18}\text{H}_{25}\text{O}_5$ $[\text{M} + \text{H}]^+$ 321.1697, observed 321.1690.

12. (R)-6,8-Dimethoxy-3-((2S,6S)-6-methyltetrahydro-2H-pyran-2-yl)methyl)isochroman-1-one (10b). Compound **10b** (88 mg) with a yield of 60% was synthesized from compound **8b** as

a foamy solid using similar procedure for the synthesis of **10a** and **11a**. $[\alpha]_D^{25} + 78.26$ (c 1.0, CHCl₃). IR ν_{\max} (film): cm⁻¹ 3015, 2931, 1704, 1598, 1218. ¹H NMR (400 MHz, CDCl₃): δ 6.39 (s, 1H), 6.31 (s, 1H), 4.59–4.52 (m, 1H), 3.91 (s, 3H), 3.85 (s, 3H), 3.63 (td, $J = 5.5, 11.0$ Hz, 1H), 3.46–3.39 (m, 1H), 3.00–2.81 (m, 2H), 2.09 (dt, $J = 7.0, 14.0$ Hz, 1H), 1.82–1.72 (m, 2H), 1.63–1.44 (m, 4H), 1.21–1.17 (m, 1H), 1.13 (d, $J = 6.1$ Hz, 3H). ¹³C NMR (100 MHz, CDCl₃): δ 164.3, 163.1, 162.8, 144.1, 107.0, 103.9, 97.7, 74.4, 73.8, 73.5, 56.1, 55.5, 40.8, 34.7, 33.2, 31.0, 23.5, 22.2. HRMS calculated for C₁₈H₂₄O₅Na [M + Na]⁺ 343.1516, observed 343.1510.

13. (S)-6,8-Dimethoxy-3-(((2S,6S)-6-methyltetrahydro-2H-pyran-2-yl)methyl)isochroman-1-one (11b). Compound **11b** (83 mg) with a yield of 58% was synthesized as a yellowish oil from compound **9b** following similar procedure for the synthesis of compounds **10a**, **11a**, and **10b**. $[\alpha]_D^{25} - 121.78$ (c 0.3, CHCl₃). IR ν_{\max} (film): cm⁻¹ 3015, 2931, 1704, 1598, 1218. ¹H NMR (400 MHz, CDCl₃): δ 6.39 (s, 1H), 6.28 (s, 1H), 4.69–4.64 (m, 1H), 3.91 (s, 3H), 3.84 (s, 3H), 3.70 (t, $J = 10.7$ Hz, 1H), 3.46–3.39 (m, 1H), 2.90–2.75 (m, 2H), 1.88–1.77 (m, 2H), 1.72–1.66 (m, 2H), 1.57–1.51 (m, 3H), 1.19–1.16 (m, 1H), 1.11 (d, $J = 6.1$ Hz, 3H). ¹³C NMR (100 MHz, CDCl₃): δ 164.3, 163.0, 144.1, 107.1, 103.8, 97.7, 73.8, 73.7, 73.0, 56.1, 55.5, 41.7, 35.5, 33.2, 31.6, 23.6, 22.1. HRMS calculated for C₁₈H₂₄O₅Na [M + Na]⁺ 343.1516, observed 343.1510.

14. Cladosporin (Compound 12). A suspension of aluminum powder (106 mg, 0.331 mmol) in dry benzene (5 mL) was treated with I₂ (1.3 g, 5.293 mmol) under argon, and the violet mixture was stirred under reflux for 30 min until the violet color disappeared. After the mixture was cooled to 0 °C, few crystals of TBAI (10.6 mg, 0.033 mmol) and phloroglucinol (208.6 mg, 1.654 mmol) were added before a solution of compound **10a** (106 mg, 0.331 mmol) in dry benzene (3 mL) was added in one portion. The resulting green-brown suspension was stirred for 30 min at 5 °C before saturated Na₂S₂O₃ solution (8 mL) and ethyl acetate (8 mL) were added. After separation of the layers, the aqueous phase was extracted with ethyl acetate. The combined organic layers were washed with brine, dried over Na₂SO₄, filtered, and concentrated in vacuo. Purification by column chromatography afforded cladosporin (compound **12**) (0.052 g) as a white solid with a yield of 54%. Melting point: 171–173 °C. $[\alpha]_D^{25} - 15.75$ (c 0.6, EtOH). IR ν_{\max} (film): cm⁻¹ 3416, 3022, 1656, 1218. ¹H NMR (400 MHz, CDCl₃): δ 11.06 (s, 1H), 7.47 (br s, 1H), 6.29 (s, 1H), 6.16 (s, 1H), 4.68 (t, $J = 9.8$ Hz, 1H), 4.12 (s, 1H), 4.01 (s, 1H), 2.89–2.75 (m, 2H), 2.00–1.94 (m, 1H), 1.87–1.81 (m, 1H), 1.70–1.63 (m, 4H), 1.35 (d, $J = 6.1$ Hz, 2H), 1.23 (d, $J = 6.7$ Hz, 3H). ¹³C NMR (100 MHz, CDCl₃): δ 169.9, 164.3, 163.1, 141.8, 106.7, 102.0, 101.5, 76.3, 68.0, 66.6, 39.3, 33.6, 30.9, 18.9, 18.1. HRMS calculated for C₁₆H₂₁O₅ [M + H]⁺ 293.1384, observed 293.1379.

15. (S)-6,8-Dihydroxy-3-(((2R,6S)-6-methyltetrahydro-2H-pyran-2-yl)methyl)isochroman-1-one (Compound 13). Compound **13** (0.031 g) with a yield of 49% was synthesized as a white solid from compound **11a** following similar procedure for the synthesis of compound **12**. Melting point: 134–138 °C. $[\alpha]_D^{25} - 100.7$ (c 0.5, CHCl₃). IR ν_{\max} (film): cm⁻¹ 3413, 3023, 1657, 1218. ¹H NMR (400 MHz, CDCl₃): δ 11.11 (s, 1H), 7.19 (br s, 1H), 6.31 (s, 1H), 6.17 (s, 1H), 4.67 (s, 1H), 4.14–4.09 (m, 1H), 3.95 (s, 1H), 2.92–2.91 (m, 2H), 2.43 (br s, 1H), 1.83–1.69 (m, 5H), 1.39–1.33 (m, 2H), 1.20 (d, $J = 6.1$ Hz, 3H). ¹³C NMR (100 MHz, CDCl₃): δ 170.0, 164.4, 163.0, 141.6, 106.7, 102.0, 101.6, 76.6, 67.4, 67.2, 37.3, 32.6, 31.5, 29.8, 19.7, 18.1. HRMS calculated for C₁₆H₂₁O₅ [M + H]⁺ 293.1384, observed 293.1379.

16. (R)-6,8-Dihydroxy-3-(((2S,6S)-6-methyltetrahydro-2H-pyran-2-yl)methyl)isochroman-1-one (Compound 14). Compound **14** (0.043 g) was synthesized with a yield of 57% as a white solid from compound **10b** using similar procedure for the synthesis of compound **12** and compound **13**. Melting point: 194–199 °C. $[\alpha]_D^{25} + 46.44$ (c 0.5, EtOH). IR ν_{\max} (film): cm⁻¹ 3416, 3022, 1656, 1218. ¹H NMR (400 MHz, CD₃OD): δ 6.23 (s, 1H), 6.20 (s, 1H), 4.74–4.67 (m, 1H), 3.63–3.58 (m, 1H), 3.52–3.46 (m, 1H), 2.97–2.86 (m, 2H), 2.07–2.00 (m, 1H), 1.84–1.77 (m, 2H), 1.67–1.53 (m, 3H), 1.28–1.18 (m, 2H), 1.13 (d, $J = 6.1$ Hz, 3H). ¹³C NMR (101 MHz, CD₃OD): δ 171.7, 166.4, 165.8, 143.6, 108.1, 102.3, 101.8, 78.0, 75.5,

75.2, 42.2, 34.5, 33.8, 32.5, 24.7, 22.6. HRMS calculated for C₁₆H₂₁O₅ [M + H]⁺ 293.1384, observed 293.1379.

17. (S)-6,8-Dihydroxy-3-(((2S,6S)-6-methyltetrahydro-2H-pyran-2-yl)methyl)isochroman-1-one (Compound 15). Compound **15** (0.037 g) was synthesized from compound **11b** with a yield of 49% as a white solid using similar procedure for the synthesis of compound **12**, compound **13**, and compound **14**. Melting point: 154–157 °C. $[\alpha]_D^{25} - 5.0$ (c 0.4, CHCl₃). IR ν_{\max} (film): cm⁻¹ 3422, 3020, 1659, 1630, 1216. ¹H NMR (400 MHz, CD₃OD): δ 6.21 (s, 1H), 6.20 (s, 1H), 4.77–4.71 (m, 1H), 3.69–3.64 (m, 1H), 3.52–3.45 (m, 1H), 2.94–2.84 (m, 2H), 1.92–1.72 (m, 4H), 1.61–1.58 (m, 3H), 1.22–1.17 (dd, $J = 4.3, 11.6$ Hz, 1H), 1.14 (d, $J = 6.7$ Hz, 3H). ¹³C NMR (100 MHz, CD₃OD): δ 171.7, 166.4, 165.8, 143.7, 108.0, 102.3, 101.7, 77.6, 75.3, 74.8, 43.0, 34.6, 34.5, 33.1, 24.8, 22.5. HRMS calculated for C₁₆H₂₁O₅ [M + H]⁺ 293.1384, observed 293.1382.

18. (R,E)-8-((tert-Butyldimethylsilyloxy)non-3-en-2-one (R3). Compound **R3** was synthesized from compound **R1** as a colorless liquid by following similar procedure for the synthesis of **3**. The compound was filtered through silica and forwarded to next step without further characterization.

19. (8R,E)-8-((tert-Butyldimethylsilyloxy)non-3-en-2-ol (R4). The compound **R4** (8 g, 82%) was synthesized (1:1 diastereomeric mixture) from compound **R3** as a white colorless oil by following similar procedure for the synthesis of compound **4**. ¹H NMR (200 MHz, CDCl₃): δ 5.67–5.52 (m, 2H), 4.26 (t, $J = 5.9$ Hz, 1H), 3.82–3.76 (m, 1H), 2.06–2.00 (m, 1H), 1.61 (s, 2H), 1.42–1.38 (m, 4H), 1.25 (d, $J = 6.3$ Hz, 3H), 1.11 (d, $J = 6.1$ Hz, 3H), 0.88 (s, 9H), 0.04 (s, 6H).

20. (8R,E)-Non-3-ene-2,8-diol (R5). Compound **R5** (3.7 g, 87%) was synthesized from compound **R4** as a colorless oil by following similar procedure for the synthesis of compound **5**. ¹H NMR (200 MHz, CDCl₃): δ 5.70–5.45 (m, 2H), 4.28–4.19 (m, 1H), 3.83–3.75 (m, 1H), 2.05–2.02 (m, 2H), 1.61 (br s, 2H), 1.49–1.40 (m, 4H), 1.24 (d, $J = 6.3$ Hz, 3H), 1.18 (d, $J = 6.2$ Hz, 3H).

21. Fragment A'. Fragment A' was synthesized from compound **R5** as a pale yellow oil by following similar procedure for the synthesis of fragment A.

22. Methyl 2,4-Dimethoxy-6-((E)-3-((2R,6R)-6-methyltetrahydro-2H-pyran-2-yl)allyl)benzoate (R6a) and Methyl 2,4-Dimethoxy-6-((E)-3-((2S,6R)-6-methyltetrahydro-2H-pyran-2-yl)allyl)benzoate (R6b). Compounds **R6a** (0.55 g) and **R6b** (0.52 mg) were synthesized with an overall yield of 53% from fragment A' and fragment B as a yellowish oil by following similar procedure for the synthesis of compounds **6a** and **6b**.

Compound R6a. ¹H NMR (200 MHz, CDCl₃): δ 6.33 (s, 2H), 5.73 (td, $J = 6.4, 15.4$ Hz, 1H), 5.53 (dd, $J = 6.1, 15.5$ Hz, 1H), 3.85 (s, 3H), 3.79 (s, 7H), 3.51–3.40 (m, 1H), 3.32 (d, $J = 6.3$ Hz, 2H), 1.80 (dt, $J = 3.1, 6.0$ Hz, 1H), 1.61–1.49 (m, 4H), 1.25 (s, 1H), 1.17 (d, $J = 6.2$ Hz, 3H).

Compound R6b. ¹H NMR (200 MHz, CDCl₃): δ 6.33 (s, 2H), 5.75–5.65 (m, 2H), 4.33 (q, $J = 3.8$ Hz, 1H), 3.86 (s, 3H), 3.79 (s, 7H), 3.35 (d, $J = 4.9$ Hz, 2H), 1.65–1.58 (m, 5H), 1.20 (s, 1H), 1.15 (d, $J = 6.4$ Hz, 3H).

23. 3-(Hydroxy((2R,6R)-6-methyltetrahydro-2H-pyran-2-yl)methyl)-6,8-dimethoxyisochroman-1-one (R7a). Compound **R7a** (0.389 g, 50%) was synthesized from compound **R6a** as a foamy solid by following similar procedure for the synthesis of compound **7a**. ¹H NMR (400 MHz, CDCl₃): δ 6.39 (br s, 1H), 6.33 (br s, 1H), 4.76–4.43 (m, 1H), 3.91 (d, $J = 5.5$ Hz, 3H), 3.85 (s, 3H), 3.74–3.28 (m, 4H), 2.75–2.63 (m, 1H), 2.11–1.94 (d, 1H), 1.85–1.82 (m, 1H), 1.61–1.48 (m, 3H), 1.24 (s, 1H), 1.17–1.08 (m, 3H).

24. 3-(Hydroxy((2S,6R)-6-methyltetrahydro-2H-pyran-2-yl)methyl)-6,8-dimethoxyisochroman-1-one (R7b). Compound **R7b** (0.397 g, 57%) was synthesized from compound **R6b** as a yellowish oil by following similar procedure for the synthesis of compound **7b**. ¹H NMR (400 MHz, CDCl₃): δ 6.38 (s, 1H), 6.31 (s, 1H), 4.66–4.39 (m, 1H), 4.12–3.97 (m, 1H), 3.89 (d, $J = 3.9$ Hz, 4H), 3.84 (s, 3H), 3.68–3.54 (m, 1H), 3.34–3.20 (m, 1H), 2.75–2.66 (m, 1H), 1.86–1.62 (m, 4H), 1.55–1.50 (m, 1H), 1.34–1.31 (m, 1H), 1.24–1.15 (m, 3H).

25. O-((S)-((S)-6,8-Dimethoxy-1-oxoisochroman-3-yl)-((2R,6R)-6-methyltetrahydro-2H-pyran-2-yl)methyl) S-Methyl Carbonodithioate (R9a) and O-((R)-((R)-6,8-Dimethoxy-1-oxoisochroman-3-yl)-((2R,6R)-6-methyltetrahydro-2H-pyran-2-yl)-methyl) S-Methyl Carbonodithioate (R8a). Compounds R8a (0.187 g) and R9a (0.18 g) were synthesized with a yield of 73% from compound R7a as foamy solids by following similar procedure for the synthesis of compounds 8a and 9a.

Compound R8a. ^1H NMR (400 MHz, CDCl_3): δ 6.38 (s, 1H), 6.28 (s, 1H), 5.96 (d, $J = 9.2$ Hz, 1H), 4.94 (d, $J = 11.6$ Hz, 1H), 4.08 (t, $J = 10.1$ Hz, 1H), 3.91 (s, 3H), 3.83 (s, 3H), 3.51 (dd, $J = 5.8$, 10.7 Hz, 1H), 3.01–2.94 (m, 1H), 2.76–2.71 (m, 1H), 2.56 (s, 3H), 1.82 (d, $J = 12.8$ Hz, 1H), 1.67–1.47 (m, 4H), 1.23–1.14 (m, 1H), 1.11 (d, $J = 5.5$ Hz, 3H).

Compound R9a. ^1H NMR (400 MHz, CDCl_3): δ 6.40 (s, 1H), 6.32 (s, 1H), 6.00 (t, $J = 4.3$ Hz, 1H), 4.77 (dd, $J = 3.1$, 11.0 Hz, 1H), 3.95 (s, 1H), 3.91 (s, 3H), 3.85 (s, 3H), 3.44 (dd, $J = 5.8$, 10.1 Hz, 1H), 3.14 (dd, $J = 11.6$, 15.9 Hz, 1H), 2.89–2.85 (m, 1H), 2.57 (s, 3H), 1.86–1.83 (s, 1H), 1.67–1.66 (m, 1H), 1.56–1.54 (m, 2H), 1.45–1.41 (m, 1H), 1.21–1.19 (s, 1H), 1.13 (d, $J = 6.1$ Hz, 3H).

26. O-((R)-((R)-6,8-Dimethoxy-1-oxoisochroman-3-yl)-((2S,6R)-6-methyltetrahydro-2H-pyran-2-yl)methyl) S-Methyl Carbonodithioate (R8b) and O-((S)-((S)-6,8-Dimethoxy-1-oxoisochroman-3-yl)-((2S,6R)-6-methyltetrahydro-2H-pyran-2-yl)-methyl) S-Methyl Carbonodithioate (R9b). Compounds R8b (0.215 g) and R9b (0.135 g) were synthesized from compound R7b with 70% yield as foamy solids by following similar procedure for the synthesis of 8b and 9b.

Compound R8a. ^1H NMR (500 MHz, CDCl_3): δ 6.39 (s, 1H), 6.31 (s, 1H), 6.21 (dd, $J = 3.4$, 6.9 Hz, 1H), 4.68 (td, $J = 2.8$, 11.6 Hz, 1H), 4.36–4.32 (m, 1H), 4.06–4.04 (m, 1H), 3.90 (s, 3H), 3.84 (s, 3H), 3.09 (dd, $J = 11.8$, 16.0 Hz, 1H), 2.87 (dd, $J = 2.3$, 16.0 Hz, 1H), 2.57 (s, 3H), 1.74–1.69 (m, 3H), 1.61–1.55 (m, 2H), 1.35–1.33 (m, 1H), 1.17 (d, $J = 6.5$ Hz, 3H).

Compound R9b. ^1H NMR (400 MHz, CDCl_3): δ 6.38 (s, 1H), 6.29 (s, 1H), 6.19 (d, $J = 9.8$ Hz, 1H), 4.86 (d, $J = 11.6$ Hz, 1H), 4.43–4.39 (m, 1H), 3.91 (s, 4H), 3.83 (s, 3H), 2.99 (dd, $J = 12.5$, 15.6 Hz, 1H), 2.74 (dd, $J = 2.4$, 15.9 Hz, 1H), 2.56 (s, 3H), 1.68–1.65 (m, 4H), 1.34 (dd, $J = 7.0$, 10.7 Hz, 2H), 1.20 (d, $J = 6.7$ Hz, 3H).

27. (R)-6,8-Dimethoxy-3-(((2R,6R)-6-methyltetrahydro-2H-pyran-2-yl)methyl)isochroman-1-one (R10a). Compound R10a (0.087 g, 64%) was synthesized from compound R8a as a yellowish oil by following similar procedure for the synthesis of compound 10a. ^1H NMR (400 MHz, CDCl_3): δ 6.40 (s, 1H), 6.29 (s, 1H), 4.68 (t, $J = 10.4$ Hz, 1H), 3.92 (s, 3H), 3.85 (s, 3H), 3.71 (t, $J = 10.7$ Hz, 1H), 3.47–3.42 (m, 1H), 2.91–2.76 (m, 2H), 1.90–1.78 (m, 2H), 1.73–1.66 (m, 2H), 1.55–1.49 (m, 3H), 1.18–1.16 (m, 1H), 1.12 (d, $J = 6.1$ Hz, 3H).

28. (S)-6,8-Dimethoxy-3-(((2R,6R)-6-methyltetrahydro-2H-pyran-2-yl)methyl)isochroman-1-one (R11a). Compound R11a (0.079 g, 60%) was synthesized from compound R9a as a foamy solid by following similar procedure for the synthesis of 11a. ^1H NMR (500 MHz, CDCl_3): δ 6.40 (s, 1H), 6.32 (s, 1H), 4.57 (ddd, $J = 3.2$, 5.7, 8.6 Hz, 1H), 3.92 (s, 3H), 3.87 (s, 3H), 3.64 (td, $J = 5.4$, 11.0 Hz, 1H), 3.46–3.42 (m, 1H), 2.98 (dd, $J = 11.4$, 16.0 Hz, 1H), 2.85 (dd, $J = 2.7$, 16.0 Hz, 1H), 2.13–2.04 (m, 1H), 1.83–1.76 (m, 2H), 1.58–1.49 (m, 4H), 1.21 (d, $J = 8.8$ Hz, 1H), 1.14 (d, $J = 6.1$ Hz, 3H).

29. (R)-6,8-Dimethoxy-3-(((2S,6R)-6-methyltetrahydro-2H-pyran-2-yl)methyl)isochroman-1-one (R10b). Compound R10b (0.103 g, 57%) was synthesized from compound R8b as a semisolid by following similar procedure for the synthesis of compound 10b. ^1H NMR (400 MHz, CDCl_3): δ 6.41 (s, 1H), 6.32 (s, 1H), 4.56–4.53 (m, 1H), 4.05–4.04 (m, 1H), 3.92 (s, 3H), 3.86 (s, 3H), 2.97–2.91 (m, 2H), 2.39–2.35 (m, 1H), 1.73–1.67 (m, 5H), 1.37–1.31 (m, 2H), 1.16 (d, $J = 6.1$ Hz, 3H).

30. (S)-6,8-Dimethoxy-3-(((2S,6R)-6-methyltetrahydro-2H-pyran-2-yl)methyl)isochroman-1-one (R11b). Compound R11b (0.087 g, 60%) was synthesized from compound R9b as a white solid by following similar procedure for the synthesis of 11b. ^1H NMR (400 MHz, CDCl_3): δ 6.39 (s, 1H), 6.29 (s, 1H), 4.59–4.54 (m, 1H), 4.07 (t, $J = 8.2$ Hz, 1H), 3.93 (br s, 1H), 3.91 (s, 3H), 3.85 (s, 3H),

2.92–2.78 (m, 2H), 1.91–1.81 (m, 2H), 1.74–1.63 (m, 4H), 1.34–1.28 (m, 2H), 1.19 (d, $J = 6.1$ Hz, 3H).

31. (R)-6,8-Dihydroxy-3-(((2R,6R)-6-methyltetrahydro-2H-pyran-2-yl)methyl)isochroman-1-one (Compound 16). Compound 16 (0.034 g, 51%) was synthesized from compound R10a as a white solid by following similar procedure for the synthesis of compound 12. Melting point: 155–158 °C. $[\alpha]_D^{25} +5.6$ (c 0.4, CHCl_3); ^1H NMR (400 MHz, CD_3OD): δ 6.21 (s, 1H), 6.20 (s, 1H), 4.74 (t, $J = 9.8$ Hz, 1H), 3.69–3.64 (m, 1H), 3.48 (dd, $J = 5.2$, 9.5 Hz, 1H), 2.93–2.85 (m, 2H), 1.88–1.73 (m, 4H), 1.60 (d, $J = 10.4$ Hz, 3H), 1.19 (d, $J = 13.4$ Hz, 1H), 1.14 (d, $J = 6.1$ Hz, 3H).

32. (S)-6,8-Dihydroxy-3-(((2R,6R)-6-methyltetrahydro-2H-pyran-2-yl)methyl)isochroman-1-one (17). The compound 17 (0.017 g, 53%) was synthesized from compound R11a as a white solid by following similar procedure for the synthesis of compound 13. Melting point: 195–197 °C. $[\alpha]_D^{25} -45.23$ (c 0.5, EtOH). ^1H NMR (400 MHz, CD_3OD): δ 6.23 (s, 1H), 6.20 (s, 1H), 4.72–4.67 (m, 1H), 3.61–3.58 (m, 1H), 3.48 (dd, $J = 5.5$, 10.4 Hz, 1H), 2.97–2.90 (m, 2H), 2.07–2.00 (m, 1H), 1.84–1.77 (m, 2H), 1.67–1.53 (m, 3H), 1.28–1.18 (m, 2H), 1.13 (d, $J = 6.1$ Hz, 3H).

33. (R)-6,8-Dihydroxy-3-(((2S,6R)-6-methyltetrahydro-2H-pyran-2-yl)methyl)isochroman-1-one (Compound 18). Compound 18 (0.021 g, 55%) was synthesized from compound R10b as a white solid by following similar procedure for the synthesis of compound 14. Melting point: 135–139 °C. $[\alpha]_D^{25} +104.19$ (c 0.2, CHCl_3). ^1H NMR (400 MHz, CDCl_3): δ 11.12 (s, 1H), 6.32 (s, 1H), 6.18 (s, 1H), 4.69–4.66 (m, 1H), 4.10–4.09 (m, 1H), 3.96 (s, 1H), 2.93–2.91 (m, 2H), 2.47–2.36 (m, 1H), 1.78–1.70 (m, 5H), 1.42–1.31 (m, 2H), 1.20 (d, $J = 6.1$ Hz, 3H).

34. (S)-6,8-Dihydroxy-3-(((2S,6R)-6-methyltetrahydro-2H-pyran-2-yl)methyl)isochroman-1-one (Compound 19). Compound 19 (0.023 g, 43%) was synthesized from compound R11b as a white solid by following similar procedure for the synthesis of compound 15. Melting point: 174–177 °C. $[\alpha]_D^{25} +16.57$ (c 0.5, EtOH). ^1H NMR (400 MHz, CDCl_3): δ 11.07 (br s, 1H), 6.30 (s, 1H), 6.17 (s, 1H), 4.69 (t, $J = 9.8$ Hz, 1H), 4.13 (br s, 1H), 4.02 (br s, 1H), 2.90–2.76 (m, 2H), 2.01–1.95 (m, 1H), 1.88–1.82 (m, 1H), 1.71–1.64 (m, 4H), 1.36 (d, $J = 6.1$ Hz, 2H), 1.24 (d, $J = 6.7$ Hz, 3H).

■ ASSOCIATED CONTENT

Supporting Information

(PDF) Molecular Formula Strings. (CSV) The Supporting Information is available free of charge on the ACS Publications website at DOI: 10.1021/acs.jmedchem.8b00565.

Coordinates information for structure representation (CIF)

Coordinates information for structure representation (CIF)

Coordinates information for structure representation (CIF)

Coordinates information for structure representation (CIF)

Molecular formula strings and some data (CSV)

Single crystal X-ray and ORTEP, protein expression and purification, thermal shift assay, aminoacylation assay, *Plasmodium falciparum* culture, crystallization, ^1H and ^{13}C NMR spectra (PDF)

Accession Codes

PDB codes are as follows: compound 12, 4HO2;¹¹ compound 13, SZHS; compound 16, SZH2; compound 17, SZH3; compound 18, SZH4. Authors will release the atomic coordinates and experimental data upon article publication.

■ AUTHOR INFORMATION

Corresponding Authors

*A.S.: e-mail, asharma@icgeb.res.in.

*D.S.R.: e-mail, ds.reddy@ncl.res.in.

ORCID

Rajesh G. Gonnade: 0000-0002-2841-0197

D. Srinivasa Reddy: 0000-0003-3270-315X

Author Contributions

^VP.D., P.B., and N.M. have contributed equally to this work. A.S. and D.S.R. designed the study. P.D. and G.R.J. produced cladospors. P.B. and M.S. performed protein purifications. P.B. and N.M. performed all enzymatic and binding assays. P.B. and N.M. crystallized PfKRS complexes and froze the crystals along with M.Y. M.Y. and K.H. collected the data sets, and M.Y. solved the crystal structures. A.S., P.B., N.M., and M.Y. analyzed the bound drugs in PfKRS. R.G.G. solved the small molecule crystal structures. All authors participated in data analyses. All authors discussed the results and contributed to the manuscript preparation.

Notes

The authors declare no competing financial interest.

ACKNOWLEDGMENTS

The authors thank the beamline staff at PROXIMA 1 and PROXIMA 2A for assistance during data collection at Synchrotron SOLEIL. P.D. and P.B. thank UGC for the award of research fellowship. N.M. and M.S. thank CSIR for fellowship. P.B., M.S., and M.Y. thank the Indo-French Centre for the Promotion of Advanced Research (IFCPAR/CEFIPRA) for travel grant to synchrotron SOLEIL for data collection experiments. We also thank Diamond Light Source for access to beamline I03 (MX14744) that contributed to the results presented here. The Wellcome Trust Centre for Human Genetics is supported by the Wellcome Trust (Grant 090532/Z/09/Z). Funding includes OE and DBT grants for work on parasite tRNA synthetases to A.S. Additionally, A.S. is supported by a J. C. Bose fellowship and via MMV funding. This work is a part of the project proposal submitted to SERB, New Delhi, India, under the special call “Theme-Based Call for Proposals Initiated by the Program Advisory Committee of Organic Chemistry” (Reference EMR/2016/004301/OC). This proposal is currently under evaluation.

ABBREVIATIONS USED

CCR2, CC chemokine receptor 2; CCL2, CC chemokine ligand 2; CCR5, CC chemokine receptor 5; TLC, thin layer chromatography

REFERENCES

- (1) McConathy, J.; Owens, M. J. Stereochemistry in drug action. *Primary Care Companion J. Clin Psychiatry* **2003**, *5*, 70–73.
- (2) Newman, D. J.; Cragg, G. M. Natural products as sources of new drugs from 1981 to 2014. *J. Nat. Prod.* **2016**, *79*, 629–661.
- (3) Nguyen, L. A.; He, H.; Pham-Huy, C. Chiral drugs: an overview. *Int. J. Biomed. Sci.* **2006**, *2*, 85–100.
- (4) Vargesson, N. Thalidomide-induced limb defects: resolving a 50-year-old puzzle. *BioEssays* **2009**, *31*, 1327–1336.
- (5) Evans, A. M. Comparative pharmacology of S(+)-Ibuprofen and (R)-Ibuprofen. *Clin. Rheumatol.* **2001**, *20* (Suppl. 1), 9–14.
- (6) Springer, J. P.; Cutler, H. G.; Crumley, F. G.; Cox, R. H.; Davis, E. E.; Thean, J. E. Plant growth regulatory effects and stereochemistry of cladosporin. *J. Agric. Food Chem.* **1981**, *29*, 853–855.
- (7) Scott, P. M.; Van Walbeek, W.; Maclean, W. M. Cladosporin, a new antifungal metabolite from *Cladosporium cladosporioides*. *J. Antibiot.* **1971**, *24*, 747–755.
- (8) Brocks, D. R.; Mehvar, R. Stereoselectivity in the pharmacodynamics and pharmacokinetics of the chiral antimalarial drugs. *Clin. Pharmacokinet.* **2003**, *42*, 1359–1382.
- (9) Hoepfner, D.; McNamara, C. W.; Lim, C. S.; Studer, C.; Riedl, R.; Aust, T.; McCormack, S. L.; Plouffe, D. M.; Meister, S.; Schuierer, S.; Plikat, U.; Hartmann, N.; Staedtler, F.; Cotesta, S.; Schmitt, E. K;

Petersen, F.; Supek, F.; Glynn, R. J.; Tallarico, J. A.; Porter, J. A.; Fishman, M. C.; Bodenreider, C.; Diagona, T. T.; Movva, N. R.; Winzeler, E. A. Selective and specific inhibition of the *Plasmodium falciparum* lysyl-tRNA synthetase by the fungal secondary metabolite cladosporin. *Cell Host Microbe* **2012**, *11*, 654–663.

(10) Khan, S.; Garg, A.; Camacho, N.; Van Rooyen, J.; Kumar Pole, A.; Belrhali, H.; Ribas de Pouplana, L.; Sharma, V.; Sharma, A. Structural analysis of malaria-parasite lysyl-tRNA synthetase provides a platform for drug development. *Acta Crystallogr., Sect. D: Biol. Crystallogr.* **2013**, *69*, 785–795.

(11) Khan, S.; Sharma, A.; Belrhali, H.; Yogavel, M.; Sharma, A. Structural basis of malaria parasite lysyl-tRNA synthetase inhibition by cladosporin. *J. Struct. Funct. Genomics* **2014**, *15*, 63–71.

(12) Sharma, A.; Sharma, M.; Yogavel, M.; Sharma, A. Protein translation enzyme lysyl-tRNA synthetase presents a new target for drug development against causative agents of leishmaniasis and schistosomiasis. *PLoS Neglected Trop. Dis.* **2016**, *10*, 1–19.

(13) Zheng, H.; Zhao, C.; Fang, B.; Jing, P.; Yang, J.; Xie, X.; She, X. Asymmetric total synthesis of cladosporin and isocladosporin. *J. Org. Chem.* **2012**, *77*, 5656–5663.

(14) Mohapatra, D. K.; Maity, S.; Rao, T. S.; Yadav, J. S.; Sridhar, B. An efficient formal total synthesis of cladosporin. *Eur. J. Org. Chem.* **2013**, *2013*, 2859–2863.

(15) Vintonyak, V. V.; Maier, M. E. Synthesis of the core structure of cruentaren A. *Org. Lett.* **2007**, *9*, 655–658.

(16) Dermenci, A.; Selig, P. S.; Domaol, R. A.; Spasov, K. A.; Anderson, K. S.; Miller, S. J. Quasi-biomimetic ring contraction promoted by a cysteine-based nucleophile: Total synthesis of Sch-642305, some analogs and their putative anti-HIV activities. *Chem. Sci.* **2011**, *2*, 1568–1572.

(17) Chatterjee, A. K.; Choi, T. L.; Sanders, D. P.; Grubbs, R. H. A general model for selectivity in olefin cross metathesis. *J. Am. Chem. Soc.* **2003**, *125*, 11360–11370.

(18) Tian, J.; Sang, D. Application of aluminum triiodide in organic synthesis. *ARKIVOC* **2015**, 446–493.

(19) Mohapatra, D. K.; Maity, S.; Banoth, S.; Gonnade, R. G.; Yadav, J. S. Total synthesis of isocladosporin and 3-epi-isocladosporin. *Tetrahedron Lett.* **2016**, *57*, 53–55.

(20) Reddy, B. V. S.; Reddy, P. J.; Reddy, C. S. The stereoselective total synthesis of isocladosporin. *Tetrahedron Lett.* **2013**, *54*, 5185–5187.

(21) McNamara, C.; Winzeler, E. A. Target identification and validation of novel antimalarials. *Future Microbiol.* **2011**, *6*, 693–704.

(22) Schlagenhauf, P. Mefloquine for malaria chemoprophylaxis 1992–1998: a review. *J. Travel Med.* **1999**, *6*, 122–133.

(23) Karle, J. M.; Karle, I. L. Crystal structure of (–)-mefloquine hydrochloride reveals consistency of configuration with biological activity. *Antimicrob. Agents Chemother.* **2002**, *46*, 1529–1534.

(24) Ding, J.; Hall, D. G. Concise synthesis and antimalarial activity of all four mefloquine stereoisomers using a highly enantioselective catalytic borylative alkene isomerization. *Angew. Chem., Int. Ed.* **2013**, *52*, 8069–8073.

(25) Fang, P.; Han, H.; Wang, J.; Chen, K.; Chen, X.; Guo, M. Structural basis for specific inhibition of tRNA synthetase by an ATP competitive inhibitor. *Chem. Biol.* **2015**, *22*, 734–744.

(26) Jain, V.; Yogavel, M.; Kikuchi, H.; Oshima, Y.; Hariguchi, N.; Matsumoto, M.; Goel, P.; Touquet, B.; Jumani, R. S.; Tacchini-Cottier, F.; Harlos, K.; Huston, C. D.; Hakimi, M. A.; Sharma, A. Targeting prolyl-tRNA synthetase to accelerate drug discovery against malaria, leishmaniasis, toxoplasmosis, cryptosporidiosis, and coccidiosis. *Structure* **2017**, *25*, 1495–1505.

(27) Jain, V.; Sharma, A.; Singh, G.; Yogavel, M.; Sharma, A. Structure-based targeting of orthologous pathogen proteins accelerates antiparasitic drug discovery. *ACS Infect. Dis.* **2017**, *3*, 281–292.

(28) Manickam, Y.; Chaturvedi, R.; Babbar, P.; Malhotra, N.; Jain, V.; Sharma, A. Drug targeting of one or more aminoacyl-tRNA synthetase in the malarial parasite *Plasmodium falciparum*. *Drug Discovery Today* **2018**, DOI: 10.1016/j.drudis.2018.01.050.

(29) Jain, V.; Yogavel, M.; Oshima, Y.; Kikuchi, H.; Touquet, B.; Hakimi, M. A.; Sharma, A. Structure of prolyl-tRNA synthetase-

halofuginone complex provides basis for development of drugs against malaria and toxoplasmosis. *Structure* **2015**, *23*, 819–829.

(30) Sharma, A.; Sharma, A. *Plasmodium falciparum* mitochondria import tRNAs along with an active phenylalanyl-tRNA synthetase. *Biochem. J.* **2015**, *465*, 459–469.

(31) Khan, S.; Sharma, A.; Jamwal, A.; Sharma, V.; Pole, A. K.; Thakur, K. K.; Sharma, A. Uneven spread of *cis*- and *trans*-editing aminoacyl-tRNA synthetase domains within translational compartments of *P. falciparum*. *Sci. Rep.* **2011**, *1*, 188.



Scalable synthesis of cladospirin

Pronay Das^{a,b}, Yash Mankad^a, D. Srinivasa Reddy^{a,b,*}

^aOrganic Chemistry Division, CSIR-National Chemical Laboratory, Dr. Homi Bhabha Road, Pune 411008, India

^bAcademy of Scientific and Innovative Research (AcSIR), New Delhi 110 025, India

ARTICLE INFO

Article history:

Received 11 January 2019

Revised 2 February 2019

Accepted 5 February 2019

Available online 6 February 2019

Keywords:

Cladospirin
Total synthesis
Anti-malarials
Mitsunobu

ABSTRACT

Cladospirin, a secondary metabolite isolated from fungal sources like *Cladosporium cladosporioides* and *Aspergillus flavus* was found to exhibit selective nano-molar activity against malarial parasite *Plasmodium falciparum* by inhibiting parasitic protein biosynthesis. In addition, this natural product has a broad range of bioactivities including, antiparasitic, antifungal, antibacterial as well as plant growth inhibition. However, it has limited availability from the natural sources for further development. Herein, we report a modified and improved synthetic route which led us to produce this potent natural product in a gram scale. Conversion of the undesired diastereomer to desired one via Mitsunobu inversion of secondary alcohol and carbon monoxide insertion reaction towards the construction of isocoumarin unit are the key features of the present synthesis.

© 2019 Elsevier Ltd. All rights reserved.

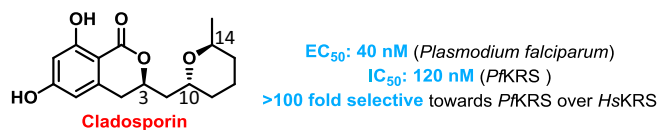
Cladospirin, also known as asperentin is a secondary metabolite found in diverse fungi including *Cladosporium cladosporioides* [1] and *Aspergillus flavus* [2] with the first isolation documented way back in 1971 by Scott and Walbeek [1]. Structurally it consists of a THP ring (2,6-disubstituted tetrahydropyran) connected to an isocoumarin moiety [1,3,4] (Fig. 1) whose complete stereochemical elucidation was reported in 1981 by Springer et. al. [2] Cladospirin was found to illustrate a broad spectrum of bio-activities (Fig. 1) such as antifungal [1], insecticidal, plant growth inhibition [2,5] and antibacterial [6], as well as anti-inflammatory activity [7]. While screening natural product library to identify inhibitors of *Plasmodium falciparum* (Pf), which happens to be the causative pathogen for malaria; Winzeler et al. identified cladospirin to display potent antiparasitic activity (~40 nM) against both blood and liver stage proliferation of the pathogen by ceasing protein biosynthesis in the parasitic cell through inhibition of cytosolic lysyl-tRNA synthetase (PfKRS) [8,9]. Besides, cladospirin was found to be >100 fold selective towards parasitic KRS as compared to human enzyme (HsKRS) [9]. Apart from PfKRS, cladospirin is known to inhibit KRSs from other species, including helminth parasites such as *Loa loa* (Ll) and *Schistosomamansoni* (Sm) [10]. By considering the promising potential of cladospirin, we have initiated a program towards it. Recently, we have accomplished the synthesis of all the possible eight stereoisomers (cladologs) of cladospirin and in collaboration with Sharma et al. we successfully deciphered the

stereochemical bases of cladologs' interaction with PfKRS through cladolog-PfKRS co-crystallization [11]. These interesting findings and impressive biological profile of cladospirin undoubtedly make it a promising candidate towards the development of novel anti-malarials. A proper bio-assessment towards drug development demands adequate quantity of the lead compound (cladospirin), which has limited access from natural sources. Hence development of an efficient and scalable synthetic strategy is worth exploring. As of today, one asymmetric total synthesis [4] followed by a formal synthesis [3] of the natural product have been documented by She et al. and Mohapatra et al. using independent and elegant ways, respectively. Following that, we have documented a synthesis of cladospirin, where we have adopted a strategy to access different isomers deliberately [11]. Although these synthetic routes to access cladospirin were documented, there is a need for new route which can provide sufficient material. Here we report a modified approach to access cladospirin in "gram-scale".

Our synthesis commenced with the known intermediate **1** (prepared through a reported protocol) which was subjected to epoxidation using mCPBA reagent to its corresponding epoxide (fragment B) as an inseparable diastereomeric mixture. The epoxide thus obtained, on Grignard reaction with commercially available 1-bromo-3,5-dimethoxybenzene (fragment A) afforded 1:1 diastereomeric mixture of alcohols (**2** and **3**) with excellent overall yield of 86%. It is worth mentioning that maintaining a low concentration of Grignard reagent (<0.5 M) is crucial for the reaction. Higher concentrations of Grignard reagent results in an unrequired dimerization product [12]. Here, in this case, we were able to separate both the diastereomers (**2** and **3**) cleanly using simple silica

* Corresponding author at: Organic Chemistry Division, CSIR-National Chemical Laboratory, Dr. Homi Bhabha Road, Pune 411008, India.

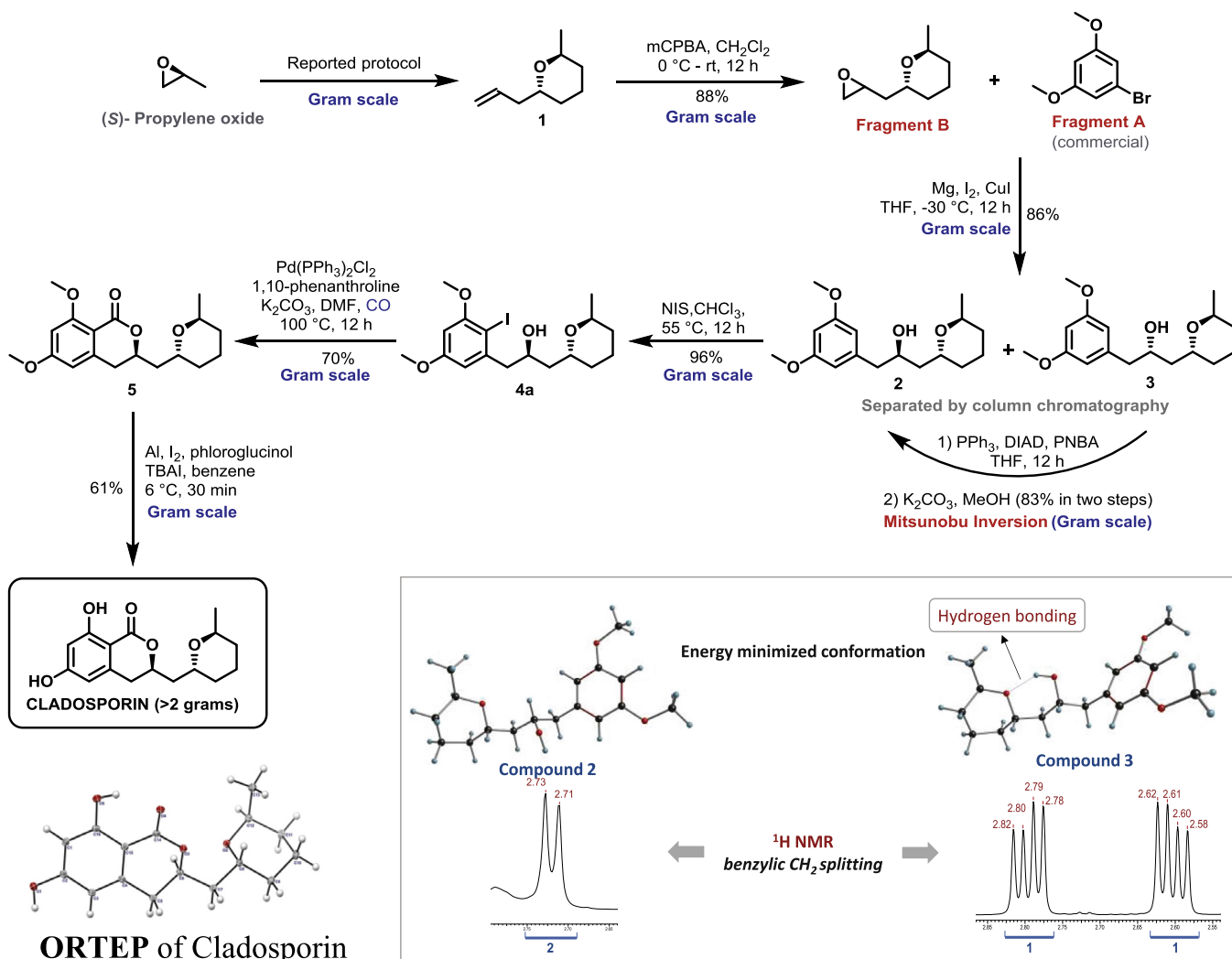
E-mail address: ds.reddy@ncl.res.in (D.S. Reddy).



Parasites		Fungus	
Parasites	IC_{50} (μ M)	<i>Penicillium</i> sp.	<i>Aspergillus</i> sp.
<i>Plasmodium yoeli</i>	0.04	<i>viridicatum</i>	<i>niger</i>
<i>Trypanosoma brucei</i>	2.05	<i>expansum</i>	<i>ochraceus</i>
<i>Leishmania donovani</i>	2.56	<i>obscurans</i>	<i>versicolor</i>
<i>Toxoplasma gondii</i>	2.63	<i>viticola</i>	<i>clavatus</i>
			<i>nidulans</i>

<i>Colletotrichum</i> sp. (Fungus)	% inhibition
<i>acutatum</i>	92.7 (30 μ g/mL)
<i>fragariae</i>	90.1 (30 μ g/mL)
<i>gloeosporioides</i>	95.4 (30 μ g/mL)

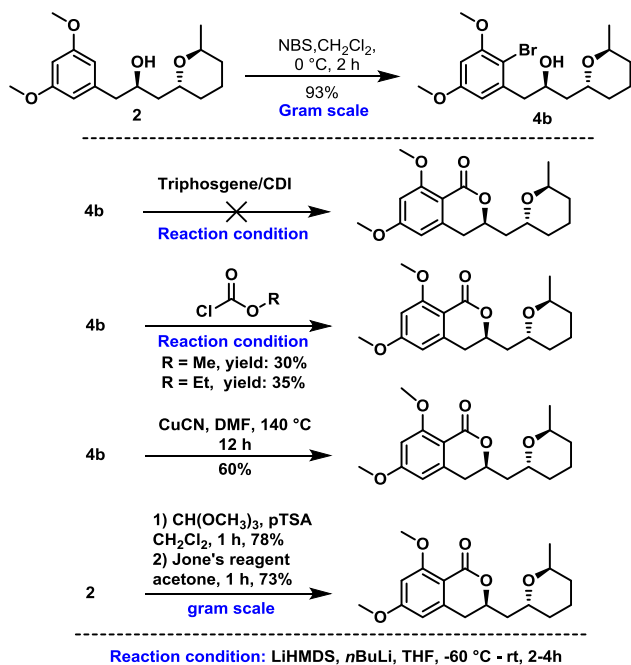
Fig. 1. Spectrum of Cladosporin bio-activities.



Scheme 1. Gram scale synthesis of cladosporin.

gel column chromatography. In this context, we made interesting observations while analyzing ^1H NMR data of these isomers where identical chemical shifts of all the concerned proton signals were

observed for both the compounds except the benzylic protons, which showed significant chemical shift difference for both. This difference in the ^1H NMR pattern could probably be explained using



Scheme 2. Alternatives towards lactonization.

energy minimized conformer of both the compounds using Gaussian. Unlike compound **2**, compound **3** was found to exhibit a hydrogen bonding interaction between the secondary alcohol and the tetrahydropyran oxygen which might be the probable cause for a constrained conformation of compound **3** and this in turn resulted in a separate splitting pattern for both the benzylic protons (Scheme 1). To make use of undesired diastereomer, compound **3** was subjected to Mitsunobu reaction protocol followed by ester hydrolysis which led to the complete inversion of the secondary alcohol center in **3** to afford the required diastereomeric alcohol **2** in good yields. Next we focused to construct the six-membered lactone present in the natural product which was envisioned using palladium catalyzed carbon monoxide insertion reaction. Accordingly, the alcohol **2** was converted to its corresponding iodo-compound **4a** in excellent yields by using *N*-iodosuccinimide (NIS) and catalytic amount of *p*TSA in chloroform solvent. The iodo-compound **4a** was treated with Pd(PPh₃)₂Cl₂, potassium carbonate and 1,10-phenanthroline in presence in DMF at 100 °C under blanket of carbon monoxide to obtain desired compound **5** in 70% yield [14]. Demethylation of compound **5** was achieved through aluminium triiodide mediated exhaustive demethylation [15] to furnish the natural product cladospirin. The spectral data of the synthesized compound was in complete agreement with the reported data [3,4]. Besides, structure and relative stereochemistry of the synthesized compound was further confirmed by single crystal X-ray diffraction analysis for an unambiguous assignment of its stereocenters. Herein, we would also like to document alternate ways/attempts to form the six-membered lactone ring of cladospirin, in particular using bromo compound **4b**. Alcohol **2** upon treatment with *N*-bromo succinimide (NBS) in CH₂Cl₂ afforded bromo compound **4b** in excellent yield. The bromo compound thus obtained treated with *n*BuLi, LiHMDS to generate corresponding dianion which was subsequently quenched with electrophiles like triphosgene, carboxydimidazole (CDI), methylchloroformate and ethyl chloroformate which did not give any fruitful results (Scheme 2). We also tried to insert copper in the carbon halogen bond followed by protodecupration to

furnish the required lactone [13]. Although we were successful in obtaining the required product **5** in a moderate yield of 60%, we were unable to reproduce comparable yields at higher scale. As an alternative, we also prepared the required lactone **5** by following She's protocol [4].

In short, we have accomplished a scalable total synthesis of cladospirin natural product. Gram-scale operations, Mitsunobu inversion to convert undesired alcohol to required one and palladium-catalyzed carbon monoxide insertion reaction to construct six-membered lactone ring are the highlights of present work. Now we have more than two grams of material in hand which is sufficient for further profiling such as in-depth assessment of the pharmacokinetics and pharmacodynamics.

Acknowledgments

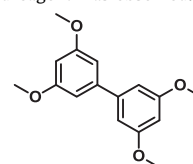
We would like to acknowledge University Grants Commission (UGC) for providing research fellowship to PD. We would also like to express our gratitude to Dr. Amit Sharma (ICGEB, New Delhi) for goading us into this project. Besides we thank Dr. Rambabu Dandela for X-ray crystallographic analysis of cladospirin and Tamal Das for conducting the energy minimization of two diastereomers. This work is a part of the project funded by SERB, New Delhi, India, entitled as "Hit to Lead Development of Potent Anti-Parasitic Natural Product Scaffold" (EMR/2016/004301).

Appendix A. Supplementary data

Supplementary data to this article can be found online at <https://doi.org/10.1016/j.tetlet.2019.02.012>.

References

- [1] P.M. Scott, W. Van Walbeek, W.M. Maclean, *J. Antibiot.* **24** (1971) 747.
- [2] J.P. Springer, H.G. Cutler, F.G. Crumley, R.H. Cox, E.E. Davis, J.E. Thean, *J. Agric. Food Chem.* **29** (1981) 853.
- [3] D.K. Mohapatra, S. Maity, T.S. Rao, J.S. Yadav, B. Sridhar, *Eur. J. Org. Chem.* **2013** (2013) 2859.
- [4] H. Zheng, C. Zhao, B. Fang, P. Jing, J. Yang, X. Xie, X. She, *J. Org. Chem.* **77** (2012) 5656.
- [5] Y. Kimura, N. Shimomura, F. Tanigawa, S. Fujioka, A. Shimada, *Z Naturforsch C.* **67** (2012) 587.
- [6] H. Anke, *J. Antibiot. (Tokyo)* **32** (1979) 952.
- [7] J.D. Miller, M. Sun, A. Gilyan, J. Roy, T.G. Rand, *ChemBiol Interact.* **183** (2010) 113.
- [8] D. Hoepfner, C.W. McNamara, C.S. Lim, C. Studer, R. Riedl, T. Aust, S.L. McCormack, D.M. Plouffe, S. Meister, S. Schuierer, U. Plikat, N. Hartmann, F. Staedtler, S. Cotesta, E.K. Schmitt, F. Petersen, F. Supek, R.J. Glynn, J.A. Tallarico, J.A. Porter, M.C. Fishman, C. Bodenreider, T.T. Diagana, N.R. Movva, E. A. Winzeler, *Cell Host Microbe.* **11** (2012) 654.
- [9] S. Khan, A. Garg, N. Camacho, J. Van Rooyen, A. Kumar Pole, H. Belrhali, L. Ribas de Pouplana, V. Sharma, A. Sharma, *Acta Crystallogr., Sect. D: Biol. Crystallogr.* **69** (2013) 785.
- [10] A. Sharma, M. Sharma, M. Yogavel, A. Sharma, *PLoS Neglected Trop. Dis.* **10** (2016) 1.
- [11] P. Das, P. Babbar, N. Malhotra, M. Sharma, G.R. Jachak, R.G. Gonnade, D. Shanmugam, K. Harlos, M. Yogavel, A. Sharma, D.S. Reddy, *J. Med. Chem.* **61** (2018) 5664.
- [12] Formation of dimeric compound (tentative structure shown below) at higher concentrations of Grignard reagent was observed.



- [13] U. Nookraju, E. Begari, P. Kumar, *Org. Biomol. Chem.* **12** (2014) 5973.
- [14] B.T.V. Srinivas, A.R. Maadhur, S. Bojja, *Tetrahedron* **70** (2014) 8161.
- [15] J. Tian, D. Sang, *ARKIVOC* **2015** (2015) 446.

DFT/NMR Approach for the Configuration Assignment of Groups of Stereoisomers by the Combination and Comparison of Experimental and Predicted Sets of Data

Gianluigi Lauro, Pronay Das, Raffaele Riccio, D. Srinivasa Reddy, and Giuseppe Bifulco*



Cite This: *J. Org. Chem.* 2020, 85, 3297–3306



Read Online

ACCESS |



Metrics & More

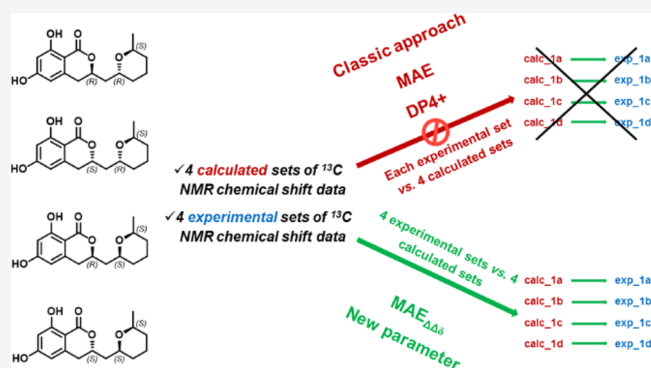


Article Recommendations



Supporting Information

ABSTRACT: Quantum mechanical/nuclear magnetic resonance (NMR) approaches are widely used for the configuration assignment of organic compounds generally comparing one cluster of experimentally determined data (e.g., ^{13}C NMR chemical shifts) with those predicted for all possible theoretical stereoisomers. More than one set of experimental data, each related to a specific stereoisomer, may occur in some cases, and the accurate stereoassignments can be obtained by combining the experimental and computed data. We introduce here a straightforward methodology based on the simultaneous analysis, combination, and comparison of all sets of experimental/calculated ^{13}C chemical shifts for aiding the correct configuration assignment of groups of stereoisomers. The comparison of the differences between the calculated/experimental chemical shifts instead of the shifts themselves led to the advantage of avoiding errors arising from calibration procedures, reducing systematic errors, and highlighting the most diagnostic differences between calculated and experimental data. This methodology was applied on a tetrad of synthesized cladospirin stereoisomers (cladologs) and further corroborated on a tetrad of pochonicine stereoisomers, obtaining the correct correspondences between experimental and calculated sets of data. The new $\text{MAE}_{\Delta\Delta\delta}$ parameter, useful for indicating the best fit between sets of experimental and calculated data, is here introduced for facilitating the stereochemical assignment of groups of stereoisomers.



INTRODUCTION

Nuclear magnetic resonance (NMR) spectroscopy is one of the pivotal analytical tools used to determine key chemical properties of organic compounds, for example, relative/absolute configurations,^{1,2} and to provide further structural information, for example, representative conformational patterns of the investigated molecules.³ In this context, the spectroscopic properties of organic compounds can be proficiently predicted by accurate quantum chemical methods.^{1,4–7} Indeed, the integration of the information from experimental and computational data can then be of fundamental importance to solve different structural issues of organic compounds. In the last decade, different studies were performed with the combination of the information from NMR spectroscopy (experimental part) and quantum mechanical (QM) calculations (predicted part) (QM/NMR integrated approach) for the successful elucidation of the configurational patterns of organic compounds.^{1,4} Also, this approach is helpful for the stereostructural assignment of natural compounds, thus representing a reliable alternative, faster and cheaper, to total synthesis.⁸ Also, the notable advances in computer science nowadays allows the performance of accurate conformational sampling and QM calculations

even on desktop computers, thus facilitating the structural elucidation process.

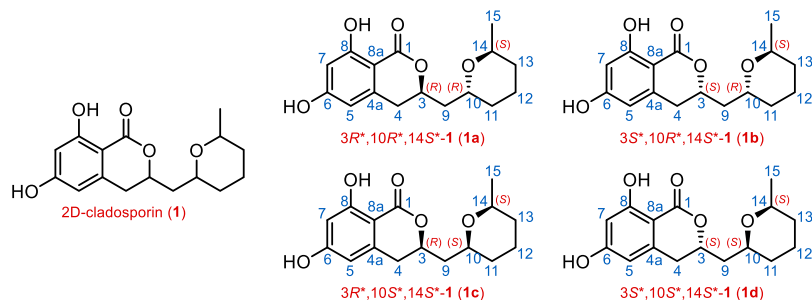
The QM/NMR integrated approach, successfully applied by different research groups and us,^{9–14} is based on the assumption that the possible theoretical stereoisomers show different NMR features (e.g., $^1\text{H}/^{13}\text{C}$ chemical shifts and J coupling constants). Once both the experimental and predicted data are collected, their comparison may be quantified using different factors, such as by the mean absolute error (MAE),¹ the corrected MAE,¹ the root-mean-square deviation (RMSD), and the correlation coefficient R and, as reported in recent studies, by more challenging statistical parameters, such as the DP4 parameter by Goodman¹⁵ and the optimized DP4+ by Sarotti.¹⁶

Specifically, the general workflow for determining the relative/absolute configurational pattern of an organic compound relies on the following two main phases:^{1,4,17}

Received: November 20, 2019

Published: January 21, 2020

Chart 1. Chemical Structures of 2D-Cladosporin (1) Reference Compound and of Cladologs 1a–1d



- generation of the ensembles of conformers to be accounted for the subsequent prediction of the chemical properties (e.g., $^{13}\text{C}/^1\text{H}$ NMR chemical shift and J coupling constants). Generally, this step foresees extensive conformational searches for all possible theoretical stereoisomers by molecular mechanics (MM) methods; subsequently, the sets of conformers are geometry-optimized by QM methods, and the contribution of each conformer to the final Boltzmann population, according to the related computed energy, is then computed;
- extraction of the values, computation of the Boltzmann-weighted final set of data, and comparison with experimental values. The computed sets of data for all possible stereoisomers are generally compared with each single set of experimental values using specific quantitative parameters (e.g. MAE, DP4, and DP4+) ^{15,16} useful for predicting the correct relative configurations (and in some cases, the absolute configurations, when coupled to other methods) of the case-study compound.

In particular, focusing on the last point, it is important to note that this methodology allows to predict the most probable stereoisomer as that featuring the best parameter value after generating a ranking (e.g., the lowest MAE value or the highest DP4+ probability). Using this approach, the results are dramatically affected by the set of stereoisomers accounted and the related sets of data: this means that if one of the theoretical isomers is excluded from the investigation, the application of this workflow anyway leads to a solution, identifying the most probable isomer among the set of accounted items. For the same reasons, if two (or more) sets of experimental data related to different isomers are available, this protocol could lead in principle to the identification of the same most probable solution, namely, the isomer whose computed data lead to the best ranked parameter values related to both the sets of experimental values. Accordingly, the assignment of the configurations of groups of stereoisomers (e.g., pairs, triads etc.) performed by comparing one-by-one each single set of experimental data to all sets of computed data could likely lead to errors. Contrarily, we speculated that accounting and comparing all sets of experimental/predicted data at the same time might be convenient for a more robust assignment.

Starting from these premises, in this study, we propose a method for the configuration assignment of groups of stereoisomers by accounting, combining, and comparing all possible sets of experimental and predicted chemical shift values in order to find the best match between the available data. As a proof of concept, we report the application of this

methodology considering four synthesized cladosporin stereoisomers (cladologs), whose related sets of ^{13}C NMR experimental chemical shift values are available, and demonstrating how this approach led to the identification of the correct correspondences between experimental and calculated sets of data.

RESULTS AND DISCUSSION

Comparing Experimental and Calculated Chemical Shift Data for Cladologs. Cladosporin is a secondary metabolite isolated from fungal sources ¹⁸ bearing three stereocenters and featuring 2R,9R,13S absolute configuration. In 2018, Reddy et al. reported a divergent synthesis of all eight possible stereoisomers based on the cladosporin 2D structure (1, Chart 1) (cladologs); also, all ^{13}C NMR chemical shift data were assigned to each specific isomer. ¹⁹ In the present study, the four cladologs featuring different relative configurations (1a–1d, Chart 1) were accounted, and then four sets of experimental data were considered for the subsequent comparison with the four calculated ones. Specifically, we named the sets of calculated data for 1a–1d as calc_1a, calc_1b, calc_1c, and calc_1d, respectively. For simplicity, the sets of experimental data, assigned in the reference study ¹⁹ (corroborated by comparison with already reported studies on cladosporin and related analogues ^{20,21}), were named for 1a–1d as exp_1a, exp_1b, exp_1c, and exp_1d, respectively.

Concerning the computation of the ^{13}C chemical shift data, after performing an extensive conformational search (see computational details, Experimental Section), the ensembles of sampled conformers were then submitted to a geometry and energy optimization step at the density functional theory (DFT) using the MPW1PW91/6-31g(d) functional/basis set. ²² Then, for each isomer, ^{13}C NMR chemical shifts were computed on the MPW1PW91/6-31g(d,p) level, ²² considering the influence of each conformer on the total Boltzmann distribution taking into account the relative energies.

Once all experimental/calculated values were available, we started employing a classic QM/NMR approach in order to confirm the assignments for 1a–1d and test this methodology when different experimental sets of data are available. Each experimental set of data was separately compared in detail with the four calculated ones; specifically, for each accounted atom, the experimental and calculated chemical shifts (δ) were compared using the $\Delta\delta$ parameter

$$\Delta\delta = |\delta_{\text{calc}} - \delta_{\text{exp}}|$$

where δ_{calc} and δ_{exp} are the calculated and experimental chemical shift values, respectively.

After calculating all $\Delta\delta$ values, the MAE values and DP4+ probabilities were computed for determining which calculated

Table 1. ^{13}C NMR MAE Values and DP4+ Probabilities Computed for the Three Functional/Basis Set Combinations Accounted in This Study Related to Compounds 1a–1d^a

	MPW1PW91/6-31g(d,p)		exp_1a set of data MPW1PW91/6-311+g(d,p)		B97-2/cc-pVTZ	
	^{13}C MAE	DP4+ probability	^{13}C MAE	DP4+ probability	^{13}C MAE	DP4+ probability
calc_1a	1.86	2.52%	2.45	0.08%	2.20	N.A. ^b
calc_1b	1.63	97.48%	2.32	99.92%	1.96	N.A. ^b
calc_1c	2.61	0.00%	4.09	0.00%	2.93	N.A. ^b
calc_1d	2.85	0.00%	4.09	0.00%	3.18	N.A. ^b
	MPW1PW91/6-31g(d,p)		exp_1b set of data MPW1PW91/6-311+g(d,p)		B97-2/cc-pVTZ	
	^{13}C MAE	DP4+ probability	^{13}C MAE	DP4+ probability	^{13}C MAE	DP4+ probability
calc_1a	2.22	0.00%	2.82	0.00%	2.58	N.A. ^b
calc_1b	1.75	100.00%	2.48	99.96%	2.10	N.A. ^b
calc_1c	2.79	0.00%	4.25	0.00%	3.15	N.A. ^b
calc_1d	3.03	0.00%	4.29	0.04%	3.39	N.A. ^b
	MPW1PW91/6-31g(d,p)		exp_1c set of data MPW1PW91/6-311+g(d,p)		B97-2/cc-pVTZ	
	^{13}C MAE	DP4+ probability	^{13}C MAE	DP4+ probability	^{13}C MAE	DP4+ probability
calc_1a	3.76	0.00%	2.83	0.00%	3.86	N.A. ^b
calc_1b	3.85	0.00%	2.32	0.00%	3.96	N.A. ^b
calc_1c	2.53	96.23%	1.88	91.24%	2.65	N.A. ^b
calc_1d	2.53	3.77%	2.13	8.76%	2.63	N.A. ^b
	MPW1PW91/6-31g(d,p)		exp_1d set of data MPW1PW91/6-311+g(d,p)		B97-2/cc-pVTZ	
	^{13}C MAE	DP4+ probability	^{13}C MAE	DP4+ probability	^{13}C MAE	DP4+ probability
calc_1a	3.83	0.00%	2.70	0.00%	3.90	N.A. ^b
calc_1b	3.93	0.00%	2.30	0.00%	4.01	N.A. ^b
calc_1c	2.63	90.63%	1.75	78.99%	2.72	N.A. ^b
calc_1d	2.57	9.37%	1.95	21.01%	2.64	N.A. ^b

^aThe correct/incorrect correspondence between experimental and calculated data are highlighted in green and orange, respectively. ^bB97-2/cc-pVTZ functional/basis set combination cannot be set in the calculation of DP4+ probability.

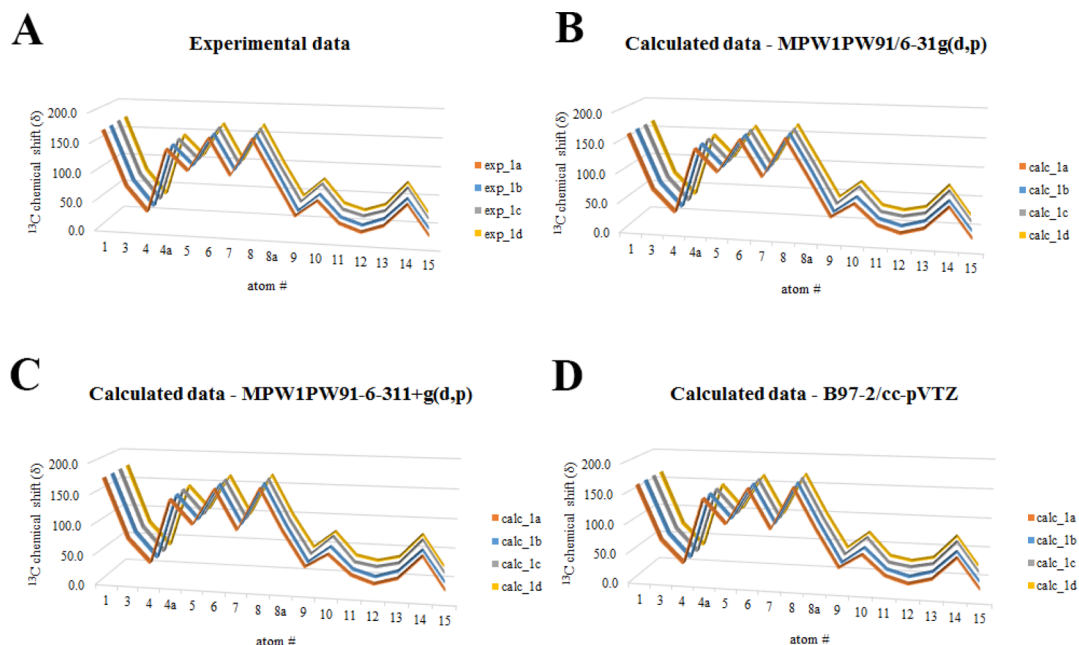


Figure 1. Line graphs related to the (a) experimental and (b–d) calculated ^{13}C chemical shift values belonging to compounds 1a–1d. In particular, concerning the computed data, those related to all three functional/basis set combinations were reported: (a) MPW1PW91/6-31g(d,p); (b) MPW1PW91/6-311+g(d,p); (c) B97-2/cc-pVTZ.

set of data fits better with the experimental one. The MAE is defined as the following

$$\text{MAE} = \frac{\sum (\Delta\delta)}{n}$$

Namely, it is the summation (\sum) of the n computed absolute δ error values ($\Delta\delta$) normalized to the number of $\Delta\delta$ errors considered (n)

The obtained data, and precisely the MAE values, highlighted uncertain results that questioned the reliability of this procedure when multiple sets of experimental data are accessible. Specifically, exp_1a set of experimental data, assigned to compound 1a, showed the best fit with calc_1b, featuring the lowest MAE values and highest DP4+ probability among the obtained rankings, thus not in accordance with the assignment reported in the reference study (Tables 1 and S1,

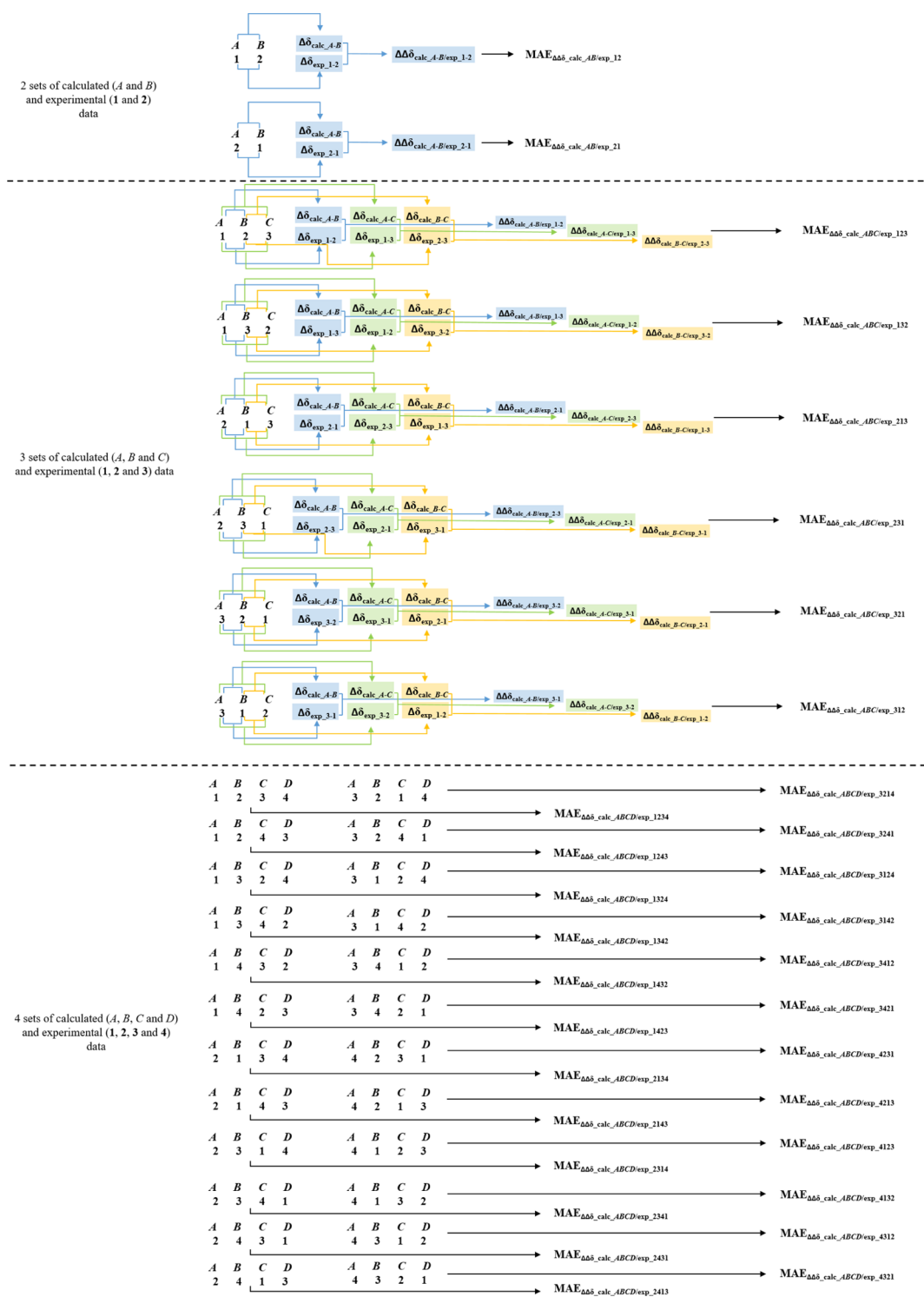


Figure 2. Possible combination alignments when two, three, and four sets of experimental/calculated data are available.

Supporting Information). Moving to the exp_1b pattern of experimental data, the lowest MAE value and highest DP4+ probability were found against calc_1b among the ranking, in accordance with the starting assignment (Tables 1 and S2, Supporting Information). The third set of experimental data exp_1c fit with calc_1c, thus in agreement with the known assignments (Tables 1 and S3, Supporting Information). Finally, exp_1d set of experimental data, assigned to compound 1d, showed the best DP4+ value with calc_1c, again not in accordance with the assignment reported in the

reference study (Tables 1 and S4, Supporting Information). Summarizing, the same calculated set of data calc_1b, related to compound 1b, showed both the best MAE values and DP4+ probabilities among the related rankings when compared to two different experimental sets of data (exp_1a and exp_1b) originally assigned to two different compounds (specifically, 1a and 1b). The same behavior was found with the calculated set of data calc_1c, related to compound 1c, showing the best MAE values and/or DP4+ probabilities among the related rankings compared to exp_1c and exp_1d experimental sets of

data. The obtained results prompted us to perform further calculations employing different levels of theory by the combination of various DFT functional/basis sets in order to obtain additional sets of computed ^{13}C chemical shift data to be compared with the experimental ones. However, both expanding the basis set from 6-31g(d,p) to 6-311+g(d,p) on the same MPW1PW91 level and considering the B97-2/cc-pVTZ functional/basis set combination,²³ the results did not show a remarkable improvement and basically confirmed what was obtained on the initial MPW1PW91/6-31g(d,p) level (Tables 1, and S5–S12, Supporting Information). The analysis of all these data highlighted that by comparing each experimental set of data against the four calculated ones separately, through the MAE and DP4+ rankings, the same theoretical stereoisomer can be predicted as the most probable one, and it is also the case if compared with different experimental sets of data. In summary, following this approach, we obtained ambiguous results that prompted us to find an alternative method to solve this issue.

In particular, an accurate analysis of the experimental sets of data and the corresponding sets of calculated ones accounting the three employed functional/basis set combinations was performed; the deep investigation and comparison of all data highlighted the high similarity of the values (Figure 1), as clearly indicated by the computed averaged RMSD considering all investigated atoms for both the experimental and computed data sets, prompting us to find an alternative methodology for solving this stereochemical issue [averaged RMSD for experimental data set = 1.542 ppm, min. RMSD = 0.112 ppm, max RMSD = 4.058 ppm; averaged RMSD for calculated data set MPW1PW91/6-31g(d,p) = 0.932 ppm, min. RMSD = 0.011 ppm, max RMSD = 3.430 ppm; averaged RMSD for calculated data set MPW1PW91/6-311+g(d,p) = 1.103 ppm, min. RMSD = 0.062 ppm, max RMSD = 3.873 ppm; averaged RMSD for calculated data set B97-2/cc-pVTZ = 0.938 ppm, min. RMSD = 0.004 ppm, max RMSD = 3.430 ppm].

Comparing all Calculated/Experimental Data: the MAE $_{\Delta\delta}$ Parameter. Accordingly, we focused on managing all available clusters of data in a different manner, specifically combining all experimental and calculated sets of data at the same time in order to achieve a more robust comparison between all values. In this scenario, different methodologies were proposed based on this concept, such as the computation of the CP3 probability as proposed by Goodman.²⁴ Specifically, this method is only applicable to pairs of stereoisomers, making its use poorly suitable when more stereoisomers must be considered. However, the CP3 approach highlighted the benefit in simultaneously accounting and comparing all experimental/calculated chemical shifts: specifically, aligned values drive the results toward the correct assignment and, accordingly, disarranged data aid in excluding incorrect stereoisomers.

In this study, we took advantage of the above concept, introducing an approach applicable on all of the available experimental/calculated sets of data. This methodology is based on building all possible combination alignment schemes between the experimental and calculated groups of values; afterward, all accounted combination alignment schemes are ranked accounting a specific parameter in order to propose the best fit between experimental and calculated patterns. It is inferable that increasing the number of accounted isomers (e.g., moving from two to three to four isomers and so on), the comparison of experimental/computed data becomes more

arduous because the number of possible combinations increases. On the other hand, the availability of a large set of comparable data should lead to a more confident and robust assignment.

In more detail, the proposed methodology can be summarized in the following steps:

(a) generate all possible experimental/calculated comparison alignments between the sets of data. Specifically, a starting fixed sequence is defined for the calculated sets used as a reference since the stereochemistry related to each of them is known a priori. Then, all possible sequences related to the experimental set counterparts, for which the related stereochemistry must be determined, are built.

For the most simple case, that is, two stereoisomers, we can assume that two sets of calculated data, named A and B, and two sets of experimental data, named 1 and 2, are available.

The possible comparison alignments are (Figure 2) as follows:

- 1) AB/12: calculated sets A and B corresponding to experimental 1 and 2, respectively;
- 2) AB/21: calculated sets A and B corresponding to experimental 2 and 1, respectively.

Thus, as the number of experimental/calculated sets increases, the number of comparison sequences increases. Indeed, with three stereoisomers, three sets of calculated, named A, B, and C, and three sets of experimental, named 1, 2, and 3, will be accounted (Figure 1). The possible comparison sequences then will be

- 1) ABC/123: calculated A, B, and C corresponding to experimental 1, 2, and 3, respectively;
- 2) ABC/132: calculated A, B, and C corresponding to experimental 1, 3, and 2, respectively;
- 3) ABC/213: calculated A, B, and C corresponding to experimental 2, 1, and 3, respectively;
- 4) ABC/231: calculated A, B, and C corresponding to experimental 2, 3, and 1, respectively;
- 5) ABC/321: calculated A, B, and C corresponding to experimental 3, 2, and 1, respectively;
- 6) ABC/312: calculated A, B, and C corresponding to experimental 3, 1, and 2, respectively;

Starting from the number of experimental/calculated sets of data (n), the final number of comparison alignments (c) is then computed with the following relation

$$c = n! \quad (1)$$

Then, for 2, 3, and 4 sets of experimental/calculated data 2, 6, and 24 possible combinations will be taken into account (Figure 2), respectively (eq 1).

(b) The differences between the chemical shift values belonging to each possible pair of calculated sets of data following the defined sequence are computed; then, the same procedure is applied to the experimental sets of data following the possible sequences (Figure 2). The obtained values will be subsequently compared, as described in the following (c) point (vide infra).

Specifically, for the above-reported case featuring two sets of calculated data (A and B) and two sets of experimental data (1 and 2),

- 1) AB/12: for each accounted atom, the difference (Δ) between each chemical shift (δ) belonging to the calculated set A and the corresponding value belonging to B is computed through the $\Delta\delta_{\text{calc}}$ parameter:

Table 2. ^{13}C NMR MAE $_{\Delta\Delta\delta}$ Values Related to the Accounted Comparison Alignments Considering calc_1a calc_1b calc_1c calc_1d Fixed Sequence and All Possible 24 Combinations Considering exp_1a, exp_1b, exp_1c, and exp_1d Sets of Data^a

MPW1PW91/6-31g(d,p) comparison alignment ^b	MAE $_{\Delta\Delta\delta}$	MPW1PW91/6-311+g(d,p) comparison alignment ^b	MAE $_{\Delta\Delta\delta}$	B97-2/cc-pVTZ comparison alignment ^b	MAE $_{\Delta\Delta\delta}$
exp_1a exp_1b exp_1c exp_1d	1.066	exp_1a exp_1b exp_1c exp_1d	1.089	exp_1a exp_1b exp_1c exp_1d	1.070
exp_1a exp_1b exp_1d exp_1c	1.120	exp_1a exp_1b exp_1d exp_1c	1.157	exp_1a exp_1b exp_1d exp_1c	1.124
exp_1b exp_1a exp_1c exp_1d	1.224	exp_1b exp_1a exp_1c exp_1d	1.291	exp_1b exp_1a exp_1c exp_1d	1.232
exp_1b exp_1a exp_1d exp_1c	1.298	exp_1b exp_1a exp_1d exp_1c	1.380	exp_1b exp_1a exp_1d exp_1c	1.308
exp_1c exp_1b exp_1a exp_1d	2.487	exp_1c exp_1b exp_1a exp_1d	2.617	exp_1c exp_1b exp_1a exp_1d	2.471
exp_1d exp_1b exp_1a exp_1c	2.515	exp_1d exp_1b exp_1a exp_1c	2.635	exp_1d exp_1b exp_1a exp_1c	2.496
exp_1c exp_1a exp_1b exp_1d	2.541	exp_1c exp_1a exp_1b exp_1d	2.674	exp_1c exp_1a exp_1b exp_1d	2.525
exp_1d exp_1b exp_1c exp_1a	2.581	exp_1d exp_1b exp_1c exp_1a	2.702	exp_1d exp_1b exp_1c exp_1a	2.568
exp_1d exp_1a exp_1b exp_1c	2.585	exp_1a exp_1c exp_1b exp_1d	2.706	exp_1d exp_1b exp_1c exp_1a	2.582
exp_1c exp_1b exp_1d exp_1a	2.601	exp_1d exp_1a exp_1b exp_1c	2.706	exp_1c exp_1b exp_1d exp_1a	2.603
exp_1a exp_1c exp_1b exp_1d	2.609	exp_1c exp_1b exp_1d exp_1a	2.725	exp_1a exp_1c exp_1b exp_1d	2.613
exp_1a exp_1d exp_1b exp_1c	2.647	exp_1a exp_1d exp_1b exp_1c	2.743	exp_1a exp_1d exp_1b exp_1c	2.650
exp_1d exp_1a exp_1c exp_1b	2.649	exp_1a exp_1c exp_1d exp_1b	2.746	exp_1d exp_1a exp_1c exp_1b	2.653
exp_1b exp_1c exp_1d exp_1a	2.656	exp_1b exp_1c exp_1d exp_1a	2.749	exp_1c exp_1a exp_1d exp_1b	2.678
exp_1c exp_1a exp_1d exp_1b	2.671	exp_1a exp_1d exp_1c exp_1b	2.773	exp_1b exp_1c exp_1d exp_1a	2.681
exp_1a exp_1c exp_1d exp_1b	2.674	exp_1d exp_1a exp_1c exp_1b	2.778	exp_1b exp_1c exp_1a exp_1d	2.688
exp_1b exp_1c exp_1a exp_1d	2.681	exp_1b exp_1d exp_1c exp_1a	2.784	exp_1a exp_1c exp_1d exp_1b	2.698
exp_1b exp_1d exp_1c exp_1a	2.691	exp_1b exp_1c exp_1a exp_1d	2.805	exp_1b exp_1d exp_1c exp_1a	2.715
exp_1a exp_1d exp_1c exp_1b	2.711	exp_1c exp_1a exp_1d exp_1b	2.812	exp_1b exp_1d exp_1a exp_1c	2.729
exp_1b exp_1d exp_1a exp_1c	2.721	exp_1b exp_1d exp_1a exp_1c	2.856	exp_1a exp_1d exp_1c exp_1b	2.734
exp_1d exp_1c exp_1b exp_1a	3.205	exp_1d exp_1c exp_1b exp_1a	3.410	exp_1d exp_1c exp_1b exp_1a	3.203
exp_1c exp_1d exp_1b exp_1a	3.236	exp_1c exp_1d exp_1b exp_1a	3.433	exp_1c exp_1d exp_1b exp_1a	3.235
exp_1d exp_1c exp_1a exp_1b	3.289	exp_1d exp_1c exp_1a exp_1b	3.496	exp_1d exp_1c exp_1a exp_1b	3.290
exp_1c exp_1d exp_1a exp_1b	3.324	exp_1c exp_1d exp_1a exp_1b	3.528	exp_1c exp_1d exp_1a exp_1b	3.328

^aThe correct comparison alignments are highlighted in green, showing their top-ranked positions also accounting different functional/basis set combinations. ^bconsidering calc_1a calc_1b calc_1c and calc_1d starting fixed sequence related to the calculated sets of data.

$$\Delta\delta_{\text{calcA-B}} = \delta_{\text{calcA}} - \delta_{\text{calcB}}$$

where δ_{calcA} and δ_{calcB} are the chemical shift values belonging to A and B sets of calculated data, respectively.

In the same way, the procedure is applied to the experimental sets, specifically computing $\Delta\delta$ between the chemical shifts belonging to 1 and 2 sets of values

$$\Delta\delta_{\text{exp1-2}} = \delta_{\text{exp1}} - \delta_{\text{exp2}}$$

where δ_{exp1} and δ_{exp2} are the chemical shift values belonging to 1 and 2 sets of experimental data, respectively. Afterward, $\Delta\delta_{\text{calcA-B}}$ and $\Delta\delta_{\text{exp1-2}}$ values will be compared (vide infra, (c) point).

It is important to note that, in this step, the differences between the calculated ($\Delta\delta_{\text{calc}}$) and experimental ($\Delta\delta_{\text{exp}}$) chemical shifts of corresponding carbons are computed for the subsequent comparison (vide infra), following the idea by Belostotskii,²⁵ Rodríguez,²⁶ and Goodman,²⁴ which highlighted the higher accuracy in comparing the differences between the chemical shifts than the shifts themselves because of the elimination of systematic errors.

(2) AB/21: again, $\Delta\delta_{\text{calcA-B}}$ group of values are computed as reported above; contrarily, for the experimental sets of data, the chemical shift differences are computed following the new sequence, namely, between 2 and 1, and leading to $\Delta\delta_{\text{calc2-1}}$ group of values. In this case, $\Delta\delta_{\text{calcA-B}}$ values will be then compared with those from $\Delta\delta_{\text{exp2-1}}$ (vide infra, (c) point).

Moving to three calculated/experimental sets of data, for each defined comparison alignment, three possible $\Delta\delta_{\text{calc}}$ and $\Delta\delta_{\text{exp}}$ sets of values can be computed after defining the combination pairs (Figure 2). For instance, considering the ABC/123 calculated/experimental comparison alignments, the following $\Delta\delta_{\text{calc}}$ and $\Delta\delta_{\text{exp}}$ sets of values can be defined for the subsequent comparison

$$\Delta\delta_{\text{calcA-B}} \text{ vs } \Delta\delta_{\text{exp1-2}}; \Delta\delta_{\text{calcA-C}} \text{ vs } \Delta\delta_{\text{exp1-3}}; \Delta\delta_{\text{calcB-C}} \text{ vs } \Delta\delta_{\text{exp2-3}}$$

In general, starting from the number of calculated/experimental sets of data (n), for each defined comparison alignment, the related number of calculated/experimental $\Delta\delta$ sets ($N_{\Delta\delta}$) to be accounted considering all possible pairs can be computed with the following relation (eq 2)

$$N_{\Delta\delta} = \sum_{k=1}^n (k-1) \quad (2)$$

Thus, for each of the 24 comparison alignments arising from 4 sets of experimental/calculated data (eq 1), 6 possible $\Delta\delta_{\text{calc}}$ and $\Delta\delta_{\text{exp}}$ sets of values can be computed after defining the related combination pairs (eq 2).

It is important to note that, following this procedure, the calculation of the differences between calculated chemical shift data ($\Delta\delta_{\text{calc}}$) allows to avoid all systematic errors arising from calibration procedures required for computing the chemical shift data from shielding the tensor values [using trimethylsilane (TMS) as the reference].

(c) Following the comparison alignments, the specific $\Delta\delta_{\text{calc}}$ and corresponding $\Delta\delta_{\text{exp}}$ group of values are then compared atom by atom using the $\Delta\Delta\delta$ parameter

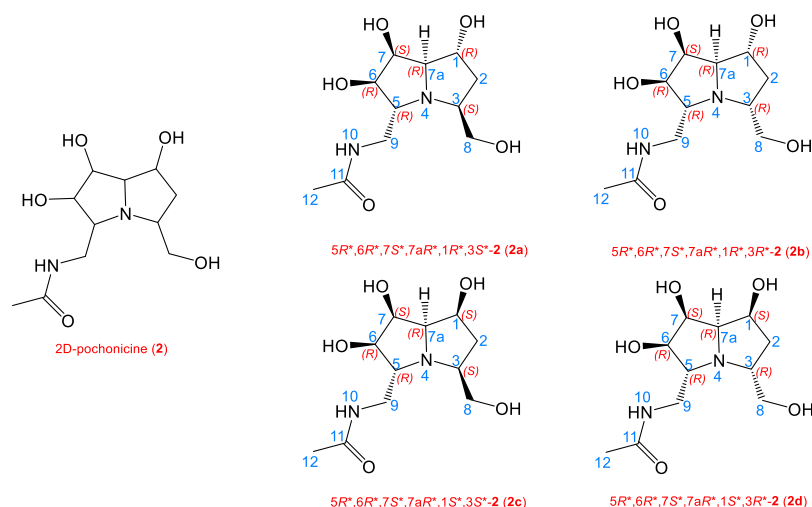
$$\Delta\Delta\delta = |\Delta\delta_{\text{calc}} - \Delta\delta_{\text{exp}}|$$

defined as the absolute difference between the $\Delta\delta_{\text{calc}}$ and $\Delta\delta_{\text{exp}}$ for each accounted atom.

In this way, the obtained $\Delta\Delta\delta$ differences are employed for detecting the similarities between calculated and experimental sets of data and then for identifying the most promising comparison alignment among all possibilities. Indeed, all computed $\Delta\Delta\delta$ values can be easily converted into a parameter that quickly indicates the best comparison alignment among all possibilities. In this study, we have defined the MAE $_{\Delta\Delta\delta}$ parameter

$$\text{MAE}_{\Delta\Delta\delta} = \frac{\sum (\Delta\Delta\delta)}{n_{\Delta\Delta\delta}}$$

Chart 2. Chemical Structures of the Four Accounted Pochonicine-Related Stereoisomers (2a–2d)

Table 3. ¹³C NMR MAE Values and DP4+ Probabilities Computed for the Three Functional/Basis Set Combinations Accounted in This Study Related to Compounds 2a–2d^a

	MPW1PW91/6-31g(d,p)		exp_2a set of data MPW1PW91/6-311+g(d,p)		B97-2/cc-pVTZ	
	¹³ C MAE	DP4+ probability	¹³ C MAE	DP4+ probability	¹³ C MAE	DP4+ probability
calc_2a	3.21	0.01%	3.16	0.00%	3.25	N.A. ^b
calc_2b	2.93	99.94%	2.71	100.00%	3.28	N.A. ^b
calc_2c	3.27	0.06%	4.27	98.85%	4.18	N.A. ^b
calc_2d	4.45	0.00%	4.59	0.00%	4.16	N.A. ^b
	MPW1PW91/6-31g(d,p)		exp_2b set of data MPW1PW91/6-311+g(d,p)		B97-2/cc-pVTZ	
	¹³ C MAE	DP4+ probability	¹³ C MAE	DP4+ probability	¹³ C MAE	DP4+ probability
calc_2a	4.55	0.00%	3.06	0.00%	2.74	N.A. ^b
calc_2b	2.12	100.00%	1.53	100.00%	1.75	N.A. ^b
calc_2c	5.09	0.00%	4.67	0.00%	4.46	N.A. ^b
calc_2d	4.48	0.00%	3.25	0.00%	2.82	N.A. ^b
	MPW1PW91/6-31g(d,p)		exp_2c set of data MPW1PW91/6-311+g(d,p)		B97-2/cc-pVTZ	
	¹³ C MAE	DP4+ probability	¹³ C MAE	DP4+ probability	¹³ C MAE	DP4+ probability
calc_2a	3.03	0.33%	3.55	0.00%	3.60	N.A. ^b
calc_2b	3.62	0.05%	2.79	0.16%	3.21	N.A. ^b
calc_2c	2.78	99.61%	3.64	99.83%	3.61	N.A. ^b
calc_2d	3.52	0.00%	3.95	0.00%	3.95	N.A. ^b
	MPW1PW91/6-31g(d,p)		exp_2d set of data MPW1PW91/6-311+g(d,p)		B97-2/cc-pVTZ	
	¹³ C MAE	DP4+ probability	¹³ C MAE	DP4+ probability	¹³ C MAE	DP4+ probability
calc_2a	4.70	0.00%	3.53	0.00%	3.08	N.A. ^b
calc_2b	3.18	71.56%	2.51	0.00%	2.64	N.A. ^b
calc_2c	5.24	0.00%	4.19	0.00%	3.75	N.A. ^b
calc_2d	3.34	28.44%	1.60	100.00%	1.47	N.A. ^b

^aThe correct/incorrect correspondence between experimental and calculated data are highlighted in green and orange, respectively. ^bB97-2/cc-pVTZ functional/basis set combination cannot be set in the calculation of DP4+ probability.

defined as the summation (\sum) of the n computed $\Delta\delta$ absolute error values ($\Delta\Delta\delta$) normalized to the number of $\Delta\Delta\delta$ errors considered ($n_{\Delta\Delta\delta}$).

Summarizing, for each possible experimental/calculated comparison alignment, the related $\text{MAE}_{\Delta\Delta\delta}$ value can be computed; finally, the lowest $\text{MAE}_{\Delta\Delta\delta}$ value among the ranking indicated the best fit between each experimental and calculated set of data.

Applying the Methodology on Cladosporine and Pochonicine Stereoisomers. The reported workflow was then applied to the four investigated cladologs (1a–1d). In this case, with 4 available sets of experimental/calculated data, 24 possible comparison alignments were taken into account (eq 1) for generating the related $\text{MAE}_{\Delta\Delta\delta}$ values (Table 2).

The calculated sets of data arising from the different combinations of functional/basis sets above reported were accounted (Table 2) in order to evaluate the applicability of the proposed procedure and to compare the results with those previously obtained. For each employed level of theory, the analysis of the data indicated that the lowest $\text{MAE}_{\Delta\Delta\delta}$ value obtained among the ranking of 24 possibilities was that related to the calc_1a calc_1b calc_1c calc_1d/exp_1a exp_1b exp_1c exp_1d comparison alignment (Table 2). On the other hand, we also computed, for each of the 24 comparison alignments, the average of the 4 possible MAE values obtained from the comparison of the calculated and experimental chemical shifts (see Table S13) instead of comparing the differences of the shifts, as proposed by us.

Table 4. ^{13}C NMR $\text{MAE}_{\Delta\Delta\delta}$ Values Related to the Accounted Comparison Alignments Considering calc_2a calc_2b calc_2c calc_2d Fixed Sequence and all the Possible 24 Combinations Considering exp_2a, exp_2b, exp_2c, and exp_2d Sets of Data^a

MPW1PW91/6-31g(d,p)		MPW1PW91/6-311+g(d,p)		B97-2/cc-pVTZ	
comparison alignment ^b	MAE _{ΔΔδ}	comparison alignment ^b	MAE _{ΔΔδ}	comparison alignment ^b	MAE _{ΔΔδ}
exp_2a exp_2b exp_2c exp_2d	2.733	exp_2a exp_2b exp_2c exp_2d	2.978	exp_2a exp_2b exp_2c exp_2d	2.672
exp_2c exp_2b exp_2a exp_2d	2.778	exp_2c exp_2b exp_2a exp_2d	3.154	exp_2c exp_2b exp_2a exp_2d	2.933
exp_2b exp_2a exp_2c exp_2d	3.745	exp_2b exp_2a exp_2c exp_2d	3.360	exp_2b exp_2a exp_2c exp_2d	3.184
exp_2d exp_2b exp_2a exp_2c	3.889	exp_2b exp_2c exp_2a exp_2d	3.620	exp_2b exp_2c exp_2a exp_2d	3.506
exp_2a exp_2d exp_2c exp_2b	3.897	exp_2c exp_2a exp_2b exp_2d	3.811	exp_2a exp_2d exp_2c exp_2b	3.725
exp_2c exp_2d exp_2a exp_2b	3.995	exp_2a exp_2c exp_2b exp_2d	3.894	exp_2c exp_2a exp_2b exp_2d	3.729
exp_2b exp_2c exp_2a exp_2d	4.001	exp_2a exp_2d exp_2c exp_2b	3.988	exp_2a exp_2c exp_2b exp_2d	3.787
exp_2b exp_2d exp_2a exp_2c	4.082	exp_2c exp_2d exp_2a exp_2b	4.173	exp_2c exp_2d exp_2a exp_2b	3.927
exp_2a exp_2b exp_2d exp_2c	4.138	exp_2a exp_2c exp_2d exp_2b	4.300	exp_2d exp_2a exp_2c exp_2b	4.073
exp_2c exp_2a exp_2b exp_2d	4.153	exp_2b exp_2d exp_2a exp_2c	4.381	exp_2a exp_2c exp_2d exp_2b	4.094
exp_2d exp_2b exp_2c exp_2a	4.184	exp_2a exp_2b exp_2d exp_2c	4.394	exp_2a exp_2b exp_2d exp_2c	4.143
exp_2a exp_2d exp_2b exp_2c	4.419	exp_2d exp_2a exp_2c exp_2b	4.408	exp_2d exp_2b exp_2a exp_2c	4.170
exp_2a exp_2c exp_2b exp_2d	4.425	exp_2c exp_2a exp_2d exp_2b	4.475	exp_2c exp_2a exp_2d exp_2b	4.217
exp_2b exp_2d exp_2c exp_2a	4.487	exp_2b exp_2a exp_2d exp_2c	4.480	exp_2d exp_2c exp_2a exp_2b	4.234
exp_2c exp_2b exp_2d exp_2a	4.543	exp_2d exp_2b exp_2a exp_2c	4.487	exp_2b exp_2a exp_2d exp_2c	4.282
exp_2b exp_2a exp_2d exp_2c	4.680	exp_2d exp_2c exp_2a exp_2b	4.517	exp_2b exp_2d exp_2a exp_2c	4.287
exp_2d exp_2a exp_2c exp_2b	4.730	exp_2b exp_2d exp_2c exp_2a	4.634	exp_2d exp_2b exp_2c exp_2a	4.314
exp_2c exp_2d exp_2b exp_2a	4.868	exp_2d exp_2b exp_2c exp_2a	4.673	exp_2b exp_2d exp_2c exp_2a	4.457
exp_2d exp_2c exp_2a exp_2b	4.875	exp_2a exp_2d exp_2b exp_2c	4.769	exp_2c exp_2b exp_2d exp_2a	4.527
exp_2c exp_2a exp_2d exp_2b	4.883	exp_2b exp_2c exp_2d exp_2a	4.776	exp_2b exp_2c exp_2d exp_2a	4.595
exp_2a exp_2c exp_2d exp_2b	5.014	exp_2c exp_2b exp_2d exp_2a	4.797	exp_2a exp_2d exp_2b exp_2c	4.681
exp_2d exp_2a exp_2b exp_2c	5.066	exp_2d exp_2a exp_2b exp_2c	4.964	exp_2d exp_2a exp_2b exp_2c	4.758
exp_2b exp_2c exp_2d exp_2a	5.259	exp_2c exp_2d exp_2b exp_2a	5.166	exp_2c exp_2d exp_2b exp_2a	5.004
exp_2d exp_2c exp_2b exp_2a	5.557	exp_2d exp_2c exp_2b exp_2a	5.284	exp_2d exp_2c exp_2b exp_2a	5.062

^aThe correct comparison alignments are highlighted in green, showing their top-ranked positions also accounting different functional/basis set combinations. ^bConsidering calc_2a calc_2b calc_2c and calc_2d starting fixed sequence related to the calculated sets of data.

In this case, we again obtained the correct comparison alignment, but the comparison with the $\text{MAE}_{\Delta\Delta\delta}$ data pointed out for the latter more discrete values and better discriminating power in identifying the correct correspondences between the data sets (see Table S13). These results strongly confirmed the applicability of the proposed methodology, highlighting with a high level of confidence the correct stereochemical assignment of groups of stereoisomers.

In order to further corroborate the proposed approach, we investigated another tetrad of stereoisomers related to pochonicine, a naturally occurring polyhydroxylated pyrrolizidine from *Pochonia suchlasporia* var. *suchlasporia* TAMA 87. In 2013, Yu et al. reported the synthesis of eight stereoisomers of pochonicine²⁷ and, in this study, we accounted the four stereoisomers with different relative configurations at C-1 and C-3 while maintaining the 5R*,6R*,7S*,7aR* configurations. In Chart 2, the four accounted stereoisomers related to pochonicine (2a–2d) are depicted.

Following the same scheme above reported for cladologs, we named the sets of calculated data for 2a–2d as calc_2a, calc_2b, calc_2c, and calc_2d, respectively, and the sets of experimental data, reported in the reference study²⁷ (corroborated by comparison with further studies on pochonicine^{28,29}), were named for 2a–2d as exp_2a, exp_2b, exp_2c, and exp_2d, respectively.

Again, employing the “classic” QM/NMR approach, the correct correspondences between the four calculated and experimental sets of data were not found considering the three functional/basis set combinations (Tables 3 and S14–S25). Conversely, the computation of the 24 $\text{MAE}_{\Delta\Delta\delta}$ values related to the comparison alignments considering calc_2a calc_2b calc_2c calc_2d sequence highlighted exp_2a, exp_2b, exp_2c, and exp_2d as the solution showing the lowest $\text{MAE}_{\Delta\Delta\delta}$ values for all three functional/basis sets employed (Table 4), thus confirming the applicability of the proposed approach.

CONCLUSIONS

In this study, we introduced an approach guiding the correct assignment of groups of stereoisomers. This methodology is based on building all possible comparison alignments between a fixed sequence from the QM/NMR calculated sets of data and all possible sequences arising from the combinations of the experimental sets of data. For each comparison alignment, the $\text{MAE}_{\Delta\Delta\delta}$ value is computed, generating a final ranking from the lowest to the highest value. Accordingly, the comparison alignment featuring the lowest $\text{MAE}_{\Delta\Delta\delta}$ value indicates the best fit between each calculated and experimental set of value, facilitating the assignment of groups of stereoisomers. We validated this approach accounting four stereoisomers of cladospirin (cladologs) and pochonicine, showing the correct assignment of each set of experimental data to the specific stereoisomer. The present approach is not limited by the number of stereoisomers to be accounted, thus representing a valuable tool for solving specific stereochemical issues. Moreover, we inserted a dedicated tab on the website of our research group (<https://computorgchem.unisa.it>) containing a tool for the straightforward $\text{MAE}_{\Delta\Delta\delta}$ computation starting from calculated and experimental data sets as input files.

EXPERIMENTAL SECTION

Experimental ^{13}C NMR Data. All experimental ^{13}C NMR chemical shift data related to compounds 1a–1d and 2a–2d were retrieved from the related reference papers,^{19–21,27–29} as reported above.

Computation of NMR Parameters. Three-dimensional starting models of compounds 1a–1d and 2a–2d were built by Maestro 10.2³⁰ and optimized by MacroModel 10.2³¹ with the OPLS force field³² and the Polak-Ribier conjugate gradient algorithm (maximum derivative less than 0.001 kcal/mol). Conformational search rounds for the above-mentioned compounds were performed using MacroModel 10.2^{30,31} on the empirical MM level. Specifically, Monte Carlo multiple minimum and low mode conformational search methods were first employed in order to explore the conformational space. Furthermore, rounds of molecular dynamics simulations were performed at 450, 600, 700, and 750 K, with a time step of 2.0 fs, an equilibration time of 0.1 ns, and a simulation time of 10 ns. All

produced conformers were then collected and analyzed in order to discard the redundant ones. Specifically, the nonredundant conformers were selected by using the “redundant conformer elimination” module of Macromodel 10.2³⁰ excluding those differing more than 12.5 kJ/mol (3.0 kcal/mol) from the most energetically favored conformation and setting a 0.1 Å RMSD minimum cutoff for saving structures. The following reported QM calculations were performed using Gaussian 09 software.³³

The obtained conformers were geometry optimized on the QM level by using the MPW1PW91 functional and the 6-31G(d) basis set. After this step, the new geometries were visually inspected in order to filter out further possible redundant conformers. Finally, the obtained conformers were accounted for the subsequent computation of the ¹³C NMR chemical shifts using the MPW1PW91/6-31G(d,p), MPW1PW91/6-311+G(d,p), B97-2/cc-pVTZ functionals/basis set combinations (see Results and Discussion and Tables S1–S12, S14–S25, Supporting Information). The final ¹³C NMR chemical shift data were computed considering the influence of each conformer on the total Boltzmann distribution and taking into account the relative energies. Calibrations of calculated ¹³C chemical shifts were performed following the multistandard approach.^{34,35} Benzene was used as the reference compound for computing sp² ¹³C NMR chemical shifts (excluding carbonyl carbons) in detail,^{34,35} whereas TMS was used for computing sp³ ¹³C chemical shift data.

The comparison of calculated and experimental data¹⁹ was performed accounting $\Delta\delta$, $\Delta\delta_{\text{calc}}$, $\Delta\delta_{\text{exp}}$, $\Delta\Delta\delta$, MAE, and MAE $_{\Delta\Delta\delta}$ parameters, as reported in the Results and Discussion section.

■ ASSOCIATED CONTENT

SI Supporting Information

The Supporting Information is available free of charge at <https://pubs.acs.org/doi/10.1021/acs.joc.9b03129>.

Calculated NMR chemical shifts with cartesian coordinates of the optimized geometries and related energies for the three employed functional/basis set combinations for the conformers of **1a–1d** and **2a–2d** (PDF)

■ AUTHOR INFORMATION

Corresponding Author

Giuseppe Bifulco – Department of Pharmacy, University of Salerno, Fisciano 84084, Italy; orcid.org/0000-0002-1788-5170; Phone: +39 (0)89969741; Email: bifulco@unisa.it; Fax: +39 (0)89969602

Authors

Gianluigi Lauro – Department of Pharmacy, University of Salerno, Fisciano 84084, Italy; orcid.org/0000-0001-5065-9717

Pronay Das – Organic Chemistry Division, CSIR-National Chemical Laboratory, Pune 411008, India; Academy of Scientific and Innovative Research (AcSIR), New Delhi 110025, India

Raffaele Riccio – Department of Pharmacy, University of Salerno, Fisciano 84084, Italy

D. Srinivasa Reddy – Organic Chemistry Division, CSIR-National Chemical Laboratory, Pune 411008, India; Academy of Scientific and Innovative Research (AcSIR), New Delhi 110025, India; orcid.org/0000-0003-3270-315X

Complete contact information is available at: <https://pubs.acs.org/doi/10.1021/acs.joc.9b03129>

Notes

The authors declare no competing financial interest.

■ ACKNOWLEDGMENTS

G.B. acknowledges the financial support of MIUR Italy PRIN 2017 project (2017A95NCJ) “Stolen molecules—Stealing natural products from the depot and reselling them as new drug candidates.” D.S.R. would like to acknowledge the SERB, New Delhi, India, for funding the project titled “Hit to Lead Development of Potent Anti-Parasitic Natural Product Scaffolds” (EMR/2016/004301). P.D. thanks the University Grants Commission (UGC) for providing research fellowship.

■ REFERENCES

- (1) Bifulco, G.; Dambruoso, P.; Gomez-Paloma, L.; Riccio, R. Determination of relative configuration in organic compounds by NMR spectroscopy and computational methods. *Chem. Rev.* **2007**, *107*, 3744–3779.
- (2) Seco, J. M.; Quiñoá, E.; Riguera, R. The assignment of absolute configuration by NMR. *Chem. Rev.* **2004**, *104*, 17–118.
- (3) Tormena, C. F. Conformational analysis of small molecules: NMR and quantum mechanics calculations. *Prog. Nucl. Magn. Reson. Spectrosc.* **2016**, *96*, 73–88.
- (4) Di Micco, S.; Chini, M. G.; Riccio, R.; Bifulco, G. Quantum mechanical calculation of NMR parameters in the stereostructural determination of natural products. *Eur. J. Org. Chem.* **2010**, *2010*, 1411–1434.
- (5) Lodewyk, M. W.; Siebert, M. R.; Tantillo, D. J. Computational prediction of ¹H and ¹³C chemical shifts: a useful tool for natural product, mechanistic, and synthetic organic chemistry. *Chem. Rev.* **2012**, *112*, 1839–1862.
- (6) Willoughby, P. H.; Jansma, M. J.; Hoye, T. R. A guide to small-molecule structure assignment through computation of (¹H- and ¹³C-) NMR chemical shifts. *Nat. Protoc.* **2014**, *9*, 643–660.
- (7) Krivdin, L. B. Computational protocols for calculating ¹³C NMR chemical shifts. *Prog. Nucl. Magn. Reson. Spectrosc.* **2019**, *112–113*, 103–156.
- (8) Kutateladze, A. G.; Holt, T. Structure Validation of Complex Natural Products: Time to Change the Paradigm. What did Synthesis of Alstofoline A Prove? *J. Org. Chem.* **2019**, *84*, 8297–8299.
- (9) Cerulli, A.; Lauro, G.; Masullo, M.; Cantone, V.; Olas, B.; Kontek, B.; Nazzaro, F.; Bifulco, G.; Piacente, S. Cyclic Diarylheptanoids from *Corylus avellana* Green Leafy Covers: Determination of Their Absolute Configurations and Evaluation of Their Antioxidant and Antimicrobial Activities. *J. Nat. Prod.* **2017**, *80*, 1703–1713.
- (10) Nadmid, S.; Plaza, A.; Lauro, G.; Garcia, R.; Bifulco, G.; Müller, R. Hyalachelins A–C, Unusual Siderophores Isolated from the Terrestrial Myxobacterium *Hyalangium minutum*. *Org. Lett.* **2014**, *16*, 4130–4133.
- (11) Dardić, D.; Lauro, G.; Bifulco, G.; Laboudie, P.; Sakhaei, P.; Bauer, A.; Vilcinskis, A.; Hammann, P. E.; Plaza, A. Svetamycins A–G., Unusual Piperazine Acid-Containing Peptides from *Streptomyces* sp. *J. Org. Chem.* **2017**, *82*, 6032–6043.
- (12) Bertamino, A.; Lauro, G.; Ostacolo, C.; Di Sarno, V.; Musella, S.; Ciaglia, T.; Campiglia, P.; Bifulco, G.; Gomez-Monterrey, I. M. Ring-Fused Cyclic Aminals from Tetrahydro- β -carboline-Based Dipeptide Compounds. *J. Org. Chem.* **2017**, *82*, 12014–12027.
- (13) Bifulco, G.; Riccio, R.; Martin, G. E.; Buevich, A. V.; Williamson, R. T. Quantum chemical calculations of ¹J_{CC} coupling constants for the stereochemical determination of organic compounds. *Org. Lett.* **2013**, *15*, 654–657.
- (14) Bagno, A.; Rastrelli, F.; Saielli, G. Predicting C-13 NMR spectra by DFT calculations. *J. Phys. Chem. A* **2003**, *107*, 9964–9973.
- (15) Smith, S. G.; Goodman, J. M. Assigning stereochemistry to single diastereoisomers by GIAO NMR calculation: the DP4 probability. *J. Am. Chem. Soc.* **2010**, *132*, 12946–12959.
- (16) Grimblat, N.; Zanardi, M. M.; Sarotti, A. M. Beyond DP4: an Improved Probability for the Stereochemical Assignment of Isomeric

Compounds using Quantum Chemical Calculations of NMR Shifts. *J. Org. Chem.* **2015**, *80*, 12526–12534.

(17) Barone, G.; Duca, D.; Silvestri, A.; Gomez-Paloma, L.; Riccio, R.; Bifulco, G. Determination of the relative stereochemistry of flexible organic compounds by Ab initio methods: Conformational analysis and boltzmann-averaged GIAO ^{13}C NMR chemical shifts. *Chem.—Eur. J.* **2002**, *8*, 3240–3245.

(18) Scott, P. M.; Walbeek, W. V.; MacLean, W. M. Cladosporin, a new antifungal metabolite from *Cladosporium cladosporioides*. *J. Antibiot.* **1971**, *24*, 747–755.

(19) Das, P.; Babbar, P.; Malhotra, N.; Sharma, M.; Jachak, G. R.; Gonnade, R. G.; Shanmugam, D.; Harlos, K.; Yogavel, M.; Sharma, A.; Reddy, D. S. Specific Stereoisomeric Conformations Determine the Drug Potency of Cladosporin Scaffold against Malarial Parasite. *J. Med. Chem.* **2018**, *61*, 5664–5678.

(20) Rawlings, B. J.; Reese, P. B.; Ramer, S. E.; Vederas, J. C. Comparison of fatty acid and polyketide biosynthesis: stereochemistry of cladosporin and oleic acid formation in *Cladosporium cladosporioides*. *J. Am. Chem. Soc.* **1989**, *111*, 3382–3390.

(21) Jacyno, J. M.; Harwood, J. S.; Cutler, H. G.; Lee, M.-K. Isocladosporin, a Biologically Active Isomer of Cladosporin from *Cladosporium cladosporioides*. *J. Nat. Prod.* **1993**, *56*, 1397–1401.

(22) Cimino, P.; Gomez-Paloma, L.; Duca, D.; Riccio, R.; Bifulco, G. Comparison of different theory models and basis sets in the calculation of ^{13}C NMR chemical shifts of natural products. *Magn. Reson. Chem.* **2004**, *42*, S26–S33.

(23) Flaig, D.; Maurer, M.; Hanni, M.; Braunger, K.; Kick, L.; Thubauville, M.; Ochsenfeld, C. Benchmarking Hydrogen and Carbon NMR Chemical Shifts at HF, DFT, and MP2 Levels. *J. Chem. Theory Comput.* **2014**, *10*, 572–578.

(24) Smith, S. G.; Goodman, J. M. Assigning the stereochemistry of pairs of diastereoisomers using GIAO NMR shift calculation. *J. Org. Chem.* **2009**, *74*, 4597–4607.

(25) Belostotskii, A. M. Calculated chemical shifts as a fine tool of conformational analysis: an unambiguous solution for haouamine alkaloids. *J. Org. Chem.* **2008**, *73*, 5723–5731.

(26) Poza, J. J.; Jiménez, C.; Rodríguez, J. J.-Based Analysis and DFT-NMR Assignments of Natural Complex Molecules: Application to $3\beta,7$ -Dihydroxy-5,6-epoxycholestanes. *Eur. J. Org. Chem.* **2008**, *2008*, 3960–3969.

(27) Zhu, J.-S.; Nakagawa, S.; Chen, W.; Adachi, I.; Jia, Y.-M.; Hu, X.-G.; Fleet, G. W. J.; Wilson, F. X.; Nitoda, T.; Horne, G.; van Well, R.; Kato, A.; Yu, C.-Y. Synthesis of Eight Stereoisomers of Pochonicine: Nanomolar Inhibition of β -N-Acetylhexosaminidases. *J. Org. Chem.* **2013**, *78*, 10298–10309.

(28) Usuki, H.; Toyooka, M.; Kanzaki, H.; Okuda, T.; Nitoda, T. Pochonicine, a polyhydroxylated pyrrolizidine alkaloid from fungus *Pochonia suchlasporia* var. *suchlasporia* TAMA 87 as a potent β -N-acetylglucosaminidase inhibitor. *Bioorg. Med. Chem.* **2009**, *17*, 7248–7253.

(29) Kitamura, Y.; Koshino, H.; Nakamura, T.; Tsuchida, A.; Nitoda, T.; Kanzaki, H.; Matsuoka, K.; Takahashi, S. Total synthesis of the proposed structure for pochonicine and determination of its absolute configuration. *Tetrahedron Lett.* **2013**, *54*, 1456–1459.

(30) *Maestro*, 10.2; Schrödinger, LLC: New York, NY, 2015.

(31) *MacroModel*, 10.2; Schrödinger LLC: New York, NY, 2013.

(32) Jorgensen, W. L.; Tirado-Rives, J. The OPLS [optimized potentials for liquid simulations] potential functions for proteins, energy minimizations for crystals of cyclic peptides and crambin. *J. Am. Chem. Soc.* **1988**, *110*, 1657–1666.

(33) Frisch, M. J.; Trucks, G. W.; Schlegel, H. B.; Scuseria, G. E.; Robb, M. A.; Cheeseman, J. R.; Scalmani, G.; Barone, V.; Mennucci, B.; Petersson, G. A.; Nakatsuji, H.; Caricato, M.; Li, X.; Hratchian, H. P.; Izmaylov, A. F.; Bloino, J.; Zheng, G.; Sonnenberg, J. L.; Hada, M.; Ehara, M.; Toyota, K.; Fukuda, R.; Hasegawa, J.; Ishida, M.; Nakajima, T.; Honda, Y.; Kitao, O.; Nakai, H.; Vreven, T.; Montgomery, J. A.; Peralta, J. E. J.; Ogliaro, F.; Bearpark, M.; Heyd, J. J.; Brothers, E.; Kudin, K. N.; Staroverov, V. N.; Kobayashi, R.; Normand, J.; Raghavachari, K.; Rendell, A.; Burant, J. C.; Iyengar,

S. S.; Tomasi, J.; Cossi, M.; Rega, N.; Millam, J. M.; Klene, M.; Knox, J. E.; Cross, J. B.; Bakken, V.; Adamo, C.; Jaramillo, J.; Gomperts, R.; Stratmann, R. E.; Yazyev, O.; Austin, A. J.; Cammi, R.; Pomelli, C.; Ochterski, J. W.; Martin, R. L.; Morokuma, K.; Zakrzewski, V. G.; Voth, G. A.; Salvador, P.; Dannenberg, J. J.; Dapprich, S.; Daniels, A. D.; Farkas, O.; Foresman, J. B.; Ortiz, J. V.; Cioslowski, J.; Fox, D. J. *Gaussian 09*, Revision A.02; Gaussian, Inc.: Wallingford CT, 2009.

(34) Sarotti, A. M.; Pellegrinet, S. C. A multi-standard approach GIAO ^{13}C NMR calculations. *J. Org. Chem.* **2009**, *74*, 7254–7260.

(35) Sarotti, A. M.; Pellegrinet, S. C. Application of the multi-standard methodology for calculating ^1H NMR chemical shifts. *J. Org. Chem.* **2012**, *77*, 6059–6065.



Herbicidal bio-assay of isocladosporin enantiomers and determination of its plausible absolute configuration

Yash Mankad¹ · Pronay Das^{1,2} · Ejaj Pathan^{2,3} · M. V. Deshpande^{2,3} · D. Srinivasa Reddy^{1,2,4}

Received: 13 June 2020 / Revised: 7 November 2020 / Accepted: 10 November 2020

© The Author(s), under exclusive licence to the Japan Antibiotics Research Association 2021

Abstract

A fungal metabolite, isocladosporin was isolated from natural fungus, *Cladosporium cladosporioides* in the mid of 90s. Due to the lack of optical rotation of isolated natural product sample, the absolute configuration of the natural product remained undetermined for more than two decades. Herein, we demonstrated an SAR study of enantiomers of isocladosporin in herbicidal bio-assay against wheat coleoptile. Using this study as a comparative tool we further proposed the plausible absolute configuration of natural isocladosporin for the first time. The assigned configuration was also supported through biogenetic precursors.

Introduction

Isocladosporin, a fungal secondary metabolite was isolated from the fungus *Cladosporium cladosporioides* way back in 1993 by Jackyno et al. [1]. This fungus also happens to be the natural production source of potent antimalarial natural product cladosporin [2]. Both the natural products feature a 2,6-disubstituted tetrahydropyran ring and a δ -valerolactone fused to a 1,3-dihydroxybenzene ring [1, 3]. Unlike cladosporin the 2,6-disubstituted tetrahydropyran ring in isocladosporin bears a *cis* geometry [1, 3]. Initial isolation report by Jackyno et al. documented two diastereomeric

structural possibility (**1'** and **2'**) of isocladosporin (Fig. 1) through 2D NMR analysis [1]. As a matter of fact, in 2012 Zheng et al. successfully synthesized **2** and the enantiomer **3** of **1'** [3]. Correlation of NMR data and melting point values of the two synthesized structures led them to conclude the relative stereochemistry of isocladosporin to be of **2** [3]. Absolute stereochemistry could not be deciphered owing to the lack of optical rotation data in literature, which in turn led to the possibility of two enantiomers (**2** and **4**), one of which is likely to be the natural product, isocladosporin. Here we determined the absolute configuration of natural isocladosporin using biological assay and the details are discussed in the present paper.

Supplementary information The online version of this article (<https://doi.org/10.1038/s41429-020-00391-1>) contains supplementary material, which is available to authorized users.

✉ M. V. Deshpande
mv.deshpande@ncl.res.in

✉ D. Srinivasa Reddy
ds.reddy@ncl.res.in

¹ Division of Organic Chemistry, CSIR-National Chemical Laboratory, Dr. Homi Bhabha Road, Pune 411008, India

² Academy of Scientific and Innovative Research (AcSIR), Ghaziabad 201002, India

³ Biochemical Sciences Division, CSIR-National Chemical Laboratory, Dr. Homi Bhabha Road, Pune 411008, India

⁴ Present address: CSIR-Indian Institute of Integrative medicine, Canal Road, Jammu 180001, India

Results and discussions

Till date, three total syntheses of one of the possible enantiomer **2** of the isocladosporin has been documented in the literature. The first total synthesis appeared from She et al. in the year 2012, where they synthesized **2** in a nine step linear fashion starting from 3,5-dimethoxybenzaldehyde and using Oxa-Pictet–Spengler reaction as a key step [3] (Fig. 2). A second highly stereoselective synthesis of **2** was reported by Reddy et al. in the following year 2013 [4]. They have highlighted a linear 12 step synthesis focusing on oxa-Michael reaction, asymmetric propargylation, and Alder–Rickerts reaction as the key steps. Following this, in the year 2016, Mohapatra et al. came up with a convergent linear synthesis of **2** in 10 linear steps with 28% overall yield

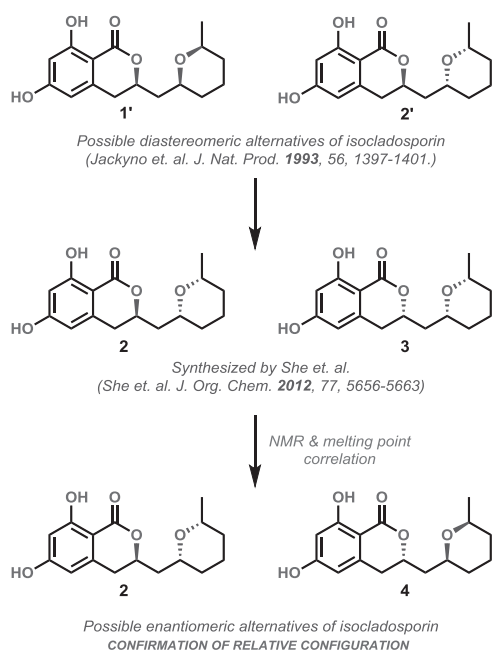


Fig. 1 Previous efforts toward structure determination of isocladosporin

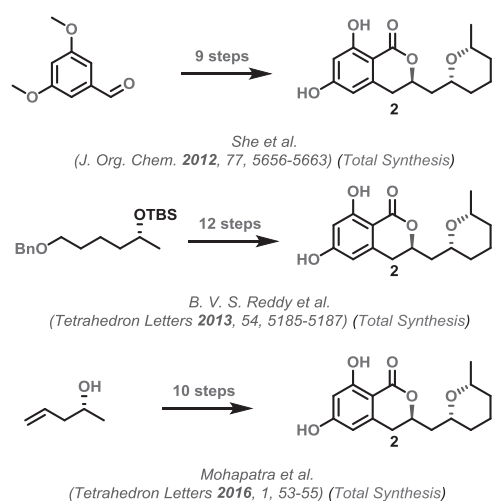
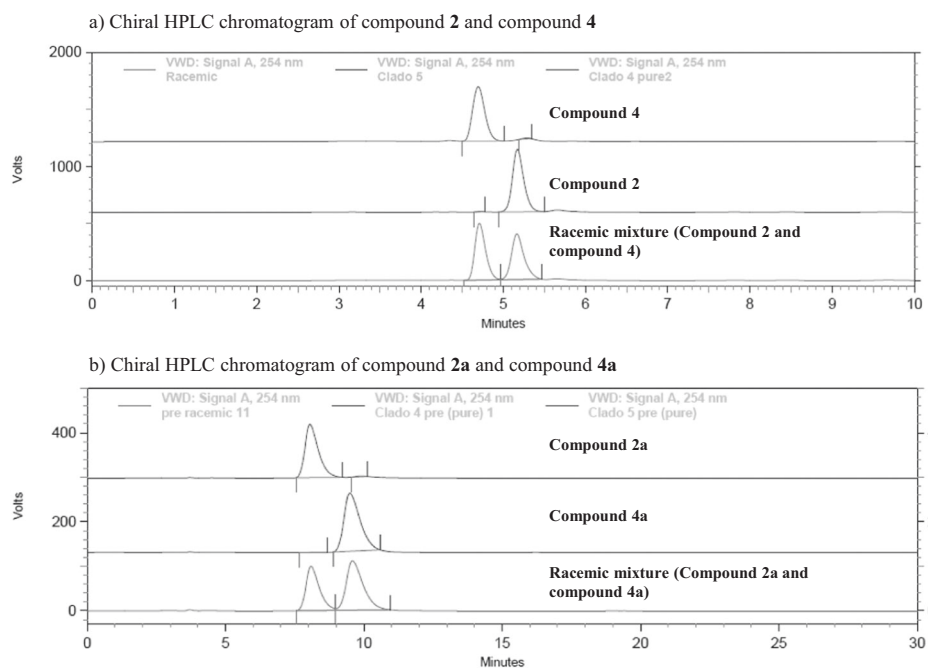


Fig. 2 Documented synthetic approaches toward isocladosporin

[5]. In a recent report from our group, we synthesized the entire stereochemical library of cladosporin in order to decipher the role of three dimensional molecular arrangement on antimalarial potency [6]. In the process of doing so, we synthesized both the possible enantiomers of isocladosporin, which happens to be the stereoisomers of cladosporin as well. We started our synthesis from commercially available chiral (*S*)-propylene oxide to access four stereoisomers and (*R*)-propylene oxide to access the rest in a divergent fashion. Owing to the lack of documented optical rotation for the natural isocladosporin, one could not directly establish its absolute stereochemical structure. Since

we have successfully synthesized both the enantiomeric possibility of isocladosporin, we planned to utilize etiolated wheat coleoptile bio-assay as a structural guiding tool to decipher the absolute stereochemistry of isocladosporin. But before plunging in to the biological assay we wished to ensure a maximum analytical and chiral purity of both the synthesized enantiomeric structures **2** and **4** as well as their immediate synthetic precursor **2a** and **4a** using high performance liquid chromatography (HPLC). All the compounds and their immediate intermediates were found to be 99% chirally pure with analytical purity >98% (Fig. 3).

Besides we did crystallize **2** and diffracted the same under X-ray generated from Cu source, so as to elucidate the absolute stereochemistry of the compound. The X-ray crystallographic data was also in complete accordance with the concerned structure [4]. Hence we could conclude an unambiguous stereochemical assignment of the related compounds on the basis of the in-depth characterization data in our hand (^1H and ^{13}C NMR, analytical and chiral HPLC, and single crystal XRD). Now, having a clear structural confirmation we aimed to decipher the absolute configuration of isocladosporin. Having no documented reports on optical rotation of the natural product we planned to take an assistance from biological assay for the purpose. In the isolation report by Jackyno et al. isocladosporin was found to inhibit the growth of etiolated wheat coleoptiles by 100% and 50% at concentrations 1000 and 100 μM , respectively. So we opted to reproduce the entire bio-assay on the two possible enantiomeric compounds of isocladosporin (**2** and **4**). Surprisingly, among the enantiomeric duo, compound **4** was found to actively inhibit the growth of coleoptiles with an inhibition of 99.1% and 68.5% at concentrations 1000 and 100 μM respectively, (Table 1, Fig. S1). On the contrary, the other enantiomer **2** was inactive or very less active (Table 1, Fig. S1). This observation led us to reasonably confirm **4** as the natural product, isocladosporin, with stereochemistry 3*S*, 10*S*, 14*S*. Having narrowed down the structural possibilities, we could further justify our confirmation through biosynthetic pathways as well (Fig. 4a) [7]. It is evident from the biosynthetic pathway that cladosporin is synthesized from linear tetraketide where the hydroxyl attached carbon (C-14) bears an *S* stereochemistry which is faithfully carry forwarded and retained in the natural product, cladosporin. Since isocladosporin is also produced from the same natural fungal source, it is reasonable to assume that the same hydroxyl stereocentre will also be reflected in the tetrahydropyran ring of isocladosporin. Now, in step 1 (Fig. 4a) the C-14 -OH does a Michael addition from the *si* face leading to an *R* stereochemistry at C-10. This Michael addition can also possibly occur from the opposite *re* face leading to the formation of a cyclic tetraketide have *cis* tetrahydropyran

Fig. 3 Chiral HPLC chromatogram of **2**, **4**, **2a**, and **4a****Table 1** Percentage inhibition in wheat coleoptile bio-assay

Sr. no.	Compound	% Inhibition at		
		10 μ M	100 μ M	1000 μ M
1.	Natural isocladosporin (unknown stereochemistry)	–	50	100
2.	Compound 2 (synthetic; 3 <i>R</i> , 10 <i>R</i> , 14 <i>R</i>)	0.9	14.4	29.7
3.	Compound 4 (synthetic; 3 <i>S</i> , 10 <i>S</i> , 14 <i>S</i>)	16.2	68.5	99.1
4.	Logran	61.3	88.3	99.9

(Fig. 4a) with an *S* stereochemistry at C-10. Now in step 2, depending on the stereochemistry at C-10, the Highly Reductive Polyketide Synthase (HR PKS) Cla2 might generate the C-3 stereocentre with a reverse selectivity to maintain the stable anti-relationship between C-10 and C-3. This in turn will generate the C-3 center with an *S* stereochemistry (Fig. 4a). This newly formed pentaketide fragment will then undergo further biotransformations to give rise to isocladosporin with a stereochemistry of 3*S*, 10*S*, 14*S* (Fig. 4b). Hence, this biosynthetic considerations also provided a possible and reasonable support to our observation.

It is worth mentioning here that while elucidating the role of stereochemistry on antimalarial potency, our group successfully identified cladosporin and unnatural enantiomer of isocladosporin (**2**) to be potent against *Plasmodium falciparum*. Like cladosporin, **2** also holds a selectivity of >100 folds toward parasitic enzyme (*PfKRS*) over that of human enzyme (*HsKRS*). In short, both natural cladosporin and

unnatural isocladosporin holds a potential toward the development of antimalarial leads with novel mode of action. On the other side, natural enantiomer **4** seems to be active for growth inhibition of certain plant fungal pathogens documented by Wang et al. [8].

Experimental section

General experimental procedures as well as experimental details and complete characterization data for all the compounds (**2**, **2a**, **4**, **4a**) are previously reported from our group [6].

Coleoptile bio-assay details

Coleoptiles bio-assay was carried out using wheat seeds as described by García et al. [9]. For instance, ~10–12 Wheat seeds (*Triticumaestivum L.*) were sown in pre-sterile Petri plates (15 cm) and moistened with water. The seeds were allowed to grow in the dark at 25 ± 1 °C for 3 days. Keeping the shoots intact, roots and caryopses were removed and shoots were placed in a Van der Weijguillotine [10]. The apical 2 mm of shoots were cut off and discarded. The 5 mm of further coleoptiles were performed under a green safe-light [11]. Compounds were pre-dissolved in DMSO (0.1%) and diluted in sterile phosphate-citrate buffer containing 2% sucrose at pH 5.6 to the final bio-assay concentration (1.0, 0.1, and 0.01 mM).

The commercial herbicide Logran was used as positive control at the same concentrations and under the same

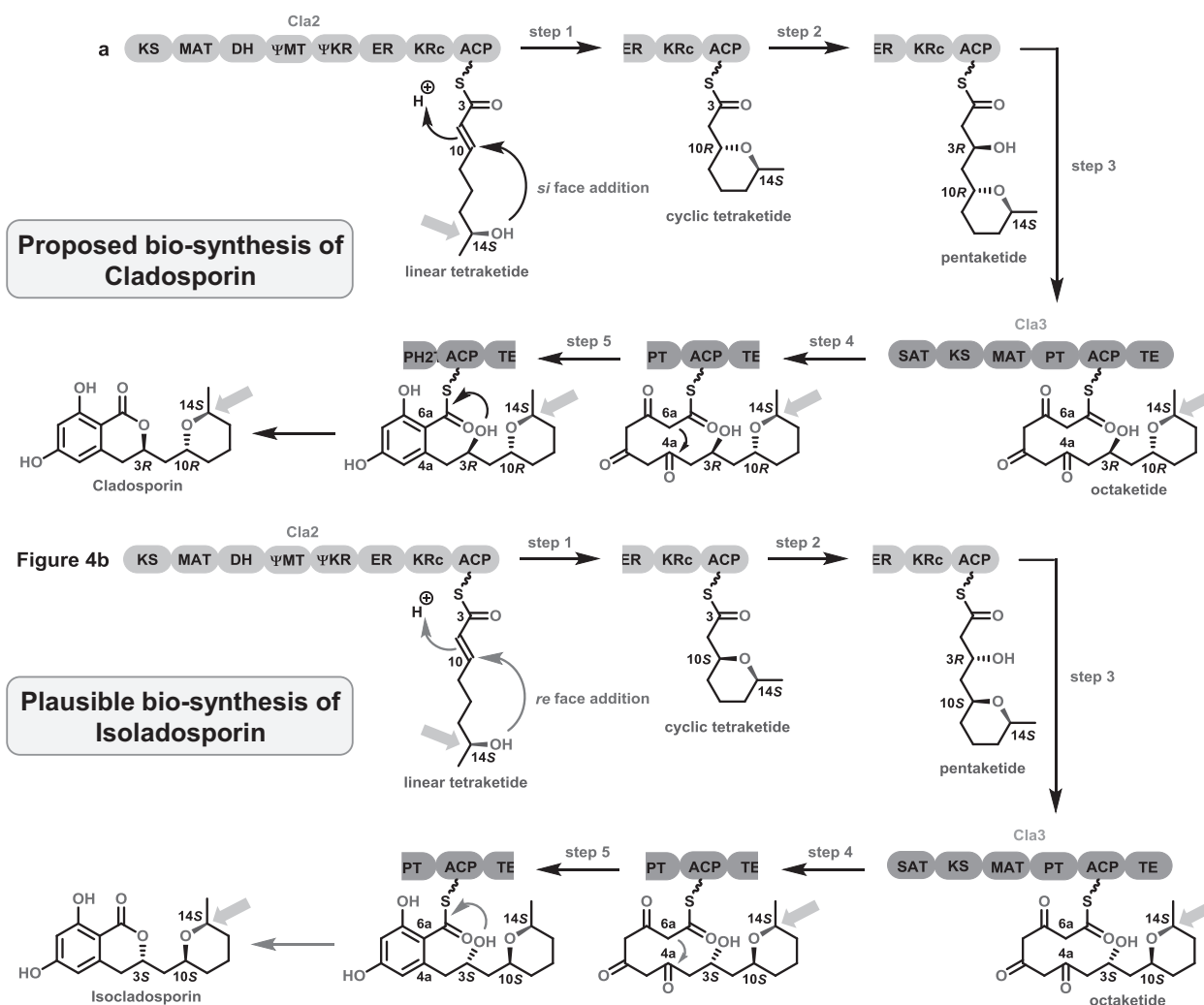


Fig. 4 **a** Biosynthetic pathway of cladosporin (figure modified from ref. 7). **b** Plausible biosynthetic pathway of isocladosporin

conditions as for test compounds [4, 12]. Buffered aqueous solutions with DMSO and without any test compound were used as a control blank for all the samples. For bio-assay, in 2 ml solution of each compound with said dilutions were dispensed in test tubes and five coleoptiles were placed in each test tube. The assay was performed in technical triplicate. The tubes were rotated at 6 rpm for 24 h at 25 °C in the dark. The coleoptiles' length were measured and data were presented as the percentage growth inhibition as compared with the buffer control. All the details of X-ray structure analysis including CIF file are available in our previous publication (see ref. [6]). We would like to mention that biosynthetic pathway is not the best option; it can only give an additional support to wheat coleoptile bio-assay in predicting stereochemistry of the natural isocladosporin.

Acknowledgements We thank Prof. Xuegong She for useful e-mail exchanges while we are sorting out discrepancies on optical rotation.

We would like to acknowledge University Grants Commission (UGC) for providing research fellowship to PD. Besides we thank Dr. Rajesh Gonnade (Center for Material Characterization, CSIR-National Chemical Laboratory, Pune) for X-ray crystallographic analysis. DSR would like to acknowledge the SERB, New Delhi, India, for funding the project titled "Hit to Lead Development of Potent Anti-Parasitic Natural Product. Scaffolds" (EMR/2016/004301).

Compliance with ethical standards

Conflict of interest The authors declare that they have no conflict of interest.

Publisher's note Springer Nature remains neutral with regard to jurisdictional claims in published maps and institutional affiliations.

References

- Jackyno JM, Harwood JS, Cutler HG, Lee MK. Isocladosporin, a biologically active isomer of cladosporin from *Cladosporium cladosporioides*. *J Nat Prod*. 1993;56:1397–401.

2. Scott PM, Van Walbeek W, Maclean WM. Cladosporin, a new antifungal metabolite from *Cladosporium cladosporioides*. *J Antibiot*. 1971;24:747–55.
3. Zheng H, Zhao C, Fang B, Jing P, Yang J, Xie X, et al. Asymmetric total synthesis of cladosporin and isocladosporin. *J Org Chem*. 2012;77:5656–63.
4. Reddy BVS, Reddy PJ, Reddy SC. The stereoselective total synthesis of isocladosporin. *Tetrahedron Lett*. 2013;38:5185–7.
5. Mohapatra DK, Maity S, Banoth S, Gonnade RG, Yadav JS. Total synthesis of isocladosporin and 3-*epi*-isocladosporin. *Tetrahedron Lett*. 2016;1:53–5.
6. Das P, Babbar P, Malhotra N, Sharma M, Jachak GR, Gonnade RG, et al. Specific stereoisomeric conformations determine the drug potency of cladosporin scaffold against malarial parasite. *J Med Chem*. 2018;61:5664–78.
7. Cochrane RVK, Sanichar R, Lambkin GR, Reiz B, Xu W, Tang Y, et al. Production of new cladosporin analogues by reconstitution of the polyketide synthases responsible for the biosynthesis of this antimalarial agent. *Angew Chem Int Ed*. 2016;55:664–8.
8. Wang X, Radwan MM, Taráwneh AH, Gao J, Wedge DE, Rosa LH, et al. Antifungal activity against plant pathogens of metabolites from the endophytic fungus *Cladosporium cladosporioides*. *J Agric Food Chem*. 2013;61:4551–5.
9. Gracia BF, Torres A, Macías FA. Synergy and other interactions between polymethoxyflavones from citrus byproducts. *Molecules*. 2015;20:20079–106.
10. Hancock CR, Barlow HW, Lacey HJ. The behaviour of phloridzin in the coleoptile straight-growth test. *J Exp Bot*. 1961;12:401–8.
11. Nitsch JP, Nitsch C. Studies on the growth of coleoptile and first internode sections. a new, sensitive, straight-growth test for auxins. *Plant Physiol*. 1956;31:94–111.
12. Macías FA, Simonet AM, Pacheco PC, Barrero AF, Cabrera E, Jiménez-González D. Natural and synthetic podolactones with potential use as natural herbicide models. *J Agric Food Chem*. 2000;48:3003–7.

Erratum

The following is corrected based on reviewer's suggestion.

Chapter 1, Section B

Page 88: The paragraph starting with "Herein, we would also like to document...gram scale operation" is repeated in the next page also.